DEFORMATION PHASES AND MINOR INTRUSIONS IN WESTERN ARGYLLSHIRE: REGIONAL IMPLICATIONS WITH RESPECT TO CALEDONIAN TECTONICS

by

Dilip Saha

A thesis submitted for the degree of
Doctor of Philosophy in the University of London

Department of Geology
Imperial College
London, SW7 2BP

May 1984

ABSTRACT

The thesis deals with the stratigraphical and structural evolution of W. Islay, Colonsay and Iona. The Colonsay Group represents a pre-Dalradian, Torridonian-like sequence which has undergone polyphase Caledonian deformation along with the basement Lewisian. The presence of an unconformity between the Lewisian and the overlying sediments is confirmed. The Colonsay Group and Bowmore Sandstone were deposited in isolated basins separated from each other and the Dalradian basin further east. They have been juxtaposed by Caledonian shortening, thrust movements, transcurrent motion along the Loch Gruinart fault and possibly a limited vertical displacement. Detrital mineralogy of the Colonsay Group and Bowmore Sandstone suggests the presence of Scourian granulites within the source.

The Dalradian is thrust over the foreland sequence of Bowmore Sandstone along the Loch Skerrols thrust. A type-I cross-girdle pattern of quartz c-axis fabric becomes well defined with increasing strain towards thrust line; fabric asymmetry reflects westward movement of the Dalradian along the thrust. Results from Loch Skerrols thrust and published data on quartz c-axis fabric elsewhere suggest a linear relationship between 'fabric strength' and Strain Intensity.

Three phases of folding (D_1 - D_3) and cleavage formation affect the Colonsay Group. Ductile deformation zones within the Islay Lewisian, folding of the Lewisian-sediment interface and local shearing in contact zone belong to D_1. A fourth phase (D_4) is represented mainly by brittle structures. Most of the minor intrusions in Islay-Colonsay-Iona are comparable to those belonging to the late- to post-Caledonian Microdiorite Suite of Smith (1979). Early lamprophyric dykes and sheets are affected by D_1 within the Lewisian and folded along with the metasediments during D_2 and D_3. The D_1-D_4 minor structures in W. Islay-Colonsay are consistent with NW-SE Caledonian compression. The penetrative deformation within the Colonsay Group is atypical of the thrust belt Torridonian of Northern Highlands and different from the style of deformation in Iona where the structure is controlled by east dipping thrust sheets forming a duplex, with the Lewisian-Torridonian contact acting as one thrust plane. Late stage brittle structures in Iona suggest NW-SE extension probably due to gravitational collapse consequent upon tectonic thickening in the region.

CONTENTS

		Page
	ABSTRACT	3
	CONTENTS	4
	LIST OF FIGURES	11
	LIST OF TABLES	20
	LIST OF MAPS	23
CHAPTER 1	LITERATURE REVIEW AND SCOPE OF THE THESIS	24
1.1	Introduction	25
1.2	Review of previous work	27
1.2.1	Early geological works on Islay	27
1.2.2	Early geological works on Colonsay	29
1.2.3	Early geological works on Iona	30
1.2.4	Later geological researches on western Argyllshire	31
1.2.5	Geophysical works	33
1.3	Scope of the present work	33
CHAPTER 2	STRATIGRAPHIC AND TECTONIC OVERVIEW	38
2.1	Introduction	39
2.2	The Lewisian	42
2.2.1	Western Islay	42
2.2.2	NE Colonsay	48
2.2.3	Iona	48
2.3	The Colonsay Group	49
2.3.1	Western Islay sediments	51
2.3.2	Sediments of Colonsay-Oronsay	61
2.3.3	Provenance of the Colonsay Group	66
2.3.4	The base of the Colonsay Group - unconformity or slide?	68

		Page
2.4	The Iona Group	69
2.5	The Bowmore Sandstone	72
	2.5.1 Introduction	72
	2.5.2 Stratigraphic subdivision and thickness	74
	2.5.3 Lithology	75
	2.5.4 Depositional environment	79
	2.5.5 Provenance	81
	2.5.6 Deformation	81
2.6	Structural history and minor intrusions	93
2.7	Major lineaments in western Argyllshire and the Malin Sea	95
	2.7.1 The Great Glen Fault System	95
	2.7.2 Fracture pattern in Colonsay and western Islay	102
	2.7.3 The Moine Thrust and the Loch Skerrols thrust	104
	2.7.4 Discussion	105
2.8	Stratigraphic Correlations	106
CHAPTER 3	STRUCTURES AT WESTERN ISLAY	110
3.1	Introduction	111
3.2	Pre-Caledonian deformation	113
3.3	Caledonian deformation within the Lewisian outcrop	113
	3.3.1 Ductile deformation zones (DDZ)	113
	3.3.2 Relative age of DDZ's	115
	3.3.3 Late structures	119
3.4	Deformation at the Lewisian-Torridonian contact	127
	3.4.1 Kilchiaran Bay area	128
	3.4.1.1 Contact zone rocks and minor structures	128
	3.4.1.2 Strain profile	133
	3.4.1.3 Microfabric	135
	3.4.2 Dun Medeir area	141

		Page
3.4.3	Port Charlotte area	142
3.4.4	Discussion	148
3.5	Folding episodes within the Colonsay Group	157
3.5.1	Succession of deformation events and minor intrusions	157
3.5.2	Early minor fold, F_1	158
3.5.3	Section across Sanaigmore Bay (F_2 and F_3 folds)	161
3.5.4	F_2 and F_3 structures from other subareas	161
3.5.5	Late structures	168
3.5.6	Axial planar fabrics	168
CHAPTER 4	THE LOCH SKERROLS THRUST - STRAIN AND MICROSTRUCTURES	178
4.1	Introduction	179
4.2	Mesoscopic structures in the thrust zone	181
4.2.1	A traverse from Loch Cam to An Carn	181
4.2.2	Bun-an-uillt area	182
4.3	Microstructural variation in a zone of strain gradient	183
4.3.1	Microstructure	183
4.3.2	Palaeostress estimate	191
4.4	Strain analysis	193
4.4.1	Background and methods	193
4.4.2	Specimen locations	196
4.4.3	Strain parameters and their values	196
4.4.4	Orientation of the finite strain ellipsoid	205
4.4.5	Displacement across the thrust zone	205
4.5	Quartz C-axis fabric	208
4.5.1	Fabric measurement and representation	208
4.5.2	The fabric pattern	210
4.5.2.1	'Matrix'	211
4.5.2.2.	'Clasts'	217
4.5.3	Fabric asymmetry	217

Page

4.5.3.1 Theoretical background 217
4.5.3.2 Asymmetry in fabrics from Loch Skerrols thrust zone 224
4.5.4 Discussion 225

4.6 Correlation between strain and degree of crystallographic preferred orientation 229
4.6.1 General statement 229
4.6.2 Point-density distribution and its variation 230
4.6.3 Fabric intensity parameter, η_3 234
4.6.4 Relationship between 'Fabric Intensity' and Strain Intensity 237

4.7 Relative age of thrusting 241

CHAPTER 5 DEFORMATION HISTORY IN COLONSAY-ORONSAY 248

5.1 Introduction 249

5.2 Outcrop pattern, folds and faults 250

5.3 Deformation at Lewisian-metasediment contact 250
5.3.1 General statement 250
5.3.2 Microstructures and strain 253

5.4 The fold phases 265
5.4.1 Episodic nature of folding and intrusion 265
5.4.2 D_1 structures 267
5.4.2.1 Early isoclinal folds 267
5.4.2.2 Other structures 271
5.4.3 D_2 structures 271
5.4.4 D_3 structures 274

5.5 Deformation and cleavage development 281
5.5.1 First axial plane cleavage, S_1 289
5.5.2 Second axial plane cleavage, S_2 293
5.5.3 Third axial plane cleavage, S_3 299

		Page
5.5.4	Spatial variation in the intensity of S_3	299
5.5.5	Relationship between metamorphism and folding	300
CHAPTER 6	LOCAL STRUCTURES IN IONA - REGIONAL IMPLICATIONS	308
6.1	Introduction	309
6.2	Deformation along the Lewisian-Torridonian contact	310
6.2.1	General features	310
6.2.2	A strain estimate	315
6.2.3	Microstructures	318
6.3	Early folds	325
6.4	West dipping shear zones and thrusts	329
6.5	Later minor structures	334
6.5.1	Reverse kinks	334
6.5.2	Asymmetric boudins	335
6.5.3	Brittle shears with a strike slip movement	343
6.6	Metamorphism	353
6.6.1	Regional/Dynamic metamorphism	353
6.6.2	Contact metamorphism	354
6.7	Discussion and summary of events	359
CHAPTER 7	CALEDONIAN MINOR INTRUSIONS	365
7.1	Introduction	366
7.2	General description	366
7.2.1	The intrusions around Port Easdale, Kiloran Bay, Colonsay	367
7.2.2	Scalasaig Diorite, Colonsay	374
7.2.3	Machire intrusion, Islay	380

Page

7.2.4 Contact metamorphic effect of the plutons 380
7.2.5 Sheet-like intrusions 381
7.2.5.1 Sheared lamprophyric sheets in Lewisian 381
7.2.5.2 Folded lamprophyres with an axial plane cleavage 385
7.2.5.3 Lamprophyres with an oblique cleavage 385
7.2.5.4 Unfoliated microdiorites 393
7.2.5.5 Felsic porphyrites 393

7.3 Mineral chemistry in plutonic intrusions 396
7.3.1 Clinopyroxene 396
7.3.2 Olivine 400
7.3.3 Biotite 401
7.3.4 Feldspar 405

7.4 Origin of oblique cleavage in intrusive sheets 405

7.5 Structural controls on the orientation of minor intrusions 412
7.5.1 Appinitic intrusions with explosion breccia 412
7.5.2 Dykes and inclined sheets 415

7.6 Comparison with Caledonian minor intrusions of Northern Highlands 416

7.7 Discussion and conclusions 418

CHAPTER 8 GENERAL DISCUSSION AND CONCLUSIONS 424

8.1 Correlation between islands 425

8.2 Basement-cover relations 426

8.3 Possible large scale structures in W. Islay-Colonsay 431

8.4 Timing of deformation in the Colonsay Group 438

8.5 Tectonic history 441

		Page
8.6	Conclusions	446
ACKNOWLEDGEMENTS		448
REFERENCES		449
APPENDICES		461
4A	Determination of 2D strain by R_f-ϕ method	461
4B	Determination of 2D strain by an algebraic method	462
4C	Test of initial randomness of strain-markers	465
4D	Determination of 3D strain	467
4E	Rotation of poles	476
4F	Estimation of point-density	488
4G	Probability distribution of point-density	498
4H	Calculation of eigenvalues of the Scheidegger's Orientation Tensor	500
4I	Linear Regression Analysis	501

LIST OF FIGURES

		Page
1.1	Location map for the Western Argyll district.	26
2.1	Lewisian outcrop in western Islay, after Survey map, 1" sheet no. 19.	41
2.2	Components of Lewisian Gneiss in the Rhinns of Islay.	45
2.3	Stratigraphic successions in W. Islay, Colonsay and Iona.	50
2.4	Sedimentary structures in the Colonsay Group.	53
2.5	Detrital mineralogy of the metasediments of W. Islay.	57
2.6	Geological map of Colonsay-Oronsay.	62
2.7	Schematic drawing showing a probable basin floor configuration during deposition of the Colonsay sediments.	67
2.8	General geological map of Iona.	70
2.9	Trough cross-bedding in flags, St. Ronan's Bay, Iona.	71
2.10	Geologic setting for the Bowmore Sandstone.	73
2.11	Detritral clasts in the Bowmore Sandstone, Blackrock area.	77
2.12	(a) Structure map of the Laggan area and schematic sections to explain the observed structures. (b) Intraformational shale breccia and bottom structure in Laggan Group. (c)Overturned cross-bedding in Laggan Group. (d) Minor iso-clinal folds in Laggan Group.	83
2.13	Axial plane cleavages in Bowmore Sandstone.	89
2.14	A cartoon showing a possible late Precambrian to early Palaeozoic scenario for the Malin Sea area.	94

		Page
2.15a	Geologic map of the Scottish Highlands to show the present position of the Moine injection complexes, the Strontian and Foyers granites and the Moine Thrust plane, from Kennedy (1946).	96
2.15b	Geologic map of the Scottish Highlands to show the former positions of Moine Injection complexes, the Strontian and Foyers granites, and the Moine Thrust plane prior to the lateral displacement along the Great Glen Fault, from Kennedy (1946).	97
2.16	Reconstruction of Scotland in the Lower Old Red Sandstone according to Garson and Plant (1972).	98
2.17	Solid geology of the Malin Sea, after Evans et al. (1980).	101
2.18	Rose-diagrams showing the azimuth of photointerpreted fractures in W. Islay and Colonsay.	103
3.1	General geologic map of W. Islay.	112
3.2	Equal-area plot showing orientations of gneissic foliations, mylonite foliation in DDZ's and azimuth of brittle shear zones with mineral veins from Islay Lewisian.	114
3.3	Morphology of ductile deformation zones (DDZ) in Islay Lewisian, Cladville.	116
3.4	Shear bands displacing mylonite foliation in Lewisian, Port Charlotte, W. Islay.	121
3.5	Late Caledonian structures in Islay Lewisian.	125
3.6	Shearing along Lewisian-Eilean Liath Grit contact, south-west of Kilchiaran Bay.	131
3.7	R_f-Ø plots for 2-dimensional strains in Crosprig Grit and Eilean Liath Grit at different distances from the Lewisian boundary.	137

		Page
3.8	Optical micrographs showing details of ribbon grains and dynamic recrystallisation along grain boundaries.	139
3.9	Quartz c-axis fabric in quartz-ribbon-mylonites, sp. 577A, Eilean Liath Grit.	139
3.10	Optical micrographs showing mylonite foliation and shear bands in basal pebbly grit, Dun Medeir, W. Islay.	145
3.11	Simplified geologic map of the Port Charlotte-Bruichcladdich area.	147
3.12	Pebbles in epidotic grits immediately overlying Lewisian Gneiss, Port an t Sruthain, Port Charlotte, W. Islay.	151
3.13	Kinematic analogue for the deformation of the Lewisian-Colonsay Group contact, W. Islay.	155
3.14	Intrafolial folds in the Colonsay Group, Rubha na-h-Airde-Moire Phyllite, W. Islay.	159
3.15	D_2 and D_3 structures from Sanaigmore Bay, W. Islay.	163
3.16	Superposition of D_2 and D_3 structures, Sanaigmore and Smaull, W. Islay.	165
3.17	Equal-area plots showing orientations of D_2 and D_3 structures from different areas, W. Islay.	167
3.18	Axial planar fabrics in the metasediments of W. Islay.	173
4.1	Geologic setting for the Loch Skerrols thrust.	180
4.2	Equal area plot of foliation poles and mineral elongation lineation in the Loch Skerrols thrust zone.	184
4.3	Microstructural changes in the Jura Quartzite with increasing strain.	185

		Page
4.4	Distribution of the aspect ratio of dynamically recrystallised grains in specimens with different Strain Intensities.	190
4.5	Localities of specimens of Jura Quartzite used for strain and fabric measurements.	197
4.6	Strain values from Loch Skerrols thrust zone. (a) Flinn plot; (b) Strain Intensity *vs.* Lode's parameter; (c) R_f-Ø plots.	201
4.7	Equal area plot showing the orientation of principal 3-dimensional strains in the Loch Skerrols thrust zone.	207
4.8	Component of displacement across the Loch Skerrols thrust due to intracrystalline slip.	209
4.9	Quartz c-axis fabric in 'matrix', Loch Skerrols thrust zone.	213
4.10	Quartz c-axis fabric in 'clasts', Loch Skerrols thrust zone.	218
4.11	Fabric asymmetry in model and natural materials deformed under simple shear.	223
4.12	Movement along Loch Skerrols thrust and its relation with asymmetry of quartz c-axis fabric.	226
4.13	Composite quartz c-axis fabric showing progressive development of an asymmetric cross-girdle pattern with increasing strain in the Loch Skerrols thrust zone.	227
4.14	Probability distribution of point-density in Series A samples.	232
4.15	Probability distribution of point-density in Series B samples.	233

Page

4.16 Distribution of point-density in a sample of quartz c-axis fabric, sp. loc. 82 and its comparison with theoretical GAMMA distribution. 235

4.17 A linear relationship between Strain Intensity (ϵ_s) and the Fabric Intensity parameters, η_3 or C. 240

4.18 Field of observed strain ellipsoids in the Loch Skerrols thrust zone and its relationship with the boundary between constriction and flattening strain for differential volume loss. 244

4.19 The effect of superposed shearing strain on the shape of an initial flattening or constriction ellipsoid. 245

4.20 Schematic drawings showing the evolution of the Islay Anticline with progressive deformation. 247

5.1 General geologic map of Colonsay-Oronsay (after Survey map) with axial traces of some F_3 folds shown. 251

5.2 Outline geological map of NE End, Colonsay. 255

5.3 Change of pebble shape and intrapebble microstructure with increasing strain. 257

5.4 Optical micrographs showing microstructures in the mylonitised pebbly grit in contact with the Lewisian Gneiss, NE end, Colonsay. 261

5.5 R_f-ϕ plots for the determination of strain in the pebbly grit, locality marked D on Fig. 5.2. 264

5.6 Early isoclinal folds in Colonsay and their refolding. 269

5.7 Equal-area plot showing the orientations of F_1 elements from different areas in Colonsay. 272

5.8 Schematic drawings to illustrate the formation of boudinage at a late stage of F_1 folding. 273

		Page
5.9	F_2 folds in Colonsay.	277
5.10	Equal-area plot showing orientation of minor structures from different parts of Colonsay.	279
5.11	F_3 structures from Colonsay.	283
5.12	Kink-like structures from Colonsay.	287
5.13	Morphology of S_1 in phyllites of Kiloran Bay, Milbuie Grit of Milbuie and semipelitic rocks of Port an Obain, Colonsay.	291
5.14	Morphology of S_2 cleavage in Oronsay Mudstone, south of Ardskenish; Limestone bands, Kiloran Bay; grits, Machrins.	297
5.15	Optical micrographs showing the relationship between metamorphic mineral crystallisation and deformation in Colonsay.	303
6.1	Equal-area plot showing the orientations of mylonite foliation and stretching lineation along the Lewisian-Torridonian contact zone, Iona.	311
6.2	East dipping shear zone in Iona and associated minor structures.	313
6.3	R_f-ϕ plot for 2D strain in contact zone and orientation of 2-dimensional principal strains, N. Iona.	316
6.4	R_f-ϕ plots for 2D strain determinations, magnitude and orientations of 3D principal strains in mylonitised basal pebbly grit, N of Marble Quarry, Iona.	317
6.5	Optical micrographs showing microstructures in deformed Lewisian-Torridonian contact zone rocks, Iona.	321

Page

6.6 An asymmetric cross-girdle pattern of quartz c-axis fabric, Sp. I9Al and its comparison with an idealised type-I cross-girdle pattern. 323

6.7 Early minor folds and axial plane cleavage, Iona. 327

6.8 West dipping shear zones and thrusts in Lewisian rocks and contact zone mylonites, Iona. 331

6.9 Reverse kinks, flagstone, St. Ronan's Bay, and schematic drawings to illustrate their evolution. 337

6.10 Asymmetric boudins and conjugate shear planes in flagstone, south of Sligeneach, and diagrammatic sketches to illustrate their formation. 341

6.11 Rose diagrams showing the orientation of brittle shears with strike slip displacement, Lewisian and Torridonian of Iona. 345

6.12 Late brittle shears (strike slip) and associated kinks in Torridonian, Iona. 347

6.13 Brittle shear zones (with or without mineral veins) in Lewisian rocks, near Port Laraichean, Iona. 351

6.14 Contact metamorphic effects of the Ross of Mull granite, Iona. 357

6.15 Distribution of major cataclastie-mylonite belts in Iona. 360

6.16 Schematic E-W cross sections showing the evolution of duplex structure in the Iona region. 362

7.1 Geologic setting for Port Easdale intrusions, Kiloran Bay, Colonsay. 369

7.2 Marginal breccia and xenoliths associated with Port Easdale intrusions, Kiloran Bay. 371

		Page
7.3	Geologic setting for Scalasaig Diorite, and Queen's Bay intrusives, Colonsay.	375
7.4	An ultrabasic xenolith within the Scalasaig Diorite, North of Colonsay Pier.	377
7.5	Geologic setting for the appinitic intrusion of Machire Bay, western Islay.	379
7.6	Photomicrographs showing microstructures of sheared-early 'lamprophyric' dykes and folded lamprophyres with an axial planar fabric.	383
7.7	Lamprophyre dykes (group C) with an oblique internal foliation, Claddich and Kilchiaran Bay, W. Islay.	387
7.8	Relationship between gneissic banding, ductile deformation zones in Islay Lewisian and the Group C dykes.	395
7.9	Unfoliated microdiorite (group D) and felsic porphryite (group E), Iona.	395
7.10	Clinopyroxene compositions in the xenoliths and host rocks of the plutonic intrusions of Scalasaig and Queen's Bay, Colonsay.	399
7.11	Feldspar compositions in the appinitic intrusions of Colonsay.	404
7.12	Orientations of group C dykes, internal foliations, and their relationship with local structures, W. Islay.	411
7.13	Equal area plot showing the orientation of group C lamprophyre dykes in the Islay Lewisian.	413
7.14	Occurrences of appinitic and basic intrusions in Scottish and Irish Caledonides. Northern Highland occurrences from Smith (1979).	422

		Page
8.1	Probable major structures in W. Islay - Colonsay.	434
8.2	Variation in the spatial development of folds in W. Islay and Colonsay.	437
4B.1.	Isotropically oriented markers in the unstrained rock. Lines drawn parallel to the two directions (arbitrarily chosen to coincide with the directions of principal strain, K_x, K_y) through the centre C of each marker define segments a_j and c_j respectively.	463
4D.1.	Equal area plot showing reference co-ordinate frame and orthogonal sections of 2D strains.	468
4D.2.	Flowchart for main program LAMBDA (a), subroutine SOLVE (b) and subroutine ORIENT (c).	473
4D.3.	Graphical representation of the cubic, $F(x) = x^3 - J_1x^2 + J_2x - J_3$, where J_1, J_2 and J_3 are the strain invariants.	475
4E.1.	Transformation of axes.	479
4E.2.	Transformation of the components of a vector.	479
4E.3.	Geometric relations for clockwise rotation of a pole around an axis OR through an angle .	479
4E.4.	Flowchart for program SPIN8.	486
4F.1.	Definition of the count-volume (nearest neighbourhood) around each grid-intersection, G. OG' is the position vector of G on the lower hemisphere. Nearest neighbourhood is defined by a cone with semivertical angle .	490
4F.2.	Relationship between spherical polar co-ordinates ($\emptyset, \gamma, 1$) and the direction cosines (l_i, m_i, n_i) of a pole considered as a unit vector $\vec{ON}_i$. The spherical polar co-ordinates are also shown in an equal-area projection.	491
4F.3.	Flowchart for program POLEV3X.	497

LIST OF TABLES

		Page
2.1	Major rock group in W. Argyll.	40
2.2	Proportions of different mineral grains in psammitic horizons of western Islay.	59
2.3	Stratigraphic groups in Colonsay-Oronsay, after Stewart (1962).	63
2.4	Modal analysis of some psammites from Colonsay (from Stewart (1962).	64
2.5	Proportions of different mineral grains in the Bowmore Sandstone.	80
2.6	Deformation events in the Bowmore Sandstone.	91
2.7	Analysis of 'illite' from Blackrock Group.	92
2.8	Correlation chart for late Precambrian-Lower Palaeozoic in W. Argyll.	109
3.1	Deformation textures in Eilean Liath Grit (at various distances from the Lewisian contact) as compared to the Crosprig Grit.	134
3.2	Strain values from near the Lewisian-sediment contact around the Kilchiaran Bay area, Rhinns of Islay.	134
3.3	The dependence of morphology of the axial plane cleavages on deformation phase and lithology.	177
4.1	Proportion of 'matrix' to 'clast' in deformed Jura Quartzite, Loch Skerrols thrust zone.	189

		Page
4.2	Dynamically recrystallised quartz grain-size and palaeo-stresses in a traverse across the Loch Skerrols thrust.	193
4.3	Table of strain values, Loch Skerrols thrust zone.	206
4.4	Point-density statistics for different C-axis fabric samples.	236
4.5	Values of Strain Intensity and Fabric Intensity in two zones of strain gradient.	239
4.6	Linear regression analysis on Strain Intensity and Fabric Intensity parameters.	240
5.1	General classification of minor structures in Colonsay and their relationship with minor intrusions.	267
5.2	Electronmicroprobe analyses of cholitoids, phyllites, north of Kiloran Bay.	305
6.1	Sequence of Caledonian events in Iona.	364
7.1	Composition of olivine in xenoliths and host rock, Scalasaigand Queen's Bay intrusives, Colonsay.	401
7.2	Electronmicroprobe analyses of biotites from xenolith and host rock, Scalasaig and Queen's Bay.	402
7.3	Mg/Fe ratios in xenolithic biotites, Scalasaig and Queen's Bay.	403
7.4	Relative age of Caledonian minor intrusions, Argyllshire and SW Inverness-shire.	419
8.1	Correlation of structures in W. Islay and Colonsay.	427
8.2	Relative age of structures in different rock groups of W. Argyllshire.	428

		Page
8.3	Deformation along basement-cover contact, W. Argyllshire.	429
4C-I	Results of tests on initial randomness of elliptical markers used in 2-dimensional strain determinations.	466
4E-I	Sense of rotation of poles obtained by executing program SPIN8.	485
4F-I	Control values to be supplied as input for different data types in program POLEV3X.	495
4F-II	Print-symbols for different ranges of point-density values.	496
4G-I	Listing of a CTUNT matrix.	499

LIST OF MAPS (in back folder)

Map I Photointerpreted fracture pattern map of W. Islay.

Map II Photointerpreted fracture pattern map of Colonsay.

Map III Structural map of W. Islay (Lewisian outcrop excluded).

Map IV Structural map of Colonsay.

Map V Structural map of Iona (Lewisian excluded).

CHAPTER 1

LITERATURE REVIEW AND SCOPE OF THE THESIS

1.1 INTRODUCTION

The Western Argyll district lies near the north-western margin of the Caledonian Orogen and forms the southwest extremity of the marginal belt so far as the Scottish Caledonides are concerned (Fig. 1.1). In each of the three islands, Islay, Colonsay and Iona, low grade metasediments occur in association with a basement that is generally assigned to the Lewisian Gneiss. In NW Scotland the Moine Thrust separates the Moine rocks of upper greenschist - amphibolite facies from the Torridonian and Cambrian of the foreland. In the region between Cape Wrath and Skye virtually undeformed foreland sediments overlie the Lewisian basement. In contrast to this, metasediments of Colonsay and western Islay are highly deformed with a history of several phases of folding and cleavage development. The Caledonian deformation of the basement which lies unconformably below these sediments is shown by the development of shear zones. Both the basement and the overlying metasediments are intruded by lamprophyric and appinitic intrusions. Moreover, the Lewisian in the Islay-Colonsay area is relatively inward in the orogen, compared to the foreland of the Northern Highlands, as if there is a left lateral offset of the basement as one traces the Caledonian marginal belt southwards through Ross of Mull and the Malin Sea area.

In the Northern Highlands the marginal belt is marked by two important lineaments - the Moine Thrust and the Great Glen Fault. The major Dalradian outcrops occur to the east of the Great Glen Fault. Undoubted outcrop of the Moine Thrust is reported from as far south as the Skye region. The Great Glen Fault can be traced for 210 kms from Tarbet Ness, in Easter Ross to the island of Mull. Several authors have suggested the continuation of these lineaments through the Malin Sea area (Evans et al. 1980, Pitcher 1969). However, the position of the lineaments in the offshore region and the displacement along them is a matter of debate in the absence of any definitive evidence. Detailed study of the local structures in western Islay, Colonsay and Iona, which forms the core of the present thesis, has apparently succeeded in putting some additional constraints on the positioning of the major lineaments in the area. Moreover, the highly involved deformation history of the rocks of western Islay and Colonsay which may in part predate the Dalradian structures of NE Islay is important when one tries to ponder on the existence and extent of any

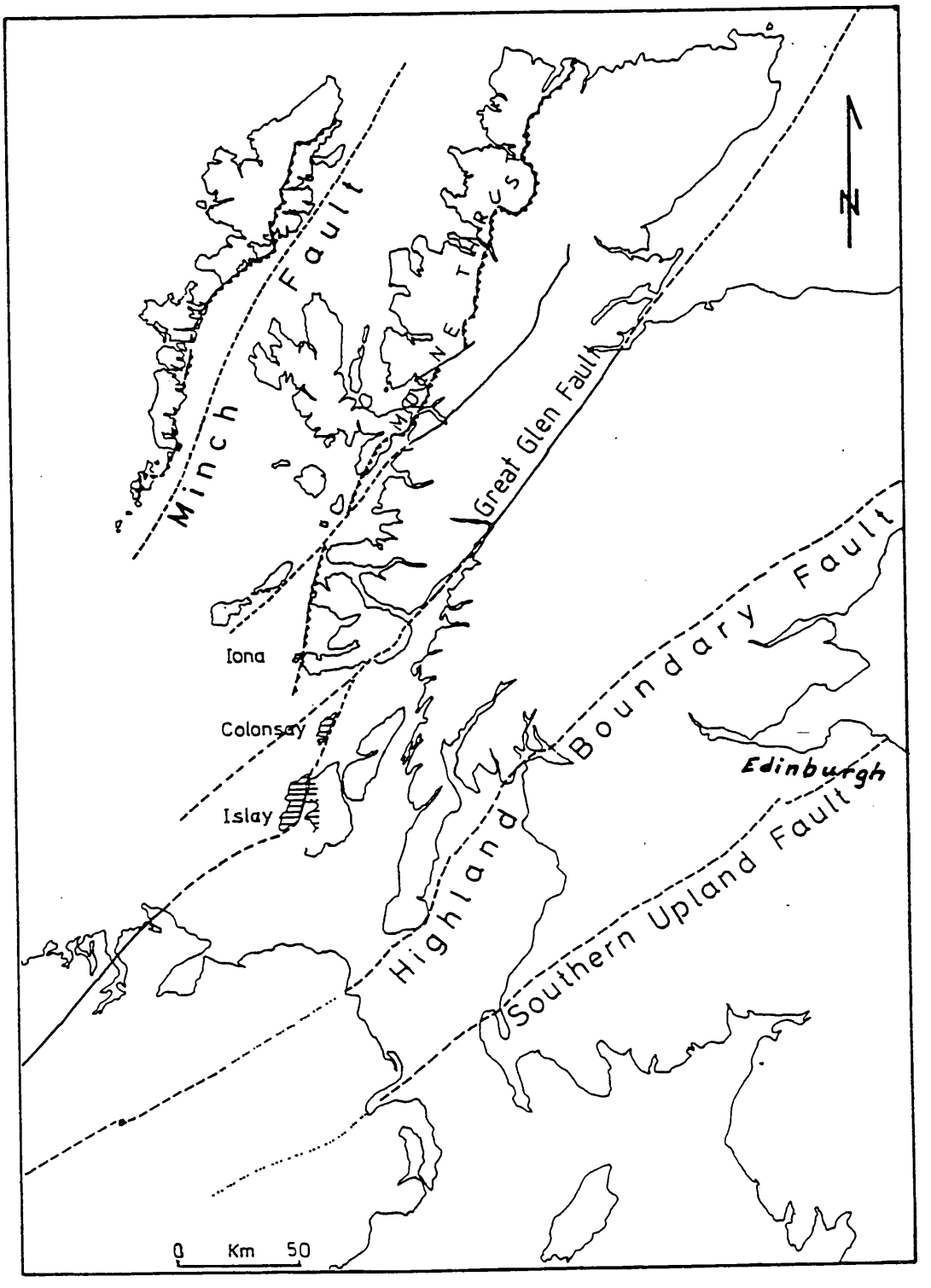


Figure 1.1. Location map for the western Argyll district. The area studied is shaded on the map.

tectonothermal events which occurred after the Laxfordian events but before the Caledonian Orogeny (sensu stricto). Thus on extended consideration present study has some bearing on the Caledonian-Appalachian continuity, and on the position of the Grenville front in the Scottish Caledonides.

Caledonian minor intrusions are well recorded in the region north of the Great Glen Fault. They have been systematically classified and show a definite grouping with respect to the Caledonian deformation events (Smith 1979). Minor intrusions showing petrographic affinities with those occurring north of Great Glen and in the Ballachullish district also occur in the area studied. It has been found that the different groups of intrusions have a distinct age relative to the local folding events. On the basis of the information gleaned from the study of the local structures and minor intrusions and from their mutual relationship, attempts have been made to put some constraints on the solution of more general problems related to the evolution of the northwest marginal belt of the Caledonian Orogen.

1.2 REVIEW OF PREVIOUS WORK

The area studied includes three islands in the Inner Hebrides - western Islay, Colonsay and Iona. Early geologic works especially those carried out in the late eighteenth and the nineteenth century treat the islands on an individual basis. In the following sub-sections these works are briefly reviewed with reference to each island.

1.2.1 Early Geological Works on Islay

Geological studies on Islay can be traced back to late 18th century. Mills (1879) first referred to the intrusive nature and basaltic character of the dolerite dykes of Islay. MacCuloch (1819) anticipated in several points conclusions reached by later workers. MacCuloch (op. cit.) compared the 'feldspathic hornblendic gneiss' on the eastern shore of the western Islay to that of Iona and the Outer Hebrides. He also referred to the conglomerate of Portaskaig and Lossit hill (NE Islay) as a primary conglomerate, correlating it with a similar rock in the Garvelloch Isles and Schehallion (boulder bed of Perthshire).

Murchison and Geikie (1861) regarded the grits and the schists of western Islay as equivalent to the lower quartz rocks (later shown to be Cambrian) of western Sutherland. However, they erroneously described the 'granitoid rocks of the southern part of the promontory (The Rhinns) as being intrusive into the grits and schists'. Thomson (1871) was the first to pronounce definitely as to the Laurentian (Lewisian) age of the gneiss of the Rhinns on the basis of the lithological resemblance to the fundamental gneiss of Sutherland and the Outer Hebrides.

With the publication of the Geological Survey (Scotland) memoir on the Geology of Islay in 1907 (henceforth to be referred to as the 'Islay memoir') considerable detail on the geology of the island became available. The memoir put on record the structural separation of the Rhinns from the eastern part of the island by the Loch Skerrols thrust. With the exception of numerous intrusive dykes, the western Islay rocks were described as of Precambrian age, the grits, shales and conglomerates representing the Torridonian and unconformably overlying the Lewisian Gneiss. The gneissic rocks occur in the southern half of the Rhinns, south of Kilchiaran and Bruichcladdich. The Bowmore grits, which comprise the isolated exposures of Blackrock, Gortan (possibly belonging to the western Islay sediments) and Laggan area, were compared with the Applecross Group on the basis of pebble composition (Wilkinson et al. 1907). The whole Bowmore group which shows signs of little penetrative deformation was regarded as younger than the Rhinns conglomerate series and the Kilchiaran slates and grits series. The rocks of E Islay (the Dalradian) are divided into a ?lower Southern Series and a Northern Series, the Beinn Bhan Quartzite and Conglomerate forming the dividing line. The Portaskaig Conglomerate which forms the lowermost unit of the Northern Series contains pebbles of gneiss resembling that from the Rhinns of Islay, of sandstone and grit like the Torridon arkose (Wilkinson et al. 1907). Thus the rocks of the Rhinns of Islay are regarded as being older than the Northern Series (in part equivalent to the Argyll Group in current nomenclature).

Bailey (1916) postulated an important dislocation along the hollow of Loch Gruinart on the ground that the Bowmore Sandstone cannot be traced west of the hollow. He suggested that the dislocation is the continuation of the Great Glen Fault and named it the Loch Gruinart Fault. Moreover, the Loch Skerrols thrust was correlated with the

Moine Thrust via a southeasterly downthrow along the Loch Gruinart Fault (Bailey op. cit.). However, a large sinistral displacement along the Great Glen Fault was unaccounted for in this hypothesis. Bailey (1916) also suggested an overturned anticlinal structure for the Dalradian sediments of NE Islay.

Green (1924) in his controversial paper suggested a synclinal structure for the NE Islay, correlated the Bowmore Sandstone with the Portaskaig Conglomerate, and regarded the latter as being overlain by and hence older than the Islay Quartzite and the rest of the Southern Series. He wrongly denounced the idea of the Loch Skerrols thrust.

1.2.2 Early Geological Works on Colonsay

Peach (1907) regarded the rocks of Oronsay, a small isolated island separated from Colonsay only during the high tide, as a continuation of the Torridonian rocks of western Islay. He argued that the alternating series of greenish and grey slates or phyllites, and schistose feldspathic grits and greywackes of Oronsay are identical in character with those seen on the promontory of Ardnave, the northern extension of western Islay.

Prior to Peach (1907), Geikie (1878) drew attention to the slight metamorphism of the Colonsay rocks as compared to the schists of the Scottish Highland, and also to the fact that at places the rocks of Colonsay are highly folded. He also described the Diorite of Scalasaig and the Syenite of Kiloran Bay, giving an account of the associated breccia, which he regarded as volcanic, and tentatively correlated with the igneous rocks of Mull.

Wright (1908), in his paper on 'The two earth movements of Colonsay', shows that the sediments of Colonsay are highly folded and are also affected by two distinct cleavages. According to Wright (op. cit.), the earlier of these is a slaty cleavage, the second a strain slip cleavage; the 'earth movements' which resulted in the production of these two cleavages were separated by a period of igneous activity, during which the diorite and syenite masses of the island and also a large proportion of the lamprophyres were intruded.

The Geological Survey (Scotland) memoir (1911) on the geology of Colonsay and Oronsay (henceforth to be referred to as the 'Colonsay memoir') records the presence of the Lewisian Gneiss covering in all somewhat less than an eighth of a square mile. The gneiss strip occur in the midst of Torridonian sediments at the north end of the island. As to the Torridonian affinities of the sediments, the memoir records:

> "The highly cleaved sediments of which Colonsay and Oronsay are for the most part built may be assumed with a fair degree of certainty to be of lower Torridonian age. They embrace a great variety of rocks, including limestones, phyllites, mudstones, banded flags, sandstones and feldspathic and epidotic grits and conglomerates. The general assemblage of types so closely resembles that of the Rhinns of Islay and the Diabaig or Lower Torridonian Group of Skye as entirely to justify the conclusion that the three districts are largely built up of one and the same group of rocks. The prevalence of feldspathic sediments, the absence of any beds which could be called a quartzite, and the abundance of epidote on various horizons mark off this group as distinct from the rocks of Jura and those parts of Islay to the east of the Loch Skerrols Thrust."

However, Craig et al. (1911) were not certain about the relationship of the Lewisian Gneiss to the surrounding sediments. They noted that the conglomerate contains not a single fragment of gneiss, but yields only quartz, quartzite and felsite (not substantiated by present study) pebbles. Craig et al. (1911) also record that the occurrence of the conglomerate affords little evidence as to the relation of the gneiss strip to the sediments.

Some details on the petrography and chemistry of the syenite intrusion at Kiloran Bay, Colonsay was given by Reynolds (1936); the nature of the quartzite xenoliths and their petrogenetic significance were also discussed in this work.

1.2.3 Early Geological Works on Iona

Early geological works on Iona have been summarised in the accounts of Anderson (1921) and Jehu (1922). The Geological Survey

memoir on the geology of Staffa, Iona and Western Mull published in 1925 draws largely from Anderson's account. About three quarters of the island of Iona is occupied by rocks which may be regarded without doubt as belonging to the Lewisian Complex. Both ortho- and para-gneisses have been reported, although the former predominates over the latter. The Iona marble belongs to the para-gneisses. Bailey et al. (1925) remark that evidence about the relative ages of the igneous and sedimentary components is inconclusive.

'Little metamorphosed black slates and grits' in the northeast of Iona, which overlie arkoses and conglomerates derived from the Lewisian Gneiss have been regarded as doubtfully Torridonian (Geikie 1889, Bailey et al. 1925). Bailey et al. (1925) observed that the basal conglomerate as a whole has been very intensely crushed, but they decline to consider any definite break or thrust along the margin. It has also been reported (Geological Survey memoir 1925) that the three small islands close to the SE shore of Iona are formed of an extension of the Ross of Mull granite which must underlie a large part of the Sound of Iona.

The granite boundary comes close to the low water line of the main island, where contact metamorphism has caused a noticeable degree of alteration in the shales and flags. Jehu (1922) ascribed the uniform 'hornfelsing of the green rocks', the thermal metamorphism of the marbles and the adjoining ortho-gneisses to the contact effect of the Ross of Mull granite.

1.2.4 Later Geological Researches on Western Argyllshire

As it appears from the above outline, the general consensus of opinion regarding the geology of Islay and Colonsay till late 1950s was centred on the following points:

(a) The Dalradian sediments of eastern Islay forming the Islay Anticline are thrust over the Bowmore Sandstone along the Loch Skerrols Thrust.

(b) The Bowmore Sandstone along with the overlying Dalradian is separated from the Islay rocks by the Loch Gruinart Fault.

(c) The rocks of Colonsay form an upward continuation of the western Islay metasediments, the whole succession unconformably overlying the Lewisian Gneiss.

(d) The southern extension of the Great Glen Fault passes through west of Colonsay; the Moine Thrust is offset by a large transcurrent displacement along the Great Glen Fault and is represented by the Loch Skerrols thrust in Islay (Kennedy 1946).

Later Amos (1959) and Stewart (1962, 1975) tried to formalise the stratigraphy of the Bowmore Sandstone and the metasediments of western Islay and Colonsay; Stewart (1975) proposed the name Colonsay Group for the whole succession covering western Islay metasediments and those of Colonsay. Although Stewart (1962) originally regarded the Colonsay Group as Torridonian, he revised his view of its stratigraphic status to probably Dalradian by invoking a slide, the Bruichcladdich Slide, at the base of the Colonsay Group in western Islay (Stewart and Hackman 1973, Stewart 1975). A critical discussion of these suggestions is reserved for the next chapter.

Three phases of deformation has been recorded in the sediments of western Islay, the major folds representing the second phase (Stewart and Hackman 1973); it was also concluded that he Islay Anticline has the same style and orientation as the second phase folds in western Islay. A NE-SW extension lineation is regarded as an ubiquitous deformation feature in western Islay (Stewart and Hackman 1973). Borradaile (1979) suggested that the first phase of deformation in western Islay predates the Dalradian structures in NE Islay. The Colonsay Group is presumed to be a Torridonian - or Moine-like sequence, older than the Bowmore Sandstone and separated from the rocks to the southeast by either a now concealed unconformity, a major tectonic boundary or both (Borradaile 1979). However, Borradaile was unable to recognise any higher clast strain in the vicinity of the Loch Skerrols thrust. He suggested from strain studies that the Islay Anticline probably originated as an open buckle which later tightened up due to compression. Fairchild (1981) questioned the overturned geometry of the Islay Anticline as proposed by Bailey (1916) and suggested that the anticline is a sinistral en

echelon anticlinorium whose axial region approximately parallels the Loch Skerrols thrust.

1.2.5 Geophysical Works

The magnetic and gravity surveys as well as the seismic reflection profiling in the Malin Sea and adjoining areas (Brewer et al. 1983, Dobson and Whittingdon 1974, Dobson et al. 1975, Evans et al. 1980, Riddihough 1968) have an important bearing on:

(a) delineating the major lineaments of the Scottish highlands extending offshore into the Malin Sea;

(b) understanding the deeper geology related to the structures at Islay, Colonsay and Iona;

(c) any attempt to reconstruct the tectonic history of the area.

The ridge of positive gravity anomaly pitching NE over the Rhinns of Islay vindicates the presence of a Lewisian basement beneath the Torridonian (Durrence 1976). Sheet 10 of the aeromagnetic map of Great Britain (diagram edition, IGS 1968) shows that a large, positive and long wavelength anomaly lies over the Islay region. It is one of the four similar positive anomalies associated with the Lewisian outcrops, viz. those of Iona, Tiree, Coll and the eastern part of Barra. The pronounced southeasterly sloping gradient of the anomaly over Islay appears from its position to be associated with the interface between the Lewisian and the overlying, largely Dalradian metasediments, and the long wavelength of the anomaly indicates that this interface extends deeply into the crust (Westbrook and Borradaile 1978).

1.3 SCOPE OF THE PRESENT WORK

The Islay region provides the meeting ground for the foreland setting of the NW Scotland and the inner Dalradian belt of NE Scotland so far as the Caledonian deformation is concerned. The structure of the metasediments of western Islay has already been described in connection with stratigraphic studies of the Colonsay Group (Stewart

and Hackman 1973), and Wright (1908) suggested two phases of 'earth-movements' affecting the Colonsay rocks. However, a comprehensive account of the deformation history of the Colonsay Group can emerge only from detailed structural analysis of the two islands on a comparative basis. With this point in mind the detailed structure of Colonsay and western Islay has been reworked.

The deformation features in the Lewisian imposed during Caledonian re-working have been examined as they are important in the understanding of the basement cover relationship in the area. Since controversies exist as to the existence and the nature of the 'Bruichcladdich Slide' (Islay memoir 1907, Stewart 1962, Stewart and Hackman 1973), the detailed fabric of the rocks of the contact zone has been analysed; some strain measurements were also carried out in this connection.

Although the Torridonian rocks of Iona rest unconformably on the Lewisian (Bailey and Anderson 1925, Jehu 1922, Stewart 1962) the basal arkosic conglomerate shows definite evidence of shearing, particularly in the southern half of the island. The Caledonian deformation in Iona has been considered from two points in view:

(a) as part of a comparison between basement cover relationship in an undoubted foreland setting and that in the Islay region which apparently forms an inner strip within the Caledonian marginal belt;

(b) in terms of variation in deformation style along the length of the marginal belt of the Caledonian orogen.

Correlation of deformation phases between geographically separated areas is always fraught with problems. Intrusive bodies cutting major and/or minor structures may provide clues to the relative ages of several phases of folds or other structures in any individual area; similar relationships in more than one area can be compared and the deformation phases can be correlated between two or more areas if the igneous bodies themselves can be matched across the areas on other grounds. The study of the minor intrusions within the Colonsay Group, the Lewisian of western Islay and the Iona Torridonian is important in this respect. Although Wright (1908) suggested that the two fold

phases in Colonsay were separated by intrusion of the syenite masses the lamprophyric dykes, the deformation history and its relationship with the igneous intrusion are more complex than was realised by the early workers. It appears that the clues provided by the relationship between structural elements of one phase or the other and the minor intrusions have not been fully exploited. The present study brings out in detail the relationship between the minor intrusions and deformation events.

Caledonian minor intrusions north of the Great Glen Fault have been classified and found to show a distinct grouping with respect to the deformation phases in the Northern Highland (Smith 1979). Minor intrusions of the present area have been compared with those described by Smith (1979). The discussion also covers the time-relations of the deformation phases in Iona and emplacement of the Ross of Mull Granite.

The Loch Skerrols thrust separates the Dalradian of NE Islay from the Bowmore Sandstone. It was suggested that the Loch Skerrols thrust might be an extension of the Moine Thrust (Bailey 1916, Kennedy 1946). However, while in Islay the Dalradian overlies the thrust, in NW Scotland the Moine rocks are thrust over the Torridonian and the Cambrian Quartzite, locally scooping up Lewisian slices along the thrust belt. The problem of such correlation will be discussed in Chapter 2. Although Borradaile (1979) did not record any higher clast strain in the vicinity of the Loch Skerrols Thrust, there is no doubt about the shearing and local mylonitisation that affects the Jura Quartzite where it is juxtaposed against the Bowmore Sandstone. On a reference cross-section of the Loch Skerrols Thrust strain measurements were made in an attempt to get a first estimate of the displacement along the zone of dislocation. Quartz c-axis orientations were measured in the same set of specimens as used for strain measurements to prepare fabric diagrams. The progressive change in the strength and pattern of preferred orientation of quartz c-axis with increasing strain has been analysed taking into consideration the statistics of directional elements and the distribution of nearest neighbour density as appear in the process of contouring pole figure diagrams. A statistical correlation between the strength parameter of the fabric, strain intensity and the ratio of the eigenvalues of the Scheidegger's

orientation tensor is discussed, together with the implications thereof.

Geophysical studies in the Malin Sea area have suggested a possible extension of the Great Glen Fault system in this area and its probable linkage with the Leannan Fault in Ireland. However, controversies exist as to the exact offshore location of the fault branches, and the nature and amount of displacement. On the assumption that this large fault system would have considerable control on the orientation of the fractures in the Colonsay Group and the Lewisian, the aerial photographs of the Rhinns of Islay and Colonsay were studied to compile maps of fracture pattern in the area. The fracture pattern thus obtained was analysed and interpreted to put some constraints on the location of the major branches of the Great Glen Fault system in the Inner Hebrides.

To summarise, the points that have been stressed in the following chapters are:

(a) detailed structural analysis in each of the three islands studied namely western Islay (Chapter 3), Colonsay (Chapter 5) and Iona (Chapter 6);

(b) study of the strain and fabric along major dislocations in the area; in particular the microstructures and strain from the Loch Skerrols thrust zone are described in Chapter 4; deformation features within the Lewisian and along the contact with the metasediments are dealt with in separate sections belonging to Chapters 3, 5 and 6;

(c) description of the minor intrusions and their relationship with the deformation phases (Chapter 7);

(d) tectonothermal implications of the metamorphic history and emplacement of the appinitic intrusions;

(e) basement cover relationship as reflected in the contrasting styles of deformation within the Lewisian and the overlying metasediments, and the deformation along the contact zones;

(f) comparison and correlation of deformation features in the three islands.

Finally, on the basis of a synthesis of the above major points, attempts have been made to comment on the tectonic setting of the Colonsay Group in the Caledonian framework and the extent of reworking of the basement in the foreland/ marginal belt during the Caledonian deformation.

CHAPTER 2

STRATIGRAPHIC AND TECTONIC OVERVIEW

2.1 INTRODUCTION

The purpose of this chapter is to provide a general account of the principal stratigraphical and structural units in western Islay, Colonsay and Iona, which will serve as a background for the more detailed structural studies that form the main part of the thesis. Much of the information summarised below is based on previous work, but the author's own observations have led to some modifications of the accepted picture which are also recorded.

The principal rock groups of the area studied are shown in Table 2.1. In Iona, undoubted Torridonian sediments of the Iona Group overlie the Lewisian (Bailey 1925, Fraser 1977, Jehu 1922, Stewart 1962, 1975). In the southern islands the Colonsay Group, which is best developed in Colonsay begins with the metasediments of western Islay which structurally overlie an assemblage of gneissic rocks. A small band of gneissic rocks is also outcropped in the northeastern end of Colonsay. Although the gneisses of Islay have been locally reworked during the Caledonian tectonothermal events, their general similarity with the Lewisian Gneiss of Iona and the Outer Hebrides is unmistakable. On geophysical grounds the Lewisian Gneiss of Inistrahull off the north coast of Ireland is reported to be connected with the gneissic outcrops in western Islay (Riddihough 1968). A series of whole rock ages of 3100-1100 m.y. has been reported from the Inistrahull gneiss (McIntyre and van Breeman 1975). More recently a Laxfordian (1710 m.y.) K/Ar date for an amphibole from the Inistrahull area has been reported (Roddick and Max 1982). The Colonsay and western Islay gneiss outcrops have a very low radioactivity (as measured by portable gamma-ray spectrometer), which suggests that they are depleted in incompatible elements. This is comparable to the character of the basement Lewisian complex west of the Caledonian front in which distinctive geochemical and isotopic signatures record depletion in incompatible elements during deep seated metamorphism at about 2700 m.y. (Smith and Watson 1983). There is, therefore, indirect evidence for the Lewisian age of the gneisses of western Islay and Colonsay.

The Colonsay Group was originally regarded as Torridonian on the basis of the similarities between some of the higher beds of the Colonsay succession and the Torridonian of Iona, Skye and Loch Carron

Table 2.1 Major rock groups in W. Argyll (no correlations implied at this point)

IONA	ISLAY	COLONSAY
Ross of Mull Granite		
	Dalradian	
	Bowmore Sandstone	
		Upper part of Colonsay Group
Iona Group	Colonsay Group (lower part)	
Lewisian Gneiss	Lewisian Gneiss	Lewisian Gneiss

(Stewart 1962). Later, the Colonsay Group was tentatively correlated with the Dalradian by invoking a slide, the Bruichcladdich Slide, at the base of the succession in western Islay (Stewart 1975, Stewart and Hackman 1973). In contrast to the Torridonian of NW Scotland, the Colonsay Group has undergone several phases of penetrative deformation; however, the metamorphic reconstitution is restricted to the lower greenschist facies - chlorite + muscovite + a brown biotite being the commonest assemblage in pelitic/semipelitic rocks.

The lower part of the Colonsay Group in western Islay is separated from the virtually unmetamorphosed Bowmore Sandstone (Amos 1959) by the Loch Gruinart fault which belongs to the Great Glen Fault system. The Dalradian of NE Islay is thrust over the Bowmore Sandstone along the Loch Skerrols thrust. An outline of the lithostratigraphy of the metasediments of western Islay and Colonsay and the Torridonian of Iona follows. A brief note on the Lewisian gneisses of the three islands is also incorporated.

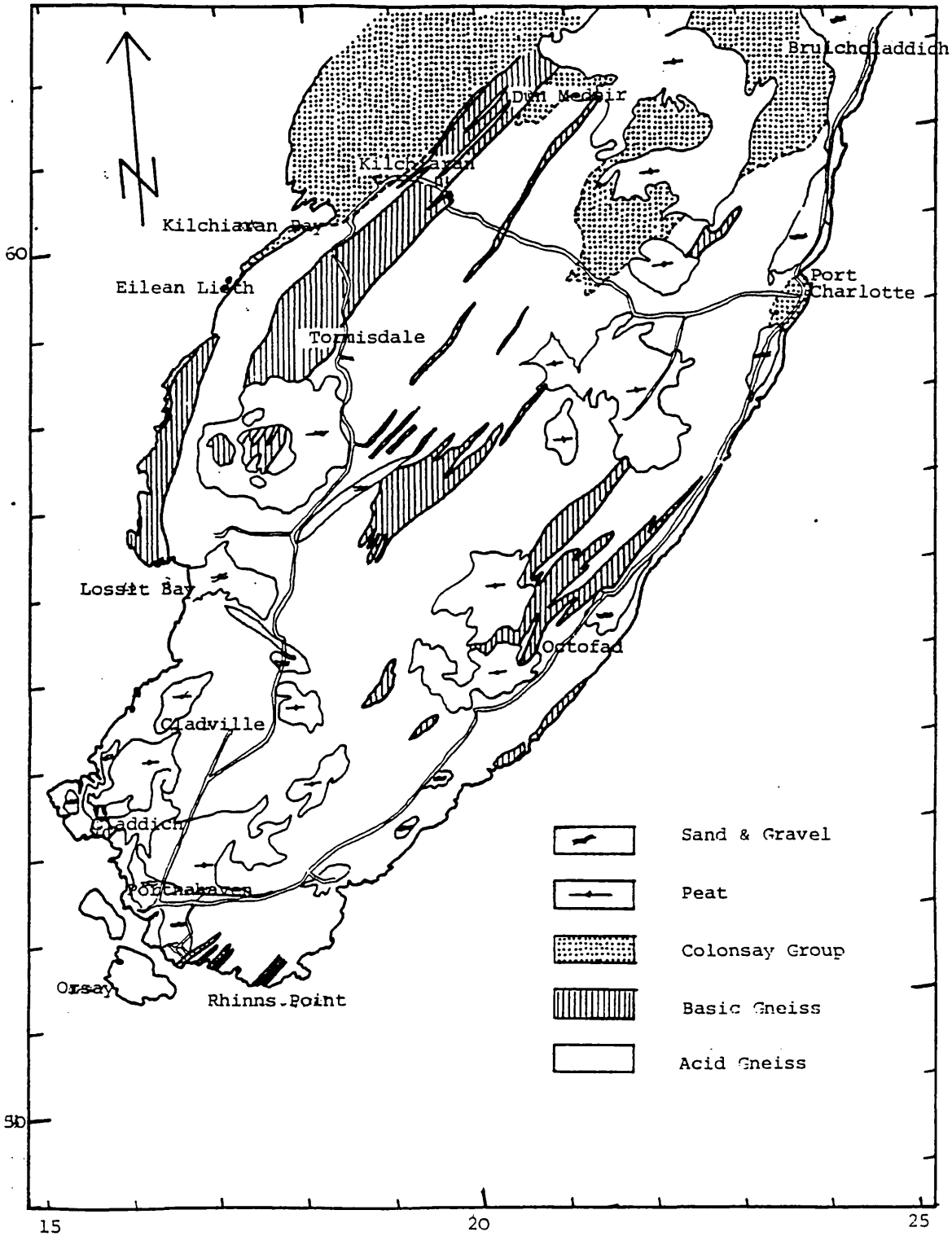


Figure 2.1. Lewisian outcrop in Western Islay, after Survey map, 1" sheet no. 19.

2.2 THE LEWISIAN

2.2.1 Western Islay

The Lewisian gneiss outcrops in western Islay roughly south of a line joining Kilchiaran Bay in the west and Port Charlotte in the east (Fig. 2.1). The rocks are generally similar to those of the western half of Iona and the Lewisian Gneiss of Inistrahull, off the northern coast of Ireland. The relationships between different gneissic components are best revealed in the coastal section between Lossit Bay and Tormisdale.

Typical outcrops around Lossit Bay show five different components (Fig. 2.2):

(a) fine grained amphibolite bands consisting chiefly of hornblende, biotite and feldspar (Fig. 2.2A); they have been widely affected by epidotisation; retrograde patches contain mainly biotite + chlorite;

(b) well foliated quartzo-feldspathic gneiss consisting mainly of feldspar + quartz + chlorite + biotite ± hornblende;

(c) 0.5-2.5 metres thick bands of coarse dioritic rock, either cutting the gneissic banding in types 'a' and 'b' (Fig. 2.2B), or parallel thereto; the rock has a porphyritic appearance with large sausuritised crystals of feldspar surrounded by smaller hornblende grains (Fig. 2.2C); some of these bands shown fine grained margins against 'a' or 'b' indicating that 'c' is a younger intrusive member within 'a' and 'b'; the feldspar grains are often ellipsoidal and their parallel alignment defines a shape fabric oblique to the general gneissic foliation;

(d) bands of hornblendite consisting solely of coarse stumpy prisms of hornblende; these bands have a cross cutting relationship with types 'a' and 'b'; in places the bands grade into type 'c' with an increase in the proportion of feldspars;

(e) cutting across all the above members are bands and veins of pegmatite (Fig. 2.2D) consisting predominantly of pink feldspar + quartz; accessories include epidote, biotite and occasionally hematite.

Figure 2.2. Components of Lewisian Gneiss in the Rhinns of Islay.

(a) Fine grained amphibolite bands (dark).

(b) Coarse dioritic bands (hammer on the left margin).

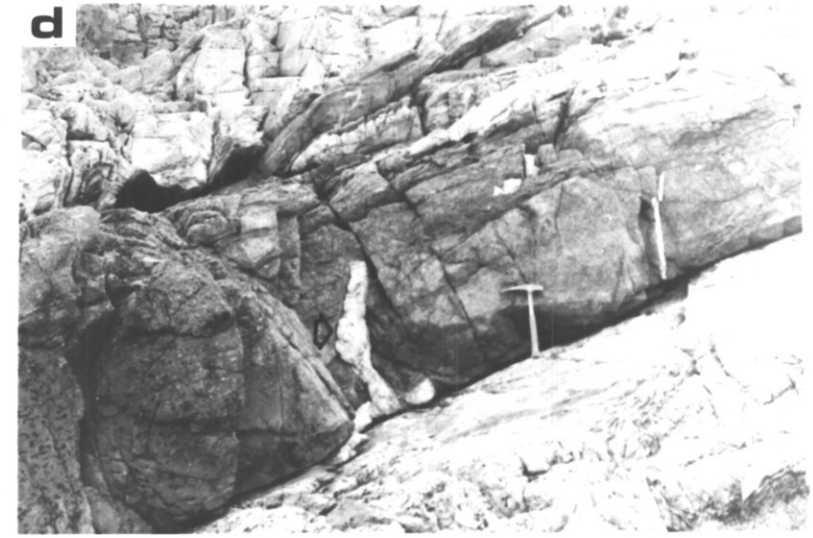
(c) Details from (b).

(d) Pegmatitic veins (arrow); notice the displacement of the vein by brittle shears.


a


b


c


d

The 'basic' gneiss tracts mapped separately (see Fig. 2.1) by early workers (Wilkinson et al. 1907) appear to be areas consisting predominantly of members 'a', 'c' and 'd' described above. Since, in the more feldspathic tracts the age relationship between 'a' and 'b' and 'c' or 'd' can be determined, the 'basic' tracts as a whole cannot be regarded as intrusive within and younger than the 'acid' gneisses (cf. Wilkinson et al. 1907). The presence of ampbibolitic member 'a' within both the groups contravenes a straightforward age grouping. However, all the above members including pegmatites (type 'e') are considered to be pre-Caledonian as all of them are transgressed by a suit of Caledonian minor intrusions comparable to those described by Smith (1979) from north of Great Glen in the Highlands. The minor intrusions will be dealt with in a later section.

A penetrative L-S fabric is found in many gneissic outcrops, especially in members 'a' and 'b'. The fabric is probably representative of Laxfordian (mid-Precambrian) deformation that these rocks suffered. However, original amphibolite facies rocks have re-equilibriated to a lower ambient temperature during Caledonian times as indicated by common reconstitution of hornblende to chlorite and/or biotite. The effect of retrogression is most marked where the gneisses are deformed in ductile to brittle Caledonian deformation zones, which are locales of mylonitisation. The latter shows an unequal development, so far as spatial distribution is concerned. In the coastal section from Cladville, south of Lossit Bay to Portnahaven and further north along the eastern coast to Port Charlotte, the gneissic rocks register a relatively higher state of deformation and show extensive retrogressive mertamorphism. The rocks exposed around Port Charlotte are so highly sheared and retrograded that they are barely recognisable as Lewisian Gneiss. However, the frequent presence of granulated hornblende in thin sections and the abundance of feldspar is in favour of grouping these sheared rocks with the Lewisian. In field appearance they are not radically different from the mylonitised Lewisian in the ductile deformation zones around Cladville, Claddich and Portnahaven. Thus the outcrops between Cladville and Portnahaven form a tie between the sheared and crushed Lewisian of Port Charlotte area and the gneisses of Lossit Bay which still preserve some of their original Lewisian characteristics.

In the one inch geological map prepared by the Survey (sheet 19, see Wilkinson et al. 1907), a 'Torridonain' patch is shown as an outlier within the gneisses in the vicinity of Portnahaven. The rocks in this supposed outlier of 'Torridonian' have been re-examined. Although the rocks appear to be quartz rich due to extensive quartz veining in the area, the petrographic characateristics are unlike those of any Colonsay Group horizon. On the contrary, presence of granulated epidotes and hornblende suggests that the rocks are probably reconstituted Lewisian Gneiss.

2.2.2 NE Colonsay

A band of gneissic rocks occur among the low grade metasediments of NE Colonsay. The general character and low radioactivity (as measured by portable gamma-ray spectrometer) compares well with the gneisses of western Islay, and hence the gneiss band is regarded as Lewisian. The gneissic band can be traced from the shore in a west-south-west direction for more than 700 metres. An unconformable relation with the pebbly grits lying immediately to the north is evident. However, the southern boundary of the gneiss outcrop is concealed by blown sands. The width of the gneissic band is probably less than a few hundred metres.

The constituent members of the gneiss include amphibolite at various stages of retrogression and pegmatoid rocks. The rock is well foliated and shows mylonitisation especially near the contact with pebbly grits. This deformation is probably an effect of local strain concentration around asperities on an uneven Lewisian-metasediment contact. A detailed discussion of the contact zone rocks is given in Chapter 5.

2.2.3 Iona

The gneissic outcrops cover nearly three-quarters of the island of Iona. From their general similarity to other Archean assemblages along the northwest coast of Scotland, these gneisses are regarded as belonging to the Lewisian complex (Bailey et al. 1925). Detailed consideration of the Lewisian geology of Iona is beyond the scope of the present thesis. In brief, both ortho- and para-gnesses have been recorded and

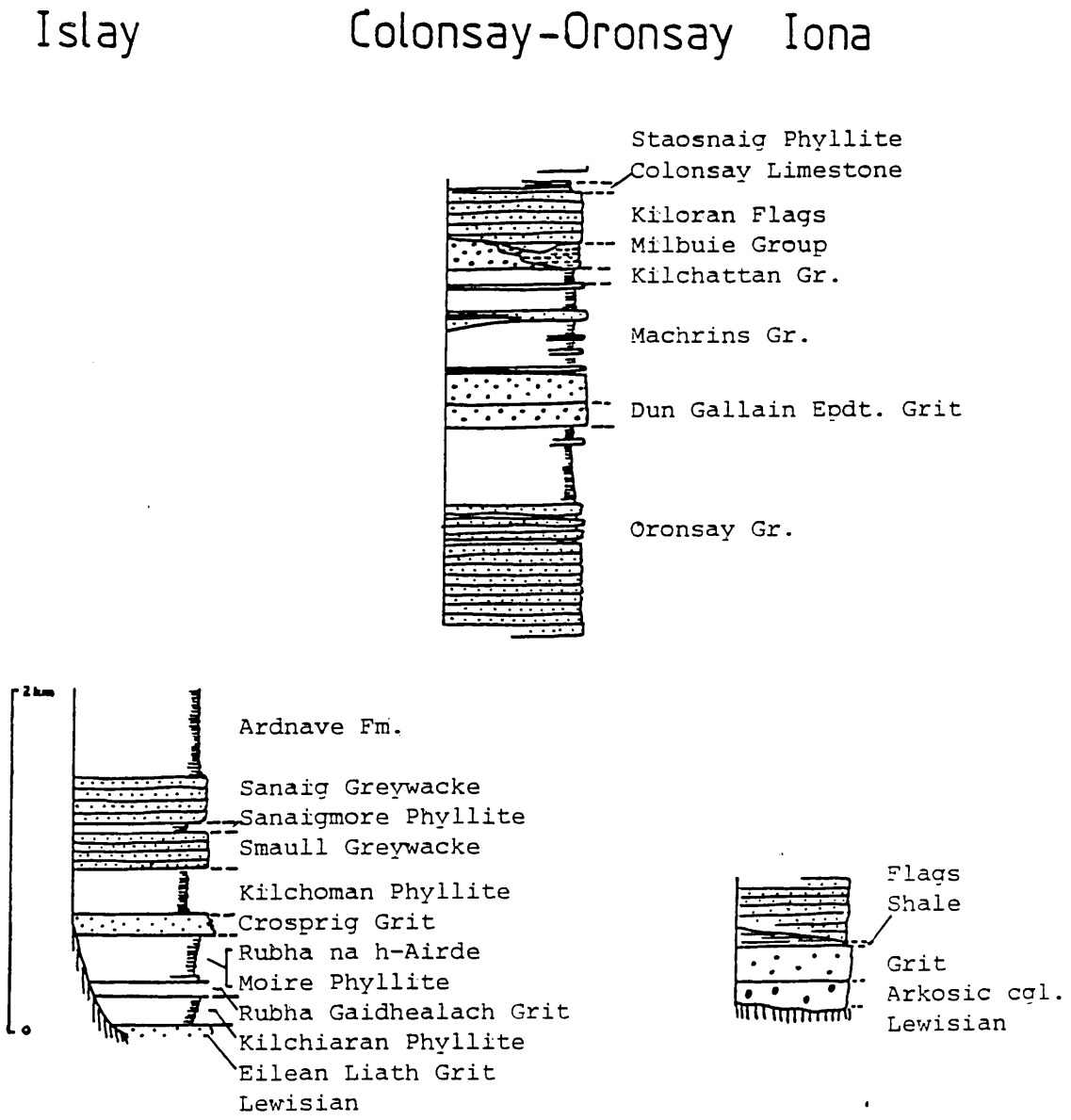
the rocks have suffered several phases of mid-Precambrian or earlier deformation (Fraser 1977). During Caledonian times, the gneisses were affected by the development of local shear zones related to westward Caledonian thrusting.

2.3 THE COLONSAY GROUP

A series of arkosic grits, locally conglomeratic, fine-grained greywackes and intercalated phyllites overlies the Lewisian in western Islay. The sediments are best exposed in the coastal section between Kilchiaran Bay and Ardnave Point. An upward continuation of this series of sediments is found in the Oronsay Greywacke and the epidotic grits, phyllites and flags of Colonsay. The total succession which is about 5 kms thick, has been named the Colonsay Group by Stewart (1975). The formations as defined by Stewart (1962, 1963) and Stewart and Hackman (1973) are shown in the stratigraphical columns of Fig. 2.3. Geological samples collected by scuba divers from the submarine exposures between Islay and Colonsay show well bedded alternations of dark grey siltstone and phyllite not unlike the Oronsay Greywacke (P.L. Barber in Evans et al. 1980). Although the rocks in western Islay and Colonsay are folded and exact correlation is difficult because the sedimentary texture of the rocks has been modified by the development of more than one cleavage, the general similarity of lithology in the two islands and the presence of submarine 'Torridonian' in the intervening area, all lend credence to the suggestion that the metasediments of western Islay and Colonsay form a single group as suggested by Stewart (1962, 1975).

The Colonsay Group shows considerable variation in sedimentary facies. A gradation from deltaic facies at the bottom to turbidite facies in the middle, and a subsequent reversal to deltaic facies have been proposed by Stewart (1962, 1963) and Stewart and Hackman (1973). The present writer accepts in a general way Stewart's lithostratigraphic divisions and boundaries and has not undertaken a detailed sedimentological study. Attention is concentrated in this chapter on features which have proved to be significant with respect to structural analysis and on new informations concerning the provenance of the Colonsay Group. Some stratigraphic comments on the key units are given in the next two subsections.

Figure 2.3 Stratigraphic successions in W. Islay, Colonsay and Iona. Successions in Islay and Colonsay after Stewart (1962) and Stewart & Hackman (1973).



2.3.1 Western Islay Sediments

2.3.1.1 The basal units

The lowest unit that comes in contact with the Lewisian south of Kilchiaran Bay is named the Eilean Liath Grit (Stewart and Hackman 1973). This is an arkosic grit with mainly quartz and feldspar clasts. The latter constitutes 50-65 per cent of the framework fraction; untwinned feldspar, probably orothclase, dominate the felsic fraction but microcline, microcline-microperthite, perthite and plagioclase are fairly common (Table 2.2).

The Eilean Liath Grit, near its contact with the Lewisian Gneiss, is sheared and quartz clasts are stretched into ribbon grains and dynamically recrystallised; a NE-SW elongation lineation is well developed. A few tens of meters northwest of the contact, the bedding dips at about 70 degrees towards northwest.

In the Kilchiaran Bay area the maximum grain diameter is about 1.5 cms. However, a conglomeratic facies in contact with the Lewisian has been descibed from the Dun Mideir area, 1.5 kms northeast of Kilchiaran House; some of the pebbles are described as having the same petrography as the Lewisian Gneiss (Wilkinson et al. 1907). The pebbles in this locality are stretched in a NE-SW direction similar to that of the stretching lineation in the Eilean Liath Grit. A basal pebbly facies is also recorded from the Port Charlotte area.

The Eilean Liath Grit is followed conformably in a northerly direction by the Kilchiaran Phyllite, which in its turn gives way to Rubha Gaidhealach Grit. The last named unit shows tabular cross-bedding and load-cast structures (Fig. 2.4). The strata are right way up, the facing in this locality being towards the northwest.

2.3.1.2 The Crosprig Grit

The great crags from Kilchoman southwestward to the sea constitute the type area. This is a coarse cream-weathering grit with clasts of quartz, feldspar and lithic composition. Noticeable are the decline of microcline, and alteration of feldspar in the framework as compared to the basal unit at Kilchiaran Bay (see Table 2.2). The proportion of matrix is also relatively high. Lithic clasts consisting

Figure 2.4. Sedimentary structures in the Colonsay Group. Field photographs taken on vertical sections except (g) which is in plan.

(a) Tabular cross-bedding in Rubha Gaidhealach Grit, Kilchairan Bay, W. Islay.

(b) Load-casts in Rubha Gaidhealach Grit, Kilchiaran Bay, W. Islay.

(c-d) Graded beds and flame structures in Sanaig Greywacke, Sanaigmore Bay, W. Islay. Strata overturned in (c).

(e) Graded beds and slump structure (bottom left) in Sanaig Greywacke, Sanaigmore Bay, W. Islay.

(f) Graded bed with a rippled top, Dun Gallain Epidotic Grits, Colonsay.

(g) Trough cross-bedding in arkosic bands, east of Balnahard, NE Colonsay. Bedding dips steeply towards east, opposite to the younging direction indicated by truncation of cross-beds.

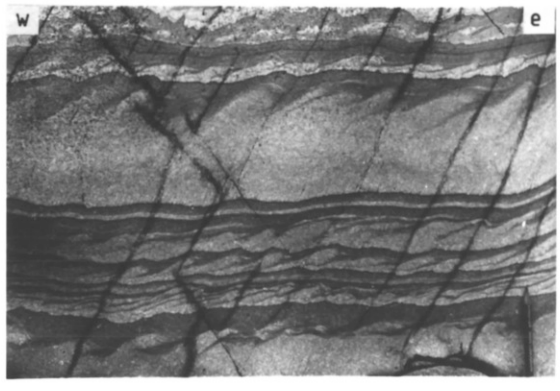


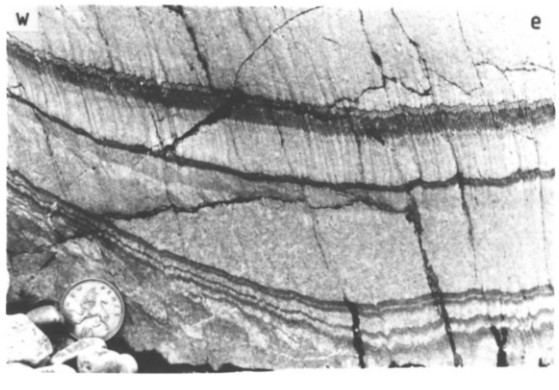




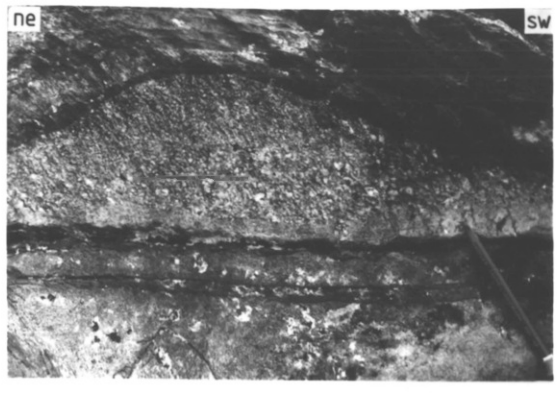
key

a	b
c	d
	e
g	f









2.4

Figure 2.5. Detrital mineralogy of the metasediments of W. Islay.

(a) Stretched pebbles in Eilean Liath Grit, southwest of Kilchiaran Bay.

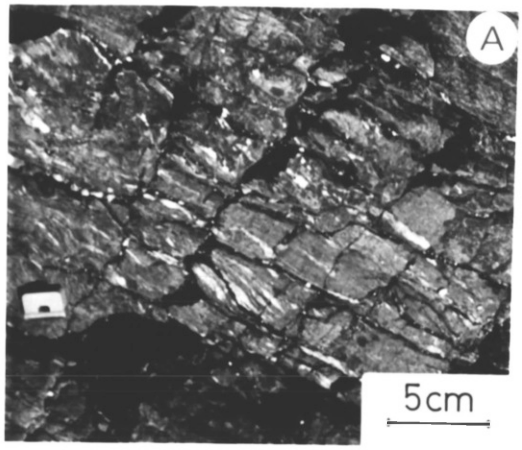
(b) Soubrounded clast of granite-gneiss, Eilean Liath Grit, south west of Kilchiaran Bay.

(c) Clast of quartzo-feldspathic granulite, Crosprig Grit, Dun Crosprig; note the inherited grain shape fabric in quartz at a high angle to the foliation in the matrix.

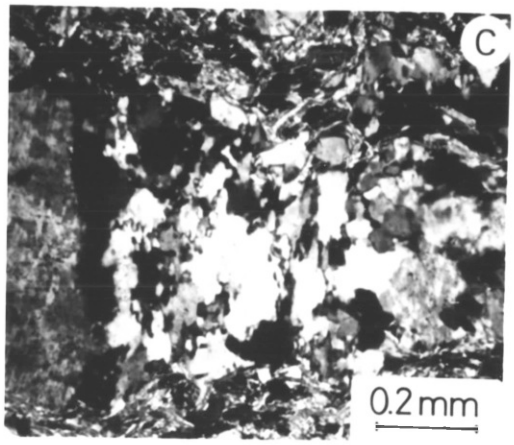
(d) Composite quartz with sutured grain boundary and stretched needles of rutile as inclusions, Crosprig Grit, Dun Crosprig.

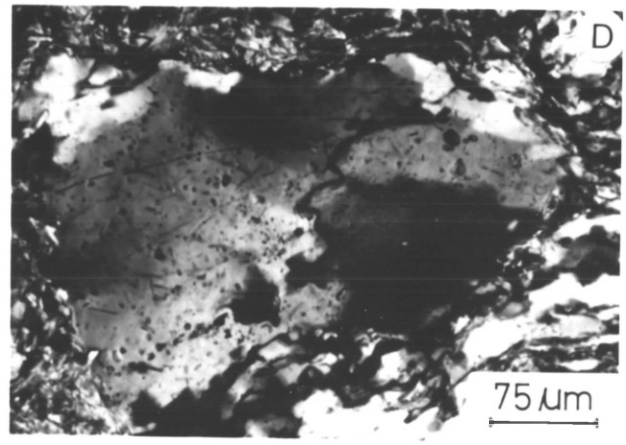
(e) Bent detrital muscovite (Mu), Crosprig Grit, Creag Mhor.

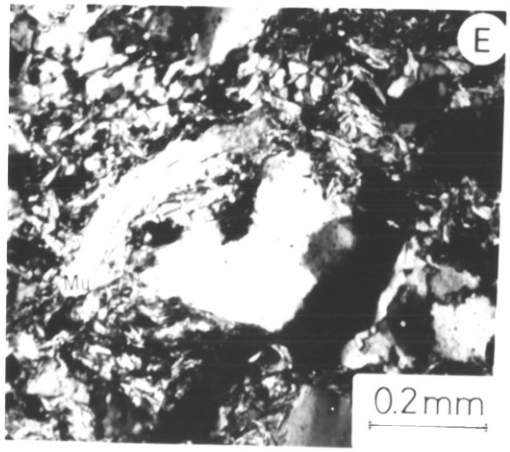
(f) Intraformational shale fragment (Sh), Smaull Greywacke, Smaull.


A
5cm


B
0.1mm


C
0.2mm


D
75 µm


E
0.2mm

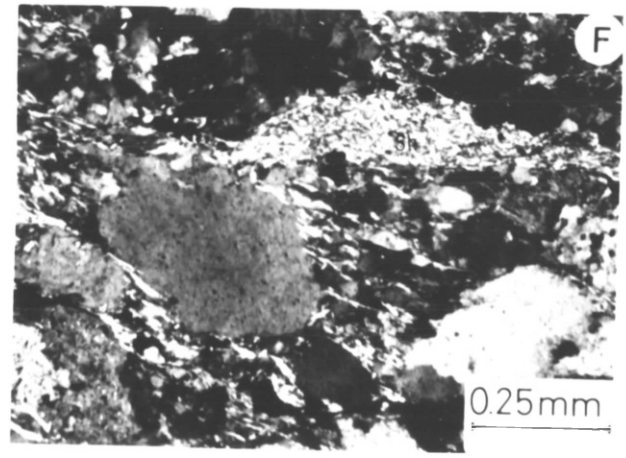

F
0.25mm

Table 2.2 Proportion of different mineral grains in psammitic horizons of western Islay

Formation	Specimen No.	FRAMEWORK COMPOSITION*							Nature of lithic fragments
		Quartz	FELDSPAR					Lithic	
			Microcline	Plagioclase	Perthite	Unspecified	Total		
Eilean Liath Grit	351	39.90	4.43	5.91	2.46	40.39	53.20	6.80	Granulite-quartz microgranite micropegmatite
	356	36.40	7.90	6.58	3.95	43.86	62.28	0.88	
Crosprig Grit	490	50.56	0.56	10.56	2.22	32.22	45.56	3.89	Granulite-quartz microgranite
	112	34.08	0.00	5.03	1.68	25.70	32.40	33.52	
Smaull Greywacke	058	49.52	0.00	5.71	6.19	11.42	23.33	27.14	Granulite-quartz shale fragments microgranodiorite
	057	50.95	0.00	8.10	10.00	12.86	30.96	18.10	

* Figures as % of total number of clasts counted, which varies from 180 to 230 in each specimen.

mainly of quartz grains and showing a distinct inherited S-L fabric are common. Some of these composite grains are of granulite quartz as indicated by the presence of quartz grains with hair-like inclusion of rutile needles (Fig. 2.5). The grains are very similar to the blue quartz described from Scourian granulites of NW Highlands (Teall in Peach et al. 1907). Single grains of blue quartz have also been recorded under the microscope.

The Crosprig Grit is regarded as the most coarse grained unit within the Colonsay Group by Stewart and Hackman (1973). However, this observation does not take into account the conglomerate patch described by Wilkinson et al. (1907) from Dun Mideir or other local occurrences of basal conglomerate (present study). Near Coul the Crosprig Grit shows distinct graded bedding. In the coastal strip southwest of Kilchoman, the grit grains show a NE-SW elongation; however, the stretching is much less marked compared to Eilean Liath Grit.

The lithology and sedimentary structures indicate a continental to deltaic facies for the sedimentary units so far described. The frequent presence of feldspar, especially microcline in the basal unit is in favour of close proximity of the source area, probably a Lewisian type basement, to the depositional basin for these units.

2.3.1.3 Turbidite facies

The transition to a deeper environment of deposition is heralded by the succession of the Kilchoman Phyllite on top of the Crosprig Grit. The Kilchoman Phyllite is about 200-300 meters thick, frequently pyritiferous and containing calcareous silty bands. Graded beds are common in the area SE of Coul Point. Slump structures have been observed in the phyllites with silty intercalations at the north end of the Machir Bay exposed at low tide.

The true greywacke of the turbidite facies is represented by the Smaull Greywacke and the Sanaig Greywacke. Graded bedding is very common in the Smaull Greywacke. A distinct increase in the proportion of matrix (30-50 per cent), and lithic fragments (18-27 per cent of the total clasts) in the framework fraction compared to Eilean Liath Grit or the Crosprig Grit, is noticeable (Table 2.2). Many of the lithic fragments are composed of fine to medium grained quartz with sutured

grain boundaries. Hair-like inclusions of rutile needles within quartz grains are common. Another interesting feature is the presence of shale fragments within the Greywacke (Fig. 2.5).

Sedimentary structures include graded bedding and flame structures (Fig. 2.4). Overturning of the flames indicates paleocurrent directions from west to east (without any corrections for tectonic tilting of the beds).

The general character of turbidite sediments is represented in the Sanaig Greywacke and the Ardnave Formation outcropping in the northern part of the Rhinns. There is a decrease in the sand-shale ratio as one traces the succession from Smaull Greywacke upwards through Sanaig Greywacke to Ardnave Formation. Carbonate grains are fairly common in the silty bands within phyllites in the Ardnave Formation. It is not unlikely that the turbidity currents themselves derived their original material from sediments building up as delta fans on mixed clastic-carbonate shoreline.

2.3.2 Sediments of Colonsay-Oronsay

2.3.2.1 Introduction

A 2 km thick succession of greywacke, mudstone, shale (now mostly phyllites) and impure limestone in Oronsay and Colonsay forms the northward and the upward continuity of western Islay sediments. The whole succession including the Oronsay Greywacke and mudstone is called the Colonsay Group after the Isle of Colonsay, where it is best developed and exposed (Stewart 1975). The succession suggested by Cunningham Craig et al. (1911) and formalised by Stewart (1962) is shown in Table 2.3. The distribution of individual units is shown in Fig. 2.6 taken from Stewart. Some problems connected with the order of succession are mentioned below.

2.3.2.2 Greywacke facies

The thickest unit is the Oronsay Greywacke group comprising a lower greywacke division and an upper laminated mudstone

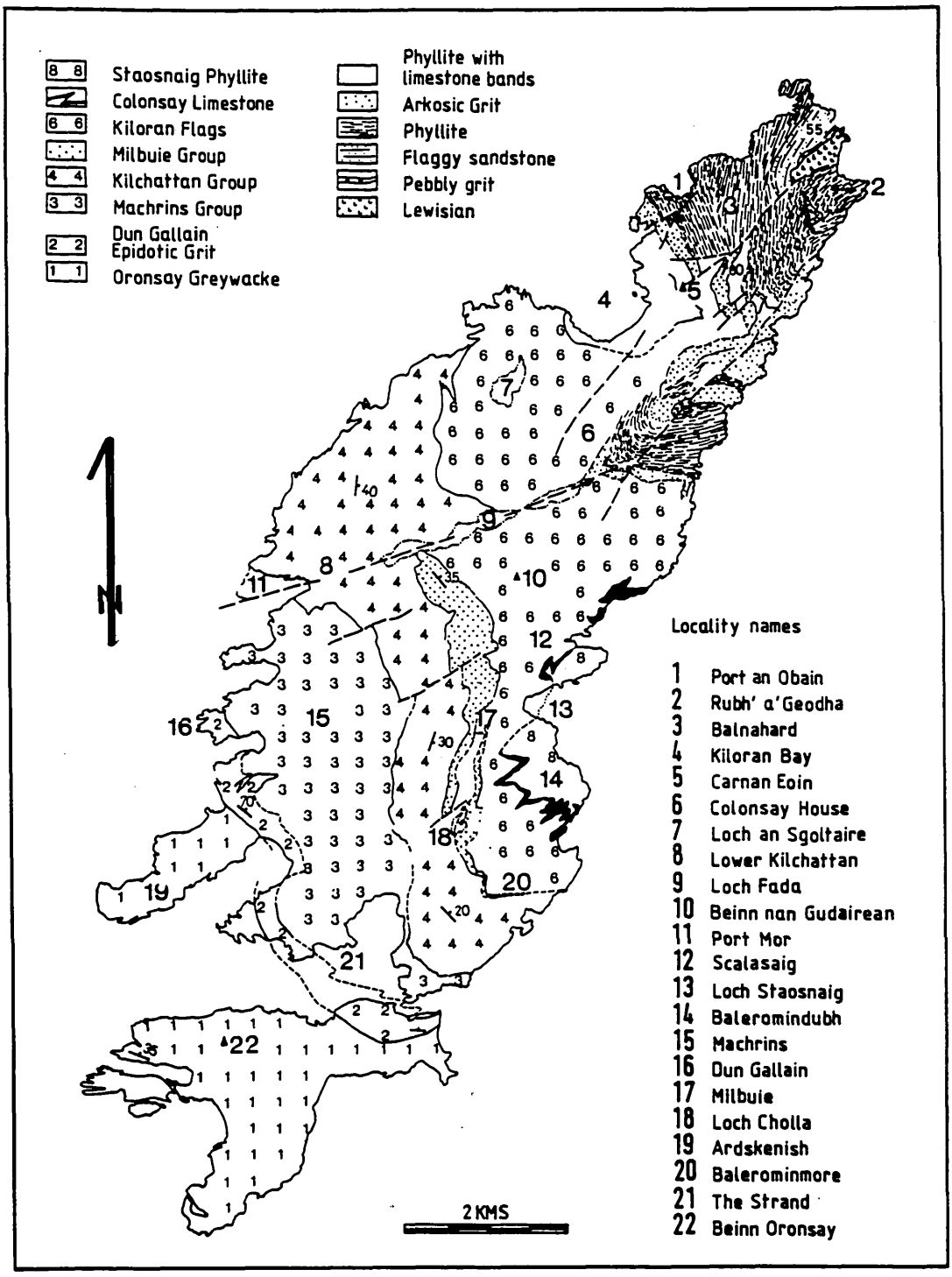


Figure 2.6. Geologic map of Colonsay-Oronsay; after Survey maps, one inch sheet nos. 27 and 35, and Stewart(1962).

Table 2.3 Stratigraphic groups in Colonsay and Oronsay, after Stewart (1962)

Name	Principal lithologies	Thickness (meters)
Staosnaig Phyllite	Fine, leaden phyllite	150+
Colonsay Limestone	Dolomitic limestone and phyllite	250-500
Kiloran Flags	Semi-pelitic flaggy sandstone; locally arkosic lenses	250-500
Milbuie Group	Siliceous phyllites with thick bands of arkose at the base, locally epidotic	100-400
Kilchattan Group	Siliceous phyllites with thick lenses of fine dark sandstone	400-1000
Machrins Group	White weathering arkoses with striped mudstone intercalations	620-660
Dun Gallain Epidotic Grits	Epidotic arkoses	120-130
Oronsay Greywacke	Greywacke turbidites and mudstones (base not exposed)	1120+

division. Sedimentary structures include common graded bedding in the lower division, and load-casts, flame structures and slump features in the Oronsay mudstone. Among the detrital grains quartz is closely followed by feldspars; larger quartz grains are often polycrystallline, showing sutured grain boundaries (Stewart 1963). It may be noted that

similar polycrystalline quartz is also present in the lower units exposed in western Islay. Various oriented sedimentary structures indicate a dominant palaeocurrent flow towards NNE (Stewart 1962).

2.3.2.3 Deltaic facies

The Oronsay Greywacke is followed upwards by the Dun Gallain Epidotic Grits. As the name suggests, these are arkosic and epidotic grits with frequent intercalations of laminated mudstones. Cross-bedding with tabular foresets is common. Graded beds with a rippled top is also found (Fig. 2.4, cf. Stewart 1962). The Machrins Group is similar to the Dun Gallain Epidotic Grits except for the much higher proportion of epidote in the latter (Table 2.4).

Table 2.4 Modal analysis of some psammites from Colonsay (from Stewart 1962)

Horizon	Modal analysis (Volume %)				
	Quartz	Feldspar	Chlorite, Sericite and stilpnomelane	Epidote	Other heavy minerals
Kiloran Flags (basal arkose)	70-76	14-23	6-8	-	0-5
Milbuie Group	39-54	16-25	10-17	10-18	0.5-1.0
Machrins Group	62-68	23-26	9	0-2	0-3
Dun Gallain epidotic Grits	40-51	21-37	9-21	3-19	-
Oronsay Group	42	30	25	3	0.3

The transition from Oronsay Greywacke to Dun Gallain Epidotic Grits probably marks the onset of a fluvio-deltaic sedimentary environment as evidenced by the sedimentary structures and general nature of the sediments. Both the Kilchattan Group and the Milbuie Group are represented by intercalations of shale and arkosic mudstones. While shales (now pyritic phyllite) predominate in the Kilchattan Group, arkoses are more common in the other group.

In the northern half of Colonsay, the psammitic bands are often lensoid and interdigitate with the shaly horizons. This is consistent with the possibility that the arkoses are channel sands and the shales interdistributary muds. One of the interesting features of the creamy arkosic bands east of Balnahard farm is the presence of trough cross-bedding, braided cross-bedding and minor slump folds, which indicate fluviatile deposition (Fig. 2.4). The beds in this area dip at about 70 degrees to the ENE; however, the sedimentary structures suggest young-ing towards west.

Although Stewart (1962) has put these arkosic sandstone bands together with leac Bhuidhe sediments in the Kilchattan Group, there are problems of correlating sediments of NE Colonsay with the rest of Colonsay succession. This will be discussed later.

2.3.2.4 Carbonate facies

An impure carbonate faceis in the Colonsay Group is represented by the Colonsay Limestone. Two outcrops have been assigned to the group - from Balerominmore to Scalasaig Bay in the southeast and the Kiloran Bay in the northwest (Cunningham Craig et al. 1911, Stewart 1962). Lithologically, the limestones in SE Colonsay range from impure phyllites with a carbonate content of about 50 per cent to almost pure carbonate rocks. Pure carbonate bands are only a few centimeters thick at best and none of these can be individually traced for more than a few tens of meters, although the carbonate group is mapped over a distance of several kilometres.

2.3.2.5 A problem with the order of succession in NE Colonsay

It has been pointed out earlier that a band of Lewisian gneiss outcrops at the NE End of Colonsay. To the north of the gneiss outcrop occur pebbly epidotic grits followed by flaggy psammites and phyllites. On the south, boundary with the sediments is concealed by sand dunes; the nearest exposure on this side is that of phyllites near Rubh a Geodha. In the survey map, the sediments surrounding the gneiss are regarded with some doubts as equivalent of Milbuie Group (t_v). Stewart (1962) put them with the Kilchattan Group (t_{iv}). It appears from dip symbols on Stewart's map and the survey map as if the sediments in the north structurally underlie the gneiss. However, present observations show that the bedding in pebbly grits immediately north of the gneiss

band dips towards northwest. Thus the sediments are unconformably overlying the Lewisian gneiss. There are some dip reversals further north, but that is due to later folding of the strata.

Between Rubh' a' Geodha and Balnahard, several arkosic sandstone bands are outcropped. These have an overall N-S trend and a steep easterly dip. However, sedimentary structures indicate that the strata are overturned and the original palaeocurrent direction was probably towards the westerly quadrant. Such a situation would be expected if the sediments were initially deposited on the western flank of a basement high. However when one considers the stratigraphic horizons in southern Colonsay, e.g., Dun Gallain Epidotic Grit and Machrins Group, the overall palaeocurrent direction is towards northeast (Stewart 1962). The westerly younging direction in Balnahard area suggests that the limestone bands around Kiloran Bay area are probably younger than the sediments surrounding the gneiss band of NE Colonsay. Although the limestone bands of Kiloran Bay represent a lithofacies similar to the Colonsay Limestone (t_{vii}) outcropped around Loch Staosnaig, the two outcrops cannot be regarded as parts of a physically continuous rock unit (cf. Cunningham Craig et al. 1911). Same lithofacies may be deposited in separated parts of a large basin if the basin floor configuration is far from a simple one. The apparent discrepancy in the sediment of younging direction between NE Colonsay and southern Colonsay as discussed above may be explained if one assumes an overlapping relationship between the sediments the two parts of the basin. A possible configuration of the basin floor which may have led to the situation is shown schematically in Figure 2.7, where the Lewisian of NE Colonsay is represented as an original high in the basin floor.

2.3.3 Provenance of the Colonsay Group

The detailed mineralogy and the palaeocurrent pattern are two important factors in the analysis of provenance of any generally clastic sedimentary group. In the lower units of the Colonsay Group feldspars form an important fraction of the framework. Of these microcline and microcline-microperthite indicate a plutonic source land, presumably a granite and/or granite-gneiss terrain. However, the frequent presence of granulite quartz and blue quartz (Fig. 2.5, Tables 2.2 and 2.4) definitely suggest that the bulk of the sediments were probably derived

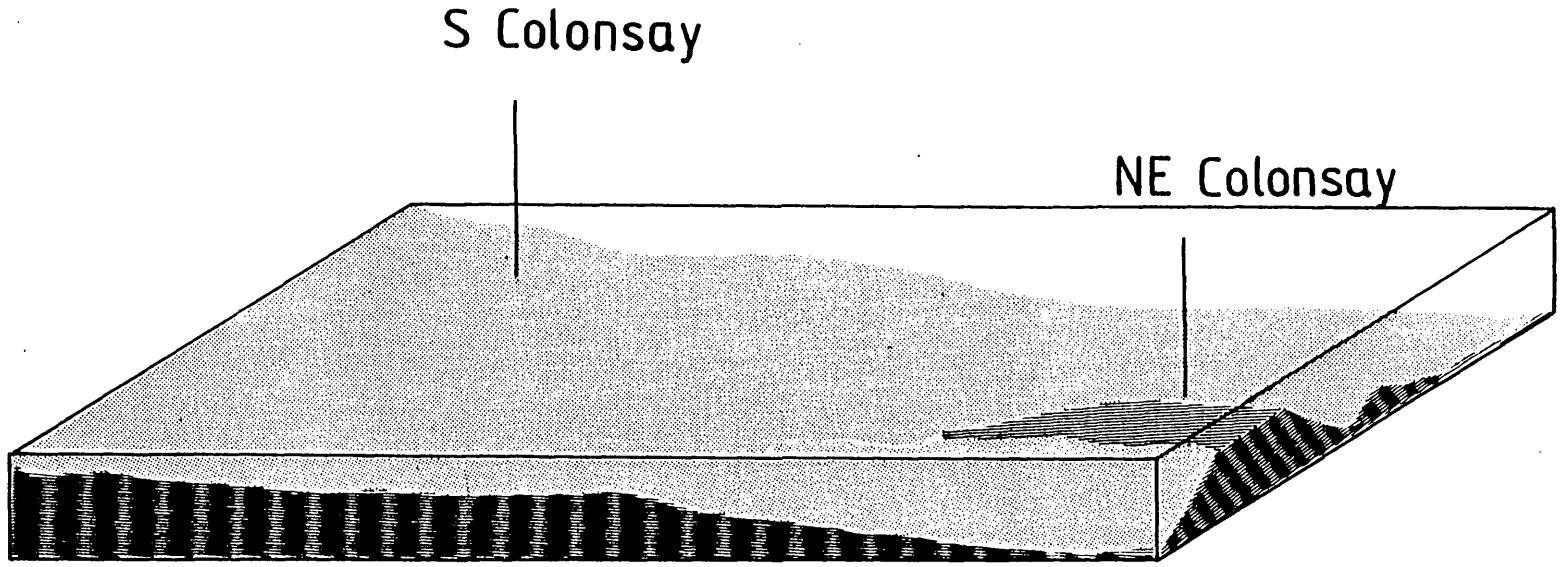


Figure 2.7. Schematic drawing showing a probable basin floor configuration during deposition of the Colonsay sediments (exaggerated vertical scale).

from granulitic gneisses, presumably a Lewisian type land source. It may be noted here that fragments of non-metamorphic acid volcanics common in Applecross Group of Torridonian have not been found in any of the Colonsay Group horizons.

The predominant palaeocurrent direction in the lower part of Colonsay Group including the Oronsay Greywacke, Dun Gallain Epidotic Grits and Machrins Grit is towards N-NE (Stewart 1962). The source area for the greater part of the Colonsay Group is most likely to have been to the south-south-west. The succession from Kilchoman Phyllite to Oronsay Greywacke represents a turbidite facies; the palaeoslope was towards north-north-east. However, it was suggested above that the sediments of northern Colonsay including those around Balnahard and Leac Bhuidhe probably represent a separate group. As indicated by sedimentary structures and general lithofacies, the rocks are fluviatile or fluviodeltaic and the sediment transport was from east to west. The occurrence of a Lewisian outcrop in the northern end of Colonsay and the unconformable epidotic grits with pebble bands on top of the Lewisian point to the possibility that these sediments were deposited on the western flank of a basement ridge.

2.3.4 The base of the Colonsay Group - unconformity or slide?

There is a controversy regarding the nature of the Lewisian-Colonsay Group contact in western Islay. Wilkinson et al. (1907) regarded the metasediments as Torridonian and unconformably overlying the Lewisian. Although Stewart (1962) originally put the Colonsay Group within the Torridonian, in his later papers (Stewart 1975, Stewart and Hackman 1973), he became more in favour of regarding the group as Dalradian. Stewart and Hackman advocated that the base of the Colonsay Group is founded on a slide, the Bruichcladdich Slide. The arguments they put forward are:

(a) the basal conglomerate as described by Wilkinson et al. (1907) is largely non-existent;

(b) the Eilean Liath Grit and the two next horizons, namely, the Kilchiaran Phyllite and the Rubha Gaidhealach Grit, wedge out against the boundary of the Lewisian;

(c) a zone of intensely sheared material intervenes between the Eilean Liath Grit and the Lewisian.

As described earlier, the Eilean Liath Grit is a coarse arkosic grit, and the clast composition is in favour of a derivation at least partly from Lewisian sources. Cross-beddings in the grit and conformably overlying Kilchiaran Phyllite indicate that the strata are right way up; the direction of younging is northwest away from the Lewisian contact. Although the development is local, a conglomeratic facies in contact with the Lewisian has been recorded from several places in western Islay, such as Dun Mideir and Port Charlotte.

As to the second argument above, it is not unlikely that the Colonsay Group was deposited on a very uneven basin floor to start with, and that the 'wedging out' of the Kilchiaran Phyllite and the Rubha Gaidhealach Grit against the Lewisian is due to stratigraphic overstepping.

There is no doubt that the contact zone is one of strain gradient. Details of strain features and strain values will be given in Chapter 3. The strain values are not high enough to warrant the suggestion that the present position of the Colonsay Group in western Islay is due to the Bruichcladdich Slide, as put forward by Stewart and Hackman (1973). The balance of evidence is in favour of an unconformable contact; of course, the contact has acted as a zone of differential displacement during the Caledonian deformation.

2.4 THE IONA GROUP

A belt of steeply dipping arkosic conglomerate, grit, shale and flaggy sandstone overlies the Lewisian Gneiss in Iona (Fig. 2.8). This group, which is over 0.5 km thick, is regarded as Torridonian (Bailey et al. 1925, Stewart 1962, Stewart 1975, Fraser 1977).

The basal bed in NE Iona consists of a boulder bed with fragments of gneiss up to 0.5 meters across, and arkosic grits with clasts of minerals derived from the gneiss, including feldspars, quartz, epidote, hornblende and mica. The sediments are unconformable on the Lewisian at the NE end of their outcrop. However, there is evidence of

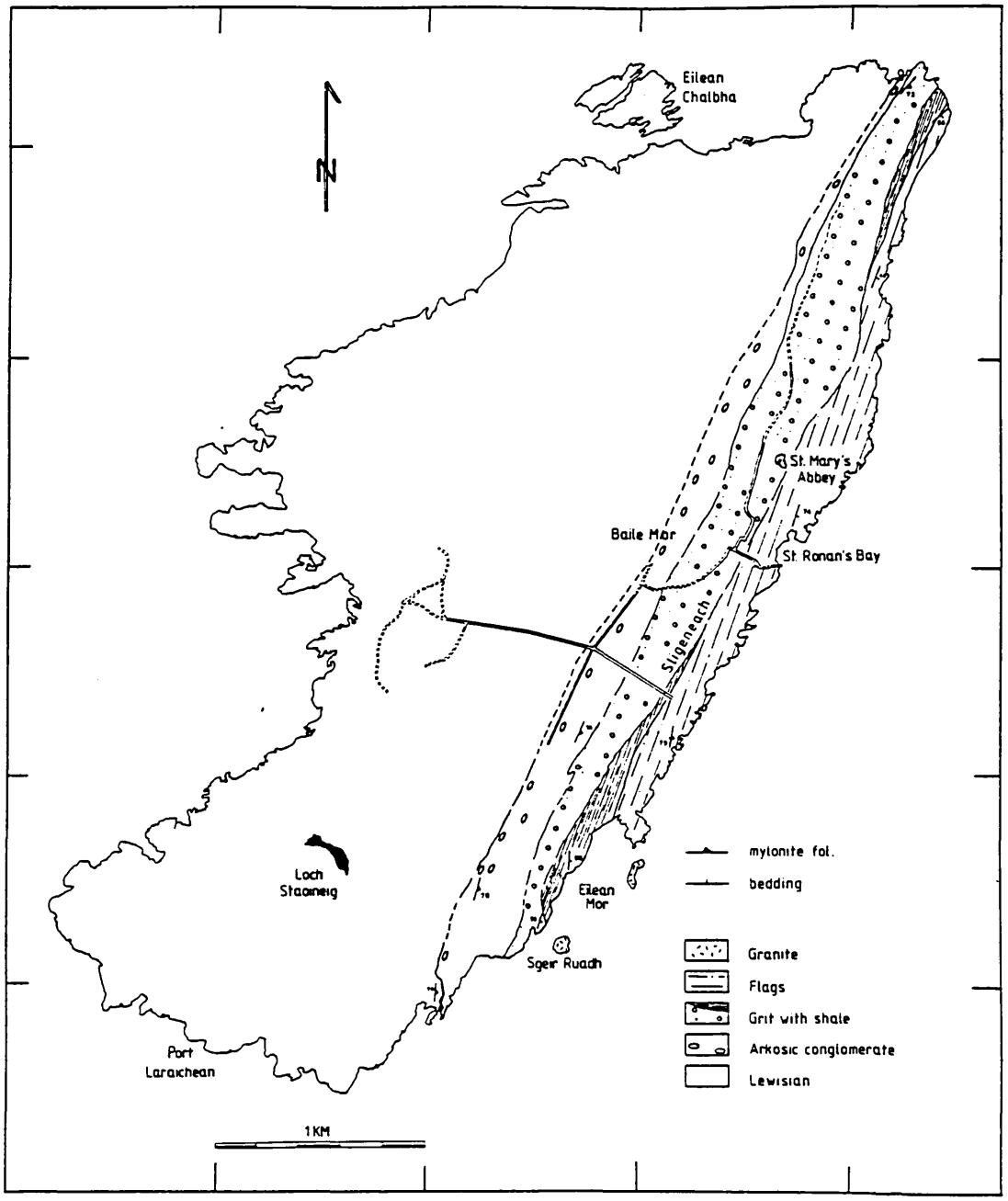


Figure 2.8. General geologic map of Iona.



Figure 2.9. Trough cross-bedding in flags, St. Ronan's Bay, Iona. Strata right way up.

shearing and mylonitisation along the contact, particularly in the southern half of the island, and also at Eilean Anaraidh, a small island north of Iona (Fraser 1977). The Lewisian-Torridonian contact will be discussed in detail in Chapter 6.

Flaggy psammites exposed along the south-eastern coastal strip are separated from the arkosic grits by wedge shaped outcrops of pelitic rocks both in the northeast and southeast part of the island (Fig. 2.8). The flaggy psammites are generally fine grained with occasional gritty bands and mudstone intercalations. Cross-bedding, particularly trough cross-bedding is fairly common (Fig. 2.9). A northerly palaeocurrent direction has been inferred by Stewart (1962) from the northeast end of the outcrop. The general younging direction is towards east away from the Lewisian rocks that occupy more than two-thirds of the island. Local overturning of cross-bedding has been reported and is probably due to minor isoclinal folding (Davidson in Fraser 1977).

In addition to shearing and mylonitisation along the Lewisian-Torridonian contact, both the flaggy psammites and the pelitic horizons show minor folds and associated axial planar cleavages. The steep dip of the Torridonian belt as a whole is probably associated with Caledonian compression. The regional metamorphic grade of the Iona group is very low (low greenschist facies), as indicated by the very fine-grained nature of the pelitic rocks except where later contact metamorphic effects are significant. The thermal effect of Ross of Mull Granite have produced local contact metamorphic minerals in the Torridonian and Lewisian close to the contact with the granite body.

2.5 THE BOWMORE SANDSTONE

2.5.1 Introduction

The Bowmore Sandstone (Amos 1959) crops out between the Gruinart hollow in the west and the Loch Skerrols thrust in the east (Fig. 2.10). Within this area the exposures are very poor and between exposures there are large expanses of alluvial deposits or raised beaches. The best exposures are found in the shore sections between the Laggan Farm and Rubh-an-t-Saile, southwest of Bowmore, and between Uisgeantisuidhe and Blackrock, west of Bridgend (Fig. 2.10). The former section will be

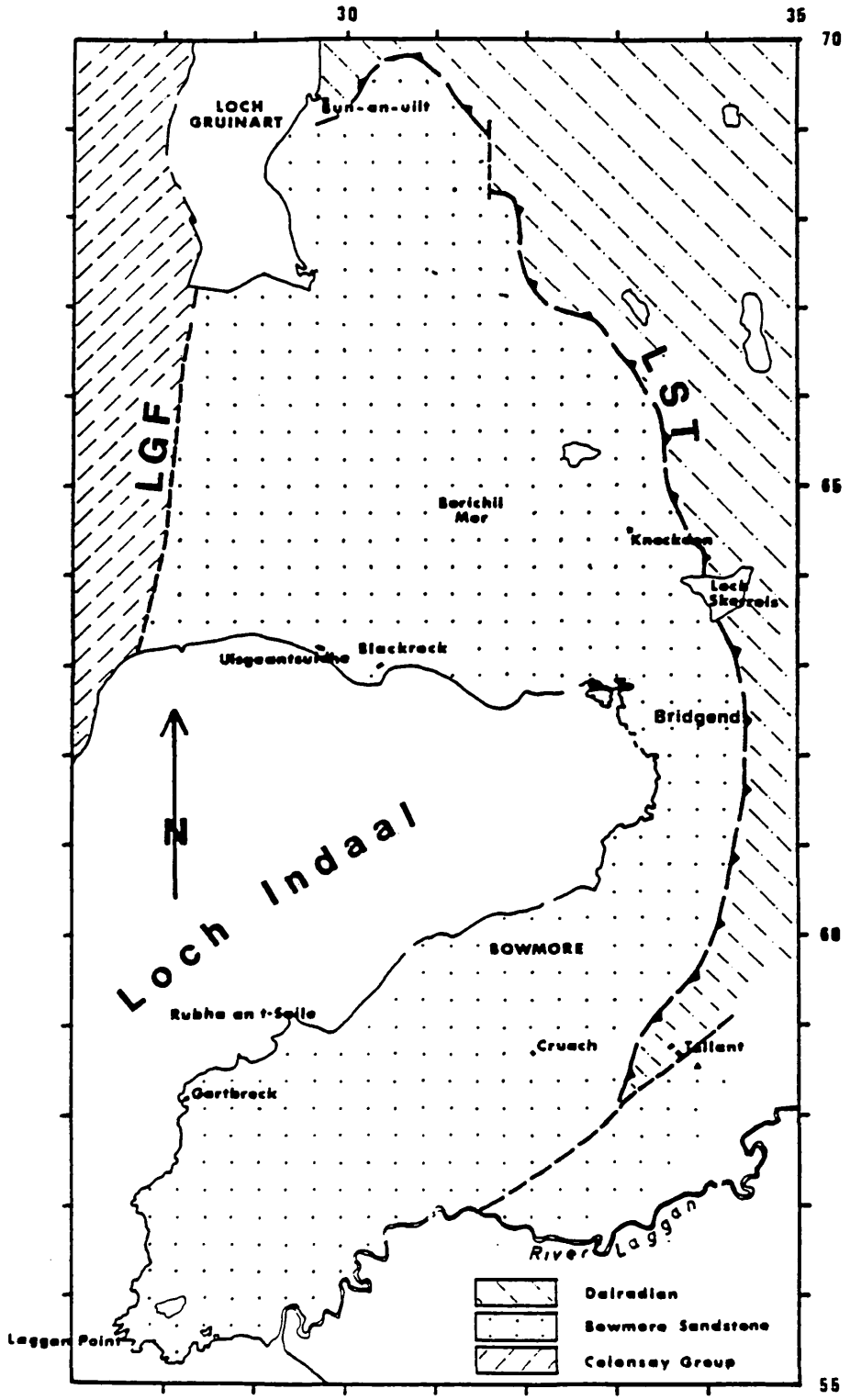


Figure 2.10. Geologic setting for the Bowmore Sandstone.

referred to as the Laggan area and the latter as the Blackrock area in the following discussion.

Although Wilkinson (1907) regarded the Gortan exposure in western Islay, one and a half kilometres north of Bruichcladdich, as belonging to the Bowmore Sandstone, careful examination by Amos (1959) and Stewart (1975), and present study indicate that the rocks seen at this exposure belong to the sediments of western Islay; more precisely, the Gortan exposure is a part of the Crosprig Grit unit within the Colonsay Group. Other exposures of the Bowmore Sandstone worth mentioning are those of Borichill-Mor, Knockdon, Carnain, Pennycraig, Crauch and Tallant Farm.

2.5.2 Stratigraphic Subdivision and Thickness

Amos (1959) subdivided the Bowmore Sandstone into the lower Laggan Group which is best exposed in the Laggan area and the upper Blackrock Group named after the exposures of the Blackrock area. The subdivisions correspond to the Laggan Flags and the Blackrock Grits respectively of Green (1924). Neither the base of the Laggan Group nor the top of the Blackrock Grop is exposed in the present area. The contact between the two groups has been described as one of conformable relationship from Knockdon and Crauch area (Amos 1959). However, the exposure in the Blackrock area is physically isolated, and its relationship with the rest of the outcrop is uncertain.

Amos (1959) estimated the minimum thickness of each of the groups at over 8000 feet (2438 meters); Stewart (1975) put the figures at over 2 kms each. Both these thickness estimates are based on the assumption that the section between Rubha-an-t-Saile and Laggan Point represent one unbroken descending sequence of strata. Although it is difficult to map individual horizons within the Laggan Group due to the lack of proper continuity of exposures and poor contrast in lithologic types, the present study shows that in the Laggan area there are alternate belts of right-way-up and overturned bedding between Rubha-an-t-Saile and Gartbreck. In addition to this, the presence of minor isoclinal folds in the exposure about 300 meters south of the Gartbreck Farm indicates that the sequence has been isoclinally folded. It follows then that there is repetition of strata in the section and the

thickness values given by Amos (1959) or Stewart (1975) are over-estimates. The exposed thickness of the Laggan Group in the Laggan area is probably not more than 500 metres and that of the Blackrock Group in the Blackrock area is around 1 km.

2.5.3 Lithology

A detailed description of the lithology of the Bowmore Sandstone has been given by Amos (1959). The salient points of Amos' description and of the present findings are enumerated below.

2.5.3.1 The Blackrock Group

The Blackrock Group consists predominantly of a coarse grained to gravelly feldspathic sandstone. The group is poorly bedded, and the bedding can be seen only where massive sandstone is interrupted by thin partings of laminated silts and/or shales. Tabular cross-bedding has been observed in such areas, the foreset is often defined by concentration of opaques. The pebble types include those of quartz (possibly derived from vein quartz or Lewisian pegmatites, showing deformation bands and dynamic recrystallization), reddened feldspar, jasper, ferruginous sandstone, quartzites with sutured grain boundaries, quartzite with ribbon quartz, and occasionally laminated silt (Fig. 2.11).

All these pebbles are enclosed in a sandy matrix which shows little signs of any penetrative deformation except local grain boundary recrystallisation. Although the pebble bands are generally only a few pebbles deep, they are widely distributed throughout the Blackrock area. This is very characteristic of the Blackrock Group for in the Laggan Group pebbly patches are only occasional. Pebbles of felsite and nordmarkite reported by Wilkinson (1907) have not been found. The texture of the ferruginous sandstone pebbles is distinctly finer than that of the surrounding matrix, and the former appears to be well sorted (Fig. 2.11); these pebbles appear red in the exposures and may be confused with the jasper pebbles.

The bulk of the Blackrock Group is a coarse, poorly sorted sandstone with clasts varying from subangular to occasionally rounded. Sand sized clasts include quartz, blue quartz, feldspars of varying

Figure 2.11. Detrital clasts in the Bowmore Sandstone. All specimens from Blackrock area.

(a) Pebble of deformed and partly recrystallised vein quartz in an undeformed matrix.

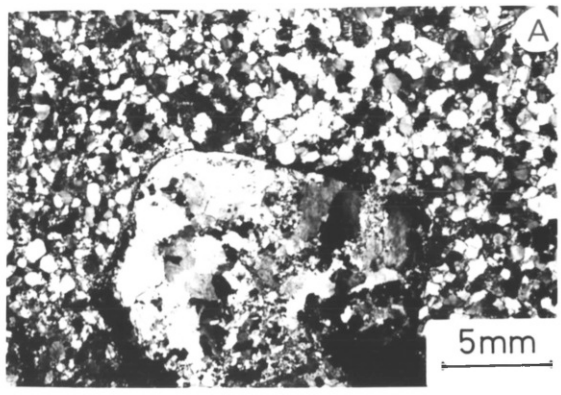
(b) Pebble of fine grained ferruginous sandstone in a coarser sandy matrix.

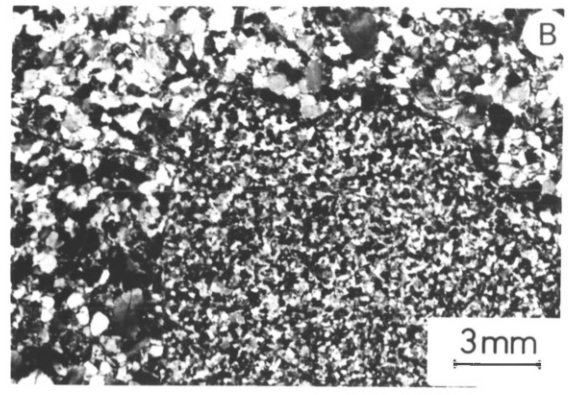
(c) Laminated silt pebble.

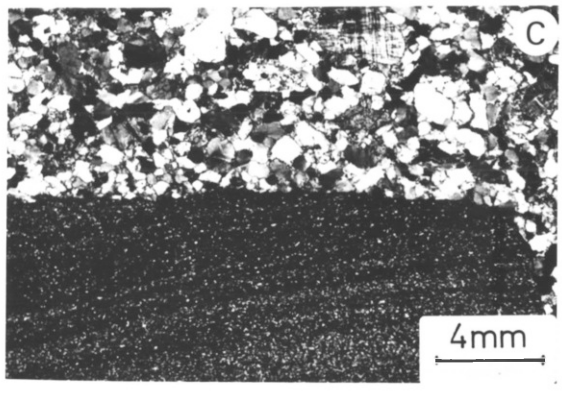
(d) Quartz clast (granulite quartz) with inherited deformation texture (centre of the micrograph). Note that the surrounding grains are free from any optical effects of strain.

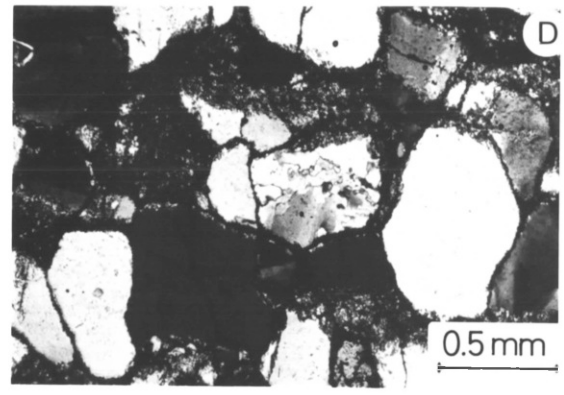
(e) Pressure solution and grain elongation in an orthoquartzite pebble.

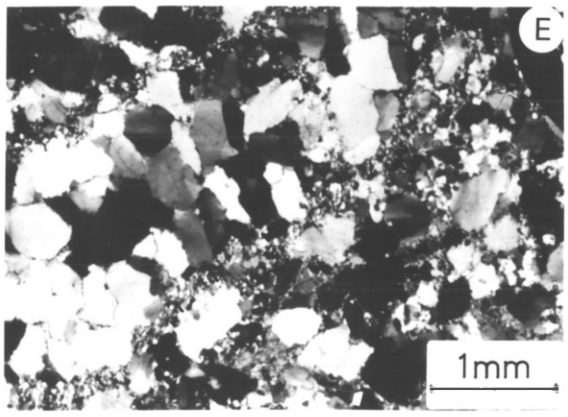
(f) Blue quartz with hair like inclusions of rutile needles.

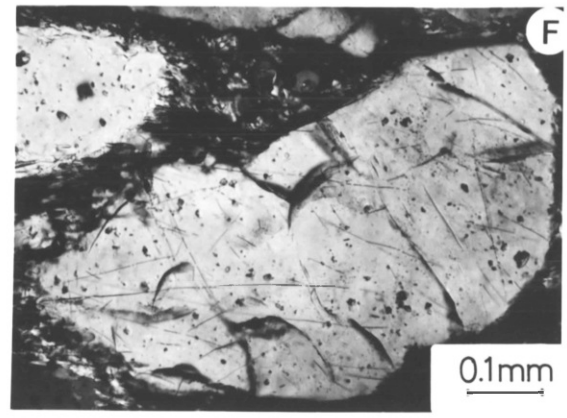

A
5mm


B
3mm


C
4mm


D
0.5mm


E
1mm


F
0.1mm

composition including perthites, microcline, orthoclase and plagioclase, epidote, opaques and mica (Fig. 2.11). The proportions of different mineral grains in a few analysed specimens are shown in Table 2.5. 'Sericite' is a common constituent often filling the gaps between the grains or as alteration products after feldspar. However, there is no appreciable alignment of phyllosilicates within the sandy facies. Carbonate grains are rare and probably diagenetic. Some of the opaques are also diagenetic.

2.5.3.2 The Laggan Group

The Laggan Group on the whole is a medium grained feldspathic sandstone with common silty and shaly intercalations (see Table 2.5 for the proportions of different mineral grains). In the section between the mouth of the river Laggan and the Laggan Farm the rocks are well bedded and commonly with a red colouration. Common sedimentary structures include tabular cross-bedding, contorted laminations, load-casts and flame structures, intraformational shale breccia and sandstone dykelets.

2.5.4. Depositional Environment

A subaqueous environment of deposition has been suggested for the Bowmore Sandstone; the general picture is one of moderately rapid deposition in shallow water with strong currents (Amos 1959). The freshness of most of the feldspar clasts is in favour of relatively short transport of the sediments. One of the interesting features is the red colouration of at least part of the Bowmore Sandstone including some pebbles of feldspar and sandstone within the Blackrock Group. This probably indicates a generally oxidizing environment of transport and deposition. Some of the pebbles might have been derived from an already existing red facies. So far as the depositional environment is concerned both the Colonsay Group and the Dalradian of NE Islay are quite distinct from the Bowmore Sandstone. The fact would be quite in agreement with a temporal and/or geographic separation of the three groups of rocks.

Table 2.5 Proportions of different mineral grains in the Bowmore Sandstone. Figures as percent of total number of clasts counted, number of clasts counted in each specimen = 180, except sp. 604 where it is 210.

Formation	Specimen No.	COMPOSITION*							Comments
		Quartz	FELDSPAR					Lithic	
			Microcline	Plagioclase	Perthite	Unspecified	Total		
BLACKROCK GROUP	BS2	60.00	6.67	2.22	7.78	20.55	37.22	2.78	Granulite quartz, blue quartz, vein quartz with recrystallization, ferruginous sandstone
	BS6	65.00	3.89	1.11	6.67	12.22	23.89	11.11	
	437	70.00	8.89	2.78	5.55	12.22	29.44	0.56	blue quartz
	487A	66.85	6.74	3.93	3.37	41.80	25.84	7.30	quartzite with pressure solution fabric
LAGGAN GROUP	594A	72.22	5.00	5.00	7.78	10.00	27.78	0	
	604	72.86	6.19	1.90	4.28	12.38	24.76	12.38	Opaques

* figures as % of total number of clasts counted

2.5.5 Provenance

Amos (1959) suggested that at least part of the terrain from which the sediments were derived was occupied by a potassic granite. However, a suite of clasts which includes blue quartz, granulite quartz with inherited shape fabric and epidote is indicative of a Lewisian type gneissic terrain as a source for at least part of the sediments. Detrital epidote is a common constituent of the Torridonian sediments of NW Scotland, presumably derived from a Lewisian basement. On the basis of the general nature of the Bowmore Sandstone, they have been compared with the Applecross Group (Wilkinson et al. 1907, Stewart 1975). Common presence of feldspars suggest that pegmatites and other acid igneous rocks must have been common within the source area.

However, the presence of jasper, ferruginous sandstone, some orthoquartzites and other sedimentary fragments in the Bowmore Sandstone indicates that the provenance must have included some supracrustal group of rocks of low metamorphic grade. Some well rounded quartz grains with high sphericity in poorly sorted sandstone must have been products of more than one cycle of deposition and transport.

One of the interesting features in some orthoquartzite pebbles is the presence of marked shape fabric, probably induced by pressure solution along quartz-quartz grain boundaries (Fig. 2.11); in one such pebble bands and veins of cataclasite are present. The implication of these features is that predating the deposition of the Bowmore Sandstone, there existed a group of sedimentary rocks which had undergone tectonic strain at low grade metamorphic conditions. One of the likely candidates to which this eroded group of rocks might belong is some representative of the Grenville rocks on this side of the Atlantic. On the other hand, if Grenville rocks in SW Argyllshire contributed detritus during the late Precambrian times, they must have been far outside the zone of granulite facies metamorphism characteristic of the Irish Grenville provinces such as the Ox Mountains inlier.

2.5.6 Deformation

Although signs of penetrative deformation are not obvious especially within the Blackrock Group, minor structures as well as large scale mapping indicate that the Bowmore Sandstone is folded and faulted. Three phases of folds have been recognised. Exposures are few and far

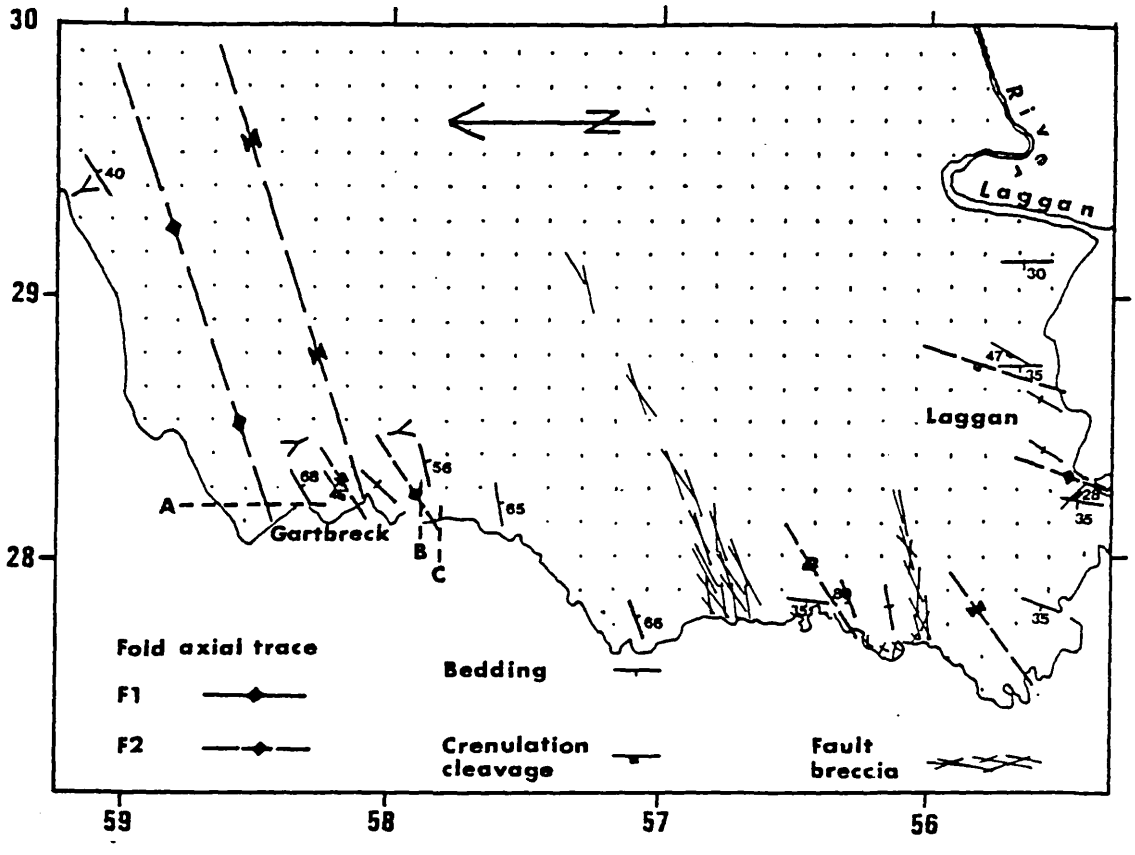
between in the area north of Bowmore. The following exposition on the structure of the Bowmore Sandstone relates mostly to the Laggan area.

Early isoclinal folds have been mapped in the area between Rubha-an-t-Saile and Gartbreck. There exists alternate belts of overturned and right-way-up bedding (Fig. 2.12). In addition to this, in an exposure 300 meters south of the Gartbreck Farm, the lamination within a silty sandstone is thrown into minor isoclinal folds (Fig. 2.12). The axial trend of these folds is ENE-WSW and the direction of overturning is towards north. A possible cross-section across the main folds and the alternative interpretations for the structures are provided in Fig. 2.12. The first of the two alternatives, i.e. the model with anticlinal antiform and synclinal synform, is favoured because the strata on the east side of the Laggan point appear to be right-way-up, and there is no evidence to suggest that the whole of the Laggan area is on the overturned limb of a larger structure.

Sandstones from the Rubha-an-t-Saile area show features of intracrystalline deformation under the microscope, such as undulose extinction, deformation bands and common grain boundary recrystallisation of quartz clasts. However, most of the feldspar grains have not suffered any mechanical breakdown or recrystallisation, except for patchy alteration to white mica. The specimens in which the observed microstructures were seen come from the overturned limb of an isoclinal fold in the Rubha-an-t-Saile area. However, the minor isoclinal folds described earlier do not bear any penetrative axial plane cleavage.

Second generation structures include asymmetric NNE folds with one near vertical limb. Such folds are common in the area between the mouth of the River Laggan and the Laggan Point. These folds are associated with an axial planar cleavage in the shaly intercalations between sandstone beds (Fig. 2.13c-d). Microstructurally, the axial plane cleavage is a crenulation cleavage which transposes an enhanced bedding parallel fabric defined by parallel alignment of extremely fine grained white micas.

The crenulation cleavage immediately west of the mouth of the River Laggan (287555) dips at 40 degrees towards WNW. West of the Laggan Farm (282553), a morphologically similar cleavage dips at 30



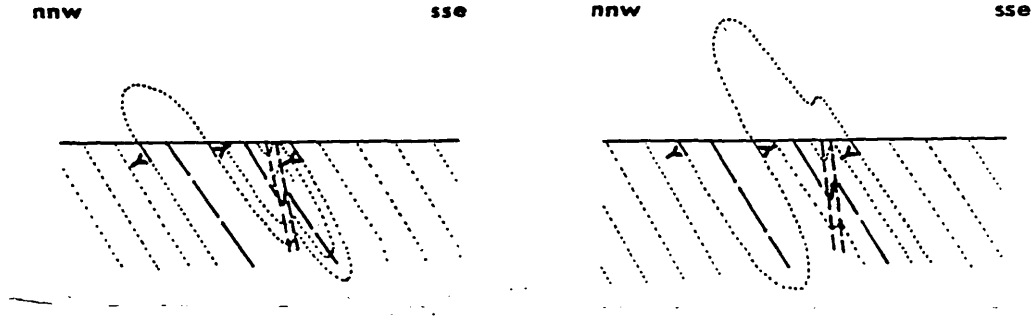


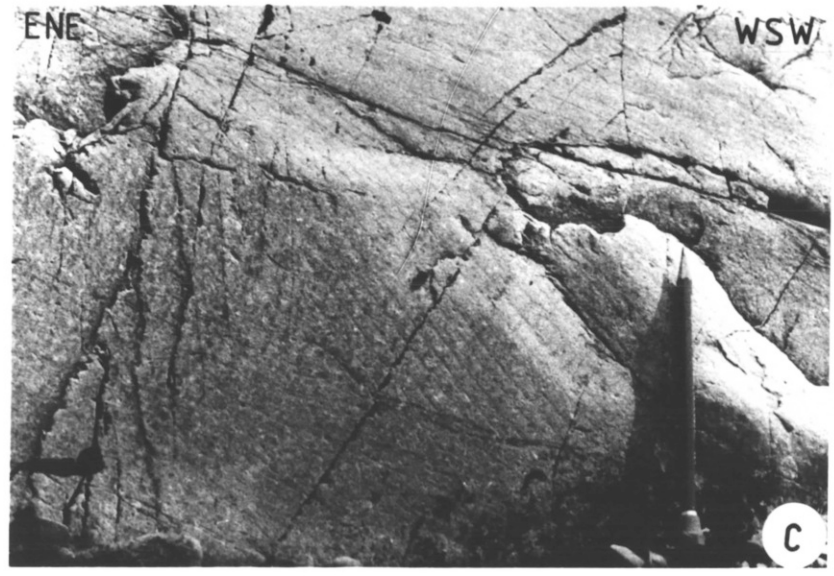
Figure 2.12. (a) Structure map of the Laggan area and schematic sections to explain the observed structures.

(b) Intraformational shale breccia and bottom structure in Laggan Group, locality 'A' in 2.12(a). The beds are right-way-up.

(c) Overturned cross-bedding in Laggan Group, locality 'B' on map in 2.12(a).

(d) Minor isoclinal folds (F_1) in Laggan Group, locality 'C' in 2.12(a).







2.12 contd.

degrees towards SW. It is highly probable that a set of late open folds on E-W axis have reoriented the crenulation cleavage associated with the second phase folds on NNE axis.

Although Amos (1959) described four phases of folding within the Bowmore Sandstone, with an E-W slaty cleavage both from the Laggan and Knockdon area, the present observations do not support Amos' structural interpretation. No penetrative E-W cleavage have been observed in the Laggan area; the only penetrative fabric is an enhanced bedding parallel fabric occurring within the shaly intercalations and probably associated with the early isoclinal folds.

It is strange that Amos (1959, p.209) regarded a monoclinal flexure (Bun na h'Aibhne monocline) as earlier than the Laggan or Cnoc Don Mhor folds, which Amos described as overturned structures. In view of the present observations Amos' Laggan fold is regarded as one of the second generation structures (F_2) near the Laggan point (Fig. 2.12). Amos regarded the Cnoc Don Mhur fold as one of his third phase of folds; the 'Laggan fold' is also grouped within the same phase. It is not possible to comment on the geometry of the Cnoc Don Mhor fold because of the poor exposure in the area (according to Amos only the overturned northern limb is visible).

Northwest of Knockdon Farm (327651) in an exposure of Laggan Group, a penetrative cleavage defined by elongation of quartz and feldspar grains and parallel alignment of phyllosilicates (Fig. 2.13a-b) strike ENE and dips at 70 degrees towards SSE. The Loch Skerrols thrust line is within 100 meters of this exposure. Notice that the mylonite foliation in the sheared Jura Quartzite around Loch Skerrols dips at 30 degrees towards east. The orientation of the penetrative cleavage in the Laggan Group rocks is comparable to that of the F_1 axial plane suggested by structures in the Laggan area (see Fig. 2.12). It is not unlikely that this cleavage is related in a general way with the F_1 folds within the Bowmore Sandstone.

In the Blackrock area the bedding is steep, dipping at 70-90 degrees towards west. Sedimentary structure (cross-bedding) indicates that the stratigraphic top is towards west. At Carnain, 1.5 kms east of Blackrock, bedding in Blackrock Grop rocks dips at 40 degrees toward

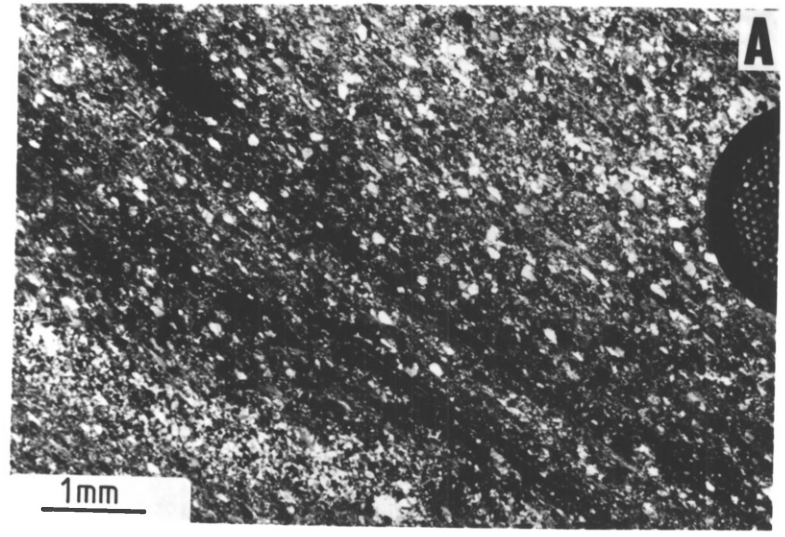
Figure 2.13. Axial plane cleavages in Bowmore Sandstone.

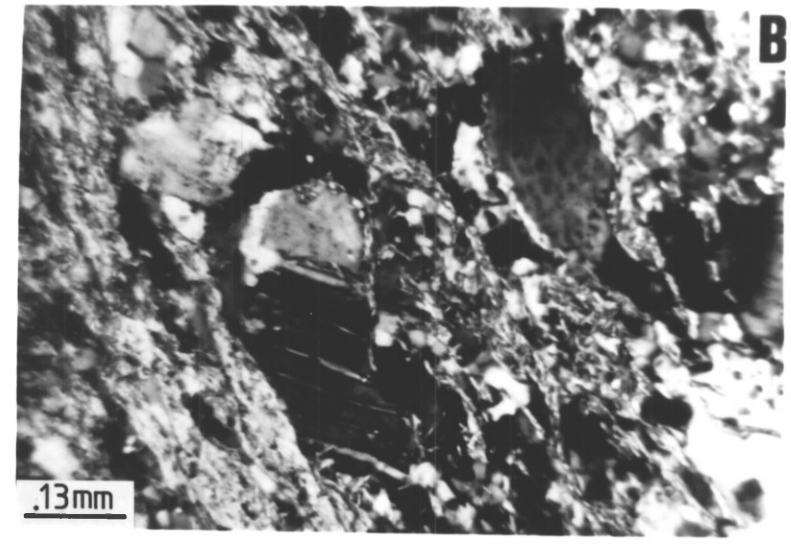
(a) Penetrative cleavages ($?S_1$) in Laggan Group, northwest of Knockdon Farm.

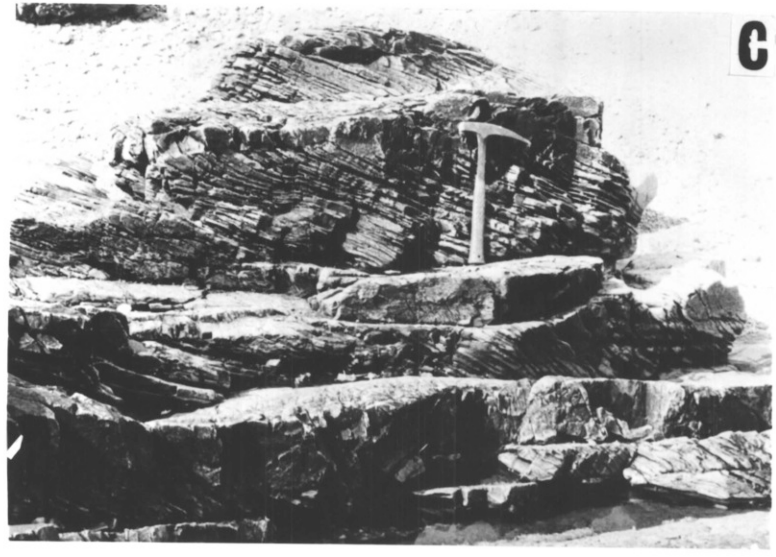
(b) Details from (a). Note elongation of clasts.

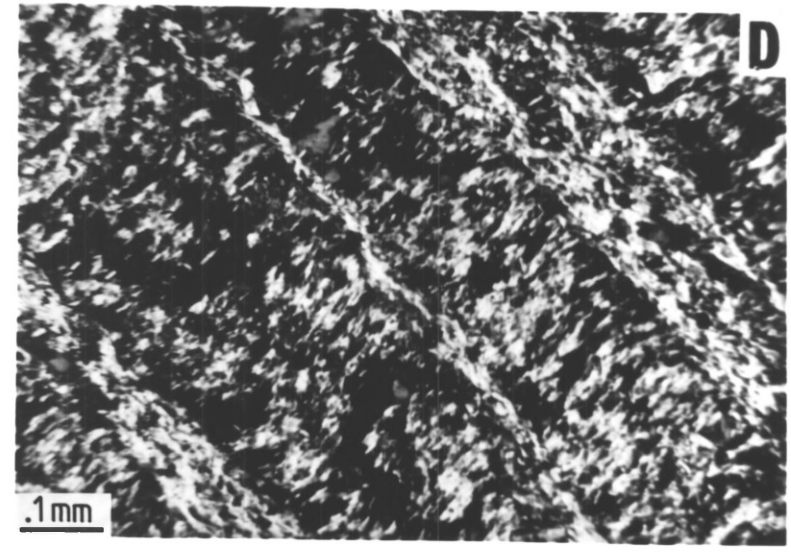
(c) S_2 cleavage in an outcrop of Laggan Group, Mouth of River Laggan. Notice cleavage refraction in alternate muddy and psammitic layers; the cleavage is far more close spaced in the former.

(d) Photomicrograph of crenulation cleavage (S_2) in the pelitic layers, locality as in (c).


A
1mm


B
.13mm


C


D
.1mm

northeast. The two outcrops may be related by a large NNE trending fold (antiform), which is comparable to F_2 structures in the Laggan area.

The main deformation events affecting the Bowmore Sandstone and the associated features are summarised in Table 2.6.

It must be emphasised here that the sequence of events put forward above is entirely with respect to the folding history of the Bowmore Sandstone. Any direct comparison with the deformation events in the Dalradian in NE Islay should be taken with a note of caution. The absence of any

Table 2.6 Deformation events in the Bowmore Sandstone

Deformation events	Fold Structure	Microstructure
D_1	Isoclinal folds between Rubha-an-t-Saile and Gartbreck	Enhanced bedding parallel fabric in pelitic bands; re-crystallisation in quartz within the Laggan Group may be associated with F_1
D_2	Close to tight folds with one near vertical limb	Crenulation cleavage in pelitic bands
D_3	Assymetric open E-W folds which reorient crenulation cleavage associated with F_2	

isoclinal folds within the Islay Dalradian seems to indicate that the F_1 folds in Bowmore are probably earlier than the 'Islay anticline' (D_{1d} of

Borradaile 1979). Since the Loch Skerrols thrust transgresses the NW limb of the 'Islay anticline', it is not unlikely that the F_2 structures within the Bowmore Sandstone predate the thrusting. With regard to the deformation events within the Colonsay Group in western Islay, D_1, D_2 events in the Bowmore Sandstone are probably parallel with the earlier events in western Islay. The E-W trend of the F_3 folds in the Bowmore Sandstone is oblique to the general Caledonian trend; however, E-W kinks are not uncommon as part of a conjugate set of kinks (latest structures) within the Colonsay Group.

It may be pointed out here that the ambient temperature at which the Bowmore Sandstone was deformed was very low even in terms of the metamorphism of the NE Islay Dalradian or the Colonsay Group. Pelitic partings within the Blackrock Group are extremely fine grained and are still shales or slates rather than phyllites. This is in contrast to the phyllites within the NE Islay Dalradian or the Colonsay Group. Within the psammites the interstitial material to detrital grains are extremely fine grained and retain some of the clay mineral chemistry. Electron microprobe analysis of a 'micaceous' mineral from such interstitial material in Blackrock Group is shown in Table 2.7. Note that the analysis shows slightly higher silica and less potassium compared to muscovite and thus the analysed mineral may be regarded as belonging to the illite group (Deer et al. 1962).

Table 2.7 Analysis of 'illite' from Blackrock Group

Element	% oxide	Formula (220)	
Si	46.545	5.638	
Al	24.425	3.487	
Ti	.298	.027	
Fe*	8.920	.904	
Cr	.138	.013	
Mg	.763	.138	
Ca	.116	.015	
Na	.121	.028)	
K	10.701	1.654)	1.682
Total	92.120		

* Total iron as FeO.

2.5.7 Tectonic Setting

The Bowmore Sandstone is juxtaposed against the Colonsay Group along the Loch Gruinart Fault (LGF). It is highly likely that the LGF represents a splay fault associated with the SW extension of the Great Glen Fault (GGF). The extension of GGF west of Colonsay named as the Colonsay fault shows a westerly downthrow; LGF shows an easterly downthrow (Evans et al. 1980). Thus the wedge of crust between the Colonsay fault and LGF is an effectively horst structure. Lensen (1958) described a method of secondary horst and graben formation associated with converging wrench faults. Application of the Lensen model for the LGF-Colonsay fault pair suggests a sinistral displacement along LGF and the Colonsay fault which is thought to be the main extension of GGF. The above-mentioned strike-slip displacements are essentially related to a pre-Mesozoic event because LGF acted as a boundary to a Mesozoic basin occurring south of the Rhinns of Islay (Evans et al. 1980).

A possible late Precambrian to early Palaeozoic scenario for the Malin Sea area is shown in the cartoon of Fig. 2.14. Assuming a sinistral displacement of a few tens of kms along LGF, the position of the Bowmore Sandstone before the displacement would be closer to the Lewisian block associated with the Inistrahull outcrop. Both the Colonsay Group and the Bowmore Sandstone were deposited in basins not far from the plausible basement high that might have existed along the line of Lewisian outcrops of Inistrahull, Rhinns of Islay and Colonsay. The early Palaeozoic position of the Islay Dalradian was probably further east, away from the basement high. The movement along the Loch Skerrols thrust during the Caledonian compression has brought the Dalradian on top of the Bowmore Sandstone.

2.6 STRUCTURAL HISTORY AND MINOR INTRUSIONS

In each of the three islands - Iona, Colonsay-Oronsay and western Islay, the metasediments have a polyphase deformation history. For reasons discussed in later chapters, the deformation is regarded as essentially Caledonian. Presence of penetrative axial plane cleavages which can be related to separate folding phases indicate that the style of deformation within the Colonsay Group is different from that of the thrust-belt Torridonian in NW Highlands. Detailed description of the structures in these islands and their implications will be given in Chapters 3-6.

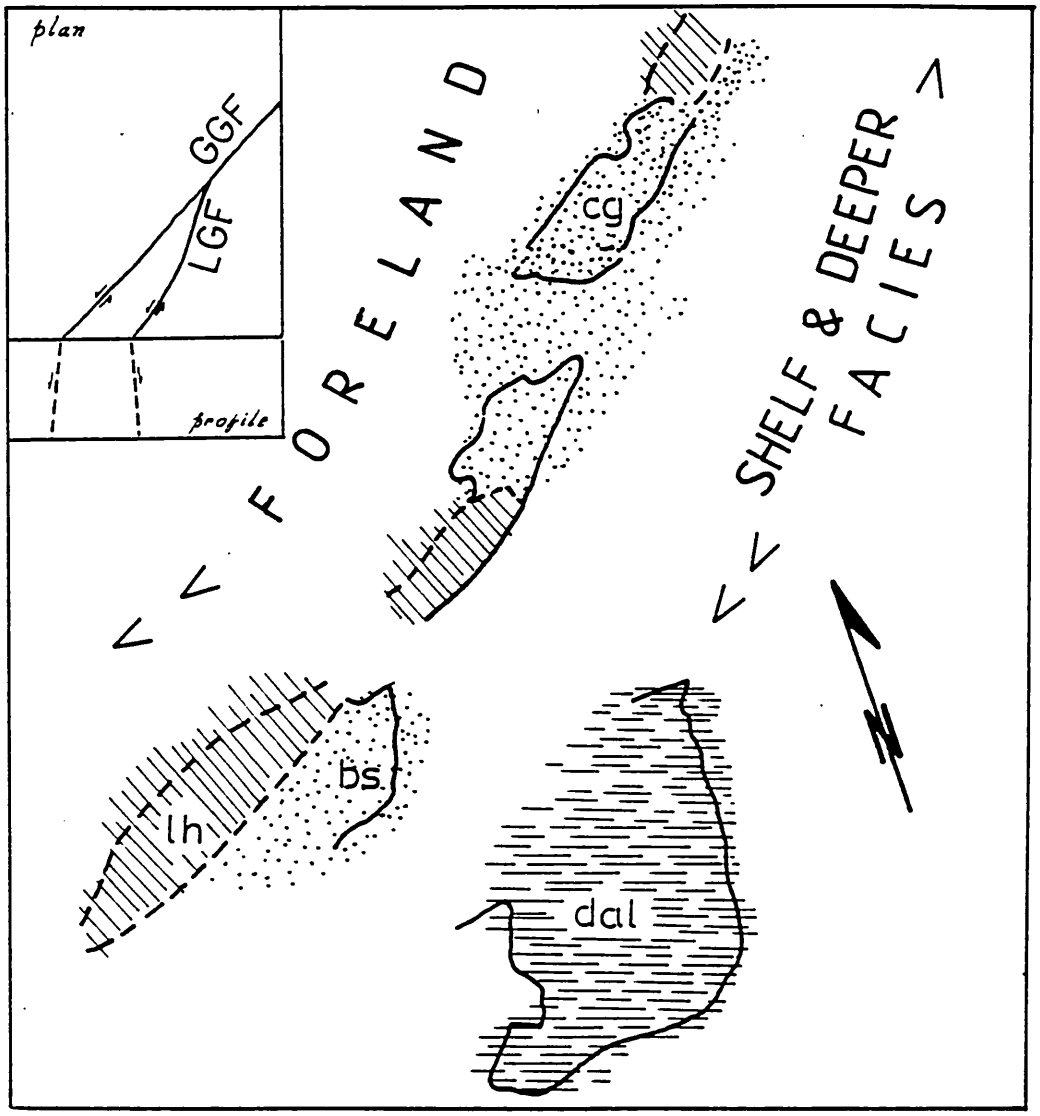


Figure 2.14. A cartoon showing a possible late Precambrian to early Palaeozoic scenario for the Malin Sea area. lew = Lewisian, cg = Colonsay Group, bs = Bowmore Sandstone, dal = Dalradian.

Inset shows the displacement along the Great Glen Fault system which juxtaposes Bowmore Sandstone against the Colonsay Group. Sinistral displacement along Loch Gruinart fault (LGF) as well as along the main branch of Great Glen Fault (GGF) produces a secondary horst structure in the area.

The metasediments and the basement Lewisian is intruded by Caledonian minor intrusions. In western Islay and Colonsay, the intrusive sheets and stocks vary from lamprophyres at various stages of alteration through appinites to felsic porphyrites. The last named type is more frequent in Iona. All the varieties have been recorded from the Lewisian in western Islay. It is interesting to note that some of the earlier minor intrusions are affected by later phases of folding and develop a strain induced fabric. A definite grouping of the intrusives with respect to deformation phases is possible. This helps, as will be shown later, in correlation of deformation phases across islands. Details on minor intrusions will be given in Chapter 7.

2.7 MAJOR LINEAMENTS IN W. ARGYLL AND THE MALIN SEA

2.7.1 The Great Glen Fault System

The Great Glen Fault (GGF) intersects mainland Scotland from the Moray Firth in the NE to the Firth of Lorne in the SW along the deep trench of Glen More. The transcurrent nature of the fault and sinistral displacement of the order of 100 kms was first suggested by Kennedy (1946). The possibility that the fault extends southwestward offshore from Mull through the Malin Sea and thence through Ireland has been suggested by several authors (Evans et al. 1980, Garson and Plant 1972, Holgate 1969, Kennedy 1946, Pitcher 1969).

NE trending faults exist in the Malin Sea area and the term Great Glen Fault system is used here to include all these faults which are presumably linked to the main fault along the Great Glen. The present location of Islay and Colonsay being roughly in line with the bearing of the GGF, a discussion on the possible location of the displacement along the major branches of the GGF system is essential to the understanding of the tectonics of the area.

Kennedy (1946) suggested a sinistral displacement of 105 kms along GGF on the basis of matching the Strontian granite with the Foyers granite, the metamorphic isograds and injection complexes on either side of Great Glen (Fig. 2.15); a post Middle Old Red Sandstone age for the movement was suggested. The line of GGF in Kennedy's reconstruction passes north of Colonsay, thus allowing the Loch Skerrols thrust to be

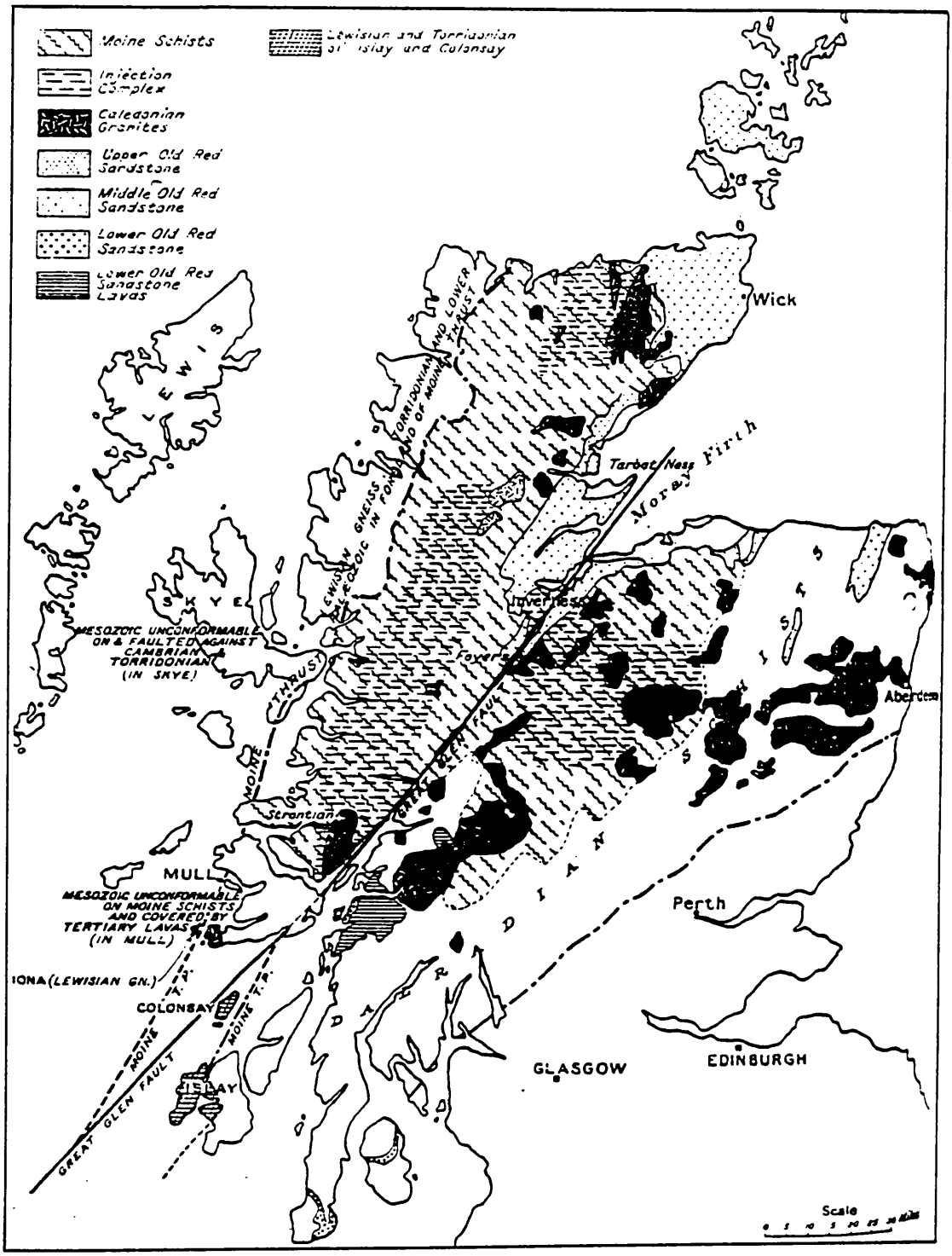


Fig. 2.15a. Geologic map of the Scottish Highlands to show the present positions of the Moine injection complexes, the Strontian and Foyers granites and the Moine Thrust plane, from Kennedy (1946).

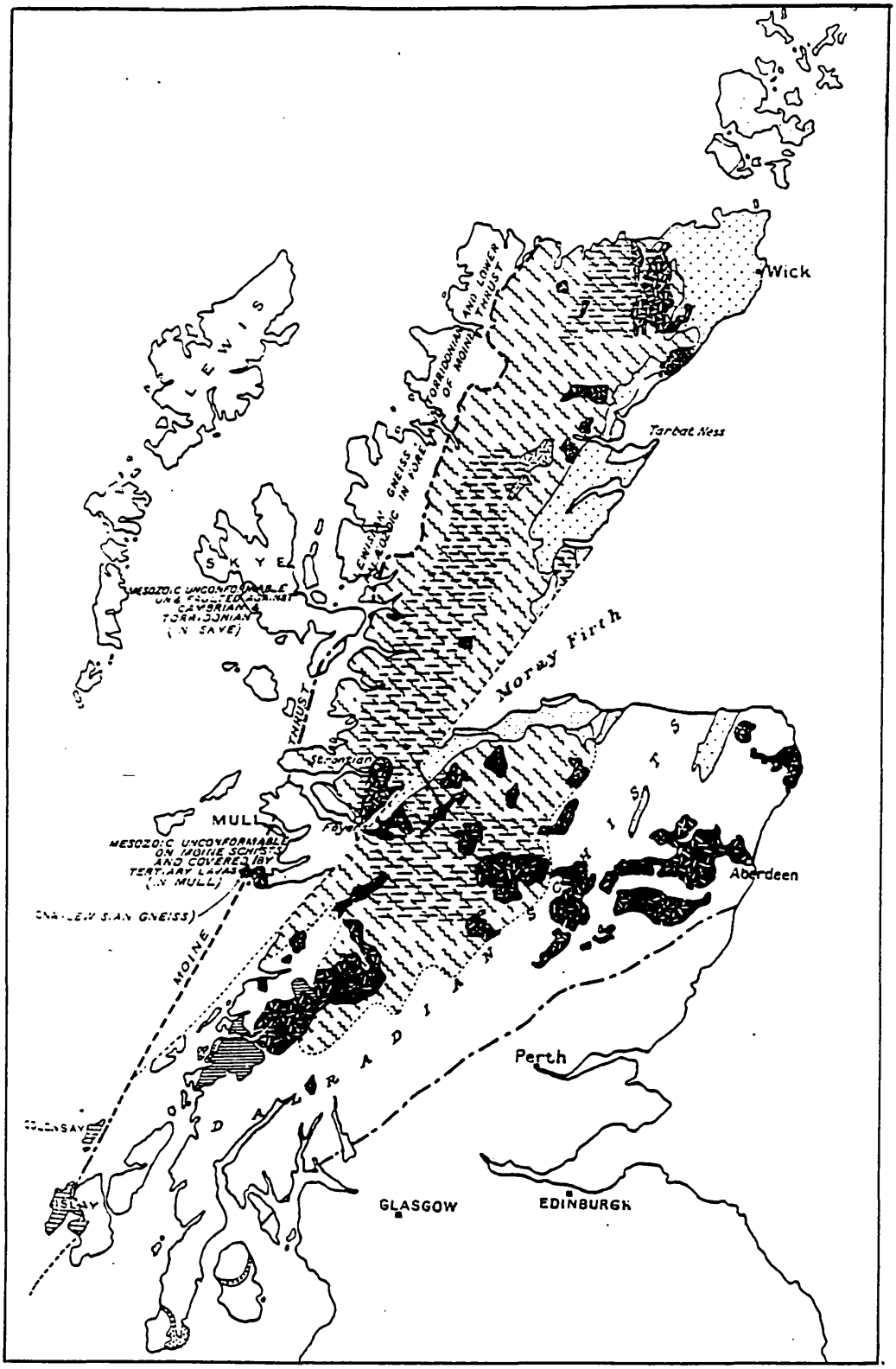


Figure 2.15b. Geologic map of the Scottish Highlands to show the former (Old Red Sandstone times) positions of Moine injection complexes, the Strontian and Foyers granites, and the Moine Thrust plane, prior to the lateral displacement along the Great Glen Fault, from Kennedy (1946). Scale and legend as in 2.15a.

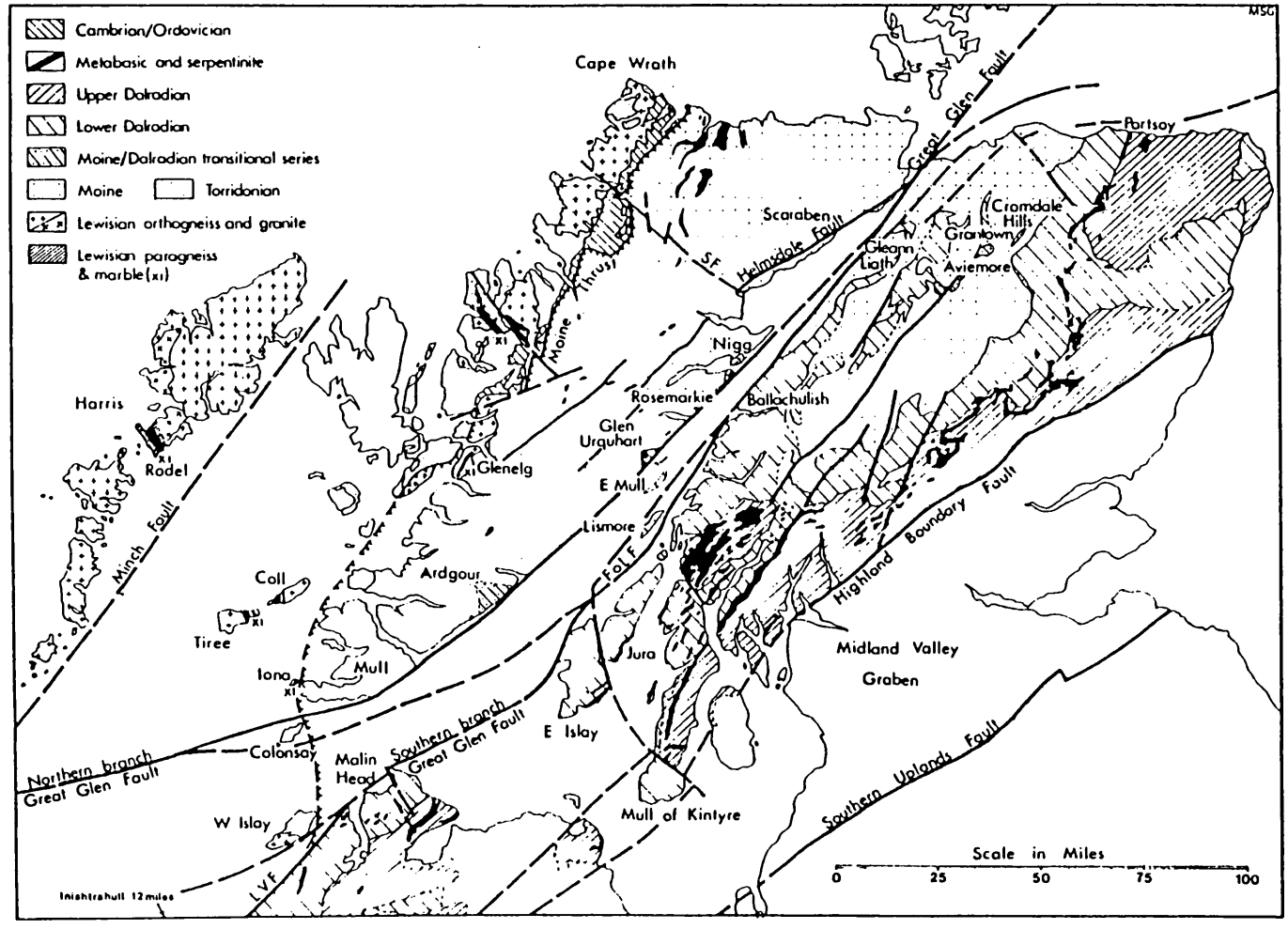


Figure 2.16. Reconstruction of Scotland in the Lower Old Red Sandstone before the postulated 75 miles dextral displacement on the Great Glen Fault and Leannan Valley Fault(LVF) and the 55 miles dextral displacement on the Minch Fault. FOLF = Firth of Lorne Fault; from Garson and Plant(1972).

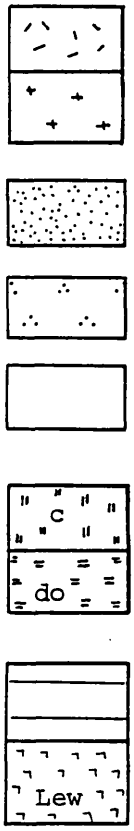
regarded as the probable southern continuation of the Moine Thrust. Holgate (1969) although essentially agreeing with Kennedy (1946) regarding sinistral displacement, suggested an additional Tertiary dextral displacement of 30 kms along the same fault line on the basis of displacement of Middle Old Red Sandstone to Mesozoic strata, Tertiary dyke swarms and ancestral pattern of the highland drainage system. In this model the sinistral displacement was revised to 134 kms, and the age of this displacement was regarded as earlier than the onset of the Middle Old Red Sandstone deposition. Holgate (1969) also suggested a dextral movement along the Firth of Lorne fault (FOLF) passing to the south of Lismore in order to match the dyke swarms on either side.

Later, the sinistral displacement along the GGF was questioned on the ground that the metamorphic zones near Foyers match equally well with the Caithness zones, which lie to the NE of Foyers and on the NW side of GGF (Garson and Plant 1972). Moreover, the apparent structural and petrographic similarity between the Strontian and the Foyers granite has been questioned both on structural and geochemical grounds (Ahmad 1967, Munro 1965). A Tertiary age for the major dextral displacement was also questioned on the ground that the aeromagnetic map of Great Britain shows no apparent Tertiary dyke displacement (Garson and Plant 1972). The sequence of movements postulated by Garson and Plant (1972) is as follows:

> A dextral movement of 121 kms occurred along the Leannan Valley Fault (Leannan Fault in Evans et al. 1980). Passing through Islay (Loch Gruinart Fault, LGF) and between Lismore and Strontian to Fort William and the Moray Firth (Fig. 2.16, the southern branch of the GGF). Simultaneously, a 88 kms dextral shift occurred along a line N of Colonsay, through eastern Mull and up the Great Glen to form the northern edge of a graben bordered to the south by the southern branch of the GGF.
>
> A further dextral displacement of 32 kms occurred along a line S of Colonsay into the FOLF southeast of Lismore. From there it traversed a wide crush belt of mylonitized Middle Old Red Sandstone and Moine rocks to the Moray Firth.

In the reconstruction of Garson and Plant (1972) the continuation of the Moine Thrust passes east of Colonsay (Fig. 2.16), but they

Figure 2.17. Solid geology of the Malin Sea area, from Evans et al.(1980).



Basic intrusion

Granitic intrusion

Assumed to be of Tertiary age unless labelled
ku = Upper Cretaceous
Cal = Caledonian

Tertiary basalt

Tertiary sediments

n = Neogene
go = Oligocene

Mesozoic and Permian sediments

k = Cretaceous t = Tertiary
j = Jurassic p = Permian

Carboniferous sediments, lavas and volcanics

Old Red Sandstone sediments, lavas and volcanics

Lower Palaeozoic & Upper Precambrian basement

Dal = Dalradian Tor = Torridonian M = Moinian

Lewisian gneiss

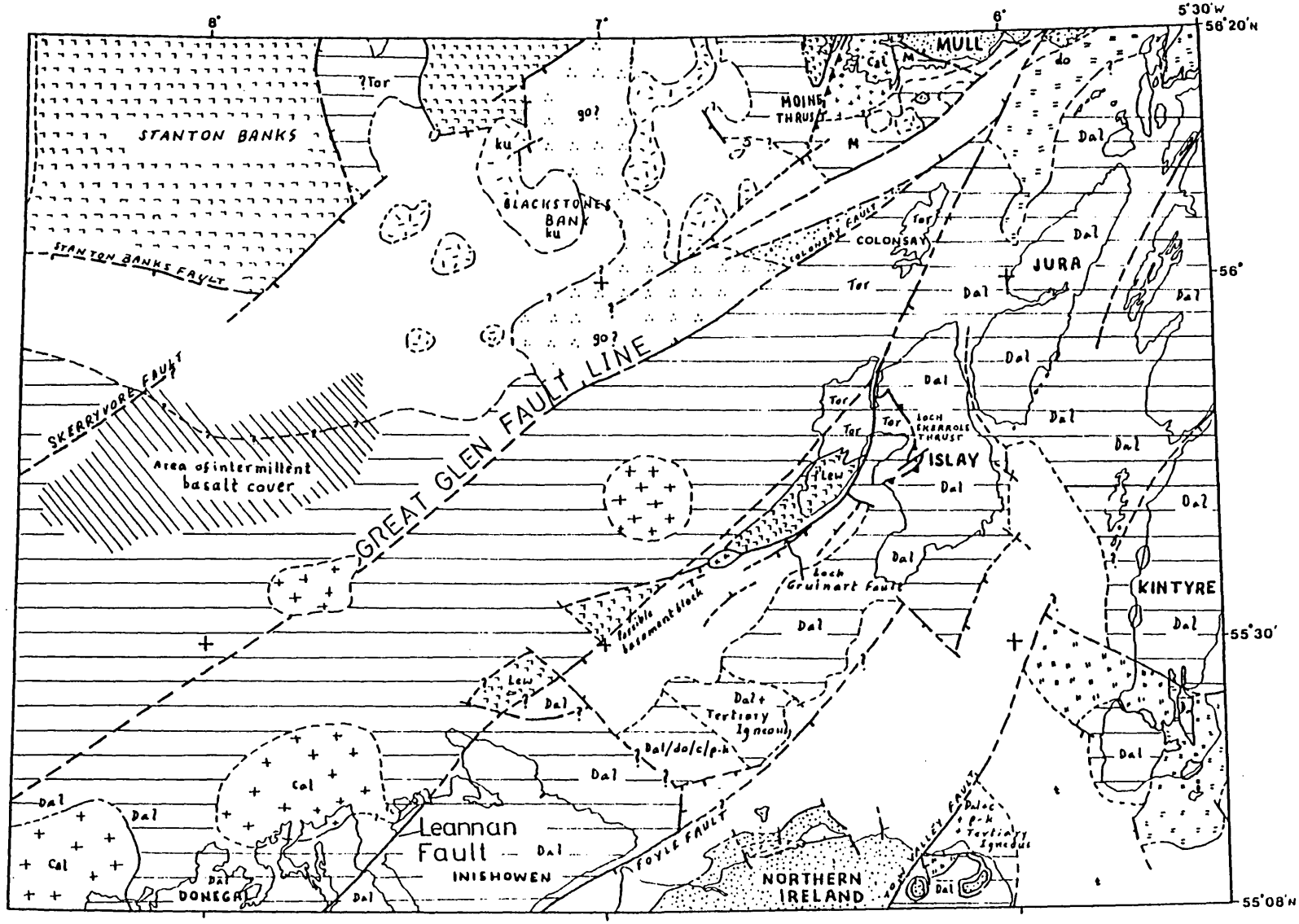
Major fault, with downthrow where known

Faulted boundary, with downthrow where known

Geological boundary

Thrust

Broken lines denote uncertainity; Universal Transverse Mercator Projection.


8°
7°
6°
5°30'W
56°20'N
56°
55°30'
55°08'N
STANTON BANKS
STANTON BANKS FAULT
?Tor
go?
ku
BLACKSTONES BANK
MOINE THRUST
M
Cal
MULL
do
Dal
COLONSAY FAULT
Tor
COLONSAY
JURA
GREAT GLEN FAULT LINE
SKERRYVORE FAULT?
Area of intermittent basalt cover
Tor/Dal
LOCH SKERROLE THRUST
ISLAY
Lew
Loch Gruinart Fault
KINTYRE
Possible basement block
Dal + Tertiary Igneous
Dal/do/c/p-h
Cal
Leannan Fault
INISHOWEN
DONEGAL
FOYLE FAULT
NORTHERN IRELAND
Dal/c/p-h + Tertiary Igneous
VALLEY FAULT

suggested that further southwads the thrust may parallel the Leannan Valley Fault separating the Lewisian of Inistrahull Island, and other submarine Lewisian rocks from areas of Dalradian and Moine gneisses in western Ireland.

A large displacement along LGF and hence along the southern branch of GGF as suggested by Garson and Plant (1972) has been questioned by Westbrook and Borradaile (1979). The major magnetic anomaly corresponding to the Lewisian outcrop and the basement in the Islay region straddles LGF, which does not fit with a displacement of more than 6-9 kms (Westbrook and Borradaile 1979).

The geological map of the Malin Sea and the adjoining area as inferred by Evans et al. (1980) from geophysical and other studies shows the major branch of GGF passing NW of Colonsay (Fig. 2.17). One of the interesting features of this map is the southeasterly downthrow along LGF, which bounds a Permo-Triassic sedimentary basin to the southeast of the Rhinns of Islay. In the reconstruction proposed by Garson and Plant (1972), a graben structure lies between the northern and the southern branch of GGF in the mainland. This would necessitate a northwesterly downthrow on the southern branch of GGF and hence on LGF. The structure of the Malin Sea as proposed from the geophysical evidence (Evans et al. 1980, Westbrook and Borradaile 1979) is contrary to the suggestion of Garson and Plant (1972).

2.7.2. Fracture Pattern in the Rhinns of Islay and Colonsay

It is highly likely that a major transcurrent fault system like the Great Glen would have some imprint on the fracture pattern of the area it transects. With this point in mind, the aerial photos of the Rhinns of Islay and Colonsay were studied to compile fracture pattern maps as deduced from the photo-lineaments in the area (see maps I and II). The essential pattern is shown in the rose diagrams of Fig. 2.18. Both in western Islay and Colonsay the pattern is bimodal with a mode either in NE or NW direction. The swarm of basic dykes at present aligned with the Tertiary volcanic and intrusive centre of SE Mull, has been traced for many miles across the Scottish mainland. Being within 50-100 kms from Mull centre, it is likely that a system of NW-SE fractures related to the emplacement of the Tertiary dykes would be

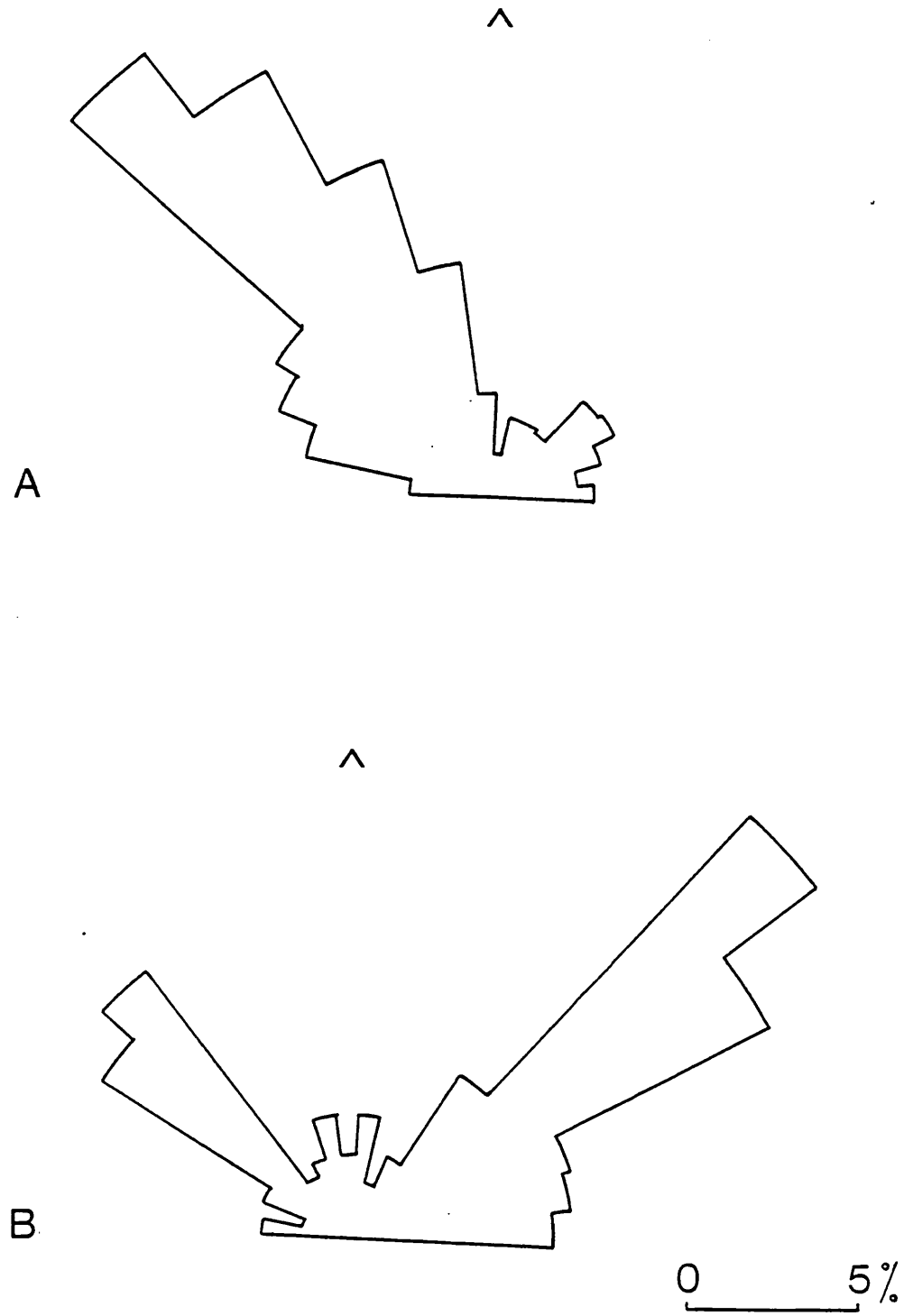


Figure 2.18. Rose-diagrams showing the azimuth of photointerpreted fractures in W. Islay (a) and Colonsay (b).

quite common in western Islay and Colonsay. Actual ground check in the area provides confirmation for the abundance of northwesterly dolerite dykes in the area. Thus the northwesterly mode in the fracture pattern can probably be excluded from further consideration. On the other hand, the northeasterly mode of photolinears probably reflect the mesoscopic fractures associated with major transcurrent faulting in the Malin Sea area. One interesting feature is the increase in abundance of northeasterly fractures in Colonsay as compared to western Islay. The pattern is more in accordance with the hypothesis that the major branch of GGF passes NW of Colonsay, and that the fault passing east of Colonsay and through the Loch Gruinart hollow (LGF) is a satellite structure.

2.7.3 The Moine Thrust and the Loch Skerrols thrust

In the NW Highlands the Moine Thrust Zone forms an important tectonic element separating the Lewisian foreland with its Torridonian and lower Palaeozoic cover from the highly deformed and reconstituted Moine rocks. The southernmost outcrop of the Moine Thrust is in Skye. However, its presence in the Sound of Iona has been suggested on the ground that while in Iona, the Torridonian Iona Group unconformably overlies the Lewisian, high grade Moine rocks occur to the SE of the Sound in the Ross of Mull. Although Kennedy (1946) and Garson and Plant (1972) differ in their reconstructions along GGF, both suggest that the logical southerly continuation of the Moine Thrust is the Loch Skerrols thrust in Islay (Figs. 2.15 and 2.16). However, there are two major difficulties in such correlation:

(a) Geophysical studies in the Malin Sea area have failed to detect any east dipping thrust that can be correlated with the southern continuation of the Moine Thrust (Brewer et al. 1983, Evans et al. 1980, Summers 1982).

(b) There is a basic difference in the tectonic setting of the Loch Skerrols thrust as contrasted with that of the Moine Thrust. In Islay the Dalradian is thrust over the Bowmore Group which is presumably Torridonian. Nowhere in NW Scotland is the Dalradian juxtaposed against the Torridonian along the Moine Thrust.

It appears that the position of the Moine Thrust south of the Sound of Iona is in doubt. The tectonics in the Islay region are rendered complex by the convergence of the N. Highland and the Grampian blocks. However, the present geographic position of Islay is further inward in the Caledonian belt as compared to the foreland setting of Iona or NW Scotland. It is not unlikely that although the Loch Skerrols thrust is related to Moine thrusting in a general way, the Loch Skerrols thrust represent a thrust higher than the Moine thrust itself, as suggested by Johnstone (1966). This question will be discussed again in the context of the structural history of western Islay.

2.7.4 Discussion

A dextral displacement along the Loch Gruinart fault (the southern branch of GGF in Garson and Plant 1972) seems to be incompatible with the results obtained from geophysical studies (Evans et al 1980, Westbrook and Borradile 1979) and photo-interpreted fracture pattern (this study). Moreover, in the reconstruction of Garson and Plant (1972) the position of Colonsay is placed to the NNW of Ardnave point in western Islay. Stratigraphic and sedimentological studies show that the Oronsay Greywacke and the sediments of S. Colonsay form an upward continuation of western Islay sediments; the dominant palaeocurrent direction for the relevant stratigraphic horizons is towards NNE (Stewart 1962).

The balance of evidence is in favour of a major sinistral displacement during the late Palaeozoic as proposed by Kennedy (1946) and Holgate (1969) with the major branch of GGF passing NW of Colonsay (Fig. 2.17). Kennedy's reconstruction places the Colonsay Group and the Lewisian of Islay more in line with the foreland rocks of northwest Scotland and Iona. This would explain the generally Torridonian nature of at least part of the Colonsay Group as well as the Bowmore Group. The Loch Gruinart fault is probably a splay structure related to GGF. If LGF is indeed a splay fault the maximum sinistral displacement along it is restricted to 25 kms, which is the distance of the north point of Colonsay from the point where LGF meets GGF south of Mull (see Fig. 2.17).

2.8 STRATIGRAPHIC CORRELATIONS

Recapitulation of relevant stratigraphic terms

The sediments of western Islay, Colonsay and Iona are generally regarded as Torridonian (Stewart 1962, I.G.S. maps of the British Isles 1966 and 1969). However, a possibility that the Colonsay Group could be Dalradian has been suggested later (Litherland 1970, Stewart and Hackman 1973, Stewart 1975). Although the name Torridonian was introduced (Geike 1982, W.H. Hudlestone in discussion of Peach and Horne 1982, Peach et al. 1907) as a time rock unit equivalent to the Torridonian Sandstone of Nicol (1866), recent works show that the Moine and the Torridonian are broadly equivalent in time (Johnstone 1975). The name 'Moine' has a regional connotation and is generally used for a succession of metasedimentary rocks which, lying to the east or southeast of the Moine Thrust, unconformably overlies the Lewisian (Johnstone 1975).

In their original type area around upper Loch Torridon, the Torridonian represents a fluviatile facies, and in parts of NW Scotland Cambrian Quartzite overlies the Torridonian. Thus the Torridonian represents a late Precambrian group of rocks the earliest of which dates back to at least 1000 m.y. (Moorbath 1969). The term Dalradian is applied to a lithologically diverse supergroup consisting of metasedimentary and metaigneous rocks of late Precambrian to Cambrian age which are younger than, and on a regional scale overlie the Moine rocks.

In western Islay, the sediments lie on top of the Lewisian Gneiss. The sequence begins with a fluviodeltaic facies. The Lewisian-sediment contact bears evidence of an original unconformity. The Oronsay Greywacke and the sediments of southern Colonsay form an upward continuation of the western Islay sediments. 'Torridonian' looking sediments have been reported from the sea-bed separating the two islands (Barber in Evans et al. 1980). The whole succession is termed the Colonsay Group (Stewart 1975).

Is the Colonsay Group Dalradian?

The sequence from the Kilchoman Phyllite to the top of the Oronsay Greywacke represents a turbidite facies which was deposited under sea

(Stewart 1962). This is in contrast to the general nature of the Torridonian sediments of NW Scotland. The latter brings into picture the possibility of correlating part of the Colonsay Group with the Dalradian. However, there are several difficulties as enumerated below:

(a) If one assumes that the Colonsay Limestone is a lithostratigraphic equivalent of the Ballachulish Limestone (Litherland 1970, Stewart 1975), the rest of the Colonsay Group underlying the Colonsay Limestone (a thickness of at least 2.5-3.0 kms) remains unaccounted for in any Dalradian column so far reported.

(b) Possible Dalradian equivalent for the Colonsay Group may be searched for higher up in the Dalradian succession. But all such correlation would be based on the assumption that the Great Glen Fault passes east of Colonsay. Geophysical evidence is in favour of the major branch of the Great Glen Fault to pass NW of Colonsay; displacement along the Loch Gruinart fault is much restricted (Evans et al. 1980, Westbrook and Borradaile 1979). Similar conclusion is also favoured by a study of the fracture pattern in the rhinns of Islay and Colonsay area.

(c) In N. Colonsay the Leac Bhuidhe sediments unconformably overlie the Lewisian, and the sequence begins with highly epidotic grit with pebble beds.

(d) The strain measurements in the Kilchiaran Bay area, western Islay does not commensurate with a large displacement necessary to bring Upper Dalradian rocks on top of the Lewisian.

On the other hand, the bulk of the Colonsay Group is derived from a Lewisian source land. Unconformable relationships between the Lewisian and the Colonsay Group are at least locally preserved. Thus the balance of evidence is in favour of regarding the Colonsay Group as sub-Dalradian possible Torridonian. And as Stewart (1962) suggested Torridonian probably represent more than one sedimentary facies.

The Bowmore Sandstone

The Bowmore Sandstone consists of the Laggan Group and the Blackrock Group. The latter is virtually undeformed and

unmetamorphosed. This is a well sorted arkosic sandstone and at least in part derived from a Lewisian like source land. There is a similarity with the Applecross Formation in the Kishorn Nappe (Stewart 1975).

The Iona Group

Although it is difficult to correlate with any particular Torridonian horizon in NW Scotland, the general fluviatile nature, unconformable relation with the Lewisian and the basal breccia-conglomerate suggest that the Iona Group belongs to the Torridonian. The stratigraphic succession in W. Argyll and their possible correlation with that in NW Scotland is summarized in Table 2.8.

Table 2.8 Correlation chart for Late Prelcambrian - Lower Palaeozoic in W. Argyll. Comparable horizons of NW Scotland are also shown

IONA	COLONSAY	ISLAY Rhinns	ISLAY E. Islay	NW SCOTLAND Foreland	NW SCOTLAND Shelf
Felsic porphyrites & vogesites	Felsic porphyrites & vogesites	Felsic porphyrites & vogesites			MINNETE SUITE
RoM+ Granite (420 ma)					
	Appinites	Appinites			MICRODIORITE SUITE (450 ma)
	Lamprophyres	Lamprophyres			
					AMPHIBOLITE SUITE (560 ma)
			DALRADIAN		
			Bowmore Sandstone	TORRIDON GR.	MOINE
	Sediments of Oronsay and S. Colonsay				
	--- overlap ---				
Iona Group	Leac Bhuidhe sediments	Rhinns of Islay sediments		SLEAT GROUP (995± 24 ma)	
LEWISIAN	LEWISIAN	LEWISIAN		L E W I S I A N	

+ Ross of Mull Granite

CHAPTER 3

STRUCTURES AT WESTERN ISLAY

3.1 INTRODUCTION

The present chapter deals with the deformation features and structural history of the Lewisian and the overlying Colonsay Group in western Islay. Although a record of Pre-Caledonian deformation remains within the Lewisian, the present study puts emphasis on Caledonian features in the basement which generally appear as ductile to brittle deformation zones (shear zones, sensu lato) and late folding and crenulation of the shear zone foliation. The nature of the contact between the Torridonian and the Lewisian has already been described in Chapter 2. Evidence for an unconformable relationship between the two groups is still preserved along the contact; however, during Caledonian movements the contact zone acted as a strain sink. The deformation features along the contact zone are described to elucidate this point.

The Colonsay Group has suffered multiple episodes of folding and cleavage development under low greenschist facies metamorphism. Different phases of folding were often separated by emplacement of minor intrusions. Detailed description of the minor intrusions is reserved for Chapter 7; however, where it is necessary to unravel the deformation history, the geometric and temporal relationship between folds and different suites of minor intrusions are briefly dealt with.

The metasediments of western Islay shows at least three phases of folding deformation. The scale at which different generations of folds are represented within the island varies. The outcrop of the lithologic boundaries is largely controlled by the second phase of folds (Fig. 3.1). These folds are overturned to the west. Relationship of these folds to possible large scale structures in western Argyllshire will be discussed in Chapter 8. In this chapter, results of structural analysis of observations on minor structures exposed along coastal strips are presented.

3.2 PRE-CALEDONIAN DEFORMATION

Pre-Caledonian deformation in Islay is restricted to the Lewisian outcrop in the southern half of the Rhinns. As has been described in Chapter 2, five major lithological components can be recognised within the Lewisian: amphibolitic gneiss, quartzo-feldspathic gneiss, coarse porphyritic diorites, hornblendites and pink pegmatites.

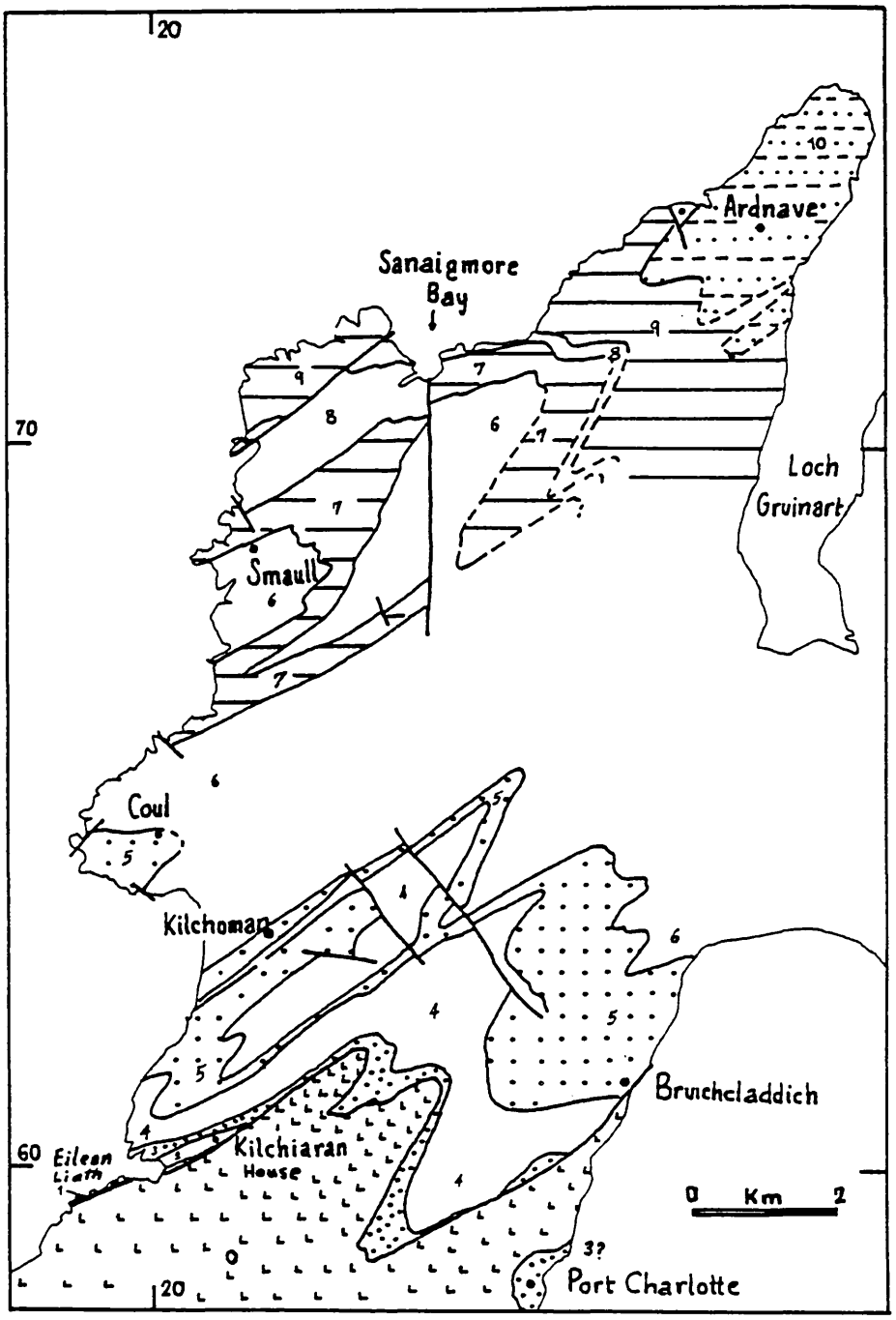


Figure 3.1. General geologic map of W. Islay, from Stewart and Hackman (1973). L = Lewisian, 1 = Eilean Liath Grit, 2 = Kilchiaran phyllite, 3 = Rubha Gaidhealach Grit, 4 = Rubha na-h-Airde Moire Phyllite, 5 = Crosprig Grit, 6 = Kilchoman Phyllite, 7 = Smaull Greywacke, 8 = Sanaigmore Phyllite, 9 = Sanaigmore Greywacke, 10 = Ardnave Formation.

The first two of these components show a well developed gneissic foliation - a penetrative L-S fabric - with a NE-SW elongation lineation. The foliation dips steeply at 60-90 degrees either to the SE or to the NW (Fig. 3.2). Under the microscope, the rocks show porphyroclasts of feldspar with pull-apart structure filled by quartz and/or calcite grains; the matrix consists of trails of biotite and chlorite replacing hornblende; quartz rich areas show ribbon grains separated by minor recrystallised grains along the boundaries of the ribbons.

The above gneissic foliation is often thrown into tight asymmetric folds. Some of the later components within the Lewisian, i.e. the porphyritic diorite bands and the pegmatites, cut across the gneissic foliation. Then the L-S fabric and tight asymmetric folds on the foliation are essentially pre-Caledonian features, probably representing one or the other Lewisian deformation events.

3.3 CALEDONIAN DEFORMATION WITHIN THE LEWISIAN OUTCROP

During the Caledonian deformation the Lewisian in W. Islay acted as a basement to the Colonsay Group. While the Colonsay Group rocks are thrown into folds and register the development of axial planar cleavages, the Lewisian responds by the formation of ductile deformation zones, a feature typical of crystalline basement rocks in orogenic belts, such as that reported from the Precambrian Blue Ridge basement rocks of Northern Virginia within the Appalachian Orogenic belt (Mitra 1978). In W. Islay, the ductile deformation zones cut across all the lithologic components within the Lewisian and also affect probable early Caledonian minor intrusions. A description of these zones follows.

3.3.1 Ductile Deformation Zones (DDZ)

In the shore section between Cladville and Claddich (National grid ref. 165545 - 160532), the gneisses show many ductile shear zones (0.25m - 1.0m wide) with a steep ESE dip. These shear zones develop in an anastomosing fashion (Fig. 3.3a). The ductile nature of the deformation zones is indicated by a gradual passage of the gneissic foliation at the outer edge of the zone to a mylonitic foliation in the centre. Most remarkable is the deformation of the porphyritic diorite bands (component 'c' within the Lewisian, see Chapter 2); a gradual

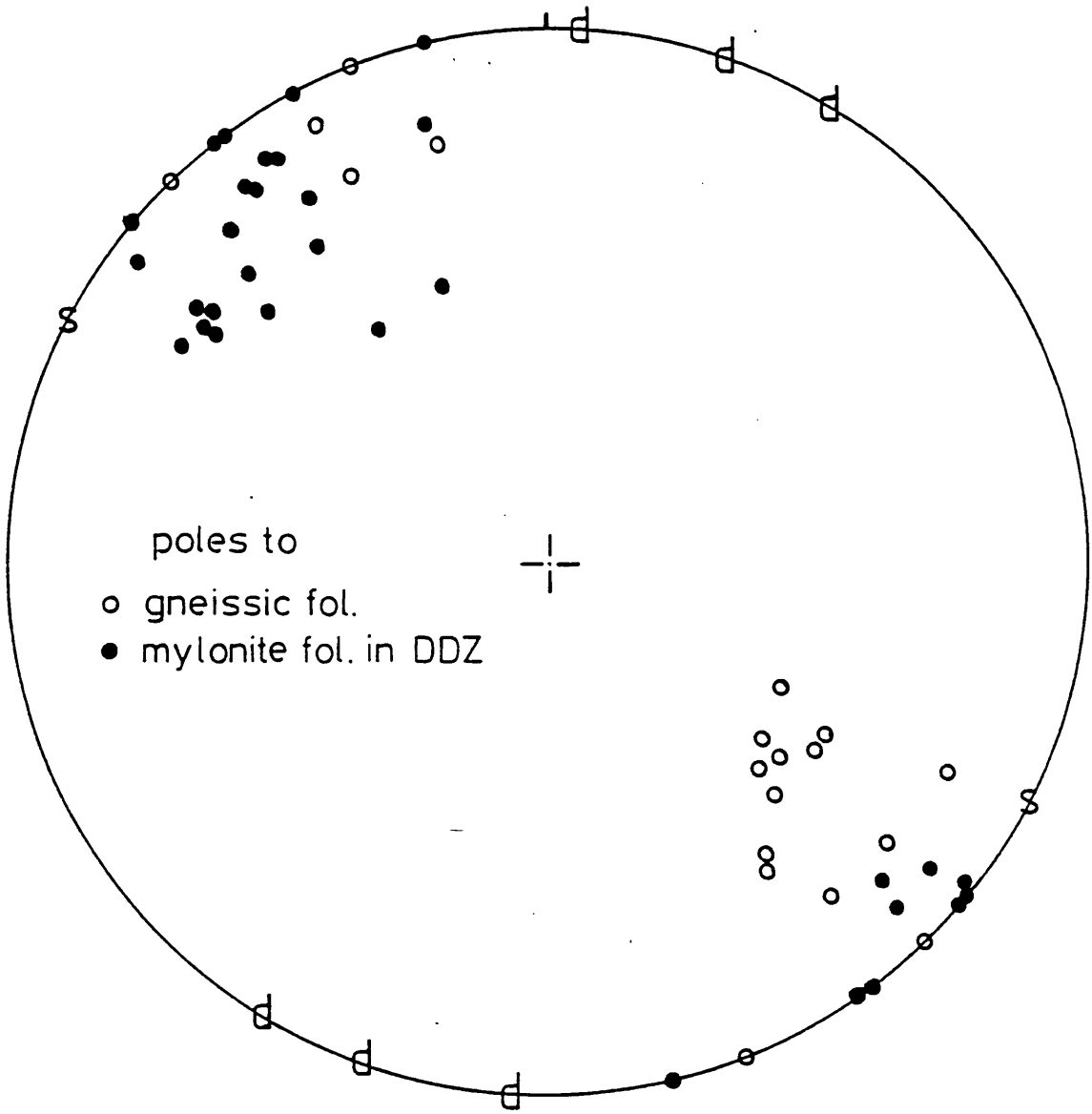


Figure 3.2. Equal area plot showing orientations of gneissic foliation, mylonite foliation in DDZ's and azimuth of brittle shear zones with mineral veins (d = dextral, s = sinistral) from Islay Lewisian.

increase in the aspect ratio of deformed phenocrysts in sections perpendicular to the foliation and parallel to the lineation is noticeable; well outside the shear zone the aspect ratio is at most 1:3, close to the shear zone the ratio is 1:6 to 1:10, and in the centre of the shear zone the phenocrysts are stretched to such an extent that they are barely recognisable as individuals (Fig. 3.3b). In thin sections, the feldspars are highly granulated at the centre of the zone and there is a gradual decrease in the overall grain size from the border to the centre of the zone; the proportion of phyllosilicates (mostly chlorite + muscovite) in the matrix also increases towards the centre. Any quartz that had been present in the parent gneiss has been thoroughly recrystallised.

The overall shape fabric within the mylonitised Lewisian in the DDZ's is L-S type with a strong linear component. The stretching lineation is subhorizontal with a NE-SW trend. This is reflected in the high aspect ratio of sausseritised feldspar grains on flat outcrops of steep DDZ's.

3.3.2 Relative Age of DDZ's

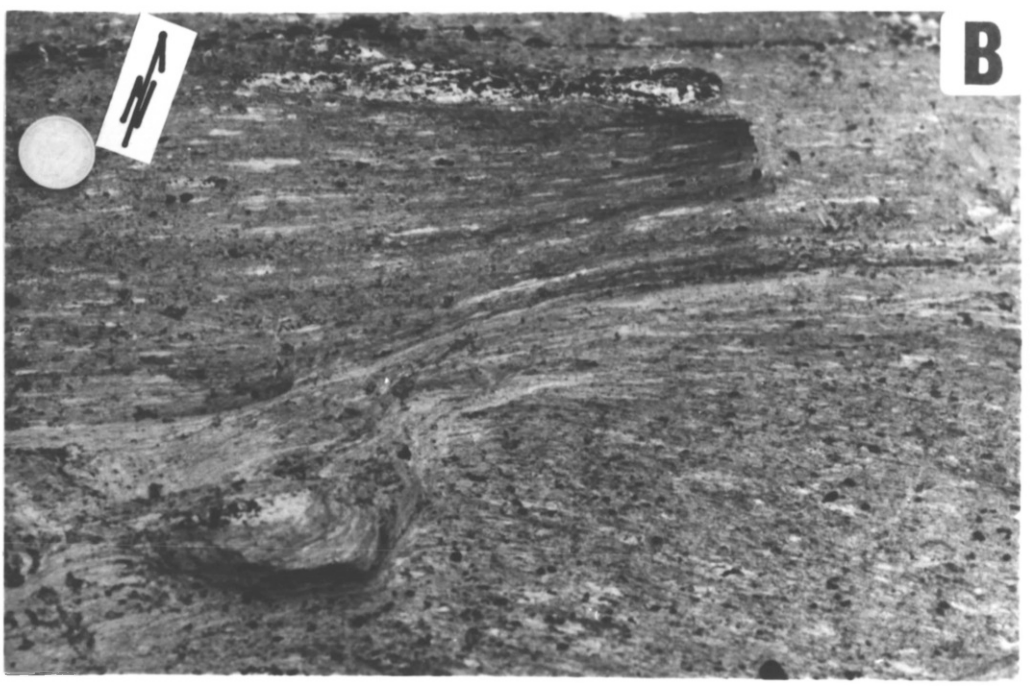
Since lamprophyre dykes with oblique foliation (group C minor intrusions, see Chapter 7 for the details) transgress the mylonite foliation in the DDZ's, it is certain that the shear zones formed earlier than the emplacement of these dykes. However, a group of epidioritic dykes is also deformed in the DDZ's. Within the zones, the dyke rocks are transformed into felts of biotite and chlorite with occasional granules of feldspar at varying stages of alteration; metallic sulfides and oxides (pyrite and hematite are the commonest) are common in these dyke rocks; in the centre of the DDZ's even the pyrite and hematite grains are streaked out parallel to the mylonite foliation. These intrusive sheets which are affected by DDZ's probably represent Caledonian minor intrusions (see Chapter 7). It appears then that the DDZ's are essentially Caledonian features; they reflect a mode of deformation that is quite common in crystalline basement complexes (Mitra 1978, Ramsay and Graham 1970). The stretching lination associated with the DDZ's is comparable with a NE-SW elongation lineation along the Lewisian-Colonsay Group contact and less conspicuously in other parts of W. Islay which as discussed in Section

Figure 3.3 Morphology of ductile deformation zones (DDZ) in Islay Lewisian, Cladville.

(a) Anastomosing nature of DDZ's.

(b) Deformation of coarse porphyritic diorites in a DDZ. Note the feldspar phenocrysts are highly stretched in the centre of the zone.


A


B

3.4.4 probably represent the earliest Caledonian deformation feature in W. Islay.

3.3.3 Late Structures

Late structures within the Lewisian in W. Islay include shear bands or extension crenulation cleavages cutting across mylonite foliation, boudinage in microdiorite dykes and in relatively coarse pegmatite slivers between DDZ's and conjugate brittle shears in the microdiorite dykes. The shear bands displacing the mylonite foliation (Fig. 3.4) probably represent later stages in the progressive deformation history of development of the DDZ's. Initiation and propagation of the DDZ's reflect local strain softening (Cobbold 1977, Mitra 1978, White et al. 1980). Once the DDZ's are well established, the induced anisotropy in the rock has a strong influence on subsequent deformation; shear bands break up this anisotropy and may at even larger strains bring about the reestablishment of more homogeneous deformation (White et al. 1980).

The microdiorite dykes were emplaced after the development of the DDZ's. Isolated dykes with NE trend in the Cladville-Claddich areas are boudinaged with an aspect ratio of 1:5 in plan (Fig. 3.5C). Where a series of subparallel dykes are separated by Lewisian gneiss with DDZ's, the dykes are traversed by a set of ENE brittle fractures (Fig. 3.5b). A complementary set of fractures with NNE shows a sinistral sense of displacement locally affecting both the gneiss and the dykes (Fig. 3.5a). The orientations of these brittle shears from the Claddich area are shown in Fig. 3.5e. Their possible mechanical and kinematic evolution is discussed below.

The early developed ductile shear zones locally extend for considerable distance (up to 10 meters) along the strike; sometimes a number of them occur in a subparallel or anastomosing fashion. This imparts a local anisotropy to the deformed crystalline basement rocks. Moreover, the presence of subparallel microdiorite dykes which cut across the gneissic banding and the foliation in DDZ's and extend for tens of meters along the strike, offers a mechanical situation analogous to a model with alternate layers of more competent and less competent material. Although at some localities a slight obliquity is seen

Figure 3.4 Shear bands displacing mylonite foliation in Lewisian, Port Charlotte, W. Islay. Photomontage prepared from micrographs taken from a thin section cut perpendicular to mylonite foliation, parallel to stretching lineation.

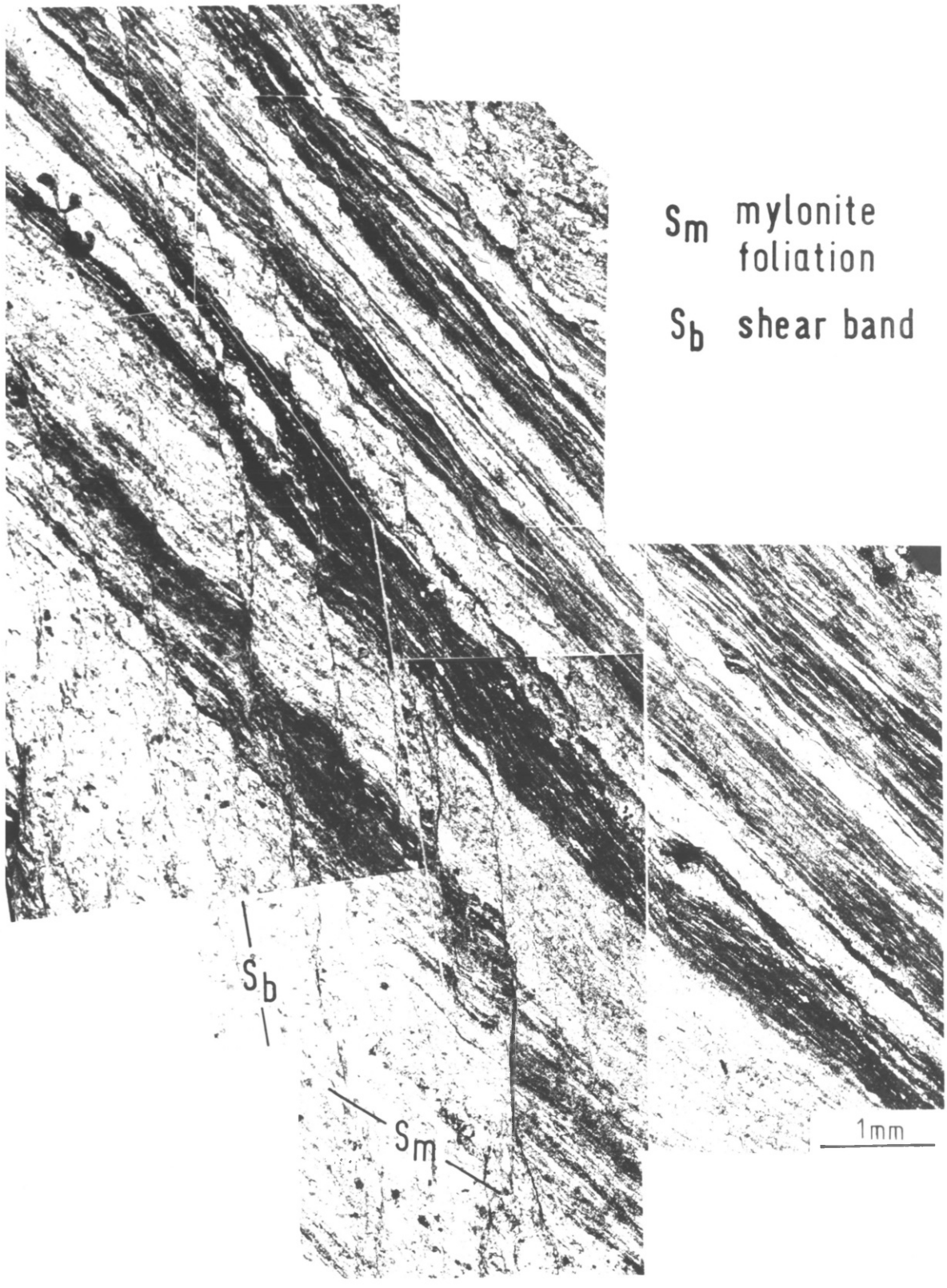

S_m mylonite foliation
S_b shear band
S_b
S_m
1mm

Figure 3.5. Late Caledonian structures in Islay Lewisian.

(a) A N-S sinistral shear zone displacing a microdiorite dyke.

(b) Boudinaged microdiorite dyke.

(c) A band of pegmatite separating DDZ's has been boudinaged during late stage deformation.

(d) A set of ESE brittle fractures in microdiorite dykes.

(e) Equal area plot showing the orientation of principal stresses (large solid circles numbered 1, 2, 3 corresponding to σ_1, σ_2, σ_3 respectively; $\sigma_1 > \sigma_2 > \sigma_3$) as deduced from the orientation of conjugate brittle shears (great circles). Poles to the plane of boudinaged microdiorite dykes are also shown (open circles); Notice concentration of these poles around σ_3, the maximum compressive stress.

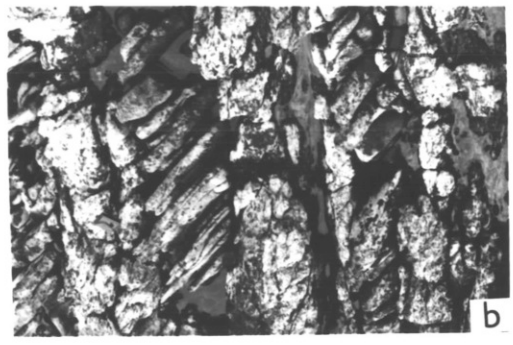
(f) A series of schematic drawings to illustrate the evolution of DDZ's and late stage structures shown in (a)-(d). While early deformation is ductile the late deformation is dominantly brittle.

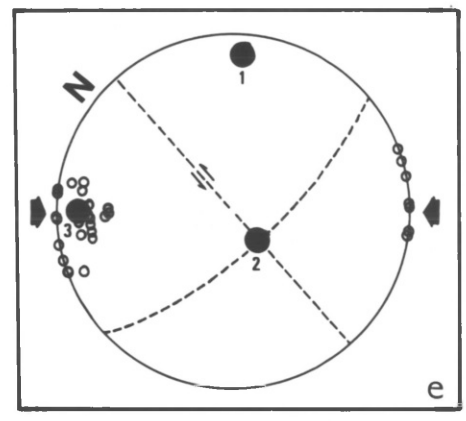
(a)-(d) field photographs (plan view) taken from Cladville-Claddich area. Geographic North on each is same as in (e).

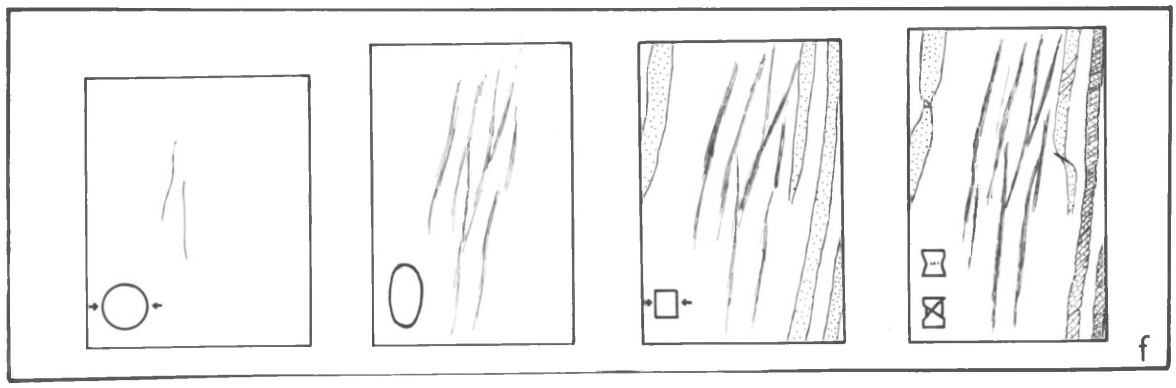












3.5

between the wall of the dyke and the gneissic foliation and/or mylonite foliation in the centre of the DDZ's, all these planar structures are steep with an average NE-SW strike (Fig. 3.2). The effect of a continued Caledonian compression from southeast can be explained in terms of the theories and experimental results put forward by Cobbold et al. (1971), (see also Cosgrove 1976). Since the compression direction is at a high angle to the direction of anisotropy (plane of mylonite foliation or dyke walls) banded structures in the form of extension crenulation cleavage, shear bands or brittle to semibrittle shear fractures develop at an acute angle to the compression direction. A sinistral displacement along N-S shear zones is compatible with overall extension subparallel to the strike of dykes and DDZ's.

The response of isolated dykes of microdiorite within the deformed gneissic rock or of bands of pegmatite within a set of subparallel DDZ's is comparable to that of a rigid layer in an 'infinite' ductile surrounding. The dyke or pegmatite band yields through the production of boudinage structure with boudin long axis (in plan) normal to the compression direction.

The overall deformation of the Lewisian in the Rhinns is a shortening in a northwesterly direction. The initial response to Caledonian deformation is manifested by the initiation and development of DDZ's.

Following the development of DDZ's the microdiorite dykes were emplaced. The response to late stage shortening was controlled by the induced anisotropy in the basement rocks due to DDZ's and subparallel dykes within the deformed gneiss (probably less competent than the dyke material under an ambient temperature of low greenschist facies). The sequence of development of these structures is shown diagrammatically in series of sketches in Fig. 3.5f.

3.4 DEFORMATION AT THE LEWISIAN-COLONSAY GROUP CONTACT

The relationship between the Lewisian and the overlying Colonsay Group has been discussed from a stratigraphic point of view in Chapter 2. It has been shown that the Colonsay Group rests on an unconformity. However, the contact zone acted as a strain sink during Caledonian

deformation; deformation features in the zone are described and discussed in this section. The actual contact is exposed in three areas in W. Islay, viz., SW of Kilchiaran Bay, the Dun Medeir area and the Port Charlotte area. Structures from these three areas are described below.

3.4.1 Kilchiaran Bay Area

3.4.1.1 Contact Zone Rocks and Minor Structures

Between Kilchiaran Bay and the small island of Eilean Liath off the coast SW of Kilchiaran Bay, and further southwest for about 100 meters, the contact between the Lewisian and the Eilean Liath Grit (basal unit of the Colonsay Group in this area) trends WSW-ENE. A zone of well foliated sheared rocks, never exceeding a few meters in thickness, straddles the contact. On a N-S traverse near Eilean Liath the succession is as follows:

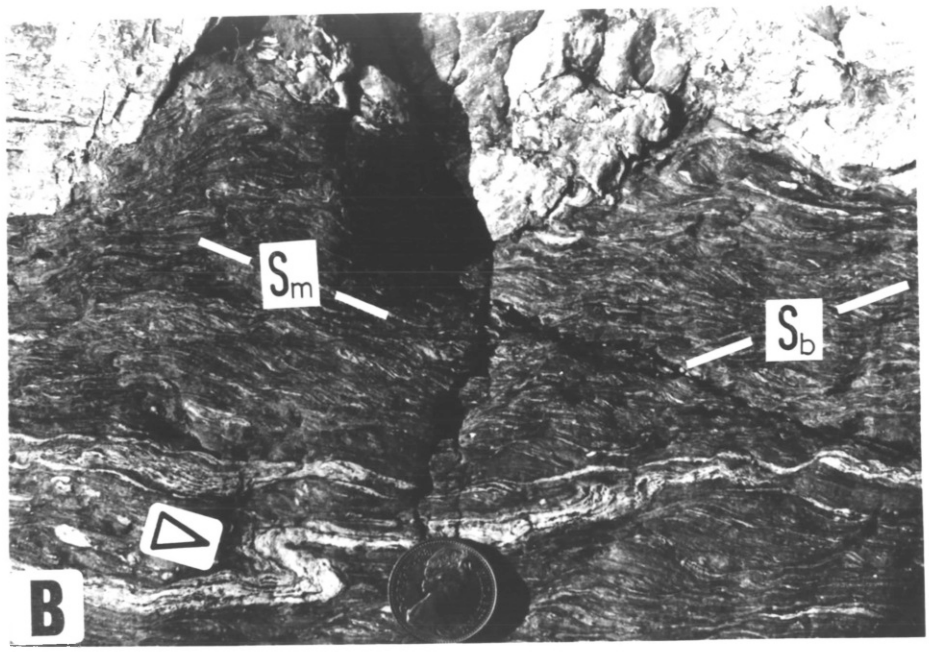
4. Coarse, thick bedded grits
3. Thinly bedded grits (5 metres)
2. Highly foliated rocks derived from both Colonsay Group and Lewisian rocks (1.5 metres)
1. Lewisian Gneiss

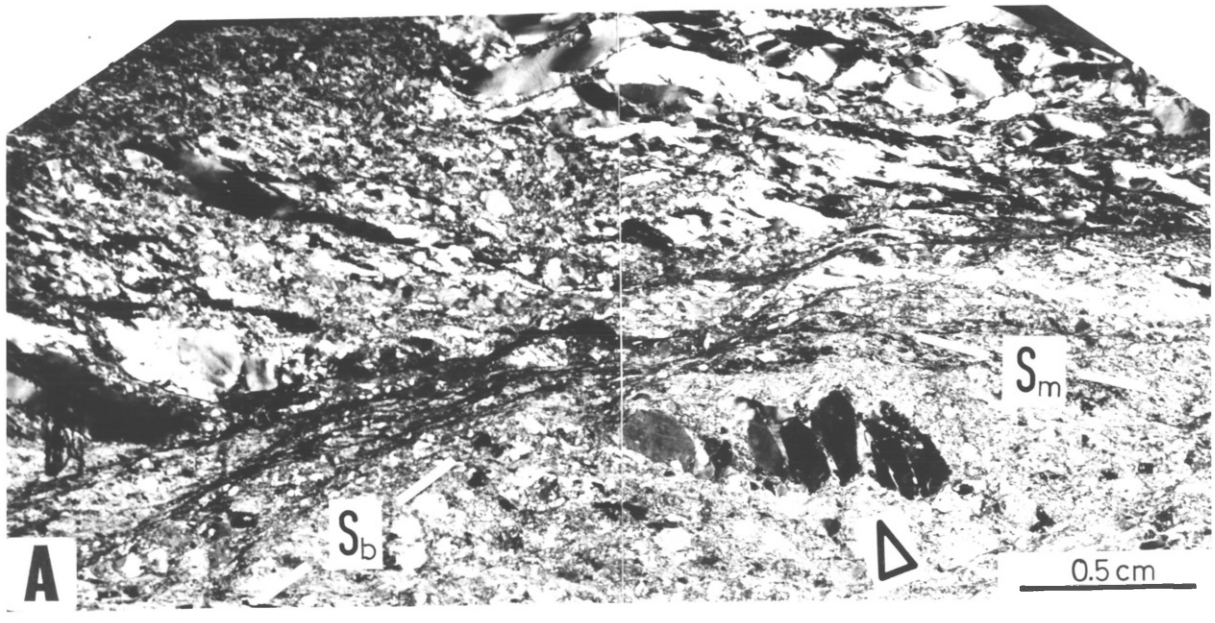
While sedimentary structures are still preserved in unit 4 above, rocks in unit 2 have all the appearance of a mylonite with a penetrative foliation trending ENE-WSW and dipping at 80 degrees NNW. The clast elongation lineation is subhorizontal with ENE-WSW trend. In thin section, the quartz grains are deformed (into ribbon grains with dynamic recrystallisation along boundaries of highly elongate subgrains or deformation bands (Fig. 3.6a). Feldspar grains are pulled apart and broken down into smaller pieces. The alignment of ribbon grains of quartz and trails of phyllosilicates define a penetrative foliation. At an acute angle to the foliation there are shear bands (Fig. 3.6b). Applying the criterion of intersection between shear bands and mylonite foliation (White et al. 1980), it appears the sense of movement is sinistral. Intrafolial folds (? sheath folds) in the shear zone have a sense of asymmetry consistent with this movement sense (Fig. 3.6b).

Figure 3.6. Shearing along Lewisian-Eilean Liath Grit contact, southwest of Kilchiaran Bay.

(a) Photomicrograph showing quartz-ribbon mylonite, Eilean Liath Grit, sp. 577A, within a few centimetres from the Lewisian contact. Note stretching of a large feldspar clast (arrow); pull aparts are filled with quartz and calcite fibres whose lengths are parallel to the long axis of ribbon quartz.

(b) Mylonite foliation and shear bands in outcrop, Eilean Liath Grit. Note the asymmetry of the intrafolial fold (arrow), which is consistent with a sinistral sense of movement deduced from the intersection of shear bands (S_b) and mylonite foliation (S_m).





3.6

Sheared Lewisian rocks, on the other hand, show extensive recrystallisation of big feldspar grains into smaller grains, and all ferromagnesian minerals have retrograded to epidote + chlorite. The shear bands offset the mylonite foliation. On the Lewisian side of the contact zone, there are pockets which show cataclastic deformation; veins and bands of cataclasite can be seen to cut across patches of recrystallised feldspar.

3.4.1.2 Strain Profile

The base of the Eilean Liath Grit is a zone of strain gradient. An increase in strain from the shore towards the contact with the Lewisian is recorded by an increase in the intensity of the L-S fabric and a reduction in the average grain size of the grit (although local pebbly patches can still be seen within a meter of the contact). Qualitatively, this increase in strain intensity can be illustrated by variations in the relative abundance of various deformation textures in quartz and feldspar clasts in specimens collected at different distances from the contact (Table 3.1). Specimens 351, 356 and 356a and 57 7 are from the Eilean Liath Grit at distances of about 10 meters, 1 meter, and a few centimeters from the contact with the Lewisian; specimen 490 is from Crosprig Grit exposed at about 1 km north of the Kilchiaran Bay.

Quantitative strain measurements were carried out on three of the set of specimens referred to in the last paragraph. Figure 3.7 shows the R_f-ϕ plots for sections cut parallel to the mineral elongation lineation and perpendicular to the foliation (XZ section) Separate plots were obtained for quartz and feldspar clasts. The principal 2D strain ratios were computed using a method described by Robin (1977) for randomly oriented markers of any shape which can be adapted for elliptical markers (see Appendix 4B for details). The orientation of the maximum principal elongation is close to the visible lineation in the specimens. As shown in Table 3.2, there is an increase in the λ_1/λ_3 ratio towards the contact so far as determinations from quartz clasts are concerned. The feldspar clasts register a much lower strain compared to quartz clasts. This illustrates the heterogeneity in the deformation at grain scale. The shape of the finite strain ellipsoid in the contact zone rocks appear to be in the constriction field. The

Table 3.1 Deformation textures in Eilean Liath Grit as compared to Crosprig Grit, Rhinns of Islay. Specimen 356a comes from a few cms from the Lewisian boundary.

	Deformation feature	Crosprig Grit Sp. No. 490	Eilean Liath Grit 351	356	356a	577
QUARTZ	Undulose extinction	++	++	++	++	++
	Deformation lamella	+	+	+	+	+++
	Ribbon grains	+	++	++	+++	+++
	Dynamic recrystallisation		++	+	+++	++
FELDSPAR	Pull aparts	++	+			++
	Intracrystalline slip *				+	++
	Recrystallisation				+	+

\+ Present ++ Common +++ Abundant
* As indicated by displacement of twin lamellae

Table 3.2 Strain values from near the Lewisian-sediment contact around the Kilchiaran Bay area, Rhinns of Islay. Note an increase in strain towards the contact as determined from shape of deformed quartz clasts.

Specimen no.	Stratigraphic Unit	Distance from the Lewisian contact (cms)	Strain ratio (λ_1/λ_3) Feldspar	Quartz
356	Eilean Liath Grit	1	2.23	11.63
351	Eilean Liath Grit	10	2.48	8.58
490	Crosprig Grit	1000	-	7.90

maximum finite strain, X, parallels the mineral elongation lineation and the microscopic foliation is close to the XY plane of the ellipsoid.

3.4.1.3 Microfabric

Thin sections prepared from samples collected from the contact zone were studied for details of the microfabric. Sheared basal pebbly rocks or grits (Eilean Liath Grit) have all the appearance of a proto-mylonite (Sibson 1977). Quartz rich areas show ribbon grains with grain boundary recrystallisation. Wilson (1975) described similar quartz ribbon mylonites from the Mt. Isa region, Australia. Ribbon grains show undulose extinction, deformation lamellae, and recrystallisation at grain boundaries or deformation band boundaries. While quartz deforms by crystal plastic mechanism, the behaviour of feldspar is brittle. Pull aparts in feldspar are common with infillings of carbonate and quartz. The direction of fibre growth of carbonates is within 5-10 degrees of the long axis of the ribbon grains. Some plagioclase grains show intragranular slip on planes at a high angle to the albite twin lamellae. The mylonite foliation, particularly in the phyllosilicate rich areas, is interacted by a set of shear bands at angles of about 37 degrees.

Quartz C-axis orientations were measured for the ribbon grains in a relatively quartz rich area within a sample from Eilean Liath Grit. The quintessence of the pattern is a point-maximum which is at 70-80 degrees to the foliation and at 80-90 degrees to the direction of maximum elongation or extension direction. There is a spread of points roughly enclosed by a small circle with an opening angle of 45-55 degrees, around the normal to foliation (Fig. 3.9). Wilson (1975) described similar quartz C-axis fabric from Mount Isa quartz ribbon mylonites, but with a smaller opening angle for the small circle. The fabric pattern could be explained in terms of a dominant slip on Basal <a> with some contributions from other slip systems such as the steep bipyramid.

The C-axis orientation of recrystallised grains of quartz at the boundary of ribbon grains is shown in Fig. 3.8b. The intensity of preferred orientation is much weaker than that of the ribbon grains. A weak maximum (2-3 x uniform) lies on a plane parallel to elongation

Figure 3.7. R_f-Ø plots for 2-dimensional strains (XZ section) at different distances from the Lewisian contact, specimens from Crosprig Grit and Eilean Liath Grit. Two-dimensional strain ratio obtained by two different methods are given below.

Specimen		Strain ratio (X/Z) 'Robin'	'Dunnet'	Loci of fixed R_i	No of markers
Feldspar	351	1.575	1.650	1.5,2.0,2.5,3.2	108
	356	1.490	1.600	1.5,1.9,2.6,3.5	142
Quartz	490	2.810	2.850	1.6,2.2,2.8,3.3	91
	351	2.927	2.950	1.6,2.2,2.9,3.3	81
	356	3.410	3.400	1.7,2.5,3.1	83

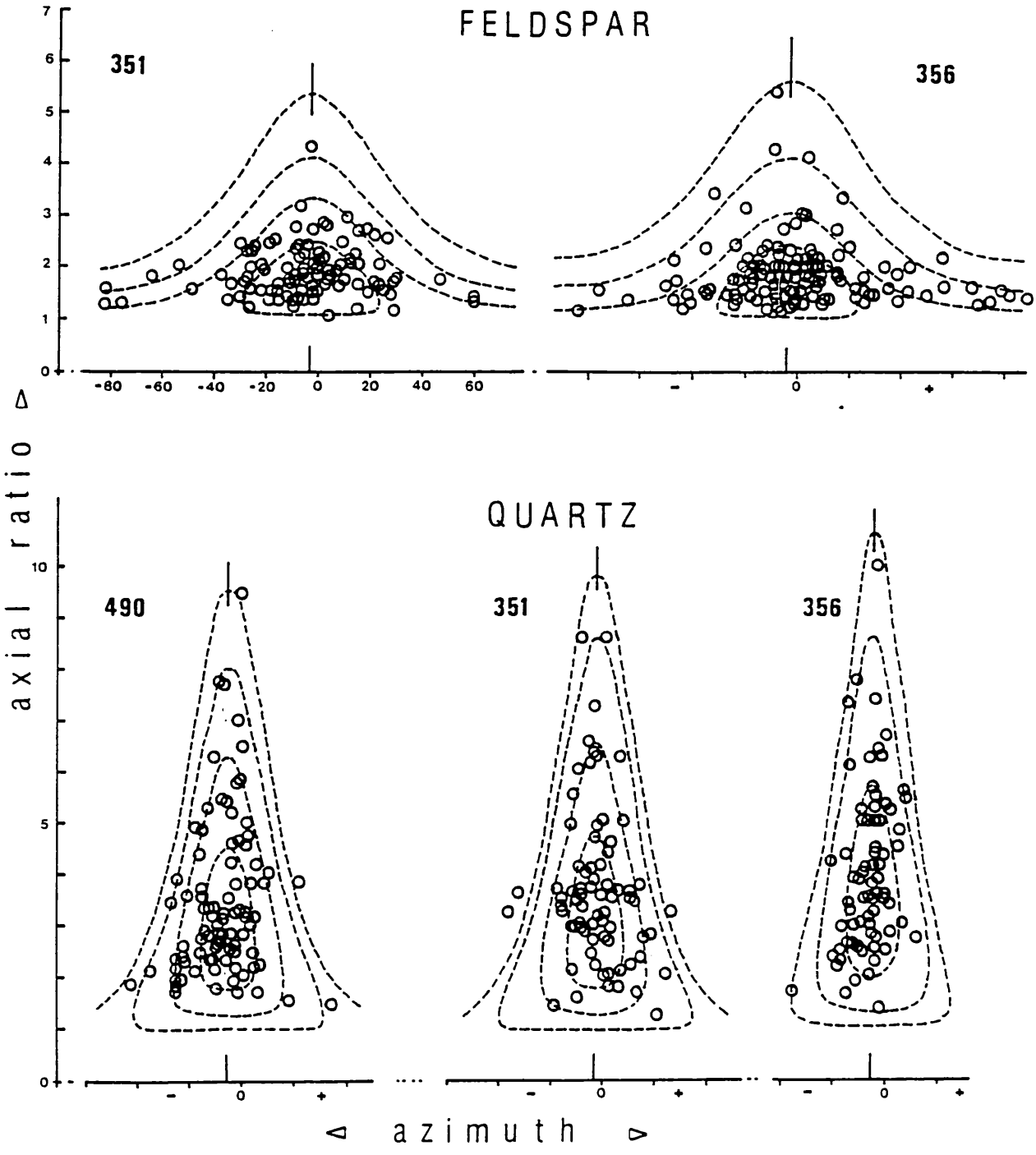

FELDSPAR
351
356
-60 -60 -40 -20 0 20 40 60
- 0 +
QUARTZ
490
351
356
axial ratio
azimuth

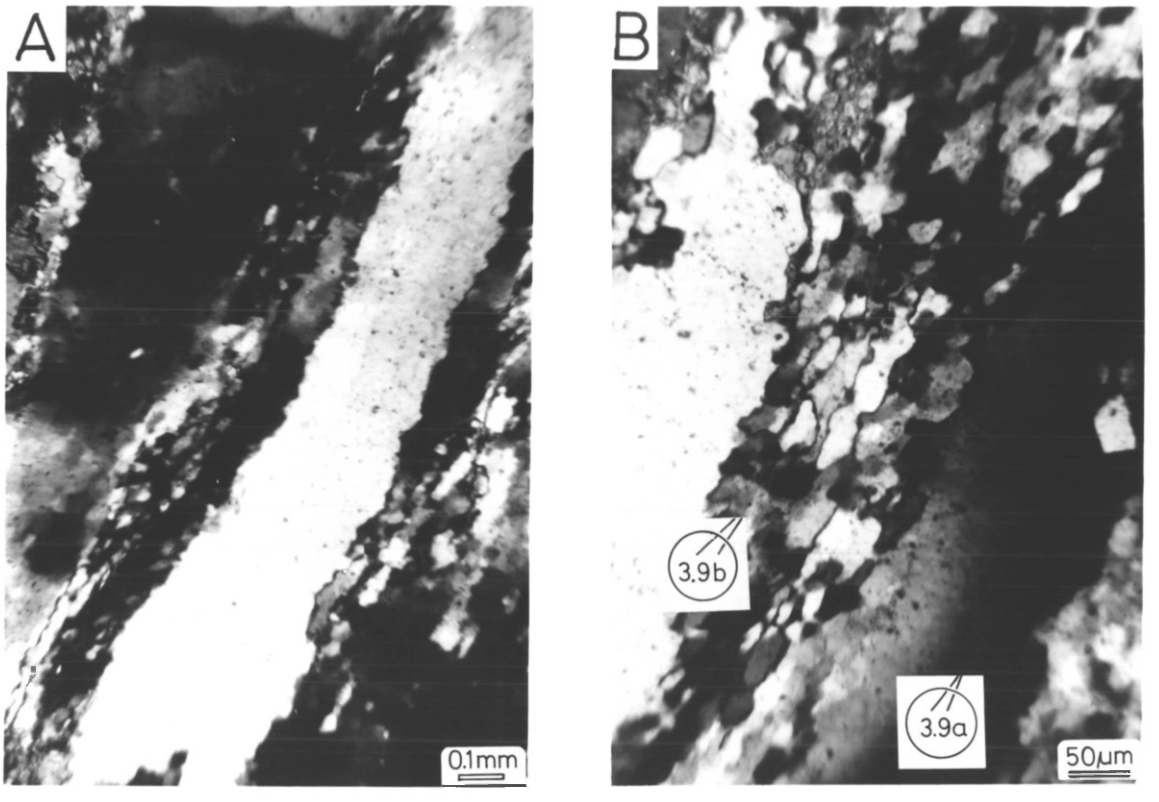
Figure 3.8. Optical micrographs showing details of ribbon grains (a) and dynamic recrystallisation along grain boundaries (b). Note elongation of some recrystallised grains.

Figure 3.9. Quartz c-axis fabric in quartz ribbon mylonites, SP577A, Eilean Liath Grit, southwest of Kilchiaran Bay.

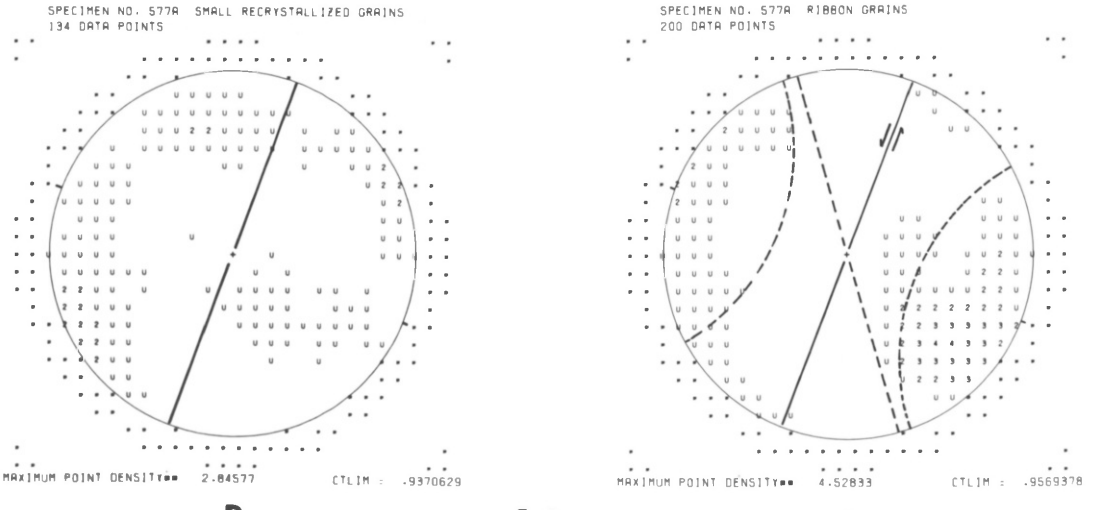
(a) Ribbon grains, on section cut parallel to stretching lineation and perpendicular to foliation (for microstructures see Fig. 3.8). The two great circles through the centre represent mylonite foliation (solid) and the shear band foliation (dashed). For detailed description of fabric see text.

(b) Recrystallised small grains at the boundary of ribbon grains. For details see text. In both (a) and (b) point-densities are in multiples of expectation (E) for uniform distribution, those below 1 x E are suppressed. Symbols mean:

print symbol	U	2	3	4	5	6	7	8	9	A	B	C	H
point-density x uniform	1-2-	3-	4 -	5 -	6-	7-	8-	9 -	10 -	11 -	12	12	above 12


A
0.1mm
B
3.9b
3.9a
50μm

3.8


SPECIMEN NO. 577A SMALL RECRYSTALLIZED GRAINS
134 DATA POINTS
MAXIMUM POINT DENSITY= 2.84577
CTLIM : .9370629
SPECIMEN NO. 577A RIBBON GRAINS
200 DATA POINTS
MAXIMUM POINT DENSITY= 4.52833
CTLIM : .9569378

B 3.9 A

lineation and perpendicular to foliation (i.e. XZ plane). However, the sample size for the fabric is small and this may not be a true representative of the fabric.

Thin sections of the Lewisian rocks immediately south of the contact show a thorough recrystallisation of the feldspar grains. Recrystallisation of feldspar is probably consequent to the pile up of dislocations in the absence of any easy slip system at the ambient (T, $\dot{e}$) (see White et al. 1980). Note that while the feldspar clasts in the Eilean Liath Grit (quartz + feldspar), behave in a dominantly brittle fashion, feldspars in the Lewisian gneiss (quartz free areas) recrystallise into smaller new grains. Production of mylonite in shear zones is associated with an overall grain size reduction. However, the deformation mechanism on a grain scale varies from dislocation glide (quartz) to cataclastic flow (feldspar in quartz + feldspar assemblage) or diffusional flow (feldspar recrystallisation in quartz-free 'hard' assemblages).

3.4.2 Dun Medeir Area

The second area is about 2.5 km NE of Kilchiaran Bay. The basal gritty and locally pebbly unit is greenish in appearance (epidotic) and contains a large proportion of phyllosilicates (mainly muscovite and biotite). Wilkinson (1907) described pebbles of gneiss, basic rock and quartz in the pebbly beds immediately overlying the dioritic gneiss. Remapping of the area confirms presence of pebble beds, with a foliation parallel to the contact with the gneiss. Recorded pebble types include quartz (composite grains), feldspar and a dark varity (? altered basic gneiss) with long axes up to a few centimeters.

The foliation is defined by alignment of micas and elongated clasts. The dip of the foliation is 35 degrees towards 146°. The clast elongation lineation is horizontal trending 049°. Although there is a distinct elongation of quartz clasts (often composite), the aspect ratio is lower than that of ribbon quartz in the Kilchiaran Bay area (see Fig. 3.10). Undulose extinction is common, but there is very little (dynamic) recrystallisation. Feldspar grains and quartz are associated with symmetrical pressure fringes with needles of quartz and chlorite; trails of mica swerve round the porphyroclasts. Pull aparts in feldspar

are only occasionally seen. Some of the opaques (? magnetite) are probably syn- to post-tectonic with respect to the foliation as would appear from the skeletal growth, angularity of grains and the sharp abutment of foliation against the opaques.

Average shapes of the pebbles suggest that the total strain ellipsoid is in the constriction field with the X axis parallel to the elongation lineation. An extension crenulation cleavage (Platt and Vissiers 1980) cutting across the penetrative foliation (Fig. 3.10) is comparable to the shear bands that transgress mylonite foliation in the contact zone rocks southwest of Kilchiaran Bay.

Between Kilchiaran House and Carn Mor (see map III) intermittent exposures of interbedded epidotic grits and laminated silts are seen. Although the actual contact with the Lewisian is not exposed, the Lewisian exposures can be seen within 10 meters from the metasediments here and there. The boundary between the two groups runs in a NE-SW direction. In this section, the sedimentary structures like cross-bedding are still preserved in the grits; however, the laminated silts are crenulated with the development of more than one crenulation cleavage. An early crenulation cleavage is subparallel to bedding and is transposed by a late cleavage. The latter is a steep structure dipping at 70-80 degrees towards 140°-150°. The axis of microscopic folds (wavelength up to 10 meters) and crenulations is horizontal with a trend of 060°.

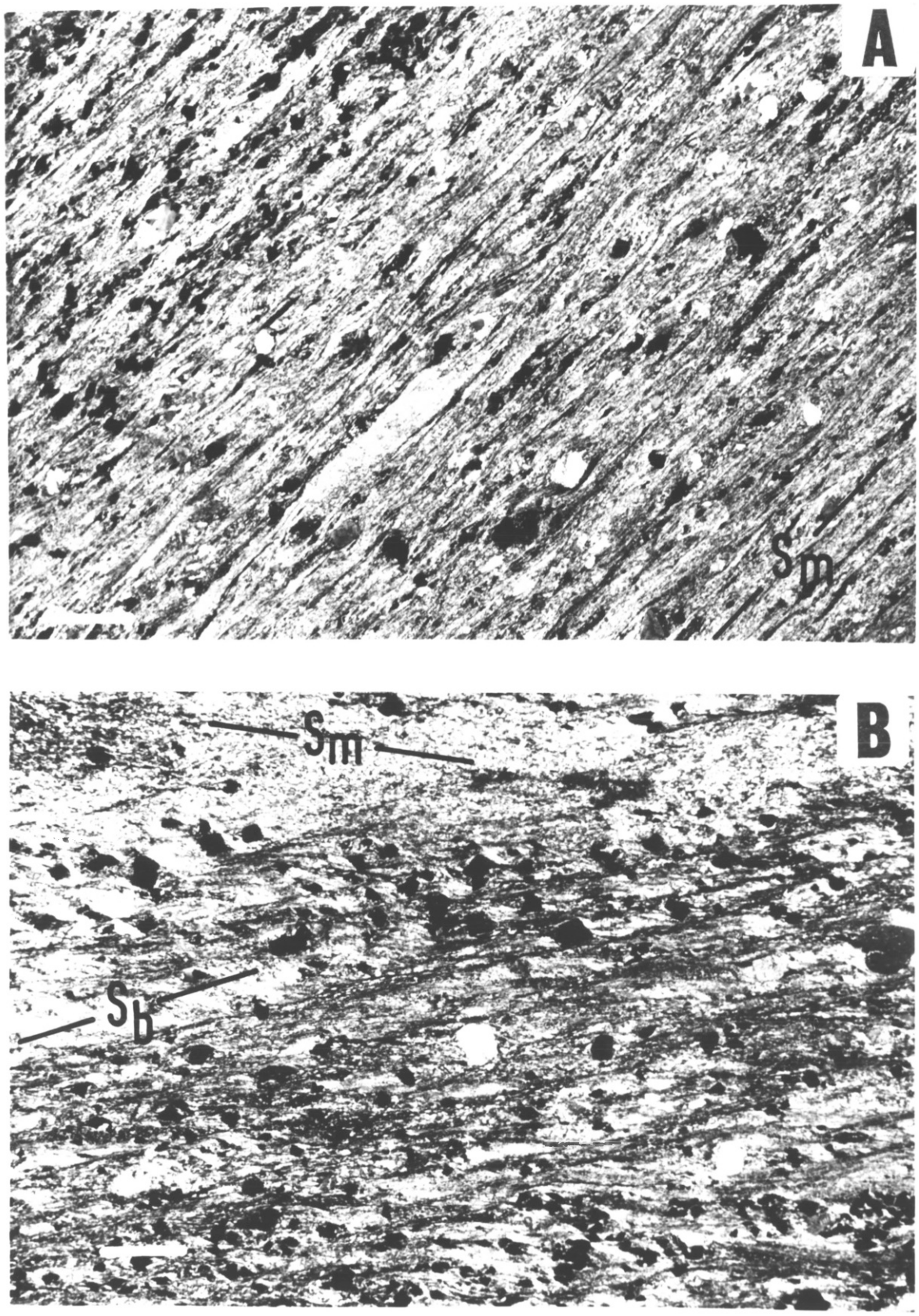
3.4.3 Port Charlotte Area

A simplified geological map of the area between Port Charlotte and Bruichcladdich is shown in Fig. 3.11. A coastal strip of fine epidotic grits can be traced from south of the lighthouse (west of Octomore) to about 1.5 km south of Port Charlotte village. In this stretch, the epidotic grits locally grade either to a slaty rock or to pebbly beds. Along the coast the metasediments locally appear to be interleaved with the Lewisian. Although local reverse faulting and thrusting cannot be ruled out, the outcrop pattern is largely due to the configuration of the coast line and relief along the coast; another contributory factor is probably the initial irregularities of the surface curved out of Lewisian on which the sediments were deposited.

Figure 3.10 Optical micrographs showing mylonite foliation (S_m) and shear bands (S_b) in basal pebbly grit, Dun Medeir, W. Islay. Scale bar is 1 mm in both (a) and (b).

(a) Mylonite foliation; the opaques formed after mylonisation.

(b) Extension crenulation cleavage or shear bands cutting mylonite foliation.



3.10

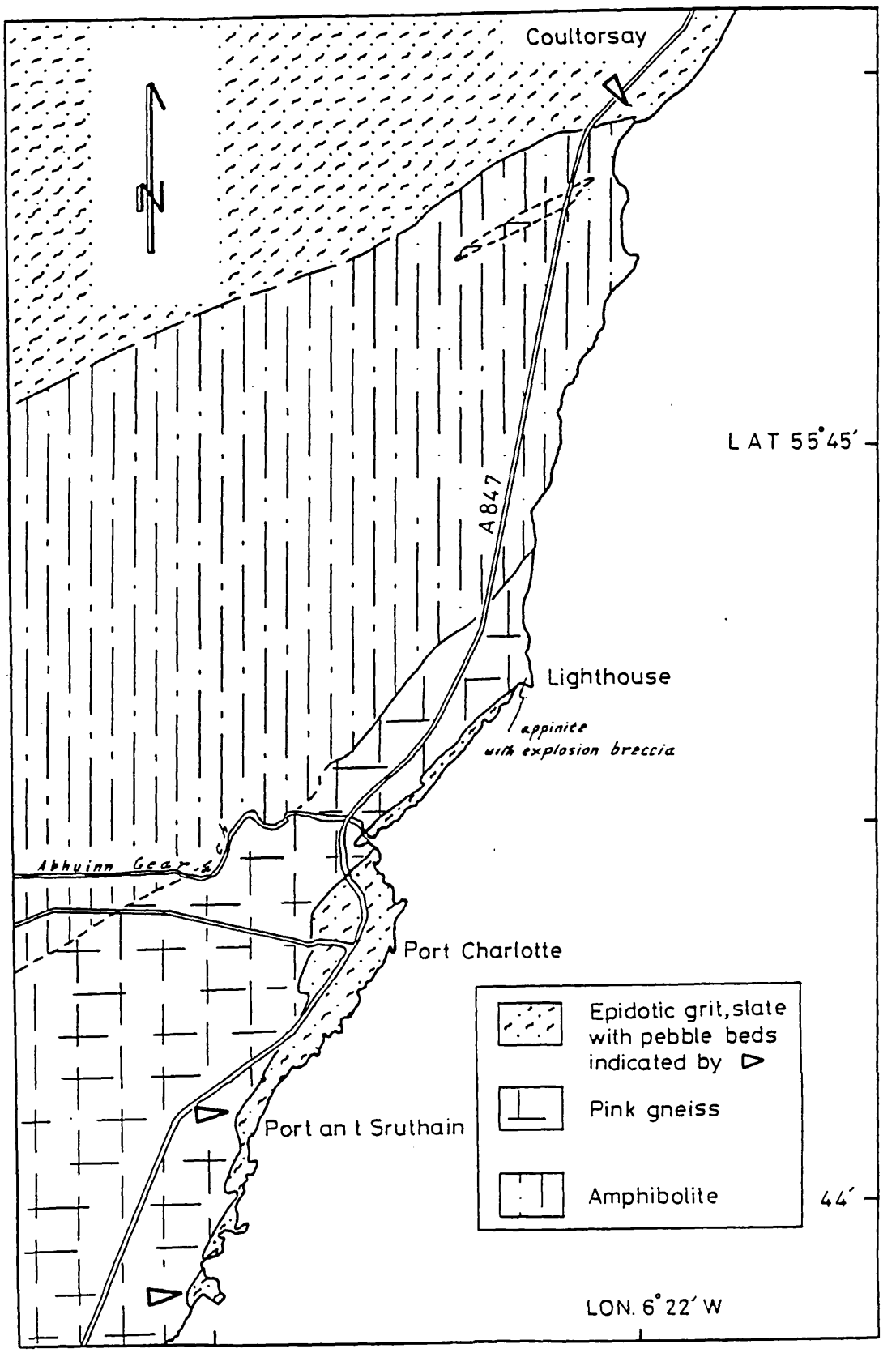


Figure 3.11. Simplified geologic map of the Port Charlotte-Bruichcladdich area.

To add to these, local shearing along the contact has produced phyllonitic rocks both within the amphibolitic Lewisian and the epidotic grits, rendering the identification of the present rock rather difficult. However, in thin sections, the sheared Lewisian shows granulated hornblendes which are not present in the grits.

Evidence for an unconformable relationship between the Lewisian and the metasediments is preserved at Port an t Sruthain (249577) and near Rudh' a' Phuirt Mhoir (248574). In the first locality, pebbly epidotic grits are in contact with a pink gneiss. Pebble types include quartz, pegmatite, epidote and epidote-quartz rock. These are set in a silty greenish matrix which shows anastomosing foliation dipping at 30 degrees towards 100° (Fig. 3.12a). The Lewisian gneiss immediately below the sediments shows an L-S fabric with a foliation dip of 50 degrees towards SE and a streaky lineation along the strike of the foliation. In the second locality the pebbles are up to 0.5 metres in long diameter which is parallel to the axis of minor open folds on foliation (Fig. 3.12b). The average foliation trend is 140° and dip 15° NE. The axes of folds and pebble long axes trend 050°.

The contact between the Lewisian and the sediments is locally sheared or affected by reverse/thrust faulting. One such reverse fault occurs north of Bruichcladdich on the shore opposite the burial ground (267615). Here, dark greenish phyllonitic rocks occur to the north of a pink gneissic band; foliation in each of the two rocks dips south at 35-45 degrees. The contact trends 072 degrees. The structure is one in which the Lewisian gneiss is thrust over the metasediments along a south dipping fault.

3.4.4 Discussion

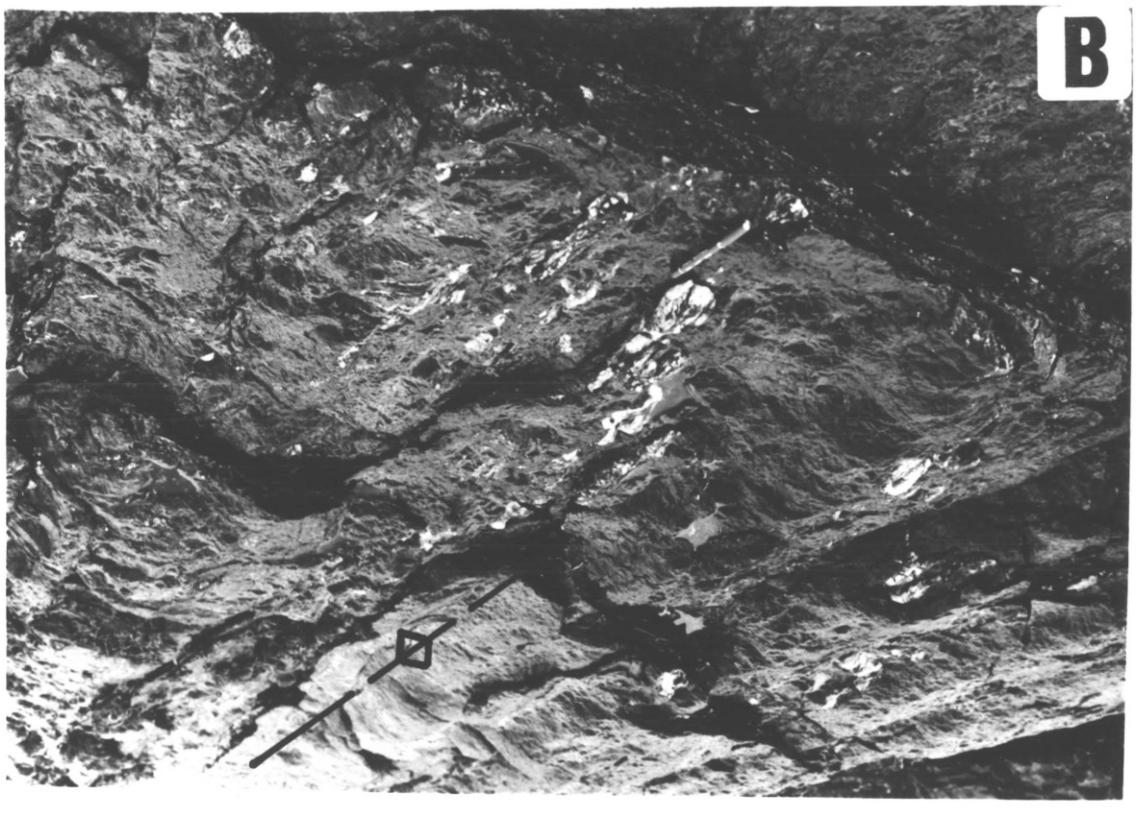
The presence of local, but widely distributed, pebble beds in contact with the Lewisian gneiss in W. Islay suggests that the Colonsay Group was unconformably deposited over the Lewisian. Probably the initial unconformity surface was not a planar one. During Caledonian compression, the whole of the Lewisian basement in W. Islay and the Colonsay Group were subjected to a shortening in a ESE-WNW direction. The mechanical situation in relation to the contact is comparable to that at an interface separating two materials with different rheological

Figure 3.12. Pebbles in epidotic grits immediately overlying Lewisian Gneiss, Port an t Sruthain, Port Charlotte, W. Islay.

(a) Pebbles of quartz and pegmatite in a matrix with anastomosing foliation.

(b) Parallelism of pebble long axes and late fold axes (F_3).





3.12

properties. In a low greenschist facies condition of (P,T) the Lewisian gneiss is probably more competent that the bedded sequence of psammites and pelites in the Colonsay Group (see Ramsay 1983). A planar surface separating a competent material from a less competent material, and subjected to shortening would respond with cuspate and lobate folds due to interface instability (Dietrich and Onat 1969, Ramsay 1967, 1983). A comparable situation within the Colonsay Group itself is illustrated in Fig. 3.13a. Here a thick psammistic layer is in contact with a fine grained argillaceous layer (Sanaigmore Greywacke). The argillaceous layer is internally bedded with concentration of clastic materials in the transition zone between adjacent beds. Along the contact the psammitic layer forms broad antiformal lobes and the argillaceous material projects as cusps into the more competent psammitic unit. The mechanical analogy can probably be extended, though on a much larger scale, to the contact between the Lewisian and the Colonsay Group in W. Islay. The boundary as mapped by the Geological Survey (1" sheet 19 and 27) is shown in Fig. 3.13d. Although in many places the boundary had to be extrapolated (due to poor exposure), the overall form of the contact is reasonably well represented. Note that the Colonsay Group rocks from cuspate synformal projections into the Lewisian substantiating the hypothesis that the Lewisian is the more competent member. However, the suggestion by Wilkinson et al. (1907) that all the folds are overturned towards the southeast is contrary to present observations. In the Kilchiaran Bay area the contact is steep ENE and bedding in the Eilean Liath Grit dips at 60-80 degrees towards NNW; in Dun Madeir area foliation parallel to the contact dips 30 degrees toward southeast, whereas in the Port Charlotte area, the local foliation dip adjacent to the contact is towards NE. Thus the folds are asymmetrical but not necessarily overturned.

The local intensification of clast elongation and development of mylonites along the contact can be explained by a dominant simple shear type deformation in localised areas. Secondary effect of the development of cusp and lobe shaped structure would be local flowage of materials, especially the incompetent ones. The local shear zones along the contact in W. Islay are thus products of a heterogeneous deformation associated with an interface instability.

Figure 3.13. Kinematic analogue for the deformation of Lewisian-Colonsay Group contact, W. Islay.

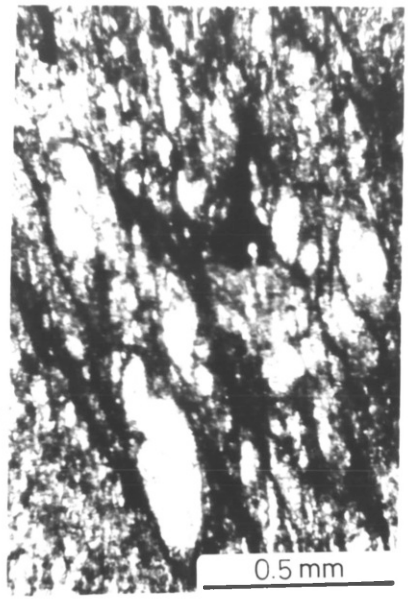
(a) Cusp and lobe structure along the contact between a thick psammitic and an argillaceous layer resulting from interface instability, Sanaig Greywacke, Sanaigmore Bay.

(b) Internal shape fabric within the argillaceous layer. Note absence of any microfolding.

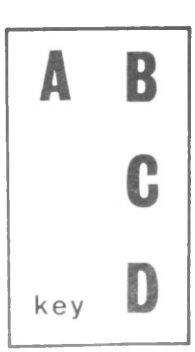
(c) Details of cusp and lobe structure in (a). The argillaceous layer (less competent) forms cuspate projections into the psammitic layer.

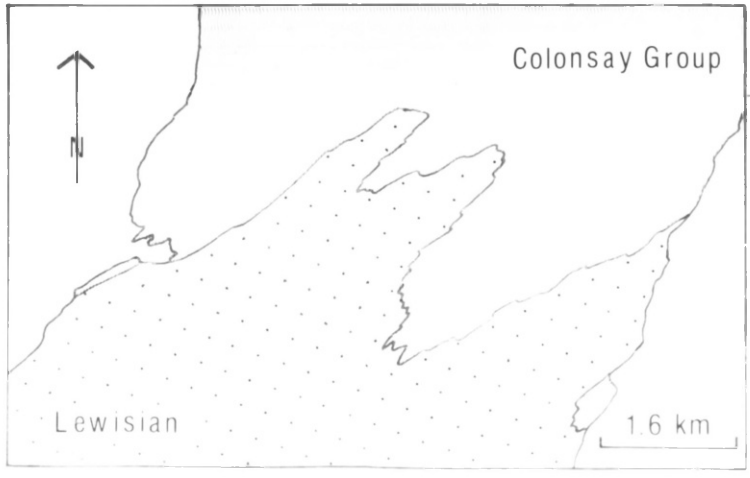
(d) Map showing the form of Lewisian-Colonsay Group interface. The Colonsay Group forms synformal cuspate projections into the Lewisian, similar to structures in (a).











3.13

In the mesoscopic example of cusp and lobe shaped structure cited above, the internal laminations within the argillaceous unit are not affected by any fold structure. On the other hand, shortening along the layer is evidenced by a grain shape fabric at a high angle to the laminations (Fig. 3.13c). The interface instability leading to cusp and lobe shaped structure developed at an early stage of progressive deformation and probably before any fold structure in the laminated unit amplified to any significant extent. Generalisation of the present argument would suggest that in the case of the Lewisian-Colonsay Group contact, the northeasterly elongation lineation was the first effect of Caledonian compression, followed by the development of folds and local shear zones and intensification of an L-S fabric along the contact. The folding of the interface (contact) probably started before any fold structure in the Colonsay Group had any appreciable amplification.

3.5 FOLDING EPISODES WITHIN THE COLONSAY GROUP

3.5.1 Succession of Deformation Events and Minor Intrusions

The succession of deformation events producing folds in bedded rocks of the Colonsay Group in W. Islay can be appraised from a study of the relationship between major and minor folds and associated structures such as axial plane cleavage and lineations. The general principles used in unravelling deformation history in areas of polyphase folding have been formulated and described by a number of workers (Friedman 1964, Ramsay 1958, 1963, 1967, Weiss 1959). Applying these principles four successive folding episodes have been recognised in the present area. Some of these folds are associated with axial plane cleavage, and the most convincing proof of the episodic nature of deformation is provided by the refolding of one or more early axial plane cleavage(s).

It has been pointed out earlier that the Colonsay Group is intruded by several groups of Caledonian minor intrusions. While one particular group of minor intrusions may predate a particular phase of folding, others may transgress folds belonging to the same phase. Thus in isolated areas where not all sets of folds or associated structures are present, the relationship with a specific group of minor intrusions, if they are available, provides a major basis for grouping the relevant structures with a specific phase of deformation. In the following

subsections the deformation episodes are referred to as D_1, D_2, D_3 and D_4 starting from the earliest, and the corresponding folds as F_1, F_2, F_3 and F_4. Axial plane cleavage, if present would be denoted by 'S' with appropriate suffix.

3.5.2 Early Minor Folds, F_1

The F_1 folds have been recorded only on a minor scale. There are isoclinal intrafolial folds and cannot be traced beyond one or two isolated hinges (Fig. 3.14). These folds are quite common in discontinuous psammitic bands within the Rubha-na-h-Airde Moire Phyllite, north of the Kilchiaran slate quarry (197602). The fold axis is subhorizontal with a NE-SW trend. The relationships between F_1 minor folds and later structures have been confirmed from coastal exposures north of Geodh nic Faidein (203600). Here an early minor isoclinal fold in alternating shale (phyllite) and grit layers is cut across by a pressure solution cleavage in grits associated with overturned folds (F_2) and a late crenulation cleavage (S_3) in phyllitic layers. The axial plane of F_1 folds locally dips at 30 degrees towards northwest (Fig. 3.14).

Major isoclinal folds have not been recorded at W. Islay. However, such folds have been mapped within the Bowmore Sandstone and are the earliest structures within the group (see Chapter 2). It is not unlikely that the minor isoclinal folds in W. Islay and the major isoclinal folds within the Bowmore Sandstone represent the same phase of deformation. In the coastal section between Kilchiaran Slate Quarry and Kilchoman the gritty horizons often show elongation of quartz and feldspar clasts in NE-SW direction parallel to the F_1 fold axis. Although the local orientation of F_2 axis is close to that of F_1, other localities where only F_2's develop do not show any appreciable clast elongation parallel to fold axis. Thus the elongation lineation is essentially related to the D_1 deformation. This elongation lineation is comparable with the elongation of clasts in the sheared zones along Lewisian-Colonsay Group contact as well as stretching lineation in the DDZ's within the Lewisian outcrop. All these features are therefore grouped with the D_1 deformation.



Figure 3.14. Intrafolial folds (F_1) in the Colonsay Group, Rubha na-h-Airde Moire Phyllite, north of Kilchiaran Slate Quarry, W. Islay.

3.5.3 Section Across Sanaigmore Bay (F_2 and F_3 Folds)

A NNW-SSE cross-section across the Sanaigmore Bay clearly brings out the fact that at least two generations of folds affect the rocks (Fig. 3.15). Both sets of folds are associated with respective axial plane cleavages. From a consideration of the relationship of similar axial planar cleavages with the minor isoclinal folds (F_1) at Geodh nic Faidein (described above), it appears that the two sets of folds at Sanaigmore are second and third generation folds, F_2 and F_3.

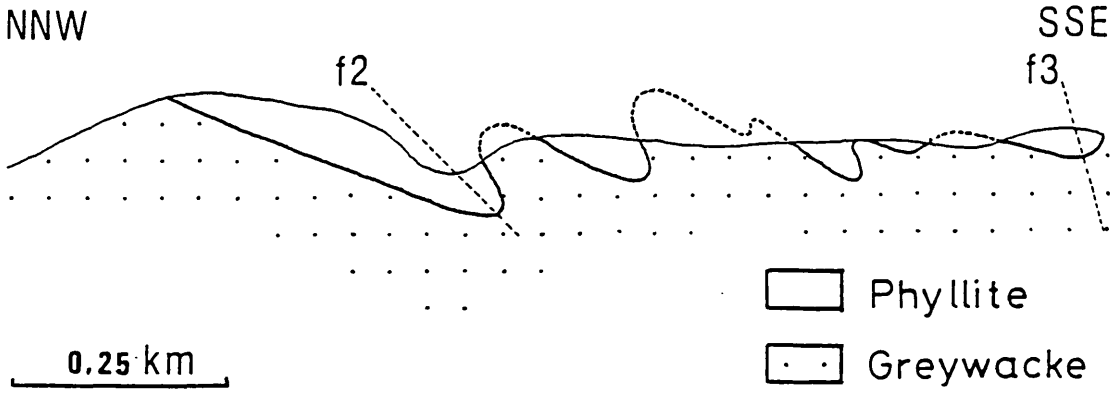
The second folds (F_2) are consistently overturned to the west. The overturned limb dips at 70-80 degrees towards SSE. The orientation of the axial plane cleavage (S_2) across the section shows considerable spread on equal area projection (Fig. 3.15b) due to refolding by F_3 folds. The F_2 axis plunges gently towards NE.

The third folds (F_3) are smaller in amplitude and wavelength than the F_2's. Their superposition is indicated by the folding of S_2 along with bedding by F_3 folds (Fig. 3.16). The F_2 folds are asymmetric, open type with a subhorizontal northeasterly plunge; the axial plane and associated cleavage (S_3) dip at 60-90 degrees SE. A group of lamprophyre sheets are also folded by S_3.

3.5.4 F_2 and F_3 Structures From Other Subareas

3.5.4.1 Loch Corr-Smaull area

Large amplitude overturned folds (F_2) with a wavelength of 50-100 meters is quite common in this section. Grit bands (Smaull Greywacke) are traversed by pressure solution seams associated with an axial plane cleavage (S_2). In the phyllites, tight minor folds of quartz segregations are associated with a crenulation cleavage; there is often a colour banding (fraction of a millimeter wide) parallel to the axial plane of F_2 minor folds (Fig. 3.16c). This banding and S2 cleavage are crenulated where F_3 folds develop. The associated crenulation cleavage (S_3) can also be observed in such areas. Superposed F_2 and F_3 minor folds are common in the cliff sections west of Smaull. Orientations fold elements and cleavages are shown in Fig. 3.17a.



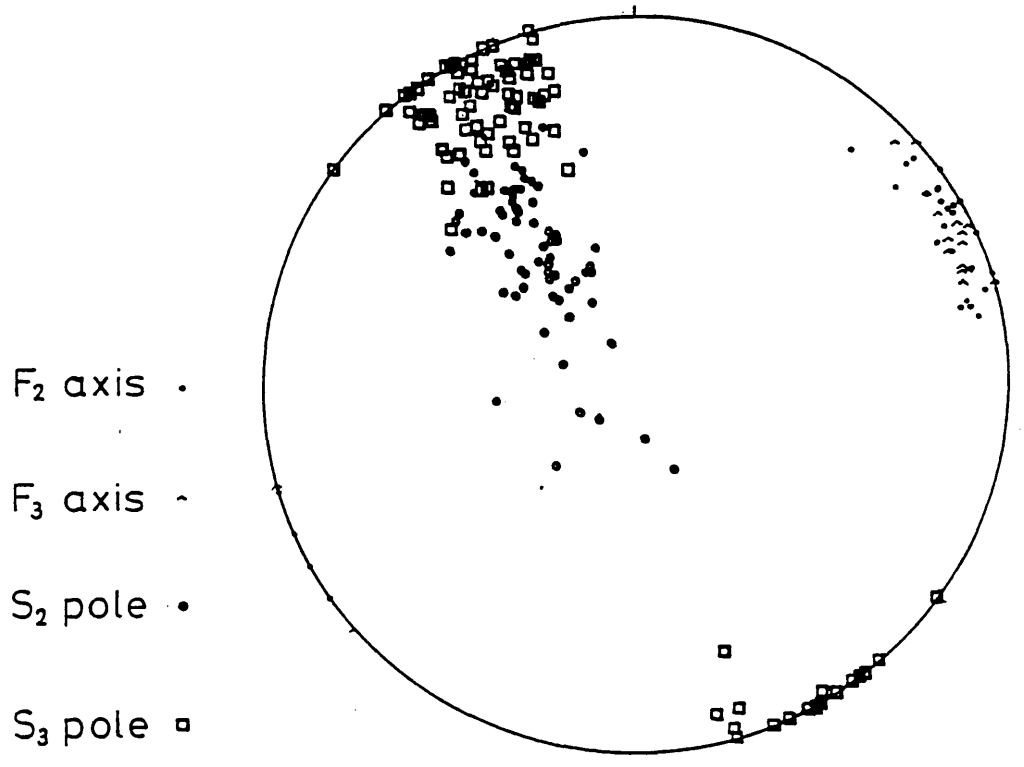


Figure 3.15. D_2 and D_3 structures from Sanaigmore Bay.

(a) A NNW-SSE cross-section across the bay.

(b) Equal-area plot showing the orientation of D_2 and D_3 structures. Spread in orientation of S_2 poles is due to refolding by F_3.

Figure 3.16. Superposition of D_2 and D_3 structures.

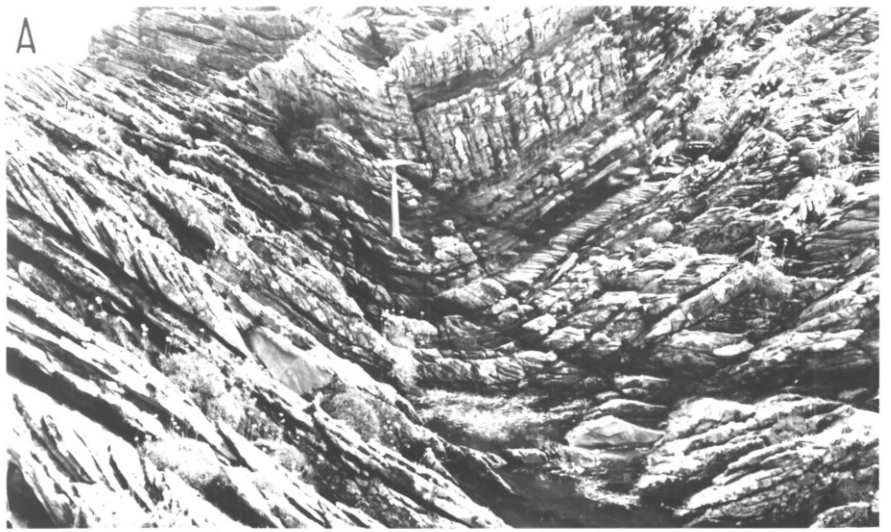
(a) An open F_3 folding showing variable orientation of S_2 cleavage on two limbs; S_3 is steep and apparent on the right limb, Sanaigmore Bay, section looking north.

(b) Type 3 interference pattern of F_2 and F_3 folds, Smaull, section looking northeast.

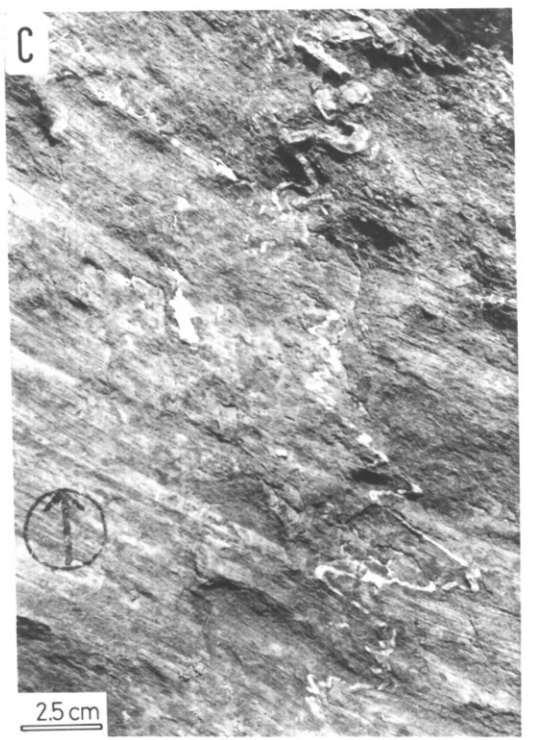
(c) S_2 cleavage and secondary colour banding parallel to the axial plane of F_2 folds, Smaull, section looking northeast.

A 3.16

B C







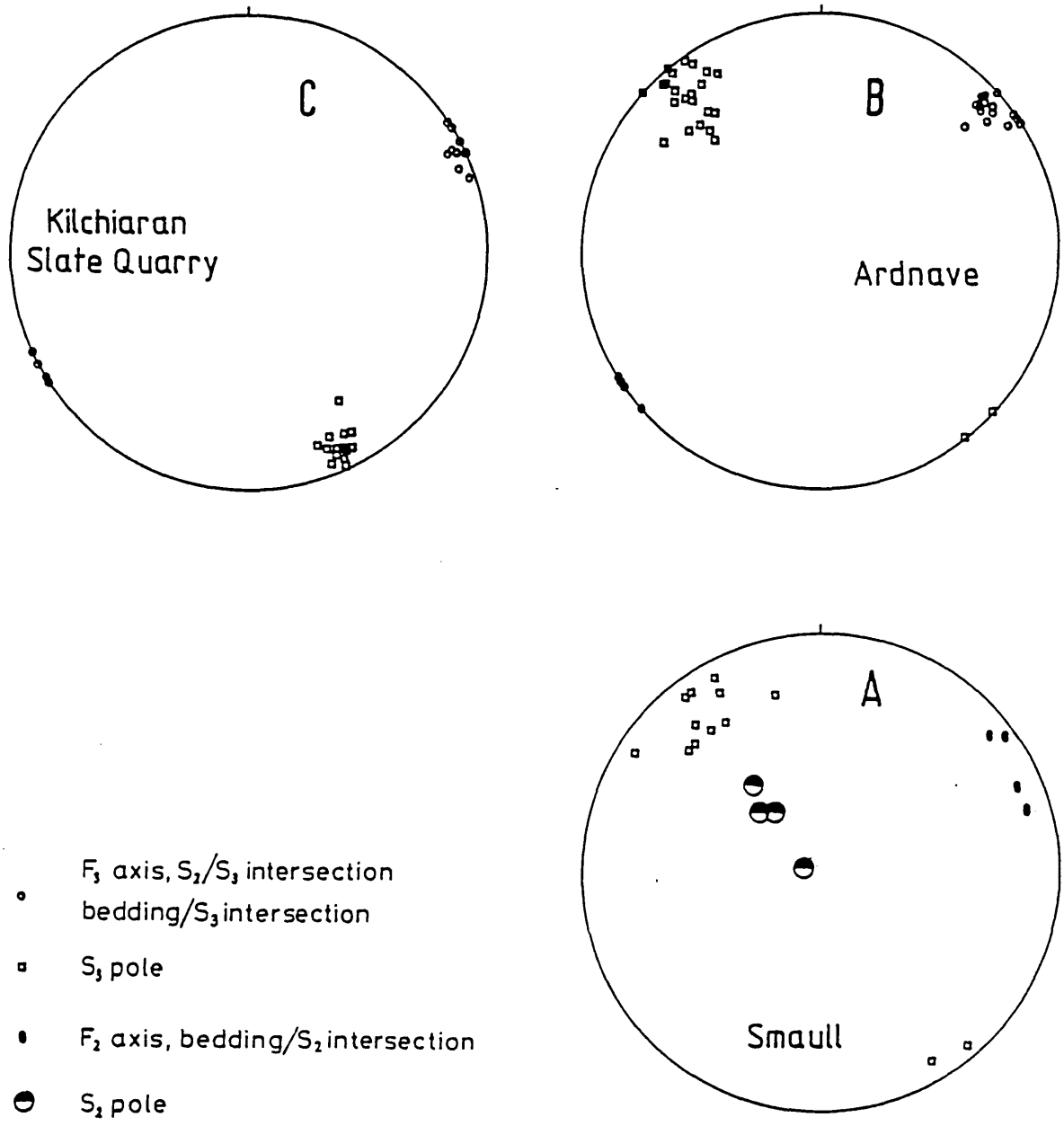


Figure 3.17. Equal area plots showing orientations of D_2 and D_3 structures from different areas, W. Islay. (a) Loch Corr-Smaull; (b) Ardnave; (c) Kilchiaran Slate Quarry.

3.5.4.2 Kilchiaran Slate Quarry Area (192602-196605)

Low amplitude second generation folds (F_2) are common here. The coastal section of the Rubha-na-h-Airde Moire Phyllite shows well developed steep crenulation cleavage (S_3). The general dip of S_3 is however towards NW. Although both at Sanaigmore and Smaull S_3 generally shows a steep dip towards SSE, on a regional scale there seems to be considerable divergence of the axial plane of F_3 structures and S_3. Orientations of S_3 and F_3 puckers are shown in Fig. 3.17c.

3.5.4.3 Ardnave Point (290748-291247)

Exposures are restricted to the coastal strip at low tide. Microscopic folds (F_2 and F_3) are common in the generally banded Ardnave Formation. Attenuated overturned limbs of minor F_2 folds are sometimes replaced by pressure solution seams (Fig. 3.18d). Secondary quartz segregations parallel to S_2 are not uncommon. S_3 crenulation cleavage transposes all earlier foliations and generally dips at 60-80 degrees towards SSE. Orientation of S_3 cleavage and associated lineations are shown in Fig. 3.17b.

3.5.5 Late Structures

Late structures in W. Islay include kink like structures with subhorizontal or east dipping kink plane (Fig. 3.18j), and steeply dipping conjugate brittle shears or kinks. The conjugate shears are represented by a dextral NE-SW set and a sinistral ESE set. Kinks on steep NE-SW planes are locally associated with a crenulation cleavage.

3.5.6 Axial Planar Fabrics

The different fold phases described above are associated with respective axial plane cleavages. Morphology of the axial plane cleavage and the intensity of their development varies with the lithology of the rocks affected as well as the intensity of a particular deformation phase. The first phase of deformation, D_1, produces a mineral elongation lineation in coarse grained clastic rocks, especially those rich in detrital quartz grains. Although this mineral elongation associated with D_1 is conspicuous along the Lewisian-Colonsay Group

contact, intracrystalline deformation of quartz grains in Crosprig Grit produces a shape fabric. The elongation is in a horizontal NE-SW direction, and parallel to the local orientation of F_1 minor folds as well as F_2 folds. Since such elongation lineation is not apparent in other exposures of F_2 folds (where F_1 is not seen), this lineation is likely to be related with D_1. In contrast to quartz grains, the feldspar clasts show pull aparts along their lengths (Fig. 3.18a). Thus the deformation mechanism is dependent on the mineralogy.

Although an elongation lineation is commonly associated with the D_1, locally a planar fabric defined by the parallel alignment of flattened clastic grains develops at a high angle to the bedding (Fig. 3.18b). Such flattening shape fabric is associated with cusp and lobe structures in Sanaig Greywacke described earlier. In pelitic units, such as the Rubha-na-h-Airde-Moire Phyllite, folds (F_1) on quartz segregations are intrafolial to the schistosity.

The axial plane cleavage (S_2) associated with the second folds is a crenulation cleavage commonly associated with close spaced pressure solution seams. In outcrops of fine grained greywackes such as those near Smaull, close spaced pressure solution seams without any obvious microfolds occur parallel to the axial plane of F_2 structures with a wavelength of a few hundred metres; S_2 cleavage in these greywackes show conspicuous cleavage refraction (Fig. 3.18c). In thin section, the pressure solution seams are characterised by a relative abundance of phyllosilicates and opaque material, probably Fe-oxides. The latter reflects the variation in grain size in graded beds so common in greywackes. In pelitic rocks the pressure solution seams are associated with mesoscopic and microfolds, the limbs of which are often attenuated due to pressure solution (Fig. 3.18d). Pressure solution appears to be the dominant mechanism for redistribution of materials associated with the S_2 cleavage formation. However, F_2 fold hinges in coarse grained quartz and carbonate segregations show deformation twins and kinks in relatively coarse calcite grains, or deformation bands, lamellae or dynamic recrystallisation in quartz grains (Fig. 3.18 e,f). Thus some degree of overlap between pressure solution and intracrystalline slip is evident in an environment of low temperature deformation.

The third cleavage (S_3) is similar to S_2 in morphology (Fig. 3.18g). However, S_3 is more common in pelitic or semipelitic units where the presence of an earlier cleavage (S_1 and/or S_2) render the rock highly anisotropic. In rocks where coarse gritty layers alternate with phyllosilicate rich layers the microfolds (F_3) develop as internal structures (Cobbold et al. 1971) within the more anisotropic phyllosilicate rich layers and a crenulation cleavage is restricted to this layer only (Fig. 3.18h). The process of development of this cleavage appears to be mineral migration (or migration of constituent ions) in response to stress gradients established during the development of buckling instabilities in anisotropic rocks (Cosgrove 1976).

The axial plane cleavage (S_4) associated with D_4 develops only locally and is restricted to pelitic rocks. Due to microcrenulations there is some alignment of mica/chlorite parallel to fold limbs. This defines the planes of local cleavage (Fig. 3.18i). Notice that compared to S_2 or S_3, material redistribution due to pressure solution is very limited in S_4.

As described above, the nature and intensity of development of the axial planar fabrics in W. Islay varies with the deformation phases. The lithologic constitution of the rocks deformed determine the deformation mechanism and the processes involved in the formation of axial plane cleavages. The relevant observations in the metasediments of W. Islay are summarised in Table 3.3.

Figure 3.18. Axial planar fabrics in the metasediments of W. Islay.

(a) Photomicrograph showing elongation of quartz clasts and pull-aparts in feldspar associated with D_1, Crosprig Grit, Dun Crosprig.

(b) Flattening of detrital grains parallel to axial plane (S_1) of cuspate and lobate folds in Sanaig Greywacke, Sanaigmore.

(c) Refraction of S_2 cleavage in Smaull Greywacke, Smaull.

(d) Attenuated F_2 limbs and pressure solution seams parallel to S_2, Ardnave Formation, Ardnave.

(e) Photomicrograph (plane polarised light) showing pressure solution seams transposing a folded quartz-carbonate vein, Ardnave.

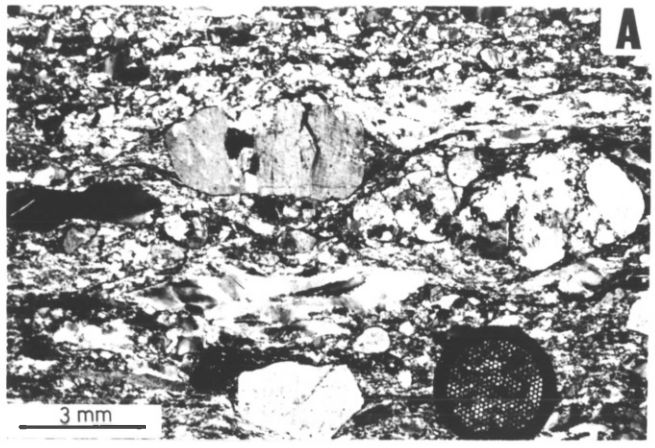
(f) Details of microstructure associated with F_2 fold hinges in quartz-carbonate vein in (e). Note twinning and kinking in calcite grains and re-crystallisation in quartz grains (arrows).

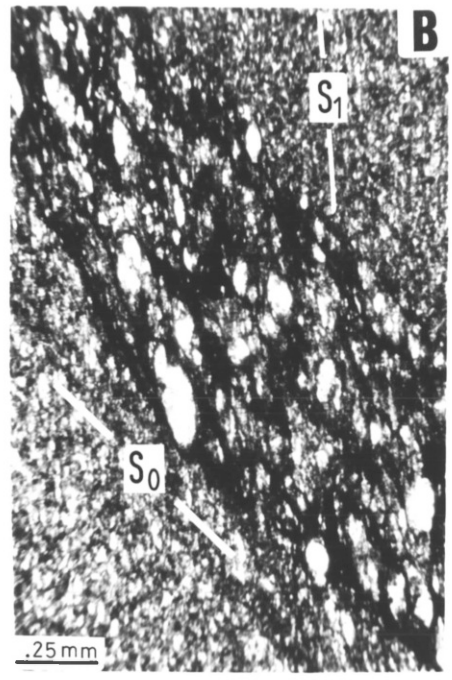
(g) Crenulation cleavage (S_3) in Ardnave Formation, NW-SE section.

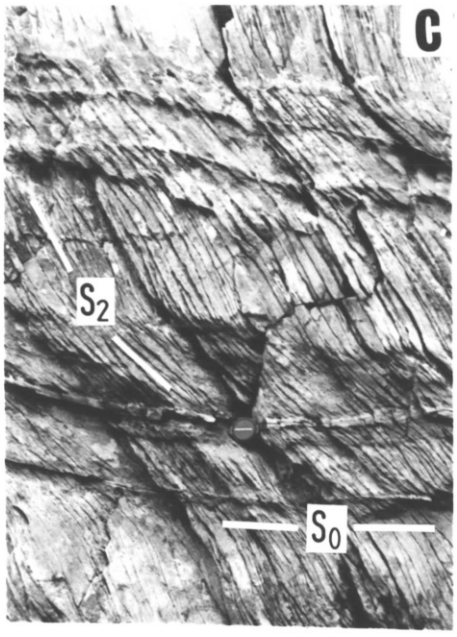
(h) Crenulation cleavage (S_3) developing as internal structures within a phyllosilicate rich layer in interbanded pelitic and coarse psammitic lithology, Crosprig Grit, Dun Crosprig. Photomicrograph in plane polarized light.

(i) Subhorizontal kinks (D_4), Smaull Greywacke, Smaull.

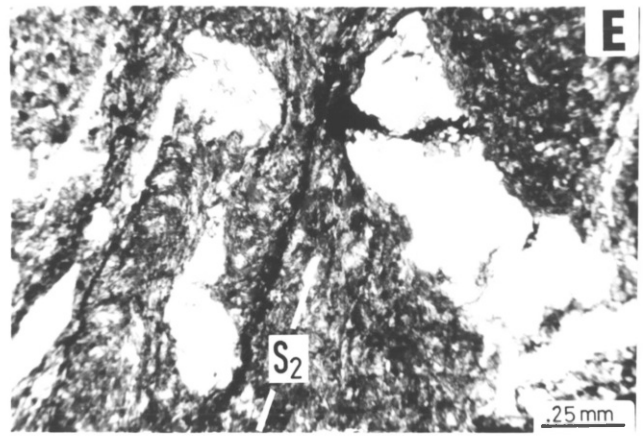
(j) Photomicrographs showing crenulation cleavage associated with D_4. Notice wide spacing of cleavage compared to (g).

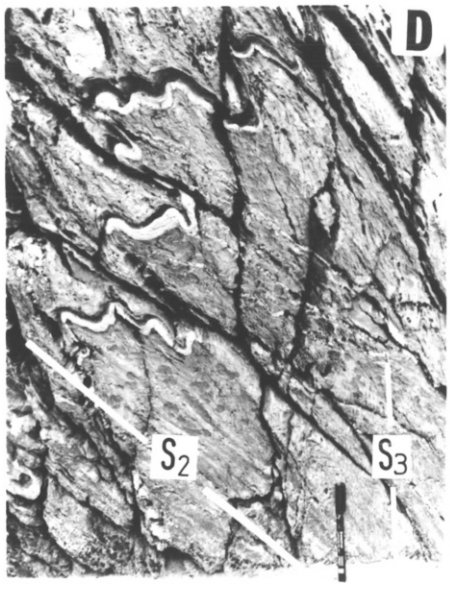




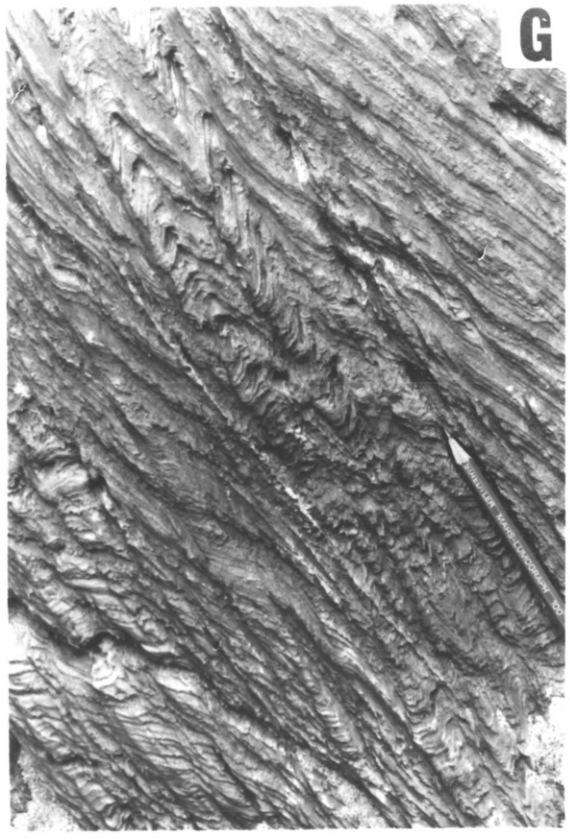


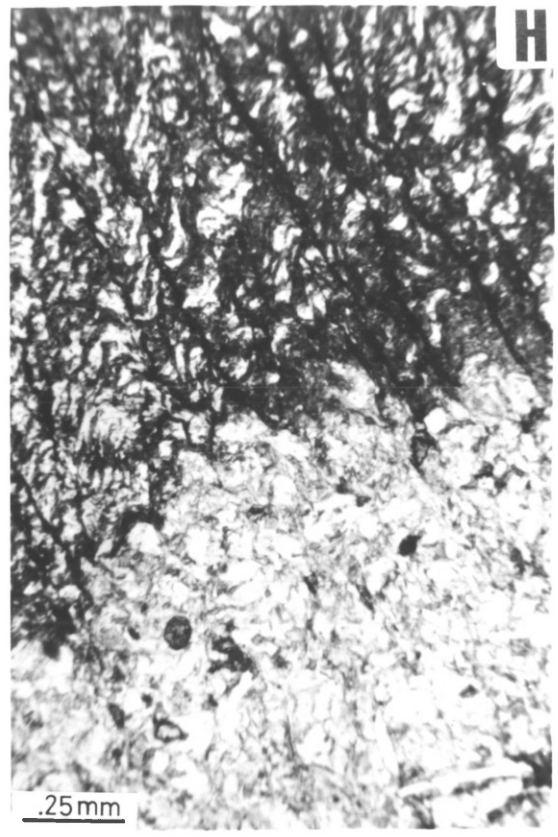
3.18



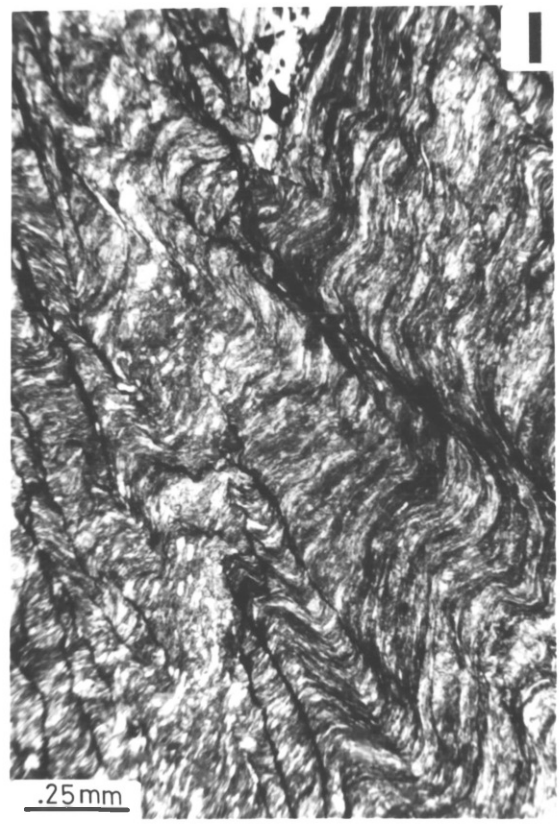












3.18 contd.

Table 3.3 The dependence of morphology of the axial plane cleavages on deformation phase and lithology

Deformation Phase	Axial Plane Fabric	Deformation Mechanism	Lithology
D_1	Elongation of mineral grains parallel to F_1 axis; schistosity in pelitic rocks with intrafolial F_1 folds	Intracrystalline slip	Quartz rich
		brittle	Feldspar-rich
	Crenulation/P.S. cleavage	Microfolding of mica, pressure solution	Thinly laminated alternate quartz-rich and mica-rich layers; fine grained greywacke
D_2		Local intracrystalline slip in coarse quartz and calcite grains	Coarse-grained quartz carbonate segregations
D_3	Crenulation/P.S. cleavage	Microfolding of micas pressure solution	Thinly laminated alternate quartz-rich and mica rich layers (relatively thick psammitic layers unaffected)
D_4	Crenulation cleavage	Local microfolding of micas	Only mica rich layers

P.S. = Pressure Solution

CHAPTER 4

THE LOCH SKERROLS THRUST - STRAIN AND MICROSTRUCTURES

4.1 INTRODUCTION

The Loch Skerrols thrust separates the Torridonian Bowmore Sandstone from the Dalradian of NE Islay (Fig. 4.1). It follows a sinuous southward course from Bun-an-Uillt on the eastern shore of Loch Gruinart and crosses Loch Skerrols, in the vicinity of which evidences for a large movement can be seen (Wilkinson et al. 1907). South of Loch Skerrols, the course of the thrust plane is less certain due to poor exposure in the area. However, near Tallant Farm the thrust plane can be seen to be shifted eastward by a normal fault. Beyond this point its course is concealed under superficial deposits, but it probably continues to the shore of Laggan Bay (Wilkinson et al. 1907).

The Loch Skerrols thrust represents a major dislocation in SW Argyllshire. Although Kennedy (1946) and Garson and Plant (1972) differ in their reconstruction along the Great Glen Fault, both these authors suggest that the logical southerly continuation of the Moine Thrust is the Loch Skerrols thrust in Islay. As discussed in Chapter 2, the major snag in such correlation is the fact that in Islay Dalradian rather than Moinian rocks lie on top of the Loch Skerrols thrust. On the other hand, Borradaile (1979) in his strain study of the Caledonides of the Islay region notes that 'greater total strains have not been recorded from the vicinity of the Loch Skerrols thrust'. Although most workers agree that there is considerable movement along the Loch Skerrols thrust, no systematic study of strain and microstructures of the thrust zone rocks has been done before. This is partly due to poor exposure along the course of the supposed thrust line. Amos (1959) notes that the thrust plane can be accurately located at the following localities:

1. About 0.5 kms southwest of Tallant farm. Here the thrust can be traced for only 50 metres.

2. Northwest of Loch Skerrols for 1.5 kms. Exposures of sheared Jura Quartzite are scattered in a narrow belt stretching from northeast of Knockdon through An Carn to Loch Drolsay at the head of River Drolsay.

3. Three-quarters of a kilometer northwest of the summit of An Carn.

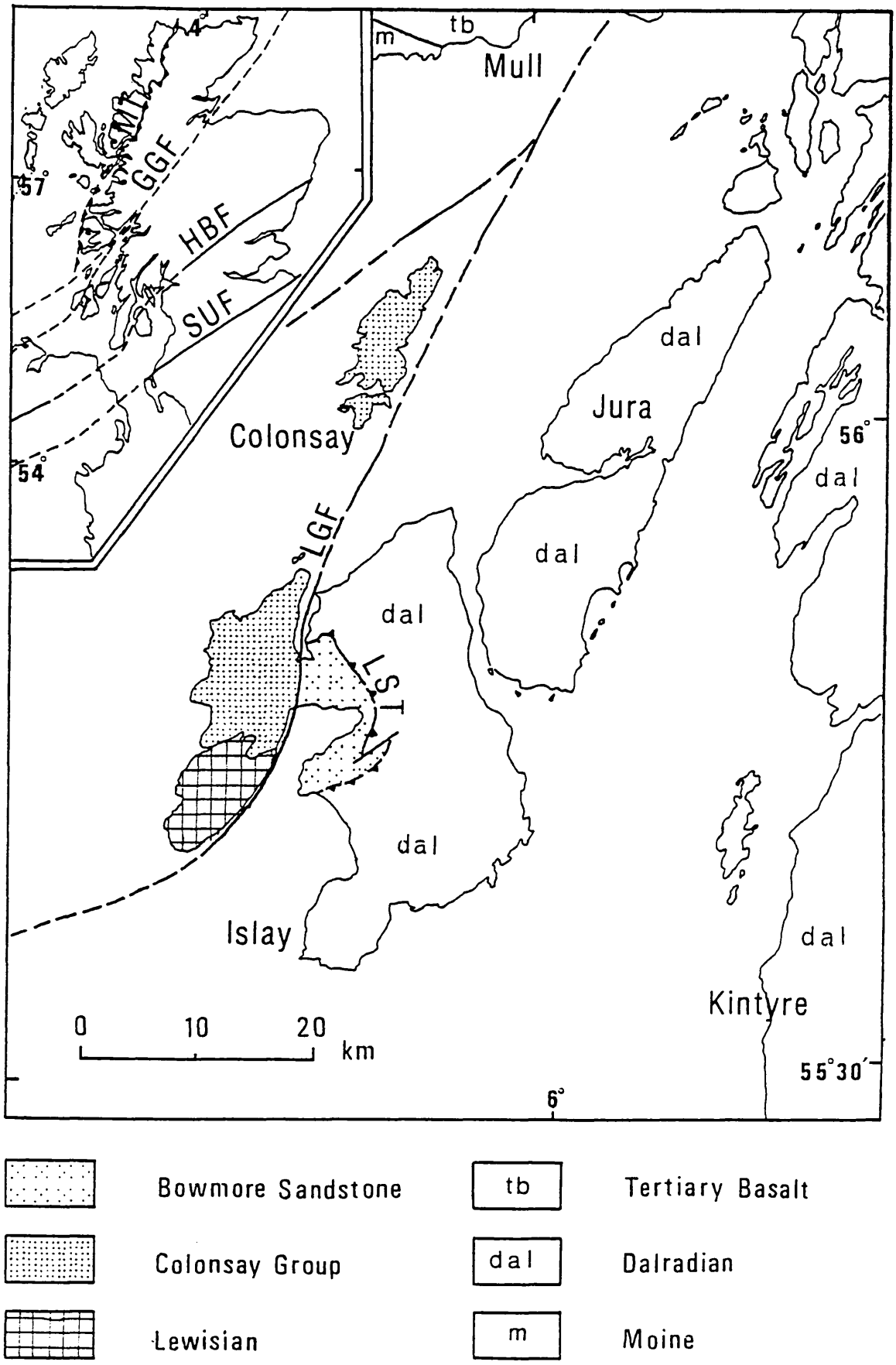


Figure 4.1. Geologic setting for the Loch Skerrols thrust. Inset shows major lineaments in Scotland. GGF = Great Glen Fault; HBF = Highland Boundary Fault; MT = Moine Thrust; LGF = Loch Gruinart Fault; LST = Loch Skerrols Thrust; SUF = Southern Uplands Fault.

4. Bun-an-uillt stream, about 0.75 kms east of the shore of Loch Gruinart.

5. East shore of Loch Gruinart, 300 metres southwest of Bun-an-uillt Farm.

The second of the above mentioned localities provides the best available place for studying the variation of strain and microstructure development across the thrust. On a traverse across the thrust plane from Loch Cam in the east to Knockdon on the west, the available exposures were studied in detail to observe and measure thrust related minor structures; specimens were collected for three-dimensional (3-D) strain measurement, and for microstructural and fabric studies. The observations and the results are described in this chapter. A new parameter based on the probability distribution of point-density in contoured fabric diagrams has been defined to measure the degree of crystallographic preferred orientation. An empirical relationship between the fabric intensity parameter and strain intensity is discussed later in this chapter. Fabric and strain data from the Loch Skerrols thrust zone and some published results are used for this purpose.

4.2 MESOSCOPIC STRUCTURES IN THE THRUST ZONE

4.2.1 A Traverse from Loch Cam to An Carn

A traverse westward from the west shore of Loch Cam to the summit of An Carn shows a gradual change in the lithologic constitution of the Jura Quartzite. Near Loch Cam and northwest of the Loch, individual clastic grains can be recognised in the exposures. The grains have a weak flattening shape fabric and their subparallel alignment defines a patchy foliation in the rock. Near River Drolsay, there is first appearance of a streaky lineation on polished parting planes in quartzite; where the clastic grains are obvious they show an apparent elongation parallel to the streaky lineation. Further west on the southern slope of the Carn, the white quartzite breaks along a low-angle southeast dipping inosculating foliation. Locally, the foliation wraps round augens of relatively undeformed quartzite. A streaky lineation is defined by parallel alignment of mica flakes.

Individual clastic grains are difficult to distinguish in hand specimen and the rock as a whole appears to be much finer grained.

The orientation of foliation and lineation in the thrust zone are shown in Fig. 4.2. The foliation has an average SSE dip at 30-40 degrees. The lineation plunges at a low angle towards SSE; note that the lineation is not exactly downdip on foliation.

4.2.2 Bun-an-uillt area

The area described below includes the stretch of intermittent exposures that straddles the high-tide level along the eastern shore of Loch Gruinart between a point about 0.5 kms southwest of Bun-an-uillt Farm and Crois-Mhor. The rocks in the southern half of the stretch are shattered and often traversed by bands and veins of breccia or fault-gouge, which may be related to a fault independent of Loch Skerrols structure.

In a small exposure about 300 metres southwest of the farm house, the intact blocks of a micaceous quartzite have all the appearances of a platy mylonite. Although the foliation is undulatory due to the presence of warps on axes plunging gently WSW, the overall dip is towards south at about 20 degrees. A streaky lineation defined by parallel grooves on polished foliation surface, and parallel alignment of white mica is persistent throughout the exposure, and has an E-W trend. The lineation is gently curved around hinges of later minor folds.

From the shore opposite Bun-an-uillt farmhouse to Crois-Mhor the exposures are of buff coloured quartzite with a penetrative foliation defined by alignment of flattened sand-sized grains in parallel planes. A streaky lineation is also observed. However, the foliation in this locality (supposedly related to shearing along the Loch Skerrols thrust) dips at 60-70 degrees towards WNW; the lineation is roughly down dip on foliation. This reversal in dip of mylonite foliation between An Carn and Bun-an-uillt is probably related to folding of the Loch Skerrols thrust plane. The E-W trend of foliation southwest of Bun-an-uillt farmhouse can be explained as due to a drag effect along an E-W fault that has displaced the Loch Skerrols thrust (Amos 1959).

4.3 MICROSTRUCTURAL VARIATION IN A ZONE OF STRAIN GRADIENT

4.3.1 Microstructure

The traverse from Loch Cam to a point half a kilometer north of Knockdon Farm reveals a zone of natural strain gradient. The traverse crosses the Loch Skerrols thrust zone. The microstructural evolution of the Jura Quartzite associated with the Loch Skerrols thrust has been studied in samples collected at varying distances from the western boundary of the Jura Quartzite in this area. The Loch Skerrols thrust separates the outcrops of Bowmore Sandstone and Jura Quartzite, but the direct contact between the two groups is not exposed in the An Carn-Knockdon area. The microstructural changes with increasing strain are listed below (Fig. 4.3). In the following discussion 'matrix' refer to the aggregate of small (30-50 μm) grains surrounding porphyroclasts of larger grains (0.5 mm and above). The larger grains are deformed sedimentary grains and described as 'clasts'. As described below through dynamic recrystallisation and attendant grain refinement of 'clasts' contribute to the 'matrix'.

1. At an overall strain intensity, G_s of 0.63, the quartz 'clasts' show undulose extinction with elongate optical subgrains; dynamic recrystallisation in quartz 'clasts', generally restricted to the grain boundaries, produces a core and mantle structure (White 1976). Although the studied samples contain less than 1 per cent feldspar grains, twin lamellae in feldspar grains are diffuse and some of these 'clasts' show pull-aparts.

2. With increasing strain (overall $G_s \sim 0.8$) the proportion of 'matrix'/'clast' increases as more and more 'clasts' are dynamically recrystallised and thereby incorporated in the 'matrix'; the recrystallised grains have straight to gently curved boundaries, except where they occur at the boundary of a relict core of porphyroclast. In the latter case, lobate grains can be seen. Some of the larger 'clasts' are broken down into subparallel ribbon grains separated by trails of fine dynamically recrystallised grains. Optical subgrains are not still obvious at the core of 'clasts'. Dynamically recrystallised grains show a weak shape fabric subparallel to the mylonite foliation.

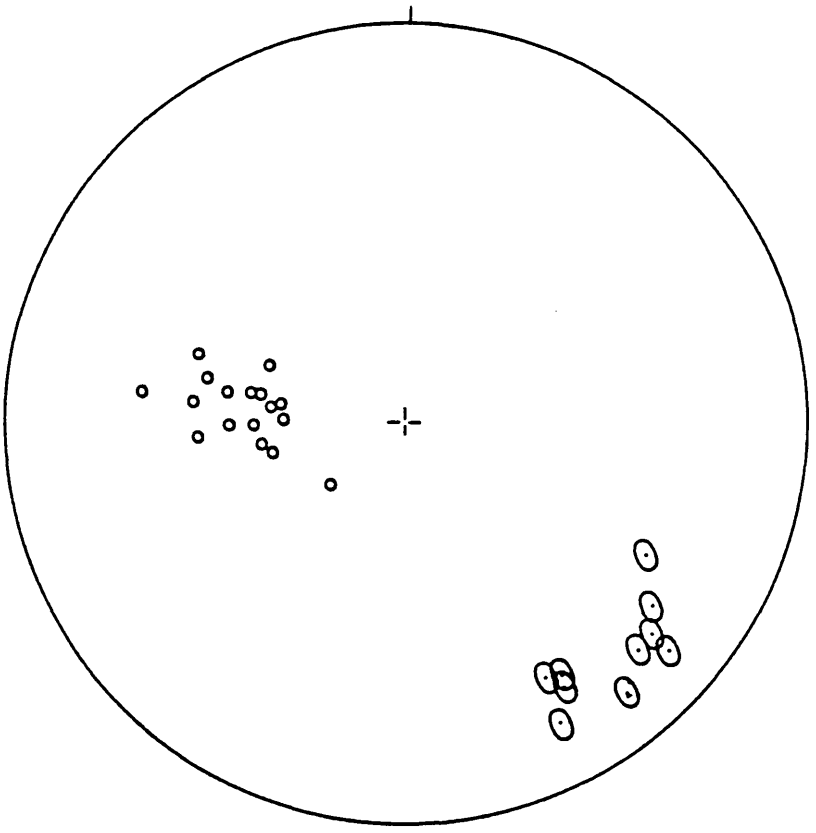
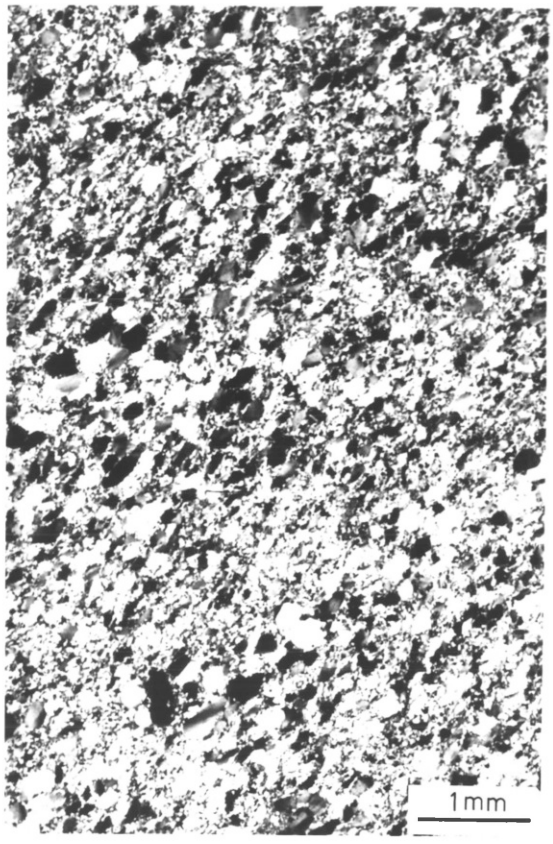
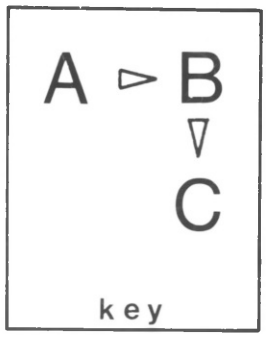


Figure 4.2. Equal-area plot of foliation poles and mineral elongation lineation in the thrust zone. Circles = poles to foliation, ellipses = lineations.

Figure 4.3. Microstructural changes in Jura Quartzite with increasing strain. a-c) with increasing strain the axial ratio of quartz clasts increases, so does the 'matrix'/'clast' ratio. Photomicrographs from sections cut parallel to lineation but perpendicular to foliation. d) At low strain dynamic recrystallisation is restricted to grain boundary; notice elongate subgrains within the large deformed grain. e) at high strain thorough recrystallisation of 'clasts' occur; notice alignment of grain boundaries.

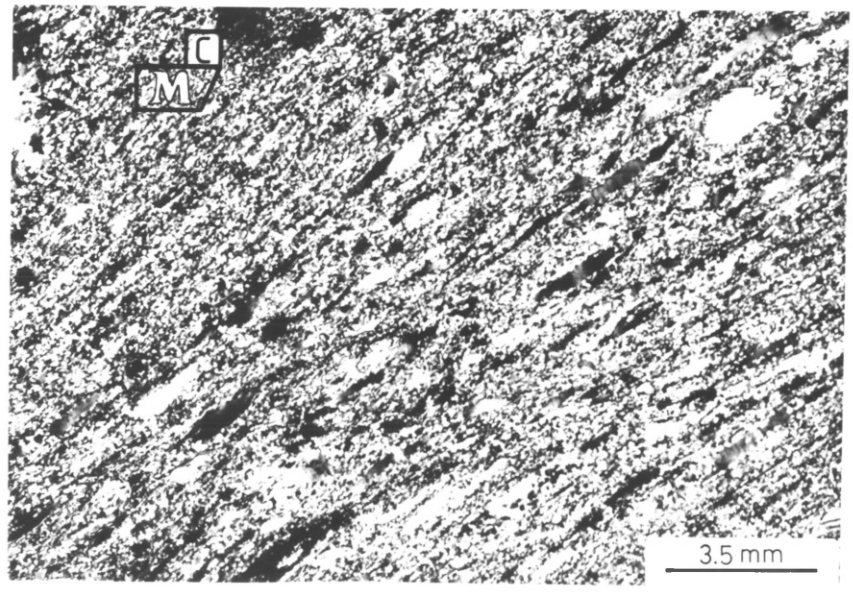




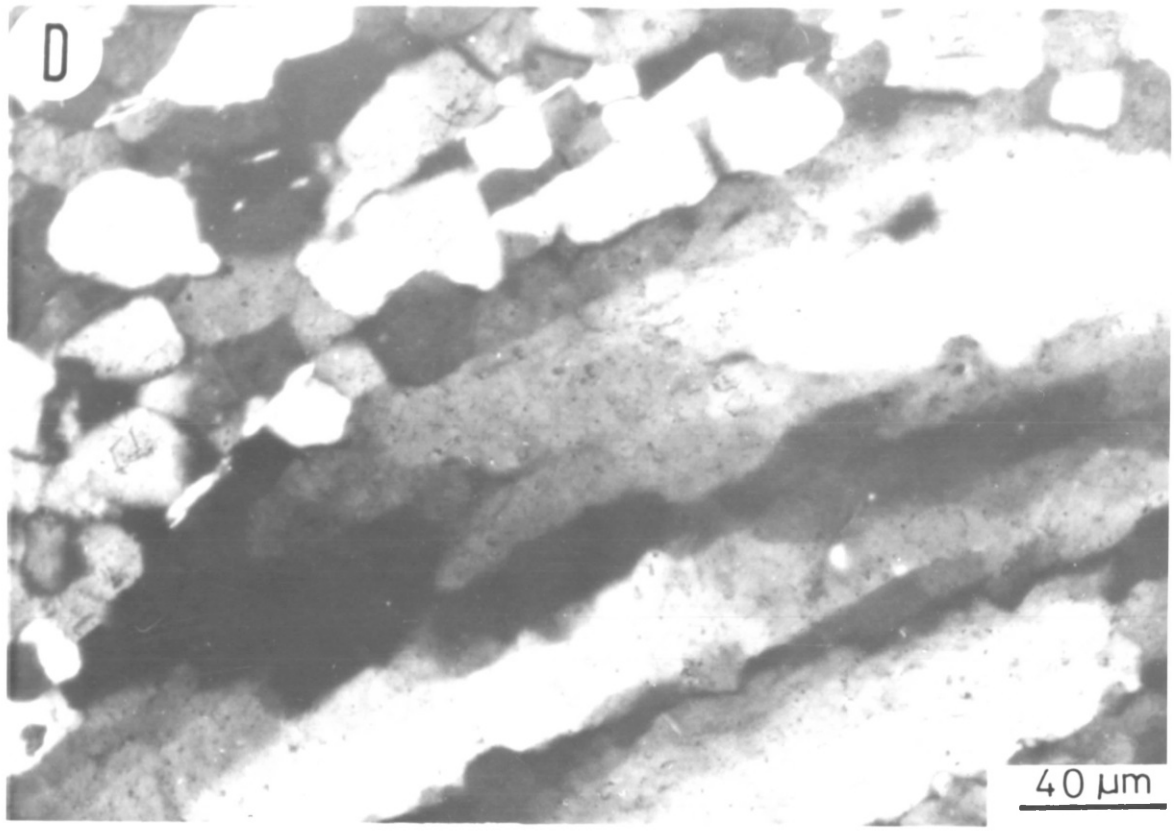


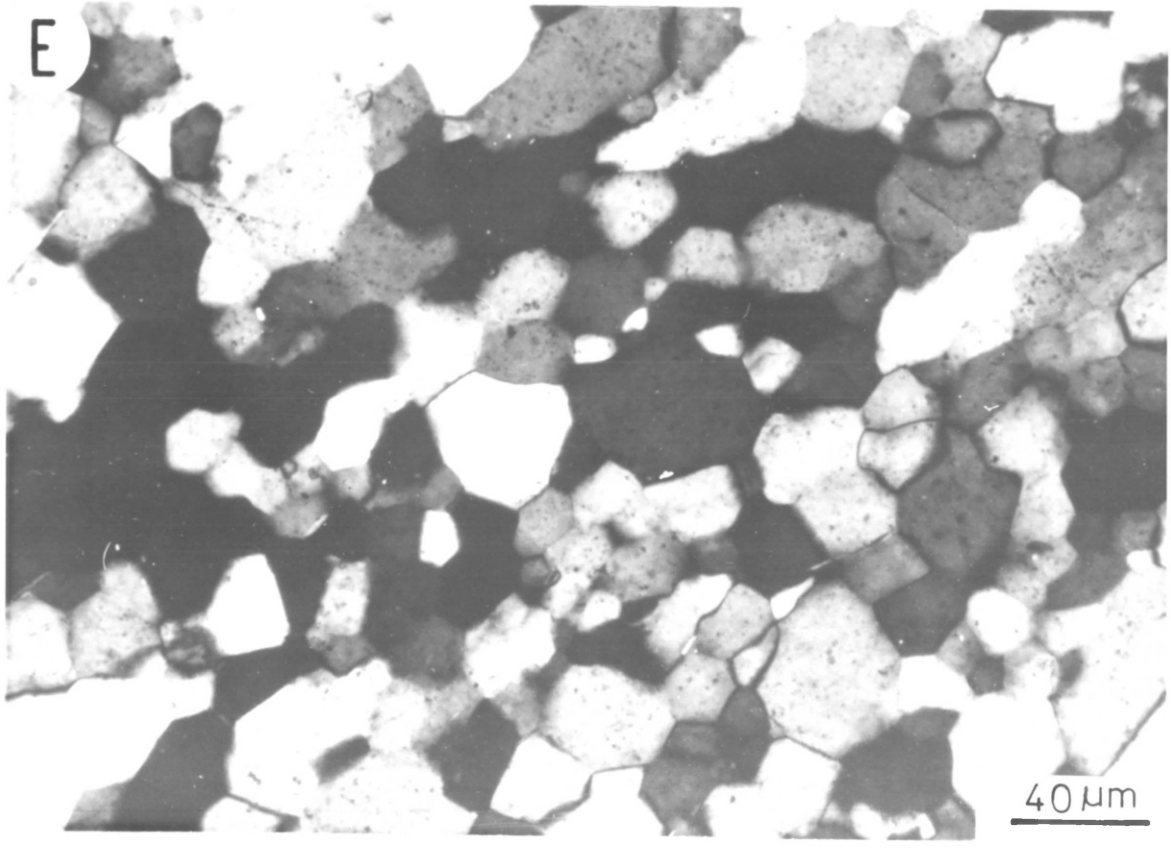
C ► Clast

M ► Matrix



4.3





4.3 contd.

3. At the highest recorded strain intensity ($\Theta_s \sim 1.3$), the proportion of 'matrix' grains is more than 85 per cent. Through recrystallisation of highly elongated clasts is common. The optical subgrains in some of the less elongated 'clasts' are polygonal in outline; grain boundaries of dynamically recrystallised grains are generally straight. Grain boundaries are often aligned parallel to each other and thus define the mylonite foliation. Some recrystallised grains are larger than average probably due to static growth.

Although the proportion of 'matrix'/'clast' increases (Table 4.1) with increasing strain, the average size of dynamically recrystallised grains does not show much variation with strain (see Table 4.2). The distribution of the aspect ratio of dynamically recrystallised grains for different samples is shown in Fig. 4.4. Optical microstructures show that the increase in the proportion of 'matrix'/'clast' is largely due to progressive dynamic recrystallisation. There is also a concommitant increase in the length of trails of white mica parallel to mylonite foliation. The apparent absence of feldspar 'clasts' in highly strained specimens is probably due to mechanical breakdown and decomposition into white mica.

Table 4.1 Proportion of matrix to clast in deformed Jura Quartzite (figures were averaged from three perpendicular sections in each specimen)

Sp. Id.	Clast %	Matrix %	Total Point Count
87	45.52	54.48	4644
86	49.31	50.69	4644
85	44.70	55.30	4644
84	44.44	55.56	4644
83	19.14	80.86	4644
82	14.73	85.27	4601
431	21.70	78.30	4644
438	25.50	74.50	4644
435	38.24	61.76	2322

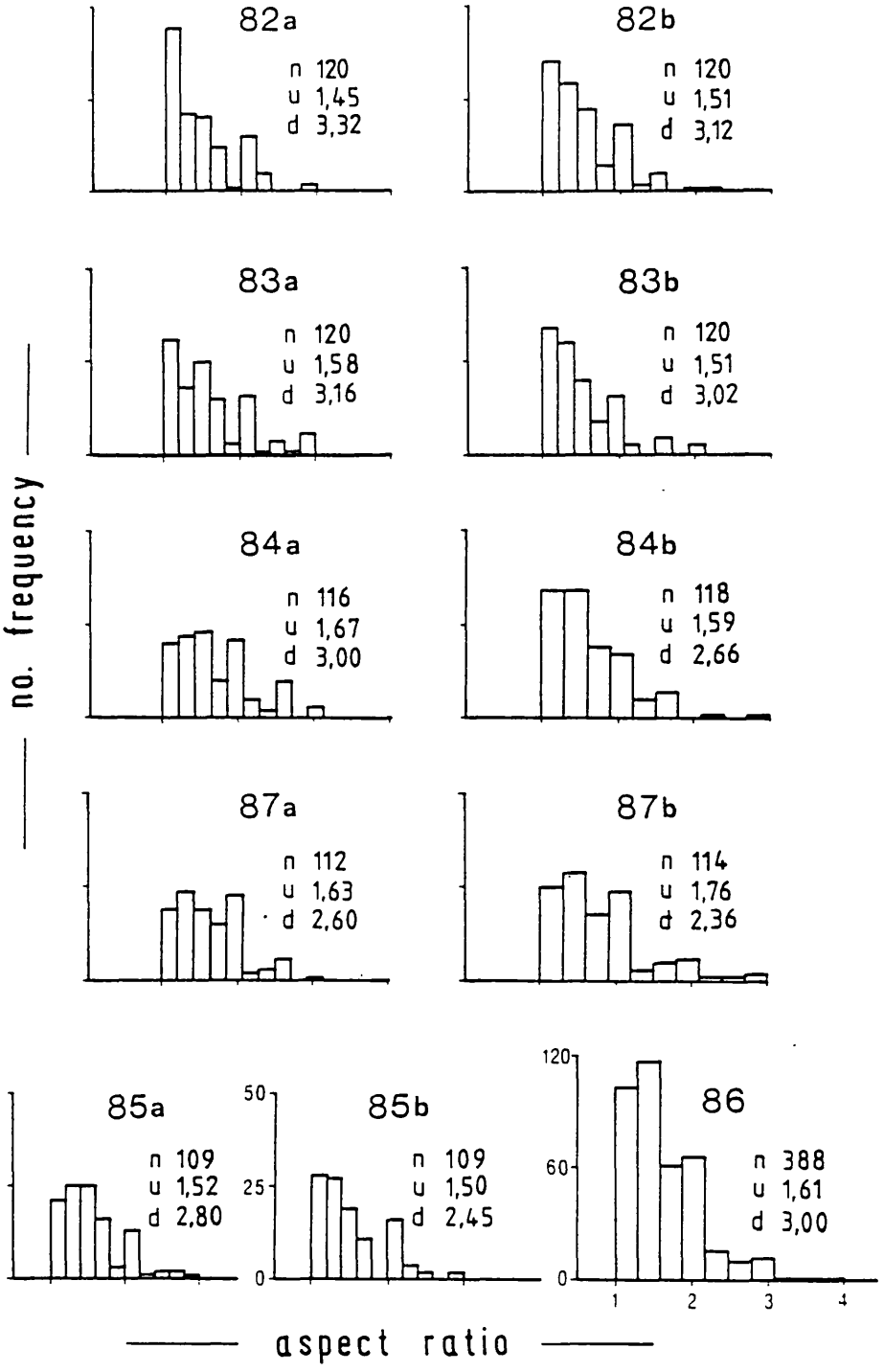


Figure 4.4. Distribution of the aspect ratio of dynamically recrystallised grains in specimens with different strain intensity. Strain values decreases from specimen no. 82 to sp. no. 87 (no. at the top of each distribution). Note that the mean aspect ratio (u) shows little change with increasing strain. d is the average grain intercept (D_j in section 4.3.2) in micrometer ocular division (1 ocular div - 12 μm). n = no. of grains measured in each thin section (a and b two mutually perpendicular thin sections in each specimen).

4.3.2 Palaeostress Estimate

Principle

Deformation induced dislocation density, subgrain size and dynamically recrystallised grain size in rocks from deeply eroded fault zones provide signatures of the differential stress that existed when the fault was active (Christie and Ord 1980, Kohlstedt and Weathers 1980, Mercier et al. 1977, Nicolas and Poirier 1976, Schmidt 1983, Twiss 1977, Weathers et al. 1979, White 1979). Experimental observations demonstrate that three microstructral elements, namely dislocation density, subgrain size and grain size, generated during steady-state deformation depend primarily on the differential stress (Mercier et al. 1977, Twiss 1977). Theoretical arguments have also been put forward to support the experimental results (Twiss 1977).

The principle has been applied by a number of workers for palaeostress estimates in thrust belts (Burg and Laurent 1978, Christie and Ord 1980, Etheridge and Wilkie 1979, Twiss 1977, Weathers et al. 1979, White 1979). It has been concluded that the dislocation density in particular is very susceptible to late overprints and the most stable palaeostress indicator is probably the recrystallised grain size (Kohlstedt and Weathers 1980, Schmid 1983). The relationship between grain size (D) and differential stress ($\delta\sigma = \sigma_1 - \sigma_3$) in deformed quartzites is given by

$$\delta\sigma = B.D^c \qquad (4.1)$$

where $\delta\sigma$ is estimated in megapascals (1 MPa = 10 Bar) and D is measured in micrometres (μm); the constant B and the exponent c have been given the following values:

B	c	ref.
603	-0.68	Twiss (1977)
381	-0.71	Mercier et al. (1977)

Application

Recrystallised grain sizes (from 'matrix') were measured for several samples collected from the Loch Skerrols thrust zone. The grain size was calculated as follows:

Mutually perpendicular longest and shortest intercepts on each grain (D_{i1} and D_{i2}) were measured in thin sections under an optical microscope and using a micrometer ocular. The geometric mean of D_{i1} and D_{i2} for each grains is averaged to give an estimate of the grain intercept in each of the two orthogonal thin sections cut from a specimen. Thus,

$$D_j = \frac{1}{n} \sum_{i=1}^{n} (D_{i1} D_{i2})^{\frac{1}{2}} \qquad (4.2)$$

where n is the number of grains measured in each thin section. The geometric mean of D_j's obtained from two mutually perpendicular thin sections is taken as the grain size (D). Although the method of grain-size measurement described above is arbitrary, for small aspect ratio of the grains (see Fig. 4.4) the grain size determined as above would be close to one calculated following a method of linear intercepts (Smith and Guttman 1953).

The differential stress values corresponding to samples collected at decreasing distances from the western boundary of the Jura Quartzite in An Carn area are shown in Table 4.2.

Although the samples correspond to different strain intensities across the Loch Skerrols thrust zone, the grain-size of the dynamically recrystallised quartz grains remains more or less the same along the traverse (Table 4.2). It may be inferred then that the differential stress did not vary much across the thrust zone. The average value of the palaeostress in the Loch Skerrols thrust zone is 54.87±3.46 MPa (calculated using equation (4.1), B and c values of Twiss (1977).

Comparison with other thrust belts

Using quartz grain-size values of Christie (1963) Twiss (1977) obtained palaeostress values of 50-130 MPa in the Moine Thrust zone. Weathers et al. (1979) determined palaeostress from deformation induced microstructures of the Moine Thrust zone from near Knockan Crag, Stack of Glencoul and the Loch Eriboil area. Determinations from grain-size in recrystallised quartz gave values of 45-56 MPa (calculated using B and c values of Mercier et al. 1977, see Eqn. (4.1)). The stress values

Table 4.2 Dynamically recrystallised quartz grain-size and palaeostress in a traverse across the Loch Skerrols thrust

Specimen location	Average grain size (μm)	Differential stress (MPa) (a) Twiss (1977)[1]	Mercier et al. (1977)[2]
87	29.47	60.41	34.49
86	35.68	53.05	30.11
85	31.19	58.12	33.13
84	33.66	55.19	31.38
83	36.81	51.92	29.44
82	38.30	50.55	28.63

(a) See text for values of B and c in Eqn. (4.1)

1 Average = 54.87±3.46

2 Average = 31.20±2.26

obtained from the Loch Skerrols thrust zone are in the lower end of the range of values for those in the Moine Thrust zone quoted above. Note that a southward decrease in the value of $\delta\sigma$ has been reported by Weathers et al. (1979). Comparable magnitudes of $\delta\sigma$ (using quartz grain-size palaeopiezometer) have been estimated from other shear zones where a ductile deformation mechanism prevailed (Kohlstedt and Weathers 1980, Twiss 1977, White 1979).

4.4 STRAIN ANALYSIS

4.4.1 Background and Methods

Two-dimensional (2-D) strain was determined for each of the three mutually perpendicular thin sections cut from hand specimens of Jura Quartzite collected at decreasing distances from the Loch Skerrols thrust (for practical purposes the western boundary of the outcrop of the Jura Quartzite is taken as within a few metres of the thrust line).

2-D strain ratios were obtained using the R_f-ϕ method (Dunnet 1969, Ramsay 1967, see Fig. 4.6 for actual plots). These strain values were cross checked using a second method - a method developed by Robin (1977), which uses strain markers of any shape including elliptical ones. Details of the methods are given in Appendix 4A and 4B. The magnitudes of the strain determined by the two methods do not differ by more than 15 per cent on an average for the measured samples. Orientations of the principal strain axes from the two methods are within a few degrees of each other. The difference is probably due to the fact that the application of R_f-ϕ method (Dunnet 1969) requires a subjective fitting of curves around a cluster of points through successive approximations.

The assumptions involved in the methods of strain determination used here are:

1. The rock underwent negligible volume change during deformation.

2. Viscosity contrast between coarse quartz grains ('clasts' used as strain markers) and the surrounding smaller quartz grains ('matrix') is insignificant.

3. Strain is homogeneous on the scale of the hand specimen.

4. The 'clasts' were initially ellipsoidal without any significant preferred orientation with respect to any of the ellipsoid axes.

Under the ambient geologic conditions, the first three assumptions above seem reasonable and no attempt was made to test them. The hypothesis of initial randomness (assumption '4' above) has been tested using methods outlined by Peach and Lisle (1979) and Robin (1977). In principle, once the 2-D strain ratio is determined using one or the other method, the set of markers can be 'undeformed' knowing that the initial shape and orientations are functions of the final shape, orientation and finite strain ratio. The strain is assumed to be irrotational. The initial orientations of the marker axes are then grouped into a number of classes and the frequency in each class is determined. For two-thirds of the samples measured the deviation from an initial isotropy is not statistically significant to reject the null

hypothesis. Details of the results of the test for initial isotropy are given in Appendix 4C.

Technique of shape measurement

Three mutually perpendicular thin sections were cut from each specimen. Where possible one of these thin sections was cut subparallel to lineation and perpendicular to foliation in the specimen. The reference directions were defined by the lines of intersections of the three orthogonal sections. The long and short diameters of the 'clasts' were measured under an optical microscope using a micrometer ocular; fluctuation of the long axis from the reference direction was obtained from the amount of stage rotation necessary to bring the long axis parallel to the reference direction. The 'clasts' are single grains of quartz which have undergone plastic deformation with varying degrees of dynamic recrystallisation. With increasing strain the peripheral subgrains progressively evolve into recrystallised small new grains (Nicolas and Poirier 1976, White 1976). The dynamic recrystallisation may lead to some alteration of the shape of the 'clasts' and introduce a bias in measurement particularly at a very high 'matrix'/'clast' ratio. However, even in the highly strained specimens, the outline of even a thoroughly recrystallised 'clast' can sometimes be recognised in plane polarised light due to the concentration of pigments or white mica along the original grain boundary.

Three-dimensional strain

The 2-D strain ratios on three mutually perpendicular sections have been combined to obtain the magnitude and orientation of three-dimensional (3-D) strain following a method proposed by Ramsay (1967). Ramsay suggested use of a desk calculator to solve the equation

$$\lambda'^3 - J_1\lambda'^2 + J_2\lambda' - J_3 = 0 \qquad (4.3)$$

which gives the relationship between the strain invariants (J_i, i = 1,3) and the principal reciprocal quadratic elongations (λ'_i, i = 1,3) in 3-D. To expedite the strain calculations an algorithm has been developed for:

(a) calculating the strain invariants (J_i, i = 1,3) from 2-D strain ratios on three orthogonal sections and the orientation of the 2-D principal strain with respect to the reference directions,

(b) a numerical solution of Eqn. (4.3) to obtain principal quadratic elongations, and

(c) orientation of the 3-D principal quadratic elongations.

Fortran programs RFPHI, RFPLOT and ROBIN were written for 2-D strain determinations. A fortran program LAMBDA implements the above algorithm for 3-D strain measurement (see Appendix 4D).

4.4.2 Specimen Locations

The locations of specimens used in strain measurement are shown in Fig. 4.5. The specimen localities numbered 82, 83, 84, 85, 86 and 87 are roughly on a traverse at right angles to the ground trace of the Loch Skerrols thrust. Specimens numbered 431, 433, 434, 435 come from the stretch of ground between Loch Sibhin and Loch Leathan. Specimen numbered 438 comes from near Bun-an-uillt on the shore of Loch Gruinart where the ground trace of the thrust is roughly E-W. Except for specimen 438 (which may be derived from Bowmore Sandstone), the specimens belong to Jura Quartzite. All specimens (except 438) have a feldspar content less than 1 per cent; specimen 438 has a higher proportion of feldspar clasts. Although the Jura Quartzite as a whole is much less feldspathic than the Bowmore Sandstone, between Crois Mhor and Gortantoid Point exposures of Jura Quartzite shows feldspar clasts approaching 0.5-1.0 cm in diameter. For the purpose of measurements only quartz clasts were considered.

4.4.3 Strain Parameters and their Values

The magnitudes of the three principal quadratic elongations are denoted by λ_i (i = 1,3). Principal natural strain parameters (G_i, i = 1,3) are calculated from λ_i, using the equation

$$G_i = \frac{1}{2}\ln(\lambda_i) \qquad (4.4)$$

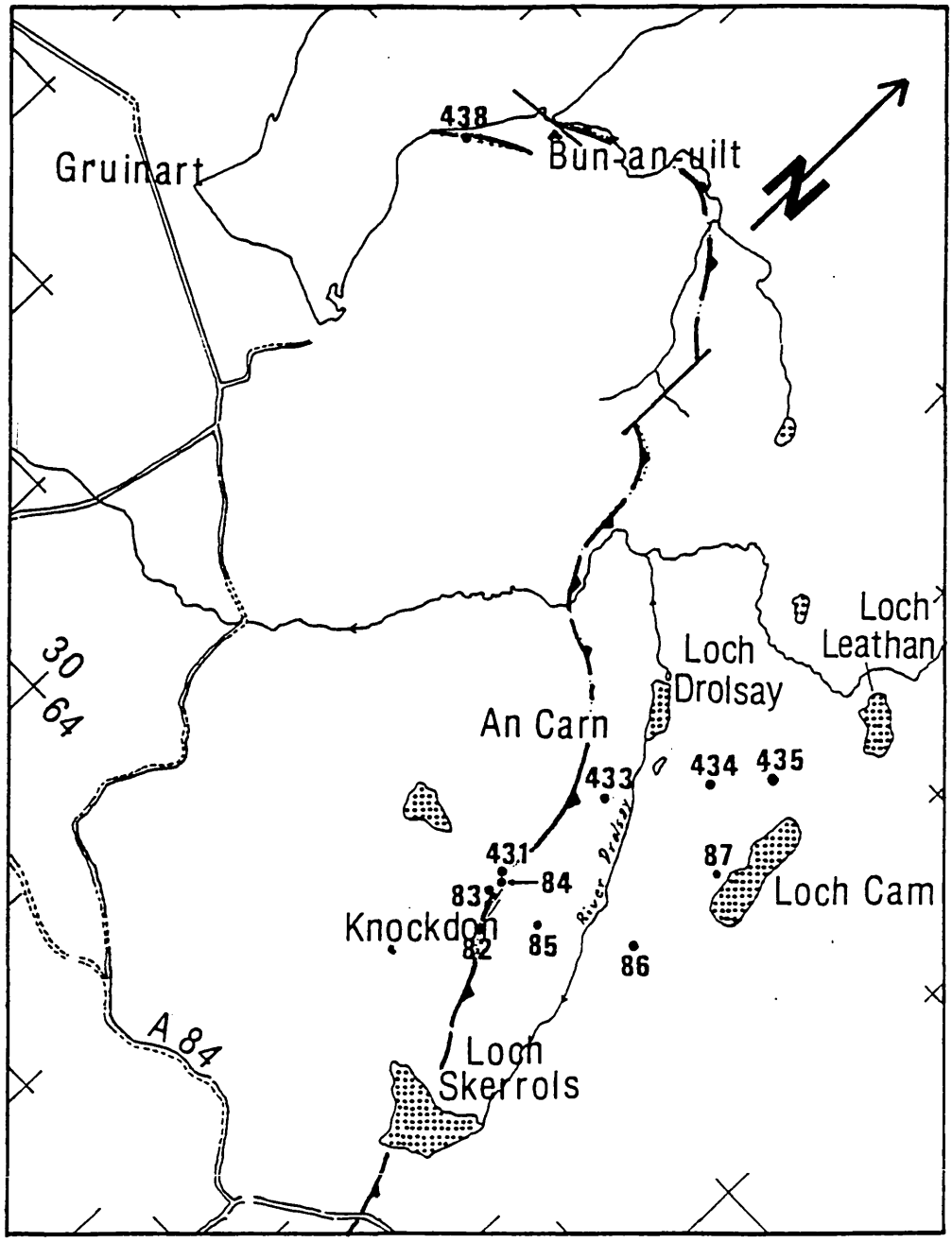


Figure 4.5. Localities of specimens of Jura Quartzite used for strain and fabric measurements.

Finite strain can be conveniently described in terms of a parameter proportional to the natural octahedral unit shear and termed strain intensity, e_s, where

$$e_s = \frac{1}{\sqrt{3}} / [(e_1-e_2)^2 + (e_2-e_3)^2 + (e_3-e_1)^2]^{\frac{1}{2}} \qquad (4.5)$$

from Miller and Christie (1981). Nadai (1963) derived the expression for the strain intensity parameter; it is proportional to the distortion of the strain ellipsoid and is useful for comparing states of strain with varying shapes of the strain ellipsoid. Moreover, the strain energy for both infinitesimal and finite strains in elastic or rigid-plastic solids can be shown to be a function of the octahedral unit shear (Nadai 1963).

The shape of the strain ellipsoid is conventionally given by the Flinn parameter, k, where

$$k = \frac{(\lambda_1/\lambda_2)^{\frac{1}{2}} - 1}{(\lambda_2/\lambda_3)^{\frac{1}{2}} - 1} \qquad (4.6)$$

On the other hand, Lode's parameter, gives the shape of the strain ellipsoid in terms of the natural strains (Hossack 1968, Miller and Christie 1981),

$$\nu = 2[(e_2 - e_3)/(e_1 - e_3)] - 1 \qquad (4.7)$$

The advantage of using Lode's parameter, ν instead of Flinn parameter, k is the fact that for all possible ranges of strain ellipsoid shape, the domain of k is given by $0 \leq k \leq +\infty$, whereas that of ν is given by $+1 \geq \nu \geq -1$.

The axial ratios of 3-D strain ellipsoids for the specimens from Loch Skerrols thrust zone are shown on a conventional Flinn plot in Fig. 4.6a and on ν-e_s plot in Fig. 4.6b. Notice that the strain intensity is higher in specimens close to the thrust line (see Fig. 4.5 for specimen locations). Higher strain-intensity is recorded in specimens 82, 83, which microstructurally approaches a mylonite. Recall that the proportion of 'matrix'/'clast' also increases with increasing e_s.

Figure 4.6. Strain values from Loch Skerrols thrust zone.

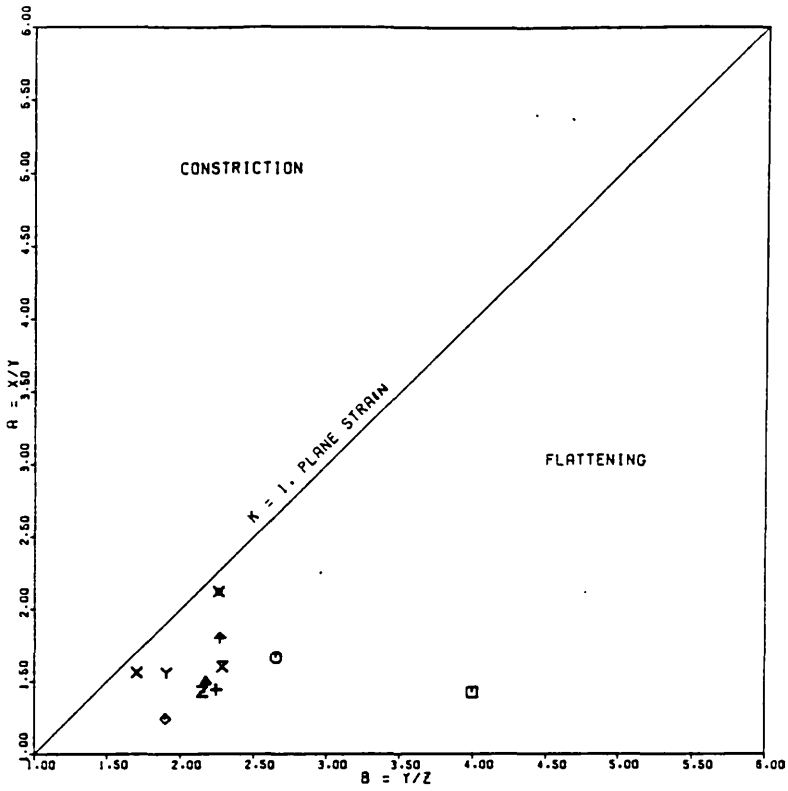
(a) 3- dimensional strain values on Flinn plot.

(b) Strain Intensity (E_s) vs. shape factor (Lode's parameter, V) plot. Note all strain values are in the flattening field.

(c) R_f-ϕ plots for each of the three orthogonal sections cut from each specimen. The loci of $R_f=F(\phi)$ for fixed R_i's shown in each plot. The values of R_i's are as given below. 2-dimensional strain ratio corresponding to each plot is given below the specimen no.

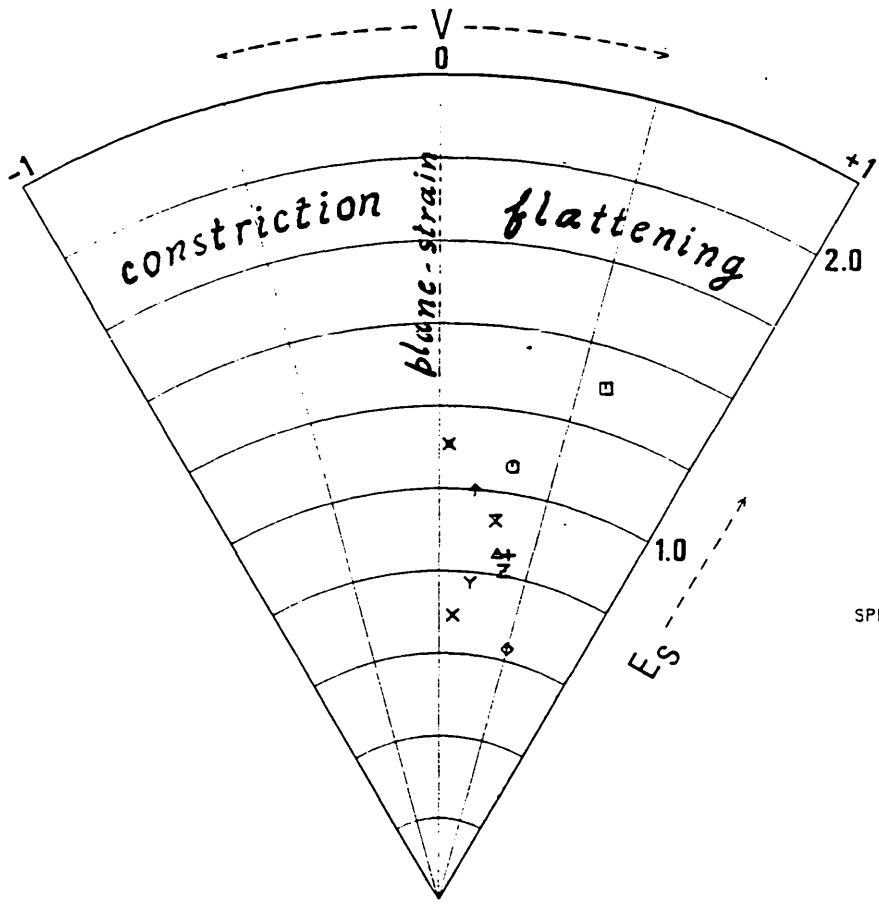
Sp.No.	R_i's	n	Sp.No.	R_i's.	n
82A	2.5,3.3	66	431A	1.7,2.4,3.1	120
82B	1.9,2.9	69	431B	1.5,1.9,2.2	120
82C	1.3,2.0,2.8	50	431C	1.5,2.0,2.5,3.2	120
83A	1.6,2.0,2.4	74	434A	1.6,2.3,2.9	120
83B	2.4,3.6	73	434B	1.5,2.0	122
83C	1.5,2.2,3.6	55	434C	1.5,2.0,2.8	120
84A	1.5,2.1	67	435A	1.6,2.0,2.4	82
84B	1.6,2.3,2.7	80	435B	1.5,1.8,2.7	120
84C	1.3,2.0,2.6	90	435C	1.4,1.9,2.6	64
85A	1.5,1.9,2.6	70	438A	2.4,3.6	122
85B	1.5,2.1,2.5	84	438B	1.5,1.9,2.2,2.6	120
85C	1.5,2.0,2.8	90	438C	1.5,2.1,2.8	120
86A	1.4,1.6,1.9	91	433A	1.8,2.2,3.0	120
86B	1.5,1.8,2.2	90	433B	1.5,1.8,2.2,2.5	120
86C	1.5,1.9,2.1	90	433C	1.5,2.0,2.6	91
87A	1.5,1.8,2.2,2.7	90			
87B	1.4,1.7,2.2	91			
87C	1.3,2.0,2.6	90			

A



SPECIMEN NO.	SYMBOL
82	⊡
83	⊙
84	△
85	+
86	×
87	◇
431	✦
433	⋈
434	Z
435	Y
438	⋈

B



SPECIMEN NO.	SYMBOL
82	⊡
83	⊙
84	△
85	+
86	×
87	◇
431	✦
433	⋈
434	Z
435	Y
438	⋈

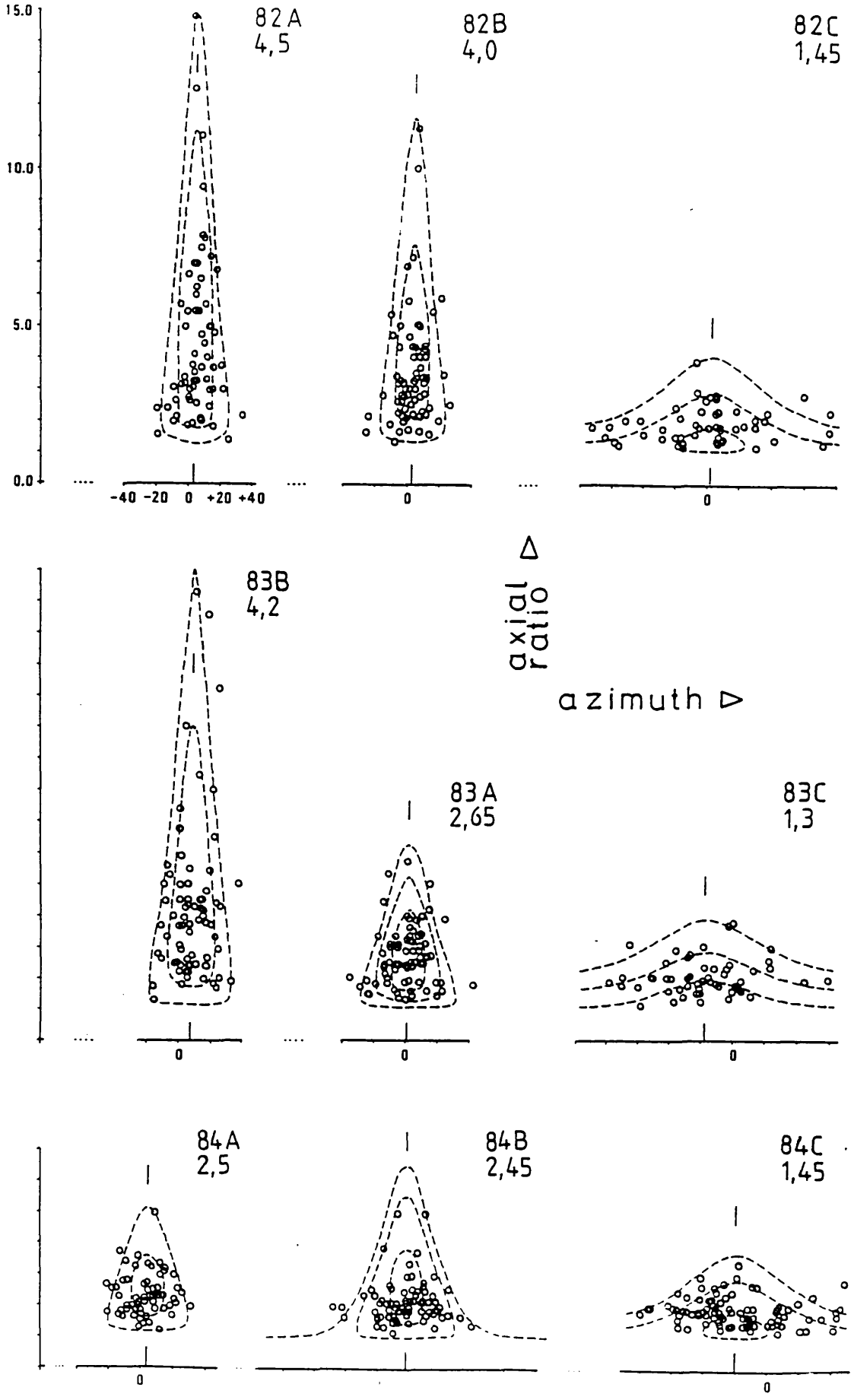

15.0
10.0
5.0
0.0
82A
4,5
82B
4,0
82C
1,45
-40 -20 0 +20 +40
0
0
axial ratio Δ
azimuth ▷
83B
4,2
83A
2,65
83C
1,3
84A
2,5
84B
2,45
84C
1,45

FIGURE 4.6C

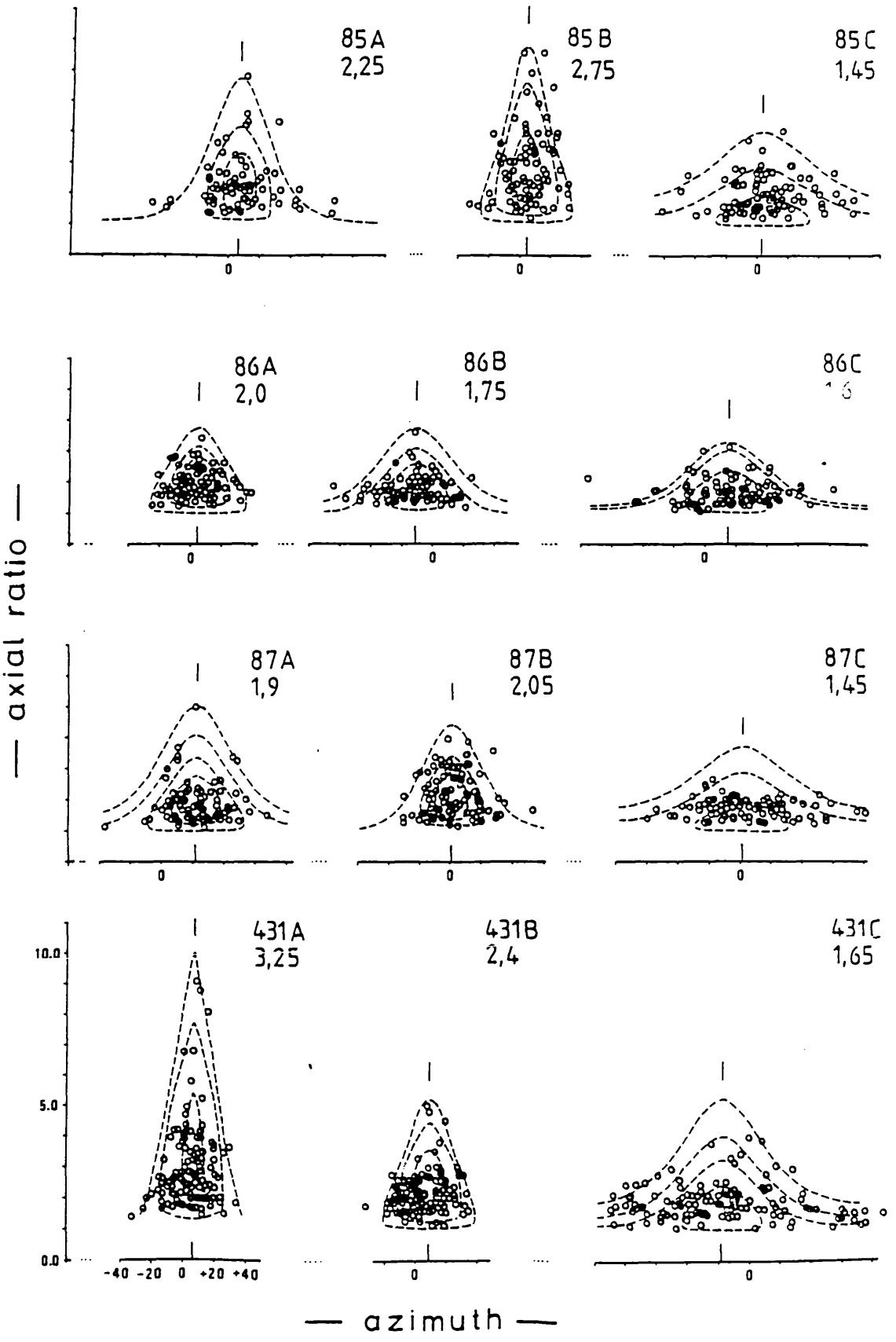


Fig. 4.6C contd.

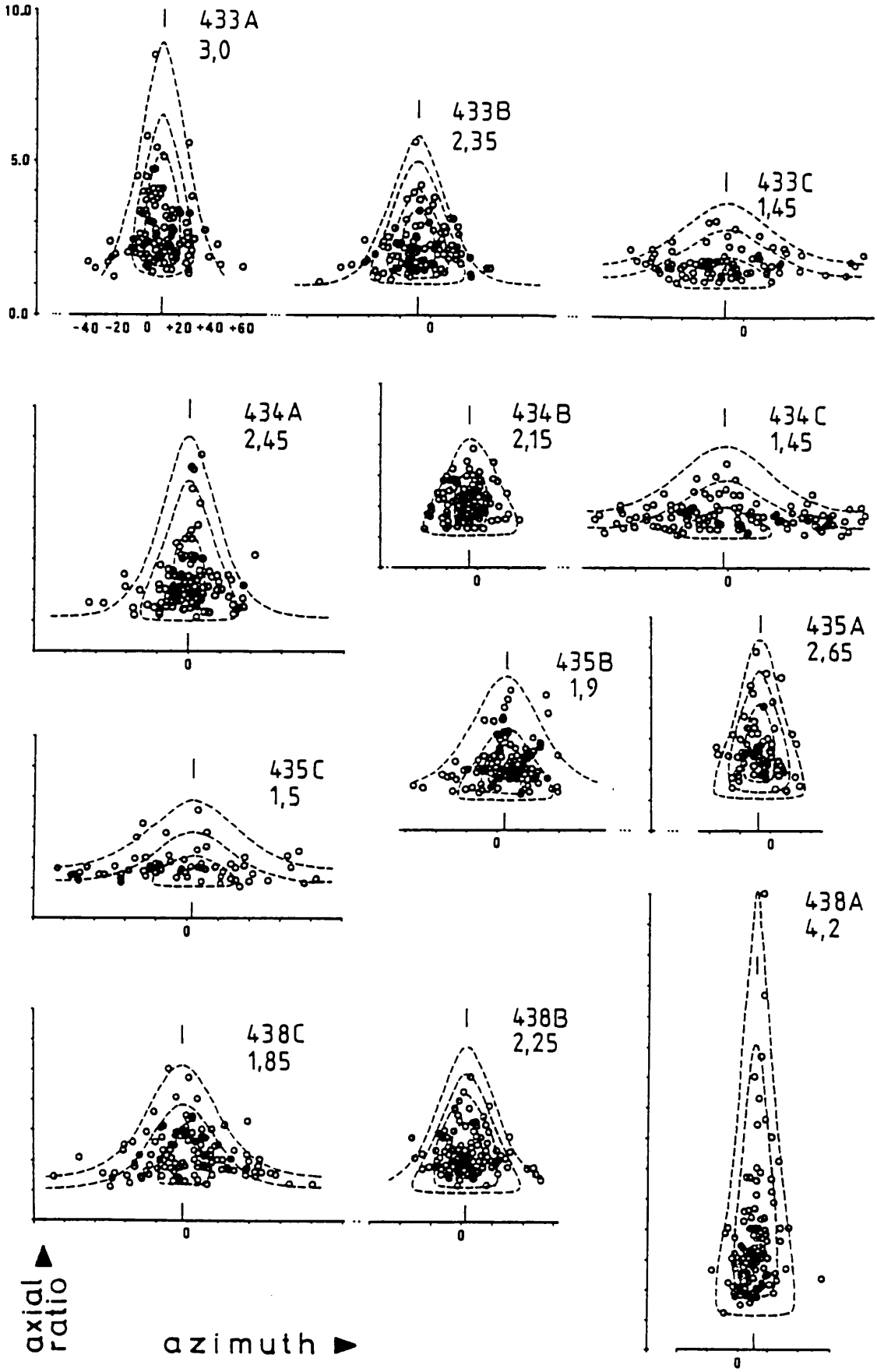


Fig. 4.6C contd.

Values of principal natural strain parameters for the measured specimens are shown in Table 4.3.

It is interesting to note that although the specimens come from a thrust zone, the finite strain ellipsoids as determined from grain shape measurement fall in the flattening field ($0<k<1$; $1>v>0$). However, there is no one to one correspondence between G_s and v values, i.e. specimens with higher G_s values do not necessarily have higher v value. In fact specimen 438 with an $G_s \sim 1.108$ has a fairly low value of $v(\sim 0.04)$ indicating that the strain-ellipsoid is closer to the plane strain field ($v = 0$). The question of the shape of the finite strain ellipsoid in the Loch Skerrols thrust zone will be discussed later.

4.4.4 Orientation of the Finite Strain Ellipsoid

Orientation of the principal quadratic elongations $(\lambda_1, \lambda_2, \lambda_3)$ are shown in the equal plot of Fig. 4.7. There is a considerable spread in the orientations of the strain axes. However, in the studied specimens the λ_1-λ_2 plane is close to the plane of foliation in the hand specimens (see Fig. 4.2 for the orientation of foliation and lineation in the thrust zone. λ_1 orientations cluster in the SSE quadrant, the value of plunge being less than 20 degrees; similar orientation of the mineral elongation lineation suggests that the lineation is probably related to the thrust movement and associated finite strain. The spread in orientation of λ_1, etc. is partly due to the sinuous course of the Loch Skerrols thrust, which has been locally reoriented due to late folding.

4.4.5 Displacement Across the Thrust Zone

The finite strain values described above are based on grain shape measurements. Optical strain features show that the changes in grain shape is caused by intracrystalline slip in quartz. Thus the measured strain gives only the component of total strain accommodated by intracrystalline slip. A minimum estimate of the displacement across the Loch Skerrols thrust can be made by considering the shear strain associated with the finite strain ellipsoid. Being restricted by the poor exposure in the area, only four specimen localities numbered 82, 85, 86 and 87 are chosen for shear strain calculations; these locations

Table 4.3 Table of strain values, Loch Skerrols thrust zone

Sp. No.	Axial ratio X : Y : Z			Natural strains ϵ_1	ϵ_2	ϵ_3	Strain intensity ϵ_s	Shape υ	k
82	1.43	1	0.25	0.70	0.34	-1.04	1.301	0.593	0.142
83	1.66	1	0.38	0.66	0.16	-0.82	1.065	0.316	0.403
84	1.50	1	0.46	0.53	0.12	-0.65	0.849	0.314	0.428
85	1.44	1	0.45	0.51	0.15	-0.66	0.852	0.376	0.357
86	1.56	1	0.59	0.48	0.03	-0.50	0.693	0.088	0.801
87	1.24	1	0.53	0.36	0.14	-0.50	0.629	0.497	0.269
431	1.80	1	0.44	0.66	0.08	-0.74	0.999	0.164	0.633
433	1.60	1	0.44	0.59	0.12	-0.71	0.929	0.276	0.468
434	1.43	1	0.47	0.49	0.14	-0.63	0.812	0.362	0.375
435	1.56	1	0.53	0.51	0.07	-0.58	0.774	0.183	0.619
438	2.12	1	0.44	0.77	0.02	-0.79	1.108	0.040	0.891

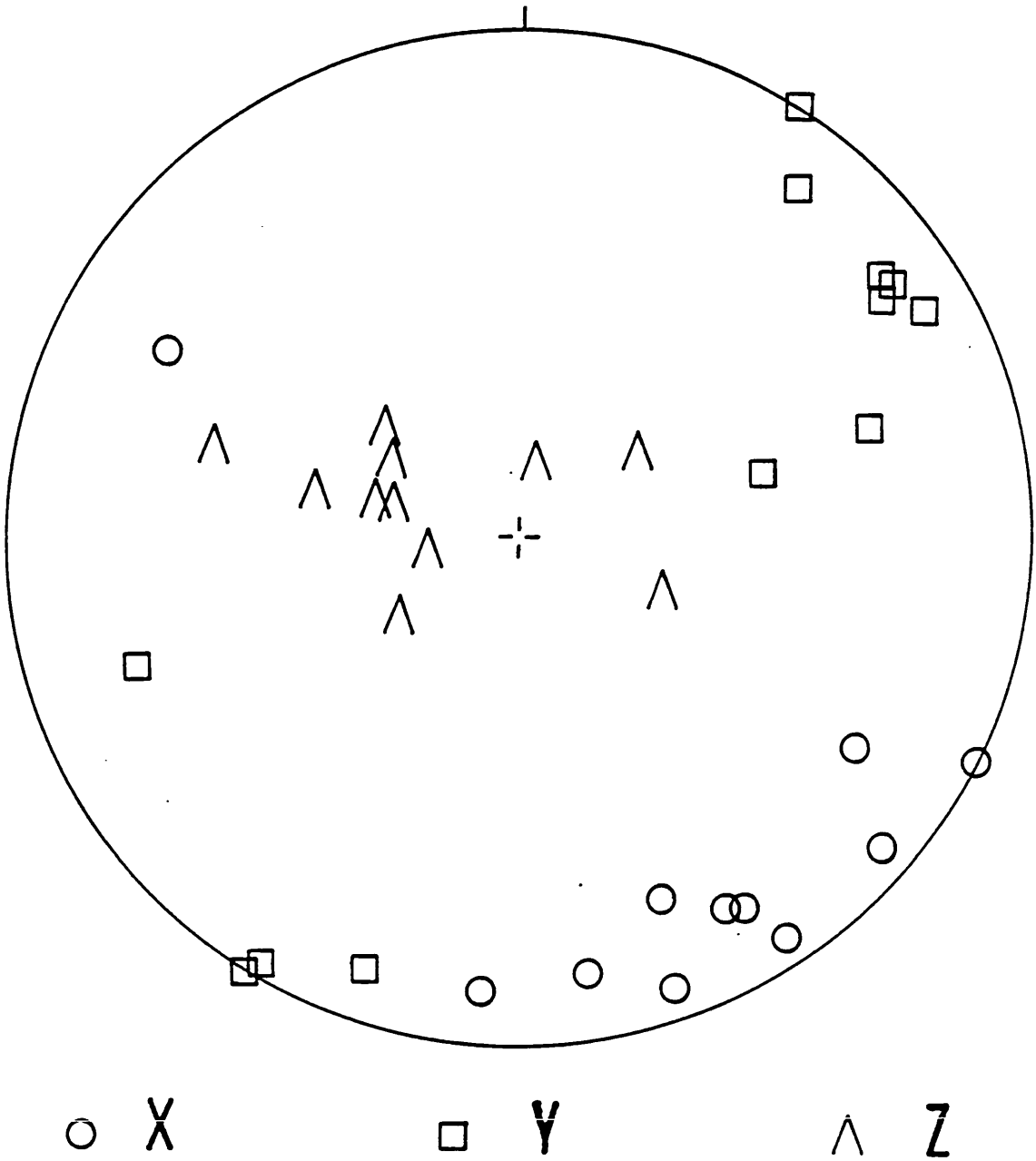


Figure 4.7. Equal-area plot showing the orientation of principal 3-dimensional strains in the Loch Skerrols thrust zone. X,Y,Z corresponds to λ_1, λ_2, λ_3 respectively.

are roughly on a traverse at right angles to the thrust line north of Loch Skerrols. The orientations of the thrust zone foliation and the λ_1-λ_2 plane of finite strain ellipsoid for these specimens is fairly close. The λ_1 direction is close to the elongation lineation. Thus the λ_1-λ_3 plane have the maximum likelihood of containing the movement direction associated with the thrust. Knowing that the displacement at each specimen locality is proportional to the maximum shear strain on λ_1-λ_3 plane, the total displacement across the thrust zone ($\approx$ a shear zone) can be obtained by integrating the displacement over the width of the zone (Ramsay and Graham 1970). Applying the principle, the displacement on a WNW-ESE profile of the Loch Skerrols thrust zone is calculated on an approximate basis (Fig. 4.8). The estimated thrust displacement north of Loch Skerrols is ~1.7 kms. It must be emphasised here that the displacement as approximated above gives only part of the thrust movement accommodated by intracrystalline slip, and does not take into account (a) components of total strain accommodated by other possible deformation mechanisms (see Borradaile 1979) and/or (b) hidden slide zones. Geological arguments favour a much larger displacement across the Loch Skerrols thrust to bring the Dalradian Jura Quartzite in contact with the Bowmore Sandstone which in many ways resemble the foreland Torridonian. Thus hidden zones of fault displacement (slide zone) in the area cannot be ruled out.

4.5 QUARTZ C-AXIS FABRIC

4.5.1 Fabric Measurement and Representation

The specimens used for fabric measurement belong to the same set used for strain determinations (see Section 4.4.2). The orientations of quartz C-axis were measured by standard universal stage techniques (Fairbairn 1949, Turner and Weiss 1963). For some of the specimens (nos. 82, 83, 84, 85, 86 and 87), C-axes were measured in each of two mutually perpendicular thin sections. Necessary rotations were implemented before comparing fabric diagrams obtained from data coming from separate thin sections (see Appendix 4E). This helps to a large extent to test the reproducibility of the diagrams. In each thin section 400 'matrix' quartz C-axis were measured; parts of the thin section containing relatively high proportion of mica are avoided, so that we are dealing essentially with a monomineralic fabric. In some of

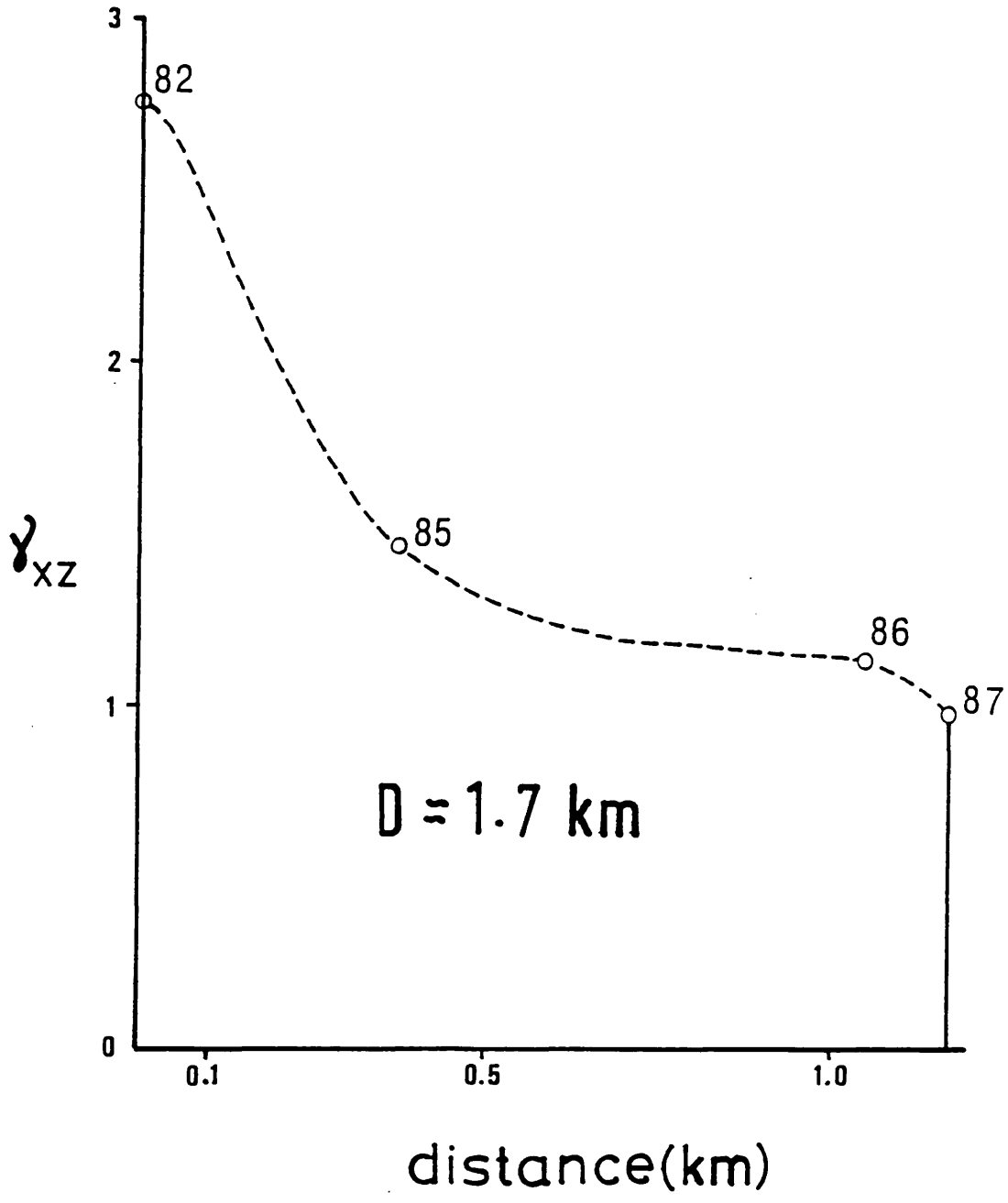


Figure 4.8. An approximation of displacement (D) across the Loch Skerrols thrust. Only the component of total strain accommodated by intracrystalline slip is taken into account.

the specimens orientations in 'clasts' were measured in addition, and plotted separately. Because of intracrystalline strain, most 'clasts' show undulose extinction, deformation bands and optical subgrains. Separate measurements were taken for different subgrains within a single 'clast'.

The preferred orientation of quartz C-axis are depicted in lower-hemisphere equal-area projections and contoured in multiples of expectation for uniform distribution. Briefly, the contouring method adopted here involves choosing a count-volume such that the expected number of poles (E) within the volume is three times the standard deviation of the number of poles that will actually fall in the area for a randomly distributed population (Kamb 1959). In the contoured pole-figure diagrams point-densities below 1 x E are suppressed. The conversion of raw-data and estimation of point-density are done by a Cyber 174 computer. A Fortran program was written for this purpose (see Appendix 4F). The program determines the size of the count-volume from the size of the sample (number of C-axis measured) and then counts the number of poles within the count-volume as the counter moves over an a priori selected grid. The numbers of poles counted at each grid-intersection are expressed as multiples of E, and printed on to an equal area plot.

4.5.2 The Fabric Pattern

As stated earlier, the 'matrix' grains and 'clasts' were measured separately for C-axis orientations. For some of the specimens measurements were made on two mutually perpendicular thin sections. In these cases, the two fabric diagrams are given different specimen no. (e.g. numeric strings '8701' and '8702' refer to two mutually perpendicular thin sections cut from the same specimen collected from location numbered 87). All C-axis orientations were rotated prior to contouring so that in individual fabric diagram the foliation trace is N-S and the mesoscopic lineation (down-plunge direction) is towards north; the structural top of the foliation is towards east (right) unless otherwise mentioned. The orientations of the principal axes of the strain ellipsoid (X, Y, Z; X>Y>Z) are also shown relative to foliation and lineation. The fabrics are described in factual terms in thiS section; interpretations are discussed in Section 4.5.3.

4.5.2.1 'Matrix'

Figure 4.9 shows quartz C-axis fabrics corresponding to specimen locations 82, 83, 84, 85, 86, 87, 431, 434, 435 and 438. Included here is also a specimen numbered CDTLSTX which comes from Bun-un-uillt area. Microstructurally it is a quartz-mica-mylonite; an advanced stage of dynamic recrystallisation makes it impossible to measure 'clasts' for grain shape fabric (hence strain values are not available).

For less deformed specimens ($0.85<G_s<0.63$; specimens 87, 86 and 84) the fabric pattern is rather diffuse. However, there is one or more point maximum (2-3 x E) lying on or close to the XZ plane (Fig. 4.9a-f). On this plane, the maximum is nearer to Z than to X. In specimens '8701' and '8401' the maxima are placed more or less symmetrically on either side of Z. In each of these specimens, the XY plane, particularly in the direction X, is associated with a very low concentration of poles.

In more deformed specimens ($1.1<G_s<0.85$; e.g. specimens 83, 85) a cross girdle pattern is apparent. The point maxima (3-4 x E) are on the XZ plane as before but the girdles intersect along Y. One of these two girdles is at a smaller angle to the YZ plane and better developed than the other. X is either pole free or associated with a very low concentration of poles. The maxima are within 30-40 degrees of Z. A submaximum is close to Y in fabric diagrams correspond to specimens '8301', '8302', '435' and '4342' (see Figs. 4.9 g-j,n,o).

In the highly deformed specimens ($G_s>1.1$; specimens 82 and 438) the fabric pattern is close to the type-I cross-girdle (Lister and Williams 1979) with point-maxima (3-5 x E) still on the XZ plane; the angle between Z and the point-maximum is less than 20 degrees. The fabric is marked by an internal asymmetry with unequal development of the two girdles (Figs. 4.9 k,l,q).

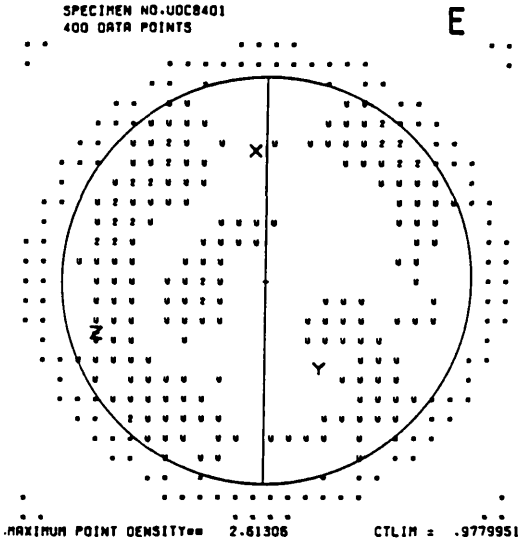
In CDTLSTX, there is an incomplete single-girdle pattern with point-maximum subnormal to the foliation (Fig. 4.9r). Assuming that the foliation represents the XY plane of the strain ellipsoid, the point maximum is within 15 degrees of Z; the offset is in the same sense as that of the better developed girdle in specimen 82.

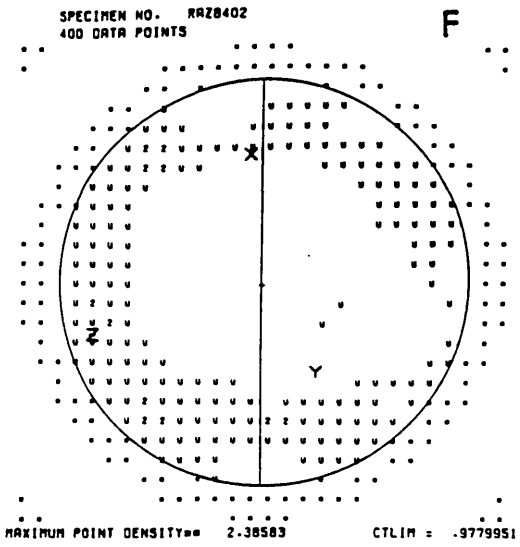
Figure 4.9. Quartz C-axis fabric in 'matrix' (a-r). In each fabric diagram X,Y,Z refer to the axes of principal finite strain (X>Y>Z); relative orientation of foliation and lineation is as shown in (s). Point-densities estimated in multiples of expectation for uniform distribution. CTLIM is inversely proportional to the count-volume. For detailed description of fabric diagrams see text. In more deformed quartzites the fabric pattern approximates a type-I cross-girdle.

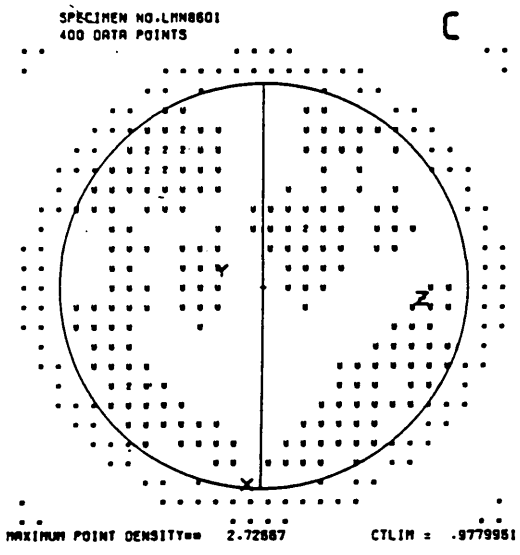
(s) Relative orientation of foliation and lineation in the fabric diagrams (a)-(r). Deduced sense of shear is indicated.

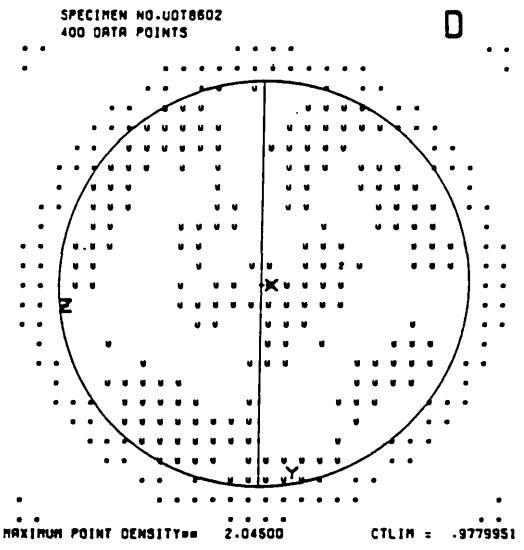
(t) A type-I cross-girdle fabric, after Lister and Williams (1979).

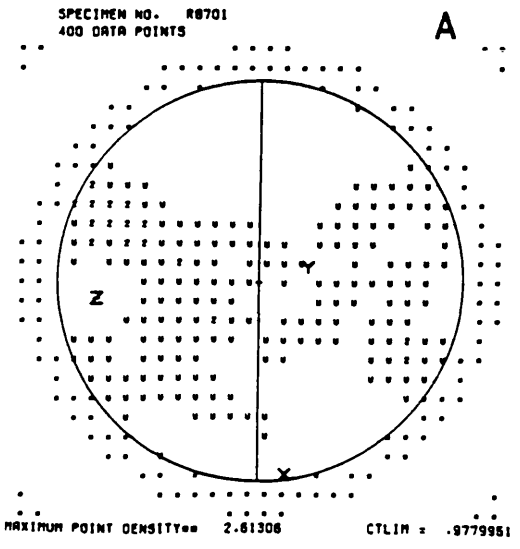
Point-density values corresponding to print-symbols within the fabric diagrams are tabled to the left of Fig. 4.9(t).

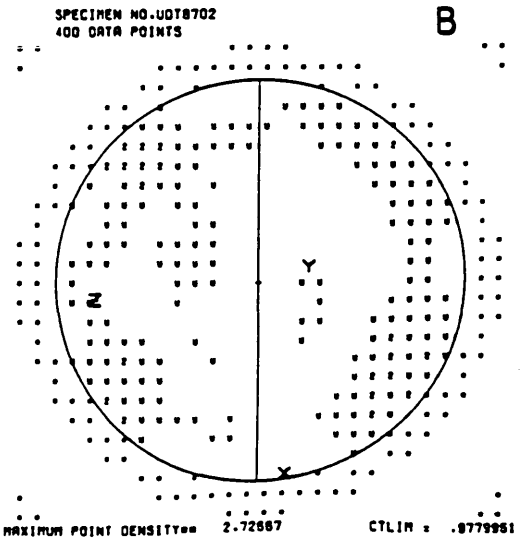

SPECIMEN NO.UOC8401
400 DATA POINTS
E
X
Z
Y
MAXIMUM POINT DENSITY= 2.61306
CTLIM = .9779951

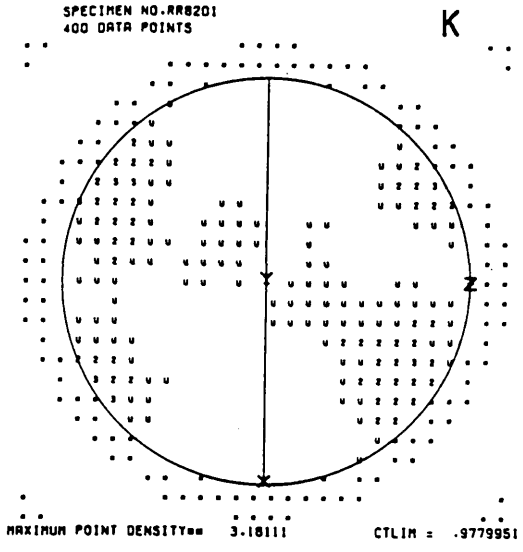

SPECIMEN NO. RRZ8402
400 DATA POINTS
F
X
Z
Y
MAXIMUM POINT DENSITY= 2.38583
CTLIM = .9779951

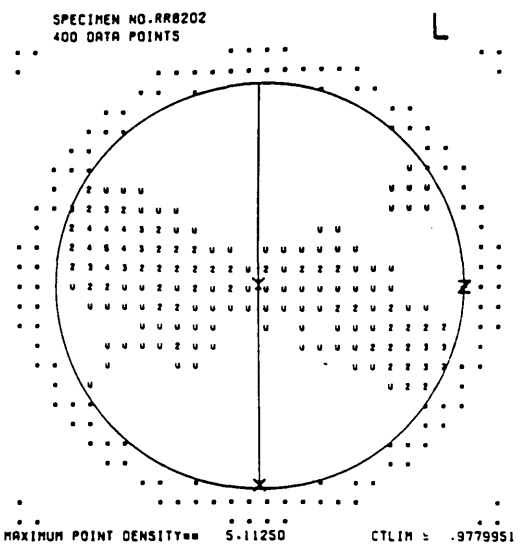

SPECIMEN NO.LMN8601
400 DATA POINTS
C
Y
Z
X
MAXIMUM POINT DENSITY= 2.72667
CTLIM = .9779951

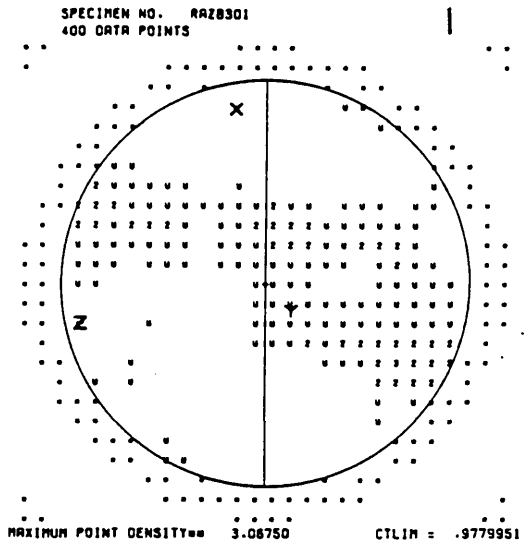

SPECIMEN NO.UOT8602
400 DATA POINTS
D
Z
X
Y
MAXIMUM POINT DENSITY= 2.04500
CTLIM = .9779951

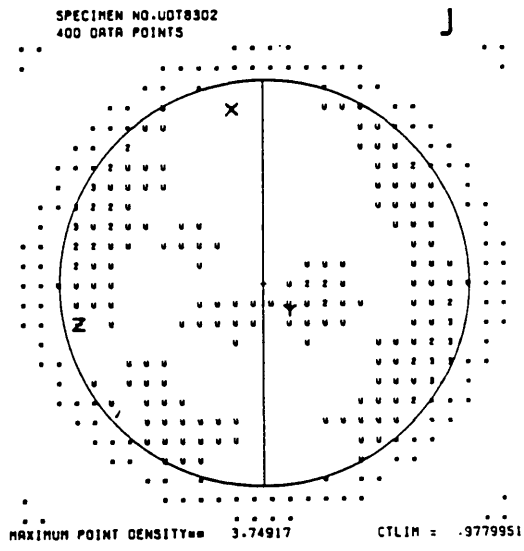

SPECIMEN NO. R8701
400 DATA POINTS
A
Z
Y
X
MAXIMUM POINT DENSITY= 2.61306
CTLIM = .9779951

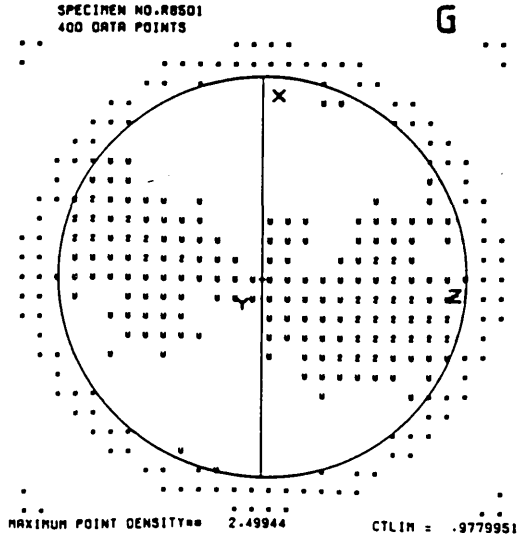

SPECIMEN NO.UOT8702
400 DATA POINTS
B
Z
Y
X
MAXIMUM POINT DENSITY= 2.72667
CTLIM = .9779951

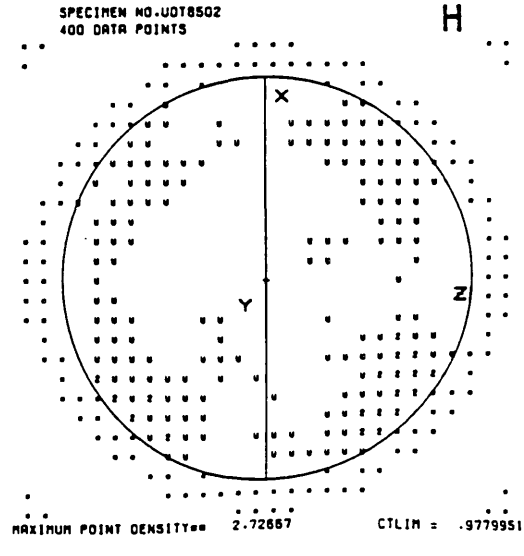

SPECIMEN NO.RR8201
400 DATA POINTS
K
MAXIMUM POINT DENSITY= 3.18111
CTLIM = .9779951


SPECIMEN NO.RR8202
400 DATA POINTS
L
MAXIMUM POINT DENSITY= 5.11250
CTLIM = .9779951

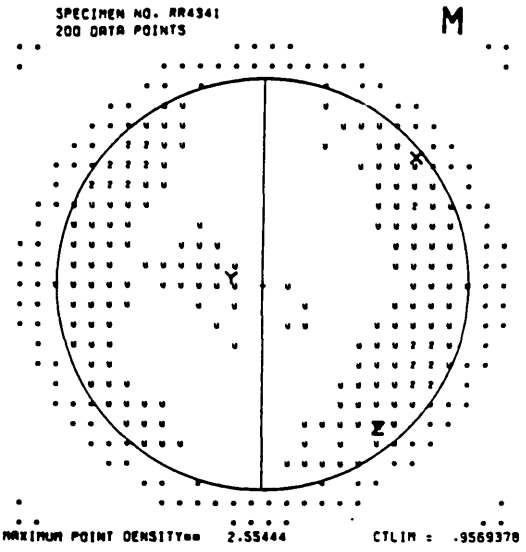

SPECIMEN NO. RAZ8301
400 DATA POINTS
I
MAXIMUM POINT DENSITY= 3.08750
CTLIM = .9779951

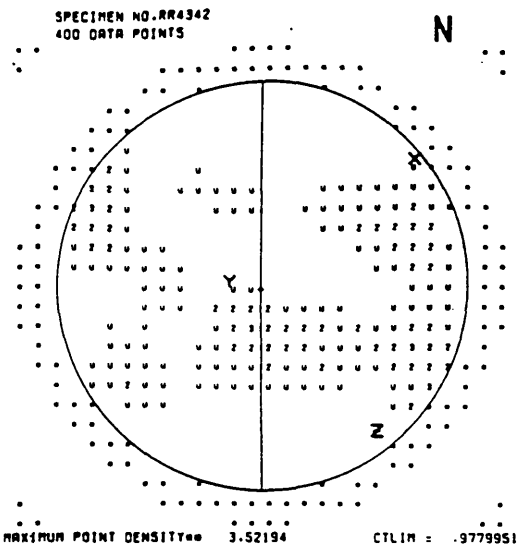

SPECIMEN NO.UOT8302
400 DATA POINTS
J
MAXIMUM POINT DENSITY= 3.74917
CTLIM = .9779951

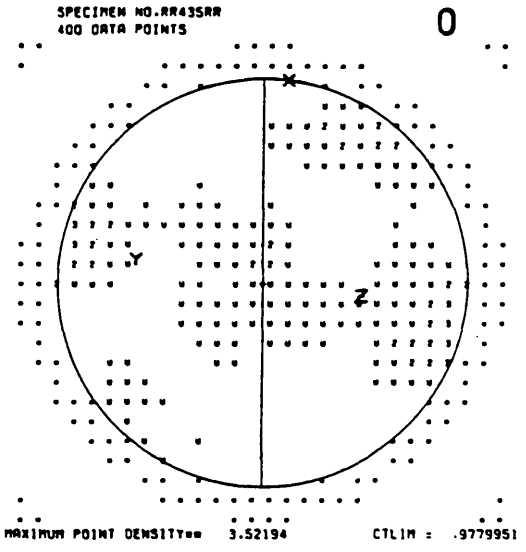

SPECIMEN NO.R8501
400 DATA POINTS
G
MAXIMUM POINT DENSITY= 2.49944
CTLIM = .9779951

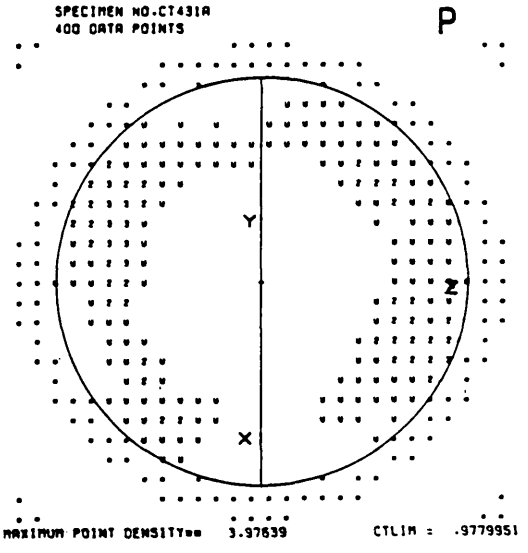

SPECIMEN NO.UOT8502
400 DATA POINTS
H
MAXIMUM POINT DENSITY= 2.72667
CTLIM = .9779951

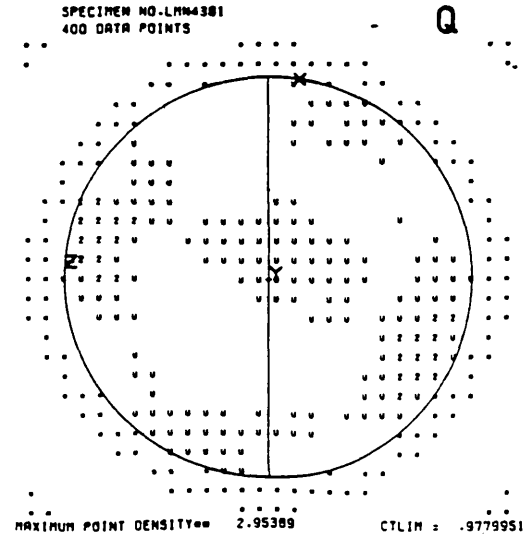
4.9 contd.

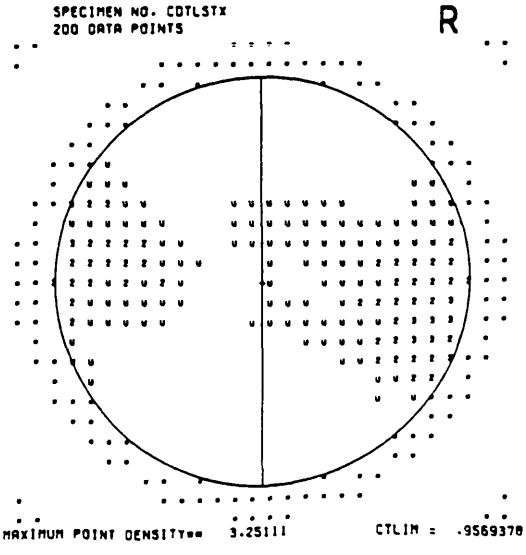

SPECIMEN NO. RR4341
200 DATA POINTS
M
MAXIMUM POINT DENSITY= 2.55444
CTLIM = .9569378


SPECIMEN NO.RR4342
400 DATA POINTS
N
MAXIMUM POINT DENSITY= 3.52194
CTLIM = .9779951


SPECIMEN NO.RR43SRR
400 DATA POINTS
O
MAXIMUM POINT DENSITY= 3.52194
CTLIM = .9779951


SPECIMEN NO.CT431A
400 DATA POINTS
P
MAXIMUM POINT DENSITY= 3.97639
CTLIM = .9779951


SPECIMEN NO.LMN4381
400 DATA POINTS
Q
MAXIMUM POINT DENSITY= 2.95389
CTLIM = .9779951


SPECIMEN NO. COTLSTX
200 DATA POINTS
R
MAXIMUM POINT DENSITY= 3.25111
CTLIM = .9569378

4.9 contd.

print symbol	point-density x uniform
U	1-2
2	2-3
3	3-4
4	4-5
5	5-6
6	6-7
7	7-8
8	8-9
9	9-10
A	10-11
B	11-12
C	12
H	above 12

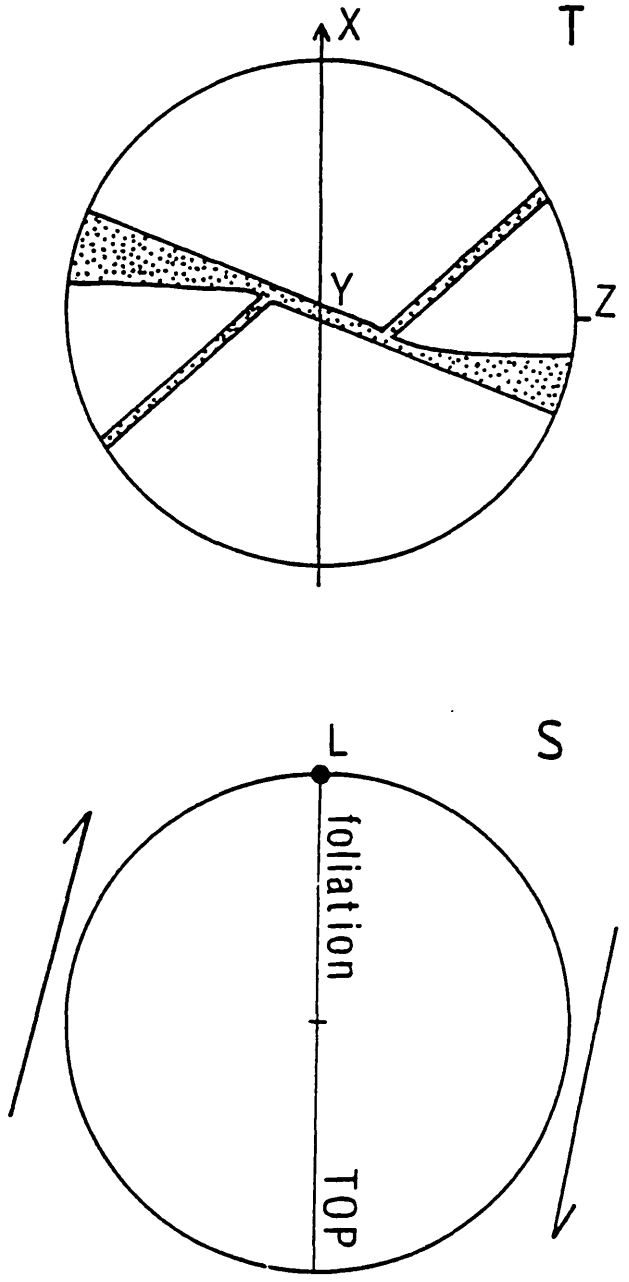


FIGURE 4.9 contd.

4.5.2.2 'Clasts'

The following observations on fabric patterns are based on single thin sections except for specimen 82. In less deformed specimens (e.g. '8601', '8502') up to 5 measurements are made on the same 'clast' to account for different subgrain orientations. In highly deformed specimens (e.g. '8301', '8201', '8202') up to 50 measurements probably correspond to one large 'clast', as the deformed porphyroclasts are marked by a subgrain structure; many of the subgrains have been rotated and dynamically recrystallised to new grains. Thus the effective sample size is smaller than in the corresponding 'matrix' fabric and the much higher point-maximum (9-11 x E) in the resulting fabric-diagrams reflect the influence of host-control. The fabric diagrams are shown in Fig. 4.10.

In '8601', a point-maximum is subnormal to the foliation. There is a right-lateral offset of the maximum with respect to foliation normal (Fig. 4.10a). In '8502', there are paired maxima one of which is stronger than the other; the maxima are on opposite sides of the foliation normal (Fig. 4.10b). Foliation top is towards west (left of the diagram) for '8502'. Both in '8502' and '8501', the foliation plane is associated with the least concentration of poles.

In '8301', paired maxima with a disposition similar to those in '8502' are found. The angle between foliation normal (Z) and the maximum is 30 degrees. The point concentration is noticeably stronger than that in '8502' or '8601'. Again, one of the maxima is stronger than the other (Fig. 4.10c). In '8201', the pattern is marked by a single maximum with a right-lateral off-set relative to YZ plane. The angle between Z and the point-maximum is 35 degrees (Fig. 4.10d). In '8202', the point maximum is slightly off from the XZ plane, but still within 30 degrees of Z and the sense of offset is similar to that in '8201' (Fig. 4.10e).

4.5.3 Fabric Asymmetry

4.5.3.1 Theoretical Background

The quartz c-axis fabric in quartzites (or model quartzites used in simulation studies) which have undergone deformation in an

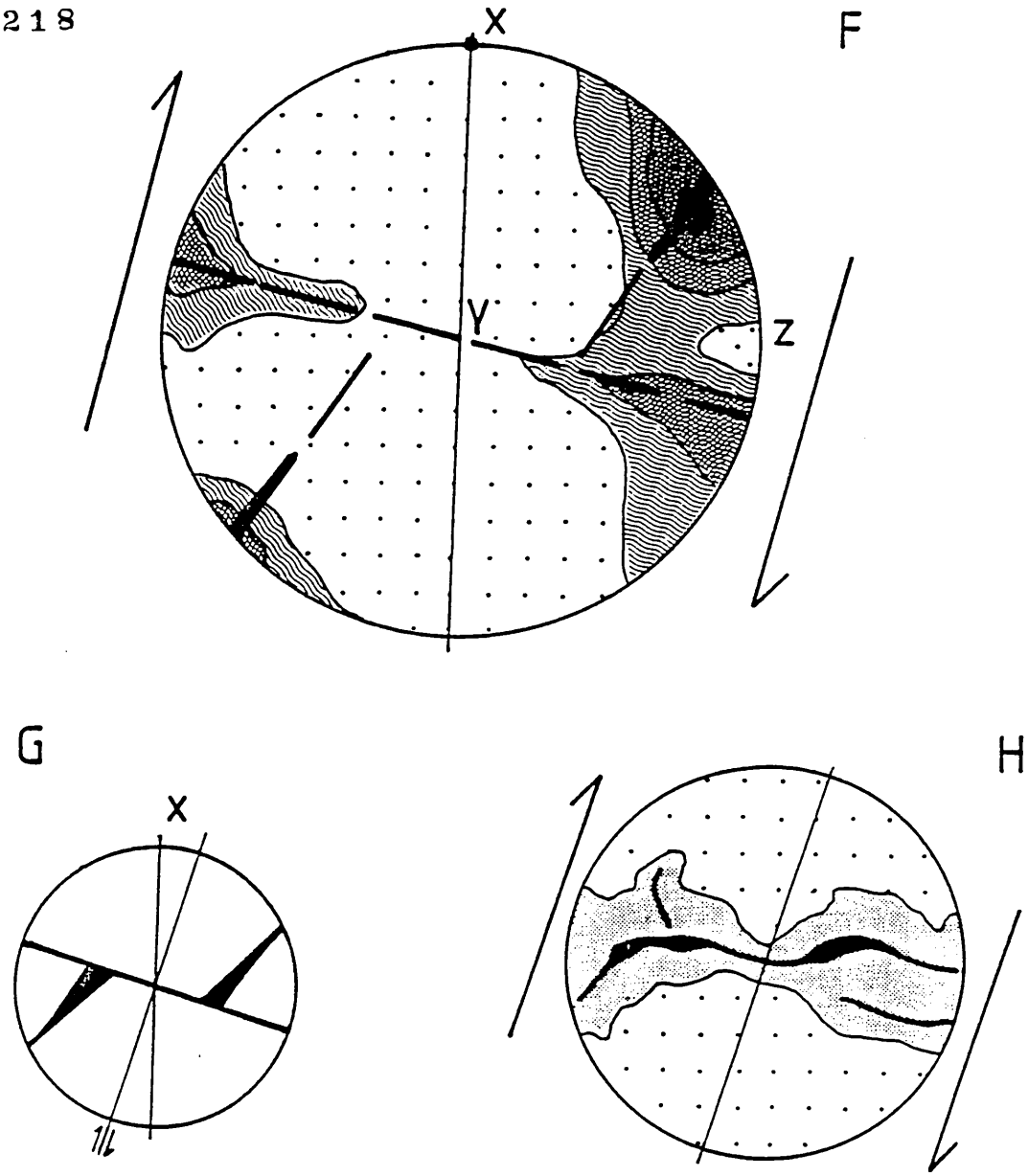
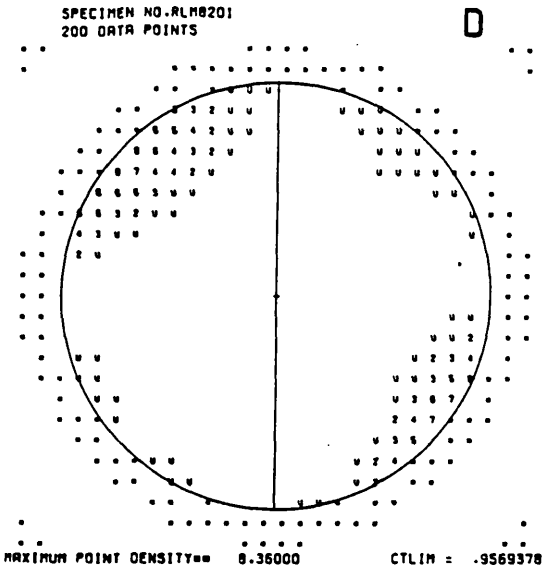


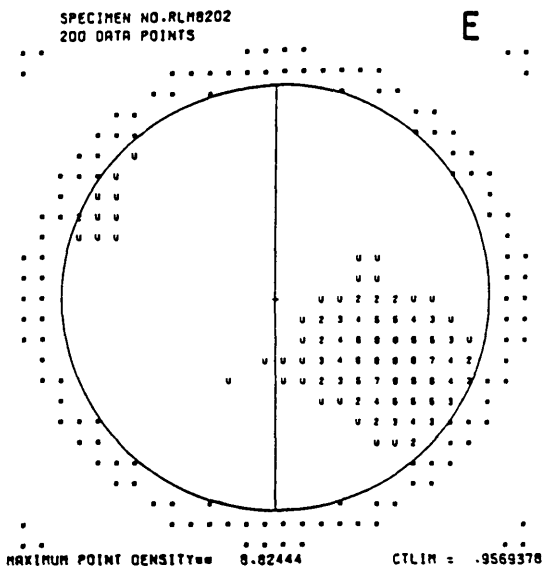
Figure 4.10. Quartz c-axis fabric in 'clasts' (a-r). For description of fabric diagrams see text. For details of contouring and relative orientation of foliation and lination see caption in Fig. 4.9 and Fig. 4.9s,t.

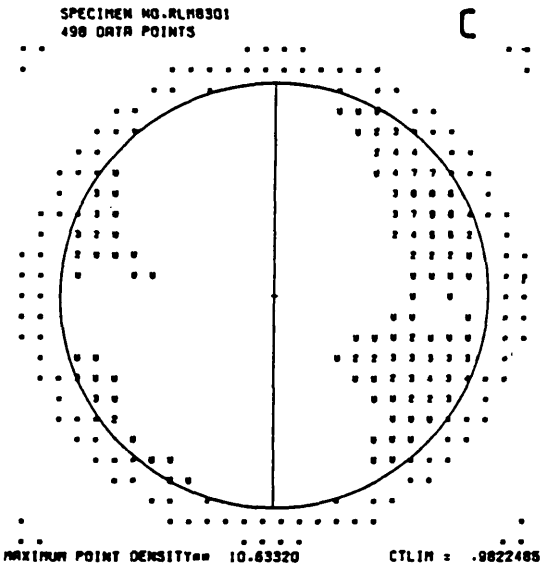
(f) Idealised fabric diagram corresponding to sp. no. RLM 8301. Note incipient girdle through Y and close to YZ plane. The stronger maximum is disposed in an anticlockwise sense from this girdle.

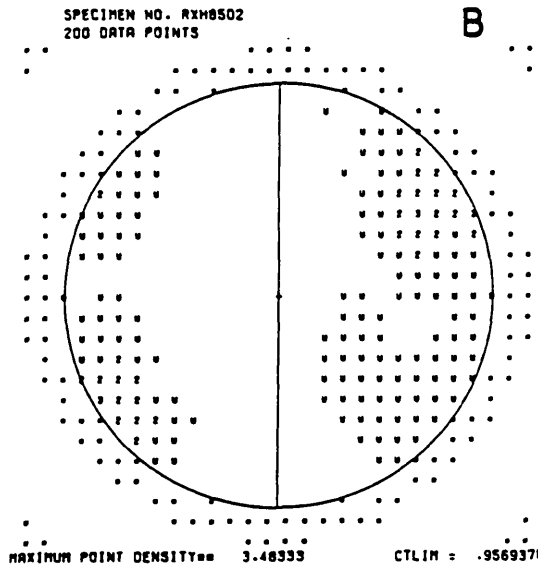
(g) A variant of type-I cross-girdle, from Lister and Williams (1979). Compare with fabric in RLM 8301.

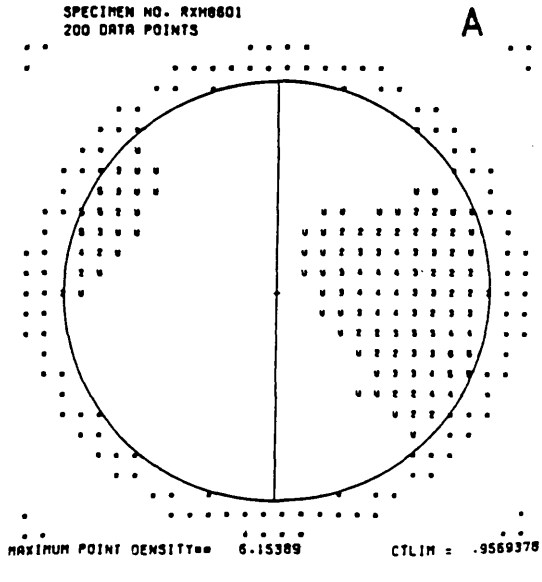
(h) Quartz c-axis fabric from a highly sheared quartz lens caught up in a narrow mylonite zone. Originally described by Carreras et al. (1977), redrawn by Lister and Williams to emphasise asymmetry in the fabric skeleton. Compare with fabric in RLM 8301.


SPECIMEN NO.RLM8201
200 DATA POINTS
D
MAXIMUM POINT DENSITY= 8.36000
CTLIM = .9569378


SPECIMEN NO.RLM8202
200 DATA POINTS
E
MAXIMUM POINT DENSITY= 8.82444
CTLIM = .9569378


SPECIMEN NO.RLM8301
498 DATA POINTS
C
MAXIMUM POINT DENSITY= 10.63320
CTLIM = .9822485


SPECIMEN NO. RXM8502
200 DATA POINTS
B
MAXIMUM POINT DENSITY= 3.48333
CTLIM = .9569378


SPECIMEN NO. RXM8601
200 DATA POINTS
A
MAXIMUM POINT DENSITY= 6.15389
CTLIM = .9569378

4.10

environment of dominant simple shear shows an asymmetry (Etchecoper 1977, Lister and Williams 1979, Schmidt et al. 1981). The major points related to the fabric asymmetry are summarised below and are illustrated in Fig. 4.11.

Etchecoper (1977) studied the progressive deformation of '2-dimensional polycrystals' and observed that for pure shear a bimodal preferred orientation develops, with the slip directions concentrating in double maximum symmetrically disposed about the extension axis (X). If (0001) [a] is assumed to be the dominant slip system in low T/T_m quartz, the corresponding point-maximum of c-axis would be symmetrically disposed about Z (the shortening axis). For simple shear a distinct asymmetry in distribution of the slip direction (and hence the C-axis) develops (Fig. 4.11 a-c). The pattern is marked by:

(a) the strongest and most sharply defined maximum disposes the slip direction within 5 degrees of the shear direction;

(b) the second weaker maximum is a broad concentration of slip directions at high angles to the axis of instantaneous shortening;

(c) the two maximum are more or less symmetrically related to the finite strain axes;

(d) the angle between the two maxima decreases with increasing finite strain.

Lister and Hobbs (1980) applied the Taylor-Bishop-Hill analysis to the problem of simulating the effect of deformation path on fabric development. Their results led to the following conclusions:

(a) The c-axis fabric formed by coaxial plane strain and progressive simple shear are rather alike at low strains and the pattern elements such as maxima or girdles are symmetrically disposed about the XY plane of the finite strain ellipsoid. However, in Model quartzite C an asymmetry in intensity distribution develops which consistently reflect the sense of shear (Figs. 4.11 d-f). Note that Lister and Hobbs (1980) defined three hypothetical model quartzites by specifying three

sets of critical resolved shear stress (CRSS) values for the dislocation glide systems. For model quartzite C the CRSS values are as follows:

Slip System	CRSS value
BASAL <A>	1.00
PRISM <A>	1.00
STEEP DIPYRAMID <C+A2>	3.00
STEEP DIPYRAMID <C+A3>	2.50

(b) At high strains asymmetry in fabric becomes quite marked, both in respect to the finite strain axes and in respect to the skeletal outline of the fabric pattern.

Note that in Figure 4.11d many c-axis plots are close to the extension axis. This is the 'kinking' orientation since the basal plane is orientated near to parallel with the shortening axis. If kinking was included in the model the maximum near X would disappear (Lister and Hobbs 1980). An idealised fabric skeleton excluding these poles near X as shown in Fig. 4.11e. This is a type-I cross-girdle c-axis fabric with unequal development of the two girdles. The internal asymmetry in the skeleton of the fabric and the sense of shear are related by the following rule:

For a dextral sense (clockwise) of shear, one girdle is perpendicular to the flow plane (plane of shear; for $\gamma > 6$ the XY plane of the finite strain ellipsoid is within 10 degrees of the flow plane) and a second weaker girdle is disposed in an anticlockwise sense from the stronger girdle.

Two natural fabrics from shear zones described in the literature are shown in Figs.4.11 g-i. Figure 4.9i shows a c-axis fabric in ice deformed in simple shear (Huddleston 1977). Two unequal maxima with a tendency to form a girdle through Y provide the essence of the pattern. The stronger maximum is perpendicular to the flow plane and the weaker maximum is disposed in an anticlockwise sense. The sample comes from a dextral shear zone. Figures 4.9g and 4.9h show the c-axis and a-axis fabric respectively in Cap de Creus mylonite (Schmid et al. 1981). A single c-axis girdle is developed and the off-set of the girdle relative to a plane normal to the foliation is in the same sense as the sense of

Figure 4.11. Fabric asymmetry in materials (model and natural) deformed under simple shear condition.

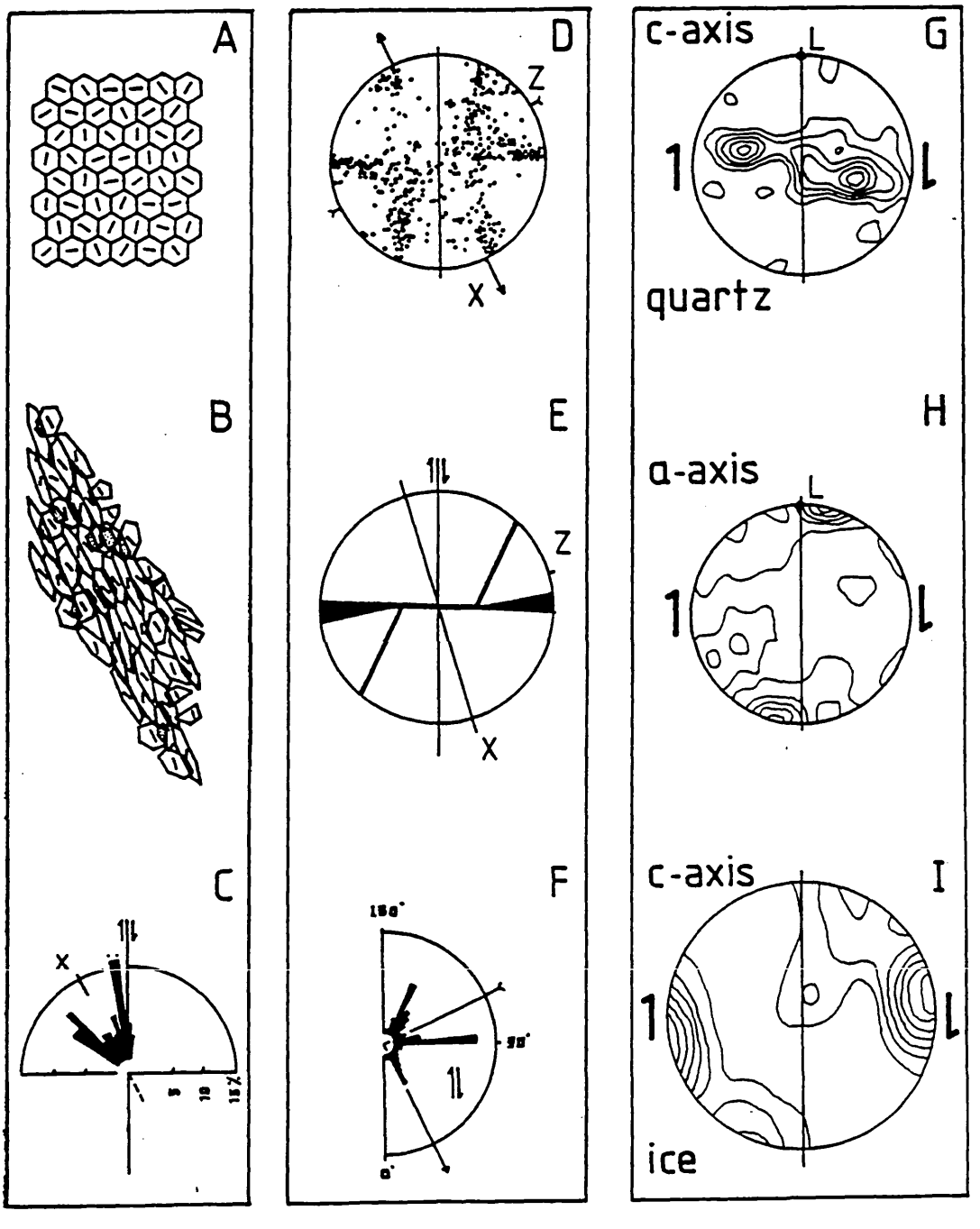
(a-c) Deformation of a '2-dimensional poloycrystal'. Slip direction randomly oriented before deformation (a), concentrated around X after deformation (b); angular distribution of slip directions with respect to X after deformation (c); from Etchecoper (1977).

(d-f) C-axis fabric in deformed Model Quartzite-C, from Lister and Williams (1979). Fabric diagram (d), idealised type-I cross-girdle with unequal development of the girdle (e) and angular distribution of the azimuth of c-axis with respect to X and the flow plane (f).

(g) Quartz c-axis fabric in Cap de Creus mylonite, from Schmid et al. (1981).

(h) Quartz a-axis fabric in Cap de Creus mylonite from Schmid et al. (1981).

(i) c-axis fabric in naturally deformed ice, from Huddleston (1977).


A
B
C
X
D
Z
X
E
Z
X
F
G
c-axis
L
1
L
quartz
H
a-axis
L
1
L
I
c-axis
1
L
ice

shear. The corresponding a-axis pattern is asymmetric in the same sense. However, caution must be employed in applying the criterion of fabric asymmetry, particularly in case of single girdle c-axis fabric, in determining the sense of shear (Passchier 1983, Simpson and Schmid 1983).

4.5.3.2 Asymmetry in fabrics from Loch Skerrols Thrust Zone

It has been suggested on geological grounds that the dislocation zone that separates the Bowmore Sandstone from the Dalradian of NE Islay is a zone of thrust movement; the displacement on an ESE dipping planar zone has moved the Dalradian westward on top of the Bowmore Sandstone. We consider below the contribution of fabric pattern in establishing the movement sense.

The essential pattern for 'matrix' quartz c-axis in the samples studied is a type-I cross-girdle which becomes increasingly assymetric with respect to the distribution of poles as the strain increases (see Figs. 4.9i-l). In highly deformed specimens (nos. 82 and 83), the girdles and point-maxima are also asymmetrically disposed with respect to the kinematic framework (the foliation, the lineation and the principal directions of finite strain axes, X,Y,Z). One of the maxima is close to Z and the strongly defined girdle is closer to the YZ plane of the finite strain ellipsoid. Application of the fabric asymmetry criteria as outlined above suggests a dextral sense of movement when the orientation of the foliation and lineation are as shown in Fig. 4.9s). Although the c-axis fabric for 'CDTLSTX' shows only a single girdle, the obliquity with respect to the foliation normal is consistent with a dextral sense of movement (Fig. 4.9r).

The c-axis fabric for 'clasts' gives a pattern of double maximum type with a grossly unequal development of the two maximum. In 'RLM8201' and 'RLM8202' (Figs. 4.10d-e) the maximum in the SE quadrant of the fabric diagram is much stronger and reflects the sense of asymmetry obtained for the corresponding 'matrix' fabric. In 'RLM 8301' (Fig. 4.10c) the maximum in the NE quadrant is stronger, but the relatively weak maximum in NW-SE quadrants is closer to Z and has an incipient tendency to form a girdle through Y. If one assumes that this incomplete girdle is perpendicular to the flow plane, then the stronger

maximum is disposed in an anticlockwise sense (see Fig. 4.10f for the idealised pattern). Lister and Williams (1979) illustrated a variant of type-I cross-girdle in which the stronger maximum is disposed in an anticlockwise sense from the feeble girdle; the latter is perpendicular to the flow plane associated with dextral movement (Fig. 4.10g). Carreras et al. (1977) described a similar quartz c-axis fabric for a highly sheared quartz lens caught up in a narrow mylonite zone (the fabric skeleton is shown in Fig. 4.10h).

Both the internal asymmetry of the fabric pattern and the asymmetry of the fabric elements with respect to the kinematic framework indicate a dextral sense of movement with the foliation plotted N-S vertical and the down-plunge direction of lineation towards north. Reorientation of the foliation and lineation to their true geographic position will make the sense of movement consistent with a westward movement of the Dalradian over the Bowmore Sandstone along the Loch Skerrols thrust (Fig. 4.12).

4.5.4 Discussion

The essential pattern of quartz c-axis fabric in the deformed quartzites of the Loch Skerrols thrust zone is a type-I cross-girdle pattern with both an internal asymmetry and an external asymmetry with respect to the kinematic axes. The external asymmetry is a reflection of a non-coaxial deformation (dominantly simple shear) along the Loch Skerrols thrust. The point-maximum close to Z, the direction of maximum finite shortening, indicates a dominant activity on the BASAL <a> slip system. For low T/T_m quartz the dominant slip system is BASAL <a> (Bouchez et al. 1983). Thus the quartz c-axis fabric from Loch Skerrols thrust zone indicates that the temperatures during deformation were low, probably in the low greenschist facies. This corroborates the temperature conditions deduced from a metamorphic mineral assemblage of chlorite + muscovite + quartz.

The progressive development of quartz c-axis fabric with increasing strain in the thrust zone is schematically shown in the composite fabric diagram of Fig. 4.13. The c-axis fabric corresponding to specimens representing strain values are colour coded with colours in the red end of the spectrum denoting higher strain. For each specimen

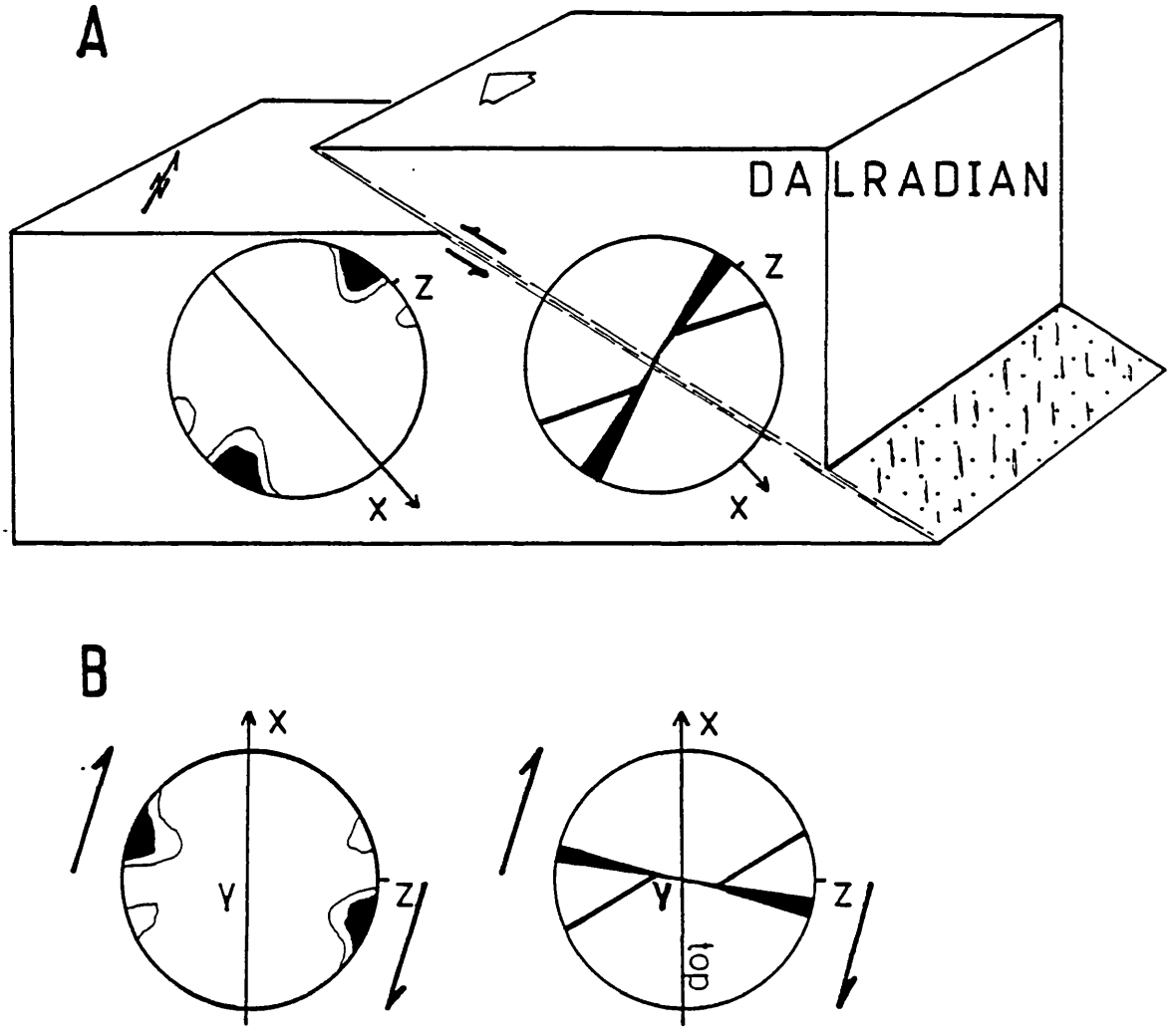


Figure 4.12. Movement along Loch Skerrols thrust and its relation with asymmetry of quartz c-axis fabric.

(a) Idealised block diagram to show the westerly movement of the Dalradian 'block'. The fabric pattern in highly deformed Jura Quartzite in their true geographic orientation on an ESE-WNW section is shown. Note that the better developed girdle in 'matrix' fabric (right) is normal to the thrust plane.

(b) Fabric pattern in 'matrix' (right) and 'clast' as they are depicted in figs. 4.9 and 4.10.

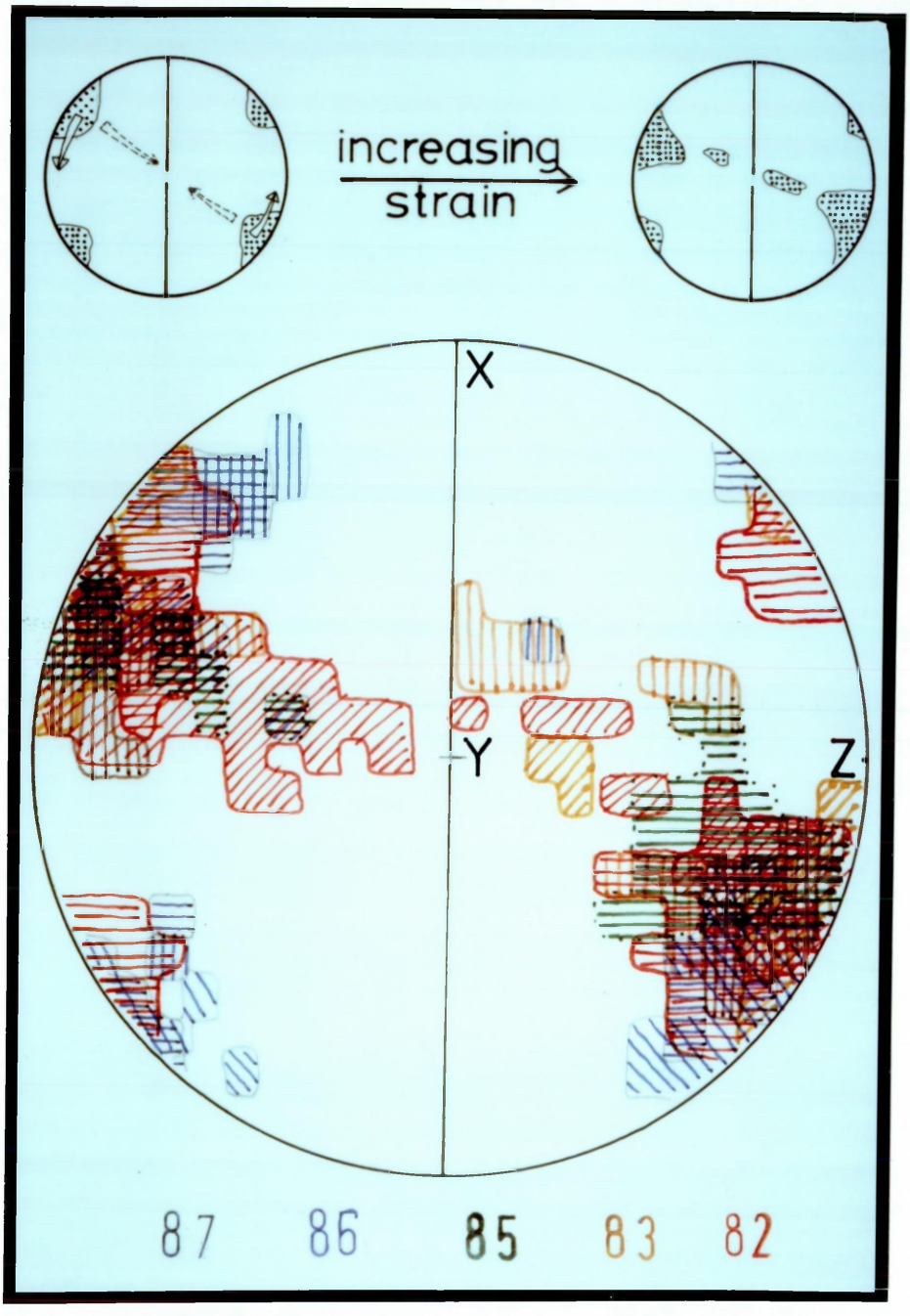


Figure 4.13. Composite quartz c-axis fabric diagram showing the progressive development of an asymmetric cross girdle pattern with increasing strain in the Loch Skerrols thrust zone. Fabrics corresponding to different strain intensities (values increasing from loc. no. 87 to loc. no. 82) are colour coded with high strain fabric represented by red end of the spectrum. Only areas of concentration above 2 x E are shown for each fabric. Note that a girdle through Y becomes well defined only at a higher strain; also there is tendency for point-maximum on XZ plane to rotate towards Z as shown in the idealised sketches on top.

only areas with concentration of poles above 2 x uniform are shown. Foliation (XY plane) is N-S and the lineation (X) is towards north. Notice that a girdle through Y and a secondary concentration near Y become defined in specimens with relatively high strain. Whereas a concentration of C-axes near Z can be explained as due to activity on basal slip system, to explain concentrations near Y and intermediate positions one needs to involve glide on other slip system, such as PRISM <a> or DIPYRAMID <a+c>. The closest approximation to the observed fabric pattern in highly deformed specimens is found in Model quartzite C (Lister and Hobbs 1980) deformed in simple shear. Although the works by Lister et al. to a certain extent predict patterns of natural quartz c-axis fabrics, the applicability is limited by the fact that in quartz-mylonites and quartz-tectonites the deformation is more often than not heterogeneous on a grain scale; Taylor-Bishop-Hill analysis conventionally assumes a homogeneous deformation.

The single slip system model (Etchecoper 1974, Bouchez et al. 1983) explains the fabric patterns observed in peridotite-mylonite or deformed ice very well, where the deformed mineral (olivine or ice) is reported to have a single slip system. The same model can be applied for low T/T_m quartz in less deformed quartzites, but deformation of quartzites at higher strains probably involves an activation of other independent slip systems in quartz in addition to a dominant BASAL <a>. It may be pointed out here that models considered by Etchecoper (1977) or Lister et al. (1978) do not consider the effect of dynamic recrystallisation with progressive deformation. In the naturally deformed quartzites described above dynamic recrystallisation has a significant contribution in producing the 'matrix' and must have had some influence on the c-axis fabric pattern.

4.6 CORRELATION BETWEEN STRAIN AND DEGREE OF CRYSTALLOGRAPHIC PREFERRED ORIENTATION

4.6.1 General Statement

Crystallographic preferred orientations in quartz-tectonites and quartz-mylonites are usually strain induced. Several studies on c-axis fabric of quartz in naturally deformed quartzites have shown qualitatively that a fabric pattern develops and becomes well defined as

the strain increases, in other words the intensity of preferred orientation varies with increasing strain (Bouchez 1977, Carreras et al 1977, Compton 1980, Marjoribanks 1976, Miller and Christie 1981). Fabric simulation studies on model quartzites have shown that the degree of lattice preferred orientation is directly related to increasing shortening (Etchecoper 1977, Lister and Hobbs 1980).

The angular distribution of lines and planes can be formally described in terms of an orientation tensor provided the distribution has a relatively high symmetry (Scheidegger 1965). A relationship between the Scheidegger's orientation tensor and the strain tensor has been derived (Cobbold and Gapais 1979); however, the relationship is strictly valid for cases where the fabric element passively rotates to its final position as a result of bulk finite strain. In the development of quartz c-axis fabric with progressive strain, the lattice elements cannot be considered as passive strain markers. Also, for fabric shapes more complicated than point-maximum, small circle or single girdle the orientation tensor and associated eigenvalues do not provide sufficient description of the nature of distribution. An attempt has been made here to study empirically the variation of the crystallographic preferred orientation as reflected in the statistical distribution of the point-density of poles. The point-density is estimated in terms of deviation from a uniform population and thus avoids problems of sample size. Some characteristics of the point-density distribution will be used to define the degree of preferred orientation (intensity parameter). Relationship of this intensity parameter with strain in some naturally deformed quartzites is discussed below.

4.6.2 Point-Density Distribution and its Variation

Two series of samples are chosen; each of these represent progressively developed fabric in an environment of strain gradient. The first series (Series A) comes from the movement zone associated with Loch Skerrols thrust. The other (Series B) includes deformed quartzites (Elba Quartzite) from the Raft River Mountain, Utah (Compton 1980). Quartzites in the Loch Skerrols thrust zone were deformed in low greenschist facies conditions. Three-dimensional strain values were obtained from measurement of grain shapes (described in Section 4.4).

The axial ratio of the strain ellipsoid varies from 1.24:1:0.527 (specimen location 87) to 1.425:1:0.25 (specimen location 82). Quartz C-axis orientation in 'matrix' of each specimen used for strain measurements were obtained (see section 4.5) and analysed for determining the nature of point-density distribution of poles. Five of the Series B samples (Elba Quartzite A, B, C, D and F) have strain ellipsoid axes ranging from 2.5:1.1:0.4 to 4.0:1.4:0.2; the quartzites were deformed under low greenschist facies condition (Compton 1980). Expt. Qzt. E (Series B) is a quartzite experimentally deformed in plane strain at 15 kbar, 800°C and e 10^{-6}/s (Tullis 1977 quoted in Compton 1980). The strain ratio for this sample is 2.0:1.0:0.5 (Tullis ibid). In Series B, published scatter diagrams showing quartz c-axis orientations on equal-area plots have been used for further analysis.

For each c-axis fabric, the point-density is estimated at each of 372 grid-intersections spread over the entire projection space. The probability (P) of getting point-density (d) equal to or less than a certain value (x uniform) is calculated (see Appendix 4G). The P-d plots gives the distribution of point-density in individual samples (Figs. 4.14 and 4.15). In each P-d plot the curve corresponding to the density distribution in a random sample from an isotropic population is also shown for comparison. The random distribution gives s-shaped curve. Even in the least deformed quartzite (specimen 87, Series A) the point-density distribution deviates from that of a random sample. The closeness of the P-d curves corresponding to two thin sections cut from each specimen (Series A) testifies to the reproducibility of the results. Whereas in the random distribution the probability of obtaining any point-density above 2 x uniform is negligibly small, even in the least deformed quartzite point-density above 2 x uniform is associated with a significant probability. With increasing strain the probability of getting higher point-density increases (Fig. 4.14); the probability of getting zero point-density also becomes appreciable at a higher strain (specimen 82). The observation that the degree of preferred orientation is partly reflected in the proportion of pole free area (Flinn 1958) is supported by these results.

The pattern of point density distribution in Series B samples (Fig. 4.15) is similar to that in Series A. The deviation from the random distribution is very marked in highly strained specimen (Elba

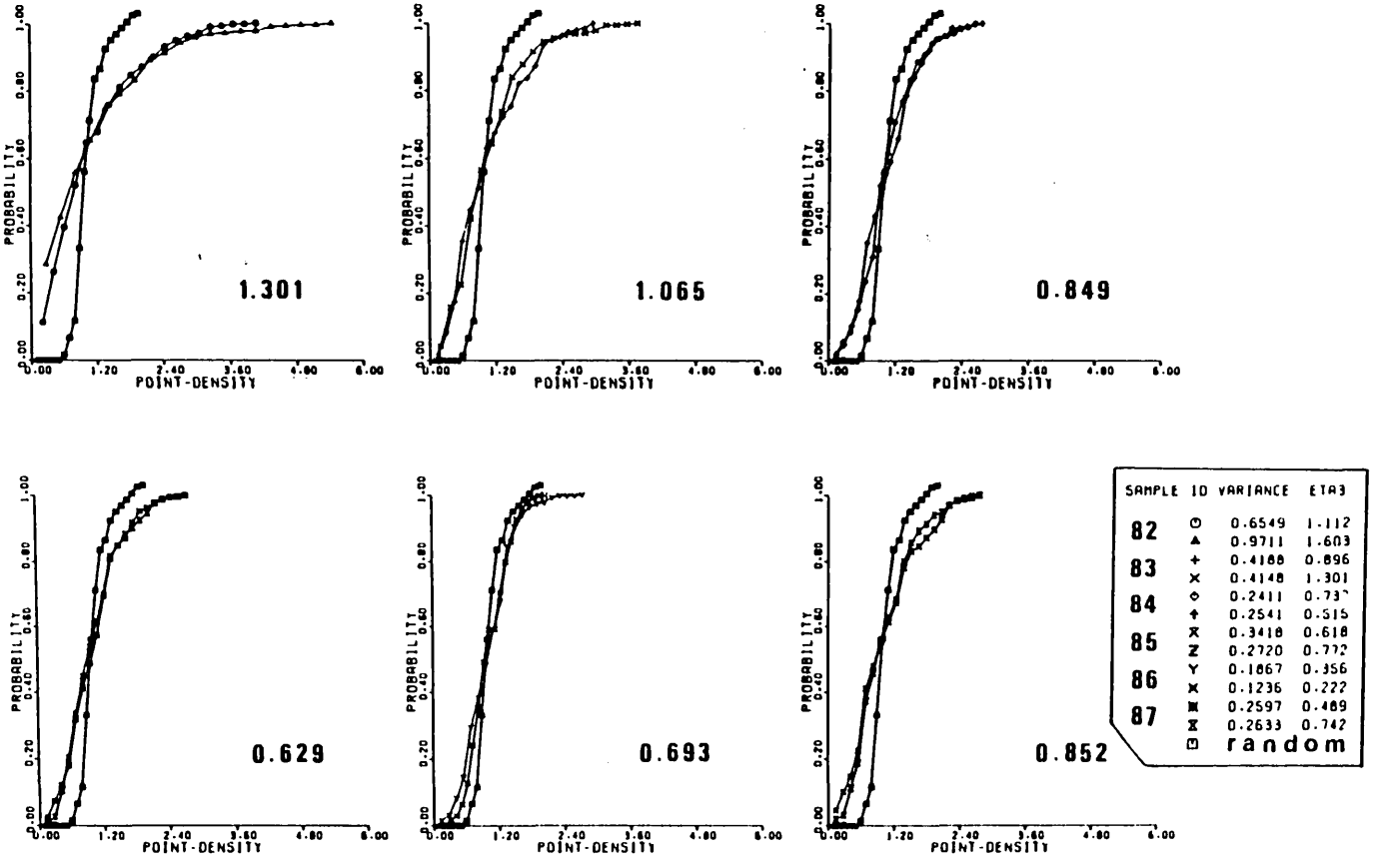


Figure 4.14. Probability distribution of point-density in Series A samples. The bold figure in each p-d plot gives the value of the Strain Intensity for corresponding specimen locality. The distribution becomes increasingly skewed with increasing Strain Intensity.

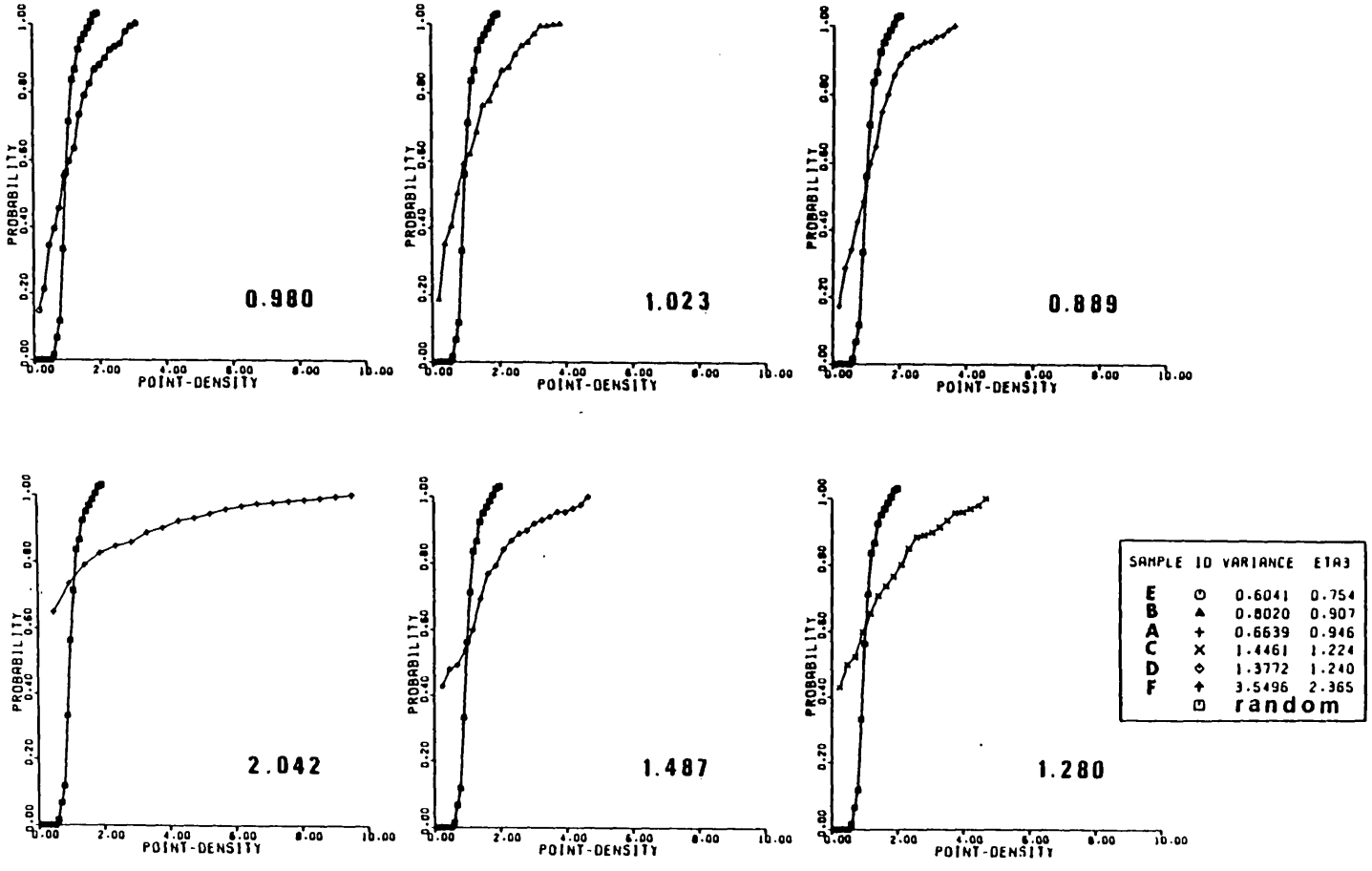


Figure 4.15. Probability distribution of the point-density in Series B samples. The bold figure in each p-d plot gives the value of the Strain Intensity, ϵ_s. For very high ϵ_s (e.g. Elba Quartzite F) the distribution is extremely skewed with the probability of getting near zero point-density > 0.5; probability of having point-density above 5 x E is greater than 10 per cent.

Qzt. F); the probability of getting near-zero point-density is 0.5. The fabric in Elba Qzt. F (not shown here) shows a single girdle with two maxima and vestiges of a cross-girdle (Compton 1980).

4.6.3 Fabric Intensity Parameter, η_3

The probability distribution of point-density reflecting the quartz c-axis preferred orientation in deformed quartzites deviates from a distribution given by a random sample from a hypothetical isotropic population. The deviation is marked by a relative increase in the probability value corresponding to a higher point-density value; concurrently with this, the probability of getting zero point-density also increases with increasing preferred orientation. In other words, the distribution becomes increasingly skewed. Thus a statistical measure of skewness can offer a measure of the degree of preferred orientation. Theoretical distributions which describe the orientation distribution in point-maximum or single girdle type fabrics has been given in Mardia (1972). However, such distribution functions are not adequate for more complex fabric types such as a cross-girdle pattern. The distribution of point-density in Type I cross-girdle fabric (described above) appears to be very similar to GAMMA distribution (Fig. 4.16). However, only a limited number of natural quartz c-axis fabrics are considered here. Hence, in the calculation of statistical parameters describing the probability distribution of the point-density we restrict ourselves to sample statistics rather than any parametric estimation based on an assumed probability density function. The sample statistics for all the samples in Series A and B are given in Table 4.4. The coefficient of skewness is of interest, because as discussed earlier this statistic describes the increasing preferred orientation in terms of deviation from a 'random' distribution. The coefficient of skewness, η_3 is given by

$$\eta_3 = \mu_3/\sigma^3 \qquad (4.8)$$

where, $\mu_3 = (1/n) \sum_{i=1}^{n} (x_i-x)^3$, the third sample moment and

$\sigma^2 = (1/n) \sum_{i=1}^{n} (x_i-x)^2$, the sample variance. In the studied

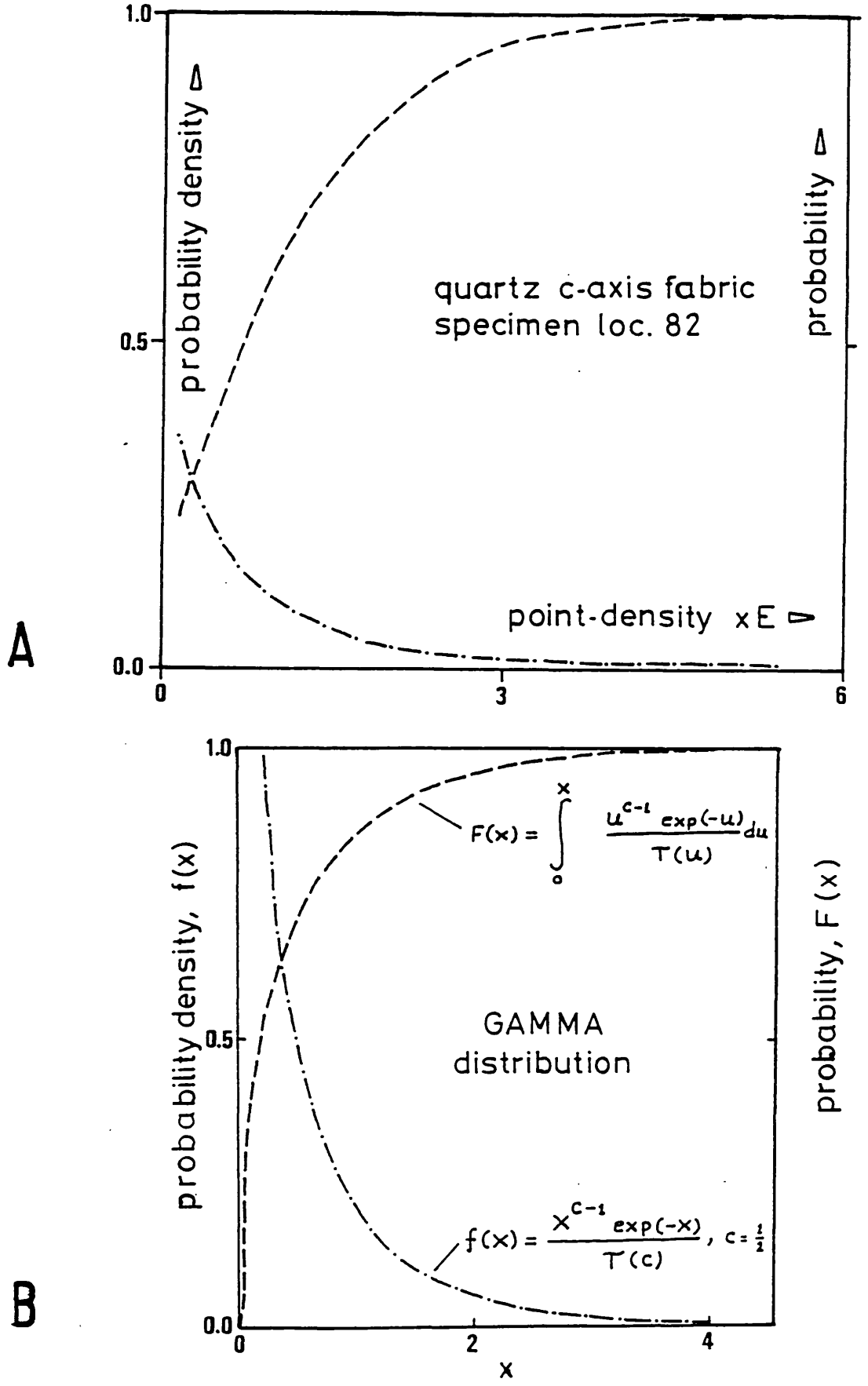


Figure 4.16. Distribution of point density in type-I cross-girdle type fabric in quartz-mylonite, specimen loc. 82, Loch Skerrols thrust zone, and its comparison with theoretical Gamma distribution (b).

Table 4.4 Point-density statistics for different c-axis fabric samples

Sample ID	Size	Mean	Variance	μ_3	Coeff. of Kurtosis	Coeff. of skewness, η_3
8201	372	1.001	0.655	0.589	3.853	1.112
8202	372	0.992	0.971	1.534	5.952	1.603
8301	372	0.999	0.419	0.243	3.087	0.896
8302	372	0.982	0.415	0.347	5.349	1.301
8401	372	0.995	0.241	0.087	3.686	0.737
8402	372	1.006	0.254	0.066	2.905	0.515
8501	372	0.988	0.342	0.124	2.679	0.618
8502	372	0.985	0.272	0.110	3.336	0.772
8601	372	0.993	0.187	0.029	3.296	0.356
8602	372	1.007	0.124	0.010	2.708	0.222
8701	372	0.999	0.260	0.065	3.073	0.489
8702	372	0.992	0.263	0.100	3.145	0.742
ELBA A	372	1.002	0.664	0.551	3.693	0.946
ELBA B	372	1.003	0.604	0.354	2.801	0.754
ELBA C	372	1.008	1.446	2.129	3.602	1.224
ELBA D	372	1.025	1.377	2.004	3.962	1.240
ELBA F	372	1.015	3.550	15.819	8.352	2.365
EXPT. E	372	1.003	0.801	0.651	2.909	0.906

samples, η_3 increases as the strain increases, the fabric pattern becomes more defined and visual judgement shows an increase in the intensity of preferred orientation. For example, η_3 values of Elba Qzt. F and Expt. Qzt. E are 2.565 and 0.907 respectively; the corresponding values for strain ellipsoid axial ratios are 0.24:1.4:4.2 and 0.5:1:2.0 respectively.

4.6.4 Relationship Between Fabric Intensity and Strain Intensity

The Orientation Tensor

Mathematically, a distribution of axes in space may be characterised by the symmetric tensor (orientation tensor) A_{ik} where,

$$A_{ik} = \frac{1}{N} a_{ik} \qquad (4.9)$$

with

$$a_{11} = \sum n_{ix}^2$$

$$a_{22} = \sum n_{iy}^2$$

$$a_{33} = \sum n_{iz}^2$$

$$a_{12} = a_{21} = \sum n_{ix} n_{iy}$$

$$a_{13} = a_{31} = \sum n_{ix} n_{iz}$$

$$a_{23} = a_{32} = \sum n_{iy} n_{iz}$$

N axes are denoted by $\vec{n}_i$, with components n_{ix}, n_{iy}, n_{iz} in x, y, z directions respectively (an orthogonal coordinate system); $\vec{n}_i$ represents unit vector in either direction of the corresponding axis (Scheidegger 1965). The distribution of the axes may be characterised by the three normalised eigenvectors of the matrix A_{ik} and the eigenvalues S_1, S_2 and S_3, $S_1 \geq S_2 \geq S_3$. Graphical representation of the eigenvalues provides a means of characterising the shape fabrics ranging from uniaxial clusters to uniaxial girdles (Woodcock 1977). Woodcock suggested that the parameter C, where

$$C = \ln(S_1/S_3) \qquad (4.10)$$

is a measure of the strength of preferred orientation.

Correlation between ϵ_s, η_3 and C

The C values were calculated for all the samples in Series A and Series B (Table 4.5) in order to test how far they correspond with the n_3 values (see Appendix 4H for computational aspect of eigenvalue calculation). As discussed above, the preferred orientation in quartz c-axis fabric of deformed quartzites is strain dependent. For 2-dimensional strain, the axial ratio of the strain-ellipse is an obvious choice for representing various intensities of strain. But, for 3-dimensional strain the ratio of the three axes of the strain ellipsoid is rather cumbersome to handle. On the other hand, the strain intensity, ϵ_3 is proportional to the octahedral unit shear (Nadai 1963, Miller and Christie 1981) and convenient for comparing finite strains falling in different fields of the Flinn plot. η_3 values for the studied samples are shown in Table 4.5; in each series there is a gradual increase in the η_3 value.

A linear regression analysis (see Appendix 4I) is applied to the set of values for ϵ_3 and η_3 (and C) to test whether a simple linear relationship between the fabric intensity parameter and the Strain Intensity exists. The results are shown in Fig. 4.17 and Table 4.6. The high value of correlation coefficient, R suggests that a first approximation to a quantitative relationship is given by the linear model

$$Y = \alpha + \beta X \qquad (4.11)$$

where X stands for ϵ_s and Y for η_3 or C.

The relationship between η_3 (or C) and ϵ_s has been established here from an empirical point of view. Any theoretical explanation of the relationship is beyond the scope of the present work. However, it may be pointed out here that the mechanical work per unit volume done by the stresses to deform an element in a plastic material is evaluated from the curve integral

$$w = 3\int \sigma \, d\epsilon + \left(\frac{3}{2}\right)\int \tau_o \, d\gamma_o \qquad (4.12)$$

to be taken along the path of straining, that is over the sequence of infinitesimal increments of strain through which the deformation has

Table 4.5 Values of strain intensity and fabric intensity in two zones of strain gradient

	Specimen	Strain intensity	Fabric intensity	
		G_s	C	η_3*
S				
E	82	1.301	1.062	1.358
R	83	1.065	0.644	1.098
I	84	0.849	0.438	0.626
E	85	0.852	0.600	0.695
S	86	0.693	0.125	0.289
A	87	0.629	0.486	0.615
S	Elba Qzt. A	0.889	1.128	0.946
E	Elba Qzt. B	1.023	1.136	0.754
R	Elba Qzt. C	1.280	1.850	1.224
I	Elba Qzt. D	1.487	2.058	1.240
E	Elba Qzt. F	2.042	3.926	2.365
S	Expt. Qzt. E	0.980	1.032	0.907
B				

* average of two subsamples in Series A

Table 4.6 Linear regression analysis on strain intensity and fabric intensity parameters

Correlation between	α	β	R*
η_3 and C	0.434	0.477	0.925
ϵ_s and C	0.656	0.360	0.943
ϵ_s and η_3	0.376	0.708	0.954

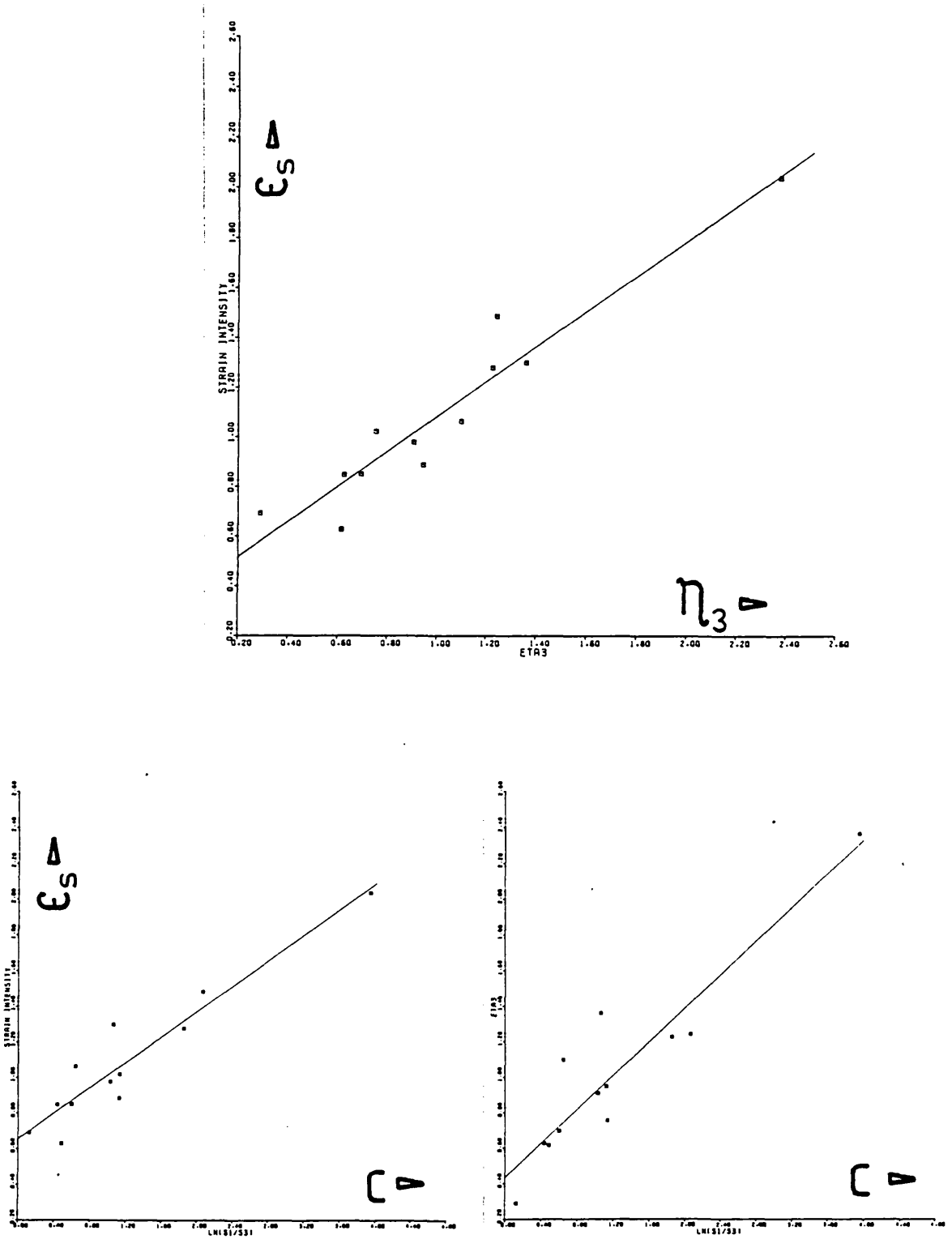


Figure 4.17. A linear relationship between the Strain Intensity (ε_s) and the Fabric Intensity parameter, η_3 or C. For slope of the regression line see Table 4.6.

passed (Nadai 1963); σ and ϵ refer to average stress and strain respectively, τ_o is the octahedral shearing stress and γ_o is the unit shear. Also

$$\epsilon_s = \frac{\sqrt{3}}{2}\gamma_o \qquad (4.13)$$

Extension of an elastic case would suggest that w (eqn. 4.12) is related to the strain energy for plastic distortion of the material. If the deformation mechanism is largely crystal plastic, i.e. conservative motion of dislocations, the driving force behind the latter is a differential in strain energy on a grain or subgrain scale.

A linear relationship between strain intensity and fabric intensity as suggested above is tested only for a limited range of strain, $0.63<\epsilon_s<2.04$. It has yet to be tested whether the relationship holds good for higher values of strain. Referring back to the fabric simulation studies of Etchecopar (1977), the results suggest that for pure shear type of deformation the fabric intensity progressively increases even at $\gamma>6$, for simple shear deformation the fabric intensity steadily increases up to a γ value of ~6, but at higher shear strain the fabric intensity remains virtually constant with progressive deformation. Only further studies on naturally deformed quartzites can prove or disprove whether the experimental results truly represent the relationship in natural fabrics. One other thing that must be emphasised here is that the quartzites considered here are almost pure quartz rocks. Since the fabric development is likely to be influenced by the presence of non-quartz phase (when the proportion of the latter is appreciable), the quartz c-axis fabric intensity in such polymineralic rocks may not be directly related to the strain intensity.

4.7 RELATIVE AGE OF THRUSTING

Two phases of folding have been recognised within the Dalradian of NE Islay (Borradaile 1979, Fairchild 1981). Fairchild (1981) described the Islay anticline as an open structure representing the first phase of Caledonian deformation in the area (D_{1d} of Borradaile 1979). The present study (also Borradaile 1979) suggests that the first phase of deformation within the Colonsay Group or Bowmore Sandstone may be earlier than D_{1d}. The Loch Skerrols thrust displaces the northwest

limb of the Islay Anticline. Not only has the Jura Quartzite been strongly deformed in the vicinity of the thrust, but members of Bonahaven Formation, north of Loch Skerrols shows a penetrative foliation with a southeast dipping elongation lineation. The latter is comparable to the elongation lineation on mylonite foliation in Jura Quartzite close to the thrust.

Minor overturned folds are observed in the interbedded phyllites and impure carbonate layers north of Loch Skerrols. However, between Crois Mhor and Gortantoid Point (the exposures are on the NW limb of Islay Anticline) the bedding in Jura Quartzite dips towards northwest. NW-SE profile through this area should therefore show the Islay Anticline as an asymmetric open fold. It is possible that the profile of the fold changes to overturned along the axial trace.

Measurement of strain and fabric in the vicinity of Loch Skerrols do show that a definite strain gradient occurs in the area and that a significant part of the strain is accommodated by intracrystalline slip (cf. Borradaile 1979). Recall that the shape of the finite strain ellipsoids as deduced from grain shape measurements shows an apparent flattening. For a simple shear type deformation in a thrust belt one would expect a plane-strain (k=1) finite strain ellipsoid if the volume is held constant during deformation. The observed shape of the strain ellipsoids in the Loch Skerrols thrust zones invites some discussion here. Three alternative hypothesis may be suggested to explain the finite strain ellipsoid shape:

(i) There was differential volume loss during deformation across the thrust.

(ii) A later deformation (D_{2d}?) following thrust movement changed the shape of a plane strain ellipsoid associated with thrust movement.

(iii) The finite strain ellipsoid as observed now is due to the combined effect of an initial constrictive or flattening deformation related to D_{1d} plus a plane strain type deformation related to thrust movement.

Figure 4.18 shows the field in which the observed strain ellipsoids lie on a Flinn plot; the boundary between the constrictive and flattening field for different volume loss are also shown. Since the field of observed strain ellipsoids crosses the lines for different volume loss, the overall deformation can be considered as falling on the boundary between constriction and flattening (i.e. plane strain for zero volume loss) only if the deformed rock had undergone different amounts of volume loss at different specimen localities. In view of similar lithology and deformation mechanism throughout the thrust zone, the proposition of different volume loss seems geologically unrealistic. Thus the hypothesis (i) above is rejected.

Minor structures in NE Islay show that a phase of deformation (D_{2d}) postdates the thrust movement. However, the effect is only local and the deformation is not penetrative enough to produce changes of shape on a grain scale. Thus the efficacy of D_{2d} in producing the observed shape of finite strain ellipsoid (hypothesis (ii)) can be questioned.

A penetrative axial plane cleavage is associated with the Islay Anticline (D_{1d}). Borradaile (1979) recorded both constrictive and flattening strain from various Dalradian horizons on either limb of the Islay anticline. An intragranular component of D_{1d} strain must have had some imprint on the Jura Quartzite which was later deformed in the Loch Skerrols thrust zone. Since, it is difficult to decide whether this initial D_{1d} intragranular strain was constrictive or flattening type, we tried to model how the final strain ellipsoid shape depends on the initial shape of the ellipsoid if the later stage of deformation (due to thrusting) is of plane strain type (simple shear). The assumption involved in the computation is that the one of the principal planes of the initial strain ellipsoid makes an angle <30 degrees with the XZ plane of the superposed strain. This seems reasonable because both the Loch Skerrols thrust and the axial plane of the Islay Anticline dip towards southeast, the axial plane being slightly steeper. Two initial k values are considered - one in the constriction field and the other in the flattening field. The shape of the final strain ellipsoid for different values of shear strain, γ are shown in Figure 4.19. Notice that for an initial flattening ellipsoid (k = 0.03) the final k value lies in the flattening field even at a very high shear strain. For an initial constrictive ellipsoid the final k value grades towards that for

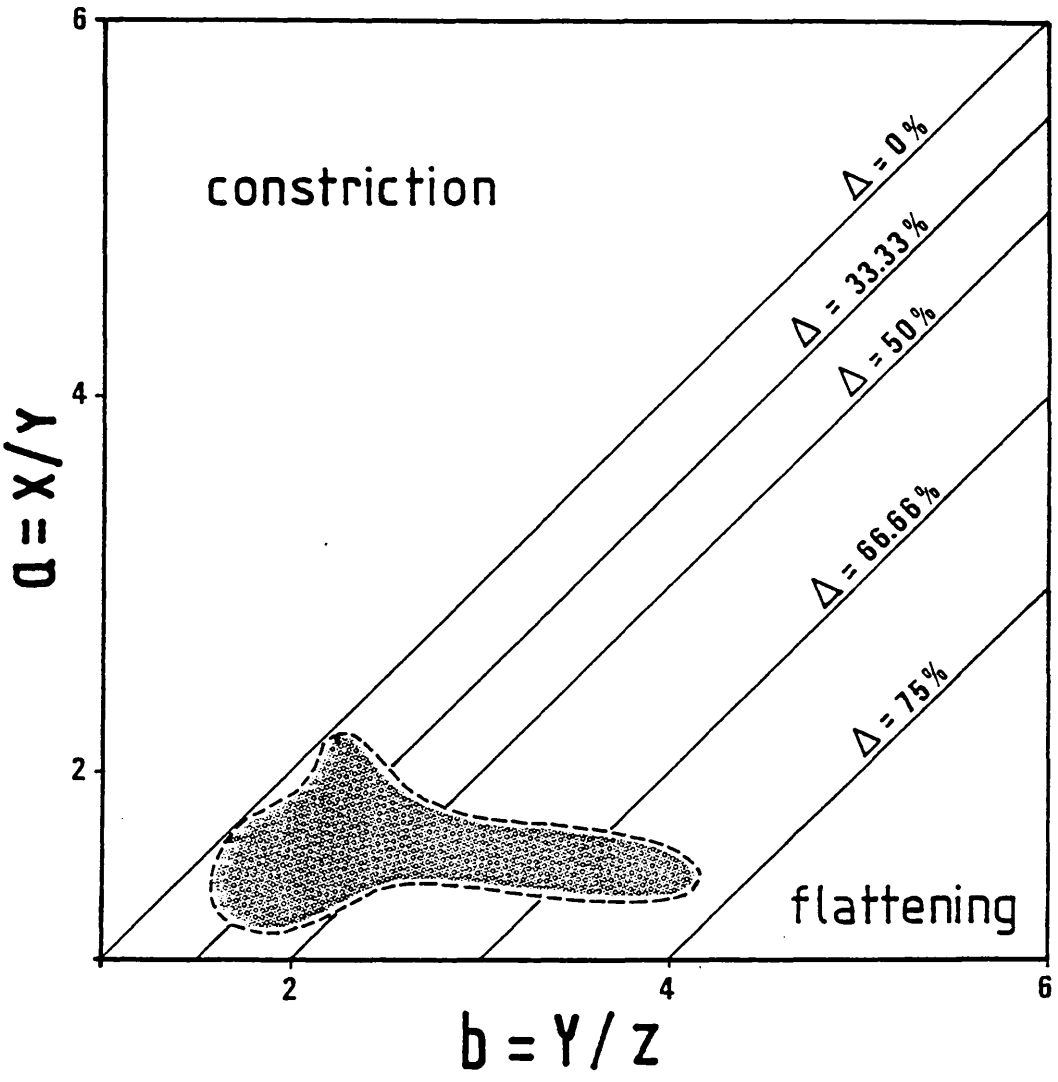


Figure 4.18. Field of observed strain ellipsoids in the Loch Skerrol thrust zone and its relationship with the boundary between constriction and flattening strain for different amounts of volume loss (Δ).

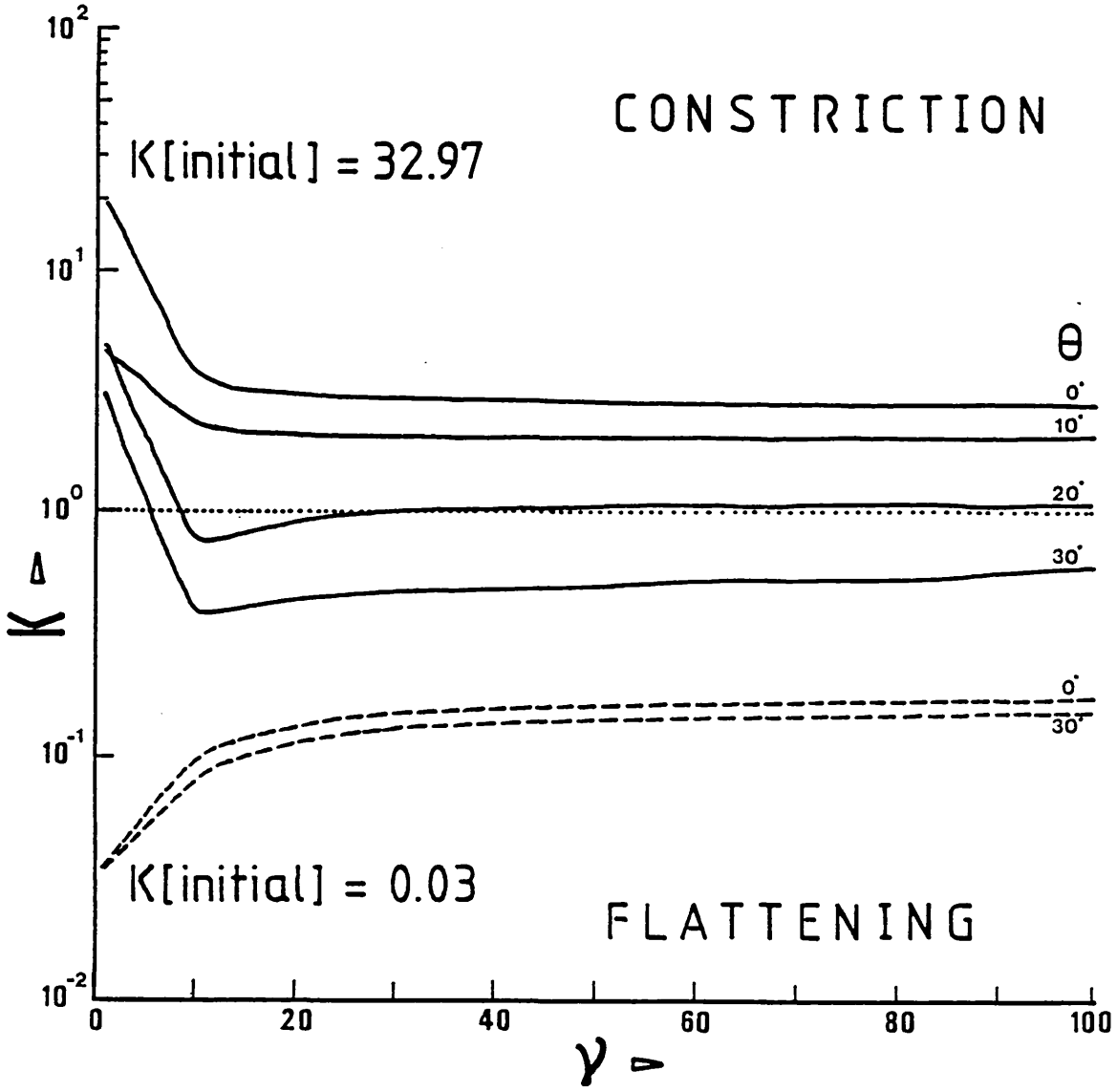


Figure 4.19. The effect of superposed shearing strain on the shape of an initial flattening (dashed lines) or constriction ellipsoid (solid lines).

a plane strain ellipsoid. Thus the third hypothesis above, particularly the alternative with an initial flattening ellipsoid, seems most reasonable.

A possible sequence of evolution of the Islay Anticline is shown schematically in the sketches of Fig. 4.20. The final profile (Fig. 4.20c) is probably true for a ESE-WNW cross section through Loch Skerrols. A difference in the shape of the profile (Fig. 4.20d) further north (through Gortantoid Point) may be due to

(a) a divergence of the movement zone from the trend of the major fold axis, and/or

(b) dissipitation of the movement along one or more slides without any significant drag effect on the NW limb of the Islay Anticline.

The picture as drawn here shows the Loch Skerrols thrust as a structure that postdates a phase of considerable amplification (but not much tightening) of the Islay Anticline. The ground-trace of the Loch Skerrols thrust shows a northward convex curvature between An Carn and Bun-an-uillt (Amos 1959). The mylonite foliation along the thrust in the latter area shows a north-north-westerly dip. Moreover, minor crenulations and brittle shears are overprinted on the mylonite foliation in this area. These show that a separate phase of folding ($?F_{2d}$ of Borradaile) locally postdates the thrusting.

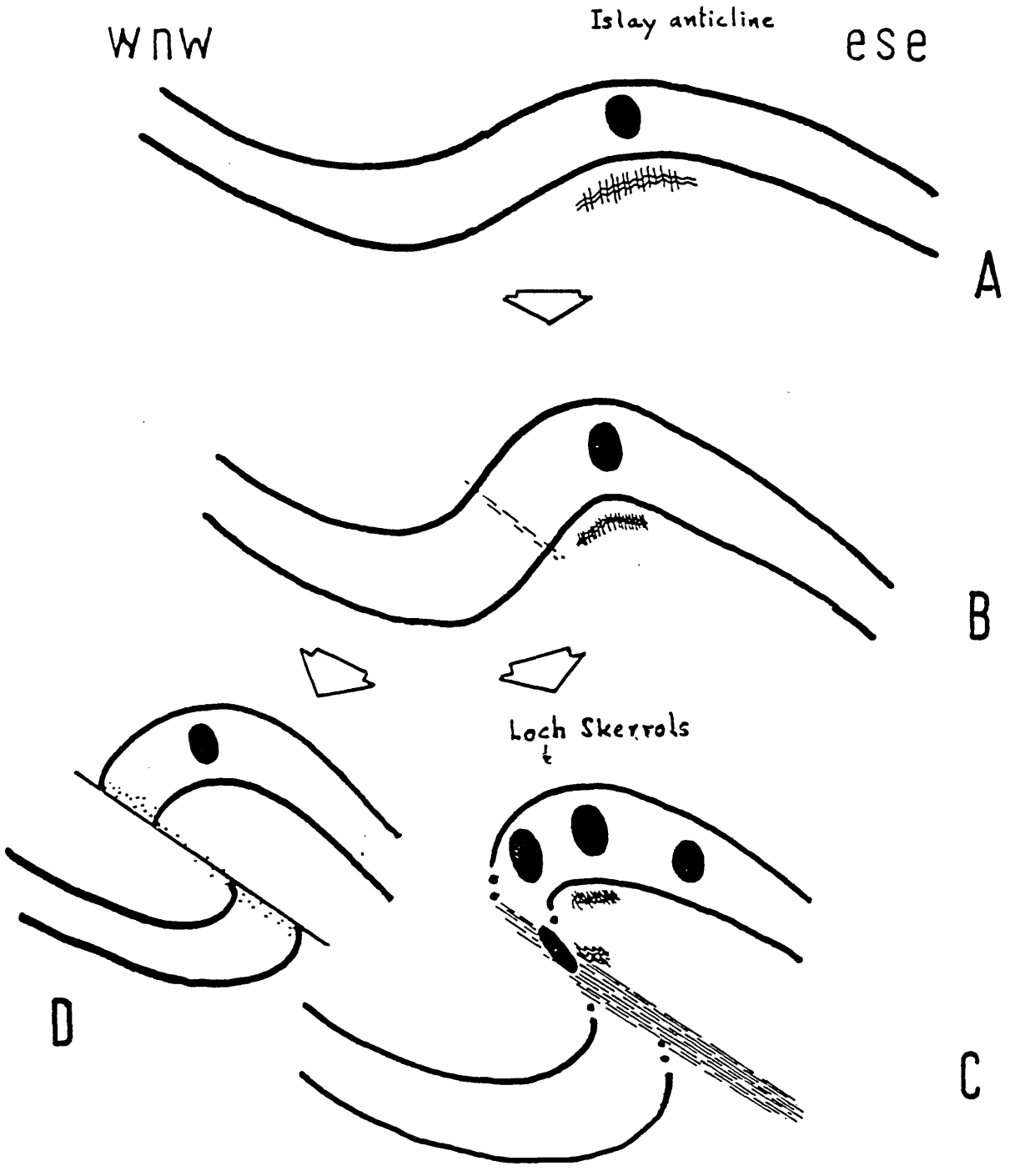


Figure 4.20. Schematic sketches showing the evolution of the Islay Anticline with progressive deformation. The Loch Skerrols thrust transgresses the western limb after considerable tightening of the fold. Two alternative paths from stage b reflects observed difference in the fold profile between Loch Skerrols and Gortartoid Point (NW Islay). Note that the footwall syncline shown here has not been mapped in the area.

CHAPTER 5

DEFORMATION HISTORY IN COLONSAY-ORONSAY

5.1 INTRODUCTION

The low grade metasediments in Colonsay and Oronsay belong to the Colonsay Group (Stewart 1975) and form an upward continuation of the succession unconformably overlying the Lewisian in W. Islay (Stewart 1962, Stewart and Hackman 1973). A gneissic band is exposed in NE Colonsay; petrographic similarity with the Lewisian gneisses elsewhere and a low radioactive content suggest that it is of much the same character and age as the Lewisian basement (Smith and Watson 1983). On its northwest the gneiss band is unconformably overlain by the sediments; the contact with the sediments in the southeast is concealed by blown sands. The sediments of NE Colonsay probably have an overlapping relationship with the rest of the Colonsay Group (see Chapter 2 for detailed discussion).

The metasediments are intruded by several suites of minor intrusions in the form of dykes, sills and small stocks and bosses. The character of the minor intrusions are similar to those of the Caledonian minor intrusions occurring in the Northern Highlands of Scotland (Smith 1979).

The metasediments in Colonsay have undergone several phases of folding. The sequence of deformation was punctuated by the emplacement of different groups of Caledonian minor intrusions. The early minor intrusions in the form of dykes and sills have been folded by later phases of folding.

Following the early works by the Geological Survey (Cunningham Craig et al. 1911, Wright 1908) the Colonsay rocks have been studied in detail from a stratigraphic point of view by Stewart 1962. The lithologic map as shown here is essentially that prepared by the survey. Results of detailed structural mapping (scale 1:10,000) are presented in this chapter. During Caledonian deformation the Lewisian-metasediment contact has undergone local shearing. Strain measurements and results from textural study of the deformed contact zone rocks are dealt with first. Study of minor structures reveals the superimposed nature of folds and associated structures. The morphology of successive axial planar cleavages varies with the style and the sequence of folding and there is a definite dependence on the lithology of the rocks affected. These questions are discussed in a later section.

5.2 OUTCROP PATTERN, FOLDS AND FAULTS

If one leaves aside outcrops occurring northeast of Kiloran Bay, the overall trend of the lithologic units is NNW-SSE. Starting from the Oronsay Greywacke unit successively younger horizons are exposed towards northeast. The Colonsay Limestone and the Staosnaig Phyllite represent the highest units in the sequence. Near Loch Fada the lithologic boundaries have only a gently curved form; the sheet dip is about 30 degrees towards east. In contrast, in the vicinity of Milbuie the boundaries take a wavy form with considerable amplitude (Fig. 5.1). Variation in the attitude of bedding and other structural elements shows that the wavy form of the outcrop is due to folding. As will be shown later, these major northeasterly folds are third generation structures (F_3). Prior to their development the broad structure appears to have been dominated by a homoclinal eastward dip except for local overturning caused by early structures (F_1 or F_2).

The sediments of NE Colonsay are unconformable to the Lewisian. The initial geometry of the lithologic boundaries was probably irregular due to the uneveness of the basin floor controlled by a local basement high. The present outcrop is rendered more complex by folding and displacement of the boundaries along faults. The structure around Kiloran Bay is controlled by late folds on axial planes with more than one orientations. South of Carnan Eoin the axial trace of a major F_3 fold runs WNW-ESE, whereas in the southern half of the Kiloran Bay NNE trending late folds occur.

A group of NE trending faults occur in northern Colonsay. The offset of lithologic bands shows that there is an apparent sinistral strike slip component of displacement. Studies of aerial photographs indicate that a major fault runs along the course of Loch Fada. The relative downthrow is on the northwesterly side. Since none of these faults is affected by folds in Colonsay, it seems that faulting post-dated the folding movement.

5.3 DEFORMATION AT LEWISIAN-METASEDIMENT CONTACT

5.3.1 General Statement

A band of gneissic rocks with a width of about 100 metres

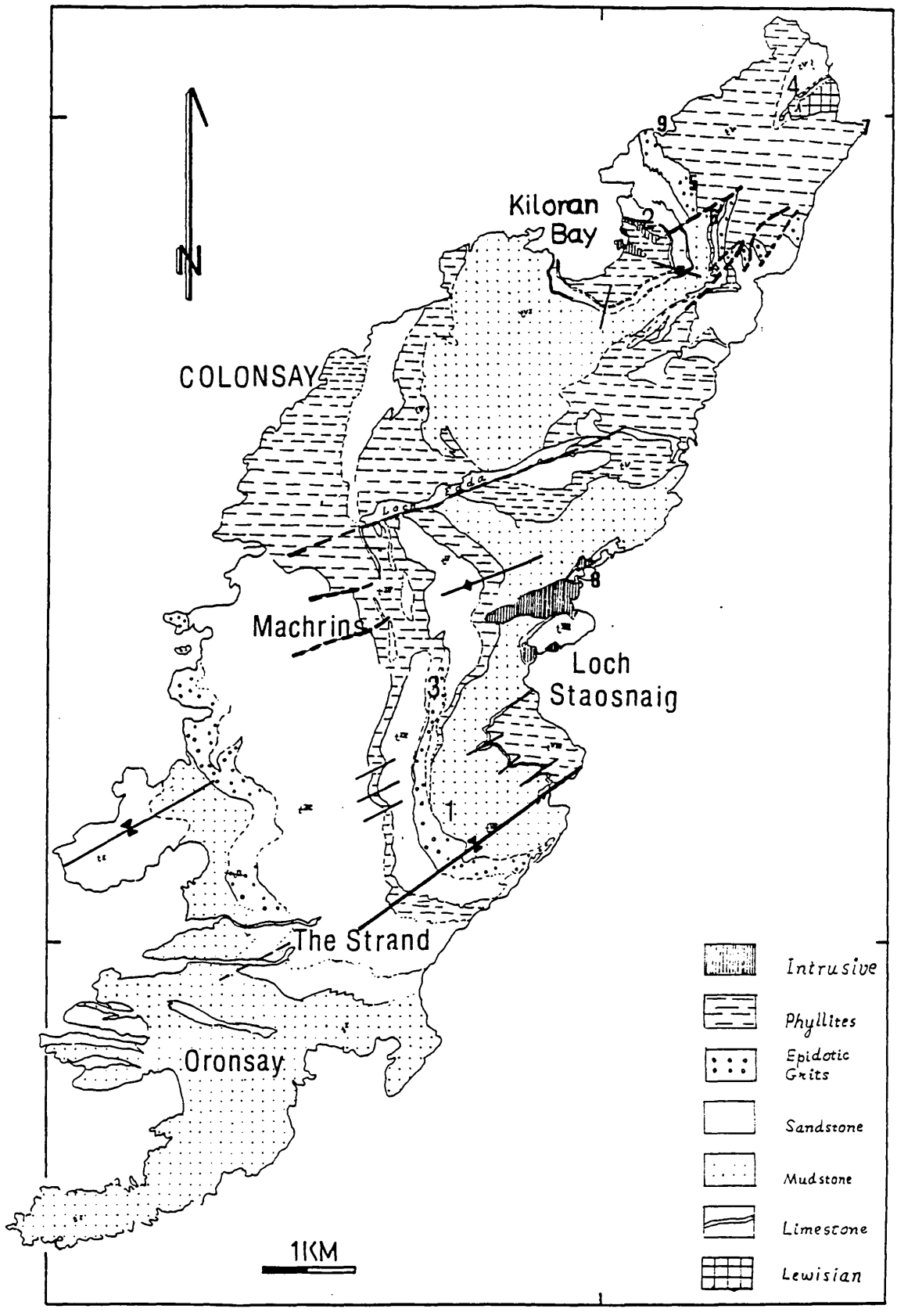


Figure 5.1. General geological map of Colonsay-Oronsay, after Survey map; axial traces of some F_3 folds shown. Locations are: 1 = Balleromínmore, 2 = Carnan Eion, 3 = Milbuie, 4 = Leac Bhuidhe, 5 = Balnahard, 6 = Bein Bhreac, 7 = Rubh a' Geodha, 8 = Colonsay Pier, 9 = Port an Obain.

outcrops in the NE End of Colonsay, around Leac Bhuidhe (Fig. 5.2). The banded gneisses have a general similarity with some of the Lewisian rocks of Iona and show a low radioactive content (as measured by portable gamma ray spectrometer). The major components of the gneiss are greenish amphibolitic bands which have retrograded to chloritic/epidotic material, and quartzo-feldspathic bands locally mylonitised to a creamy white platy rock. Remnants of coarse pegmatitic material can still be recognised in places.

A coarse gritty horizon with pebble bands occur to the north of the gneiss; the sequence at grid intersection (425 003) is as follows (Stewart 1962):

Flags

	(zone C	15m of dark blue-green mudstone
	(	containing abundant quartz-
	(	segregations. Gritty streaks
	(	appear near the lower contact
Leac Bhuidhe	(	
sediments	(zone B	10-13m of quartzite
	(	conglomerate
	(	
	(zone A	4-5m of dark blue mudstone with
	(	bands of pebbly sandstone

Sheared Gneiss

By far the commonest pebbles are those of olive green quartzite with a white crust. Other common pebble types are feldspar, epidote and granulite quartz.

Rocks along the contact particularly towards its western end, bear the evidence of localised shearing. The pebbly layers show a distinct shape fabric with the short axes of the pebbles at a high angle to the mesoscopic foliation. The Lewisian gneiss as well as the gritty rocks locally grades into white platy mylonite with a streaky lineation that plunges at a low angle either towards NNE or SSW.

Since the conspicuous mylonite foliation within the Lewisian and the pebbly grit dips towards SE, it appears as if the Lewisian is thrust over the sediments. However, towards the northeastern extremity of the grit band pebbles are less deformed, and the original compositional layers defined by the variation of grain size and pebble-matrix ratio dip towards NNW. Moreover, in detail the mylonite foliation is oblique to the overall trend of the contact which runs parallel to the bedding strike at the northeast end (Fig. 5.2). An unconformable contact between overlying Leac Bhuidhe sediments and the underlying Lewisian is thus confirmed. The relationship with the sediments to the south of the gneiss band is obscured by sand dunes. The nearest exposure of phyllites to the south is in the southern section of Balnahard Bay.

5.3.2 Microstructures and Strain

A westward increase in strain along the contact is associated with a narrowing of the gneiss and grit outcrops (Fig. 5.2) and is reflected in the micro-structure of the rocks. At the ENE extremity, the bedding is preserved and dips NNW. With the appearance of a pebble shape fabric, bedding becomes no longer recognisable and the visible foliation dips at about 55 degrees towards the southeast. Near the western end of the band, on joint surfaces normal to the foliation, the pebble axial ratio approaches 15:1. The matrix material surrounding the pebbles has the appearance of a quartz-feldspar-mica mylonite. In thin sections, the pebbles themselves show variation in microstructures with increasing strain as illustrated in Fig. 5.3. The majority of the pebbles are of schistose quartzite with varying proportions of phyllosilicates and carbonate material. In the less deformed pebbles there are two distinct modes of grain size of quartz grains. Larger grains, 1-2 mm across with undulose extinction, deformation bands and deformation lamellae are surrounded by finer (20-30 μm) grains which themselves are sometimes undulose. Some of the smaller grains are probably derived from syntectonic recrystallisation of the larger grains, as evidenced by the grain boundary recrystallisation of some deformed larger grains. The proportion of larger grains decreases as the pebbles becomes more deformed.

In the highly deformed pebbly grits, the smaller grains of quartz, together with mica with or without carbonates, make up the whole

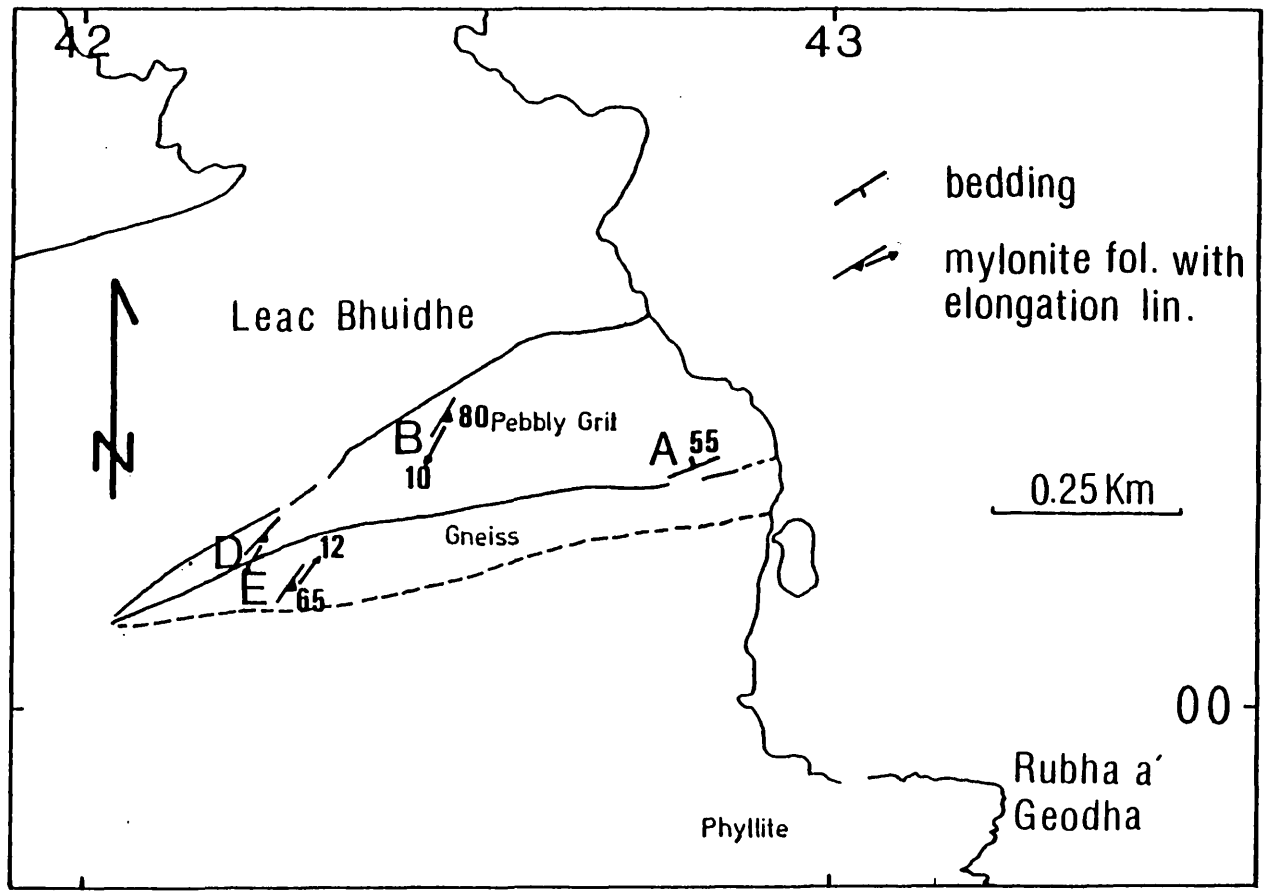
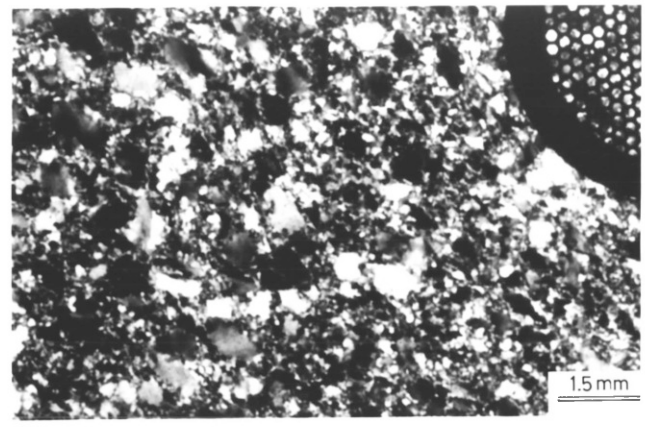


Figure 5.2. Outline geological map of NE End, Colonsay.

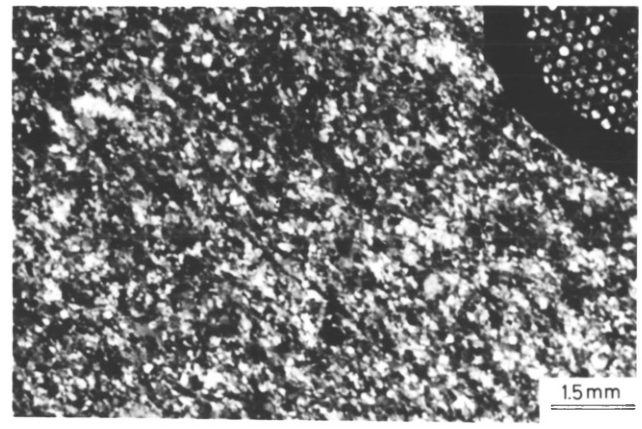
Figure 5.3. Change of pebble shape (left column) and intrapebble microstructure (right column). Follow arrows for increasing strain. Aspect ratio of pebbles low (top left) at lower strain, locality A on map in Fig. 5.2, and high at a higher strain, locality D on map in Fig. 5.2.

Within the pebbles, the proportion of dynamically recrystallised grains increases with increasing strain, localities A, B, D (top right, centre right and bottom right respectively) on map in Fig. 5.2. Optical micrographs from XZ section of pebbles.




1.5 mm




1.5 mm

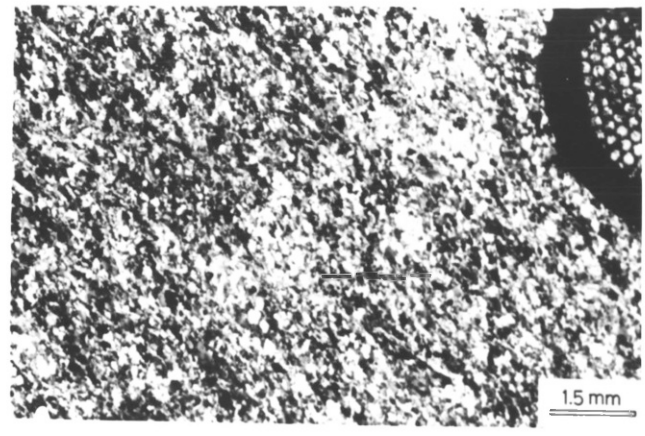
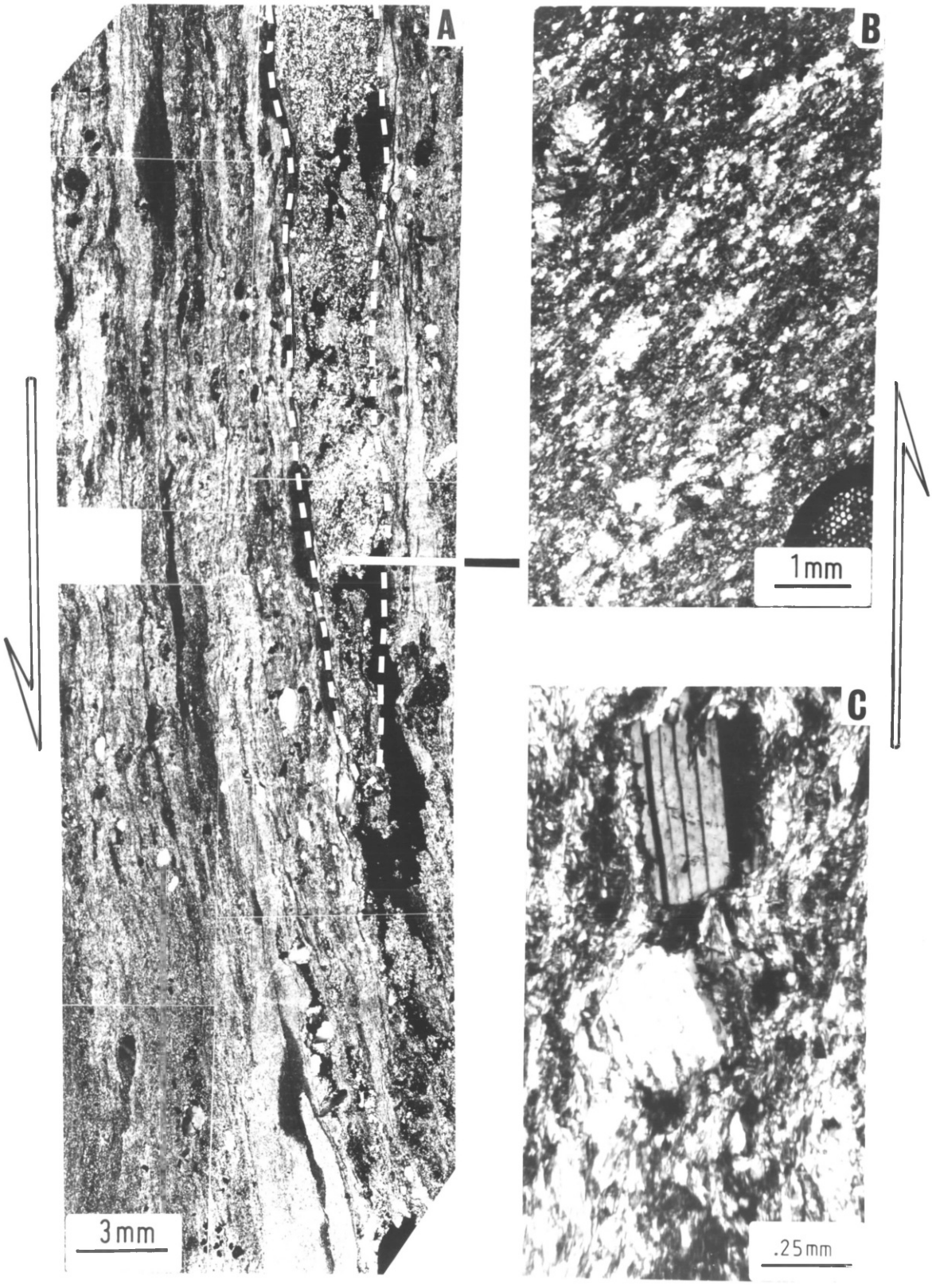

1.5 mm

Figure 5.4. Optical micrographs showing microstructures in mylonitised pebbly grit in contact with the Lewisian gneiss, NE End, Colonsay. All photographs from a thin section cut parallel to elongation lineation and perpendicular to foliation.

(a) Photomontage showing general mylonite foliation and pebble elongation (outlined); internal foliation with the pebble is oblique to the pebble boundary and mylonite foliation.

(b) Intrapebble foliation defined by parallel alignment of elongated small quartz grains. Obliquity of the intrapebble foliation is consistent with a sinistral strike-slip motion.

(c) Pull apart in plagioclase filled with fibrous chlorite. Notice rotation of fragment again indicating sinistral shear.



5.4

of the pebble. Even the smaller grains have an elongation at a small angle to the pebble long axis. The microstructures within a mylonitised grit is shown in Fig. 5.4a. The rock is a quartz-feldspar-mica mylonite. White feldspar and some ferromagnesian minerals (mostly epidote) behave in a brittle fashion, the quartz is deformed by crystal plastic mechanism. Isolated quartz clasts (single grains of quartz up to a mm across) show undulose extinction with deformation bands and local grain boundary recrystallisation. The feldspar and epidote grains are pulled apart or broken down into smaller pieces, some of which are rotated (Fig. 5.4c). The pull apart in feldspar is locally filled up with fibrous chlorite. Within the streaked out pebbles of quartzite, occasional relicts of larger grains are stretched into ribbon grains; the dynamically recrystallised grains show an elongation which is oblique to the boundary of the pebble and to the mylonite foliation outside the pebble (Fig. 5.4 a,b). The general mylonite foliation is defined by the alignment of the phyllosilicates, a significant fraction of which is probably derived from alteration of the feldspars, and by the alignment of the stretched pebbles. The obliquity of the shape fabric in the dynamically recrystallised grains within the distorted pebbles to the general mylonite foliation indicate a sinistral sense of movement parallel to the mylonite foliation. Rotation of some of the pulled apart feldspar also indicates a similar sense of movement. Note that the features shown in Fig. 5.4 are from thin sections cut parallel to the stretching lineation and perpendicular to the foliation. The stretching lineation is subhorizontal (NE-SW) and thus a dominant strike slip movement is indicated.

A strain estimate

Two-dimensional finite strain-ratios were determined from pebble axial ratio and fluctuation (R_f, ϕ) at a locality marked 'D' on Fig. 5.2, which shows a simplified map of the northeast end of Colonsay. The orientation of two joint surfaces and of the microscopic lineation is shown in Fig. 5.5a. One of these joints is perpendicular to the mesoscopic lineation. Pebble axial ratios were measured on photographs of the joint faces. R_f-ϕ plots for the two sections are shown in Fig. 5.5b,c. Assuming that the average pebble elongation would be close to the X-axis of the finite strain ellipsoid, one of the joints (which dips NNE) is close to the YZ plane of the strain ellipsoid. The other joint surface close to X-axis but a non-principal section of the strain ellipsoid.

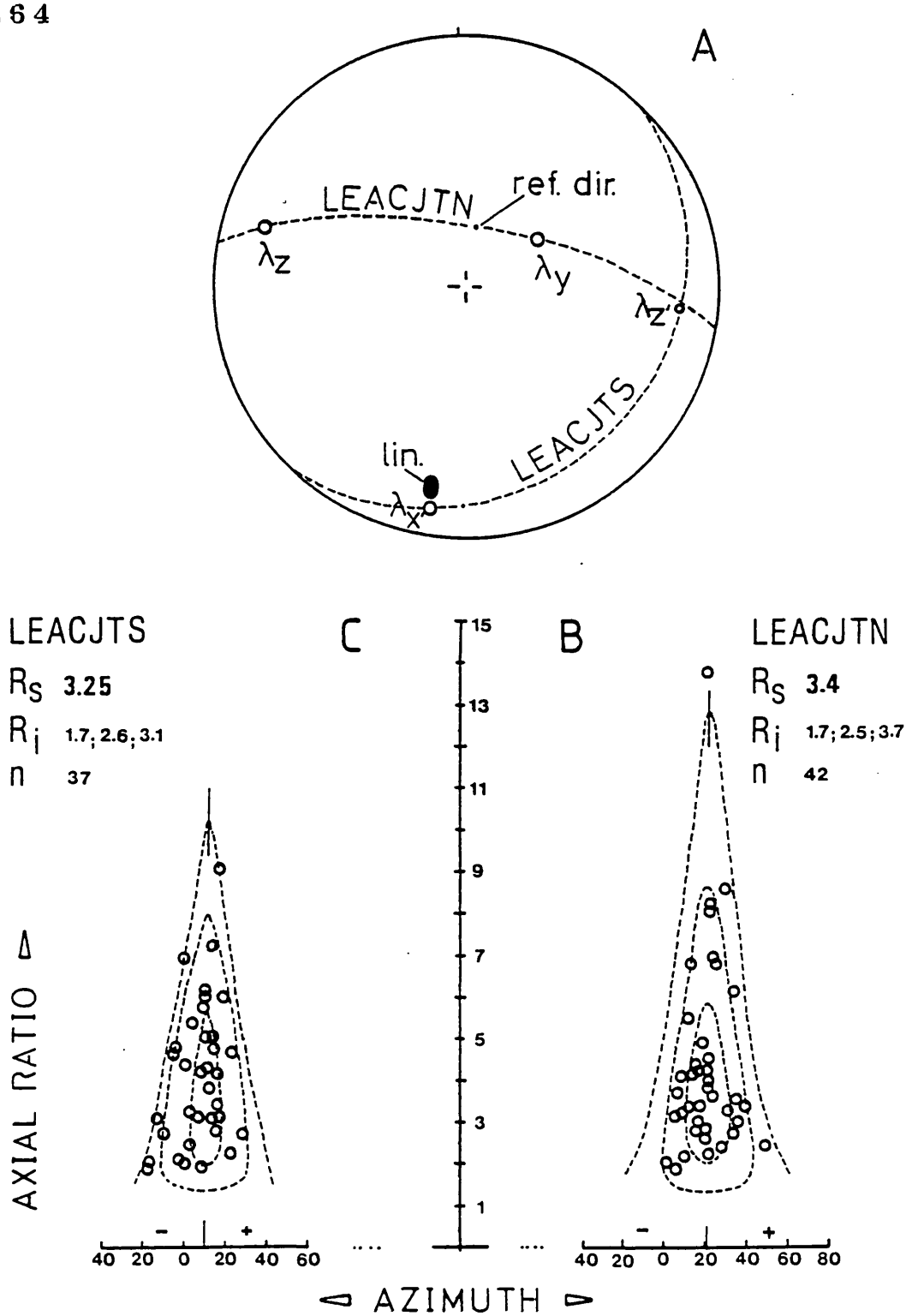


Figure 5.5. R_f-Ø plots for the determination of strain in the pebbly grit, locality marked D on Fig. 5.2.

(a) Equal-area plot showing the orientation of joint faces on which the pebble axial ratios were measured, and the principal quadratic elongations calculated from 2-dimensional strain measurements.

(b) R_f-Ø plot from joint face marked LEACJTN on (a). Strain ratio is 3.4 (YZ section).

(c) R_f-Ø plot from joint face marked LEACJTS on (a). Strain ratio is 3.25.

The 3-dimensional strain ratio is obtained by: first, calculating λ_z, in terms of R_{yz} ($=\sqrt{\lambda_y/\lambda_z}$) and then obtaining λ_x, ($\sim\lambda_x$) in terms of R_{yz}; the ratio λ_x/λ_z, is known from R_f-ϕ plot. The 3-dimensional strain ratios determined are - 1.28:1:0.30. The maximum shearing strain on XZ plane is 2.04. The direction of maximum shortening (Z) is in the NW quadrant with a low plunge (Fig. 5.5a). The finite strain ellipsoid falls in the flattening field (for zero volume strain), k = 0.1176.

A flattening type strain ellipsoid is apparently inconsistent with a dominant simple shear type deformation deduced from microstructures. However, the apparent inconsistency can be resolved by incorporating a volume strain, an initial flattening strain and/or a superimposed flattening strain following the simple shear type movement. The last alternative is supported by local crenulations of the mylonite foliation and associated development of an axial planar cleavage.

5.4 THE FOLD PHASES

5.4.1 Episodic Nature of Folding and Intrusion

The general outcrop form of the metasediments in Colonsay, at least in the southern region (including Oronsay) is controlled by simple antiforms and synforms trending in a NE-SW direction. However, when one looks at the minor structures at individual outcrops, the presence of refolded folds, cleavages and lineations suggests that the area has undergone a polyphase folding history. More than one axial plane cleavage can be observed in most exposures of pelitic/semipelitic rocks. To establish a structural history of the area the minor structures in different parts of the island have been studied in detail. On the basis of general appearance and form alone, one may distinguish several categories of minor structures; the differentiation of minor structures becomes more significant when their geometric relationships are considered. This analysis helps not only in recognition of structures of one kind or the other but also in relegating these structures to their proper place in the time bound sequence of deformation episodes.

Geometric criteria which are useful in determining the time relationship between various minor structures have been discussed by a

number of workers (Ramsay 1967, Turner and Weiss 1963, Wilson 1983). The essential criteria are listed below:

(A) Relationship between two foliations:

(i) A foliation parallel to the axial plane of a fold is later than one on which the fold develops; a crenulation cleavage is nearly always a secondary structure, and is parallel to the axial planes of micropuckerings on an earlier foliation.

(ii) A planar foliation transverse to a fold hinge is generally later than the foliation on which the fold develops.

(B) Relationship between a foliation and a lineation:

(i) The axis of a fold (including micropuckering) is later than the foliation on which the fold develops.

(ii) Lineation curving round the hinge of a fold:

(a) rectinlinear segments non-coplanar - lineation earlier than the folding event;

(b) rectilinear segments coplanar - the lineation may be either earlier or later than the folding event; if other criteria, such as folding of a foliation containing the lineation, are available, deductions can be made.

(C) Refolding relationships - when two folds show mutual interference, the axial plane and/or axis of the older is folded by the younger.

On the basis of one or more of the criteria listed above, it was possible to distinguish structures of successive generations from one another in Colonsay-Oronsay. In isolated exposures, recognition of structures of a particular generation is often guided by the orientation of the structural elements as well as by their morphologic characters. One added advantage in Colonsay is the presence of minor intrusions which locally transgress the metasediments. Although as a broad group, the majority of the sills and dykes of Colonsay belong to the Appinite Suite (Smith 1979), some of these dykes and sills cut across even the latest structural elements, whereas others are themselves folded or display a strain induced fabric. A temporal grouping of the minor

intrusions is possible on the basis of their relationship with folds and axial plane cleavages of different generations. The structural analysis of different subareas followed by their correlation throughout the island shows that in Colonsay-Oronsay there are at least three phases of folding and cleavage development. The folding events and the nomenclature of associated structures, together with a grouping of the minor intrusions relative to fold phases are shown in Table 5.1.

Table 5.1 General classification of minor structures in Colonsay and their relationship with minor intrusions

Deformation Phase	Fold Style		Axial Plane Cleavage		Minor Intrusion
D_3	F_3	Kinks or open to close folds	S_3	Quartz segregation parallel to kink plane Fracture or crenulation/P.S. cleavage	Felsic porphyrite Kiloran Syenite Scalasaig Diorite (explosion breccia)
D_2	F_2	Overturned folds	S_2	Crenulation/P.S. cleavage	Microdiorites Early lamprophyre sheets
D_1	F_1	Isoclinal folds	S_1	Crenulation cleavage, schistosity	

P.S. = pressure solution

5.4.2 D1 Structures

5.4.2.1 Early Isoclinal Folds

Isoclinal folds with wavelength varying from a few centimeters to a few meters have been recorded from Port Mor, Bein Bhreac and Northeast end of Northern Colonsay, and in the outcrops of Kilchattan Phyllite between Loch Fada in the NW and Milbuie in the southeast. Many of these minor isoclinal folds and associated axial plane cleavage (S_2) are refolded by later structures (Figs. 5.6a-b). In Bein Bhreac, east of the Balnahard farm, compositional layers in creamy feldspathic grits are thrown into isoclinal folds (Fig. 5.6c) with an axial plane cleavage

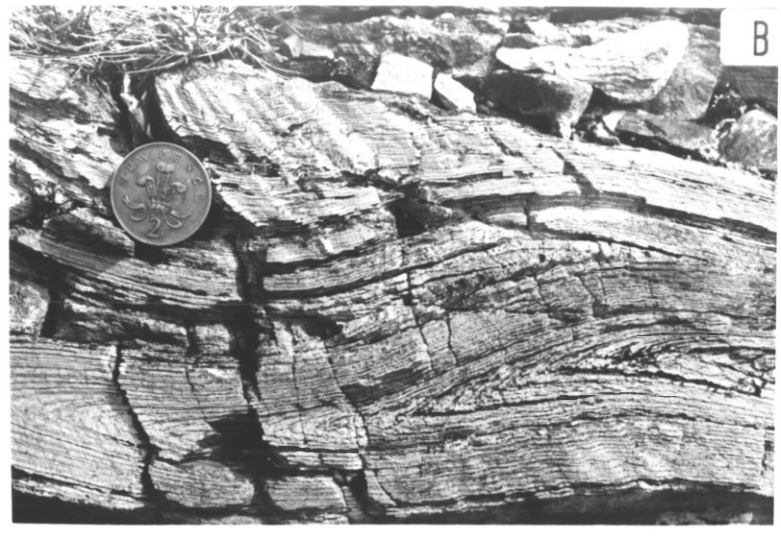
Figure 5.6. Early isoclinal folds (F_1) in Colonsay.

(a-b) Refolded F_1 structures, Milbuie. In both the field photographs F_3 minor folds are superimposed on F_1 folds. The difference in interference pattern is due to variable orientation of F_1 elements with respect to F_3 and the orientation of the outcrop face. (b) on a NE-SW cross-section; (a) on a flattish outcrop. Axis of F_3 folds in (b) plunges 32° towards 125°.

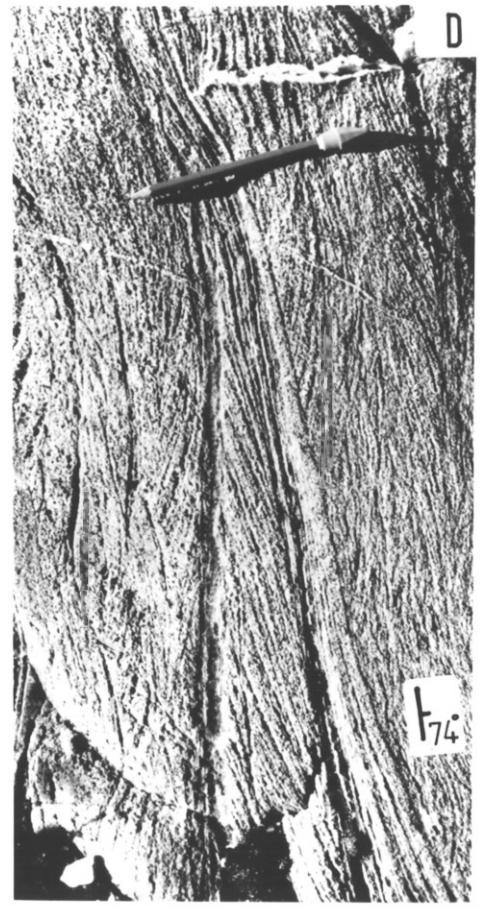
(c) Isoclinal folds in white arkosic grit, Balnahard.

(d) Local overturning of cross-beds due to F_1 folds, grit bands east of Balnahard.


A


B


C
0.5m


D
F74

defined by the alignment of strained feldspar and quartz clasts. The clast elongation lineation is parallel to the fold axis which plunges at 10 degrees towards north. In this area the grits are locally overturned as indicated by the truncation of foreset laminae of cross-beds in a direction opposite to the dip of beds (Fig. 5.7d).

Orientation of the F_1 folds varies from one subarea to the other as one would expect in an area of multiphase folding. In the Kiloran Bay area, the bedding-schistosity (S_1) intersection has an E-W trend (near zero degree plunge) compared to the northerly plunge east of Balnahard. In the Milbuie area, the F_1 axis plunges at 20 degrees towards southeast; the axial plane (or S_1) dip varies from 30 - 50 degrees towards east (Fig. 5.7).

5.4.2.2 Other Structures

Early isoclinal folding in Colonsay is accompanied by a clast elongation parallel to the fold axis, e.g. the lineation observed in Beinn Bhreac. In the same area the axial plane cleavage (S_1) is defined in grits by a grain shape fabric of feldspar and quartz clasts. Presumably S_1 is the XY plane of the finite strain ellipsoid associated first phase of deformation. In sections perpendicular to F_1 axis (X) one would expect a subsidiary stretching of more competent layers at a late stage of folding, if the ratio of Y:Z is sufficiently high. A model situation is illustrated in Fig. 5.8. In areas where F_1 folds are well developed and the lithologic variations provide enough competence contrast, more competent sandy layers are stretched to produce boudin like structures. Such structures have been recorded from Callileach Uragaig, southwest of Kiloran Bay. Boudins in thick gritty layers within the Machrins Group are also observed in the Machrins area. The folding of early boudinaged layers by F_2 folds (Fig. 5.9a) confirms that the extensional structures were indeed formed during the D_1 phase of deformation.

5.4.3 D_2 Structures

A group of asymmetric overturned folds belong to this generation. F_2 folds have been recorded from (a) the stretch of outcrops between Machrins and Carn Glas in the south, (b) southwest section of Kiloran

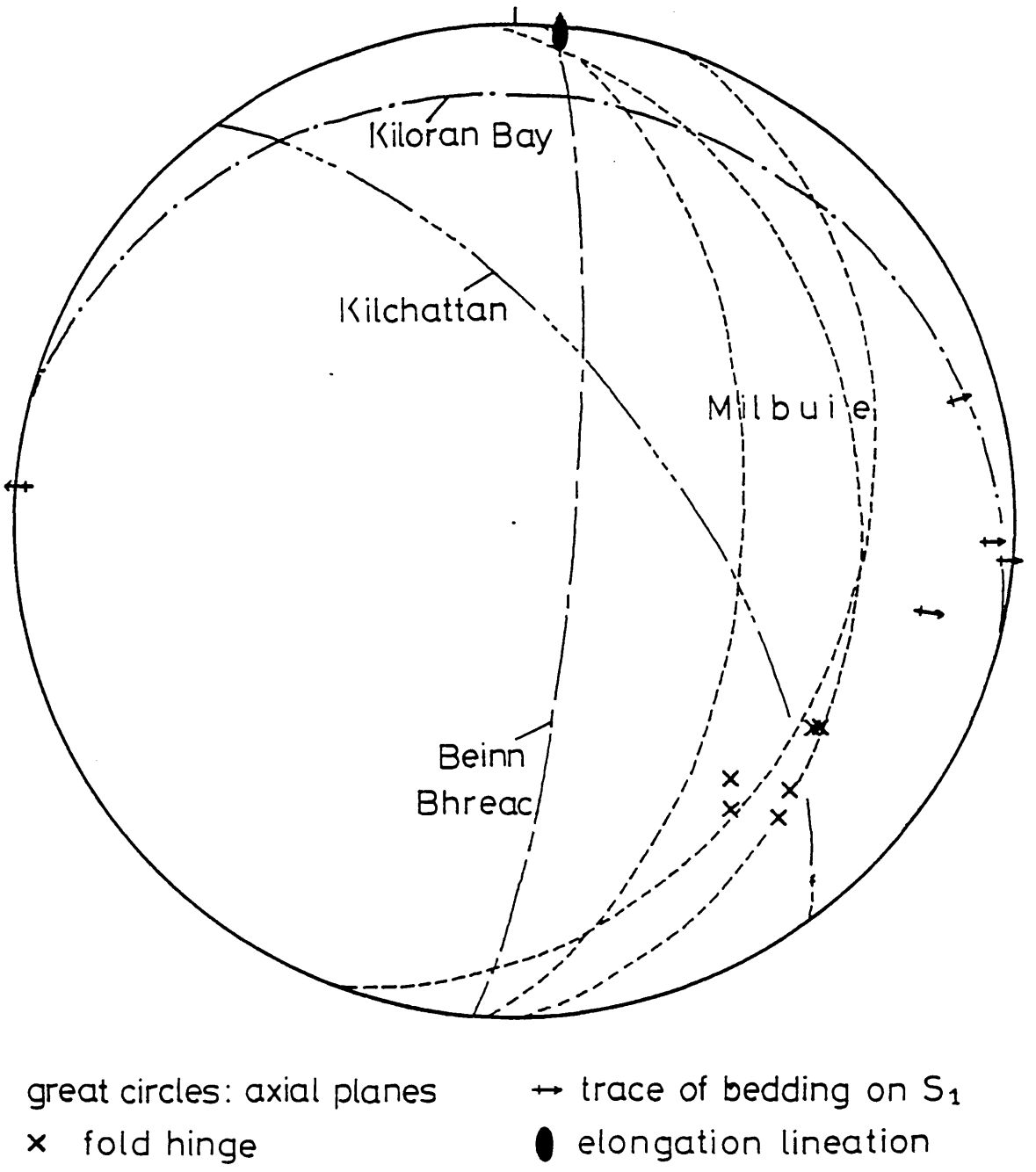


Figure 5.7. Equal-area plot showing the orientations of F_1 elements from different areas in Colonsay.

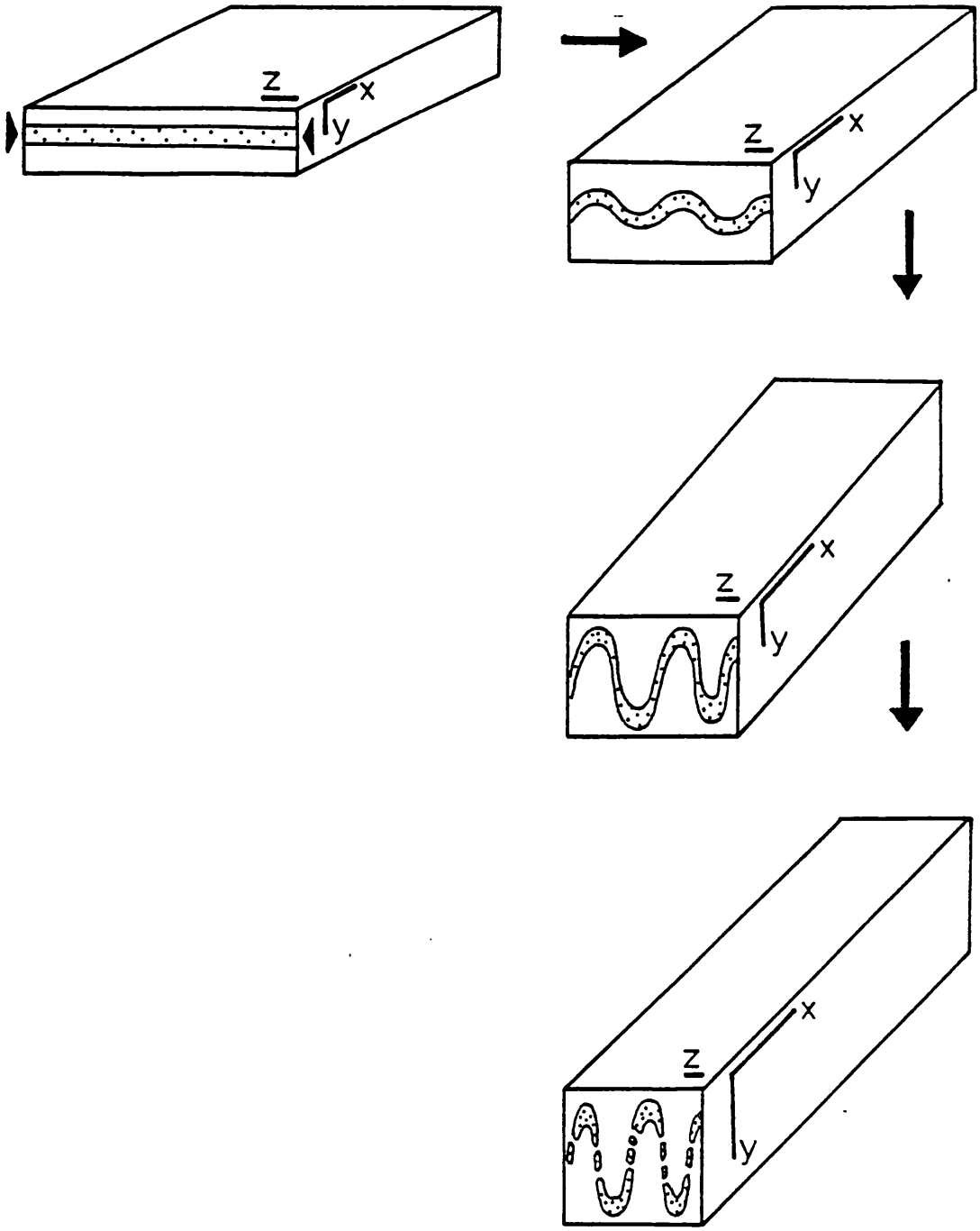


Figure 5.8. Schematic drawings to illustrate the formation of boudinage at a late stage of F_1 folding. With increasing limb-dip and tightening of the folds the limbs assume a position suitable for secondary layer parallel extension.

Bay, (c) Port an Obain and (d) between Balnahard and Rubh' a' Geodha in NE Colonsay. West of the Coast Guard station in Machrins, a boudinaged grit layer is thrown into a series of overturned folds with considerable amplitude (Fig. 5.9a). The surrounding phyllitic/muddy layers show a pressure solution or a crenulation cleavage axial planar to the F_2 folds. Elsewhere in Machrins, the F_2 folds have a lesser amplitude than the one described, but the overturned geometry and accompanying axial plane cleavage is ubiquitous. Notice that in contrast to the F_1 fold hinges, F_2 hinges on gritty layers show hardly any clast shape fabric. Any axial planar cleavage, S_2, in such lithology is a pressure solution cleavage.

The orientations of F_2 elements are shown in Figure 5.10a. There is a noticeable contrast in the orientation of F_2 structures from different areas; this is due to the deflection of all earlier structure by F_3 folds, which control the overall outcrop pattern in Colonsay.

F_2 folds not only deform the bedding, F_1 structures and axial plane cleavage associated with F_1, but also a group of early 'lamprophyrye' sheets. These intrusives have been largely altered to a carbonate + phyllosilicate bearing rock with relict feldspar grains. In the area west of Rubh a' Geodha in NE Colonsay, the phyllites are traversed by many sheets of lamprophyres subparallel to the schistosity in the country rock. The intrusive sheets are thrown into overturned folds with an axial planar cleavage that develops both in the country rock and in the dyke rock. The trend of the axial plane cleavage is ENE, dip varies from 35 to 50 degrees SE.

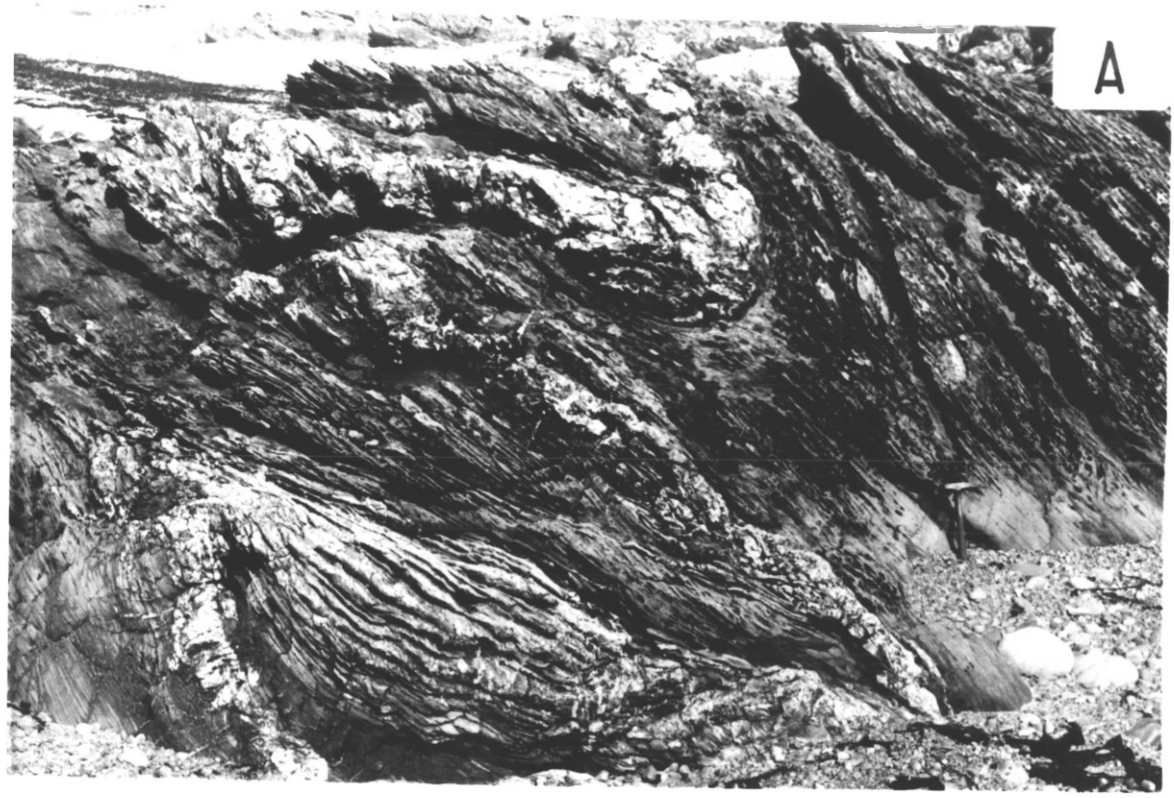
5.4.4 D_3 Structures

Major folds which develop considerable amplitude are seen in the southeastern half of the island, particularly in the area between Milbuie and the Strand separating Colonsay from Oronsay. Minor folds which deform both the schistosity (S_1) and the axial plane cleavage (S_2) associated with F_2 folds are common in many exposures throughout the island. The pattern of outcrop around Kiloran Bay, along with the systematic variation in the orientation style of minor folds shows that a major NNW-ESE trending fold controls the structure in the northern half of the bay while northeasterly folds control the structure in the

Figure 5.9. F_2 folds in Colonsay.

(a) Boudinaged grit layer folded by F_2 folds, south of Coast Guard station, Machrins.

(b) Overturned F_2 folds in grit, Machrins. Note that the axial plane cleavage is well developed only in shaly bands.





5.9

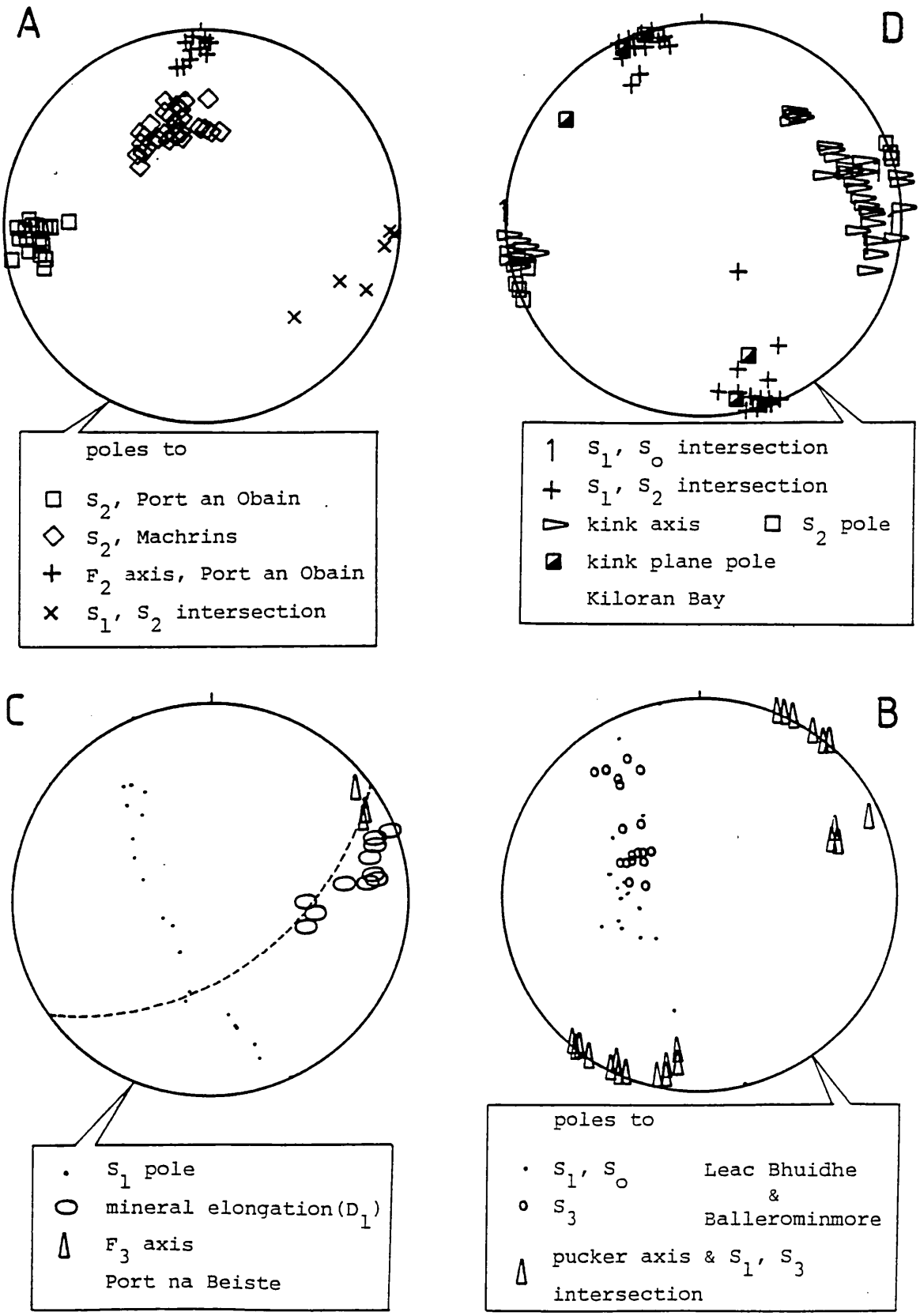


Figure 5.10. Equal-area plots showing orientation of minor structures from different parts of Colonsay.

(a) F_2 and S_2 from Port an Obain and Machrins.

(b) Early structures in F_3 domains, Leac Bhuidhe and Ballerominmore.

(c) Third folds at Port na Beiste, SE Colonsay.

(d) Minor structures at Kiloran Bay.

southern half (the structure around Kiloran Bay is discussed in Chapter 7 in relation to minor intrusions). Minor F_3 structures vary from open asymmetric folds to kinks; folds become tighter and more symmetrical along the axial region of major F_3 folds (Fig. 5.11). The majority of the structures have an axial trend in the NE quadrant with the axial plane dipping steeply southeast. However, locally the F_3 structures have other orientations, e.g. Kiloran Bay (see above) and the area between Beinn Bhreac and Cnoc na Faire in NE Colonsay. In the latter area a set of kink planes trend ENE and dip at 25-45 degrees towards SSE. That these structures are actually late in the sequence of deformation phases is shown by their superposition on F_2 structures (Fig. 5.12a).

A Major F_3 Fold in SE Colonsay

The variation in altitude of schistosity and compositional layers (bedding) across a traverse from the west of Balleromínmore to Port na Beiste clearly shows that a major NE tending synform controls the outcrop of the lithologic units (Fig. 5.1, see also map IV). The associated minor folds also show a systematic variation in style. West of the axial trace the minor folds are asymmetric, open and 'S' shaped in cross-sections looking down plunge. Near the axial region minor folds are tighter and become more symmetrical. At Port na Beiste folds with a wavelength of the order of a few tens of meters are common and there is a crenulation cleavage parallel to F_3 axial plane in pelitic rocks. In general F_3 folds and the associated axial plane cleavage, S_3 is well developed throughout the coastal strip from Rubh' a' Geodh in the north to the Strand in the south.

Lamprophyric dykes with oblique internal foliation are uncommon in Colonsay. At a few places where they have been recorded relationship with local folds suggest that the internal foliation probably formed during late-D_2 to D_3 stage. Microdiorite/appinitic dykes are common in Colonsay. Some of these are locally folded by D_3 structures. Thus these dykes were emplaced before the D_3 deformation. However, there is no appreciable axial planar fabric associated with these folded microdiorite dykes.

Kink Structures

Some of the F_3 structures in their geometry and mode of development are akin to kinks rather than sinusoidal folds. In the southern half of the Kiloran Bay, the phyllites and flaggy rocks are often traversed by late kinks on NNE trends. The kinks are associated with brittle shears which develop in conjugate sets (Fig. 5.12d). In the area east of Beinn Bhreac the phyllites and semipelitic rocks are traversed by kinks. The orientations of the kink plane varies from exposure to exposure and sometimes even in the same exposure. A vertical set of kinks trends 056°. An inclined set varies in orientation but on an average dips at 30 degrees towards south. A set of quartz veins occur parallel to the latter set of kink planes; the quartz fibres grow at high angles to the vein wall suggesting that cracks opened up parallel to the kink planes (Fig. 5.12 b-c).

As a whole, kink-like minor structures in Colonsay develop after the first and second phase of folds and associated axial plane cleavages were formed. The presence of well developed earlier cleavages as well as of a bedding parallel fabric renders the rocks sufficiently anisotropic to favour kink formation at a later stage. The geographic variation in the orientation of kink planes is probably controlled by the local orientation of the direction of anisotropy with respect to the shortening direction. It has been pointed out earlier that the orientation of schistosity which controls the anisotropy varies from one part of the island to another. Even some of the major F_3 folds may have been initiated before the formation of the kinks.

5.5 DEFORMATION AND CLEAVAGE DEVELOPMENT

All the three phases of folds described above are associated with axial plane cleavages. The morphology of the cleavage belonging to each phase of deformation is to a certain extent lithology dependent. There is also a control of strain heterogeneity on the intensity of cleavage development and its spatial variation. In this section the morphology of the axial planar cleavages, their variation with fold phases and their relationship with intensity of fold development are discussed by looking at the deformation microstructures of the mineral phases involved. Some comments are also made regarding the deformation mechanisms involved. Local relationships between metamorphic minerals

Figure 5.11. F_3 structures from Colonsay.

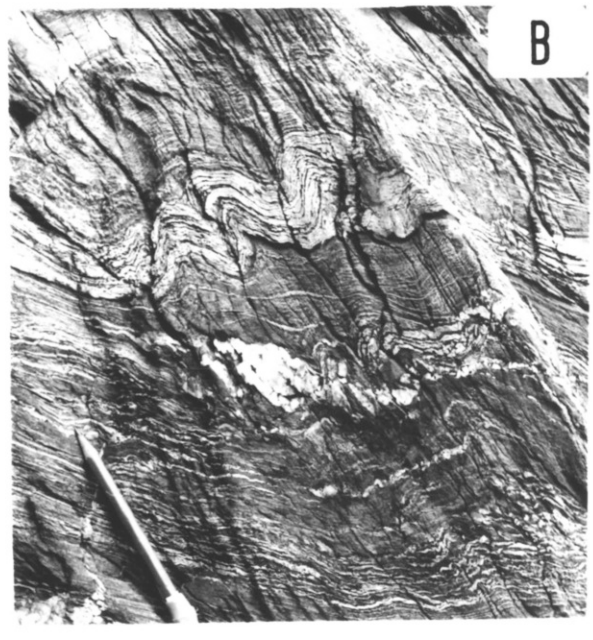
(a) On the east coast, northeast of the Strand.

(b) Milbuie.

(c) Southeast of Carnain Eoin, Kiloran Bay area.

Note that an axial plane cleavage becomes better developed in the southeastern part of the island.





5.11

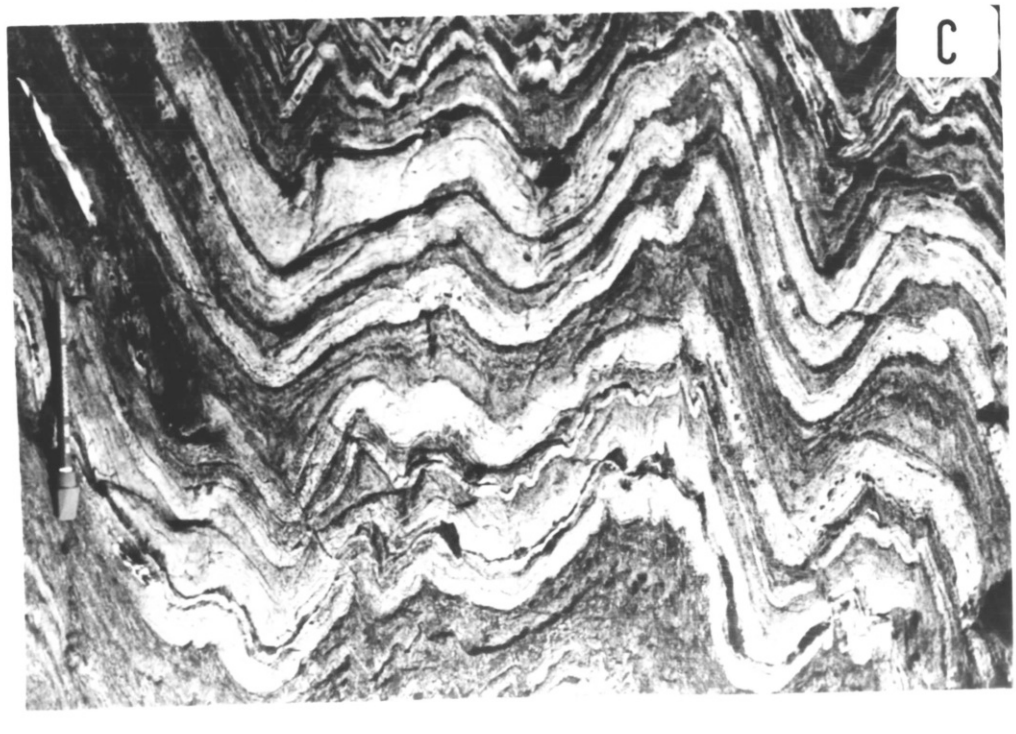


Figure 5.12. Kink-like structures from Colonsay.

(a) Late kinks superposed on an asymmetric F_3 fold, NE Colonsay.

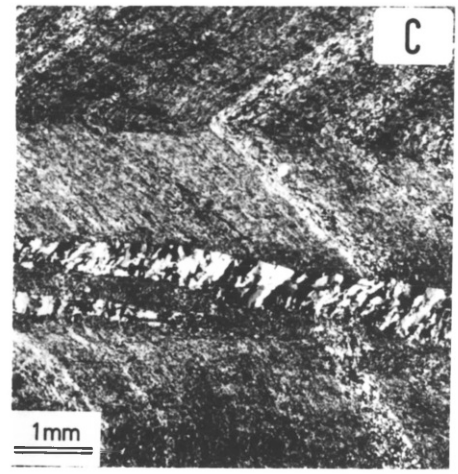
(b) Quartz veins parallel to gently inclined kink planes.

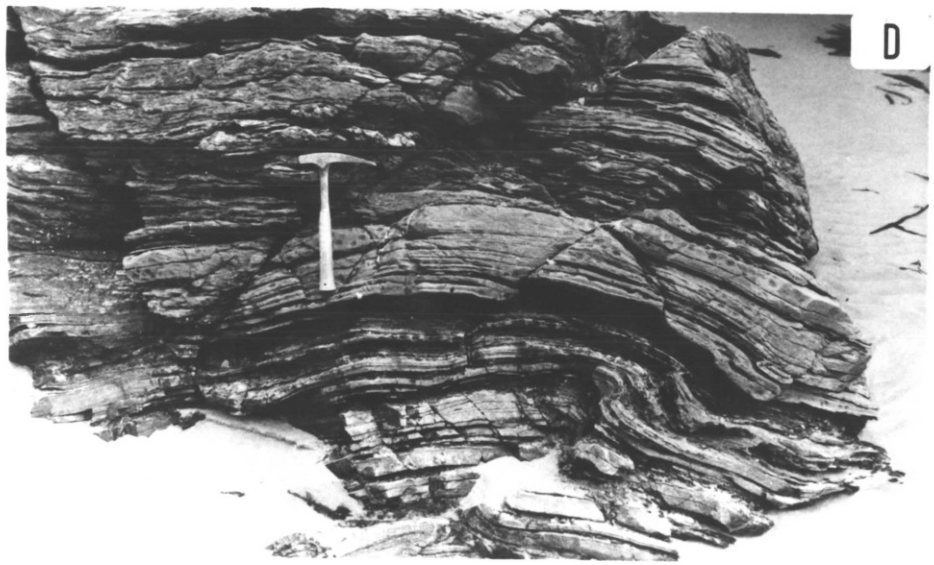
(c) Optical micrograph showing details of a quartz vein in (b); note that the quartz fibres grow at a high angle to the vein wall.

(d) Conjugate brittle shears parallel to axial plane of kinks, south of Kiloran Bay.









5.12

and different axial planar cleavages are illustrated with a few examples.

5.5.1 The First Axial Plane Cleavage, S_1

The isoclinal folds of first generation (F_1) are associated with an axial plane cleavage which develops equally well in most of the rock types exposed in Colonsay. However, the morphology of the cleavage varies depending on:

(a) the grain size of the rocks affected,

(b) the presence of an earlier bedding parallel fabric (it is not uncommon to have a pre-tectonic alignment of phyllosilicates parallel to bedding in thinly laminated units), and

(c) the proportion of phyllosilicates to mineral phases such as quartz and feldspar (the dominant rock types in Colonsay are quartzo-feldspathic grit, mudstones and shales metamorphosed to phyllites).

In very fine grained rocks such as the mudstones of Oronsay, the cleavage is defined by close spaced (30-140 μm) pressure solution (P.S.) seams which anastomose around elongated pods of quartz + feldspar + phyllosilicate grains, or single grains of quartz or feldspar. The P.S. seams themselves consist of aligned fine grained micas and chlorites and some concentration of Fe-rich material as indicated by a brown colouration under the microscope. The phyllosilicates are generally very fine (20-30 μm) and in areas between two relatively widely spaced P.S. seams the alignment of the flakes is poor. Individual quartz or feldspar grains are usually strain free, although occasional larger grains may show undulose extinction. Locally larger flakes of mica and chlorite grow across the P.S. cleavage indicating that the metamorphic mineral formation probably post-dated the initiation of the first cleavage (S_1).

In rocks where alternate phyllosilicate and quartz rich bands are affected by the F_1 folds, (Kilchattan Phyllite, Milbuie epidotic grits and phyllites), the axial plane cleavage starts as a crenulation

Figure 5.13. Morphology of S_1, Colonsay.

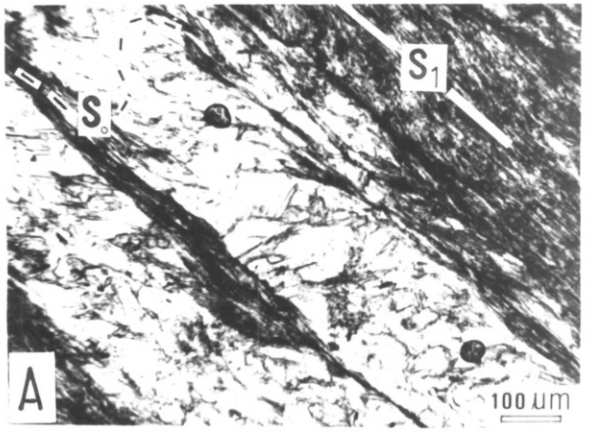
(a-b) Transposition of bedding (S_o) parallel fabric to produce a secondary banding parallel to S_1.

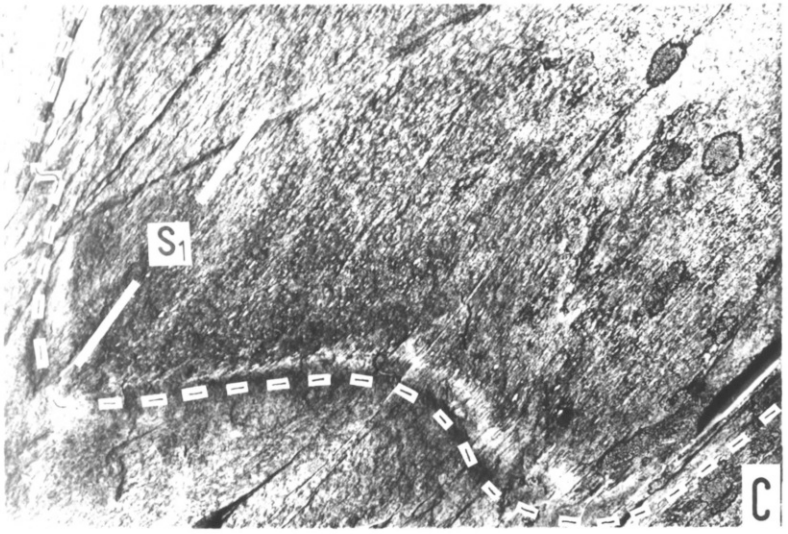
(a) Photomicrograph from phyllites, Kiloran Bay;

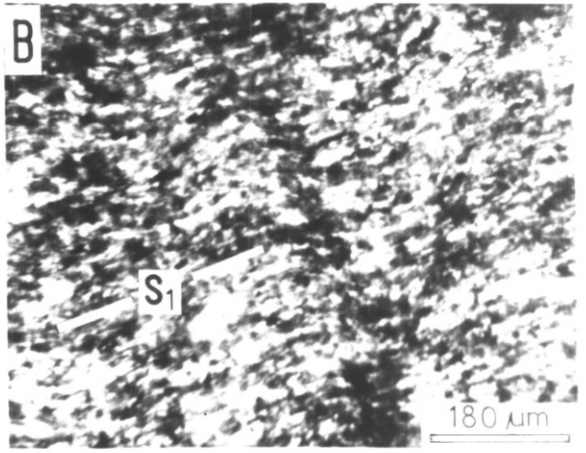
(b) Details of phyllosilicate rich band in (a); no microfold hinges are apparent.

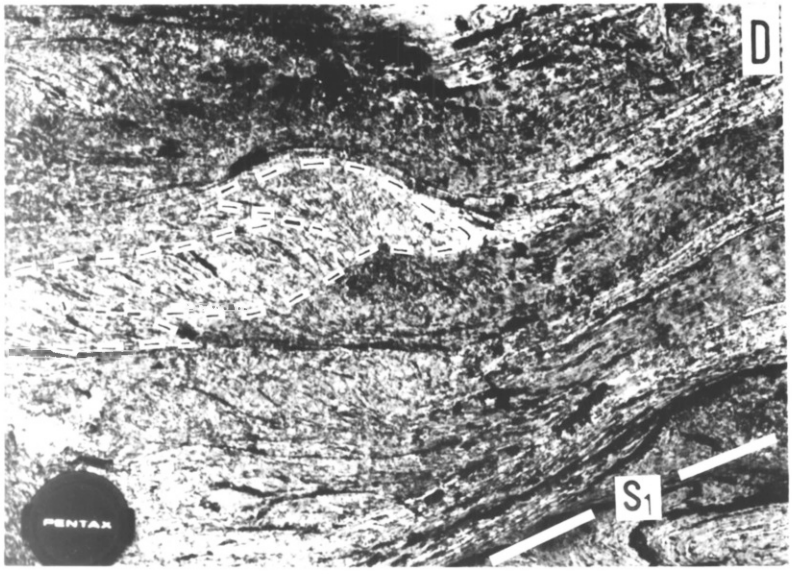
(c) Flattening of detrital quartz and feldspar grains parallel to S_1; Milbuie Grit, Milbuie.

(d) Semipelitic rocks, Port an Obain.


S1
S2
A
100 µm


S1
C


B
S1
180 µm


D
S1
PENTAX

cleavage. With increasing deformation and amplification of microfolds, the bedding parallel compositional layering is transposed to form a secondary banding parallel to the axial plane of relict F_1 hinges (Fig. 5.13 a,d); in bands originally rich in phyllisilicates S_1 is a schistosity with parallel alignment of mica flakes without any trace of microfold hinges (Fig. 5.13b). Even in secondary bands rich in phyllosilicates, the flakes are arranged in a parallel fashion and microfold hinges are not apparent in magnifications up to x400. Only in bands composed of quartz + sparse mica (+chlorite) can relict F_1 hinges be identified.

In rocks composed dominantly of quartz + feldspar (grit bands east of Balnahard, Milbuie epidotic grits), isoclinal F_1 folds are traversed by a penetrative axial plane cleavage. The foliation is defined by parallel alignment of elongated quartz lenses and feldspar grains (Fig. 5.13c). Larger feldspar grains show undulose extinction, pull aparts, and fractures in several directions with consequent granulation of larger grains; infillings of quartz in pull aparts are also recorded. Deformation features in quartz grains include undulose extinction with subgrain structure, deformation bands, and dynamic recrystallisation. Along the hinges of F_1 folds the quartz lenses are thoroughly recrystallised dynamically into small grains (40-50 μm). In thin sections cut parallel to the clast elongation lineation and perpendicular to the foliation, the dynamically recrystallised grains are themselves slightly flattened (with undulose extinction) and are aligned parallel to the axial plane cleavage. Recall that the deformation at Lewisian-metasediment contact in NE Colonsay produces local mylonitisation in grits and there is an well developed grain shape fabric in the sheared grits (see Section 5.3).

5.5.2 Second Axial Plane Cleavage, S_2

The morphology of S_2 varies from a crenulation cleavage in quartz + mica rocks (grain size 40-100 μm) to a pressure solution cleavage in fine grained rocks (e.g. mudstone member of Oronsay Greywacke unit) or in carbonate bearing rocks (impure limestone bands in Kiloran Bay). In folded early 'lamprophyric' dykes there is an axial plane cleavage which can be traced from the surrounding crenulated phyllites into the dyke rock. In the dyke rock, the axial plane cleavage is defined by a shape

fabric in carbonate grains plus pressure solution seams with a concentration of phyllosilicates. In Colonsay these folded early 'lamprophyres' are highly altered; petrographically they consist of carbonates, altered feldspars (including plagioclase), phyllosilicates and opaques.

In quartz + mica + chlorite bearing metasedimentary rocks, S_2 is a crenulation cleavage with alternate microlithons rich in quartz and mica (+ chlorite). In the quartz rich microlithons, F_2 hinges defined by alignment of mica + chlorite are still preserved; the bent mica (chlorite) flakes show undulose extinction (no polygonisation of mica grains around F_2 hinges).

In fine grained rocks (e.g. Oronsay Greywacke) the cleavage (S_2) in the outcrop has all the appearances of a pressure solution cleavage without any sign of minor folds between P.S. seams (Fig. 5.14a). In graded beds such pressure solution cleavage shows a cleavage refraction. The angle between the bedding and cleavage becomes more acute in finer grained material and the apparent spacing of the P.S. seams diminishes with a reduction in grain size.

In carbonate bearing rocks (e.g. impure limestone bands around Kiloran Bay), S_2 develops as a P.S. cleavage which is axial planar to overturned minor folds (Fig. 5.14b). In thin section, carbonate (calcite) grains show common twinning and kinking. Quartz grains are usually free from optical effects of strain except occasional undulose extinction, and so are the muscovite (+ chlorite) grains. Irregular P.S. seams (<10 μm wide) traverse the rock with an average spacing of 400 μm (Fig. 5.14c).

In folded lamprophyric dykes the cleavage is of pressure solution type; however, under the microscope there is also an elongation of carbonate grains parallel to the cleavage. Deformation twins, kink bands and some recrystallisation are common in the carbonate grains. Feldspars show undulose extinction.

In relatively coarse quarzto-feldspathic rocks (e.g. Machrin Grits, Dun Gallain epidotic grits or Milbuie grit), S_2 appears as a widely spaced P.S. cleavage near F_2 fold hinges, while a crenulation

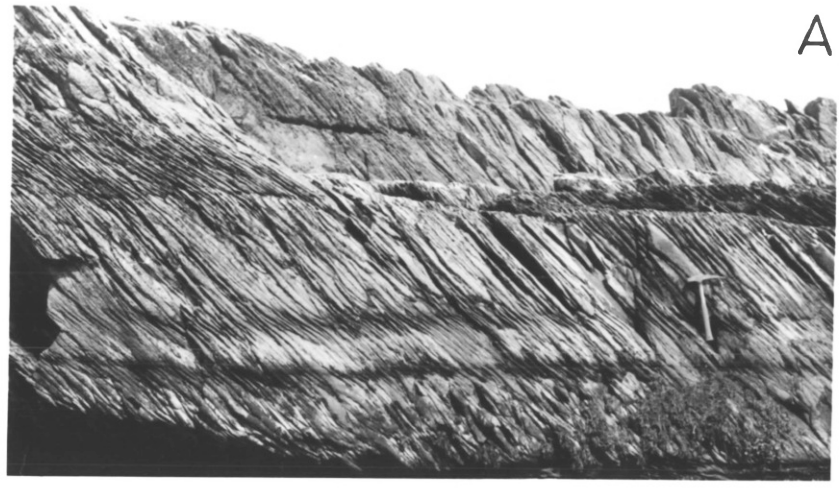
Figure 5.14. Morphology of S_2 cleavage.

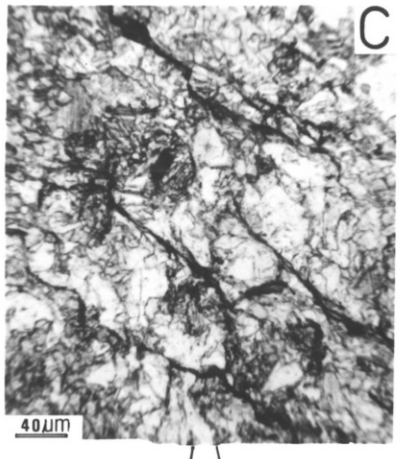
(a) Cleavage refraction in Oronsay Mudstone, south of Ardskenish.

(b) Pressure solution cleavage in limestone bands, Kiloran Bay. Note the folded quartz rich layer (bottom) which was boudinaged prior to F_2 folding.

(c) Micrograph (plane polarised light) showing pressure solution seams in limestone. Details from (c) is shown in the photomicrograph of the bottom left corner. Note twinning and kinking of calcite grains.

(d) Details from an F_2 hinge in Fig. 5.9(b). Detrital grains do not show any apparent shape fabric. Compare with Fig. 5.13(c).











5.14

cleavage is well developed in pelitic intercalations; grit bands show only spaced P.S. cleavage, there is no appreciable clast elongation parallel to the axial plane of the fold (Fig. 5.14d). This style is in sharp contrast to that of the axial plane cleavage associated with F_1 folds (compare Figs.5.13c and 5.14d).

5.5.3 The Third Axial Plane Cleavage, S_3

In the western and northern half of the island, axial plane cleavage associated with F_3 folds is developed only in pelitic rocks where S_1 or S_2 cleavage is already well developed. However, in the southeastern half of the island, especially the coastal strip between Scalasaig and the Strand, F_3 folds are widespread and the associated axial plane cleavage is well developed. In pelitic rocks, the morphology of S_3 is that of a crenulation cleavage. Microlithons consisting of a stack of one or more microfold hinges are separated by very thin (<5 μm) P.S. seams or plane fractures. There is an apparent displacement across such P.S. seams. Micas in the fold hinges show undulose extinction but no polygonisation. In folded quartzo-feldspathic grit layers the axial plane cleavage appears as a fracture or P.S. cleavage (Fig. 5.11c).

5.5.4 Spatial Variation in the Intensity of S_3 Cleavage

It has previously been suggested that the 'second cleavage' and the 'second folding' vary in intensity of development from west to east across the island (Colonsay Memoir, 1911). However, a closer look at outcrops of pelitic rocks even close to the west coast shows that two well developed cleavages are present, the earlier one being axial planar to isoclinal F_1 folds and the later cleavage associated with F_2 folds. It transpires that the early workers did not recognise that there are at least three phases of folding and cleavage development in Colonsay. While the second folding (F_2) and the associated axial plane cleavage (S_2) is more or less evenly developed in the island, the third phase of folding (F_3) and the associated cleavage (S_3) does increase in intensity of development from west to east.

5.5.5 Relationship between Metamorphism and Folding

The common assemblage of muscovite + chlorite + quartz ± epidote in pelitic rocks suggests that the overall metamorphic condition during Caledonian deformation in Colonsay was that of low greenschist facies (thermal metamorphism due to minor intrusions is commented on in Chapter 7). North of Kiloran Bay, the phyllites commonly contain chloritoid porphyroblasts (see Table 5.2 for microprobe analyses). The localised development of chloritoid is probably related to the bulk chemistry of the sediments. Chloritoid occurs only in rocks with an Al_2O_3 content in excess of the quantity present in micas and epidote; the rocks must also have a high Fe^{2+}/Mg^{2+} ratio (Halferdahl quoted in Miyashiro 1973). Although the range of lithostatic pressure for the formation of chloritoid is very wide, it is an indicator of the low temperature (chlorite to staurolite zone) part of the Barrovian sequence (Miyashiro 1973).

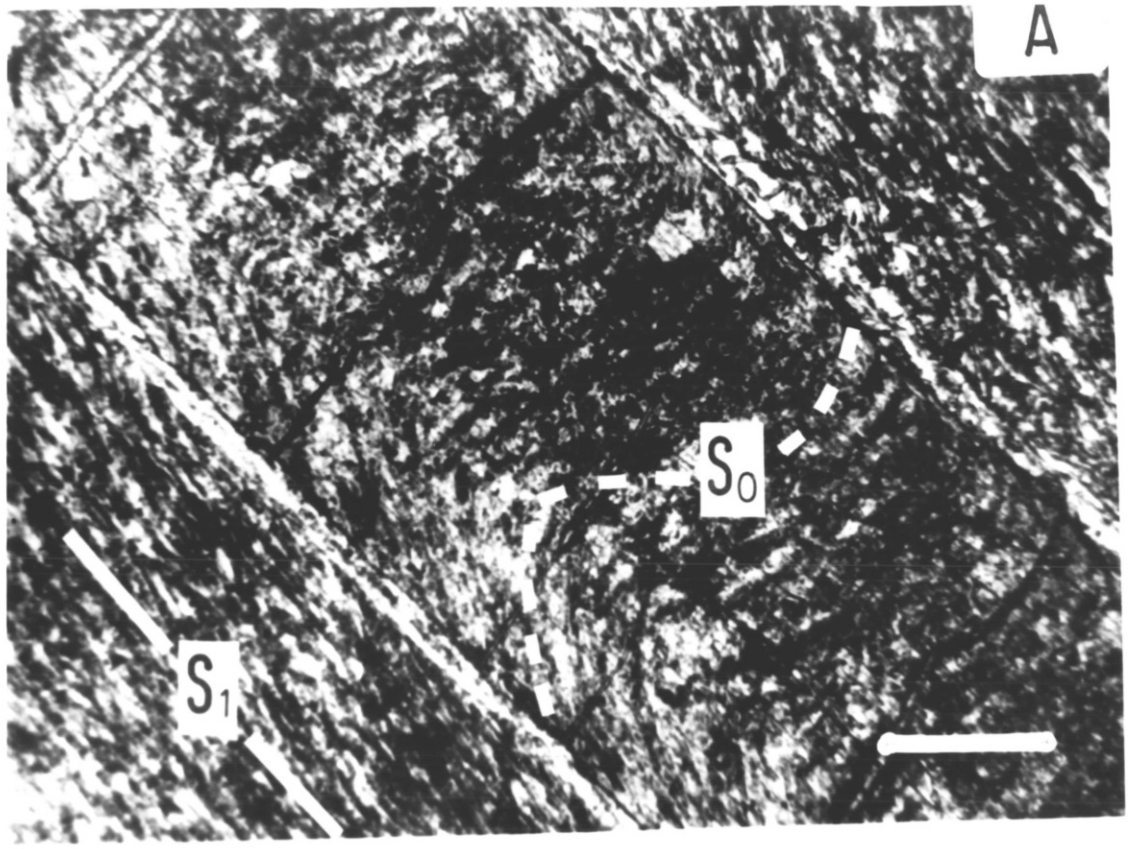
The relationship between the porphyroblasts and the microfolds of one generation or the other throws some light on the temporal relationship between metamorphic mineral formation and deformation. In thin sections cut from samples with F_1 fold hinges, porphyroblasts of chloritoid can be seen to replace a folded bedding parallel early fabric (Fig. 5.15a). In other areas where the axial plane cleavage associated with F_1 folds are refolded by F_2's, large chloritoid crystals themselves are bent into microfolds (Fig. 5.15b). The relationships illustrated in Fig. 5.15 clearly shows that the formation of chloritoid post-dated the initiation of F_1 folds and associated cleavage; the second phase of folding post-dated the chloritoid formation.

In other specimens exhibiting S_1 cleavage, large crystals of muscovite + chlorite occur transverse to the S_1 cleavage. Moreover, in F_1 microfold hinges the phyllosilicates are polygonised. In contrast to this, across F_2 hinges bent flakes of muscovites and chlorites show an undulose extinction confirming that the peak of metamorphic crystallisation separated the two folding events, F_1 and F_2.

Figure 5.15. Optical micrographs showing the relationship between metamorphic mineral crystallisation and deformation.

(a) A chloritoid crystal replacing folded bedding parallel fabric (S_o). Scale bar is 100 μm.

(b) Folded chloritoid crystals and S_2; scale bar is 250 μm.


A
S_0
S_1


B
S_2

Table 5.2 Electron microprobe analyses of chloritoids, North of Kiloran Bay

	1	2	3	4	5	6
Na_2O	0.038	0.024	0.063		0.014	0.123
MgO	1.749	1.667	1.789	1.724	1.718	1.591
Al_2O_3	39.477	39.900	38.871	39.702	40.021	39.256
SiO_2	23.789	23.970	22.962	23.710	23.667	23.608
K_2O	-	-	.049	.021	.058	.046
CaO	-	-	-	.052	-	-
TiO_2	0.046	0.043	3.599	-	-	.066
Cr_2O_3	0.039	-	.006	-	-	.098
MnO	0.957	1.032	.984	1.166	1.145	.973
FeO*	25.341	24.966	24.377	25.253	24.998	24.943
NiO	-	-	-	-	-	-
Total	91.436	91.601	92.700	91.628	91.621	90.703
No. of ions per 14 (O,OH) OH not included						
Si	2.008	2.014	1.913	1.999	1.992	2.009
Al	3.928	3.952	3.817	3.945	3.970	3.937
Ti	.003	.003	.225	-	-	.004
Fe	1.789	1.755	1.698	1.780	1.760	1.775
Mg	.220	.208	.222	.216	.215	.202
Mn	.068	.073	.069	.083	.081	.070
Cr	.003	-	-	-	-	.006
Ni	-	-	-	-	-	-
Na	.006	.004	.010	-	.002	.020
K	-	-	.005	.003	.006	.005
Ca	-	-	-	.004	-	-

Analyses 1-9 sp. 231/82

Table 5.2 Chloritoid Analyses (Cont.)

	7	8	9	10
Na_2O	.090	.093	.349	.192
MgO	1.785	1.684	1.837	1.500
Al_2O_3	39.744	39.977	39.909	35.513
SiO_2	23.691	23.802	23.583	21.160
K_2O	.027	.088	.034	-
CaO	.108	-	.109	.010
TiO_2	-	.095	.153	9.462
Cr_2O_3	.026	-	.061	.085
MnO	1.188	1.021	1.025	.932
FeO*	26.093	26.467	26.092	23.323
NiO	.169	-	-	-
Total	92.923	93.227	93.153	92.178
No of ions per 14 (O,OH), OH not included				
Si	1.981	1.982	1.966	1.786
Al	3.917	3.925	3.922	3.533
Ti	-	.005	.009	0.600
Fe	1.825	1.843	1.819	1.647
Mg	.223	.209	.228	0.189
Mn	.084	.072	.072	.067
Cr	.001	-	.004	.005
Ni	.001	-	-	-
Na	.015	.015	.056	.031
K	.003	.009	.004	-
Ca	.009	-	.009	.001

Analysis 10. From Sp. 232/82

Table 5.2 Chloritoid Analyses (Cont.)

	11	12	13	14	15
Na_2O	.076	-	-	-	.033
MgO	1.701	1.357	1.549	1.721	1.531
Al_2O_3	41.240	40.255	40.635	41.123	40.608
SiO_2	24.203	23.858	24.168	23.935	24.009
K_2O	-	-	.016	-	-
CaO	-	-	.014	.027	-
TiO_2	.100	.064	-	.049	-
Cr_2O_3	.016	.011	-	.143	-
MnO	1.173	1.173	.1.90	.812	1.158
FeO*	25.242	25.122	24.708	25.067	24.679
NiO	-	.173	-	-	.025
Total	93.752	92.016	92.438	92.878	92.043
Si	1.986	1.999	2.009	1.980	2.004
Al	3.990	3.977	3.982	4.009	3.999
Ti	.006	.004	-	.003	-
Fe	1.733	1.761	1.718	1.734	1.723
Mg	.208	.169	.192	.213	.190
Mn	.081	.084	.084	.057	.082
Cr	.001	-	-	.009	-
Ni	-	.001	.010	-	.003
Na	.012	-	-	-	.005
K	-	-	.015	-	-
Ca	-	-	.001	.002	-

Analyses 11-15, Sp. 166/81

* Total iron as FeO

CHAPTER 6

LOCAL STRUCTURES IN IONA - REGIONAL IMPLICATIONS

6.1 INTRODUCTION

A steeply dipping assemblage of arkosic conglomerate, grit, shale and flaggy psammites overlies the Lewisian Gneiss in Iona: these sediments are regarded as Torridonian (Stewart 1975). Their eastern limit is the Moine Thrust which is supposed to pass through the Sound of Iona (Clough 1911, Fraser 1977). The location of the Moine Thrust in the Ross of Mull region is postulated on the ground that while in the Ross of Mull the metasediments (Moine) are in the amphibolite facies with a mineral assemblage of garnet + kyanite + sillimanite, the general metamorphic grade of the Iona sediments is that of low greenschist facies (disregarding the effect of the late thermal metamorphism). Both the Moine rocks in the Ross of Mull and the sediments of SE Iona are affected by a thermal metamorphism associated with the intrusion of the Ross of Mull Granite.

The Torridonian in Iona has been remapped (see map V). Although the broad structure is that of an easterly dipping and eastward-facing homoclinal sequence, local overturning is indicated by the presence of overturned cross-bedding and overturned isoclinal folds on a mesoscopic scale. The presence of sheared rocks along the Lewisian-Torridonian contact and of other zones of dislocation within the Lewisian itself suggests, as will be shown later, that the deformation style is that of a thrust belt. In the following section the deformation along the contact is described. The minor structures within the Torridonian and their relationship with the thrusting movement are described in the subsequent section. One striking feature about the Torridonian in Iona is the steep altitude of both the planar fabric in the dislocation zones and the early axial plane cleavage in the sediments. One possible explanation is that shortening of the belt took place after thrust movements. The late Caledonian structures in Iona are discussed with this point in mind. The timing of the Ross of Mull Granite intrusion and associated contact metamorphism is relevant to this question. Although lamprophyric dykes (Microdiorite Suite, Smith 1979) are rather uncommon in Iona, felsic-porphyrite dykes are common both within the Torridonian and the Lewisian. These dykes lend themselves as relative time markers in the sequence of deformation events.

6.2 DEFORMATION ALONG THE LEWISIAN-TORRIDONIAN CONTACT

6.2.1 General Features

In NE Iona, a coarse boulder bed overlies the Lewisian gneiss. Much of the material forming the rock unit immediately overlying the Lewisian is undoubtedly derived from the Lewisian basement. Although metre-size boulders such as those seen in the northeast have not been recorded elsewhere along the contact, pebbles of feldspars, epidote and quartzo-feldspathic gneiss up to a few cms across are not uncommon in the lowest unit throughout the island. There is no doubt that an original unconformable relationship between the sedimentary sequence of eastern Iona and the Lewisian is preserved. However, even in the northernmost outcrop of the conglomeratic horizon, the matrix surrounding the large gneissic boulders shows a weakly developed L-S fabric. The foliation dips at 70 degrees towards ESE, the clast elongation lineation is downdip on this foliation. The Lewisian gneisses below the contact show little sign of any penetrative shearing apart from local shatter zones; the gneissic banding and the pre-Torridonian epidote veins (Fraser 1977) and pegmatites are generally preserved.

Tracing the contact towards SSE one observes an increase in the L-S fabric in the contact zone rocks. Both the Torridonian and the Lewisian gneisses in the vicinity of the contact are affected by mylonitisation. In the area NE of Marble Quarry, the Lewisian immediately below the contact is highly foliated with a streaky lineation plunging downdip on foliation. The pebbles in the conglomerate immediately overlying the Lewisian are drawn into spindle shaped forms also with a down-dip elongation. The rock has all the appearances of a mylonite. In general the effect of mylonitisation along the contact increases towards the south. In southern Iona not only the basal conglomerate unit but also the grits overlying it show effects of mylonitisation.

The general orientation of the mylonite foliation and associated elongation lineation is shown in Fig. 6.1. The stretching direction is down-dip on a steep ESE dipping zone of displacement. The arrangement can be explained in terms a westerly up dip movement of the Torridonian along the contact zone. On a mesoscopic scale the same sense of movement is indicated by displacement of quartz segregations in the zone of mylonite (Fig. 6.2).

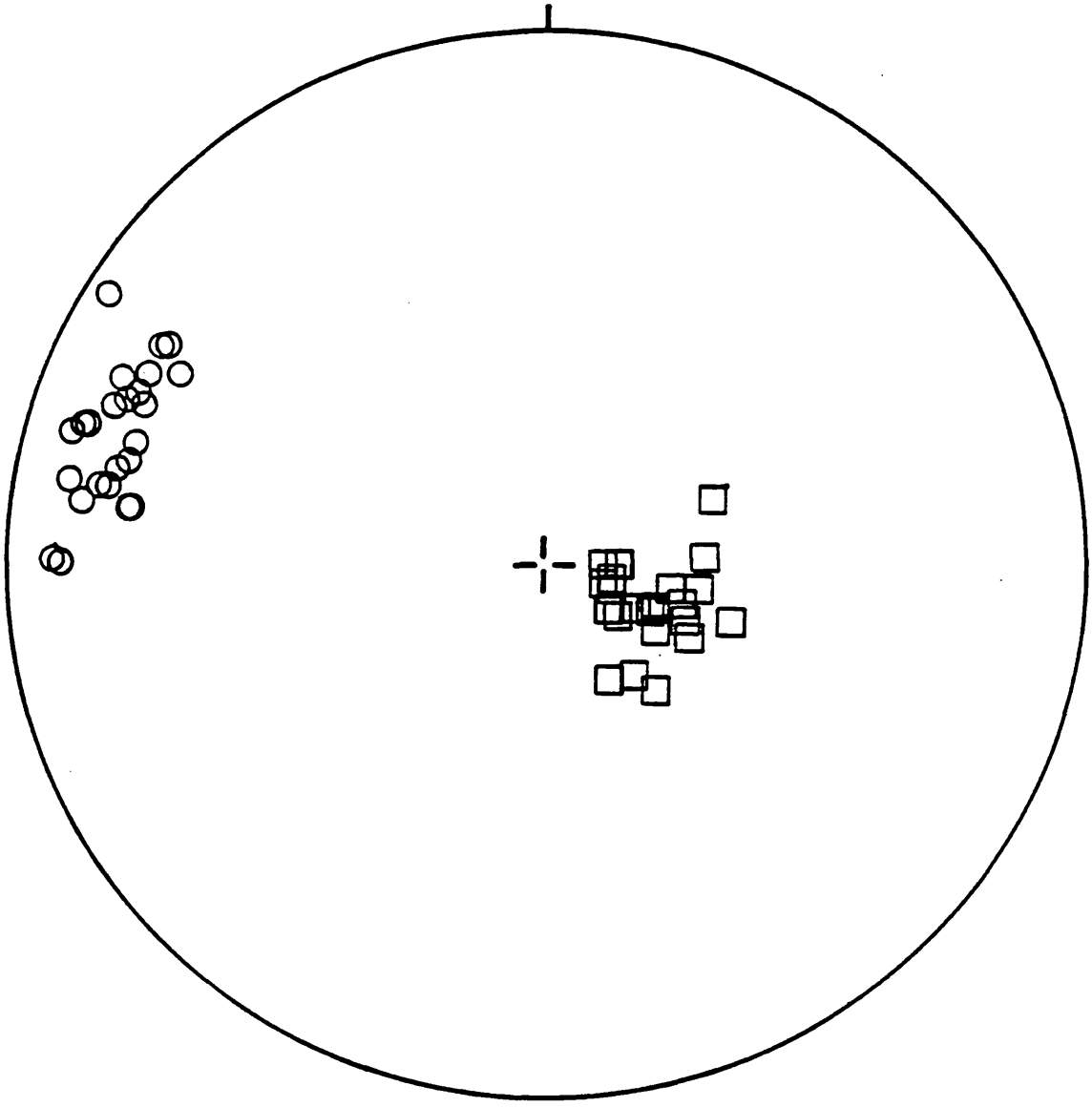


Figure 6.1. Equal area plot showing the orientation of mylonite foliation and the stretching lineation along the Lewisian-Torridonian contact zone. poles to foliation - circles, lineation - squares.

Figure 6.2. East dipping shear zones in Iona.

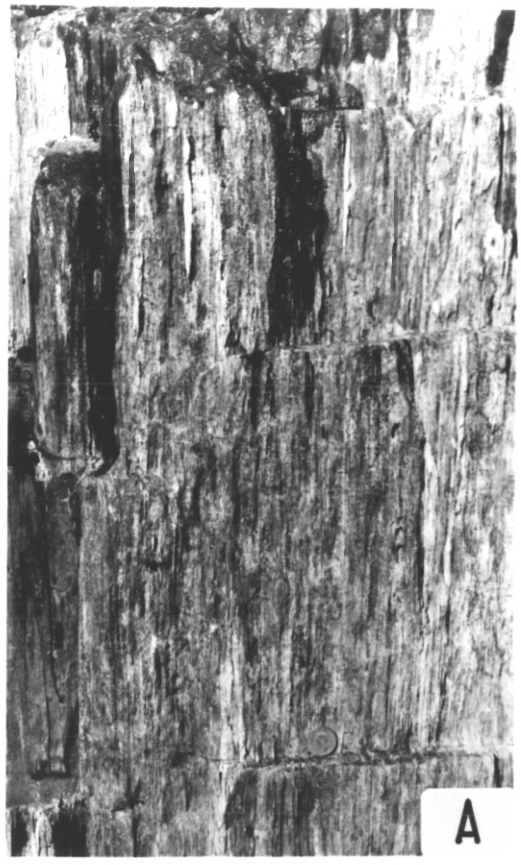
(a) Mylonites with a stretching lineation plunging down dip on foliation, Basal pebbly grit, Southern Iona.

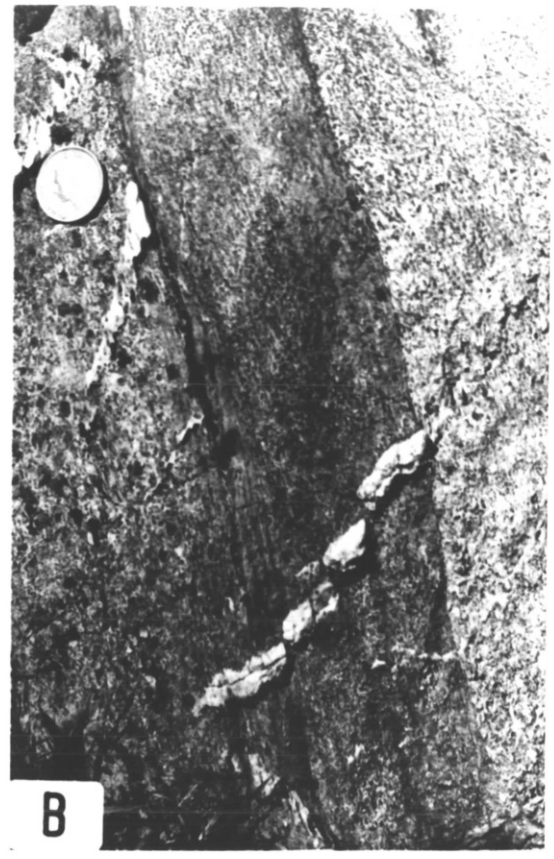
(b) Thrust sense discrete slip displacing quartz segregations, mylonitised basal pebbly grit.

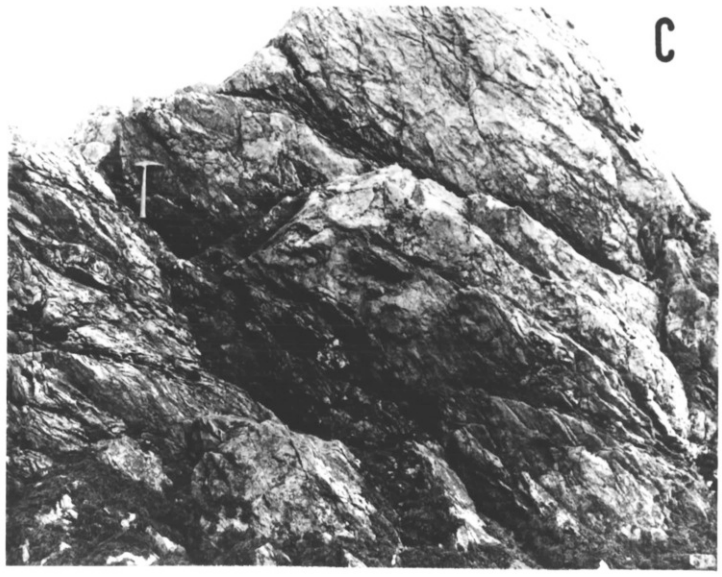
(c) Brittle shear zones within the Lewisian, Calva.

(d) Cataclasites in Lewisian, northwest Iona.

All field photographs on approx. E-W sections.









6.2

The Lewisian-Torridonian contact as mapped by the Geological Survey appear to bend on itself in the form of an overturned fold in the region of Baile Mor (Fig. 1 in Bailey et al. 1925). Bailey et al. suggested that there is a major folding of the contact. The question has been discussed by Fraser (1977). Fraser's mapping and the present remapping shows that there is no dip reversal in the area to account for folding. Apparent discrepancies between the survey map and the author's map are probably due to a mistaken identification of sheared Lewisian rocks as Torridonian in this area.

Belts of sheared and crushed rocks with shear zone foliation dipping steeply towards ESE have also been recorded within the Lewisian. The shear zone rocks vary from fault gouges to cataclasites with a well developed foliation (Fig. 6.2b).

6.2.2 A Strain Estimate

In northeast Iona 2-dimensional strain ratios for Torridonian psammites were determined from the measurement of grain shape of detrital quartz in thin sections. On a section cut perpendicular to the foliation but parallel to lineation (XZ section) the strain ratio is 1.9. Corresponding R_f-ϕ plots is shown in fig. 6.3. Field observation shows that the strain is generally much higher in southern Iona. Three-dimensional strain was calculated from measurements on pebble-shapes from an area north of the Marble Quarry. Pebble axial ratios were measured on photographs of outcrop faces parallel to the foliation and joint surfaces perpendicular to foliation and lineation. The R_f-ϕ plots are shown in Figure 6.4. 3-dimensional strain was calculated by assuming that the XY plane of the strain ellipsoid is parallel to the mesoscopic foliation. The axial ratio of the fine strain ellipsoid is 3.59:1:0.42. The shape of the ellipsoid (K = 1.87) suggests that the rocks were probably deformed in plane strain with a component of uniaxial constriction. The orientation of the principal 3-D strains are shown in Fig. 6.4c. The direction of stretching, X, plunges steeply (60 degrees) towards ESE and is close to the dip direction of the mylonite foliation. The calculated value of maximum shearing strain (γ) on XZ section is 4.2; the angle between γ and X is ~7 degrees.

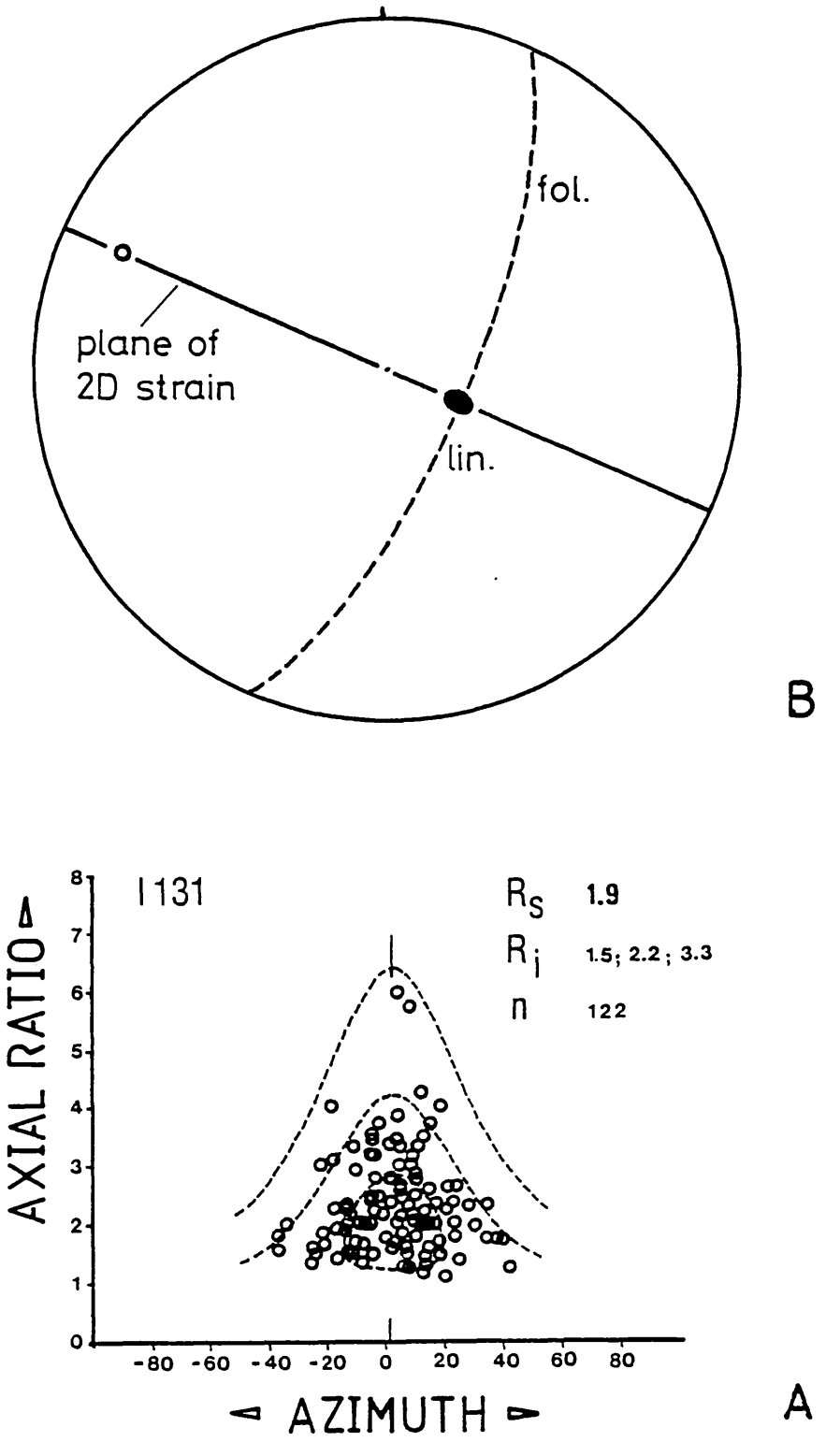


Figure 6.3. Strain in the contact zone, N. Iona. (a) R_f-Ø plot, strain ratio on XZ section is 1.9; (b) Equal area plot showing the orientation of foliation, elongation lineation and the section of 2-dimensional strain-measurement.

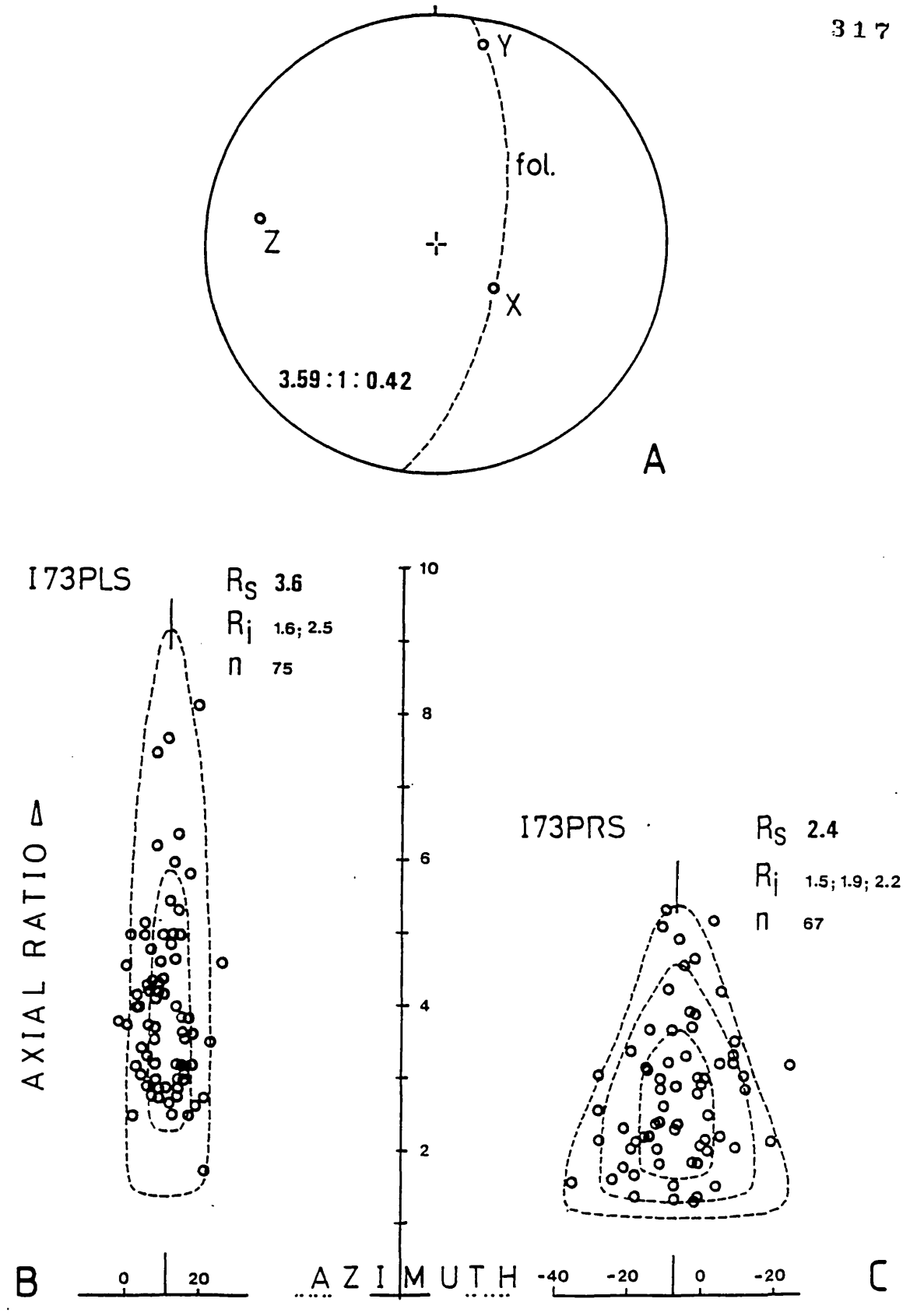


Figure 6.4. Strain in mylonitised basal pebbly grit, N. of Marble Quarry, Iona.

(a) Equal area plot showing the orientation of principal strain axes (X>Y>Z). Great circle (dashed) gives the orientation of local foliation. (b-c) R_f-Ø plots for sections parallel to (XY) and perpendicular to foliation (YZ), specimens I73PLS and I73PRS respectively.

6.2.3 Microstructures

In less strained rocks along the Lewisian-Torridonian contact, elongated quartz grains show undulose extinction, deformation lamellae and deformation bands. Most of the deformation lamella are of sub-basal orientation. Some composite quartz grains show a granulitic texture probably inherited from the parent Lewisian. Feldspars and epidote deform by fracturing and pull aparts; the latter are often filled with quartz + chlorite. Detrital micas are kinked. On the other hand, fine grained phyllosilicates which appear to have formed during deformation show local parallel alignment, trails of phyllosilicate anastomose around angular fragments of altered feldspar, epidote or slightly elongated clasts of quartz (Fig. 6.5a).

In more sheared rocks elongated clasts of quartz are recrystallised to a large extent. The preservation of features such as the core and mantle structure, curved to slightly sutured boundaries between adjacent grains within a clast and undulose extinction of some of these grains (Fig. 6.5b), suggest that original clasts probably suffered dynamic recrystallisation during mylonitisation. During the contact metamorphic effect of the Ross of Mull Granite, the rocks have suffered a static recrystallisation which is indicated by the presence of strain-free large grains and triple-point grain junctions.

The c-axis orientation of recrystallised quartz clasts in a measured sample is shown in Fig. 6.6. Although the overall preferred orientation is rather weak, the pattern is that of a cross-girdle with an asymmetry with respect to the foliation and lineation. One of the girdles is subnormal to the foliation and the lineation; the second girdle is shifted in an anticlockwise sense from the first. The asymmetry of the cross girdles can be interpreted (Lister and Williams 1979) to indicate a right lateral shear parallel to foliation (the stretching lineation (down-plunge) is plotted on the north point in the equal-area diagram, top of the foliation is towards east). Similar asymmetric cross-girdles have been described from quartz-mylonites of other thrust belts (see Chapter 4). Notice that the point-maxima lie close to the XZ plane (and Z) of the strain ellipsoid (assuming that the stretching lineation corresponds to X and the foliation parallels the XY plane).

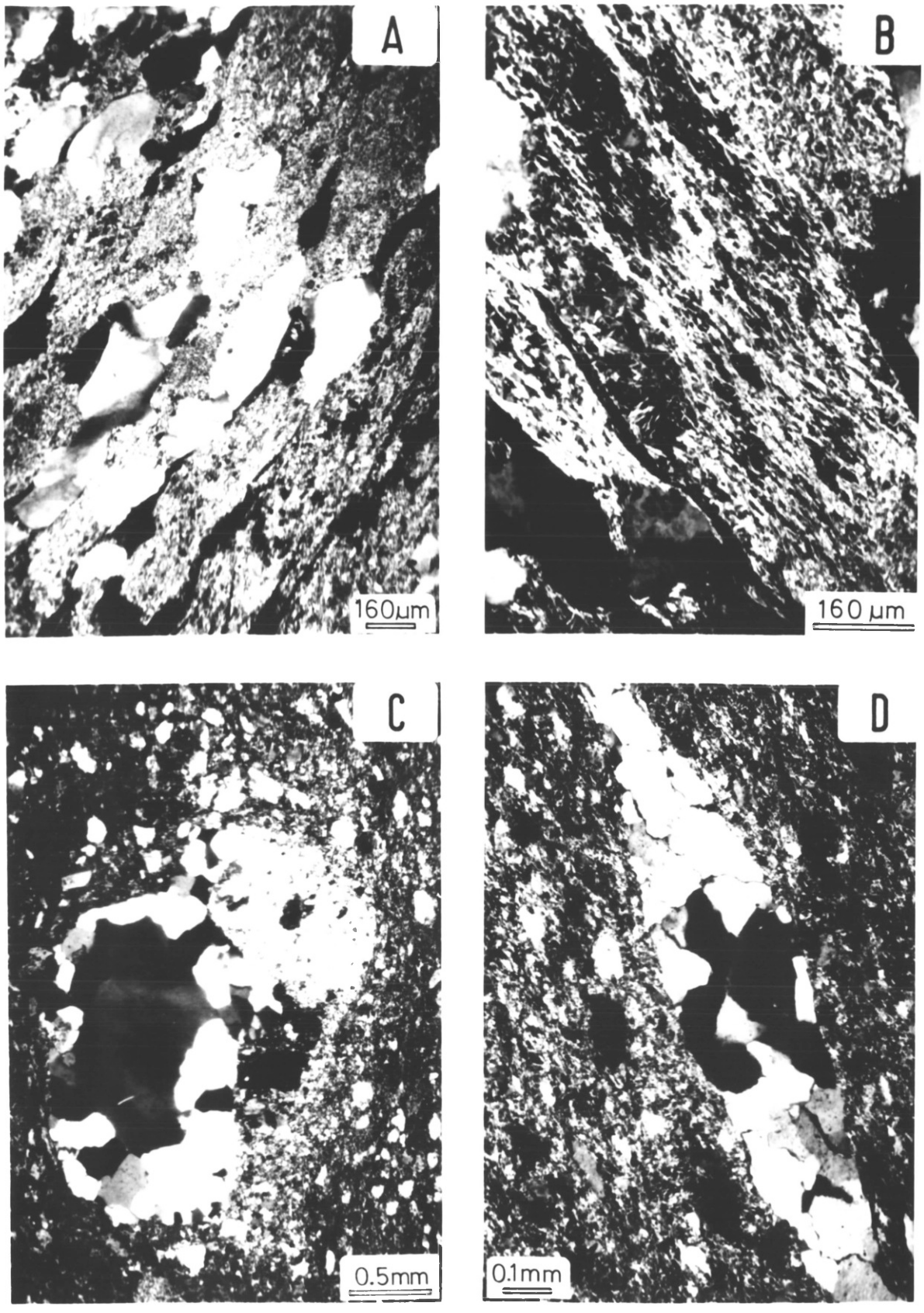
Figure 6.5. Optical micrographs showing microstructures in deformed contact zone rocks, Iona.

(a) Deformed quartz grains showing undulose extinction, but no recrystallisation, grits, N. Iona.

(b) Details of foliation in the matrix of (a); micas anastomose around relict feldspar fragments.

(c) Core and mantle structure in deformed quartz clasts, S. Iona.

(d) Thorough recrystallisation of elongated quartz clasts, specimen I9A1 (used for quartz c-axis fabric measurement), mylonitised pebbly grit, S. Iona.



6.5

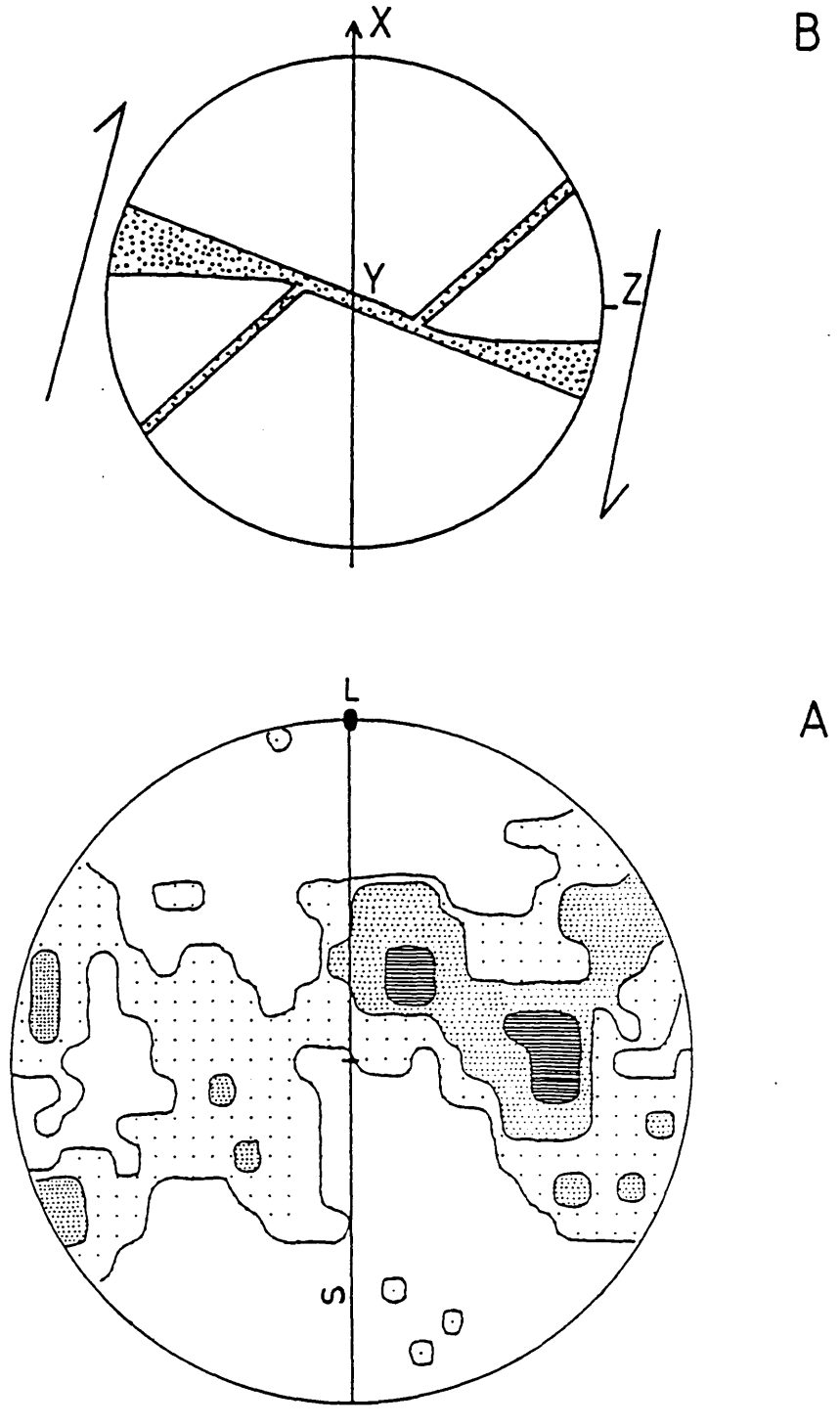


Figure 6.6. An asymmetric cross-girdle pattern of quartz c-axis fabric, Sp. I9A1. Compare with an idealised type-I cross-girdle pattern (b). Foliation top (S) is towards right, lineation (L, down plunge direction) is towards north. 214 quartz c-axis. Contours 1, 1.5 and 2 x E, expectation for uniform distribution. Maximum point-density 2.54 x E.

Although the fabric asymmetry corresponds to a thrust sense of movement along the contact zone, the fabric is relatively weak compared to the strain determined from pebble shapes in an adjacent area. Two factors probably contribute to this:

(a) The deformed rock is a feldspar-mica-quartz mylonite; only part of the total strain is accommodated by intracrystalline slip in quartz. The 'softer' fine-grained phyllosilicates probably accommodates a large portion of the total strain.

(b) The static recrystallisation due to the thermal effects of the Ross of Mull Granite has a randomising effect on the fabric.

6.3 EARLY FOLDS

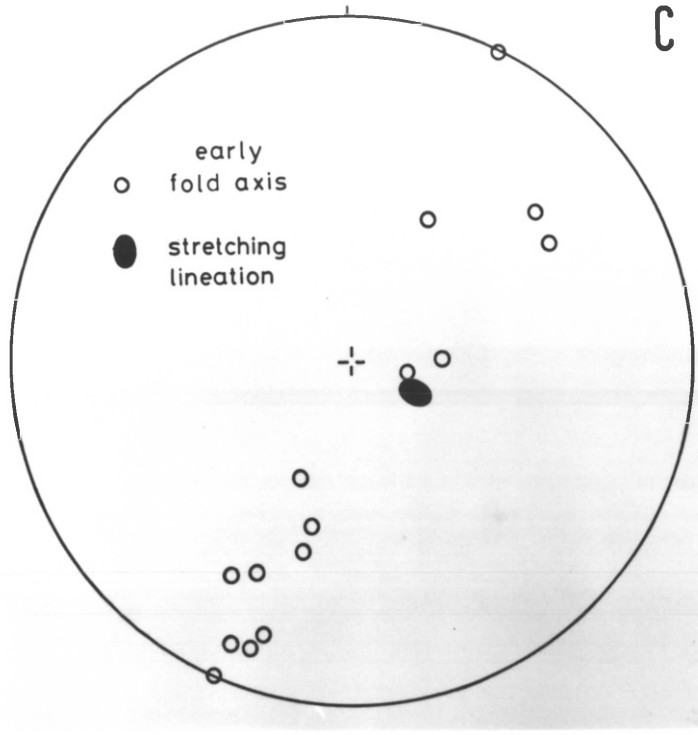
Overturned to isoclinal folds up to a few meters in wavelength have been recorded in the shale band of NE Iona. Here a compositional layering (bedding) within the shale is folded and transposed along an axial plane cleavage. The layers are stretched and detached into lensoid bodies (Fig. 6.7a). The axial plane cleavage dips steeply (70-80 degrees) towards ESE and the fold axis plunges gently towards northeast. Crenulation cleavages transposing fine laminations parallel to bedding have been recorded from other areas of Torridonian sediments (Fig. 6.7b). When mapped over a larger area, the intersection lineation parallel to the minor fold axis plunges at various angles towards the NE or SW. A striking feature is the orientation of occasional tight folds within the sheared contact zone rocks. These folds have a reclined attitude with the axial plane subparallel to the mylonite foliation and the fold axis close to the elongation lineation. The orientations of the measured early fold axes are shown in Fig. 6.7c. The spread in orientation can be explained if one assumes that these folds developed before the thrusting movement in Iona. In an ideal ductile shear zone an early lineation would be deformed so that the final orientations fall on a girdle through the movement direction and the initial orientation of the lineation (Ramsay 1967). Although the recorded orientations are limited in number, the spread of the fold axes orientations through the stretching lineation in the contact zone is consistent with the hypothesis that these folds were

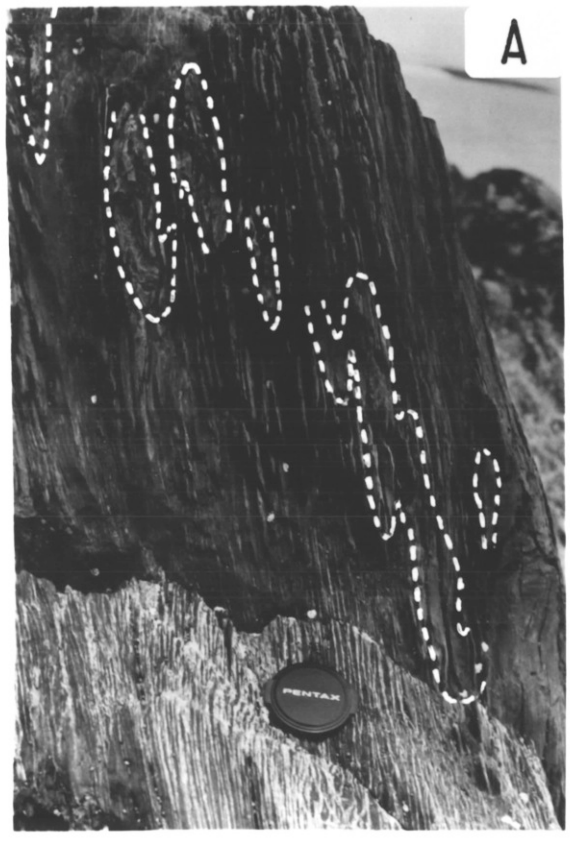
Figure 6.7. Early minor folds and axial plane cleavage.

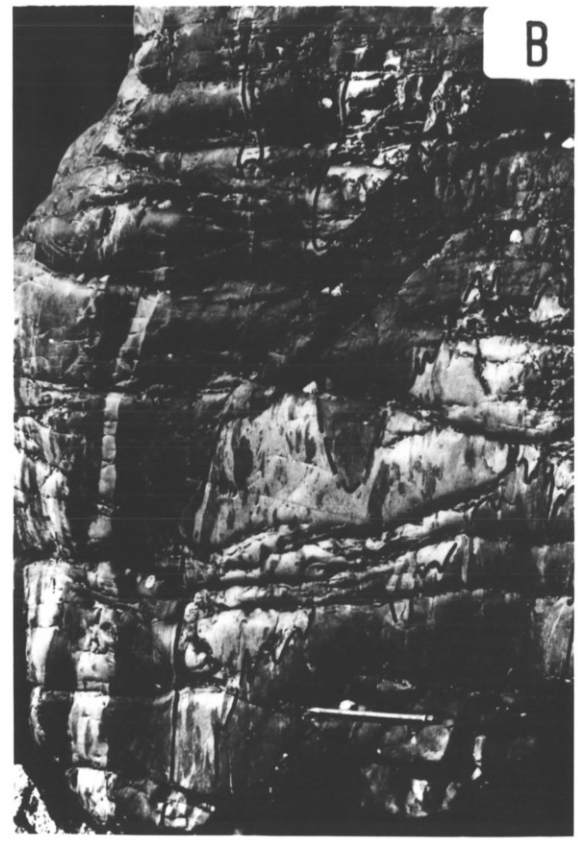
(a) Detached fold hinges (outlined) on an E-W section, Slates, NE Iona.

(b) Plan view of fold hinges in muddy intercalation within grit, Southern Iona.

(c) Equal area plot showing the spread in orientation of early fold axis in Iona. Average stretching lineation in the mylonite belt is also indicated.







6.7

early and were reorientated during the thrusting movement in Iona (cf. Fraser 1977), for similar examples of reorientation of fold axis elsewhere, see Berthe and Brun 1980, Bryant and Reed 1969 and Escher and Watterson 1974).

Apart from the folds described above, quartz segregations in the mylonites of the contact zone take a folded form. In thin section, the mylonite foliation is axial planar to the microfolds on quartz segregations. These folds probably developed due to amplification of initial perturbations during the mylonitisation process. The initiation of the early folds, their subsequent amplification and the thrust movement which locally reorient the folds may represent different stages of a continuous process of shortening of the belt.

6.4 WEST DIPPING SHEAR ZONES AND THRUSTS

The shear zones and mylonites so far described can be related to westerly movement on east dipping thrusts. Although no large thrusts with easterly movement have been recorded from the Torridonian belt, west dipping thrusts do exist within the Lewisian. One such thrust has been mapped in the area west of Port Laraichean (grid ref. 258 218, see map V). The rocks above and below the thrust plane are distinctly different; those above the thrust have a significantly higher proportion of pink, coarse quartz-feldspathic bands; mafic hornblende rich bands are more common in the rocks below the thrust (Fig. 6.8a). Lenses of coarse ferromagnesian minerals (hornblendite) lie subparallel to the thrust zone. Such lenses are cut by brittle shear zones in which the mafic minerals show a reduction in grain size and alteration to serpentinuous or chloritic material (Fig. 6.8b). West dipping unsealed fractures are common in the vicinity of this thrust. The deformation in the Port Laraichean thrust is semi-brittle to brittle, whereas other west dipping shear zones within the Lewisian show the development of cataclasites (Fig. 6.8d-e).

Within the belt of mylonites near the Lewisian-Torridonian contact, there are sigmoidal dilation veins which can be kinematically interpreted as west dipping shear zones (Fig. 6.8c). Minor west dipping shear zones are not uncommon in other Torridonian outcrops further east. The Ross of Mull Granite also shows a set of prominent west dipping

Figure 6.8. West dipping shear zones and thrusts in Lewisian rocks and contact zone mylonite, Iona.

(a) West dipping thrust within the Lewisian, west of Port Laraichean.

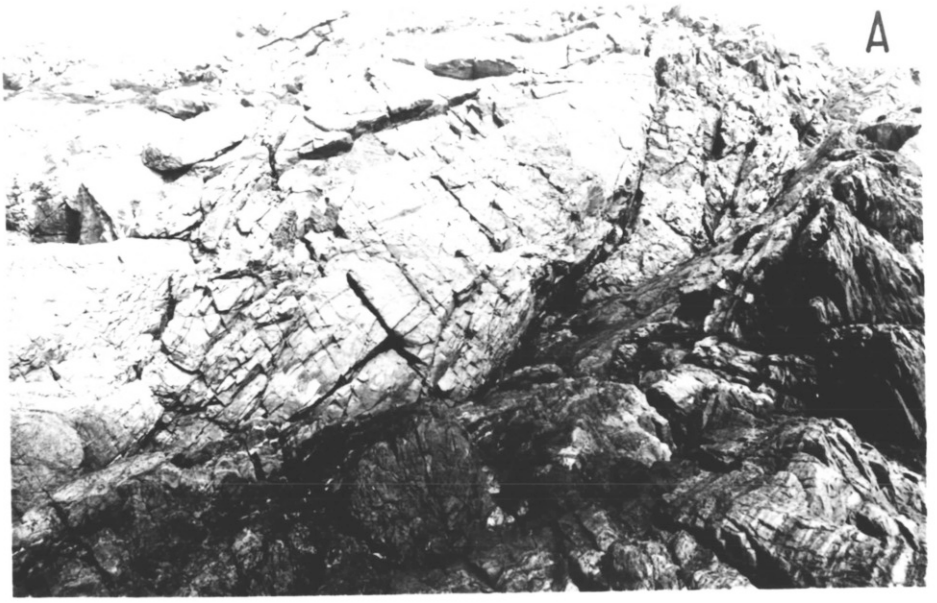
(b) Veins of breccia material in hornblendite lense lying along the thrust zone in (a). Note reduction in grain size within the breccia-vein compared to coarse surrounding rock.

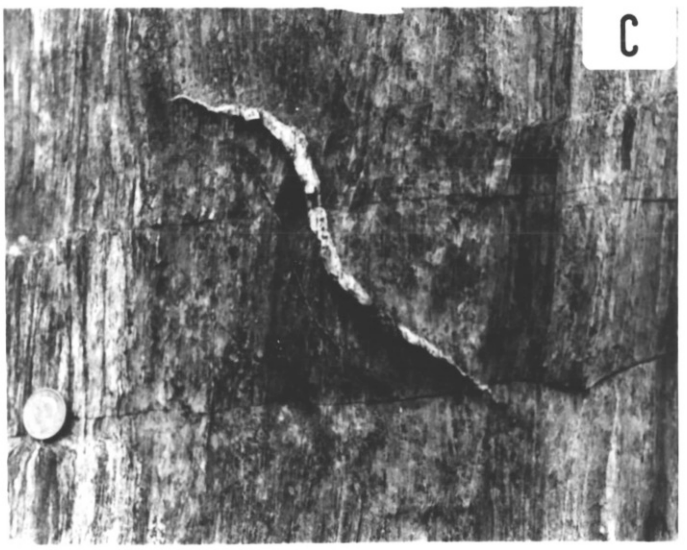
(c) Tabular zone of sigmoidal dilation veins, mylonitised grit, Lewisian-Torridonian contact zone, Southern Iona.

(d) Sheeted brittle shear zones, St. Columbas Bay, S. Iona.

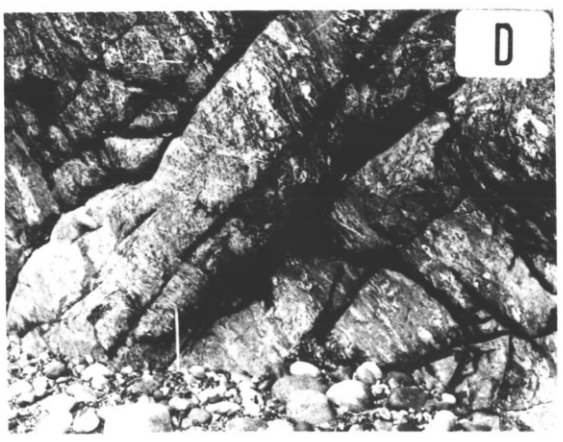
(e) Details of brecciation along one of the brittle shears in (d).

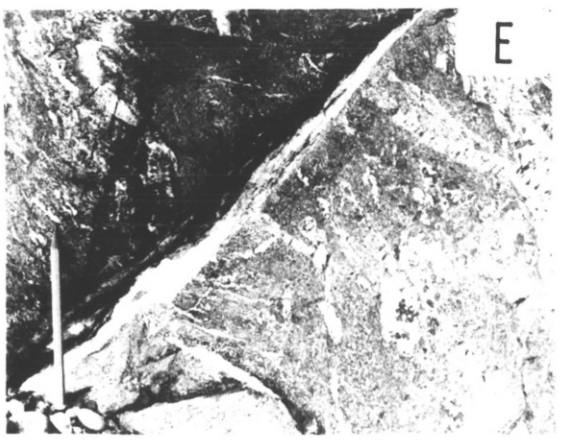
(f) Equal area plot showing orientation of west dipping shear zones and related structures.

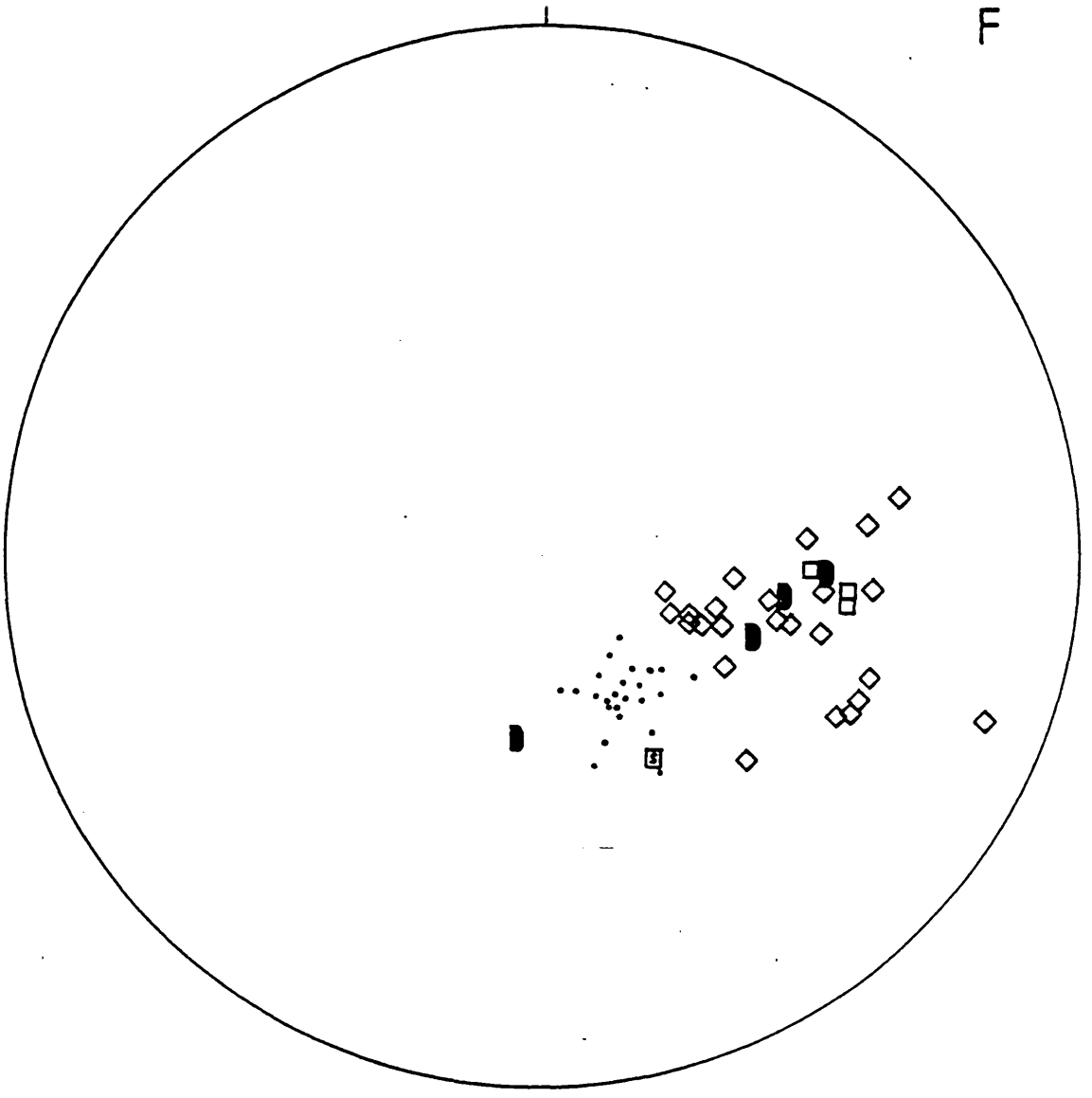

A


C


B


D


E



Poles to

◇ brittle shear zones in Lewisian; ◗ felsic porphyrite dykes • shear fractures in Torridonian, Sligeneach; ◻ shear joints in granite; ◘ zone of sigmoid dilation veins.

6.8 contd.

master joints. Shear sense displacements along some of these joints are indicated by slickensides and en echelon dilation cracks.

In terms of the models of shorterning across an orogenic belt, the west dipping shear zones in Iona could be interpreted as either, (a) conjugate shear zones or, (b) structures related to backthrusting. In terms of a conceptual model while conjugate shear zones are co-eval so far as the timing of the structures are concerned, the back thrusts are later than the forward moving thrusts. In Iona, the relative age of the west dipping structures are central to the question of fitting the observations to any conceptual model.

The presence of west dipping shear zones cutting across mylonites in the contact zone and of master joints within the Ross of Mull Granite indicates that the movements on the west dipping shear zones and thrusts continued after mylonitisation along the Lewisian-Torridonian contact. The balance of evidence is in favour of regarding the west dipping shear zones and thrusts in Iona as structures associated with backthrusting. Several small-scale examples of opposed dip thrust complexes occur at Kempie Bay in the Moine Thrust Zone; similar backthrusts and folds also occur at Assynt above flat decoupling horizons in the Lewisian Gneiss as well as in the bedded Cambrian rocks (Coward and Knipe 1981). The Iona examples are regarded as analogues of these structures.

6.5 LATER MINOR STRUCTURES

Reverse kinks on gentle ESE dipping planes, asymmetric boudin-like structures, normal kinks on alternate sets and steep brittle shears are included in this group.

6.5.1 Reverse Kinks

The reverse kinks have been recorded from flagstones on the east coast. The kinks develop on laminations parallel to bedding. They are 'S' shaped on sections looking south and often there are discrete slips parallel to the kink plane (Fig. 6.9 a-b). The local altitude of foliation (bedding) is 60 degrees toward east-south-east.

It is difficult to explain how ESE dipping reverse kinks would initiate under a horizontal/subhorizontal ESE-WNW compression (Caledonian) if the attitude of the foliations during the initiation of kinks was the same as its present steep altitude. Two possible situations which may explain these kinks are:

(a) A local shortening in a subvertical direction after the foliation assumed a steep altitude. However, other minor structures described later shows that the rocks were subjected to a layer parallel extension rather than shortening after the foliation assumed a steep altitude.

(b) The reverse kinks could have been generated by layer parallel shortening when the foliation was still dipping at a gentle/moderate angle towards east. One set of kink plane would have initiated (see Fig. 6.9c) with gentle dip towards west. If the steepening of the foliation in Iona Torridonian is due to rotation of internal structures within a thrust sheet, initially west dipping reverse kinks would be reoriented to their present east-dipping attitude. As will be suggested in Section 6.7, the present steep attitude of the Iona Torridonian probably resulted from a stacking of thrust sheets, with a stacking and thrust propagation towards west leading to steepening of the thrust sheets. Alternative (b) is therefore preferred.

6.5.2 Asymmetric Boudins

These develop as internal structures within the flaggy rocks and have been recorded on the east coast between Sligeneach and the Marble Quarry area. In cross-sections the boudins have a rhombic outline and adjacent boudins are offset with respect to one another (Fig. 6.10a). The bedding trace within individual boudins has been rotated to a steeper attitude. These boudins are controlled by a set of shear planes parallel to the one side of the boudin rhomb. A conjugate set of steep fractures have been recorded in the same exposure or in separate exposures (Fig. 6.10b). This conjugate set of fractures are either vertical (trend NNE) or dipping steeply (75-90) towards WNW. The displacement along them is consistent with a layer parallel extension.

Figure 6.9. Reverse kinks, flagstone, St. Ronan's Bay.

(a) Discrete slips parallel to kink plane.

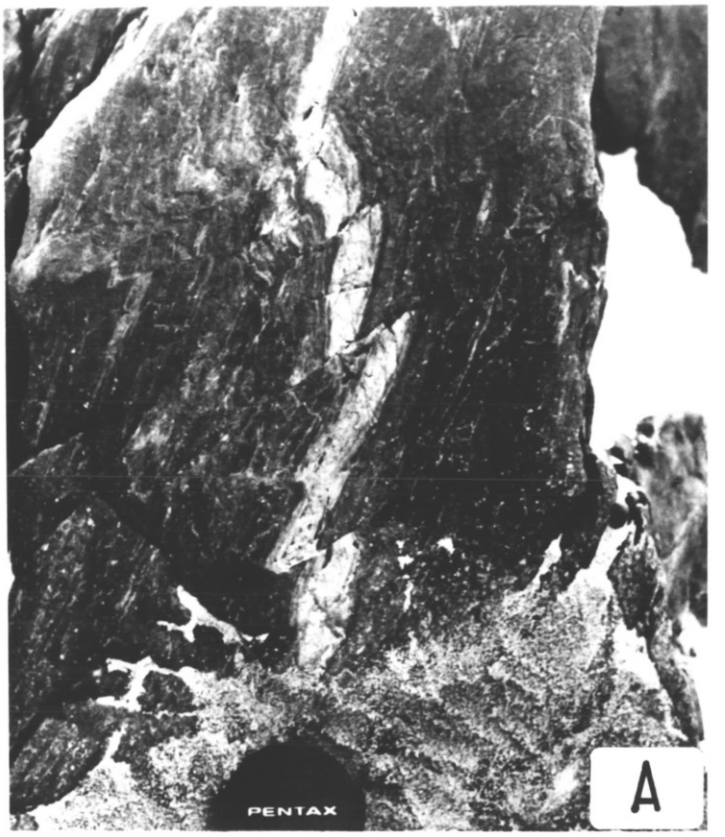
(b) S-shaped kinks on sections looking south.

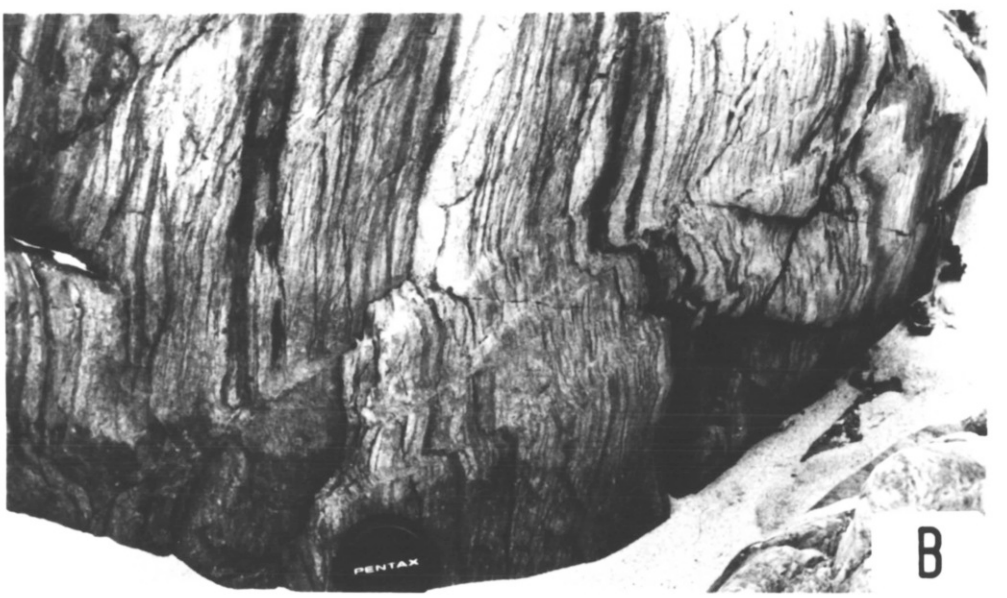
(c) Schemating drawings to illustrate the evolution of reverse kinks under an E-W compression, and subsequent steepening of foliation due to internal rotation within thrust sheets (see Fig. 6.16).

e

W

6.9





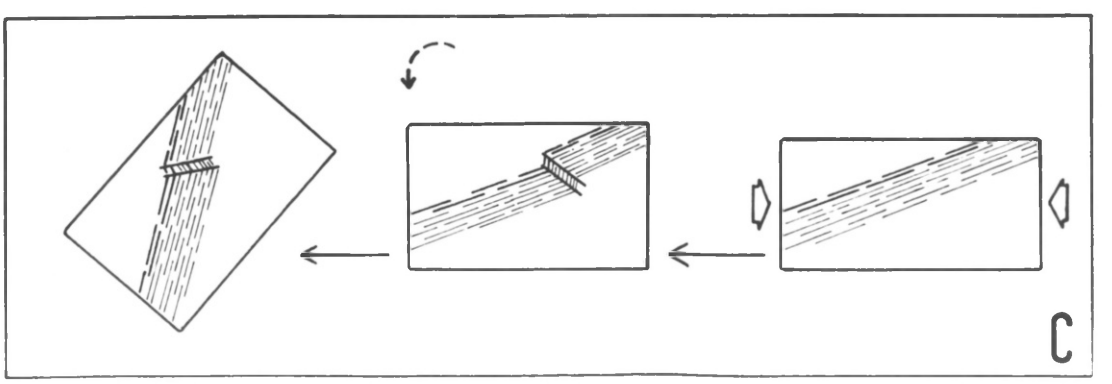


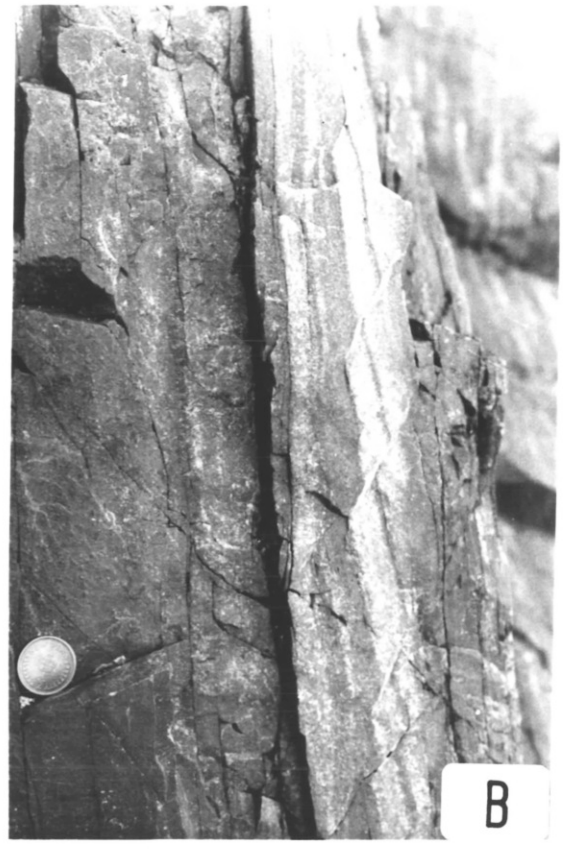
Figure 6.10. Asymmetric boudins and conjugate shear planes in flagstone, south of Sligeneach. All on approx. E-W sections looking north.

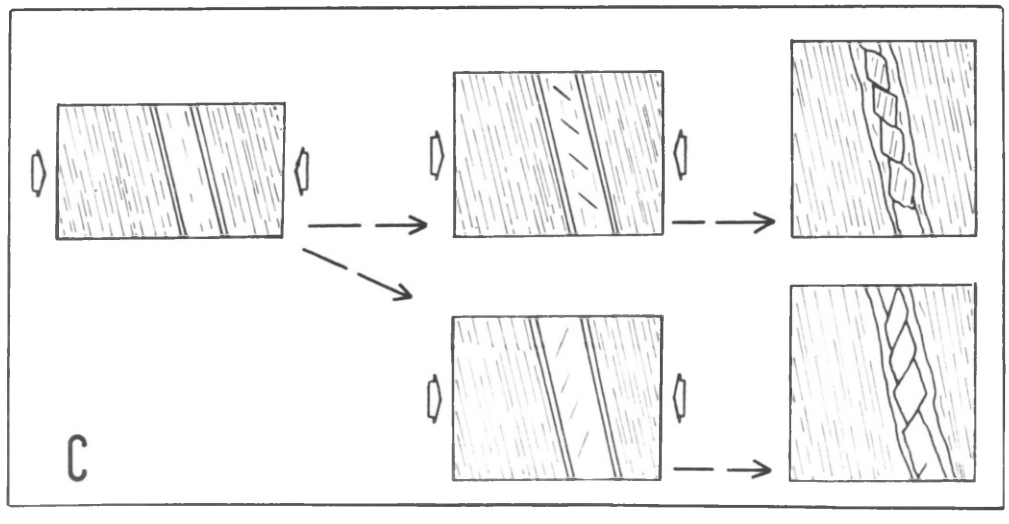
(a) Asymmetric boudins as internal structure within a relatively thicker layer within flaggy rocks. Note that the layer itself has internal laminations which are rotated during boudin formation.

(b) A conjugate set of brittle shears displacing bedding in flagstone. The structure is restricted to a relatively coarse gritty layer.

(c) Diagrammatic sketches showing the kinematic evolution of asymmetric boudins controlled by conjugate sets of slip planes.







6.10

The asymmetric boudins and the associated conjugate shears are comparable to normal kinks (Cobbold et al. 1971, Platt and Vissers 1980) which develop when the direction of compression is subnormal to the direction of anisotropy. The anisotropy in the present case is probably the result of a thin lithological layering parallel to bedding. The structures probably developed as a result of a continuing ESE-WNW horizontal/subhorizontal compression after the early foliation was steepened due to thrust movements. The probable kinematic evolution of the structures is illustrated in Fig. 6.10c.

6.5.3 Brittle Shears with a Strike-Slip Sense of Movement

Brittle shear zones with a steep attitude which displace early foliations and bedding are apparently the latest structures in the Iona Torridonian. Although the azimuth of these steep (80-90 degrees dip) shears varies, the dominant directions are towards N-S and E-W (Fig. 6.11). The N-S set shows a dextral strike slip movement, whereas the E-W set shows a sinistral sense of movement. Sometimes a shear zone grades into an asymmetric fold (kink): a dextral shear zone grades in a 'Z' shaped fold (Fig. 6.12).

Fractures and shear zones of similar orientation have been recorded from the Lewisian outcrops; on the whole the E-W set appears to be more common within the Lewisian (Fig. 6.11). Note that these dominant orientations are consistent with measurements on photo-interpreted fractures in Iona (Fig. 2.14c in Fraser 1977). However, these fractures and shear zones within the Lewisian can be divided into two groups:

(a) Fractures and shear zones (dominant strike-slip movement) which are filled with epidote and quartz veins.

(b) Fractures and shear zones which are generally unsealed but occasionally with quartz segregations.

Shear zones in group (a) usually show dextral displacement along an E-W set and sinistral displacement along a N-S set. The geometric relationship between shear zones of the two groups (Fig. 6.13) shows that the shear zones with mineral veins (group 'a') are earlier than

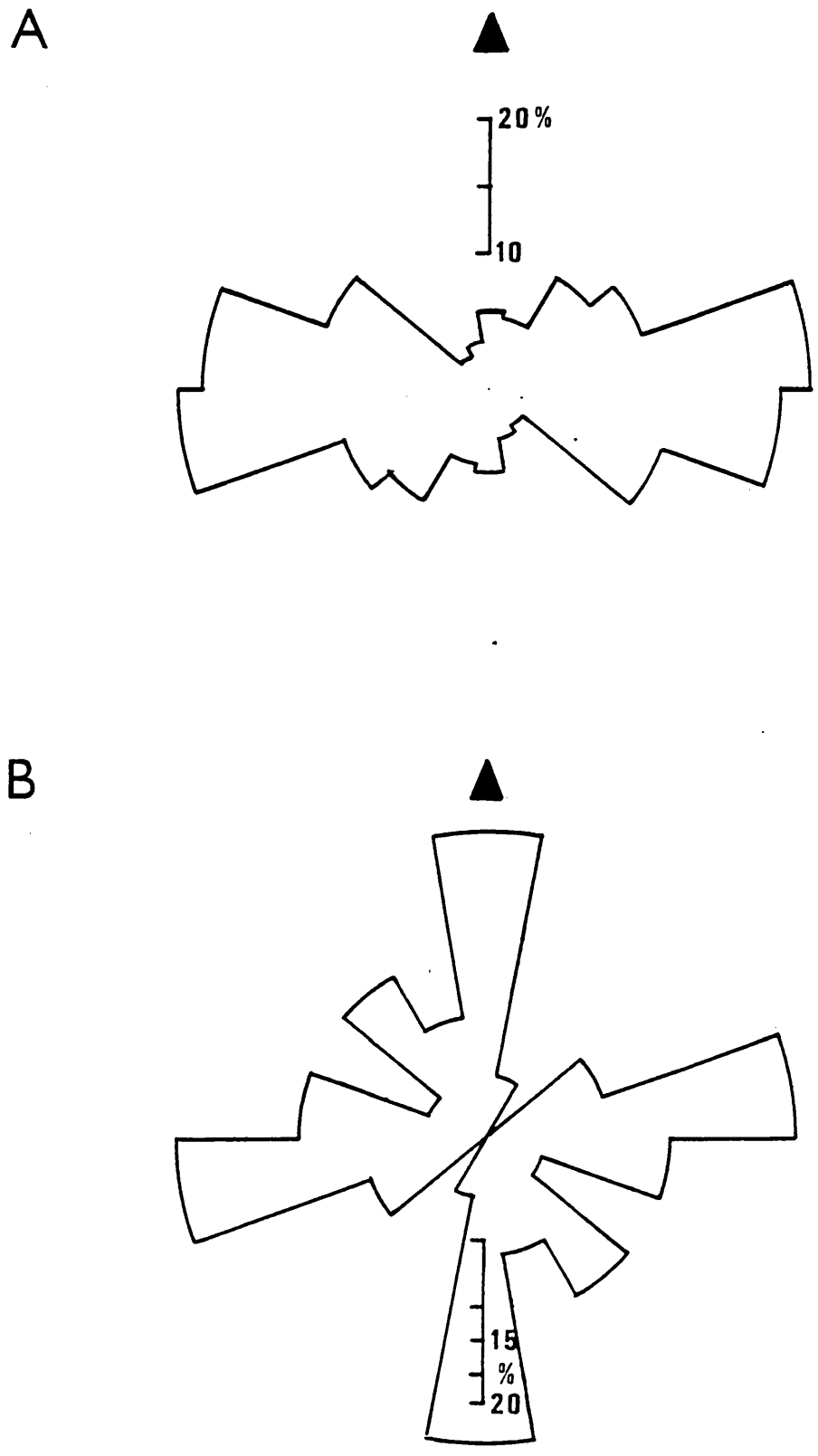


Figure 6.11. Rose-diagrams showing the azimuth of brittle shears (with strike slip displacement) in Iona. (a) 211 measurements from Lewisian outcrops. An E-W set is more common. For sense of displacement see text. (b) 22 measurements from Torridonian, St. Ronan's Bay. E-W set shows a sinistral displacement; N-S set dextral.

Figure 6.12. Late brittle shears (strike-slip) and associated kinks in Torridonian, Iona.

(a) A 'Z' kink grades into a dextral shear zone.

(b) An E-W sinistral shear zone.

Both plan view, north towards the top of the page.

6.12



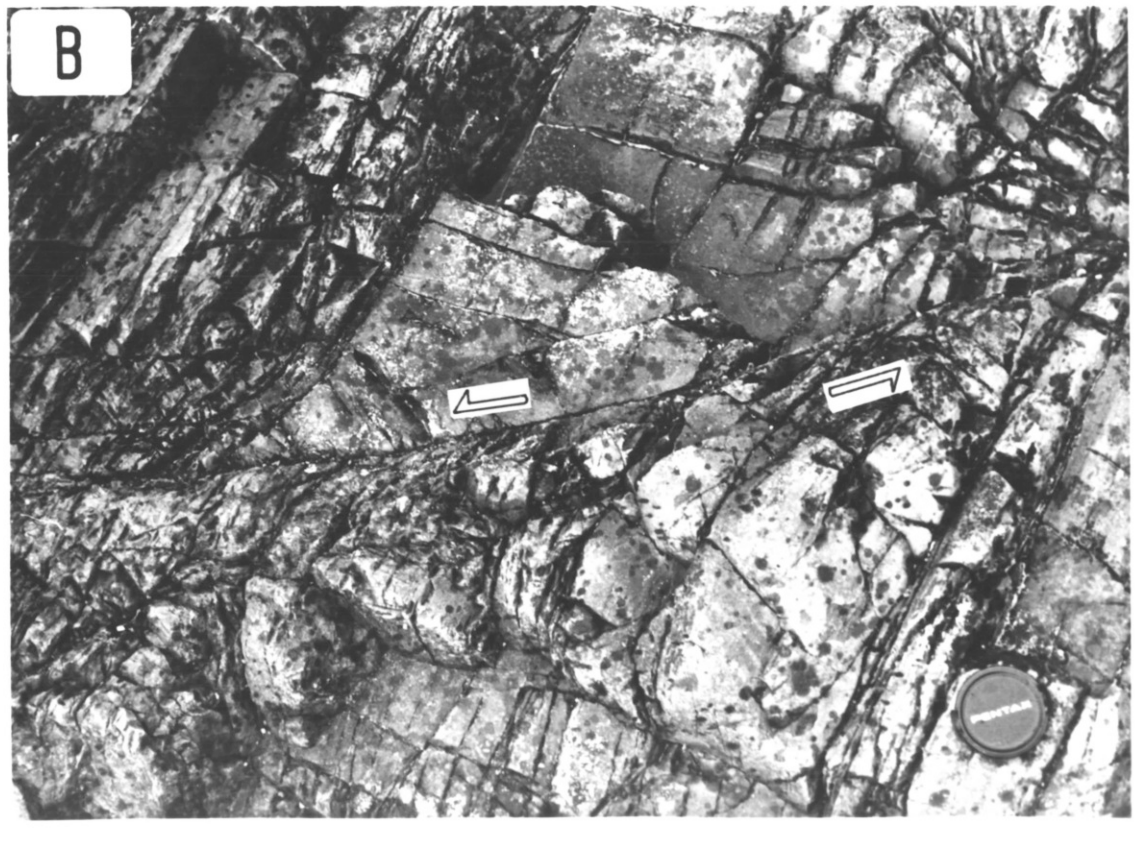


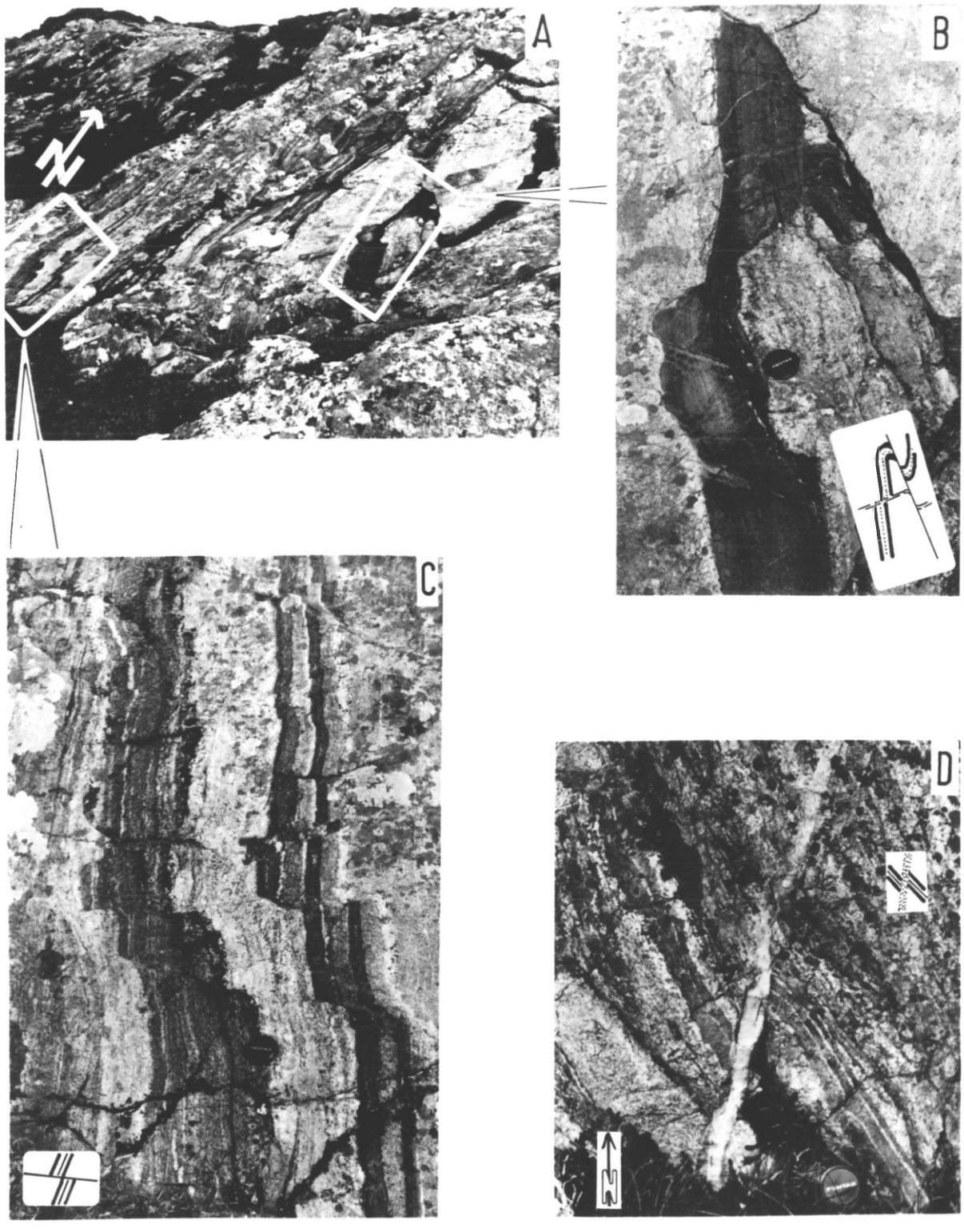
Figure 6.13. Brittle shear zones (strike-slip) in Lewisian rocks, near Port Laraichean.

(a) Outcrop showing conjugate sets of brittle shears belonging to two generations.

(b) An early dextral E-W set with epidote veins displaced by a late (Caledonian) dextral N-S brittle shear (see inset for the idealised picture).

(c) A late E-W set with sinistral movement.

(d) An early (?late Precambrian) sinistral NNE shear zone filled with quartz vein.


A
B
C
D
N

those belonging to Group 'b'. In the later group the sense of movement is sinistral on an E-W set but dextral on a N-S set (Fig. 6.13 a-c).

The Lewisian in NW Scotland suffered conspicuous epidote-mineralisation before the deposition of the Torridonian (Bailey et al. 1925, Fraser 1977). The mineralised shear zones within the Iona Lewisian probably formed before any Caledonian movement in NW Scotland. The brittle shears of similar orientation within the Torridonian are late Caledonian as they displace earlier Caledonian structures. If these are indeed conjugate brittle shears, their kinematic interpretation would suggest an extension in the NW-SE quadrants and a compression in the NE-SW quadrants. The situation is rather difficult to explain in terms of a horizontal ESE compression (Caledonian). One possibility is that these later brittle shears are secondary effects of a local extension forced by a gravitational collapse of a thickened thrust pile (see Coward 1982, 1983, cf. Johnson 1956). However, structures in Iona alone cannot prove or disprove such a hypothesis and further considerations are beyond the scope of the present thesis. Whatever may be the origin of these later brittle shears, it seems that older sets of pre-Torridonian fractures control their orientation.

6.6 METAMORPHISM

The Torridonian in Iona were subjected to a low grade regional metamorphism before the emplacement of the Ross of Mull Granite. On its eastern side, the latter has conspicuous contact metamorphic effect on the Moine in the Ross of Mull. The western boundary of the granite pluton is within a few tens of meters of the southeast coast of Iona and contact metamorphic effects on the Iona rocks (mainly in the development of spots) have been recorded (Jehu 1925, Fraser 1977).

6.6.1 Regional/Dynamic Metamorphism

In pelitic rocks of NE Iona the mineral assemblage is chlorite + phengite + quartz; here contact metamorphic effects are not obvious. The rocks are slaty rather than phyllitic. The axial plane cleavage associated with the early overturned isoclinal folds is defined by a parallel alignment of phyllosilicates, and detrital quartz and feldspar clasts are generally elongated parallel to the foliation.

Where there is a local development of a crenulation cleavage associated with the late kinking (kinks on gentle east dipping planes), the micas are generally bent over such micro-fold hinges and show optical effects of strain.

The effect of mylonitisation along the contact zone is a general reduction in grain size of the gritty rocks. Deformed quartz clasts usually show deformation lamellae in basal or sub-basal orientation indicating deformation in a low T/T_m situation (Nicolas and Poirier 1976). The pull aparts in feldspar are filled with quartz + chlorite again attesting to a low ambient temperature during deformation. The sheared Lewisian show a common development of chlorite parallel to the mylonite foliation. Chlorite is probably produced by retrograde effects on original hornblende or other ferromagnesian minerals.

The observations described above can be explained as due to a very low greenschist facies condition of metamorphism. The peak of metamorphic reconstitution post-dates the earliest folding and was probably reached during the mylonitisation along the Lewisian-Torridonian contact. The later deformation features (the reverse kinks on ESE dipping planes, asymmetric boudins etc.) post-date the low-grade metamorphic reconstitution.

6.6.2 Contact Metamorphism

Contact metamorphic effects associated with the Ross of Mull pluton are superimposed on the regional metamorphic effects described above. The contact effects are lowest in the north within the Torridonian outcrop and increases towards the southeast of the island. Apart from the sheared rocks immediately below the Torridonian and the outcrops in the vicinity of the Marble Quarry area, the Lewisian is unaffected.

The pelites in the thermal aureole grade from spotted slates to hornfelses with common porphyroblasts. The latter are best developed in the exposures close to the granite skerries of Sgeir Ruadh and Eilean Mor off the southeast coast (275223). In the spotted slates/ phyllites, the matrix of the rock outside the spots consists of brown biotite plus muscovite with or without some quartz and feldspar. Although mica

flakes have been recorded at various angles to the original foliation (slaty cleavage), a large proportion of micas are still parallel to slaty cleavage thus enhancing the early foliation. The spots themselves are elliptical in outline. In thin sections the margins are frayed (Fig. 6.14a-b). Although there is a crude alignment of the spots in outcrop faces, the axial ratio of the ellipses never exceed 2.6:1. In thin sections, these spots show large prisms of muscovite and brown biotite similar to those outside the spots except that they are larger. In some thin sections of spotted slates collected from south of Sligeneach, large plates of cordierite enclose muscovite and biotite in a poikiloblastic fashion. There is usually a greater concentration of muscovite and biotite around the rim of such poikiloblasts. Interestingly, the mica prisms within spots have their lengths oriented more commonly parallel to the long axis of the elliptical spots and the original slaty cleavage (Fig. 6.14b). The observed texture is probably an effect of anisotropy of the original slates, facilitating greater diffusion of mineral forming materials parallel to the original slaty cleavage, than in a perpendicular direction. The crude parallel alignment within the spots is as common in spots of low ellipticity as it is in those with higher ellipticity.

In the hornfelses, the porphyroblasts include cordierite, andulsite and staurolite. Of these, andulsite is most obvious in the exposures. Prisms of andulsite with squarish cross-sections grow up to 2-3 centimeters and are oriented randomly (Fig. 6.14c). In thin sections some of these andulsite prisms show chiastolitic inclusions. There is usually a concentration of mica flakes round the boundary of the andulsite porphyroblasts. Small muscovite and biotite also occur as inclusions. In the hornfelses, the muscovites are usually oriented in a random fashion.

The association of staurolite with andalusite or andalusite with cordierite and muscovite suggests that the highest temperature in the contact aureole in Iona is of the order of 600 - 650° (see Miyashiro 1973). The isotherms in the aureole probably dropped towards northeast and northwest from the outcrop of hornfelses mentioned above (grid ref. 275 223). Since the thermal effects are geographically associated with the Ross of Mull pluton, the contact metamorphism is late Caledonian and post-dates both the early folding and mylonitisation in Iona (see also

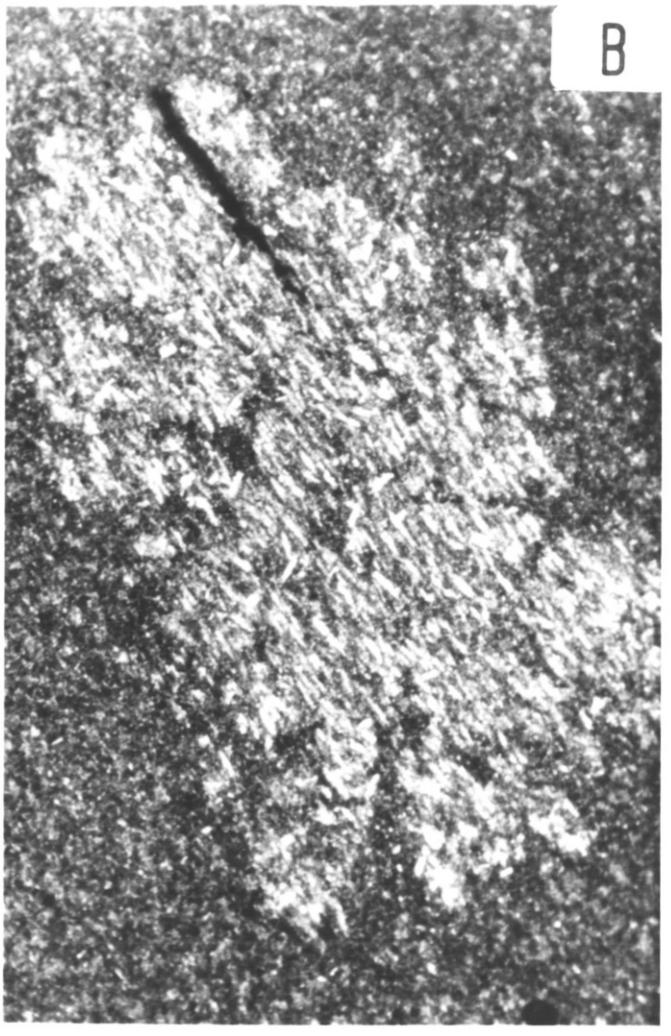
Figure 6.14. Contact metamorphic effects, Iona.

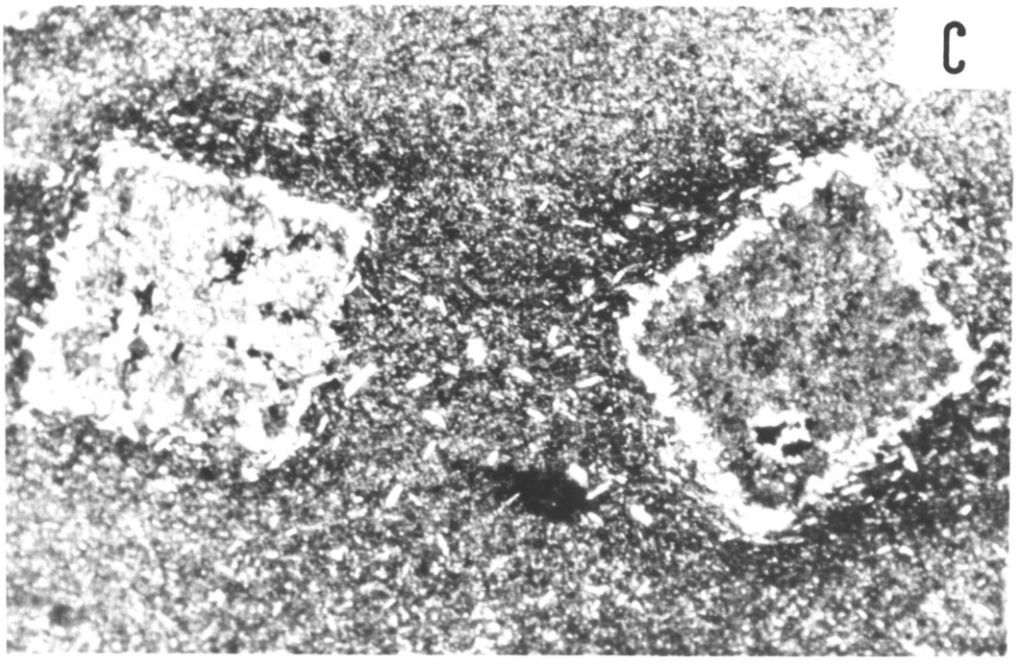
(a) Spotted slates, Sligeneach. Note slight elongation of the spots parallel to foliation.

(b) Optical micrograph showing details of a contact metamorphic spot in (a). Notice alignment of mica prisms parallel to the long axis of the spot (2 mm long).

(c) Optical micrograph showing squarish cross-sections of andalusite prisms, hornfelsed slate, southern Iona (one side of the andalusite cross-section is 5 mm).


A


B


C

Fraser 1977). The question of relative timing with respect to later minor structures in Iona is discussed in the next section.

6.7 DISCUSSION AND SUMMARY OF EVENTS

The Lewisian in Iona is part of the foreland in the Scottish Caledonides (Watson 1975). Epidote veining and pegmatisation accompanied a late Precambrian but pre-Torridonian deformation in the Lewisian (Bailey et al. 1925, Fraser 1977). In Iona this deformation is manifest in the mineralised shear zones and fractures within the Lewisian. These are interesting as they appear to have controlled the orientation of late Caledonian brittle shears with a dominant strike-slip sense of movement.

The Torridonian sediments of NE Iona were unconformably deposited over the Lewisian; some of the materials of the basal pebbly/boulder beds were derived from the local Lewisian as indicated by the petrography.

A group of "lamprophyre" dykes have been recorded in the Iona Torridonian. However, these "lamprophyres" (probably belonging to the Microdiorite Suite of Smith 1979) are rather more uncommon than those in Islay or Colonsay. The lamprophyres predate the intrusion of Ross of Mull Granite (Fraser 1977). This is indicated by a flattening fabric in the dyke rock plus a contact metamorphic effect by the pluton (Fraser 1977). Although the 'lamprophyres' probably post-dated the mylonitisation observed in Iona, their relationships are not clear enough to be decisive.

The presence of mylonite belts along the Lewisian Torridonian contact and of belts of sheared Lewisian rocks further west (one such prominent cataclasite belt crops out in Eilean Chalbha off the NW coast and continues inland in a southwesterly direction, see Fig. 6.15), suggests that we are dealing with a thrust belt. The general geology of the area and the minor structure details in Iona can be explained in terms of a duplex structure in the region. The supposed Moine Thrust east of the Iona Torridonian is the easternmost thrust (disregarding the possibility of any thrusts within the Moine in the Ross of Mull); the other major thrust horizons being the Lewisian-Torridonian contact and

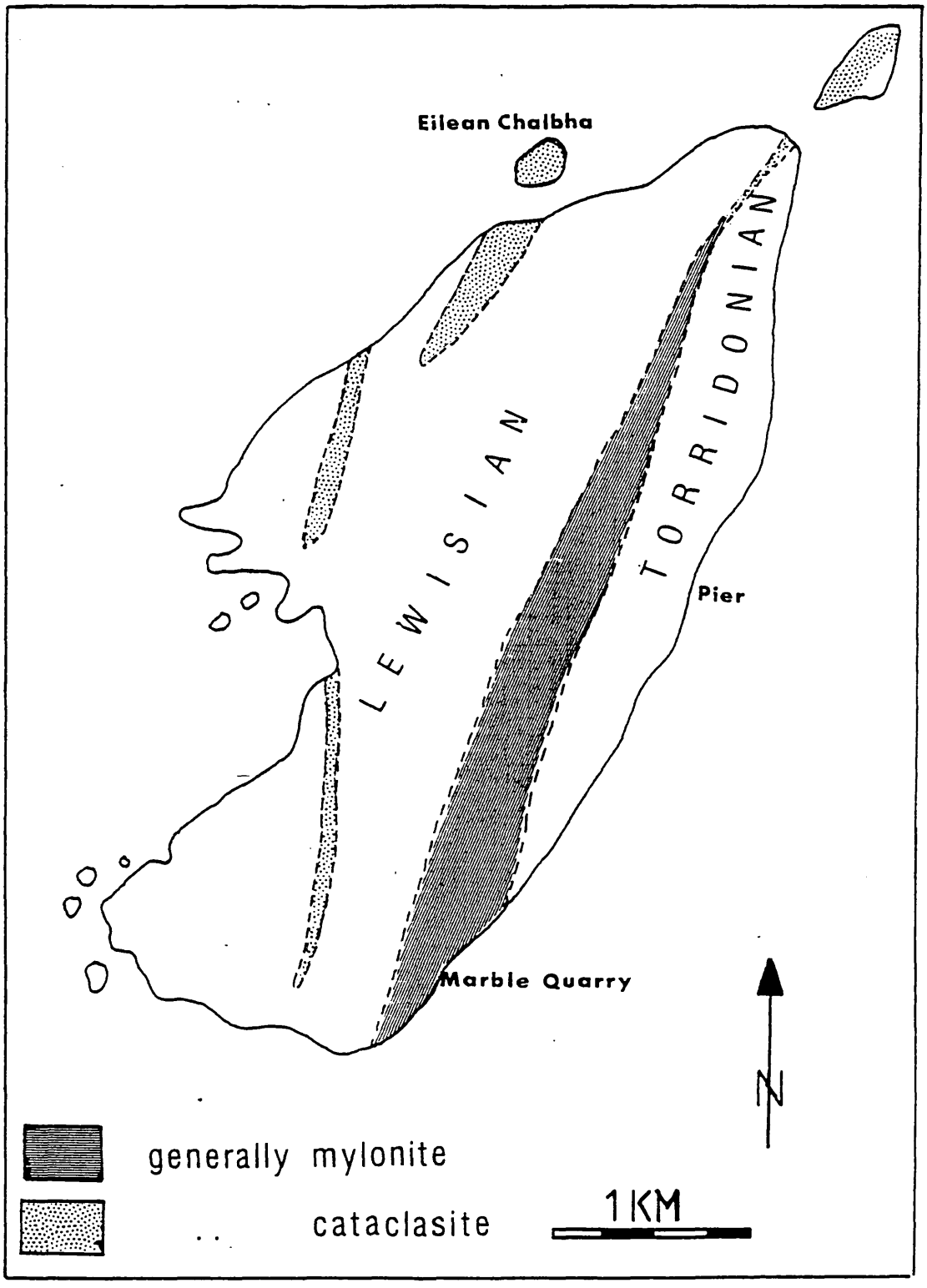


Figure 6.15. Distribution of major cataclastite-mylonite belts in Iona.

those associated with the zones of cataclastics within the Lewisian. Presumably the thrust propagation was in a westerly direction. The movement along the Lewisian-Torridonian contact and associated mylonitisation is later than the movement along the Moine Thrust itself. If one assumes that the frontal thrusts are lystic in form and develop successively westward, the steepening of the Torridonian belt in Iona can be explained as due to rotation of internal structures within a thrust sheet (Fig. 6.16). This would also help in explaining the origin of the asymmetric boudines as structures comparable to extension kinks after the belt was steepened up (Section 6.5.1). A late Caledonian shortening along a subhorizontal ESE direction would induce a foliation parallel extension.

The early folds in Iona formed prior to the mylonitisation along the Lewisian-Torridonian contact. These are probably products of a layer parallel shortening in the Torridonian below the supposed Moine Thrust. It is not certain whether these early folds formed before the movement along the Moine thrust, or after it or during the movement itself. In the deformation history of the Ross of Mull Moine thrusting was active during the third phase of folding (D_{m3}, Rilley 1966 quoted by Fraser 1977). D_{m3} folds have a style and orientation similar to the early folds of NE Iona where there is no apparent effect of shearing related to the thrusting along the Lewisian-Torridonian boundary zone.

Fraser (1977) recorded two phases of isoclinal to tight asymmetric folds (D_{t1} and D_{t2}) in the Torridonian. D_{t1} was regarded as associated with mylonitisation along the contact and D_{t2} as deforming the D_{t1} cleavage; D_{t2} fold axes are described as having a moderate to steep SSE plunge and the axial plane as having a N-S trend and steep easterly dip. The mylonite foliation in Iona is a steep one and a shortening in an ESE direction would have produced a foliation parallel extension rather than a shortening to produce D_{t2} folds on mylonite foliation. The grouping of structures proposed by Fraser (1977) does not seem to be consistent with the observations as recorded earlier. The picture appears more consistent if one regards a group of isoclinal-tight folds as the earliest Caledonian structure in Iona predating the mylonitisation. This would not only explain the variable orientation of the early fold axes which assume a steeper orientation in the mylonite belt or in the vicinity of it (see Section 6.3). Some

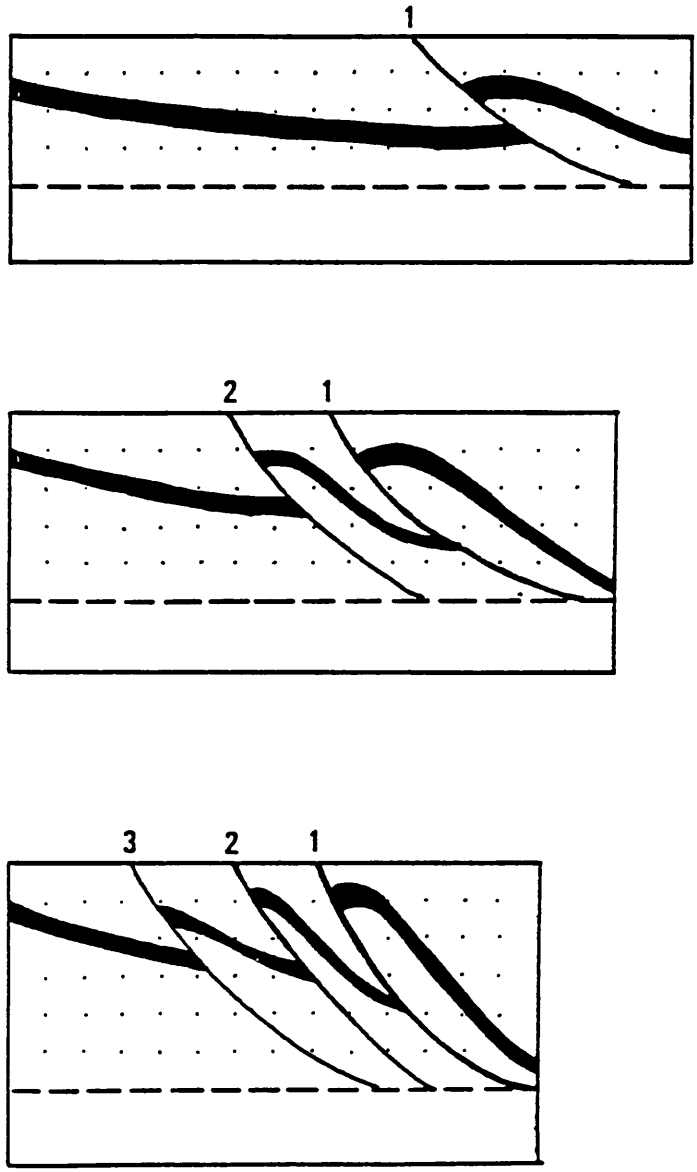


Figure 6.16. Schematic E-W cross-sections (not to scale) showing the evolution of duplex structure in the Iona region. Numerals increase from old to younger thrusts. Note steepening of internal structure within an early formed thrust sheet.

folds must have formed during the progressive shearing associated with mylonitisation and are results of passive amplification of initial perturbations on quartz segregations or locally on the foliation itself. Folds in mylonite belts would have their axes aligned close to the stretching lineation (Carreras et al. 1977, Berthe and Brun 1980) if the shearing strain is sufficiently high. Although recorded by Fraser as D_{t2} structures, minor fold axes form the Marble Quarry area plot close to the orientation of the stretching lineation (Fig. 14.2c in Fraser 1977). Such F_{t2}'s should be regarded as produced during the mylonitisation rather than after it.

As shown earlier, the west dipping thrusts and shear zones have formed later than the mylonitisation. The question is whether they formed earlier or later than the intrusion of the Ross of Mull pluton. The granite body in the Ross of Mull does show a set of prominent west dipping joints and brittle shear zones with a movement sense opposite to that along the Moine Thrust or along mylonite belt along the Lewisian-Torridonian contact. Such parallelism of orientation of this set of structures within the granite and in Iona may be a coincidence, or, alternatively 'backthrusting' on a limited scale started before the emplacement of the granite and continued till after the solidification of the granite.

Felsic porphyrite dykes are quite common in the Iona Torridonian and Lewisian and have also been recorded in the Ross of Mull Granite around Fionnphort. Interestingly the dykes have an orientation subparallel to the west dipping shears and joints both in S. Iona and in the Ross of Mull (Fig. 6.8). The dykes probably followed a 'weakness' in the country rocks produced by an earlier set of structures. Near Port Laraichean in SW Iona one such porphyrite dyke is dextrally displaced by a N-S trending shear zone (fault). Clearly the late brittle shears (and kinks) formed after the emplacement of the felsite dykes. The sequence of events as interpreted from the present observations and discussed above is summarised in Table 6.1.

Table 6.1 Sequence of Caledonian events in Iona

N-S and E-W brittle shears with strike-slip displacement	
West dipping shear zones and thrusts;	Felsic porphyrites
Asymmetric boudins on a steepened early foliation	
Other East dipping shear zones and thrusts in the Lewisian	Ross of Mull Granite
Mylonitisation and thrusting along the Lewisian-Torridonian boundary; folds in the mylonite belt, downdip stretching lineation	Microdiorites (lamprophyres)
Reverse kinks (K.P. and associated slip planes reoriented to gentle ESE dipping orientation	Movement along Moine Thrust
Early folds initially on a gentle NNE-SSW orientation; stretching lineation parallel to fold axis	

K.P. = kink plane

CHAPTER 7

CALEDONIAN MINOR INTRUSIONS

7.1 INTRODUCTION

A comprehensive account of the Caledonian minor intrusions in the Northern Highlands has been given by Smith (1979) who established their sequence and distribution. Sheets of lamprophyres and felsic porphyrites as well as several plutonic bodies of supposed Lower Old Red Sandstone age have been described from Colonsay Group of Colonsay and W. Islay (Wilkinson et al. 1907, Cunningham Craig et al. 1911, Reynolds 1936) and felsic porphyrite dykes are common in Iona. The minor intrusions of Colonsay and Islay occur to the south of the main branch of the Great Glen Fault which passes through the northwest of Colonsay. In the geological history of the islands the intrusions form important time markers and provide clues for the correlation and comparison of deformation events across the islands. On the other hand, the local structures often control the locales of minor intrusions. The present chapter puts emphasis on these two aspects. A comprehensive petrologic account of the igneous intrusions is beyond the scope of present work. However, some interesting observations bearing on the petrologic affinity of the plutonic intrusions of Colonsay, so far unrecorded, are described. It should also be mentioned that in addition to the lamprophyres and felsic porphyrites described from the metasediments of W. Islay by previous writers, similar dykes and sills also occur within the Lewisian and the present discourse provides a first report on them. Appinitic intrusions with explosion breccia have also been discovered in W. Islay.

The plan of this Chapter is to start with a general description of the intrusions of the area under two headings - the plutonic stocks and bosses, and the sheet like intrusions. A discussion on the structural controls on the orientation of minor intrusions which follows is intended to provide some general lessons on the mode of emplacement of syn- to post-tectonic intrusions in orogenic belts. In a later section, the local intrusions are compared with the Caledonian minor intrusions in the Northern Highlands. Some regional implications of the present observations are pointed out in the concluding section.

7.2 GENERAL DESCRIPTION

On the basis of the geometry of the intrusions the Caledonian minor intrusions of W. Argyllshire can be grouped under two headings -

the stock like intrusions and the sheets. The former include the plutonic intrusions of Kiloran Bay, Balnahard, Loch Staosnaig and Queens Bay in Colonsay, and the intrusions at the northend of Machire Bay near the lighthouse of Bruichcladdich in W. Islay. These intrusions are somewhat elongated in shape with their long axis not exceeding 1 km. Some of these intrusions are briefly described below. The sheet like intrusions include both dykes and inclined sheets and their thickness is usually less than a meter. Some dykes can be traced along strike for a few tens of meters. A classification and description of the sheets is given in the later part of this section.

7.2.1 The intrusions around Port Easdale, Kiloran Bay

An excellent petrologic account is provided by Reynolds (1936). Although Reynolds described the intrusions around Port Easdale as two separate bodies, these may be part of the same intrusion with selvages of the country rock interrupting the exposure of the intrusive. A further elongated mass outcrops on the cliffs north of Port Easdale (Fig. 7.1, compare with Fig. 1 in Reynolds 1936). The intrusive bodies are elongated in a WNW-ESE direction and are associated with xenolithic and breccia material along their margins. The distribution of the xenoliths and the breccias is far from uniform. The best exposures of breccias are on the southern side of Port Easdale. Here a marginal zone of 'hybrid' rocks with partly digested xenoliths of mainly psammitic material in a dark matrix are followed outwards on the southern side by a band of breccia material.

The breccia fragments vary in size from a few centimeters to a meter. The fragments are angular and are tightly interlocked without any apparent matrix (Fig. 7.2a). Fragments of phyllite, psammites and occasionally carbonates have been observed. Most of these can be petrographically matched with the metasediments around Kiloran Bay. Some of the larger phyllite fragments show a crenulation cleavage rucked on the schistosity. It is highly likely that brecciation was due to a high fluid pressure associated with the intrusive magma. The compact nature of the breccia suggests a high confining pressure during the emplacement of the intrusives.

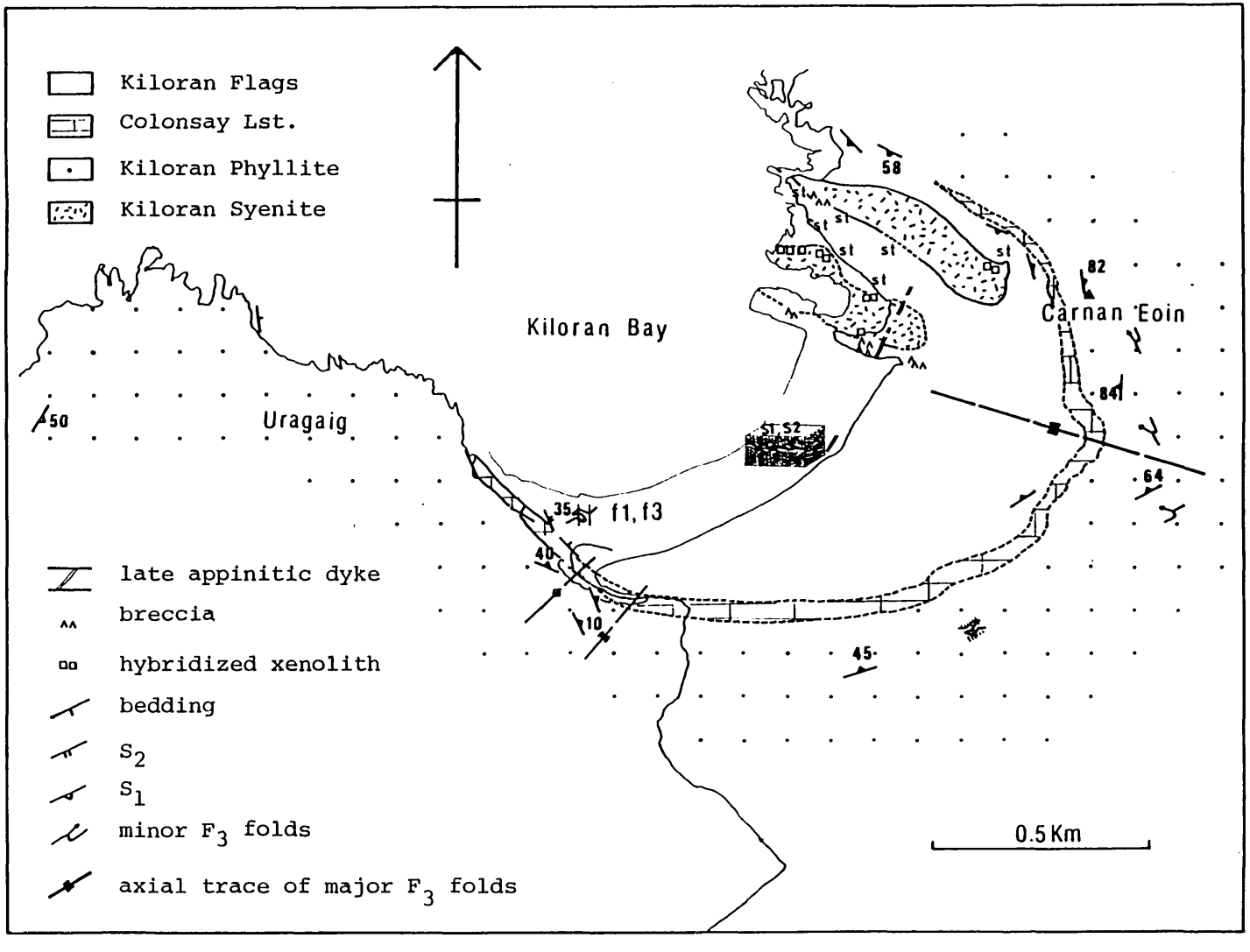


Figure 7.1. Geologic setting for the Port Easdale intrusions, Kiloran Bay, Colonsay. Chloritoid occurrences indicated by 'st'.

Figure 7.2. Marginal breccia and xenoliths associated with Port Easdale intrusions, Kiloran Bay.

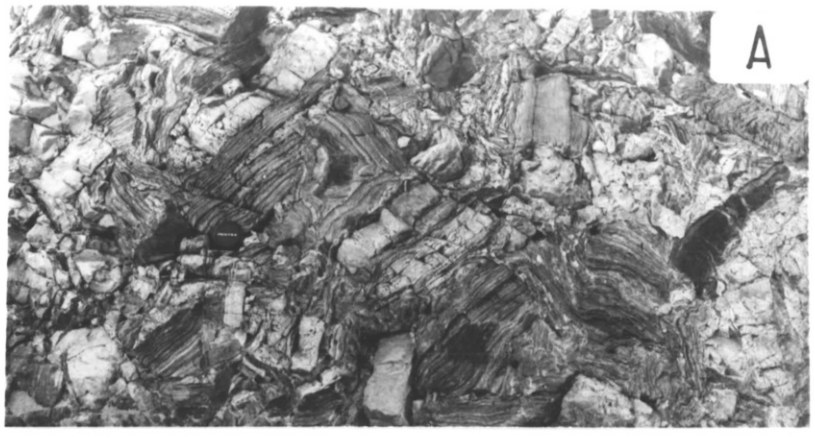
(a) Marginal breccia.

(b) Xenoliths in the hybrid zone.

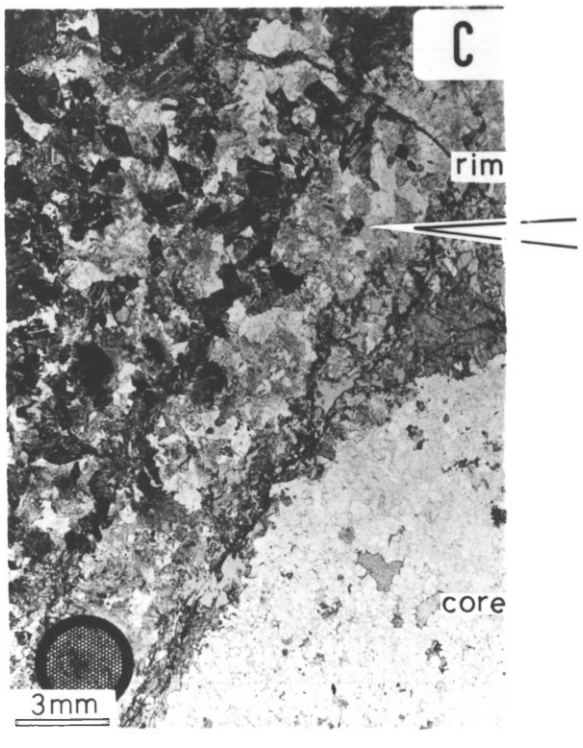
(c) Photomicrograph showing the petrography of a 'quartzite' xenolith. Reaction with the intrusive magma produces an inner syenitic and outer hornblendite rim.

(d) Photomicrograph showing details of micrographic intergrowth in the syenitic rim.

7.2









The xenoliths in the hybrid zone are interesting. They include mainly well rounded 'quartzite' fragments which vary in diameter from a few centimeters to less than a meter (Fig. 7.2b). Some of the xenoliths are separated by a pale 'halo' from the surrounding matrix. Examination of thin sections from a selection of xenoliths shows that the relatively unaltered core consists of over 95% of quartz. Some are made of large single grains (>1 cm) with strain shadows and probably derived from vein quartz. Others show large undulose grains in a matrix of finer quartz grains, the boundaries of which are sutured. In the latter type, grains of feldspar (perthite or graphitic intergrowth of feldspar + quartz) and carbonates and patches of chlorite are present. The cores of the xenoliths are surrounded by an inner rim consisting of graphic intergrowth of quartz and feldspar with hornblende, biotite and carbonate. This is followed on the outerside by a zone of hornblendite which grades into the matrix surrounding the xenoliths (Fig. 7.2 c-d). A detailed description is given by Reynolds (1936).

The main igneous rock at Port Easdale varies from a quartz bearing syenite to more basic kindreds with an increase in the proportion of hornblende and biotite. Late stage alteration of hornblende and biotite to chlorite is common. Carbonate grains with deformation twins occur either as a dispursed phase or as veins within the syenitic rock. Pyrite is a common accessory in the igneous rock as well as some of the xenolithic fragments.

Near the eastern boundary of the Port Easdale intrusion, a dark green fine grained dyke about a meter wide cuts across the pink syenite mass. The dyke can be traced further SSW where it cuts across the marginal breccia band and continues into the country rock (Fig. 7.1). The dyke rock is of microdioritic composition.

Roundness of xenoliths

The roundness of some quartzite xenoliths in the Port Easdale intrusions is striking. Cunningham Craig et al. (1911) regarded these pebbles as exotic and attributed the roundness to erosion of materials derived from a loose surface formation, which had fallen into a fissure and pipe. However, the scarcity of rounded pebbles in the marginal breccia band, the occurrence of the most rounded pebbles near the main

igneous body and the 'hybrid' rims that surround the pebbles do suggest that the roundness of the xenoliths may have been caused by the action of the intrusive magma (Reynolds 1936).

The source of these 'quartzite' xenoliths is rather uncertain. They are different in petrographic nature from any of the Colonsay Group psammites exposed in Colonsay. It has been suggested that the 'quartzite' pebbles are indistinguishable from pebbly Jura Quartzite which is thrust over the Bowmore Sandstone in Islay (Cunningham Craig et al. 1911). Some of the pebbles are not unlike the 'quartzite' pebbles in the conglomerate horizon that unconformably overlies the Lewisian in NE Colonsay. While the occurrence of quartz grains in two distinct size modes makes the xenolithic cores texturally similar to some pebbly quartzites of sedimentary origin, similar textures may result from deformation of a coarse, rather equigranular pure quartz rock of any origin. Similar texture has been observed in deformed quartz rich bands in the Lewisian and some quartz-granulite clasts within the psammitic horizons of the Colonsay Group exposed in W. Islay. The most remarkable features are the sutured grain boundaries, the two modes of sizes of the grains and the optical strain features especially in the larger grains. It is not unlikely that some of these pebbles have been brought up by the magma from a Lewisian type crust that floors the Colonsay Group sediments. The preferential survival of fragments consisting of quartz only is probably due to refractory nature of a pure quartz rock compared to one that consists of quartz + feldspar ± other ferromagnesian minerals.

7.2.2 Scalasaig Diorite, Colonsay

The intrusive body around Scalasaig is relatively large in size with an areal extent of about 0.3 square kilometers from Colonsay Pier (Fig. 7.3). The main Scalasaig intrusion is associated with a marginal breccia similar in character to that of Kiloran Bay. The main breccia band is exposed on the northwest side of the intrusive.

Petrographically the intrusive seems to be relatively basic compared to the Port Easdale intrusions. Although the overall composition is that of an augite diorite, variation to more basic compositions is reflected in the related increase in the proportion of

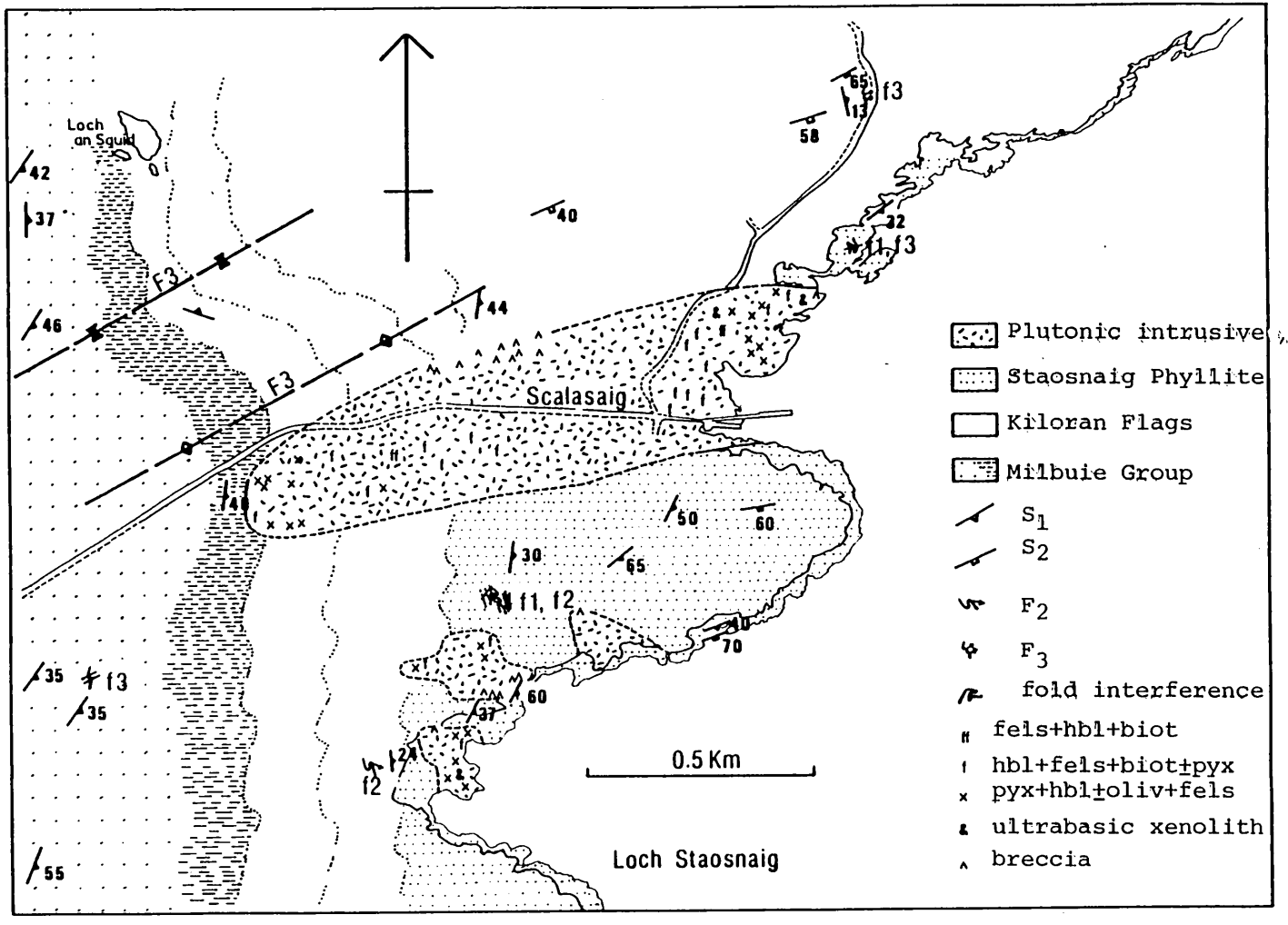


Figure 7.3. Geologic setting for Scalasaig Diorite and Queen's Bay intrusives, Colonsay. Spatial variation in the petrography of the intrusive rocks are shown.



Figure 7.4. An ultrabasic xenolith within the Scalasaig Diorite, North of Colonsay Pier.

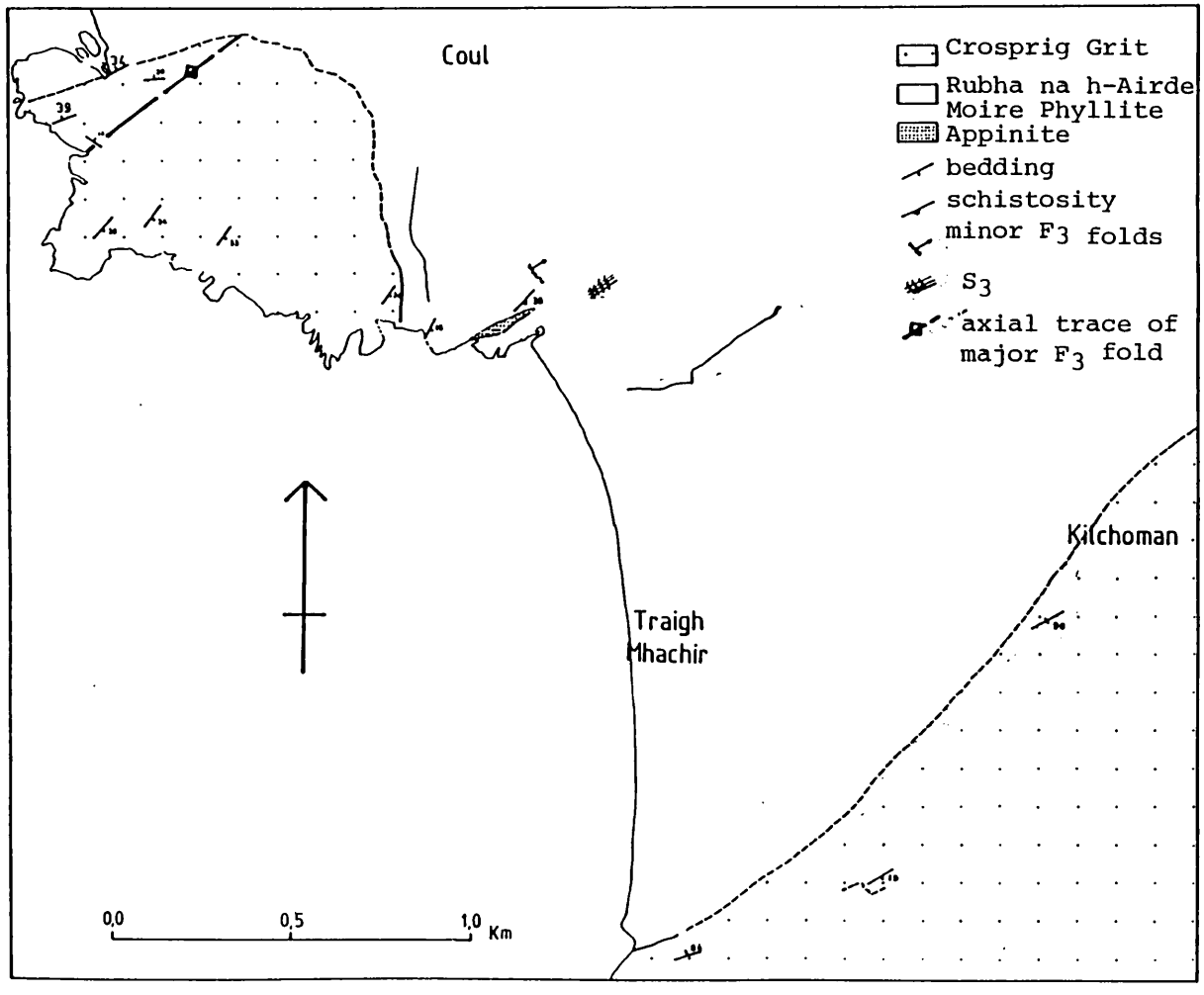


Figure 7.5. Geologic setting for the appinitic intrusion of Machire Bay, western Islay.

olivine, phlogopitic biotite and diopsidic augites compared to hornblende and alkali feldspar. The petrographic variation is schematically shown in Fig. 7.3. In addition to this spatial gradation to different petrographic types, some basic/ultrabasic xenoliths have been recorded near the northeastern margin of the body (Fig. 7.4).

Some smaller intrusions exposed on the shores of Loch Staosnaig (Queens Bay) have an overall picritic composition. However, xenoliths of mica-peridoties are common. Some of the xenoliths at Queens Bay show what may be regarded as igneous layering. Some observations on the mineral chemistry of these xenoliths are presented in a later section.

7.2.3. Machire intrusion, Islay

An appinitic intrusion with associated explosion breccia occur at the north end of Machire Bay, south of the Coul Farm (Fig. 7.5). The greater part of the intrusion is exposed only during low tide. The main igneous rock is similar to the Kiloran Syenite. The rock body is unfoliated and elongated in a ENE direction. The intrusion is much smaller than the Colonsay intrusions.

A similar intrusion and associated explosion breccia occurs near the lighthouse of Bruichcladdich on the eastern shore of the western Islay. The intrusion is a small one covering only an area of about 100 square metres.

7.2.4 Contact Metamorphic Effects

With reference to the Scalasaig Diorite, the Survey Memoir (Cunningham Craig et al. 1911) recorded contact phenomena converting grey limestone to a greenish white marble and black phyllites to a lustrous phyllite with the production of new mica. Although the memoir recorded spotting in the phyllites around Loch Staosnaig, the present mapping did not show any evidence of spotted phyllites. On the other hand, the phyllites in the vicinity of the Port Easdale intrusions have an apparent spotted appearance which the writer at first ascribed to a contact effect. Microscopic examination shows that the spots contain porphyroblasts of chloritoid (see Table 5.2 for analyses). There is no apparent change in the size of phyllosilicates (chlorite + muscovite) or

their orientation in the vicinity of the porphyroblasts compared to the surrounding mass. Microstructural relationships (described in Chapter 5) show that the chloritoids grew after the first folding in Colonsay and were themselves folded by microfolds belonging to a second phase of deformation. Geological relationships in and around Kiloran Bay show that the plutonic intrusions in this area formed after at least the first two phases of folding. The constituent minerals of the Kiloran Syenite, excepting carbonate grains, show little signs of deformation and the same holds true for intrusions of Scalasaig or Queens Bay.

Thus it appears that the chloritoids as described earlier are products of a regional metamorphism of the Colonsay sediments, the peak of which was attained before the emplacement of Port Easdale intrusions. The highest temperature in the contact aureole of the Kiloran Syenite mass must have been below the breakdown point of chloritoid.

7.2.5 Sheet-like Intrusions

Various sills and dykes of biotite-lamprophyres, microdiorites and felsite-porphyrites are included in this group. The thickness of the sheets varies from a few centimeters to a few meters. For descriptive purposes, the intrusive sheets may be classified into:

A) Sheared 'lamprophyric' sheets in Lewisian.
B) Folded lamprophyres with an axial plane cleavage
C) Lamprophyres with an oblique cleavage.
D) Unfoliated microdiorites.
E) Felsic porphyrites.

7.2.5.1 Sheared Lamprophyric Sheets in Lewisian

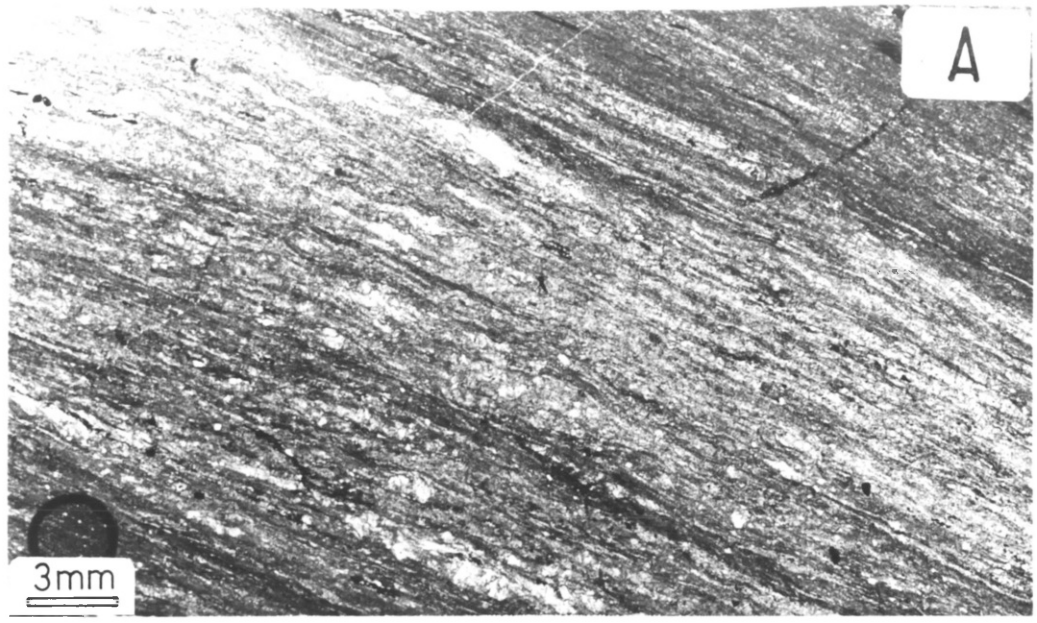
Intrusive sheets of this group have been recorded in the Lewisian of W. Islay. A cross-cutting relationship with the gneissic banding is preserved in areas away from ductile shear zones. Within the shear zones the dyke rock itself develops an L-S fabric comparable to the general shear zone foliation (Fig. 7.6a). In thin sections, the rock consists of a fine grained aggregate of biotite, chlorite and granular feldspar at various stages of alteration. This group of intrusives are distinguished from the amphibolitic component of the

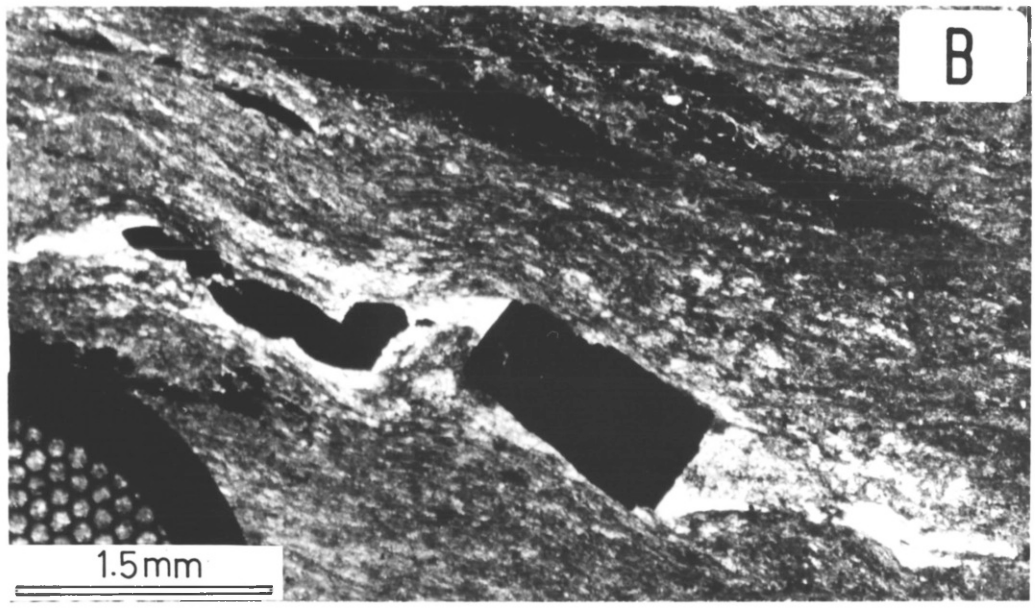
Figure 7.6. Photomicrographs showing petrography of Group A and Group B intrusive sheets.

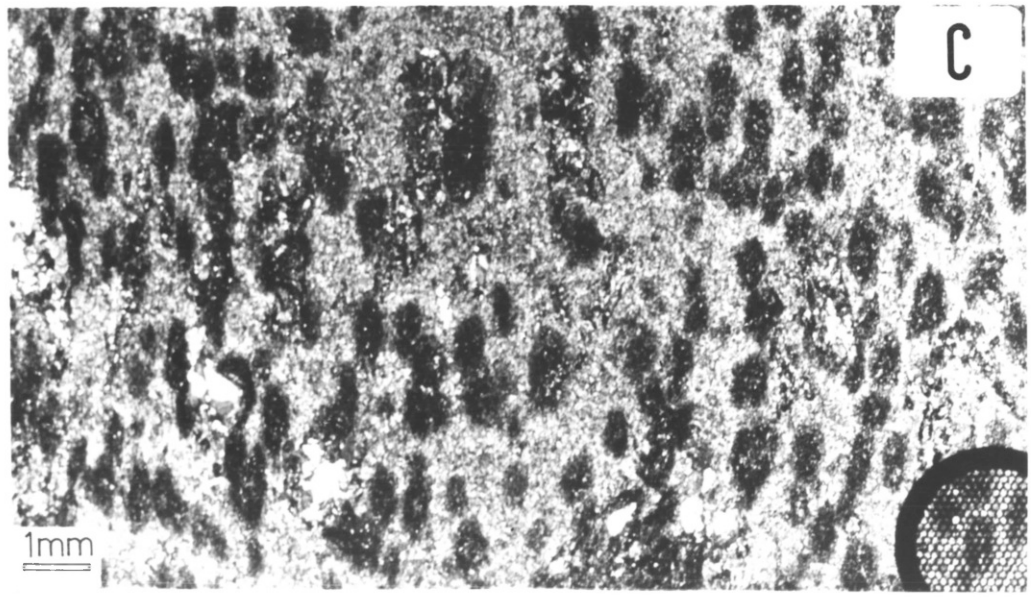
(a) Sheared early 'lamprophyric' dykes, group A, Cladville, Rhinns of Islay.

(b) Stretched pyrite (centre) and hematite (top) in sheared group A dyke, Cadville, Rhinns of Islay.

(c) Flattened spots parallel to axial plane cleavage (S_2) in folded group B dykes, N. Colonsay.







7.6

Lewisian, by the common presence of granular epidote in the latter and the common presence of opaques (haematite + pyrite) in the former. In the ductile shear zones, the opaques are usually stretched, pull aparts in pyrite are normally filled with quartz + chlorite (Fig. 7.6b).

7.2.5.2 Folded 'lamprophyres' with an axial plane cleavage

Folded lamprophyres are common the northern part of Colonsay. Sporadic occurrences have now been recorded from W. Islay as at the northern end of Machire Bay and at Sanaigmore Bay. Some of the folds in dykes near Rubha a' Geodha in Northern Colonsay are overturned in style and a penetrative cleavage runs parallel to the axial plane of the folds. There are flattened ellipsoidal spots parallel to the axial plane cleavage. Northeast of Port an Obain, a crenulation cleavage (S_2) in the enclosing phyllites passes into a penetrative axial planar foliation in a folded intrusive sheet. The folds on the intrusive sheet are open to close folds, and in thin section dark elliptical spots show parallel alignment (Fig. 7.6c). Similar flattening of spots in folded dyke rocks have been observed in the north end of Machire Bay, Islay; however, local mesoscopic structures suggest that these are associated with F_3 folds rather than F_2 as in Colonsay. One common feature of these folded intrusive sheets is their highly altered nature. Under the microscope, relict feldspars, calcite and a fine chloritic/micaceous material makes up most of the rock. Some of the spots are filled with granular calcite, but in others there is little apparent difference between the spots and the surrounding mass, except that in plane polarised light the spots appear darker.

A pre-F_2 age is certain for the folded and cleaved dykes in northern Colonsay. The Islay example must have been earlier than local F_3 folds.

7.2.5.3 Lamprophyres with an oblique cleavage

These group of dykes are characterised by an internal foliation which is oblique to the dyke walls (Fig. 7.7a). Most common occurrences have been recorded in Kilchiaran Bay area, on the cliffs south of Lossit Bay and in the Cladville area west of Portnahaven in Islay. Usually several sheets occur in a parallel fashion in individual exposures, the

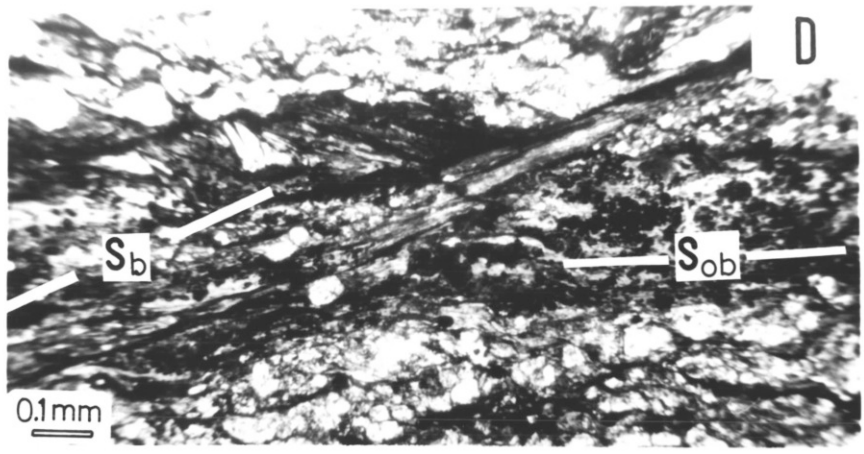
Figure 7.7 Lamprophyres (Group C) with an oblique cleavage.

(a) Group C lamprophyres within the Lewisian, Claddich, W. Islay. Note that the obliquity of the internal foliation is consistent with a dextral (strike slip) sense of shear (see sketch on right).

(b) Photomicrograph showing the internal foliation of the dyke in (a).

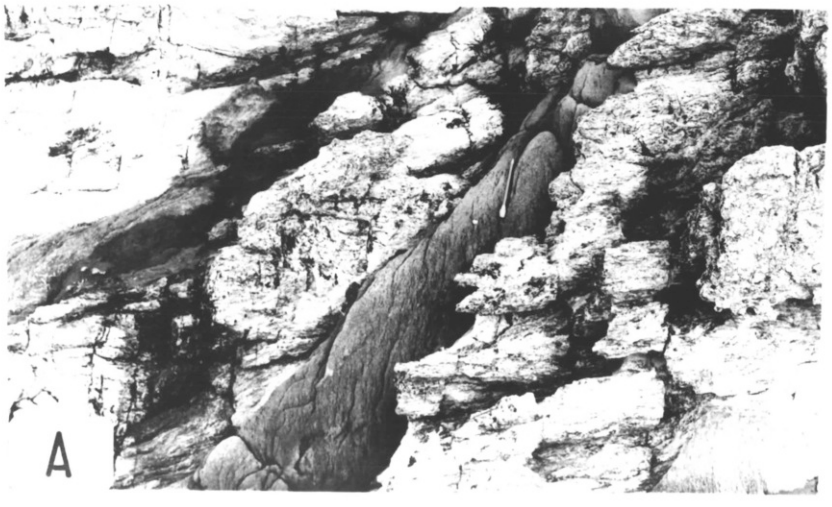
(c) Crenulated internal foliation in a group C dyke, Rubha-Gaidhealach Grit, Kilchiaran Bay, W. Islay.

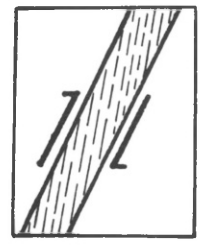
(d) Photomicrograph showing the morphology of internal foliation (S_{ob}) of the dyke in (c). Crenulations are partly due to shear bands (S_b) displacing S_{ob}.











7.7

thickness of each sheet varying from a few centimetres to about a meter. Very thin sheets (3-4 cm wide) are sometimes devoid of the internal foliation. Some of the dykes can be traced up to 150 metres along their strike.

In thin sections the rock type varies from one in which primary porphyritic biotite is enclosed in a very fine groundmass to one where streaks of granular feldspar alternate with sheafs of biotite + chlorite. The oblique foliation is defined by a parallel alignment of the porphyritic biotites or the sheafs of biotite and chlorite (Fig. 7.7b). Anastomosing pressure solution seams often traverse the feldspathic streaks. Carbonates and pyrite are commonly present in these rocks.

One interesting feature about these dykes is the consistent sense of obliquity of the internal foliation. In all the observed cases, the trace of internal foliation in plan intersects the dyke walls in such a way that the acute angle between the foliation and dyke wall point in the sense of a right-handed shear (see Fig. 7.7a). The angle of obliquity reaches a maximum of 38 degrees and there is little deviation of this obliquity from the dyke wall to the centre in individual sheets. In some thicker sheets of Kilchiaran Bay, the oblique foliation has a crenulated appearance (Fig. 7.7c). Some of the apparent crenulation may be due to the anastomosing nature of the foliation, but in thin section the foliation is sometimes displaced along discrete 'band' structures akin to shear bands or extension crenulation cleavage (Fig. 7.7d).

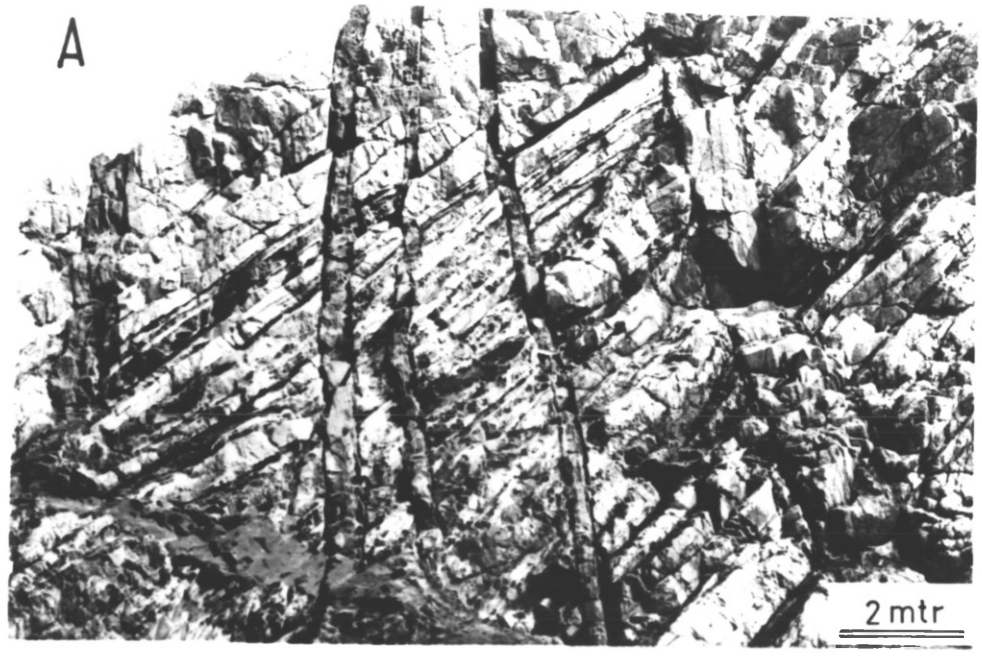
In the section between Losit Bay and Portnahaven group C dykes frequently cut the Lewisian banded gneiss (Fig. 7.8a) and some of these dykes follow the ductile shear zones within the Lewisian. Although the overall trend of the shear zones and the dykes are not much different (see Fig. 7.8c), in detail, the mylonite foliation in the shear zone terminates against the dyke wall (Fig. 7.8b) indicating an intrusive relationship. Notice that these dykes are different from the group A intrusive sheets which are themselves sheared along with the enclosing Lewisian gneiss.

Figure 7.8 Relationship between gneissic banding, ductile deformation zones (DDZ) in the Islay Lewisian and the group C dykes.

(a) Group C dykes cutting Lewisian banding on an NW-SE cross-section, south of Lossit Bay. Notice absence of any apparent displacement of gneissic banding across dyke walls.

(b) Obliquity of the internal foliation in the dyke (parallel to length of the marker pen), dyke wall and the foliation in the DDZ, plan view, Claddich.

(c) A group C dyke within a DDZ, Claddich.


A
2 mtr


B


C

7.2.5.4 Unfoliated microdiorites

These group of dykes are characterised by their relict igneous texture, usually that of a mesocratic microdiorite with hornblende, feldspar of albite-oligoclase composition and biotite (Fig. 7.9). Carbonates and pyrite (± chalcopyrite) are common accessories. Hornblende and biotite are often altered to chlorite. Some of the thicker dykes show xenoliths near the dyke walls, which can be matched with the country rock.

These dykes are widely distributed both in W. Islay and in the northern half of Colonsay. In some outcrops foliated biotite lamprophyres are truncated by thicker sheets of unfoliated microdiorite indicating that at least some of the microdiorites are later than the dykes with oblique internal foliation. On the other hand, some microdiorite dykes themselves are buckled into open asymmetric folds, as at Port an Obain and Kiloran Bay. Local structural relationships indicate a late age for these folds. There is no associated axial planar foliation in the dyke rocks.

At Port Easdale, northwest Colonsay, a microdioritic dyke cuts across the Kiloran Syenite and the associated breccia band (Fig. 7.9a, see also Fig. 7.1). The microdiorite dykes as a group probably were emplaced over a protracted period of time. While the relatively early formed dykes are folded by the last phase of folding, others have post-dated these.

7.2.5.5 Felsic porphyrites

Dykes of this group are more common in Iona. A few dykes of similar composition have been observed within both the Lewisian and the Colonsay Group sediments in W. Islay and in Colonsay. In southern Iona, the felsic porphyrites are characterised by phenocrysts of zoned feldspar, biotite and quartz set in a fine matrix consisting of granular quartz and feldspar. The quartz 'phenocrysts' have a rounded outline often with corroded and enlarged margins and sometimes consist of several grains locked together (Fig. 7.9c). In view of the fact that quartz is usually the last in the sequence of mineral crystallisation from a magma, some of these large quartz grains are probably incorporated as xenocrysts by the ascending magma.

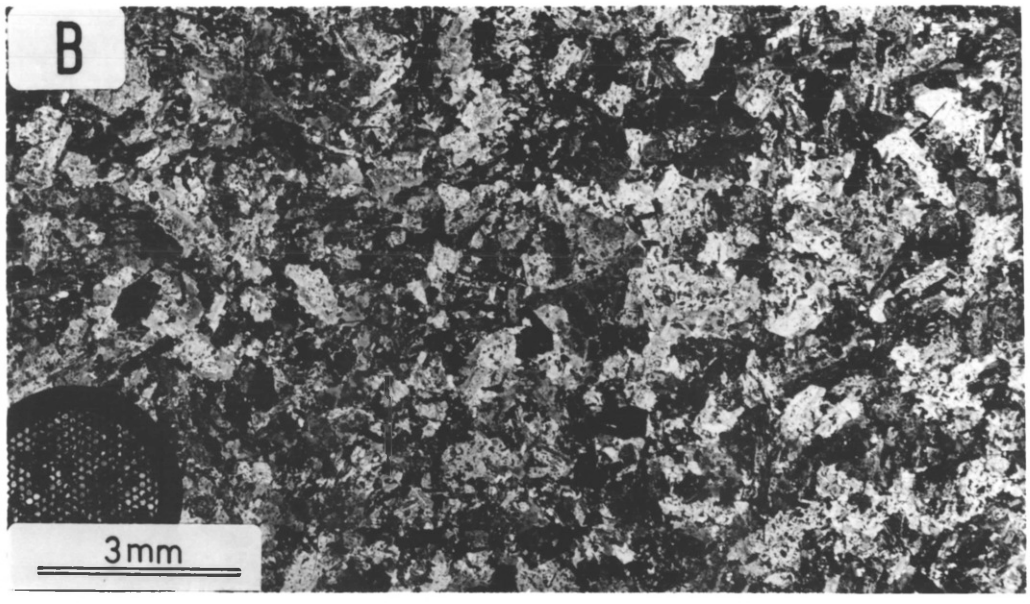
Figure 7.9. Unfoliated microdiorite (group D) and felsic porphyrite (group E) dykes.

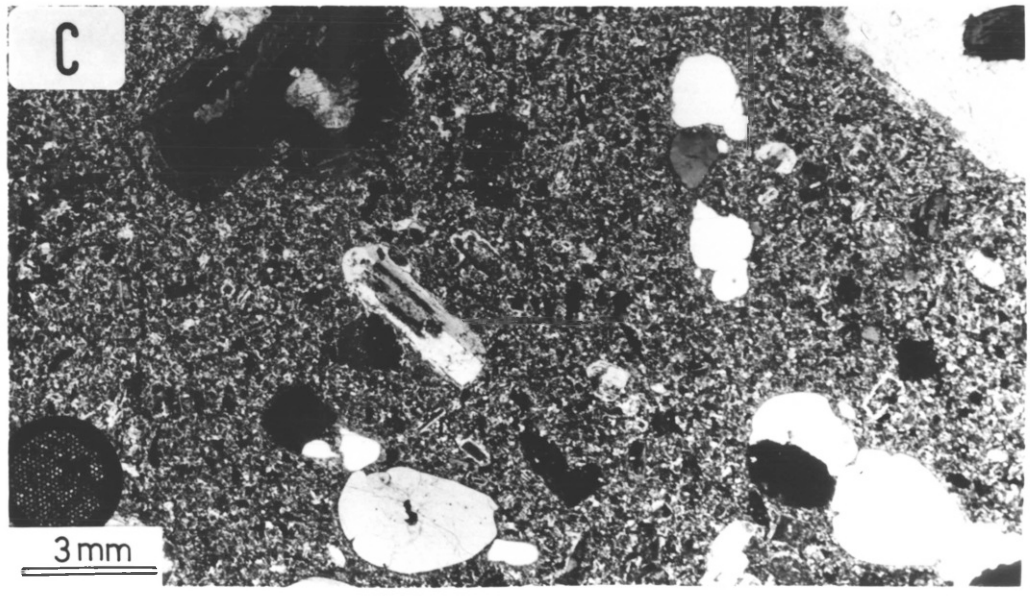
(a) A group D dyke cutting across marginal breccia band associated with Port Easdale intrusions, Kiloran Bay, Colonsay.

(b) Photomicrograph showing the petrography of the dyke in (a).

(c) Photomicrograph showing petrography of felsic porphyrites, St. Columba's Bay, Iona. Note the corroded quartz xenocrysts.


A


B
3mm


C
3mm

Felsic porphyrites have been recorded from the Ross of Mull granite and west dipping dykes of this group are quite common near Fionnphort. Noticeably these dykes in southern Iona, as well as Ross of Mull have an orientation which follows west dipping fractures, shear zones and joints in the surrounding rocks (see Chapter 6). At Port Laraichean, SW Iona, a porphyrite dyke is displaced by two parallel N-S trending fault zones. The apparent displacement indicates a dextral movement. These faults have an orientation and sense of movement comparable to the late Caledonian brittle shears observed elsewhere in Iona (both within the Lewisian and the Torridonian).

7.3 MINERAL CHEMISTRY IN PLUTONIC INTRUSIONS

The plutonic intrusions of Scalasaig and Queens Bay (Colonsay) contain xenoliths which are basic to ultrabasic in composition. Results of electron microprobe analysis of individual minerals in some polished thin sections prepared from the xenoliths and the host are presented here. A few analyses of feldspars from xenoliths and host syenite of Kiloran Bay are also given. These are significant in ascertaining the nature of the parent magma from which the intrusives derived, or the source of the xenoliths.

7.3.1 Clinopyroxenes

In the general mass of the Queens Bay intrusions, both olivine and clinopyroxenes occur as phenocrysts within a groundmass consisting of laths of plagioclase and granular pyroxene and biotite. The clinopyroxene phenocrysts are often zoned. Although there is a relative Fe-enrichment towards the rim, the range of composition is equivalent to a few mole per cent of Hedenbergite (Hd). The range of composition of the phenocrysts and small grains in the groundmass is shown in Fig. 7.10c. While the phenocrysts are in the field of Diopside (Poldervaart and Hess 1951), the smaller grains are mostly in the Salite field with one of the analysed minerals straying into the Calcic Augite field. Although there is a progressive Fe-enrichment through differentiation the range of composition is rather restricted - from $Wo_{48}En_{45}Fs_{6}$ to $Wo_{42.5}En_{38.5}Fs_{19}$. Notice that there are no pyroxenes in the Enstatite-Ferrosilite field.

Figure 7.10. Clinopyroxene compositions in the xenoliths and host rocks of the plutonic intrusions of Scalasaig and Queen's Bay, Colonsay.

(a) Pyroxenes from xenoliths in Scalasaig occurrence.

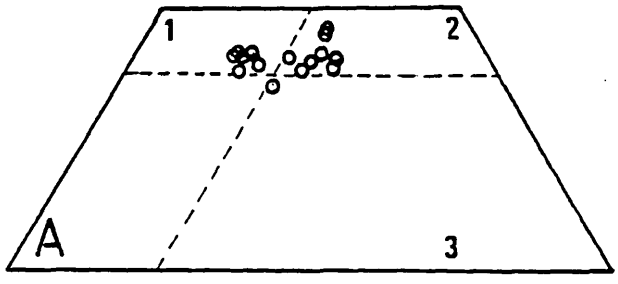
(b) Pyroxenes from xenoliths in Queen's Bay occurrence.

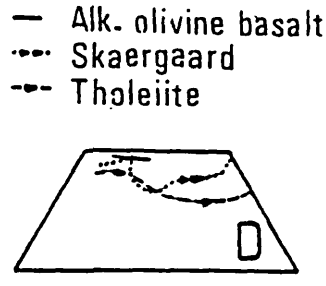
(c) Pyroxenes from the host rock, Queen's Bay intrusive. Larger phenocrystic grains - squares, small grains in the groundmass - circles.

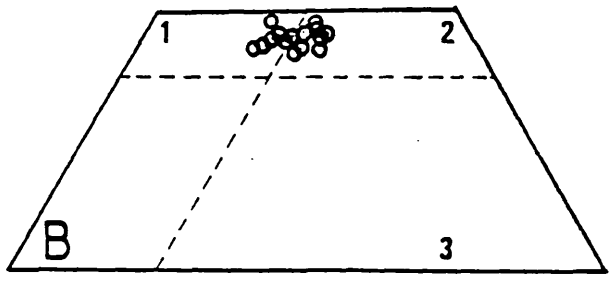
(d) Clinopyroxene trends in basaltic magmas, from Wilkinson (1951). Note that the range of composition in (a)-(c) indicate a similarity with alkali-olivine basalts.

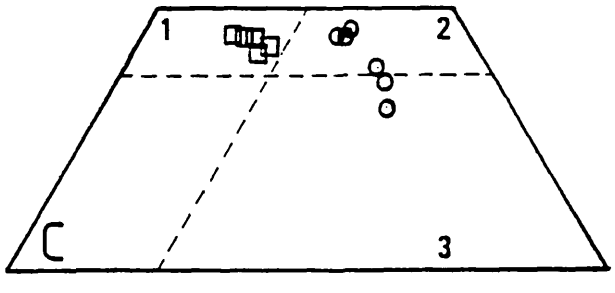
(e) Position of the total field in (a)-(c) (dark corner) in the pyroxene quadrilateral.

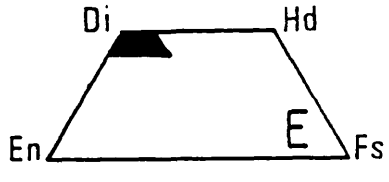
In (a)-(c) the Diopside, parts of Salite and Augite fields (Potdervaart and Hess, 1951) are indicated by numerals 1, 2, 3 respectively.


1
2
A
3


— Alk. olivine basalt
Skaergaard
Tholeiite
D


1
2
B
3


1
2
C
3


Di
Hd
En
E
Fs

Petrographically two types of xenoliths have been distinguished from Queens Bay. One is a mica peridotite with granular (2-4 mm) olivine and biotite and subordinate clinopyroxenes (type I). Pyroxenes show occasional progressive zoning. Although olivines show secondary alterations to serpentinous material either throughout or along fractures, many grains are fresh and there is no record of any reaction rim. The second type of xenoliths consists of large grains (1-2 mm) of olivine and clinopyroxenes with interstitial biotite and feldspar ± pyroxene (type II). Xenoliths recorded from the northeastern part of the Scalasaig intrusion are of the second type.

The pyroxene compositions in the xenoliths are shown in Fig. 7.10 a-b. Again the composition is highly restricted falling on either side of the boundary between the Diopside and Salite fields. The range of composition in the Queens Bay xenolith is from $Wo_{49}En_{43}Fs_{8}$ to $Wo_{47}En_{41}Fs_{12}$. In the Scalasaig occurrence, the range is from $Wo_{46}En_{47}Fs_{7}$ to $Wo_{46}En_{40.5}Fs_{14.5}$. The variation of Ca content in the analysed samples is equivalent to 5 mole percent of Wollastonite (Wo) in each locality. The Queens Bay occurrences show slightly more calcic pyroxenes.

On the whole the range of composition lies parallel to the Di-Hd join. The pyroxenes in the xenoliths and the phenocrystic pyroxenes in the host rock in Queens Bay have similar composition. Although the smaller interstitial grains in the groundmass (probably the late forming crystals in the progressive fractionation process) are relative Fe-rich the composition is mostly in the Salite field.

7.3.2 Olivine

Modal olivine is rare in the main igneous rock of the Scalasaig intrusion. The Queens Bay intrusion contains phenocrystic olivines, but the mineral is most common in the xenoliths occurring within these intrusions. None of these olivines show any reaction rim with pyroxene. Serpentinous alteration along fractures is common. Concentration of granular opaques along the boundaries of the crystals is probably due to secondary alteration.

The composition of analysed olivines in terms of the proportion of forsterite to fayalite molecules are given in Table 7.1. The range of composition is restricted to the crysolite field (Fa_{23}-Fa_{26}). This is comparable to the composition of the earliest olivines in the differentiated Black Jack sill, New South Wales, which is petrogenetically related to the alkali-olivine basalts (Wilkinson 1956). There is little difference in composition between olivines in the xenoliths and the rare phenocrysts within the main igneous rock.

Table 7.1 Composition of olivine in xenoliths and the host rock, Scalasaig and Queens Bay

Analysis	1	2	3	4	5	6	7	8
Mole % Mg	75.20	74.93	76.00	76.63	76.26	76.47	76.34	77.60
Mole % Fe	24.80	25.07	24.00	23.37	23.74	76.34	23.66	22.40

Analyses 1-5 from xenolith in the Scalasaig intrusion
Analyses 6,7 from xenoliths in the Queens Bay intrusion
Analysis 8 from the main igneous rock, Queens Bay.

7.3.3 Biotites

Biotites in the xenoliths are richer in Mg^{2+} compared to the biotites in the main igneous rock at Queens Bay. Compare analysis 1 and 2 in Table 7.2. Of the 19 analysed biotites from xenoliths, only 5 show Mg/Fe ratio marginally less than 2:1 (Table 7.3). The average ratio is 2.35. Thus the biotites in the xenoliths are essentially phologopitic whereas the late formed biotites in the host rock are Fe-rich biotites. The phlogopitic composition of the biotites suggests crystallisation from a basic and ultrabasic magma (Engel and Engel 1951). Relatively early crystallisation of Mg-rich biotites in the xenoliths is probably due to a higher H_2O content of the magma.

Table 7.2 Electron microprobe analyses of biotites from xenolith (sp. 300A) and host rock (sp. QBH4), Scalasaig

	Oxide	QBH4 Analysis 1	300A Analysis 2 (xenolithic)
	Na_2O	-	-
	MgO	11.026	15.488
	Al_2O_3	14.415	15.008
	SiO_2	35.904	37.346
	K_2O	9.853	9.903
	CaO	.025	.032
	TiO_2	3.980	4.410
	Cr_2O_3	.032	.357
	MnO	.250	.008
+	FeO	19.411	12.357
	NiO	-	-
	Total	94.895	95.281
	No. of atoms per 24 (O,OH)		
	Si	5.107	5.539
	Al	2.417	2.624
	Ti	.426	.492
+	Fe	2.309	1.533
	Mn	.030	.001
	Mg	2.417	3.424
	Cr	.004	.042
	Ni	-	.024
	K	1.788	1.874
	Ca	.004	.005

+ Total iron as FeO

Table 7.3 Mg/Fe ratio in xenolithic boitites

Analysis	1	2	3	4	5	6
Mole % Mg	72.37	67.41	71.80	75.22	63.74	74.24
Mole % Fe	27.62	32.58	28.20	24.78	36.25	25.76

Analysis	7	8	9	10	11	12	13
Mole % Mg	72.12	73.44	72.40	65.70	67.60	73.45	73.59
Mole % Fe	27.88	26.56	27.60	34.30	32.40	26.55	26.41

Analysis	14	15	16	17	18	19
Mole % Mg	64.37	72.34	66.14	67.59	65.34	66.15
Mole % Fe	35.63	27.66	33.86	32.41	34.66	33.85

Analyses 1-11 from specimen 300A, Scalasaig
Analyses 12, 13 from specimen QBX2, Queens Bay
Analysses 14-19 from specimen QBB3, Queens Bay
Calculated from the results of electron microprobe analysis.
Average Mg/Fe = 2.35±0.418

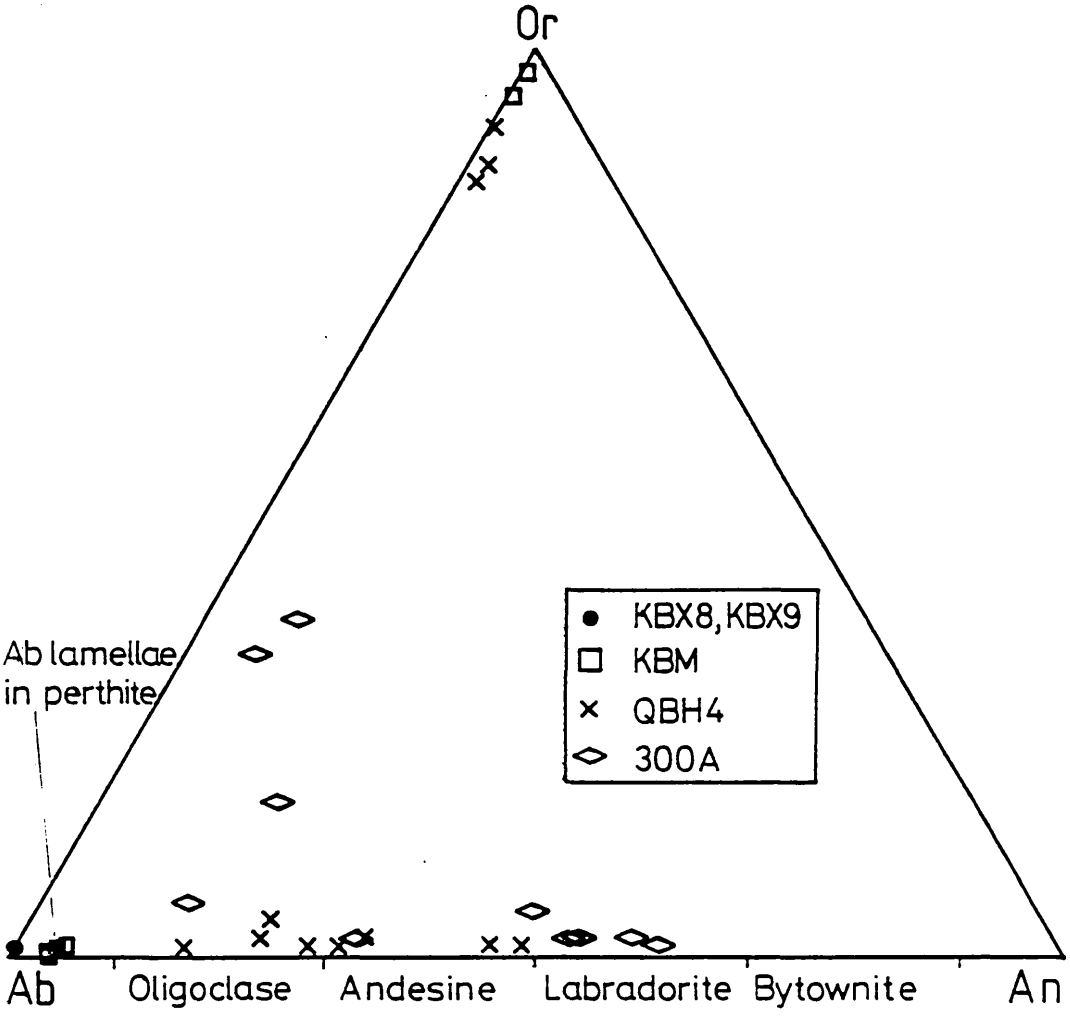


Figure 7.11. Feldspar compositions in the appinitic intrusions of Colonsay. Specimens KBX8, KBX9 are 'quartzite' xenoliths from Port Easdale intrusion. KBM = host rock of Port Easdale intrusion. QBH4 = host rock of Queen's Bay intrusions. 300A = xenolith from Scalasaig Diorite.

7.3.4 Feldspar

Whereas type I xenoliths (see the section 7.3.1) are essentially devoid of feldspars, both alkali feldspar and plagioclase occur as interstitial material in type II xenoliths from Queens Bay intrusive. The main igneous rock in Scalasaig and Queens Bay contain both alkali feldspar and plagioclase usually in the ground mass surrounding phenocrystic olivine and pyroxene, or in association with hornblende in the dioritic patches. In contrast, the intrusions at Kiloran Bay show a preponderance of alkali feldspar over plagioclase.

The compositions of analysed feldspar are shown in Fig. 7.11. Whereas plagioclase in the xenoliths is labradoritic, that within the main igneous rock at Queens Bay is of oligoclase-andesine composition. There is also a marked contrast in the composition of the alkali feldspars. In the xenoliths, the feldspar is more Na-rich than Or_{40}. Some of these compositions are in the anorthoclase field suggesting crystallisation in the High Albite-Sanidine series (Deer et al. 1966). In the main igneous rock, the alkali feldspars plot either towards the orthoclase corner with Na-feldspar content up to Ab_{15}, or are albitic. The presence of two species of alkali feldspar, and which are not necessarily perthitic indicate crystallisation at a lower temperature from a residual liquid. Notice that the feldspars from the Kiloran Bay syenite are either nearly pure albites or are close to orthoclase in composition. Some of the K-spar is pethitic.

In the reaction rims bordering 'quartzite' xenoliths of Port Easdale albitic feldspar occur in micrographic intergrowths with quartz. Textural evidence indicates that a local melt of albite-quartz (or Na-K feldspar-quartz eutectic composition was produced due to the resorbtion of quartz from 'quartzite' xenoliths into the surrounding magma (see also Reynolds 1936). The minimum temperature from Albite-Quartz eutectic is 1062° (Schairer and Bowen 1947). The ambient temperature of the surrounding magma must have been higher than this. The significance of these mineral compositions will be discussed later.

7.4 ORIGIN OF OBLIQUE CLEAVAGE IN INTRUSIVE SHEETS

The origin of oblique cleavage in intrusive sheets has been discussed by several workers (Allaart 1976, Berger 1971, Davidson and

Park 1978, Rees 1979, Smith 1979, Talbot 1980, Watterson 1968). The foliation within such sheets is interpreted as due to a shear parallel to the boundary of the dykes. Localisation of the fabric within dyke walls provides a reason for treating the development of internal deformation of the dykes as comparable to that in the ductile shear zones of Ramsay and Graham (1970). More generally, deformation within the dykes may be regarded as related to banded strain perturbations within the regional strain field (Cobbold 1977). The initiation of such perturbations in the present case is likely to have been related to a material heterogeneity. The dyke rock was evidently more ductile (less competent) than the surrounding country rocks.

In the Islay examples, the oblique cleavage is best developed around Kilchiaran Bay and between Lossit Bay and Portnahaven. In the Kilchiaran Bay area the dykes transect bedded psammites with intercalations of phyllites. In the southern part of W. Islay, the country rock is Lewisian gneiss which shows interbanding of pegmatitic, granitic and amphibolitic rocks. Both the metasediments and the Lewisian have suffered ductile deformation prior to the emplacement of the dykes. However, the deformation post-dating the intrusion of dykes can be best explained by assuming that the lamprophyric dykes were less competent at the time of deformation than the surrounding country rocks, i.e. the psammites or the Lewisian gneiss. It may be mentioned here that in the northern part of W. Islay some inclined lamprophyre dykes show an oblique cleavage where the surrounding country rock is a phyllite with thin psammitic bands or quartz veins. Lower competence of the intrusive sheets may be due to one or more of the following factors:

(a) the dyke rock was hotter than the country rock at least during the initial stage of deformation.

(b) Greater fluid content of the dyke rocks.

(c) A strain softening mechanism was active because of the mineralogy or developing fabric.

The magmas from which the dyke material was derived must have been at a higher temperature than the metasediments of lower greenschist facies condition. However, the temperature difference between the dyke rock and the country rock was not great even immediately after

intrusion. The general absence of chilled margins is relevant here. In Islay late stage metasomatic and retrograde alteration are common in the lamprophyres attesting to a higher fluid content. Much of this fluid was probably intergranular. The presence of biotites, chlorites or calcite would indeed facilitate deformation because of the presence of easy glide systems in these minerals.

Within the confines of the dyke boundaries the deformation was more or less homogeneous as indicated by the near constant attitude of oblique cleavage from dyke margin to dyke centre even in dykes as thick as 1 metre. The dyke was evidently consolidated before the bulk of the strain was imposed (see also Smith 1979). The preferred orientation of biotites/chlorites which contributes to the formation of the internal foliation is strain imposed.

The kinematic situation can be partly explained in a way similar to strain modification of angular density distributions (March 1932, Owens 1973). An experimental model relevant to the present problem is suggested by Rees (1979). Rees considered the orientation of grains in a sheared dispersion and suggested that the preferred orientation of long and short axis is due to two contributing factors which are not mutually exclusive: (1) the varying angular velocity of non-equidimensional grains as they rotate due to shearing; and (2)grains tend to take up attitudes such as that minimum angular momentum is transferred during collisions as they are sheared past each other. The relative size of the 'marker' grains and those of the dispersed media has an important influence on the relative contributions of the two factors and hence on the final preferred orientation. The dominance of intergranular collisions (factor 2 above) would lead to an obliquity between the direction of preferred orientation of the long axes and the direction of flow even at a higher strain. On the other hand, the predominance of factor 1, would result in a convergence of the direction of preferred orientation with the flow direction as strain increases. With respect to the finite strain ellipsoid, the long axis of the grains would tend to align themselves parallel to the X axis. The angle between the latter and the shear direction is dependent on the magnitude of the strain (Flinn 1962, Ramsay 1967, Talbot 1980).

The obliquity of the internal foliation with respect to the dyke walls for measured Islay examples is shown in Fig. 7.12. Although the

total number of measurements is limited, in all cases except one the obliquity in steeper sheets can be interpreted as due to a dextral strike slip movement parallel to the dyke wall. On vertical sections cutting these dykes, there is no apparent displacement of gneissic banding or bedding in quartzite across the dyke walls (see Fig. 7.8a). This is consistent with a dominant strike slip movement in these dykes. On the other hand in some gently inclined lamprophyre sheets of Northern Rhinns (W. Islay), the obliquity of the internal fabric is apparent on vertical sections alone; the internal foliation is steeper than the dyke wall indicating a northwesterly thrust sense shear parallel to the dyke wall (this is comparable to the movement sense in the more common set of SE dipping sheared microdiorites described from N. of Great Glen, (Smith 1979).

The obliquity of the internal fabric in the measured cases varies between 16 degrees and 38 degrees. The modal value being around 30 degrees. The obliquity is defined as the angle between the poles of the internal foliation and the dyke wall. There is no direct correlation between the angle of obliquity, thickness of the dykes or the azimuth of strike or dip of the dyke wall. In fact, the measured cases show a smaller fluctuation in the azimuth of the dyke wall (15 degrees) compared to the variation in the obliquity of the internal fabric (22 degrees). The limited range of orientation of the dykes may suggest that these dykes themselves rotated to a final preferred orientation due to a regional strain and that the shearing parallel to the dyke walls has arisen from the rotation of the sheets (see Talbot 1980). However, if the shearing was consequent upon a rotation of the sheets themselves, then one would expect opposite sense of shearing on dykes which were initially inclined in opposite directions from the final orientation (ideally XY plane of the bulk strain ellipsoid). North of Kilchiaran Bay (W. Islay) several near parallel dykes are spatially associated with a large F_3 fold (wavelength 300 meters). Although the axial plane of the fold is quite close to the average dyke orientation in this locality, the dykes dip on either side of the axial plane. But, the sense of obliquity of the internal foliation is persistently the same, viz., one consistent with a dextral strike-slip parallel to dyke walls. This observation is contrary to what one would expect if the situation was that proposed by Talbot (1980). It seems at least in the Islay examples, the shearing in the dyke rocks is induced by material

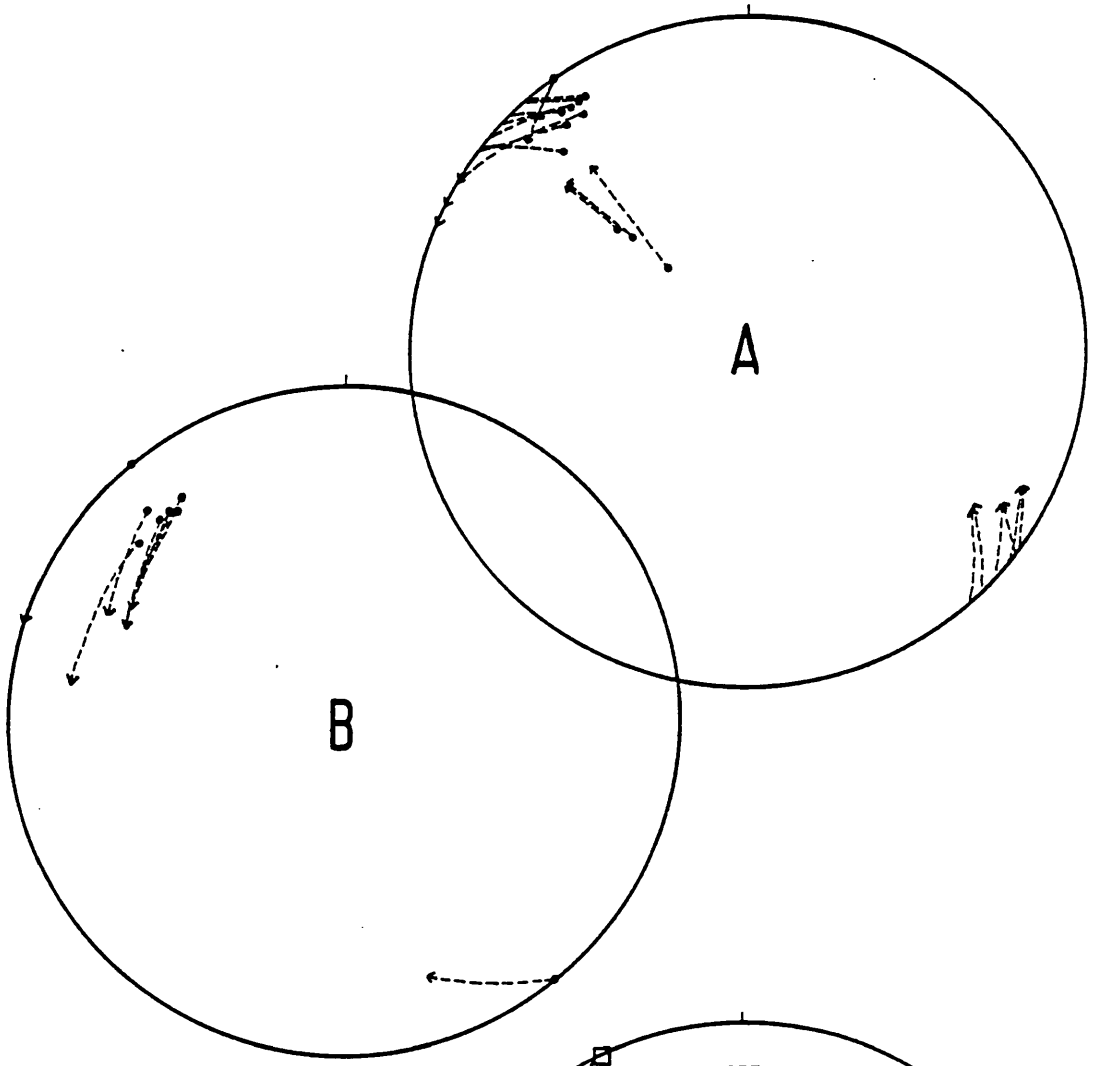
Figure 7.12 Orientation of group C dykes and their internal foliation, W. Islay.

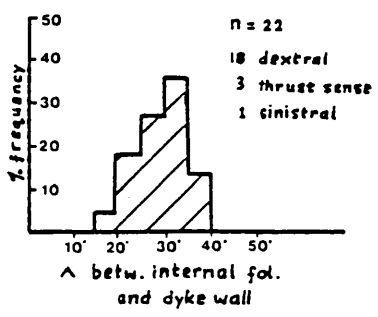
(a) Equal area plot showing poles to dyke wall (dots) and internal foliation (arrowhead), Kilchiaran Bay and three inclined sheets from northern Rhinns.

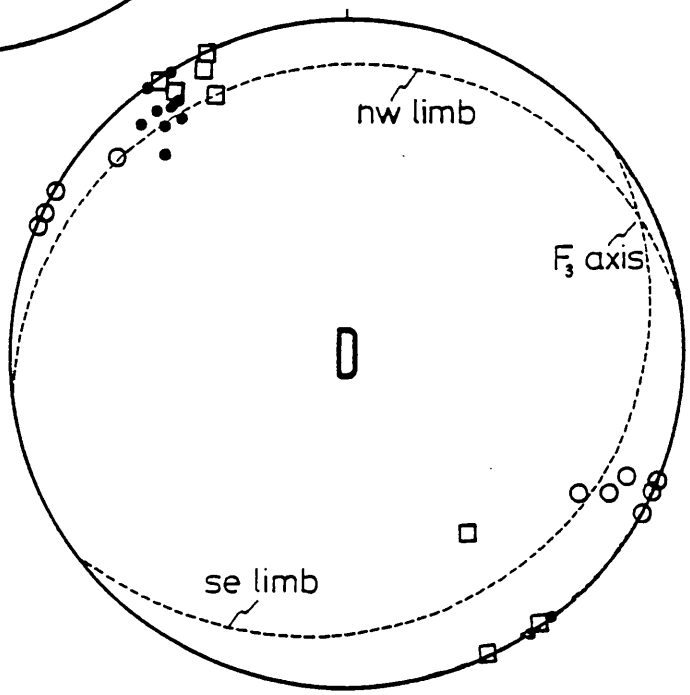
(b) From Cladville.

(c) Frequency distribution of the 'obliquity' of the internal foliation for dykes plotted in (a)-(b).

(d) Equal-area plot showing the geometric relationship between a major F_3 fold, axial plane cleavage (squares), dyke orientation (solid circles) and oblique internal foliation (open circles), north of Kilchiaran Bay. The internal foliation in all the measured dykes is consistent with a dextral (strike slip) sense of shear.


A
B


C
50
40
30
20
10
% frequency
n = 22
18 dextral
3 thrust sense
1 sinistral
10'
20'
30'
40'
50'
^ betw. internal fol.
and dyke wall


nw limb
F3 axis
D
se limb

heterogeneity, the flow parallel to dyke walls resulting from a boundary condition imposed by an initial restricted range in orientation of the dykes relative to the regional stress system.

Under suitable circumstances, the orientation of regional stress system can be derived from observations on the orientation of intrusive sheets and their internal fabric (Berger 1971, Davidson and Park 1978). The basic assumptions are:

(a) The resolved shear stress parallel to dyke walls exceeds a certain critical value for effective shearing. This will occur most effectively when the coefficient of resolved shear stress is greatest, that is when σ_3 (maximum compressive stress) is at 45 degrees to the slip direction and σ_2 lies on the slip plane normal to slip direction.

(b) The sense of shear on individual sheets depends on their orientation relative to the principal stress ($\sigma_1 > \sigma_2 > \sigma_3$, extensional stresses reckoned positive).

The most noticeable feature about the intrusive sheets with oblique fabric in Islay is their limited range of orientation and the predominant dextral sense of shear parallel to dyke walls. For subvertical dykes with an average strike of 070°, a subhorizontal orientation of σ_3 with a bearing of 125° would produce most effective dextral shear parallel to the dyke wall. Although this is not the best orientation for a thrust sense movement on SE dipping dykes, the resolved component parallel to the dip of dyke wall would be relatively large. A subhorizontal ESE maximum compressive stress (σ_3) is consistent with the regional Caledonian trend.

7.5 STRUCTURAL CONTROLS ON THE ORIENTATION OF MINOR INTRUSIONS

7.5.1 Appinitic Intrusions with Explosion Breccias

Plutonic intrusions of Colonsay, viz. the Kiloran Syenite, Scalasaig Diorite and the smaller syenitic intrusions of Islay are referred to under this heading. The twin intrusions of Port Easdale, Kiloran Bay and the Scalasaig Diorite body are elongated parallel to

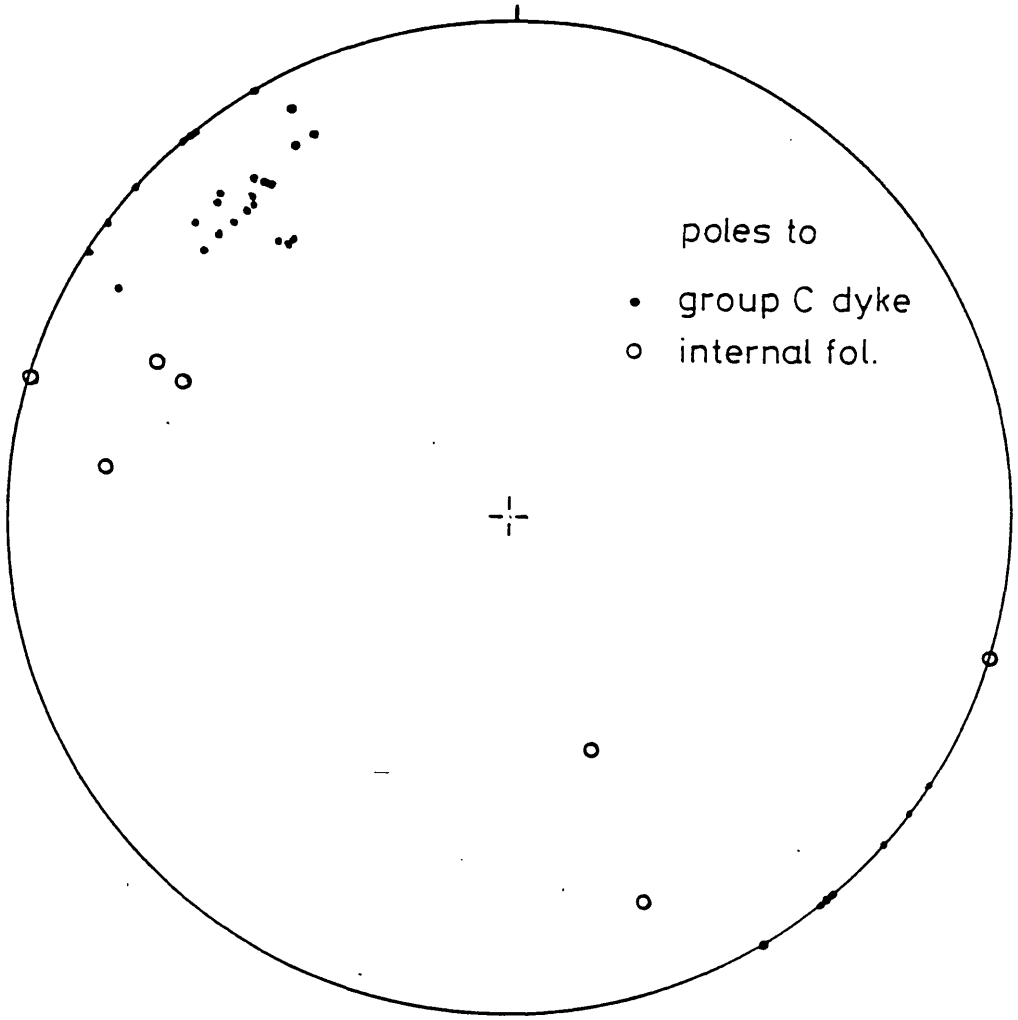


Figure 7.13. Equal area plot showing the orientation of lamprophyre dykes (group C) in the Islay Lewisian.

local major folds (see Figs. 7.1 and 7.3). The Machire Bay intrusion is too small in outcrop to be correlated with any major fold structure. However, the longer dimension is evidently parallel to the trend of minor F_3 folds (Fig. 7.5). While the local F_3 fold trend around Scalasaig is ENE-WSW that of the northern half of Kiloran Bay is ESE-WNW. It has been pointed out earlier that late folds in Colonsay probably developed as what might be regarded as members of a conjugate set. Geological evidence suggests that the major fold in the northern part of Kiloran Bay is an F_3 structure (see Chapter 5). The Scalasaig Diorite body closely follows the axial trace of an F_3 antiform. The outcrop of the Port Easdale intrusion does not extend as far as the fold closure on a limey band (Fig. 7.1), but a subterrenean extension cannot be ruled out. The fold geometry in this case is, however, that of a synform with one steep limb and the fold axis plunges at a moderate angle. Although a preference to fold axial region is apparent so far as spatial localisation of intrusions are concerned, there is no obvious correlation with antiformal or synformal structure (see also Bowes and Wright 1967).

The fold axial regions are usually areas of stress and strain concentrations and consequent development of fractures (if a brittle failure occurs) and/or cleavage development. These would certainly provide easier paths for the emplacement of an ascending magma. It may be pointed out here that the appinitic intrusions at Colonsay as well as Islay are immediately surrounded by phyllitic rocks. The association may be a coincidental one. However, such localization may be facilitated by the fact that a shale (parent rock for phyllites) would have a higher fluid content (mainly as lattice H_2O) than a psammite. During progressive regional metamorphism, the transition from shale-slate-phyllite would likely to expel considerable volume of fluid increasing the possibility of a higher fluid pressure in the immediate environment. The production of marginal breccias is probably a result of higher fluid pressure of the magma coupled with the effect of locally generated excess fluids. The compact nature of the marginal breccias associated with these intrusions suggest that they were produced under a reasonably high confining pressure.

7.5.2 Dykes and Inclined Sheets

The early lamprophyric dykes cut across the gneissic banding and are themselves sheared in the ductile shear zones in the Lewisian of W. Islay. The lamprophyres with an oblique cleavage show a preferred orientation (Fig. 7.13) within the Lewisian. The most common observed dyke orientation is that which trends around 050° and dips between 75-90 degrees either towards northwest or southeast. A similar orientation is observed for the unfoliated microdiorites, and felsic porphyrite dykes of southern Rhinns. Within the metasediments of western Islay steeper sheets with ENE trend have been observed in the section between Kilchiaran Bay and Machire Bay. At Kilchiaran Bay, the foliated lamprophyres are parallel to the axial plane of a major F_3 fold. In the northern part of the Rhinns, specially within the phyllitic rocks early dykes follow a penetrative foliation (S_1) and those with a subhorizontal attitude are themselves folded by later folds. Early lamprophyre and microdiorite sheets in Colonsay show similar relationships.

Although the number of observations is limited, a NE-ENE (Caledonian) trend is apparent for the sheet like intrusions. Some of the group B lamprophyres have followed the ductile shear zones previously formed within the Lewisian. Noticeable features about these dykes are their near-straight and parallel boundaries. In some cases several of these dykes occur in a parallel fashion within an expanse of a few tens of meters, as if the dykes have followed some sheeted fracture zones. Although the possibility of rotation of dykes towards a finite orientation due to bulk strain cannot be ruled out for early formed dykes, the control of pre-existing fractures on late microdiorite and felsite dykes is noticeable. The unfoliated microdiorites in southern Islay have suffered only the last increments of regional strain and the deformation features on them are largely in the brittle field (see Chapter 4). Yet their consistent orientation is noticeable. It may be recalled here that on the photo-interpreted fracture pattern of Islay and Colonsay (see Chapter 2), one mode of fracture azimuth is between 045°-065°. Although most of these fractures are probably related to the movement along the Great Glen Fault system, some of these may date back to an earlier part of the Caledonian deformation history.

The control of pre-existing fractures or tabular zones of ductile or brittle deformation on the orientation of post-tectonic intrusions is well illustrated by the felsic porphyrite sheets of

southern Iona and the Ross of Mull. Here, the dykes follow west dipping shear zones, fractures and joints within the Lewisian, Torridonian and the Ross of Mull Granite.

7.6 COMPARISON WITH CALEDONIAN MINOR INTRUSIONS OF NORTHERN HIGHLANDS

Three suites of minor intrusions are important as significant igneous episodes in the magmatic history of the N. Highlands Caledonides, the early tectonic Amphibolite Suite, the late to post-tectonic Microdiorite Suite and the post-tectonic Minette Suite (Smith 1979). The Microdiorite Suite includes some felsic porphyrites and appinites. The intrusions of the main Amphibolite Suite post dated the first phase of regional deformation in the N. Highlands; the lower and upper limits of intrusion are provided by the age of the Carn Chuinneag granite, c.560 Ma and the late Caledonian Pegmatite Suite, C.450 Ma (Smith 1979). The early intrusions (group A sheets) which have been deformed with the country rocks in the ductile shear zones within the Lewisian outcrop, W. Islay are petrographically different from the Amphibolite Suite intrusions described from N. Highlands. However, most of these early intrusions have lost their original igneous texture. Moreover, the country rocks in N. Highlands have been deformed in the amphibolite facies and the prevailing metamorphic condition in W. Islay was in the low greenschist facies. On the other hand, the ductile shear zones in the Lewisian of W. Islay have formed early in the local structural history. Thus on the basis of the relative age with respect to local deformation phases, the group A sheets are early-tectonic, and may be comparable with the members of the Amphibolite Suite of Smith.

Folded lamprophyres with an axial plane cleavage (group B sheets) and lamprophyres with an oblique cleavage (group C sheets) post-date the first phase of deformation in W. Argyllshire. The group B sheets are locally folded by F_2 folds (Colonsay) and group C sheets cut across the ductile shear zones within the Lewisian of W. Islay. These are comparable to the microdiorite intrusions of Loch Garry, which were deformed under fairly ductile conditions and before the end of Caledonian tectonism (Fettes and Macdonald 1978, Lawrie 1961, Smith 1979). The upper age limit of the group C sheets in W. Islay is that of local F_3 folds. The 'sheared microdiorites' of N. Highlands (equivalent

to group C in Argyllshire) cut the 450 Ma pegmatites and are older than the Strontian and Ross of Mull granites (Smith 1979). The age of the Ross of Mull granite is C.420 Ma (Beckinsale and Obradovitch 1973). While some of the unfoliated microdiorites (group D) in Colonsay are deformed by late folding (F_3) which produces open assymetric folds without any penetrative axial planar fabric, others transgress all Caledonian minor structures. The intrusion of group D sheets began towards the concluding stages of the Caledonian tectonism and continued after it.

The appinitic stocks of Colonsay and W. Islay have preserved their igneous texture and showed little sign of any deformation. It may be recalled here that some of the semipelitic fragments in the marginal breccia associated with these plutons show both S_1 and S_2 cleavages. The relative time of intrusions of these plutons would fall in the same period as the group D sheets, possibly towards the later end.

The felsic porphyrite dykes (group E) cut across all early structures in Islay and Colonsay and locally cut sheets belonging to groups described in the preceding paragraphs. Chilled margins are noticeable in many of the group E dyke. The country rocks must have been relatively cool during their intrusion. The relationship between the Minette Suite and the rocks of the fold belt indicate that the region had stabilised and that Caledonian deformation had ceased when these dykes were intruded (Smith 1979). One may be tempted to correlate the group E dykes in W. Argyllshire as equivalent of the Minette Suite in N. Highlands. However, some of the felsic-porphyrite dykes in Iona are displaced by late brittle shears. Whether these structures represent late 'hiccups' of the Caledonian tectonism or are later post-Caledonian structures localised along pre-existing zones of weakness is a matter of debate. However, the lower age limit of group E sheets can definitely be fixed at C.420 Ma, the age of the Ross of Mull granite. The latter is cut across by the felsic porphyrite dykes in Fionnphort (Ross of Mull).

The discussion in the preceding paragraphs shows that in W. Argyllshire, there was an early phase of intrusion. After this, the microdioritic sheets were intruded over a protracted period of time in the deformation history. Their deformation varies from a ductile to a

brittle regime and encompasses local F_2, F_3 folding and a brittle phase which probably post-dated F_3 folding. The age relationships are tentatively summarised in Table 7.4.

7.7 DISCUSSION AND CONCLUSIONS

The general geologic setting, petrography and structural features of the minor intrusions in Islay, Colonsay and Iona (W. Argyllshire) indicate that the majority of these intrusions are comparable to the intrusions belonging to the Microdiorite Suite in N. Highlands, north of Great Glen. The general observation that the Microdiorite Suite is late to post-tectonic with respect to regional Caledonian deformation (Smith 1979) is upheld by the observations in W. Argyllshire. However, some lamprophyric dykes in Islay and Colonsay are involved in the F_2 folding of the area suggesting either, the period of intrusion of the whole suite was protracted, or that the folding phases cannot be matched in time across the total Caledonian belt. Group A intrusive sheets are involved in the earliest phase of Caledonian deformation in W. Islay. In contrast to this, the intrusions belonging to Amphibolite Suite in N. Highlands post dated the emplacement of Lewisian slices into the Moine rocks of Sutherland, the intrusion of Carn Chinneag granite and the formation of Ardgour granitic gneisses (Peacock 1977). Widespread examples of individual intrusions cross-cutting the oldest fabric in the Moine country rocks show that the suite post-dated the first phase of regional deformation (Smith 1979). The observations in W. Islay with respect to Group A sheets implies either these are unique to this part of Caledonian belt, or the ductile shear zones in W Islay formed later than the first phase of regional deformation in N. Highlands. One must bear in mind that the Moine rocks of N. Highlands are known to have a pre-Caledonian deformation and metamorphic history (the Morarian event, c.750 m.y. or c.1000 m.y.) and the first phase of regional deformation may, at least in part, represent the pre-Caledonian event. The second alternative would be consistent with folding of group B sheets by local F_2 folds. Two assumptions are inherent in this deduction - (a) the representatives belonging to a particular suite are products of relatively short-lived igneous event, and (b) the 'peaks' of folding deformation (fold phases) are separated by relatively weaker 'background' deformation.

Table 7.4 Relative age of Caledonian minor intrusions

SW Inverness-shire (Smith 1979)			Argyllshire (present study)	Other probable equivalents
Minor intrusions	Major intrusions			
MINNETTE SUITE	RATAGAIN			
		D_4	Felsic porphyrites of Iona (Group E)	
Felsic porphyrite-MICRODIORITE-Appinite Suite	ROSS OF MULL STRONTIAN		Unfoliated microdiorite sheets (Group D)	
Early felsic porphyrite suite of Cluanie	CLUANIE	D_3	Scalasaig Diorite, Kiloran Syenite Machire intrusion	Appin district intrusions intrusions, associated with Ardara Pluton, Donegal
LATE CALEDONIAN PEGMATITE SUITE			Lamprophyres with oblique cleavage (Group C)	
		D_2	Folded lamprophyres with AP cleavage (Group B)	
		D_1	Early minor intrusions	
AMPHIBOLITE SUITE				(Group A)

The appinitic stocks of Colonsay bring out some interesting points in petrogenesis and the relationship between magmatism and tectonism. The mineral chemistry of these rocks suggest their affinity with an alkali-olivine-basalt magma. Geochemistry of appinites from the type area (Ballachulish dt.) indicates that the rocks are due to the differentiation of a basic magma; closeness with a calc-alkaline suite is noticeable except for the higher K_2O content of the appinites (Wright and Bowes 1979). Some of the xenoliths in these intrusions show a very high Mg/Fe ratio in olivines and biotites indicating that these may be either fragments brought from the lower crust, if not mantle, or very early formed cumulates within the deep seated magma chamber. Even within the confines of a small island such as Colonsay the appinitic intrusions show a range of composition from basic (Queens Bay) to acid-intermediate (Port Easdale). Although normal crystal fractionation can produce a range of composition in the resulting fractions, the importance of contamination of materials in the upper crust is indicated by the xenoliths of Port Easdale intrusions. The high fluid content of the magma at certain stages of intrusions of these appinitic stocks is probably due to the influence of fluids derived from sediments undergoing tectonism and regional metamorphism. Wright and Bowes (1979) suggests that the high K_2O content is probably allied to the high volatile content.

The partial melting of 'quartzite' xenoliths to produce an Albite-Quartz eutectic, in the Port Easdale intrusions suggests that the temperature in the magma surrounding the xenoliths must have been in the region of around 1050°C. Such high temperature of the magma suggests basic magmatic source. It may be mentioned here that partial melting associated with appinitic intrusions has been reported from Appin district and the high contact temperature is attributed to a convective circulation of the magma (Platten 1982). On geochemical grounds the appinitic intrusions associated with the Ardara pluton, Donegal are regarded as being derived from the mantle (Hall 1967). Although a high temperature for the intrusive magma is suggested for the Colonsay appinites, the apparent absence of conspicuous thermal metamorphic effect in the surrounding country rocks invites some comments here. For a simple model the initial contact temperature (T_c) in the immediate vicinity of an igneous intrusion is given by:

$$T_c = \frac{1}{2} T_o$$

where, T_o is the initial temperature of the magma in the intrusive (Jaeger 1964). As discussed earlier, although porphyroblasts of chloritoid occur in the vicinity of Port Easdale intrusion, the spatial association is one of coincidence. The chloritoids formed as a product of regional metamorphism, the peak of which was between local F_1 and F_2 fold phases. The Port Easdale intrusions are post-F_2. It appears that the temperature in the contact aureole was not high enough to favour any metamorphic reaction leading to breakdown of chloritoid. Experimental investigations (Ganguly 1968, Ganguly and Newton 1968, Halferdahl 1961, Hoschek 1969, Richardson 1968) shows that Fe-chloritoid by itself could be stable over all the pressure range ($P_s = P_{H_2O}$) up to 20 kb and up to 500-700°C depending on P_{O_2}. In natural rocks reactions with associated minerals could decrease the break-down temperature (Miyashiro 1973). Taking the temperature value in the lower end of this range, one can say that the highest aureole temperature associated with the appinitic intrusions of Colonsay was probably less than 500°C. In fact, the resorbtion of the xenoliths in a basic magma could have taken place at a greater depth in the crust and the emplacement of the appinitic intrusions into the pelites of the Colonsay Group may have taken place when the magma has re-equilibriated to a relatively lower temperature. The apparent textural similarity of some 'quartzite' xenoliths from Colonsay with deformed quartz-granulites should be recalled here.

If the appinitic intrusions are indeed derived from magmas coming from deep within the crust, if not the mantle, the presence of some deep crustal fracture system would facilitate their emplacement in the upper levels of the crust. The distribution of appinitic intrusions in the Scottish and Irish Caledonides are shown in Fig. 7.14. The close spatial association of appinitic intrusions with late-to-post-Caledonian granite plutons (e.g. the Strontian Granite, the Rogart Granite) north of Great Glen has been discussed by Smith (1979). In Fig. 7.14 the major lineaments in the Caledonian belt are also shown. Empirically, the distribution of the appinitic and basic intrusions show spatial association with the Great Glen fault line on a regional scale. The significance of Great Glen fault as a deep crustal structure in the Caledonian belt can not be overemphasised. It is possible that the Great Glen fault system acted, at least in part, as a 'channel way' for

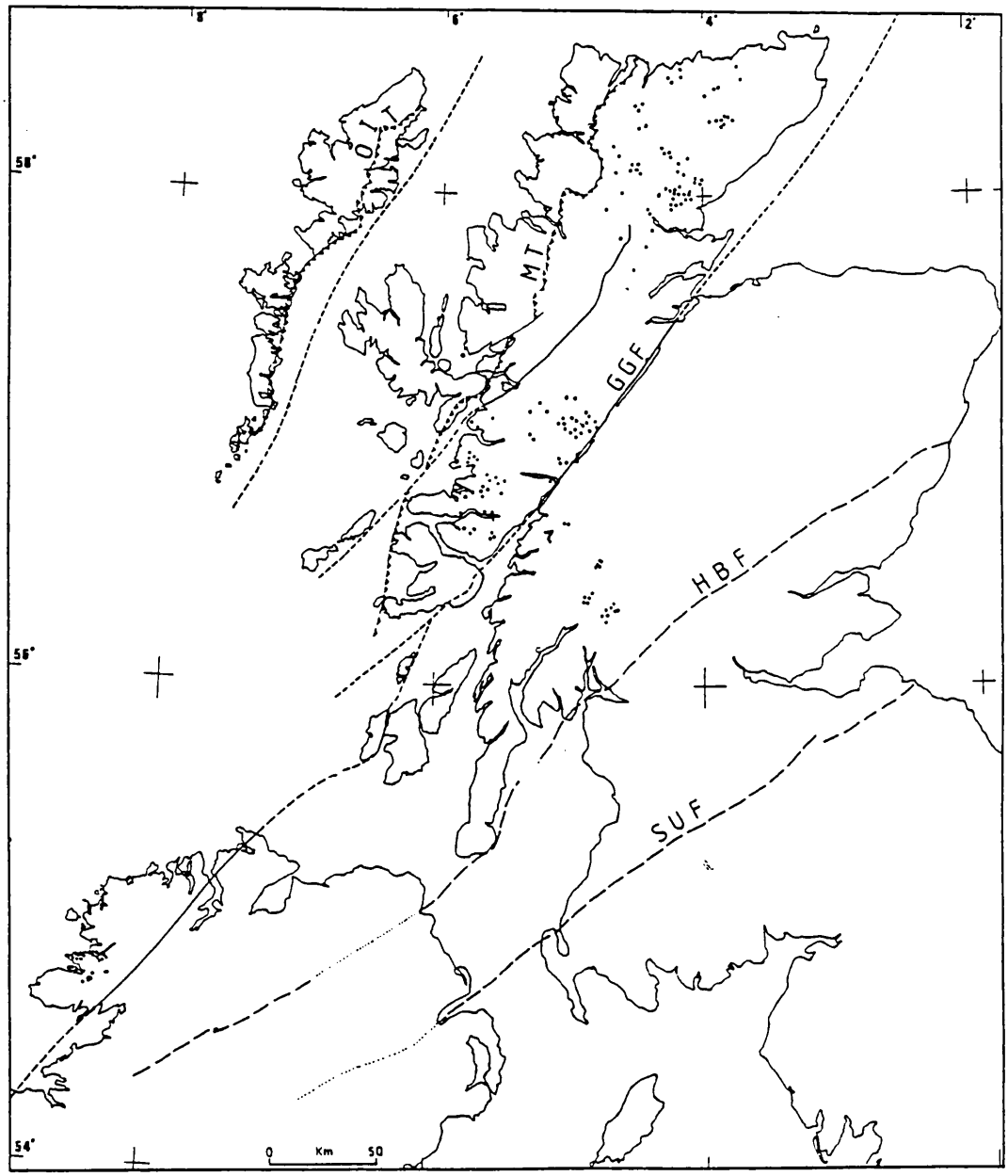


Figure 7.14. Occurrences of appinitic and basic intrusions in Scottish and Irish Caledonides. Northern Highland occurrences from Smith(1979). OIT = Outer Isles Thrust; MT = Moine Thrust; GGF = Great Glen Fault; HBF = Highland Boundary Fault; SUF = Southern Uplands Fault.

the ascending magma that gave rise to the late-to-post-tectonic intrusions including the appinites in the Caledonian belt. Some appinites are also located on transverse deep fractures in N. Highlands (Watson 1984).

One basic difference of the felsic porphyrite dykes and the earlier minor intrusions is the almost ubiquitous presence of chilled margins in the former. It is clear that these intrusive sheets (Group E) were emplaced when the host rock was relatively cool. The felsic-porphyrites of W. Argyllshire were emplaced after the stabilisation of the Caledonian belt and probably re-equilibriation of the rocks to a much lower temperature. This is consistent with the general post-tectonic character of these intrusions. However, there is a distinct control of pre-existing structures on the orientation of these intrusive sheets, as discussed earlier.

CHAPTER 8

GENERAL DISCUSSION AND CONCLUSIONS

8.1 CORRELATION BETWEEN ISLANDS

The islands of Islay and Colonsay are geographically separated. On sedimentological and stratigraphic grounds, the metasediments of Colonsay-Oronsay are thought to be an upward continuation of the metasediments of western Islay, which also unconformably overlie the Lewisian (Stewart 1962, Stewart 1975, Stewart and Hackman 1973). The whole succession of metasediments is united as the Colonsay Group (Stewart 1975). Although no major fold structure can be physically traced from western Islay to Oronsay and Colonsay, the general similarity in orientation and style of mesoscopic structures, as well as of mappable folds, in each island suggests the possibility of correlation of these structures. The most convincing evidence for the time-equivalence of structures across the islands comes from the relationship of the local structures with the Caledonian minor intrusions. This point has been stressed in Chapter 7 (see especially Table 7.4). The relationship with appinitic intrusions does indicate that the deformation events that produced axial planar cleavages in the Colonsay Group were largely complete before the emplacement of these minor intrusions. Structural analysis in Islay and Colonsay has shown that several phases of folds and axial planar cleavages are present. In Colonsay, the F_2 folds affect the group B intrusive sheets and produce a flattening fabric in dyke rock parallel to the axial plane of F_2 folds. The intrusive sheets with oblique cleavage (Group C) are syn- to post-D_3 in W. Islay. Appinitic stocks are post D_3 both in Islay and Colonsay. The felsic porphyrite dykes post-date most deformation features in W. Islay and Colonsay.

Moving to Iona, all the minor structures except the west dipping shear zone and late brittle structures were formed before the intrusion of the Ross of Mull Granite. Comparisons with structures in the Colonsay Group can be drawn from the relationship of the appinites on a regional scale with respect to the post-tectonic Caledonian granites. The appinites are earlier than most of these intrusions including the Ross of Mull Granite. Since the appinites in Colonsay and W. Islay post-date D_3 phase, the minor structures other than later brittle structures in Iona may be comparable to those related to D_1-D_3 phase in W. Islay and Colonsay. A tentative correlation for structures in the three islands is shown in Tables 8.1 and 8.2. The relative age of structures in Bowmore Sandstone and NE Islay Dalradian is also shown in

Table 8.2. Such correlation must be regarded as highly tentative as diachronity of deformation in geographically separated areas cannot be ruled out.

8.2 BASEMENT-COVER RELATIONS

In each of the three regions, W. Islay, Colonsay and Iona, evidence of an unconformable relationship is preserved (cf. Stewart 1975, Cf. Stewart and Hackman 1973). However, during Caledonian shortening these boundaries acted as strain sinks. This is evident in the presence of local zones of strain gradients, in shearing of the contact zone rocks to produce mylonitic rocks and as in Islay, in folding of the interface between the Lewisian and the Colonsay Group. The deformation features along the contacts are summarised in Table 8.3.

In W. Islay, the Lewisian has an outcrop which occupies several square kilometers. The boundary between the Lewisian and the overlying Colonsay Group has an overall trend which is transverse to the NE-SW Caledonian strike. A competence contrast between the crystalline basement and the metasediments led to an interface instability, when the rocks were subjected to shortening subparallel to the originally flattish boundary. The Colonsay Group rocks form cuspate synformal projections into the Lewisian indicating that the Lewisian acted as a more competent member. The local intensification of clast elongation and development of mylonitic rocks along the contact is probably a secondary effect of the heterogeneous deformation that resulted from the existence of asperites on the boundary surface as well as from differential flowage of the more ductile Colonsay Group rocks. Kilchiaran Bay, Dun Medeir and the areas around Port Charlotte and Bruichcladdich provide locales of higher strain and mylonitic rocks.

The internal deformation within the Lewisian takes a different form from that within the Colonsay Group. Whereas the Colonsay Group rocks are folded and refolded with associated development of axial planar cleavages, the basement deforms with the production of ductile-brittle shear zones separated by areas of low strain. A mode of deformation not uncommon in crystalline basement rocks (see Mitra 1978). A homogeneous bulk shortening of the crystalline basement could be achieved by DDZ's in several directions. In W. Islay the present

Table 8.1 Correlation of structures in W. Islay and Colonsay

Deformation Phase	Intrusive Marker	Style and orientation of mesoscopic folds and related structures	
		W. Islay	Colonsay
D_4	Felsic porphyrite	Kinks, brittle shear zones; orientation variable	Kinks, brittle shear zones; variable orientation, locally conjugate
D_3	Microdiorites without any internal foliation Appinites	Open asymmetric folds, AP Cl locally developed in the hinge region and short limbs; subhorizontal ENE axis, AP dips steeply towards SSE. Boudinage in microdiorite dykes	Open/close folds, AP Cl better developed in the eastern part of the island; subvertical AP Cl trends ENE. Axis and AP orientation Kiloran Bay in conjugate sets; AP's NE and ESE. Folds on microdiorite dykes without any AP Cl.
D_2	Microdiorite/ lamprophyres with oblique Cl	Overturned folds with WNW vergence; NE-ENE fold axis; AP Cl P.S. or Cr. Cl. type, refolded in domains of F_3	Close/overturned folds; Axis and AP orientation variable; P.S. or Cr. Cl. parallel to AP in group B B dykes
	Lamprophyres with a flattening shape fabric		
D_1		Minor isoclinal folds, AP orientation variable; Axis parallel to a subhorizontal NE-SW stretching lineation	Isoclinal folds, clast shape fabric in psammites parallel to AP Cl; stretching lineation locally parallel to F_1 axis. Boudinage in competent layers
	Early lamprophyres		

AP Cl = Axial Plane Cleavage
P.S. = Pressure Solution
Cr. Cl. = Crenulation Cleavage

Table 8.2 Relative age of structures in different rock groups of W. Argyllshire

Colonsay Group +	Bowmore Sandstone	Dalradian	Iona Torridonian/ Lewisian	Major events and intrusives in Scottish Caledonides
D_4			N.S. and E.W. brittle shear zones/kinks	FELSIC PORPHYRITES
			West dipping shear zones (? backthrusting)	
			Extension kinks	ROSS OF MULL GRANITE (c.420 m.y.)
			Other E-dipping shear zones and thrusts	
D_3	Late folds			APPINITES (c.430-470 m.y.)
		F_{2d}*	Mylonitisation and thrusting along Lewisian/Torridonian boundary	
D_2	F_2 folds and axial plane cleavage in pelitic inter-calations			
		Loch Skerrol thrust ?Islay Anticline (F_{1d}*)	Isoclinal folds Gentle NNE-SSW axis	MOINE THRUSTING
D_1	Isoclinal folds			

+ For details within the Colonsay Group see Table 8.1. * Nomenclature after Borradaile (1979)

Table 8.3 Deformation along basement-cover contact

	W. Islay	Colonsay	Iona
Nature of original contact	Unconformity	Unconformity	Unconformity
Kinematic analogue	Interface instability	?	Ductile shear zone
Dominant sense of displacement	Strike-slip	Strike-slip	Thrust
Finite strain ellipsoid X>Y>Z	Constriction λ_x/λ_z = 11.6 X horizontal NE on subvertical XY plane	Flattening λ_x/λ_z = 18.7 X has a small pitch on steep SSE dipping XY plane	Constriction λ_x/λ_z = 72.5 X down dip on steep ESE dipping XY plane
Maximum width of mylonite belt	1.5 metres	5 metres	250 metres
Relative age of deformation in the local time scale	Pre- to syn-F_1	Pre- to Syn-F_1	Post-F_1
Quartz C-axis fabric	Small circle in ribbon grains, weak in recrystallised grains	Not determined	Asymmetric cross-girdle in recrystallised grains

orientation of the DDZ's is concentrated around a steep NE-SW plane and the stretching direction is consistent with dextral strike slip movement in most of the DDZ's. It is possible that DDZ's initially of varying orientation might have rotated to a finite orientation during progressive deformation. The anastomosing appearance of the DDZ's may be due to this process.

The outcrop of the Lewisian in Colonsay is very restricted in extent. Unconformable relationships are evident in the NE corner of the Lewisian band. Again, the strain varies along the contact. Higher pebble strain and mylonitised pebbly grits and Lewisian are exposed towards the southwestern end of the contact. As in W. Islay, the orientation of the fabric suggests a dominant strike-slip motion.

The tectonic situation in Iona is different. The structure can be compared to a thrust zone with several thrust sheets structurally lying one above another (duplex structure). The Moine thrust passing through the Sound of Iona brings Moine rocks on top of the Iona Torridonian. The latter is thrust over the Lewisian along the Lewisian-Torridonian contact. Several belts of steep E-dipping cataclasites/mylonites occur within the Lewisian block and may divide internal thrust sheets within the Lewisian. Other E-dipping thrusts west of Iona in the Sea of Hebrides cannot be precluded. The Lewisian-Torridonian contact acted as a thrust zone lying at the base of the Torridonian sheet. A traverse across the contact shows that both the Lewisian and the overlying pebbly grits are involved in the mylonitisation related to thrusting and that they share a common fabric in which the linear element is oriented down-dip. There are also belts of sheared rocks lying further to the west within the basement but parallel to the Lewisian-Torridonian contact. The internal deformation of the Islay Lewisian started early in the sequence of deformation phases and at least initially a ductile mode of deformation was operative. In contrast, the belts of sheared rocks within the Lewisian of Iona suggests a more brittle type of deformation taking place at a later stage in the sequence of westward propagation of the Caledonian thrusts (see Chapter 6). A tentative correlation of structures in the three regions shows that the thrust sense shear zones along Lewisian/ Torridonian boundary in Iona is later than the dominant strike-slip shear zones of W. Islay and those along the Lewisian-Colonsay Group

contact. In W. Islay and Colonsay the fabrics in these shear zones are locally overprinted by crenulation cleavage associated with later phases of folding. In Iona mylonites along Lewisian/Torridonian contact is affected by late brittle deformation (extension kinks, brittle shear zones with sigmoidal dilation veins)

8.3 POSSIBLE LARGE SCALE STRUCTURES IN W. ISLAY-COLONSAY

An account of minor structures in the Colonsay Group has been given in Chapter 3 and Chapter 5. The largest mappable folds within the confines of the islands have wavelengths of the order of a few hundred metres and none of the axial traces can be traced for more than 1 km or so. In this section, the possible existence of larger scale structures and their geometrical relation with the observed structures in Islay and Colonsay are discussed. Theoretical analysis and experimental works show that the dominant wavelength of folds in a buckled multilayer material depends among other factors on the relative thickness of layers with different viscosities or competence contrast (Biot 1961, 1963, 1964, Biot et al. 1961, Ramberg 1961, 1963, 1964, Ramsay 1967). A thick competent layer surrounded by less competent material is most likely to produce large wavelength folds (Ramsay 1967). Recalling the lithologic character of the Colonsay group, one may argue that the arkosic or greywacke units with phyllites above and below, may provide a situation comparable to that of some model materials considered in theoretical and experimental analyses of fold initiation and development considered by Biot, Ramberg and Ramsay among others. Following these analyses, it may be deduced that an apparent absence of very large scale structures is due to the lack of any suitable marker horizon which might have acted as a thick competent 'layer'. On the other hand, the tracing of continuous outcrops of the rocks in question is hindered by geography (mapping is limited to the confines of individual islands), and by lateral displacements along later faults. Thus the possible existence of large scale structures which may involve rocks in both Islay and Colonsay plus the submarine area to the east and west of and between these islands, cannot be ruled out.

One geometric way to predict large scale structures is to consider the relationship between congruous folds of different orders. Noting that the F_2 folds in W. Islay are in general overturned towards

WNW one may suggest that all the Colonsay Group rocks probably lie on the normal limb of an anticline or syncline which is also overturned to the northwest (Fig. 8.1a).

The stratigraphic and tectonic situation for the Colonsay Group may be broadly compared to that of the thrust-belt Torridonian of NW Highlands, especially in the western Ross-shire area. In the area around Loch Hourn, Lochalsh and Loch Carron the Torridonian rocks are disposed in westward facing fold nappes bounded by the Moine thrust in the east and the Kishorn thrust on the west (Barber 1965, Cheeney and Mathews 1965, Coward and Whaley 1980). If similar tectonics apply for the W. Argyllshire, one may postulate the existence of a thrust to the west of Islay and Colonsay, so that the observed folds within the Colonsay Group may be regarded as internal structures within a thrust sheet. An easterly bounding thrust may be an extension of the Loch Skerrols thrust or any other eastward-dipping line of dislocation in the region. The plausibility of such a speculative model can be tested by comparing the details of Colonsay Group structures with those in western Ross-shire. The large folds, e.g. the Lochalsh fold, within the Kishorn nappe, lack any widely developed penetrative cleavage (cf. early isoclinal folds in Bowmore Sandstone) and a penetrative shearing fabric is evident only in the overturned limb in the vicinity of the Moine thrust (Barber 1965, Cheeney and Mathews 1965, Coward and Whaley 1980). In contrast to this, a penetrative axial plane cleavage is always present with F_2 folds in W. Islay and Colonsay.

When one considers the geographical variation in the tightness of the F_3 folds and intensity of S_3 cleavage, a systematic picture is noticeable in Colonsay where the amplitude of F_3 folds increases on a NW-SE traverse. Although the morphology as well as the intensity of the S_3 cleavage is to a certain extent lithology dependent, the axial planar cleavage is most conspicuous along the SE coast of Colonsay in all lithological types (Fig. 8.2). The variation in the style of minor F_3 folds in Colonsay may be related to the presence of a major synformal structure whose axial trace should pass close to the eastern coast of Colonsay. The S-shaped down plunge profile (looking northeast when the fold axis is horizontal) of all F_3 structures in Islay is consistent with such a large scale structure. If such a synform does indeed exist, the wavelength of the largest F_3 structures should be in excess of 10

kilometres (the distance from coast to coast across western Islay is 7 km) because the F_3 folds in W. Islay and Colonsay (excepting those along the eastern coast) are consistently asymmetrical though not overturned, S-folds with axial planes dipping at 70-90 degrees towards SSE.

The observed variation in the intensity of development of F_3 and S_3 cannot be related to any major thrusts passing west of Islay and Colonsay. The possible influence of a thrust in the east can be put forward only with some reservations. The reactivation of older normal faults as high angle reverse/thrust faults has been considered to explain certain features of the Caledonide orogen and related foreland deformation (see Stewart 1982). The F_3 structures in Colonsay Group may have been generated by the footwall shortening related to such thrust movements.

However, several points can be brought against a model of thrust zone and associated fold nappes in W. Argyllshire.

(a) In contrast to the Lewisian in the thrust sheets of NW Highlands (e.g. the Moine nappe or the Kishorn nappe), the Islay Lewisian is relatively undeformed and the Colonsay Group sediments unconformably overlie the Lewisian. The Lewisian in Islay is more likely to be autochthonous or at least para-antochthonous than to be part of a far-travelled nappe.

(b) The internal deformation within the Lewisian shows steep NE-SW ductile deformation zones with a dominant strike slip sense of displacement. Contrast this with an ESE plunging lineation in the Kishorn nappe which is related to westerly movement along the thrusts (Coward and Whaley 1980). The overall stretching direction in Colonsay and W. Islay is subhorizontal NE-SW.

(c) Early formed axial planar cleavages (S_1 and S_2) are penetrative especially in pelitic and semipelitic lithology, and no zonal distribution such as that seen with respect to D_3 is evident. Penetrative fabrics are restricted below the Moine Thrust elsewhere.

If we recall the structures of Iona, thrusting along the Lewisian-Torridonian contact reorients early gently plunging (NNE-SSW)

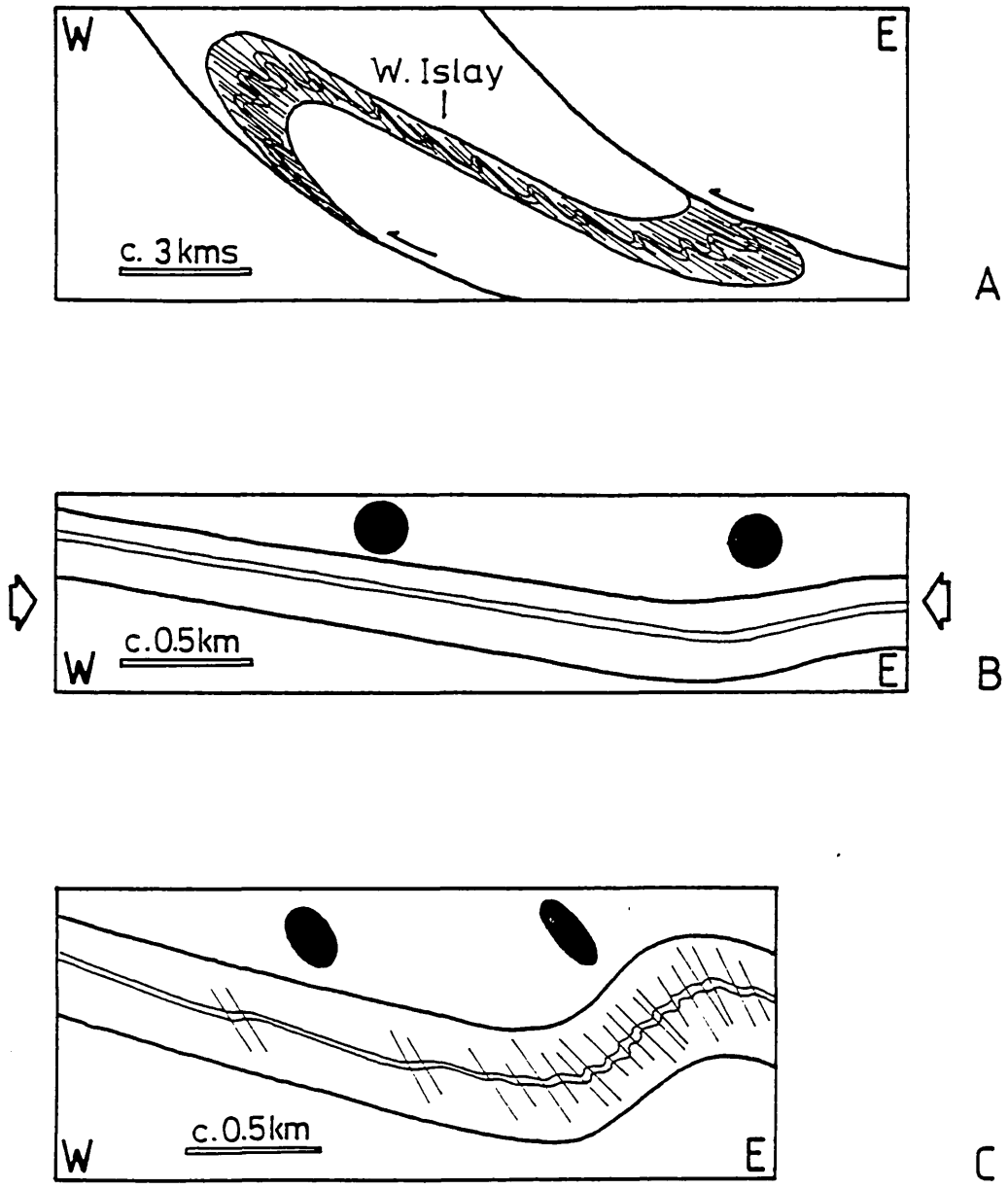


Figure 8.1 Probable major structures in W. Islay - Colonsay.

(a) A speculative cross-section showing F_2 structure and associated thrusts.

(b) A major asymmetric F_3 synform at an early stage, note that the short limb makes a smaller angle with the compression direction.

(c) Preferential development of small scale folds preferentially in the short limb of (b) with progressive deformation.

(d) A mesoscopic F_3 fold showing preferential development of microcrenulation and S_3 cleavage near the hinge and in the short limb. Compare with (b) and (c).



8.1d

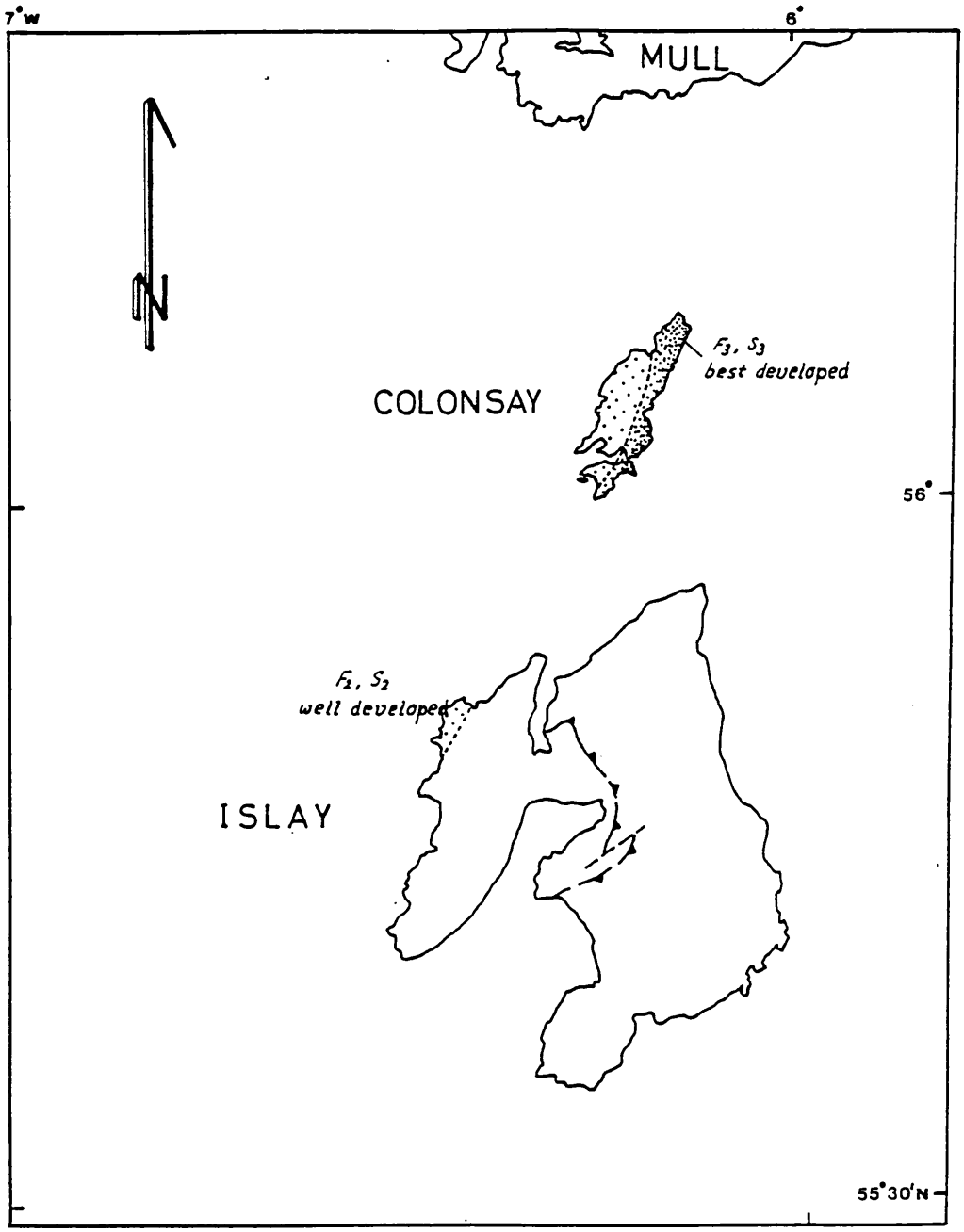


Figure 8.2. Variation in the spatial development of folds in W. Islay and Colonsay. The density of stipples varies qualitatively with the variation in the intensity of F_3 and S_3 in Colonsay (after Wright 1907).

fold axes to a steeper orientation parallel to the stretching direction in the mylonite belt. In Islay and Colonsay although the S_2 cleavage and F_2 axial planes show a spread in orientation in domains of F_3 structures, F_2 and F_3 axes are nearly co-axial. The spread in orientation of S_2 cleavage can be explained as a result of refolding relationships (see Chapter 3, section 3.5.3). These contrasts emphasise the differences in tectonic history between Colonsay-Islay and Iona.

Coming back to the variation in the intensity of F_3 and S_3 in the Colonsay Group, an alternative explanation can be put forward. A closer look at F_3 folds (of wavelengths 1 cm to 1 metre) and associated axial planar cleavages shows that the cleavage is best developed in the hinge region and the short limb of the asymmetric folds (Fig. 8.1d). Such folds and axial plane cleavage have been recorded from Sanaigmore Bay (c. 2 km from the west coast of the Rhinns) and from Smaull (within 100 metres of the west coast). The large scale geographic variation may be similarly related to the disposition of a large asymmetric structure where the short limb is favourably oriented for larger layer parallel shortening during progressive deformation (Fig. 8.1b). A schematic cross-section of such a large scale structure and possible variations in strain and cleavage development are shown diagrammatically (Fig. 8.1c).

The above discussion shows that the Lewisian and overlying late Precambrian metasediments in W. Argyll display a mode of deformation which in many ways is different from that in the marginal Caledonian thrust nappes of NW Highlands. Although both the basement and overlying Colonsay Group appear to be autochthonous or paraautochthonous, a penetrative folding deformation dominates the scenario. The late deformation (D_3) in the Colonsay Group may be related to a footwall response of a major thrust movement east of Colonsay and Islay. But the earlier structures formed as a general response of the local rocks to a Caledonian compression. While the Lewisian basement deforms by the formation of ductile deformation zones, the overlying sediment prism is thrown into folds with northwest vergence.

8.4 TIMING OF DEFORMATION IN THE COLONSAY GROUP

The metasediments of W. Islay and Colonsay form a link, at least in a geographical sense, between the metamorphic Caledonides of the N.

Highlands and those of NW Ireland. Widespread open to tight folding in the N. Highlands on steep NE-SW axial planes are generally assigned to the Caledonian Orogeny (Powell 1974). However, there are also folds on other axial planes. As a broad generalisation, these folds are asymmetric, with westerly vergence, in the west, but more upright in the central Moines (Johnson et al. 1979). The general orientation of F_2 and F_3 folds in W. Islay and Colonsay (see Chapter 3 and Chapter 5) is comparable to the dominant direction of those belonging to the Caledonian Orogeny. The ENE trend of the F_3 fold axis in Islay is consistent with a general swing of the Caledonide strike from NE-SW to E-W as one passes from the N. Highlands to W. Ireland.

A polymetamorphic history has long been suggested for the Moines (Read 1961). Although there still exists some debate as to the exact dating, one or two late Precambrian tectonothermal events - Grenville and/or Morarian, are well established in the deformation history of the Northern Highland Moines (Brewer et al. 1979, Brook et al. 1976, Gilletti et al. 1961, Johnson et al. 1979, Long and Lambert 1963, Pidgeon and Johnson 1973, van Breeman et al. 1974). The areal extent of the Proterozoic orogeny is still unclear (Johnson et al. 1979). Also in doubt is the continuation of the Proterozoic orogen to the south of the Great Glen (Johnson et al. 1979, cf. Piasecki and van Breeman 1979). This point coupled with the observation that the Proterozoic structures may include major close to tight folds with SE vergence involving Moine and Lewisian rocks (Ramsay 1963, Simony 1973) would be against any suggestion of Grenvillian or Morarian affinity of the deformation in the Colonsay Group. However, the association of the Colonsay Group with the Lewisian outcrops in SW Argyllshire is a point to be reckoned with.

Although the stratigraphic status of the Colonsay Group is as yet unresolved, recent remapping in W. Islay and Colonsay confirms an unconformable relationship between the supposed Lewisian and the overlying Colonsay Group (Stewart 1962, cf. Stewart and Hackman 1973, cf. Stewart 1975, Wilkinson et al. 1907). In W. Argyllshire, the Lewisian rocks are also affected by the local polyphase deformation. It has been argued earlier (see Chapter 3) that the ductile deformation zones (DDZ) in the W. Islay Lewisian are probably contemporaneous with the D_1 structures within the Colonsay Group. Comparing the Islay situation with the fact that in the NW Highland, the Morar division

rocks locally overlie the Lewisian unconformably (Peach et al. 1910, Ramsay 1958), one can consider the possibility of an older age (Proterozoic) for at least the earlier phases of local deformation in W. Argyllshire. The geologic history of the lamprophyric intrusions in W. Argyllshire is relevant here. It has been shown (see Chapter 7) that many of the sheet-like intrusions within the Colonsay Group and Islay Lewisian are petrographically very similar to the late Caledonian minor intrusions occurring north of Great Glen (see Smith 1979). Several groups of similar minor intrusions are recognised in W. Argyllshire (see Chapter 7), and the majority of the intrusive sheets are affected by local F_2 and/or F_3 folding. Some assume a deformation induced penetrative fabric. As discussed earlier these folded minor intrusions can be compared with the earlier members of the Microdiorite Suite of Smith (1979). The age of the Microdiorite Suite is late Caledonian north of Great Glen. Even allowing for some spread in timing of these Caledonian minor intrusions, the F_2 onward deformation in W. Argyllshire should be clearly regarded as Caledonian (s.s.). The paradox of DDZ's in the Lewisian and early isoclinal folds in the Colonsay Group (D_1 in local history) can be reconciled if we recall that some early 'lamprophyric' intrusive sheets are themselves stretched out in the DDZ's. Notice also that the late pegmatites which cut across earlier Lewisian elements are also involved in these DDZ's. Even if one argues that these pegmatites are the counterpart of old pegmatites within the Moine in N. Highlands, rather than of Laxfordian pegmatites, the D_1 deformation in W. Islay postdates their emplacement. Thus, even the early folds within the Colonsay Group should probably be regarded as Caledonian.

An estimate of the upper age limit of the folding deformation in W. Argyllshire can be had from the timing of the appinitic intrusions. As has been pointed out earlier, the deformations that produced axial planar cleavages in the Colonsay Group were complete before the emplacement of the appinitic stocks. On a regional scale the appinites antedates the late-/post-Caledonian granites, e.g. the Ross of Mull Granite (c. 420 Ma; Smith 1979). D_2 and D_3 in W. Argyll should therefore have been completed by c.420 Ma. The last hiccups of Caledonian Orogeny probably lingered after the emplacement of the Ross of Mull Granite as evidenced by the west dipping shear zones and brittle

shears with strike slip movement in Iona; the probable equivalents in Colonsay and W. Islay are those grouped together as local D_4.

This account would probably be incomplete without any mention of the relative age of deformation of the Bowmore Sandstone or the Dalradian in NE Islay. The style of deformation within the Bowmore Sandstone is different from that in the Dalradian (see Chapter 2 and Chapter 4). The early isoclinal folds within the Laggan Group are missing in the Dalradian. Accepting the view that the Islay Anticline is D_{1d} in the sequence of deformation of the Dalradian (Roberts and Treagus 1977), one interpretation would be to regard the isoclinal folds within the Bowmore Sandstone as earlier than D_1 deformation in the Dalradian. On the other hand, a palinspastic reconstruction that takes into account the movement of the Dalradian along Loch Skerrols thrust and subsequent transcurrent motions along the Great Glen Fault systems, would separate the Bowmore Sandstone from the Dalradian basin during Late Proterozoic - early Palaeozoic times. Correlation of fold phases in geographically separate rock groups is always fraught with problems. Although the style of deformation is different, it is possible that the early isoclinal folds in the Laggan Group are broadly contemporaneous with the Dalradian D_{1d} phase. On sedimentological grounds, the Bowmore Sandstone is regarded as equivalent to the Applecross Torridonian (Stewart 1975, Wilkinson et al. 1907) and its proximity to the Lewisian basement in the Inistrahull - W. Islay region (see discussion in Chapter 2) is consistent with a foreland setting of Torridonian basins. On the basis of a similar tectonic setting of the Colonsay Group, at least the lower part of it, the early isoclinal folds in Bowmore Sandstone are tentatively grouped with the F_1 minor folds in W. Islay. It is suggested then that although there is an apparent difference in the age of deposition of the Colonsay Group, the Bowmore Sandstone and the Dalradian of NE Islay, the folding deformation within these groups are essentially manifestations of polyphase Caledonian Orogeny (the equivalent of Grampian Orogeny in the Highlands).

8.5 TECTONIC HISTORY

The Colonsay Group of sedimentary rocks were deposited over the Lewisian during late Proterozoic times. The lower part of the succession is fluviatile and grades upward into turbidites (delta slope;

Stewart 1962). The composition of the detrital grains suggests that much of the material was derived from a Scourian basement. Comparing the group with the foreland Torridonian of NW Scotland, it is suggested that the Colonsay Group was deposited in a small ensialic basin, presumably fault bounded (see Stewart 1982). The difficulty in providing a lithostratigraphic correlation between the Colonsay Group rocks and any other known late Proterozoic successions outside W. Islay and Colonsay points to a restricted extent of the depositional basin. The Bowmore Sandstone was deposited in another such basin. Taking into account a wrench movement along the Loch Gruinnart fault, a palaeographic separation between the Bowmore Sandstone and the Colonsay Group is imperative. Comparing the detrital grain composition of these two groups, it appears that the provenance of the Bowmore Sandstone included some deformed low-grade supracrustal rocks in addition to Scourian gneisses.

In Stewart's model, the Torridonian basins in NW Scotland originated through rifting of a continental crust during late Proterozoic times: the rifting is thought to be due to the initiation of an Iapetus-related ocean (Stewart 1982). It has been argued on geochemical grounds that the source areas for the Stoer Group (c.968 Ma) and the Torridonian Group (c.777 Ma) are different (Moorbath 1969), and that the Torridonian is genetically unrelated to the Grenville Morarion orogen (Johnson 1975, Stewart 1982). The separation between the Bowmore Sandstone and the Colonsay Group on geological grounds compares well with the postulated differences between the Stoer Group and the Torridon Group. In fact the Bowmore Sandstone has long been compared with the Applecross Formation on lithological grounds (Wilkinson et al. 1907). If the dating of the Morarian orogeny (800-700 Ma) is true (Johnson 1975) and if the Torridonian rifting did precede this, then the rifting must have given way to collisional tectonics postulated for the origin of Morarian nappes (Johnson 1975). And the initiation of the proto-Atlantic (Dewey 1969, Dewey and Kidd 1974) must have followed all these Proterozoic tectonothermal events. The implication is that the rifting supposedly necessary to form the Torridonian basins must be unrelated to the opening of the Iapetus in late Proterozoic-Early Cambrian times. Conversely, part of the Upper Torridonian detritus could have been derived from uplifted Grenville/Morarian orogen rocks (cf. O'Nions et al. 1983). Some supposedly Grenville tectonothermal

events in NW Scotland are dated at c.1024 Ma (Brewer et al. 1979), which is older than the dates for some Torridon Group rocks in NW Scotland (Moorbath 1969).

In this context, one must take into account the fact that the present-day outcrops of the 'older' Moine rocks are very much restricted in the Scottish and Irish Caledonides. It is possible that much of these later Proterozoic metasediments related to Grenville Orogen have been eroded away and found their way into some foreland successions, such as the Bowmore Sandstone, or alternatively into Dalradian basins (cf. O'Nions et al. 1983). These deductions are highly speculative and in view of the doubts about the reliability of palaeocurrent data from complex folded strata, a latitude of uncertainty would be there as regards the source land mass with respect to the depositional basins of late Proterozoic (Torridonian). Recall that although an easterly or northeasterly palaeocurrent direction is apparent for some formations within the Colonsay Group (Stewart 1962), no such definite clustering of palaeocurrent directions is evident from the Bowmore Sandstone (Amos 1959).

During the late Precambrian the Dalradian environment evolved from a relatively stable subsiding shelf into a series of fault bounded blocks and basins (Anderton 1982). The general features of the Lower Dalradian (Appin Group) are consistent with a range of shelf to marine marginal environment (Harris et al. 1978). The upper Dalradian registers a change to deep water turbidite and basinal facies; the change to deep water sedimentation has been interpreted as due to the initiation of major syndepositional faulting in Argyll Group times (Harris et al. 1978; Anderton 1979). This increase in tectonic instability can be interpreted as an associate of continental rifting which led to the inception of the Iapetus Ocean at the end of the Precambrian or the base of Cambrian (Anderton 1982). Subduction in early Ordovician initiated the closing of the Iapetus Ocean. The deformation of the Dalradian Supergroup and the D_2 onward deformation in the Moine record the effect of this subduction and closing of Iapetus (Grampian orogeny). The foreland basement and cover in NW Scotland is usually free from effects of any penetrative deformation related to the Caledonian Orogeny (s.s.), but shortening across the upper crust has

been achieved by major thrusts such as the Outer Hebrides thrust or the Flannon thrust.

In W. Argyllshire the juxtaposition of the Appin Group and Argyll Group rocks against the supposedly Torridonian Bowmore Sandstone calls for transportation of rocks from the inner part of the orthotectonic basin towards the foreland in the form of fold nappes. Evidently this happened as the strata in the Dalradian basin were squeezed due to the gradual closing of the Iapetus. The total amount of displacement along the base of the Dalradian nappe is a matter for speculation. But a study of the Loch Skerrols thrust zone which separates the Dalradian from the Bowmore Sandstone does indicate that a zone of strain gradient occurs in this area. Strain and fabric measurements indicate a similarity with other Caledonian thrusts in the NW Highlands. On the other hand, the mode of deformation within the Colonsay Group is atypical of the thrust zone Torridonian of NW Scotland. Penetrative folding deformation is recorded in at least three phases of folding and associated axial planar cleavages are developed. Minor intrusions comparable to those described from north of Great Glen (Smith 1979) are involved in this deformation. This justifies inclusion of these fold phases affecting the Colonsay Group as essentially Caledonian (s.s.).

The high grade metamorphism of the Dalradian and Moine rocks exposed over most of the Highland indicates that there was a tectonic thickening of the Highland rocks during the Grampian Orogeny. The unroofing of the Highland metamorphic complexes was accompanied by a progressive decline in regional temperatures. The regional decline of temperatures was associated with well-documented changes in deformation style, penetrative ductile deformation giving way to inhomogeneous deformation and ultimately to block movements. The main fracture systems of the Highlands were established during this Late Orogenic period (Watson 1984). A NE-SW set dominates the fracture system in the Highlands and finds expression in the Great Glen fault system. The change from a regime dominated by transverse shortening to one of sinistral strike slip motion took place in the highlands at 430-425 Ma, roughly coinciding with the elimination of the Iapetus Ocean in Late Silurian times (Watson 1984).

The Great Glen Fault system can be traced from north Scotland through W. Argyll into Ireland. On a regional scale this fault system follows an arcuate course from N-S in Shetland to E-W in western Ireland. On geological grounds a net sinistral displacement of 100 km is suggested (Kennedy 1946, Smith and Watson 1983, for other possibilities, cf. Garson and Plant 1972, cf. van der Voo and Scotese 1981). South of the Appin district the GGF seems to branch into a number of splays. The 'main' fault probably passes northwest of Colonsay while a splay runs offshore along the SE coast of Colonsay to become the Loch Gruinart fault (LGF) in the Islay region (Evans et al. 1980). It has been argued earlier that the photointerpreted fracture pattern from W. Argyllshire is consistent with the above suggestion. Lateral displacement along the LGF during post-orogenic block movements brought the Bowmore Sandstone and the Dalradian nappe against the Colonsay Group and underlying Lewisian of W. Islay.

One final point that needs consideration in this section is the metamorphism of the Colonsay Group rocks. The metamorphic grade is that of low greenschist facies and postdates D_1 deformation in W. Islay and Colonsay. Assuming an average geothermal gradient of 25°C/km, the depth of the rocks at present level of exposure during late Caledonian time can be estimated at 12km. This brings in the question of an overburden which has since been unroofed. Tectonic thickening during transverse shortening of the Caledonian belt partly explains the overburden for such metamorphism. However, comparing with the tectonic situation in the Highlands, a horizontal westward transport of material as thrust sheets could have increased the thickness of the crust. For such purposes, one can invoke a hypothetical Moine nappe or a greater westward extent of the Dalradian nappes. If such a thrust sheet (or a pile of thrust sheets) did indeed exist during Late Caledonian times, these must have since been eroded out. The presence of virtually unmetamorphosed Bowmore Sandstone on the opposite side of LGF calls for a vertical displacement between the two blocks, in addition to the lateral displacement apparent along LGF. Alternatively, the W. Islay-Colonsay block may have had a cover of early Palaeozoic rocks, such as those occurring in the foreland of NW Scotland.

8.6 CONCLUSIONS

1. The Colonsay Grop was deposited unconformably over the Lewisian in Late Proterozoic. The provenance of the sediments included Scourian gneisses. The source for the Bowmore Sandstone included some deformed supracrustal rocks in addition to Scourian rocks. Differences in the detrital mineralogy and the style of deformation suggest a palaeogeographic separation between the Bowmore Sandstone and the Colonsay Group at the times of deposition and folding. The separation is consistent with geologic evidence for a left lateral displacement along the Loch Gruinart fault during Devonian-Carboniferous times (see chapter 2).

2. A photointerpreted fracture pattern study suggests that the main branch of Great Glen fault passes west of Colonsay and the Loch Gruinart fault is a splay in the Great Glen Fault systems.

3. The effects of Grampian Orogeny in W. Islay and Colonsay are recorded in at least 3 phases of folds and associated cleavage development. A fourth late Caledonian phase produces mainly brittle structures.

4. Both the overlying metasediments and the basement Lewisian were deformed. While the late Proterozoic metasediments are thrown into folds, mostly with a westerly vergence, the basement deformed by the formation of ductile to brittle deformation zones.

5. The tectonic situation in W. Islay and Colonsay is atypical of the foreland rocks of NW Highlands. The local structures in the Highlands including those in Iona can be explained in terms of a westward movement of successive thrust sheets which may or may not have carried fold nappes. In W. Islay and Colonsay the 'Torridonian' suffers penetrative folding deformation while the basement shortened by the development of ductile deformation zones. The deformation style is different from the thrust belt Torridonian of Northern Highlands.

Higher penetrative deformation of the Colonsay Group rocks with respect to Torridonian further north may be related to the initial distribution of the 'microcontinents' (Dewey 1969) with respect to the Iapetus Ocean; the closing of the ocean during the caledonian orogeny

must have reshuffled, telescoped together and laterally displaced these 'microcontinents' and associated sedimentary basins.

6. The Loch Skerrols thrust represent a zone of major strain gradient in the area. The quartz C-axis fabric in the thrust zone quartz-mylonites is an asymmetric type-I cross-girdle. The fabric asymmetry is consistent with a westward transport of the Dalradian along the Loch Skerrols thrust. A linear relationship between strain intensity and degree of quartz C-axis preferred orientation has been observed.

7. The minor intrusions in W. Argyllshire can be compared with the Caledonian minor intrusions north of Great Glen. Several groups of minor intrusions have been recognised and they bear specific relationships with respect to the local deformation phases. Only a small number of early lamprophyres are involved in local D_1 deformation; some are folded in a ductile manner during D_2 or D_3; a great majority of minor intrusions post dates D_3, thus comparing well with the late Caledonian Microdiorite Suite (see Smith 1979). The appinitic stocks of Colonsay and W. Islay are post-D_3, whereas many of the felsic porphyrites postdate the late brittle phase of deformation lumped together as local D_4.

8. Mineral chemistry of the appinites suggests an affinity with the alkali-olivine basalts; high Mg/Fe ratios as well as high K_2O content (as apparent from mineral chemistry) compares well with other appinitic intrusions in the Caledonian belt. The locales of appinites are related to the late Caledonian fracture sets (see also Watson 1984). Geometric control of earlier structures on the orientation of sheet like intrusions in W. Argyllshire is also evident.

ACKNOWLEDGEMENTS

Prof. Janet Watson initiated me to Scottish Geology, encouraged me every time during the last three years and a half (including when I was sidetracked into computing!) and took the task of correcting my English and Geology in the manuscript. I am indebted to her for all these.

I have benefited from discussions with Drs. John Cosgrove, J-P Latham, Mike Norton, and other friends in Structural Geology Research, and Dr. D.I. Smith and Mr. G.S. Johnstone of IGS. M/s Colin Leach and Nick Royall helped in EMP work. Mr. Alan Jones taught me 'high-tech' ways of making thin sections. My thanks to all of them.

I am grateful to Mr. Adolfo Cash, Ms. Grace Lau and Mr. Nick Morton of Photography for instructing me in basics of photography and providing an express service during the final lap. Many thanks, Nick!

Mrs. Elizabeth Jenks went through my 'good and bad' handwriting while typing this thesis. My special thanks to her. Thanks are also due to people in Islay, Colonsay, Iona and Ross of Mull for providing accommodation and logistic support during field-work.

Life would have been far more worse without my Bengali friends in London, particularly Siddheswar da who has shared woes of overseas life, and Avijit and Sukanta who have cheered me up in many desolate moments with their rare spirit!! This work would have been impossible without the financial support from the Government of West Bengal (India) in the form of a state-scholarship. I can but thank my country folks who unknowingly toil for the expensive education of a priviledged few!

REFERENCES

Ahmad, M.V. 1967. Some geophysical observations on the Great Glen Fault. Nature, 213, 275-277.

Allart, J.H. 1967. Basic and intermediate igneous activity and its evolution of the Julianehab Granite, South Greenland. Meddelser om Gronland, 175, 136.

Amos, B.J. 1959. Geology of the Bowmore district. Unpublished Ph.D Thesis, Univ. of London.

Anderson, E.M. 1921. In Summary of Progress for 1920. Mem. Geol. Survey, 1921, p.31.

Anderton, R. 1979. Slopes, submarine fans, and syndepositional faults: sedimentology of parts of the middle and upper Dalradian in the SW Highlands of Scotland. In The Caledonides of the British Isles - Reviewed. Geol. Soc. London Sp. Pub. 8, 483-488.

Anderton, R. 1982. Dalradian deposition and the late Precambrian-Cambrian history of the N Atlantic region: a review of the early evolution of the Iapetus Ocean. J. Geol. Soc. London, 139, 421-431.

Bailey, E.B. 1916. The Islay Anticline. Q.J. Geol. Soc., London, 69, 280-305.

Bailey, E.B., Anderson, E.M., Burnett, G.A., Richey, J.E., Lee, G.W., Wright, W.B., Wilson, G.V. and Thomas, H.H. 1925. The Geology of Staffa, Iona and Western Mull. Mem. Geol. Survey, HMSO, Edinburgh.

Barber, A.J. 1965. The history of the Moine Thrust zone, Lochcarron and Lochalsh, Scotland. Proc. Geol. Assoc., 76, 215-242.

Beckinsale, R.D. and Obradovich. 1973. Potassium-argon ages for minerals from the Ross of Mull, Argyllshire, Scotland. Scott. J. Geol., 9, 147-156.

Berger, A.R. 1971. Dynamic analysis using dykes with oblique internal foliations; Bull. Geol. Soc. Amer., 82, 781-786.

Berthe, D. and Brun, J.P. 1980. Evolution of folds during progressive shear in the South Armorican shear zone, France. J. Struct. Geol., 2, 127-133.

Biot, M.A. 1961. Theory of folding of stratified viscoelastic media and its implication in tectonics and orogenesis. Bull. Geol. Soc. Amer., 72, 1595-1620.

Biot, M.A. 1963. Theory of stability of multilayered continua in finite anisotropic elasticity. J. Franklin Inst., 276, 128-153.

Biot, M.A. 1963. Internal buckling under initial stress in finite elasticity. Proc. Roy. Soc. London, 273A, 306-326.

Biot, M.A. 1964. Theory of internal buckling of a confined multilayered structure. Bull. Geol. Soc. Amer. 75, 563-568.

Biot, M.A., Ode, H. and Roever, W.L. 1961. Experimental verification of the folding of stratified viscoelastic media. Bull. Geol. Soc. Amer., 72, 1621-1630.

Borradaile, G.J. 1979. Strain study of the Caledonides in the Islay region, SW Scotland: implications for strain histories and deformation mechanisms in greenschist. J. Geol. Soc., London, 136, 77-88.

Bouchez, J.L. 1977. Plastic deformation of quartzites at low temperature in an area of natural strain gradient. Tectonophysics, 39, 25-50.

Bouchez, J.L, Lister, G.S., and Nicolas, A. 1983. Fabric asymmetry and shear sense in movement zones. Geologische Rundschau, 72, 401-419.

Bowes, D.R. and Wright, A.E. 1967. The explosion-breccia pipes near Kentallen, Scotland, and their geologic setting. Trans. Roy. Soc., Edinburgh, 67, 110-143.

Brewer, M.S., Brook, M. and Powell, D. 1979. Dating of the tectonometamorphic history of the southwestern Moine, Scotland. In The Caledonides of the British Isles - Reviewed. Geol. Soc. London Sp. Pub. 8, 129-137.

Brewer, J.A., Mathews, D.H., Warner, M.R., Hall, J., Smythe, D.K. and Whittington, R.J. 1983. BIRPS deep seismic reflection studies of the British Caledonides. Nature, 303, 206-210.

Brook, M., Powell, D. and Brewer, M.S. 1976. Grenville age for rocks in the Moine of Northwestern Scotland. Nature, 260, 515-517.

Bryant, B. and Reed, J.C. 1969. Significance of lineation and minor folds near major thrust faults in the Southern Appalachians and the British and Norwegian Caledonides. Geol. Mag., 106, 412-429.

Burg, J.P. and Laurent, Ph. 1978. Strain analysis of a shear zone in a granodiorite. Tectonophysics, 47, 15-42.

Carreras, J., Estrada, A. and White, S.H. 1977. The effect of folding on the C-axis fabric of a quartz-mylonite. Tectonophysics, 39, 3-24.

Cheeney, R.F. and Mathews, D.W. 1965. The structural evolution of the Tarskavaig and Moine nappes in Scotland. Scott. J. Geol., 1, 256-281.

Christie, J.M. and Ord. A. 1980. Flow stress from microstructures of mylonites: examples and current assessment. J. Geophys. Res., 85, 6253-6262.

Clough, C.T. 1911. In the Geology of Colonsay and Oronsay with part of the Ross of Mull. Mem. Geol. Surv, 1911, p.77.

Cobbold, P.R. 1977. Description and origin of banded deformation structures. I. Regional strain, local perturbations, and deformation bands. Can. J. Earth Sci., 14, 1721-1731.

Cobbold, P.R. 1977. Description and origin of banded deformation structures. II. Rheology and growth of banded perlturbations. Can. J. Earth Sci., 14, 2510-2523.

Cobbold, P.R., Cosgrove, J.W. and Summers, J.M. 1971. Development of internal structures in deformed anisotropic rocks. Tectonophysics, 12, 25-53.

Cobbold, P.R. and Gapais, D. 1979. Specification of fabric shapes using an eigenvalue method. Bull. Geol. Soc. Amer., 90, 310-312.

Compton, R.R. 1980. Fabrics and strains in quartzites of a metamorphic core complex, Raft River Mountains, Utah. Geol. Soc. Amer. Mem. 153, 385-398.

Cosgrove, J.W. 1976. The formation of crenulation cleavage. Q.J. Geol. Soc., London, 132, 155-178.

Coward, M.P. 1982. Surge zones in the Moine Thrust Zone of NW Scotland. J. Struct. Geol., 4, 247-256.

Coward, M.P. 1983. The thrust and shear zones of the Moine Thrust Zone and the NW Scottish Caledonides. J. Geol. Soc., London, 795-811.

Coward, M.P. and Knipe. R.J. 1981. A discussion on the origin and significance of backfolds and backthrusts. Tectonic Studies Group, AGM (abstr.), Oxford, 1981.

Coward, M.P. and Whaley, J.S. 1980. Textural and fabric studies across the Kishorn Nappe, near Kyle of Lochalsh, Western Scotland. J. Struct. Geol., 1, 259-273.

Cunningham Craig, E.H., Wright, W.B. and Bailey, E.B. 1911. The Geology of Colonsay and Oronsay, with part of the Ross of Mull. Mem. Geol. Survey, HMSO, Edinburgh.

Davidson, L.M. and Park, R.G. 1978. Late Nagssutoqidian stress orientation derived from deformed granodiorite dykes north of Holsteinborg, West Greenland. J. Geol. Soc., London, 135, 283-289.

Deer, W.A., Howie, R.A. and Zussman, J. 1962. Rock forming minerals, Vol. III. Sheet Silicates. Longmans, London.

Deer, W.A., Howie, R.A. and Zussman, J. 1966. An introduction to the Rock Forming minerals. Longmans, London.

Dewey, J.F., 1969. Evolution of the Appalachian/Caledonian orogen. Nature, 222, 124-129.

Dewey, J.F. and Kidd, W.S.F. 1974. Continental Collisions in the Appalachian-Caledonian orogenic belt and variations related to complete and incomplete suturing. Geology, 2, 543-546.

Dietrich, J.H. and Onat, E.T. 1969. Slow finite deformation of viscous solids. J. Geoph. Res., 74, 129-154.

Dobson, M.R. and Evans, D. 1974. Geological structure of the Malin Sea. J. Geol. Soc., London, 130, 475-478.

Dobson, M.R., Evans, D. and Whittington, R. 1975. The offshore extensions of the Loch Gruinart Fault, Islay. Scott. J. Geol., 11, 23-35.

Dunnet, D. 1969. A technique of finite strain analysis using elliptical particles. Tectonophysics, 7, 117-136.

Durrence, E.M. 1976. A gravity survey of Islay, Scotland. Geol. Mag., 113, 251-261.

Engel, A.E.J. and Engel, C.G. 1960. Progressive metamorphism and granitisation of the Major Paragneiss, NW Adirondack Mtns., N.Y., Part II: Mineralogy. Bull. Geol. Soc. Amer., 71, 1.

Escher, A. and Watterson, J. 1974. Stretching fabrics, folds and crustal shortening. Tectonophysics, 22, 223-231.

Etchecoper, A. 1977. A plane kinematic model of progressive deformation in a polycrystalline aggregate. Tectonophysics, 39, 121-139.

Etheridge, M.A. and Wilkie, J.C. 1979. The geometry and microstructure of QP mylonite zones - a field test of the recrystallised grain-size palaeopiezometer, analysis of actual fault zones in bedrock. Open File Rep. 179-1239, 448-504, U.S. Geol. Survey, Mento Park, California.

Evans, D., Kenolty, N., Dobson, M.R. and Whittington, R.J. 1980. The geology of the Malin Sea. IGS report 79/15. HMSO London.

Fairbairn, H.W. 1949. Structural petrology of deformed rocks. Addison-Wesley, Reading, Mass.

Fairchild, I.J. 1981. The structure of NE Islay. Scott. J. Geol. 16, 189-197.

Fettes, D. and MacDonald, R. 1978. Glen Garry vein complex. Scott. J. Geol., 14, 335-358.

Flinn, D. 1958. On tests of significance of preferred orientations in three dimensional fabric diagrams. Journ. Geol., 66, 526-539.

Flinn, D. 1962. On folding during three dimensional progressive deformation. Q.J Geol. Soc., London, 118, 385-428.

Fraser, F. 1977. The geology of Iona. Unpublished PhD thesis, Univ. of St. Andrews, Edinburgh.

Friedman, J. 1964. Pattern of folded folds in the Appalachian Piedmont along Susquehanna River. Bull. Geol. Soc. Amer., 75, 621-638.

Fukunga, K. and Hostetler, L.D. 1973. Optimization of k-Nearest-Neighbour density estimates. IEEE Trans. Info. Theory, IT-19, 320-326.

Ganguly, J. 1968. Analysis of the stabilities of chloritoid and staurolite and some equilibria in the system $FeO-Al_2O-SiO_2-H_2O-O_2$. Amer. J. Sci. 246, 277-298.

Ganguly, J. and Newton, R.C. 1968. Thermal stability of chloritoid at high pressure and relatively high oxygen fugacity. J. Petrol., 9, 444-466.

Garson, M.S. and Plant, J. 1972. Possible dextral movements on the Great Glen and Minch faults in Scotland. Nature Phy. Sci., 240, 31-35.

Geikie, A. 1889. Recent researches into the Origin and age of the Highlands of Scotland. Nature, 40, 322-323.

Geikie, J. 1878 (1882). Notes on the Geology of Colonsay and Oronsay. Trans. Geol. Soc., Glasgow, 6, 157.

Gilletti, B.J., Moorbath, S. and Lambert, R.St.J. 1961. A geochronological study of the metamorphic complexes of the Scottish Highlands. Q.J. Geol. Soc., London, 117, 233-272.

Green, J.F.N. 1924. The structure of the Bowmore-Port Askaig dt. of Islay. Q.J. Geol. Soc., London, 80, 72.

Halferdahl, L.B. 1961. Chloritoid: its composition, X-ray and optical properties, stability and occurrence. J. Petrol., 2, 49-135.

Hall, A. 1967. The chemistry of appinitic rocks associated with the Ardara Pluton, Donegal, Ireland. Contr. Min. Pet., 16, 156-171.

Harris, A.L., Baldwin, C.T., Bradbury, H.J., Johnson, H.D. and Smith, R.A. 1978. Ensialic basin sedimentation: the Dalradian Supergroup. In: Bowes, D.R. and Leake, B.E. (eds.). Crustal Evolution in NW Britain and Adjacent Regions, 115-138. Seel House Press, Liverpool.

Hastings, N.A.J. and Peacock, J.P. 1974. Statistical Distributions. Butterworths, London.

Holgate, N. 1969. Palaeozoic and Tertiary transcurrent movements on the Great Glen Fault. Scott. J. Geol., 5, 97-139.

Hoschek, G. 1969. The stability of staurolite and chloritoid and their significance in the metamorphism of pelitic rocks. Contr. Min. Pet., 22, 208-232.

Hossack, J.R. 1968. Pebble deformation and thrusting in the Bygdin area (S. Norway). Tectonophysics, 5, 315-339.

Huddleston, P.J. 1977. Progressive deformation and development of fabric across zones of shear in glacier ice. In Energetics of Geological Processes, ed. S. Saxena and S. Bhattacharji, Springer-Verlag, New York.

Huddleston, P.J. 1980. The progressive development of inhomogeneous shear and crystallographic fabric in glacial ice. J. Struct. Geol. 2, 189-186.

Jaeger, J.C. 1964. Thermal effects of intrusions. Rev. Geophys. 2, 443-466.

Jehu, T.J. 1922. The Archaean and Torridonian formations and the Later Intrusive Igneous rocks of Iona. Trans. Roy. Soc. Edin., 53, 166.

Johnson, M.R.W. 1956. Conjugate fold systems in the Moine Thrust zone in the Loch Carron and Coulin Forest area, Wester Ross. Geol. Mag., 93, 345-350.

Johnson, M.R.W. 1975. Morarian Orogeny and Grenville belt in Britain. Nature, 257, 301-302.

Johnson, M.R.W., Sanderson, D.J. and Soper, N.J. 1979. Deformation in the Caledonies of England, Ireland and Scotland. In The Caledonides of the British Isles - Reviewed. Geol. Soc. London Sp. Pub., 8, 165-186.

Johnstone, G.S. 1975. The Moine Succession. In A Correlation of the Precambrian rocks in the British isles. Geol. Soc., London Sp. Rep. No. 6, 30-42.

Kamb, W.B. 1959. Ice petrofabric observations from Blue Glacier, Washington, in relation to theory and experiment, J. Geophys. Res., 64, 1891-1909.

Kennedy, W.Q. 1946. The Great Glen Fault. Q.J. Geol. Soc. London, 102, 41-76.

Kohlstedt, D.L. and Weathers, M.S. 1980. Deformation induced microstructures, palaeopiezometers and differential stresses in deeply eroded fault zone. J. Geophys. Res., 85, 6269-6285.

Krumbein, W.C. and Graybill, F.A. 1965. An Introduction to Statistical Models in Geology. McGraw-Hill, New York.

Lawrie, T.R.M. 1961. Scottish Highlands and Islands. Mem. Geol. Surv. Summ. Prog. for 1960, 45-47.

Lensen, G.J. 1958. A method of graben and horst formation. J. Geol. 66, 579-587.

Lister, G.S. and Hobbs, B.E. 1980. The simulation of fabric development during plastic deformation and its application to quartzite: the influence of deformation history. J. Struct. Geol., 2, 355-370.

Lister, G.S., Patterson, M.S. and Hobbs, B.E. 1978. The simulation of fabric development in plastic deformation and its application to quartzite: the model. Tectonophysics, 45, 107-158.

Lister, G.S. and Williams, P.F. 1979. Fabric development in shear zones: theoretical controls and observed phenomena. J. Struct. Geol., 1, 283-297.

Litherland, M. 1970. The stratigraphy and structure of the Dalradian rocks around Loch Creran, Argyll. PhD thesis, Univ. of Liverpool.

MacCulloch, J. 1819. The Western Islands of Scotland, Vol. II, Vol. III Plate 22. General map of the Western Isles and Map of Islay, Jura, Colonsay, Oronsay.

McIntyre, R.M., van Breeman, O., Bowes, D.R. and Hopgood, A.M. 1975. Isotopic studies of the gneiss complex, Inistrahull, Co. Donegal, Sci. Proc. Roy. Dublin Soc., 5A, 301-309.

March, A. 1932. Mathematische Theorie der Regelung nach der Korngestalt bei Affiner Deformation. Z. Krist., 81, 285-297.

Mardia, K.V. 1972. Statistics of directional data. Academic Press, London.

Marjoribanks, R.W. 1976. The relation between microfabric and strain in a progressively deformed quartzite sequence from Central Australia. Tectonophysics, 32, 269-293.

Mercier, J.C., Anderson, D.A. and Carter, N.L. 1976. Stress in the lithosphere, inferences from steady state flow in rocks. Pure Appl. Geophys., 115, 199-226.

Miller, D.M. and Christie, J.M. 1981. Comparison of quartz microfabric with strain in recrystallized quartzite. J. Struct. Geol., 3, 129-141.

Mills. A. 1790. Some account of the strata and Volcanic Appearances in the North of Ireland and Western Islands of Scotland. Phil. Trans. Roy. Soc., 80, 73.

Mitra, G. 1978. Ductile deformation zones and mylonites: the mechanical processes involved in the deformation of crystalline basement rocks. Amer. J. Sci., 278, 1057-1084.

Mitra, G. 1979. Ductile deformation zones in Blue Ridge basement rocks and estimation of finite strains. Bull. Geol. Soc. Amer., 90, 935-951.

Miyashiro, A. 1973. Metamorphism and metamorphic belts. George Allen and Unwin, London.

Monro, D.M. 1982. Fortran 77. Edward Arnold, London.

Moorbath, S. 1969. Evidence for the age of deposition of the Torridonian sediments of northwest Scotland. Scott. J. Geol. 5, 154-170.

Munro, M. 1965. Some structural features of the Caledonian granitic complex at Strontian, Argyllshire. Scott., J. Geol., 1, 152-175.

Murchison, R.I. and Geikie, A. 1861. On the altered rocks of the Western Islands of Scotland, and the North-Western and Central Highlands. Q.J. Geol. Soc., 42, 206.

Nadai, A. 1963. Theory of flow and fracture of solids. McGraw-Hill, New York.

Nicolas, A. and Poirier, J.P. 1976. Crystalline plasticity and solid state flow in metamorphic rocks. Wiley-Interscience, New York.

Nye, J.F. 1957. Physical Properties of Crystals. OUP, Oxford.

O'Nions, R.K., Hamilton, P.J. and Hooker, P.J. 1983. A Nd isotope investigation of sediments related to crustal development in the British isles. Earth and Planet Sci. Let., 63, 229-240.

Owens, W.H. 1973. Strain modification of angular density distributions. Tectonophysics, 16, 249-261.

Passchier, C.W. 1983. The reliability of asymmetric c-axis fabrics of quartz to determine sense of vorticity. Tectonophysics, 99, T9-T18.

Peach, B.N. 1907. In Wilkinson et al. 1907. The Geology of Islay. Mem. Geol. Survey, HMSO, Glasgow.

Peach, B.N., Horne, J., Woodward, H.B., Clough, C.T., Harker, A. and Wedd, C.B. 1910. The geology of Glenelg, Lochalsh and southeast part of Skye. Mem. Geol. Survey, U.K.

Peach, C.J. and Lisle, R.J. 1979. A Fortran IV program for the analysis of tectonic strain using deformed ellptical markers. Computers and Geosciences, 5, 325-334.

Peacock, J.D. 1977. Metagabbros in granitic gneiss, Inverness-shire, and their significance in the structural history of the Moines. Rep. IGS No. 77/20.

Phillips, F.C. 1971. The use of stereographic projection in structural geology. Edward Arnold, London.

Piasecki, M.A.J. and van Breeman, O. 1979. The 'Central Highland granulites': cover-basement tectonics in the Moine. In The Caledonides of the British Isles - Reviewed, Geol. Soc. London Sp. Pub. 8, 139-144.

Pidgeon, R.T. and Johnson, M.R.W. 1973. Isotopic evidence for 'early' events in the Moines. In Pidgeon, R.T., MacIntyre, R.M., Sheppard, S.M.F. and van Breeman, O. (eds.), Geochronology and isotope geology of Scotland. Scottish Univ. Res. and Reactor Centre, East Kilbridge, Glasgow.

Pitcher, W.S. 1969. North-east trending faults of Scotland and Ireland and chronology of displacements. Mem. Am. Assoc. Petrol. Geol. 12, 723-773.

Platt, J.P. and Vissers, R.L.M. 1980. Extensional structures in anisotropic rocks. J. Struct. Geol., 2, 397-410.

Platten, I.M. 1982. Partial melting of feldspathic quartzite around late Caledonian minor intrusions in Appin, Scotland. Geol. Mag, 119, 413-419.

Poldervaart, A. and Hess, H.H. 1951. Pyroxenes in the crystallisation of basaltic magma. J. Geol., 59, 472-489.

Powell, D. 1974. Stratigraphy and structure of the western Moine and the problem of Moine orogenesis. J. Geol. Soc., London, 130, 575-593.

Ramberg, J. 1961. Contact strain and folding instability of a multilayered body under compression. Geol. Rund., 51, 405-439.

Ramberg, J. 1963. Fluid dynamics of viscous buckling applicable to folding of layered rocks. Bull. Amer. Assoc. petrol. Geol., 47, 484-515.

Ramsden, J. and Cruden, D.M. 1979. Estimating densities in contoured orientation diagrams. Bull. Geol. Soc. Amer., 90, 229-231.

Read, H.H. 1961. Aspects of the Caledonian magmatism in Britain. Proc. Liverpool Manchester Geol. Soc., 2, 653-683.

Rees, A.I. 1979. The orientation of grains in a sheared dispersion. Tectonophysics, 55, 275-287.

Reynolds, D.L. 1936. Demonstrations in petrogenesis from Kiloran Bay, Colonsay. I. The transfusion of quartzite. Min. Mag., 24, 367-407.

Richardson, S.W. 1968. Staurolite stability in part of the system Fe-Al-Si-O-H. J. Petrol., 9, 468-488.

Riddihough, R.P. 1968. Magnetic surveys off the north coast of Ireland. Proc. Roy. Irish Acad. 66B, 27-41.

Roberts, J.L. and Treagus, J.E. 1977. Polyphase generation of nappe structures in the Dalradian rocks of the southwest Highlands of Scotland. Scott. J. Geol., 13, 237-254.

Robin, P.Y.F. 1977. Determination of geologic strain using randomly oriented strain markers of any shape. Tectonophysics, 42, T7-T16.

Roddick, J.C. and Max, M.D. 1983. A Laxfordian age from the Inistrahull Platform, County Donegal, Ireland. Scott. J. Geol., 19, 97-102.

Schairer, J.F. and Bowen, N.L. 1947. The system anorthite-leucite-silica. Bull. Soc. Geol. Finlande, 20, 67-87.

Scheidegger, A.E. 1965. On the statistics of bedding planes, grain axes, and similar sedimentological data. U.S. Geol. Survey Prof. Paper 525-C, C164-C167.

Schmid, S.M. 1983. Microfabric studies as indicators of deformation mechanisms and flow laws operative in Mountain Building. In Mountain Building Processes, ed. K.J. Hsu, Academic Press, London.

Schmid, S.M., Casey, M. and Starkey, J. 1981. An illustration of the advantages of a complete texture analysis described by the orientation distribution function (ODF) using quartz pole figure data. Tectonophysics, 78, 101-118.

Sibson, R.H. 1977. Fault rocks and fault mechanisms. J. Geol. Soc., London, 133, 191-213.

Simony, P.S. 1973. Lewisian sheets within the Moines around 'The Saddle' of northwest Scotland. J. Geol. Soc. London, 129, 191-210.

Simpson, C. and Schmid, S.M. 1983. An evaluation of criteria to determine the sense of movement in sheared rocks. Bull. Geol. Soc. Amer., 94, 1281-1288.

Smith, D.I. 1979. Caledonian minor intrusions of the N Highlands of Scotland. In The Caledonides of the British isles - Reviewed, Geol. Soc., London Sp. publ. No. 8.

Smith, C.S. and Guttman, L. 1953. Measurement of internal boundaries in three-dimensional structures by random sectioning, Trans. AIME, 197, 81-87.

Smith, D.I. and Watson, J. 1983. Scale and timing of movements on the Great Glen Fault. Geology, 11, 523-526.

Starkey, J. 1970. A computer program to prepare orientation diagrams. In: Paultish, P. (ed.). Experimental and Natural Rock Deformation: Proceedings of the International Symposium, Darmstadt, 1969. Springer-Verlag, Berlin.

Stauffer, M.R. 1966. An empirical statistical study of three dimensional fabric diagrams as used in structural analysis. Can. J. Earth Sci., 3, 473-498.

Stewart, A.D. 1962. On the Torridonian sediments of Colonsay and their relationship to the main outcrop in northwest Scotland. Liverpool Manchester Geol. J. 3, 121-156.

Stewart, A.D. 1962. Greywacke sedimentation in the Torridonian of Colonsay and Oronsay. Geol. Mag., 99, 399-419.

Stewart, A.D. 1975. 'Torridonian' rocks of Western Scotland. In The Correlation of the Precambrian rocks of British isles. Geol. Soc., London, Sp. Rep. No. 6, 43-51.

Stewart, A.D. 1982. Late proterozoic rifting in NW Scotland: the genesis of the 'Torridonian'. J. Geol. Soc., London, 139, 413-420.

Stewart, A.D. and Hackman, B.D. 1973. Precambrian sediments of W. Islay. Scott. J. Geol., 9, 185-201.

Summers, T.P. 1982. A seismic study of crustal structure in the region of the Western Isles of Scotland. Unpublished PhD thesis, Univ. of Durham.

Talbot, C.J. 1980. Obliquely foliatekld dykes as deformed incompetent single layers. Bull. Geol. Soc. Amer., 93, 450-460.

Thompson, J. 1877. On the Geology of the island of Islay. Trans. Geol. Soc., Glasgow, 5, 200.

Tullis, J. 1977. Preferred orientation of quartz produced by slip during plane strain. Tectonophysics, 39, 87-102.

Turner, F.J. and Weiss, L. 1963. Structural analysis of metamorphic tectonites. McGraw-Hill, New York.

Twiss, R.J., 1977. Theory and applicability of a recrystallized grain size palaeopiezometer. Pure Appl. Geophys. 115, 227-244.

van der Voo, R.J. and Scotese, C. 1981. Palaeomagnetic evidence for a large (>2000 km) sinistral offset along the Great Glen fault during Carboniferous time. Geology, 9, 583-589.

Watson, G.S. 1970. Orientation statistics in the Earth Sciences. Bull. Geol. Instn. Univ. Upsala N.S. 2, 73-89.

Watson, J. 1975. The Lewisian Complex. In Precambrian, Geol. Soc. London. Sp. Pub. 6, 15-29.

Watson, J. 1984. The ending of the Caledonian orogeny in Scotland. J. Geol. Soc., London, 141, 193-214.

Watterson, J. 1968. Plutonic development of the Ilordleq area, South Greeland: Part II. Late kinematic basic dykes. Meddr. Gronland, 185, 104.

Weathers, M.S., Bird, J.M., Cooper, R.F. and Kohlstedt, D.L. 1979. Differential stresses determined from deformation induced microstructures of the Moine Thrust Zone. J. Geophys. Res., 84, 7495-7509.

Weiss, L.E. 1959. Geometry of superposed folding. Bull. Geol. Soc. Amer., 70, 91-106.

Westbrook, G.K. and Borradaile, G.J. 1978. The geological significance of magnetic anomalies in the region of Islay. Scott. J. Geol., 14, 213-224.

White, S.H. 1976. The effects of strain on the microstructures, fabrics and deformation mechanisms in quartzite. Phil. Trans. Roy. Soc., London, 283A, 69-86.

White, S.H. 1979. Grain and sub-grain size variation acorss a mylonite zone. Contrib. Mineral. Petrol., 70, 193-202.

White, S.H., Burrows, S.E., Carreras, J., Shaw, N.D. and Humphreys, F.J. 1980. On mylonites in ductile shear zones. J. Struct. Geol., 2, 175-187.

Wilkinson, J.F.G. 1956. The olivines of a differentiated teschenite sill near Gunnedah, New South Walws. Geol. Mag., 93, 441-

Wilkinson, J.F.G. 1956. Clinopyroxenes of alkali-basalt magma. Amer. Min., 41, 724.

Wilkinson, S.B., Teall, J.J.H. and Peach, B.N. 1907. The Geology of Islay. Mem. Geol. Survey, HMSO, Glasgow.

Wilson, G. 1983. Introduction to small scale geological structures. George Allen and Unwin, London.

Wilson, C.J.L. 1975. Preferred orientation in quartz ribbon mylonites. Bull. Geol. Soc. Amer., 86, 968-974.

Woodcock, N.H. 1977. Specification of fabric shapes using an eigenvalue method. Bull. Geol. Soc. Amer., 88, 1231-1236.

Wright, W.B. 1908. The two earth-movements of Colonsay. Q.J. Geol. Soc., London, 64, 297.

Wright, A.E. and Bowes, D.R. 1979. Geochemistry of the appinite suite. In The Caledonides of the British Isles - Reviewed. Geol. Soc., London Sp. Publ. Sp. Publ., 8, 679-704.

APPENDIX - 4A

DETERMINATION OF 2D STRAIN BY R_f-ϕ METHOD

The method is after Ramsay (1967) and Dunnet (1969). It has been shown that the axial ratio, R_f, of elliptical markers after a homogeneous finite strain is given by:

$$R_f = F(R_i, R_s, \phi) \qquad (4A.1)$$

where,

R_i = initial undeformed marker axial ratio
R_f = final deformed marker axial ratio
R_s = finite strain axial ratio
ϕ = angle between the marker long axis and the direction of maximum principal 2D strain.

The exact relationship in (4A.1) can be expressed as

$$\text{Cos } 2\phi = \frac{R_i(R_f^2 + 1) \pm 2(R_i^2 + 1)R_s R_f}{R_i(R_f^2 - 1)(R_s^2 - 1)} \qquad (4A.2)$$

(Dunnet 1969).

Equation (4A.2) relates two measurable parameters R_f and ϕ to the initial shape ratio, R_i and strain ratio R_s. For any set of values of R_i and R_s the locus of $R_f = F'(\phi)$ will reflect only variation in the initial orientation of the marker. Then a suite of particles of constant initial shape but variable orientation, will have after deformation, R_f/ϕ parameters which lie on a 'hyperbolic' curve around the finite strain value.

Specific values of R_i and R_s substituted in equation (4A.2) allow construction of theoretical $R_f = F'(\phi)$ curves which can be directly compared to R_f-ϕ plots derived from measured data.

APPENDIX - 4B

DETERMINATION OF 2D STRAIN BY AN ALGEBRAIC METHOD

The method is after Robin (1977). Consider a number of markers, having various outlines within a planar section through an unstrained and isotropic rock. A centre C can be determined for each marker (Fig. 4B.1). Consider now two orthogonal directions within the section, designated x and y. Let the intercepts on each marker parallel to x and y through C be a_j and c_j respectively. The condition for isotropy is:

$$\prod_{j=1}^{N} \frac{a_j}{c_j} = \frac{a_1}{c_1} \times \frac{a_2}{c_2} \times \ldots \frac{a_j}{c_j} \times \ldots \frac{a_n}{c_n} \simeq 1 \qquad (4B.1)$$

Since the directions x and y are arbitrary they can be chosen to coincide with the principal directions of strain. Let the principal quadratic elongations for a homogeneous strain undergone by the rock be K_x and K_y. The intercepts a_j and c_j for jth marker become a_j' and c_j' after strain given by:

$$a_j' = K_x^{\frac{1}{2}} a_j; \quad c_j' = K_y^{\frac{1}{2}} c_j. \qquad (4B.2)$$

Therefore:

$$\prod_{j=1}^{n} \frac{a_j'}{c_j'} = \left(\frac{K_x}{K_y}\right)^{\frac{n}{2}} \prod_{j=1}^{n} \frac{a_j}{c_j} \qquad (4B.3)$$

or using (4B.1)

$$\sum_{j=1}^{n} \log \frac{a_j'}{c_j'} = \frac{n}{2} \log \frac{K_x}{K_y} \qquad (4B.4)$$

The ratio of principal quadratic elongations K_x/K_y can therefore be obtained from (4B.4). The intercepts a_j' and c_j' are measured on n markers in the planar section, the ratios a_j'/c_j' are calculated and their logarithmic average is proportional to axial strain ratio.

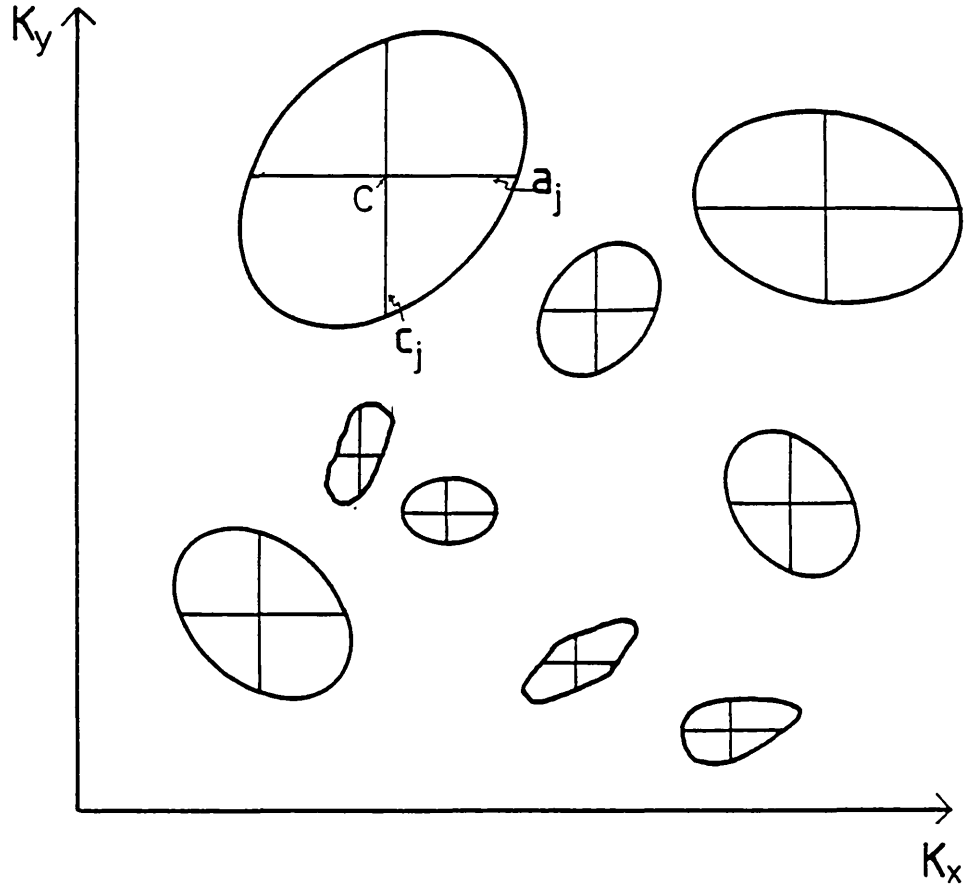


Figure 4B.1. Isotropically oriented markers in the unstrained rock. Lines drawn parallel to the two directions (arbitrarily chosen to coincide with the directions of principal strain, K_x, K_y) through the centre C of each marker define segments a_j and c_j respectively.

The method requires that the principal directions of strain x and y be known. In principle, equation (4B.4) is evaluated for all azimuths from 0-180 degrees and the direction which gives maximum value for K_x/K_y is chosen.

Ramsay (1967) and Dunnet (1969) have proposed a method to calculate the strain from the final axial ratio, R_j and axis orientations, ϕ_j, of initially randomly oriented ellipses (see Appendix 4.A). However, for practical purposes a subjective fitting of curves around a cluster of points (R_j-ϕ_j plot) has to be made and this may involve errors. Application of Robin's method for elliptical markers is fairly straightforward. The ratio a'_j/c'_j (eqn. (4B.4) can be calculated from R_j and ϕ_j by:

$$\frac{a'_j}{c'_j} = \left(\frac{\tan^2\phi_j + R_j^2}{R_j^2\tan^2\phi_j + 1} \right)^{\frac{1}{2}} \qquad (4B.5)$$

Once the ratios of n ellipses are calculated with (4B.5) from R_j and ϕ_j eqn. (4B.4) can be used to estimate the strain ratio. For ellipses, trials to find the direction which maximises eqn. (4B.4) can be done numerically, without new measurements on the planar section. A new origin (reference direction) for the orientation angles ϕ_j, i.e. a new x direction, can be tried by simply adding a uniform value (e.g. 1°, 2°, ...) to all ϕ_j, and repeating the above calculations.

Based on the above principles a Fortran program ROBIN is written to calculate the 2D strain ratio and the direction of 2D principal strain.

APPENDIX - 4C

One of the assumptions involved in 2D strain determination using R_f-ϕ or algebraic method (Robin 1977) is that the long axis of the markers are initially distributed randomly on the plane of section. Computer program THETA written by Peach and Lisle (1979) is used for testing the initial randomness of grain/pebble long axis in samples used for strain measurements in Loch Skerrols thrust zone, Lewisian-Torridonian contact zone in Iona and the Lewisian-Colonsay Group contact in Islay. The results are presented in Table 4C-I.

TEST FOR INITIAL RANDOMNESS

TABLE 4C-I

SPECIMEN NO.	FREQUENCY IN EACH 18 DEGREE CLASS. RANGE: -90 TO +90										NPTS	EXPECTED NO.	CHI-SQUARE	D. OF F.	P*
DTA8201	1.0	5.0	5.0	11.0	8.0	14.0	10.0	4.0	4.0	4.0	66	6.6	21.88	8	.01 - .001
DTA8202	2.0	8.0	8.0	9.0	8.0	12.0	11.0	6.0	2.0	3.0	69	6.9	16.65	8	.05 - .02
DTA8203	7.0	4.0	6.0	5.0	5.0	6.0	5.0	4.0	2.0	6.0	50	5.0	3.60	8	.90 - .80
DTA8301	5.0	8.0	14.0	4.0	8.0	10.0	10.0	8.0	3.0	4.0	74	7.4	14.38	8	.10 - .05
DTA8302	1.0	2.0	6.0	13.0	10.0	14.0	11.0	9.0	5.0	2.0	73	7.3	27.96	8	< .001
DTA8303	4.0	7.0	5.0	8.0	2.0	6.0	6.0	7.0	5.0	5.0	55	5.5	4.82	8	.80 - .70
DTA8401	3.0	4.0	12.0	12.0	3.0	7.0	14.0	6.0	2.0	4.0	67	6.7	25.99	8	.01 - .001
DTA8402	5.0	7.0	12.0	10.0	6.0	9.0	12.0	9.0	7.0	3.0	80	8.0	9.75	8	.30 - .20
DTA8403	5.0	7.0	7.0	20.0	9.0	2.0	9.0	9.0	13.0	9.0	90	9.0	23.33	8	.01 - .001
DTA8501	5.0	6.0	8.0	9.0	9.0	8.0	5.0	10.0	6.0	4.0	70	7.0	5.43	8	.80 - .70
DTA8502	4.0	6.0	8.0	15.0	9.0	14.0	13.0	5.0	2.0	7.0	83	8.3	21.22	8	.01 - .001
DTA8503	3.0	8.0	13.0	13.0	7.0	10.0	9.0	11.0	5.0	11.0	90	9.0	10.89	8	.30 - .20
DTA8601	12.0	4.0	11.0	13.0	10.0	9.0	13.0	9.0	7.0	3.0	91	9.1	12.19	8	.20 - .10
DTA8602	9.0	11.0	9.0	15.0	6.0	9.0	11.0	11.0	2.0	7.0	90	9.0	12.22	8	.20 - .10
DTA8603	1.0	8.0	14.0	13.0	5.0	9.0	12.0	10.0	9.0	10.0	91	9.1	14.60	8	.10 - .05
DTA8701	8.0	7.0	7.0	14.0	11.0	13.0	4.0	13.0	8.0	5.0	90	9.0	12.44	8	.20 - .10
DTA8702	3.0	9.0	7.0	13.0	12.0	11.0	9.0	12.0	9.0	6.0	91	9.1	9.55	8	.30 - .20
DTP8703	2.0	8.0	13.0	12.0	6.0	2.0	10.0	18.0	11.0	8.0	90	9.0	24.44	8	.01 - .001
DTP438C	11.0	10.0	14.0	15.0	15.0	12.0	14.0	10.0	10.0	9.0	120	12.0	4.00	8	.90 - .80
DTP438B	11.0	8.0	10.0	17.0	8.0	5.0	17.0	20.0	8.0	16.0	120	12.0	19.33	8	.02 - .01
DTP438A	6.0	7.0	20.0	12.0	12.0	21.0	24.0	8.0	7.0	5.0	122	12.2	36.03	8	< .001
DTP435C	8.0	2.0	6.0	7.0	6.0	7.0	6.0	9.0	7.0	6.0	64	6.4	4.75	8	.80 - .70
DTP435B	6.0	8.0	19.0	21.0	8.0	13.0	14.0	13.0	8.0	10.0	120	12.0	18.67	8	.02 - .01
DTP435A	4.0	3.0	11.0	13.0	13.0	5.0	10.0	8.0	5.0	10.0	82	8.2	15.32	8	.10 - .05
DTP434C	9.0	11.0	8.0	13.0	15.0	11.0	14.0	9.0	18.0	12.0	120	12.0	7.17	8	.70 - .50
DTP434B	10.0	8.0	10.0	11.0	9.0	22.0	14.0	18.0	8.0	12.0	122	12.2	15.54	8	.05 -.02
DTP434A	11.0	10.0	7.0	15.0	16.0	18.0	13.0	15.0	7.0	8.0	120	12.0	11.83	8	.20 - .10
DTP433C	7.0	8.0	11.0	11.0	4.0	5.0	18.0	8.0	12.0	7.0	91	9.1	16.36	8	.05 - .02
DTP433B	4.0	7.0	17.0	19.0	11.0	18.0	14.0	12.0	8.0	10.0	120	12.0	18.67	8	.02 - .01
DTP433A	4.0	6.0	8.0	23.0	13.0	17.0	16.0	15.0	12.0	6.0	120	12.0	27.00	8	< .001
DTP431C	17.0	7.0	10.0	12.0	10.0	12.0	17.0	15.0	12.0	8.0	120	12.0	9.00	8	.50 - .30
DTP431B	3.0	11.0	12.0	15.0	8.0	10.0	32.0	15.0	9.0	5.0	120	12.0	48.17	8	< .001
DTP431A	4.0	13.0	7.0	20.0	11.0	19.0	21.0	8.0	10.0	7.0	120	12.0	27.50	8	< .001
I73PLSP	1.0	3.0	9.0	14.0	10.0	7.0	14.0	8.0	5.0	4.0	75	7.5	23.27	8	.01 - .001
I73PRSP	2.0	5.0	8.0	11.0	7.0	9.0	9.0	7.0	4.0	5.0	67	6.7	9.87	8	.30 - .20
DTFP356	9.0	15.0	18.0	14.0	18.0	15.0	14.0	11.0	12.0	16.0	142	14.2	5.32	8	.80 - .70
DTFP351	9.0	14.0	11.0	11.0	8.0	18.0	9.0	9.0	6.0	13.0	108	10.8	9.96	8	.30 - .20
DTQP356	1.0	12.0	8.0	13.0	8.0	18.0	9.0	4.0	6.0	4.0	83	8.3	27.24	8	< .001
DTQP351	5.0	4.0	10.0	10.0	19.0	6.0	7.0	15.0	1.0	4.0	81	8.1	33.69	8	< .001
DTQP490	3.0	8.0	7.0	13.0	10.0	15.0	19.0	9.0	3.0	4.0	91	9.1	28.01	8	< .001

D. OF F. = DEGREES OF FREEDOM * PROBABILITY LEVEL IN CHI-SQUARE DISTRIBUTION. FROM FISHER & YATES (1963).

APPENDIX - 4D

The theoretical background for the calculation of the magnitude and orientation of 3D strain ellipsoid from 2D strain ratios on three non-principal orthogonal sections XY, YZ and ZX has been given by Ramsay (1967).

Equations for 3D strain

Following notations are used here

k = reciprocal quadratic elongation
K = quadratic elongation
c = shear strain x k
t = angle between principal strain axis and reference direction (one of X, Y, and Z)

An appropriate suffix is added to the symbol to indicate a particular direction or plane.

Let us assume that we know the 2D principal strain ratios (R_1,R_2,R_3) on three orthogonal sections, XY, YZ, ZX, which are <u>not</u> the principal sections of the strain ellipsoid. The lines of intersections between any pair of planes, i.e. the directions X,Y,Z serve as the axes on a rectangular cartesian coordinate frame (Fig. 4D.1). On each plane the angle, t_x,t_y or t_z, between the maximum 2D quadratic elongation, K_{xy1},K_{yz1} or K_{zx1}, and the coordinate axis X,Y or Z, is known.

The equations representing the state of strain on XY,YZ and ZX sections have been given by Ramsay (1967).

Section XY:

$$k_x = k_{xy1}\cos^2 t_x + k_{xy2}\sin^2 t_x \qquad (D.1)$$

$$k_y = k_{xy1}\sin^2 t_x + k_{xy2}\cos^2 t_x \qquad (D.2)$$

$$c_{xy} = (k_{xy2} - k_{xy1})\sin t_x \cos t_x \qquad (D.3)$$

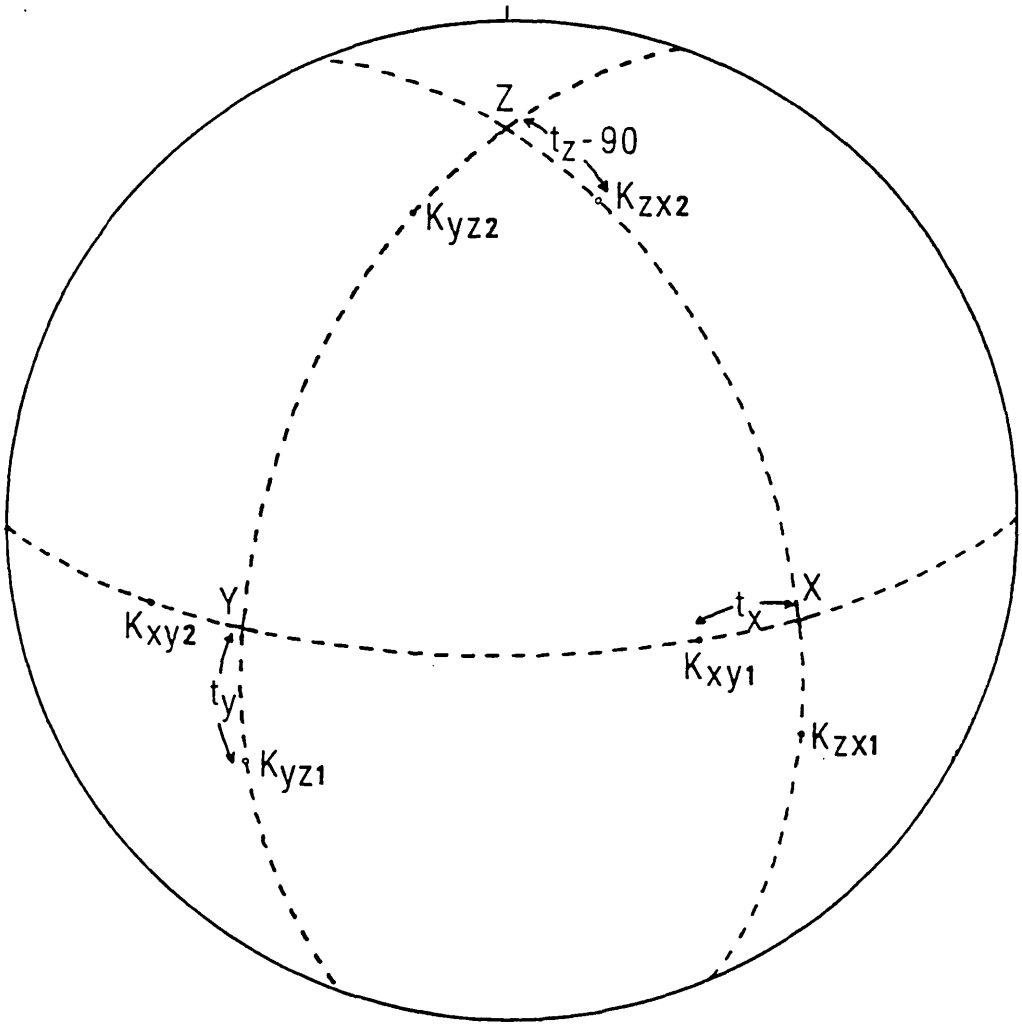


Figure 4D.1. Equal area plot showing reference co-ordinate frame and orthogonal sections of 2D strains.

Section YZ:

$$k_y = k_{yz1}\cos^2 t_y + k_{yz2}\sin^2 t_y \qquad (D.4)$$

$$k_z = k_{yz1}\sin^2 t_y + k_{yz2}\cos^2 t_y \qquad (D.5)$$

$$c_{yz} = (k_{yz2} - k_{yz1})\sin t_y \cos t_y \qquad (D.6)$$

Section ZX:

$$k_z = k_{zx1}\cos^2 t_z + k_{zx2}\sin^2 t_z \qquad (D.7)$$

$$k_x = k_{zx1}\sin^2 t_z + k_{zx2}\cos^2 t_z \qquad (D.8)$$

$$c_{zx} = (k_{zx2} - k_{zx1})\sin t_z \cos t_z \qquad (D.9)$$

where K_x, k_y and k_z represent the reciprocal quadratic elongations along X,Y and Z respectively; c_{xy}, c_{yz} and c_{zx} are related to the shearing strain, by $c = \gamma k$, adding suffixes for appropriate sections.

Since only the 2D strain ratios are known, to obtain the 3D strain picture, equations (D.1-9) have to be rewritten to express the quantities on the left hand side in terms of the same 2D strain ratio, say $R_1 = k_{xy2}/k_{xy1}$. This can be done first by eliminating k_y from eqns. (D.2) and (D.4)

$$k_{yz1} = \frac{k_{xy}(\sin^2 t_x + R_1 \cos^2 t_x)}{\cos^2 t_y + R_2 \sin^2 t_y} \qquad (D.10)$$

and similarly values of k_{yz2}, k_{zx1} and k_{zx2} may be obtained in terms of k_{yz1}. Substitution of $k_{yz1}, k_{yz2}, k_{zx1}$ and k_{zx2} thus obtained in equations (D.1-9) will give $k_x, k_y, k_z, c_{xy}, c_{yz}$ and c_{zx} in terms of k_{xy1}, the input values being those of R_1, R_2, R_3, t_x, t_y and t_z.

Once $k_x, k_y, k_z, c_{xy}, c_{yz}$ and c_{zx} have been determined, the problem is to find the values of 3D principal reciprocal quadratic elongations and their orientation with respect to the arbitrarily defined coordinate axes. The equation of the strain ellipsoid in terms of the six elements $k_x, k_y, k_z, c_{xy}, c_{yz}$ and c_{zx} is given by:

$$k_x X^2 + k_y Y^2 + k_z Z^2 - 2c_{xy}XY - 2c_{yz}YZ - 2c_{zx}ZX = 1 \qquad (D.11)$$

Analytically, the magnitude of k_1, k_2 and k_3 can be obtained by finding the length of the common normal to the sphere,

$$X^2+Y^2+Z^2=R^2 \qquad (D.12)$$

and the ellipsoid represented by the equation (D.11) The solution is obtained by differentiating equations (D.11) and (D.12) and then comparing differential co-efficients which are related to the gradients of the common normal (see equations (D.15a-c). On the other hand the principal reciprocal quadratic elongations, k_1, k_2 and k_3 are three roots of the cubic,

$$k^3-J_1k^2+J_2k-J_3=0 \qquad (D.13)$$

where

$$J_1=k_1+k_2+k_3=k_x+k_y+k_z \qquad (D.14a)$$

$$J_2=k_1k_2+k_2k_3+k_3k_1$$
$$= k_xk_y+k_yk_z+k_zk_x-c_{xy}^2-c_{yz}^2-c_{zx}^2 \qquad (D.14b)$$

$$J_3=k_1k_2k_3$$
$$= k_xk_yk_z-2c_{xy}c_{yz}c_{zx}-k_xc_{yz}^2-k_yc_{zx}^2-k_zc_{xy}^2 \qquad (D.14c)$$

from the properties of strain invariants (Ramsay 1967).

To obtain the orientations of k_1, k_2 and k_3, one can substitute the values of $k_i (i=1,3)$, in the following sets of equations:

$$(k_x-k_i)X-c_{xy}Y-c_{zx}Z=0 \qquad (D.15a)$$

$$-c_{xy}X+(k_y-k_i)Y-c_{yz}Z=0 \qquad (D.15b)$$

$$-c_{zx}X-c_{yz}Y+(k_z-k_i)Y=0 \qquad (D.15c)$$

Solution of the simultaneous equations (D.15.a-c) gives the coordinates of the end point of the principal axes of the strain ellipsoid. Thus one gets three sets of values for (X,Y,Z), each satisfying

$$X_i^2+Y_i^2+Z_i^2=K_i \quad (i=1,3) \qquad (D.16)$$

Direction cosines of the 3D principal quadratic elongations are obtained from

$$l_i = X_i / k_i \qquad \text{(D.17a)}$$

$$m_i = Y_i / k_i \qquad \text{(D.17b)}$$

$$n_i = Z_i / k_i \quad (i=1,3) \qquad \text{(D.17c)}$$

A method of numerical solution of equation (D.13) is coded in subprogram SOLVE. This is called from the main routine LAMBDA after the strain invariants have been computed (eqns. (D.14a-c), for essentials of LAMBDA see flowchart in Fig. 4D.2A. The algorithm for subprogram SOLVE is given below (Fig. 4D.2B). Subprogram ORIENT computes the orientation of k_i with respect to X,Y,Z; equations (D.15-17) are used (Fig. 4D.2C).

Subprogram SOLVE

The subroutine provides an algorithm for the numerical solution of a cubic equation, all three roots of which are positive real numbers. The relevant equation is

$$f(x) = x^3 - J_1 x^2 + J_2 x - J_3 = 0 \qquad \text{(D.18)}$$

where J_1, J_2 and J_3 represent the strain invariants. For a numerical solution of the equation we follow the method of graphically representing f(x) in f(x)-x space and try to define the neighbourhood of at least one of the points where

$$f(x) = x^3 - J_1 x^2 + J_2 x - J_3$$

and f(x)=0 intersect. Figure 4D.3 shows that the intermediate root of equation (D.18) lies between two values of x, each of which satisfies f'(x)=0.

$$\text{But, } f'(x) = \frac{d}{dx} f(x) = 3x^2 - 2J_1 x + J_2 \qquad \text{(D.19)}$$

We also notice that f(x) changes sign in the domain $x_1 < x < x_2$, where x_1 and x_2 are the roots of the quadratic equation, $3x^2 - 2J_1 x + J_2$. These roots are given by

$[J_1 \pm \sqrt{(J_1^2 - 3J_2)}]/3.$

The crux of the problem lies in computing values of f(x) in the range $x_1 < x < x_2$ and determining the turning point where f(x) changes sign from positive to negative. We can start with a value $x = x_1$ and gradually increase the value of x in small increments, say δx. By choosing a sufficiently small value of δx, and by locating the turning point in f(x), the intermediate root can be determined to an acceptable level of accuracy.

The subprogram starts with the setting of some control values of NITR and OUTLUP which will ultimately determine the size of δx (see flowchart in Fig. D.2B). In the actual Fortran program, NITR=1000 and OUTLUP=3. For 2D strain ratios not exceeding 10, 3000 iterations are sufficient to get a solution which differs from the actual root by less than 0.0001. For more stringent accuracy, the value of OUTLUP and/or NITR can be appropriately increased. Steps 4-18 perform the operation of finding the intermediate root. There are two DO LOOP's in this sequence. The first one sets off with the hexagonal box with a '7' inside. The assignments in box 8 are repeated NITR times to get successive values of x in the range $x_1 < x < x_2$ and to calculate the corresponding values of f(x). The second DO LOOP (the start of which corresponds to the hexagonal box with '11' inside) checks the sign of the quotient (W) obtained by dividing each value of f(x) by the next, and thus brackets the neighbourhood where a change of sign in f(x) occurs.

Once the intermediate root has been determined with sufficient accuracy, the other roots can be found by solving the quadratic

$$x^2 + (k_2 - J_1)x + (J_1^2 - J_1 k_2 + J_2) = 0 \qquad (D.20)$$

Steps 15-18 execute this in the subprogram. The value of the three roots are in the storage locations associated with the subscripted variable X, and are returned to the main program LAMBDA.

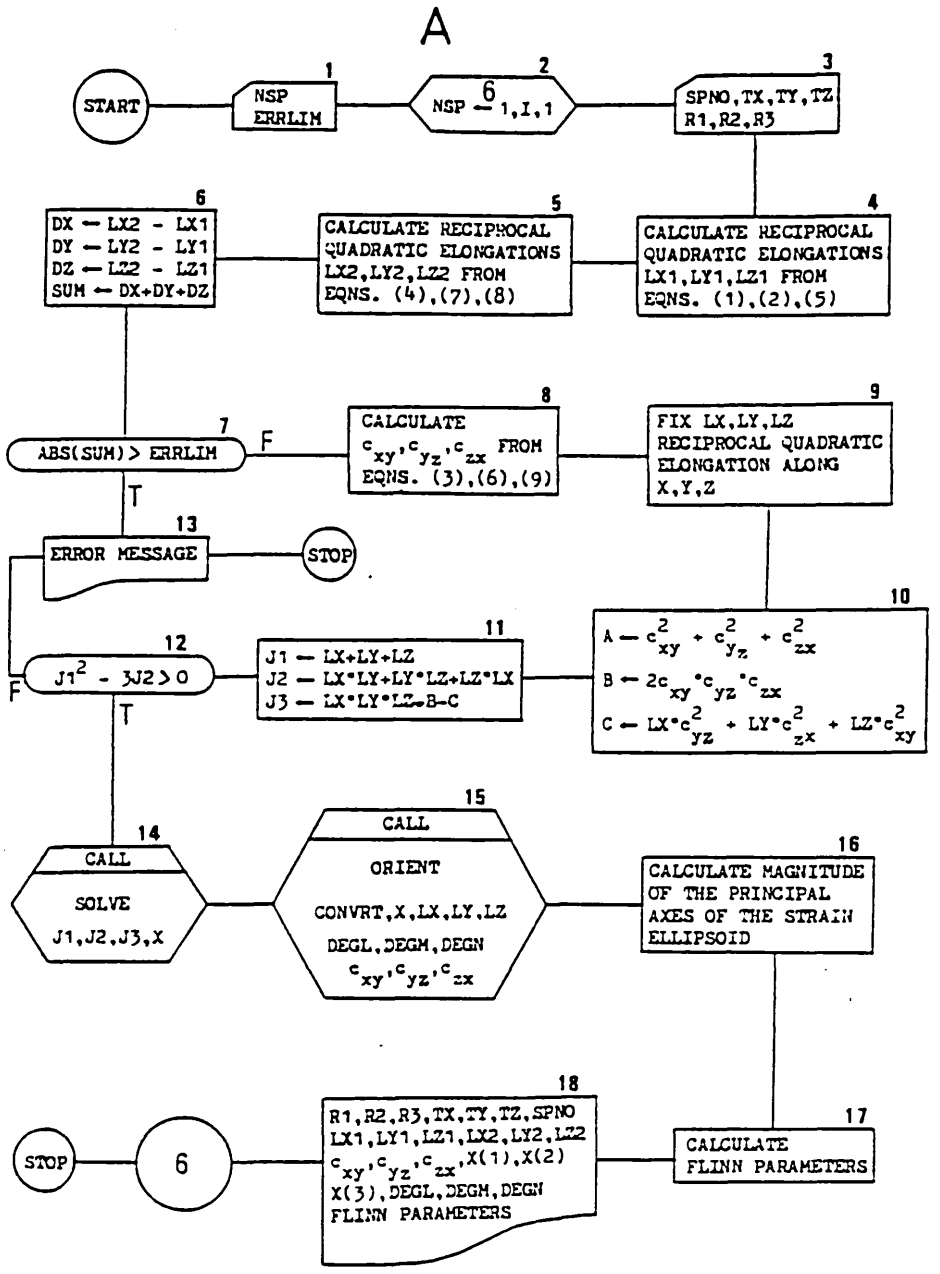


Figure 4D.2. Flowchart for main program LAMBDA (a), subroutine SOLVE (b) and subroutine ORIENT (c).

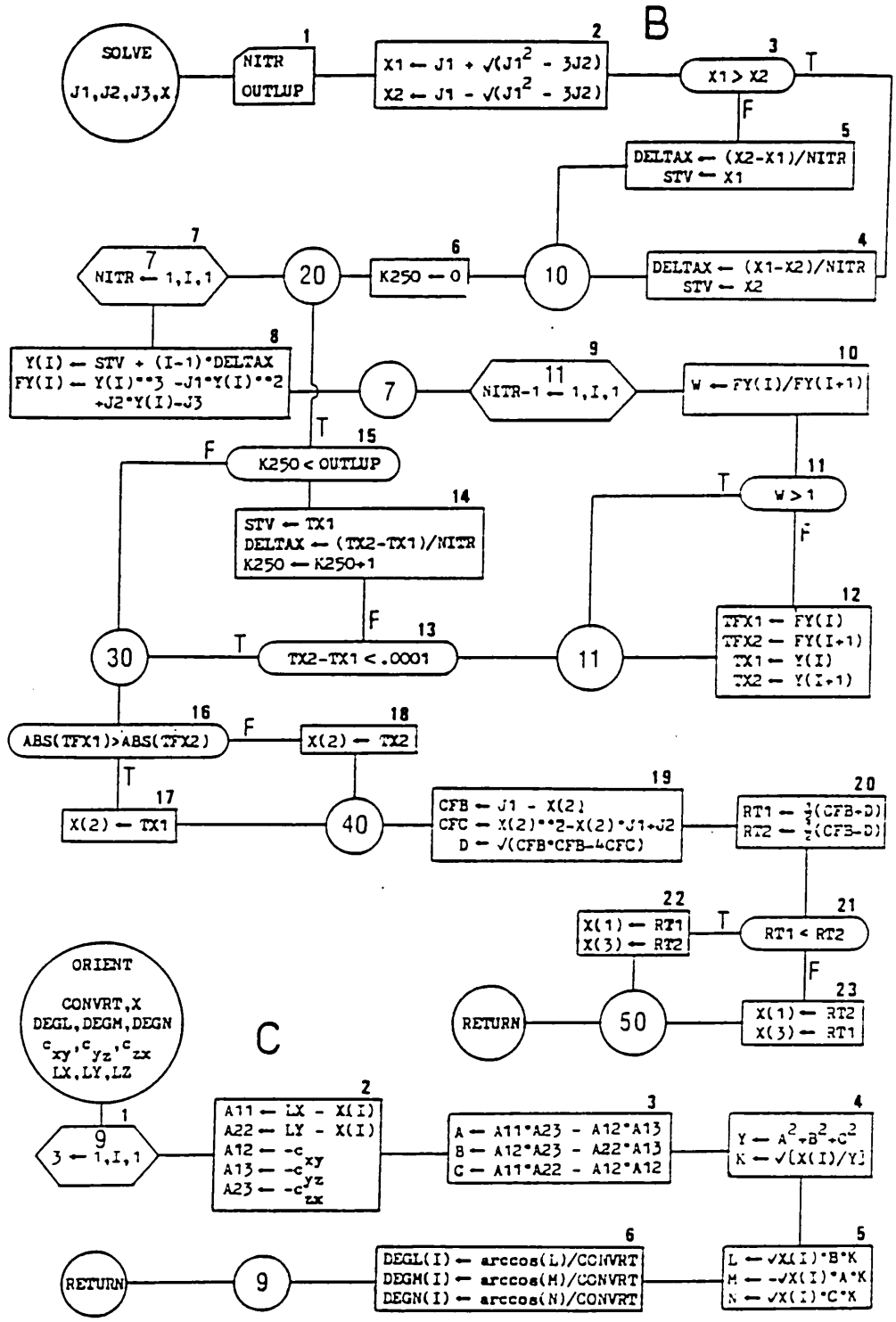


FIGURE 4D.2 contd.

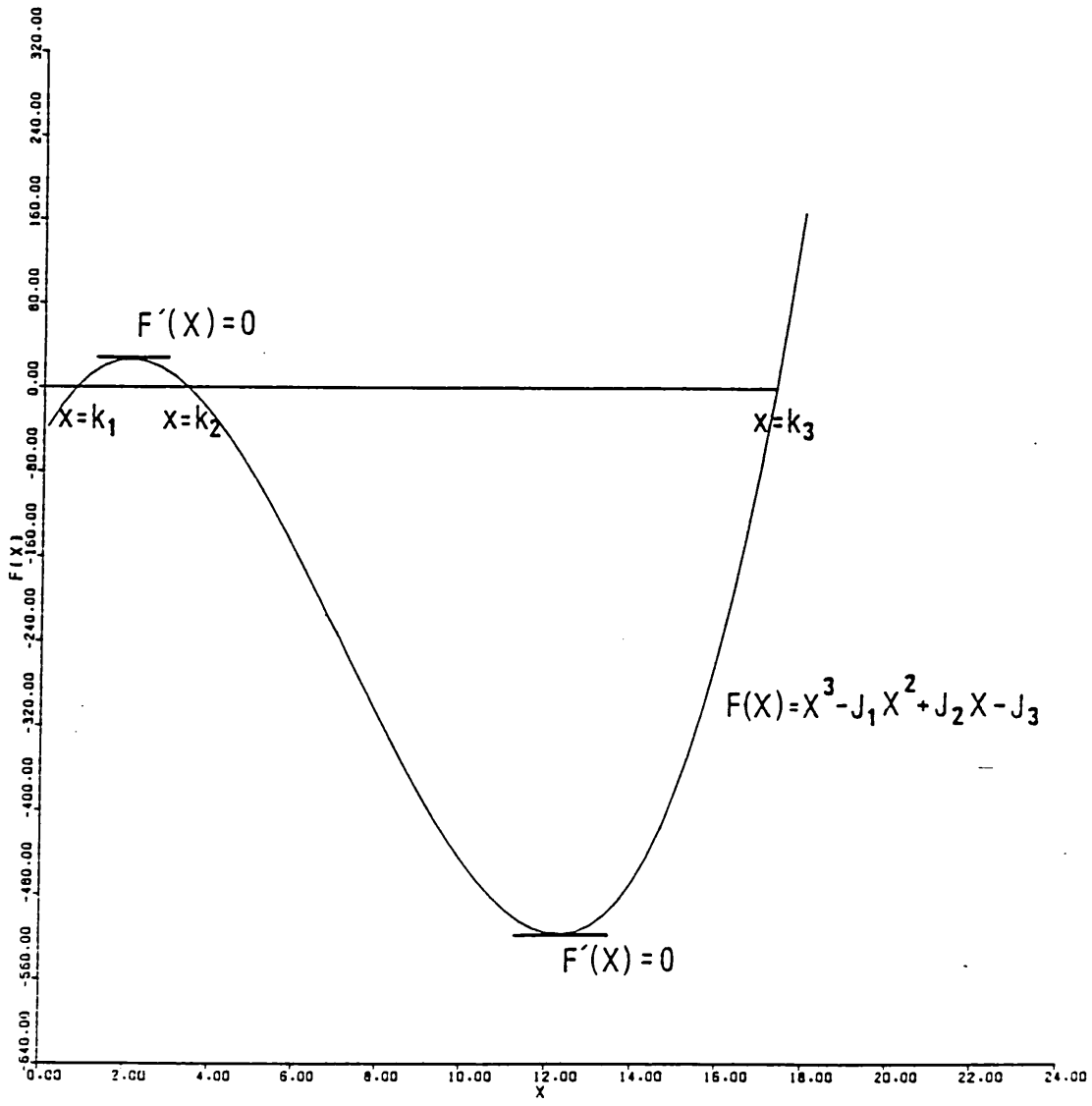


Figure 4D.3. Graphical representation of the cubic,
$F(x) = x^3 - J_1 x^2 + J_2 x - J_3$,
where J_1, J_2 and J_3 are the strain invariants.

APPENDIX - 4E

ROTATION OF POLES

Graphical methods of rotation of poles around an axis are known to geologists for a long time (Fairbairn 1949, Phillips 1971). However, the procedure can be tedious and time consuming if a large number of poles are to be handled and if more than one rotation is necessary. Considering the geometry of rotation of each poles around an axis, Starkey (1970) wrote FORTRAN programs (subroutines ROT8 and OST3) for automated rotation of poles. For a 'general' orientation of the rotation axis and the pole, Starkey's method involves solution of oblique spherical triangles. Since the subroutine OST3 has 18 references to trigonometric functions and for each pole of general orientation OST3 has to be called twice, the program is rather inefficient (see Monro 1982) for situations involving single or multiple rotation of hundreds/ thousands of poles. An alternative algorithm is presented below.

Geometry of Rotation

Consider each pole as a unit vector, $\vec{p}_i$, in the X-Y-Z rectangular cartesian co-ordinate space. In the reference hemisphere, X is horizontal north, Y is horizontal east and Z is vertical downwards. Co-ordinates of the end point of $\vec{p}_i$ is therefore equal to the direction cosines of $\vec{p}_i$ with respect to X,Y,Z.

Instead of considering the rotation of each pole around the axis separately, the reference axes are rotated. The operation is equivalent to a transformation of axes (Nye 1957). If the initial set of axes are given by X,Y,Z and the rotated set by X',Y',Z' then the angular relations between the axes may be specified by drawing up a table of direction cosines:

		'Initial' X	Y	Z
'Rotated'	X'	a_{11}	a_{12}	a_{13}
	Y'	a_{21}	a_{22}	a_{23}
	Z'	a_{31}	a_{32}	a_{33}

(E.1)

a_{ij} is defined as in Fig. 4E.1.

Orientation of the rotated pole in terms of its direction cosines can be obtained by considering the transformation of vector components. Let the components of $\vec{p}_i$ with respect to X,Y,Z be p_1,p_2,p_3 (Fig. 4E.2) and with respect to X',Y',Z' be p'_1,p'_2,p'_3. p'_1 is obtained by resolving p_1,p_2,p_3 along the new direction X'. Thus

$$p'_1 = p_1\cos\hat{XX}' + p_2\cos\hat{YX}' + p_3\cos\hat{ZX}'.$$

Hence from (E.1)

$$p'_1 = a_{11}p_1 + a_{12}p_2 + a_{13}p_3 \qquad \text{(E.2.1)}$$

and similarly,

$$p'_2 = a_{21}p_1 + a_{22}p_2 + a_{23}p_3 \qquad \text{(E.2.2)}$$

$$p'_3 = a_{31}p_1 + a_{32}p_2 + a_{33}p_3. \qquad \text{(E.2.3)}$$

Thus if the transformation matrix, a_{ij} and the initial orientation of the poles (p_1,p_2,p_3) are known, the final orientations (p'_1,p'_2,p'_3) can be easily obtained from (E.2.1-3).

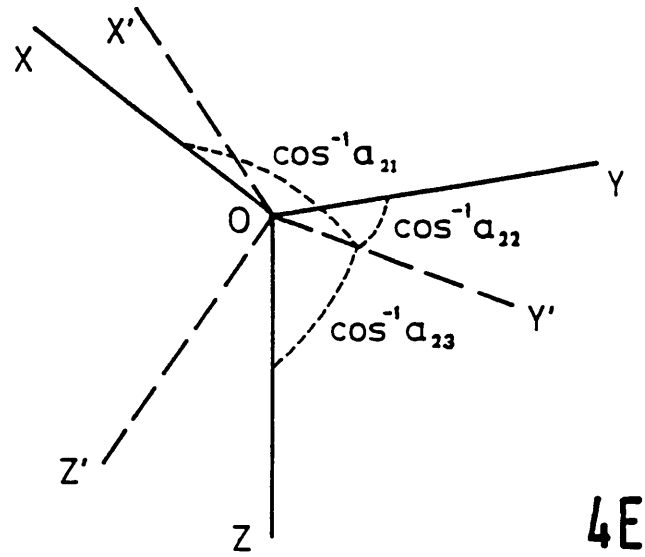
The transformation matrix, a_{ij}

Let the rotation axis be represented by another unit vector, $\vec{R}$ with components l,m,n along X,Y,Z respectively. Consider the rotation of $\vec{X}(|X|=1)$ around R. If the components of $\vec{X}$ are l_i,m_i,n_i before and l_f,m_f,n_f after rotation, and the plane angle between $\vec{R}$ and $\vec{X}$ is α then from the scalar product of two unit vectors

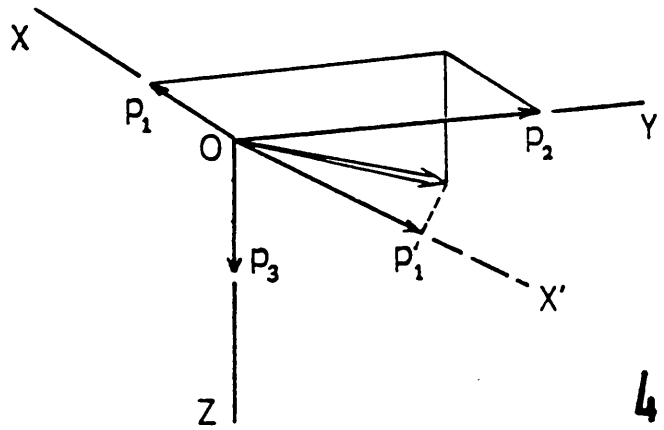
Figure 4E.1. Transformation of axes.

Figure 4E.2. Transformation of the components of a vector.

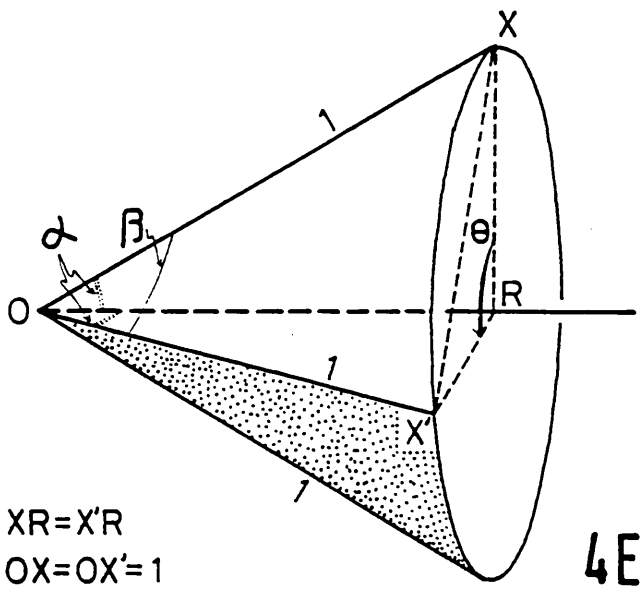
Figure 4E.3. Geometric relations for clockwise rotation of a pole around an axis OR through an angle θ.



4E.1



4E.2



XR=X'R
OX=OX'=1

4E.3

$$\cos\alpha = ll_i + mm_i + nn_i \qquad (E.3)$$

Since the plane angle between $\vec{R}$ and $\vec{X}$ remains constant during rotation

$$ll_f + mm_f + nn_f = \cos\alpha \qquad (E.4)$$

The angle, β, between $\vec{X}$ and $\vec{X}'$ can be obtained by considering the plane triangles with sides formed by $\vec{X},\vec{X}'$ and normals drawn from the end points of $\vec{X},\vec{X}'$ on to the rotation axis (Fig. 4E.3).

$$\cos\theta = \frac{2XR^2 - XX'^2}{2XR^2} \qquad \text{from triangle XRX'.}$$

$$XX^2 = 2XR^2(1-\cos\theta)$$

$\cos\beta = 1-\frac{1}{2}XX^2$ from triangle XOX' (Fig. 4E.3).

$$\therefore \cos\beta = 1-[\sin^2\alpha(1-\cos\theta)]\,. \qquad (E.5)$$

Now from the scalar product of $\vec{X}$ and $\vec{X}'$

$$l_i l_f + m_i m_f + n_i n_f = \cos\beta\,. \qquad (E.6)$$

From the properties of direction cosines

$$l_f^2 + m_f^2 + n_f^2 = 1\,. \qquad (E.7)$$

By solving the simultaneous equation (E.4), (E.6) and (E.7) l_f, m_f and n_f can be obtained. Thus the final orientation of the co-ordinate axes and the transformation matrix a_{ij} can be obtained. One must remember however that (E-7) is a second degree equation and algebraic solution of (E.4); (E.6) and (E.7) gives more than one set of solutions if $\vec{R}$ does not coincide with one of X,Y,Z or certain other special cases to be described below. The correct solution for our problem must satisfy the Kronecker delta (Nye 1957), i.e.

$$a_{ik}a_{jk}=0 \quad \text{for } i\neq j, \qquad (E.8)$$

using dummy suffix notation.

Special cases of rotation

From computational aspects algebraic or numerical solution of (E.4), (E.6), (E.7) to obtain a_{ij} can be profitable only if the rotation axis, $\vec{R}$, is oblique to the co-ordinate axes. This situation is referred to as a 'general' case in the earlier paragraphs. When $\vec{R}$ coincides with one of X,Y, or Z, (E.4), (E.6) or (E.7) are identical and one of l_f, m_f or n_f must be equal to 1($\cos\alpha=\cos 0=1$). Hence, in these situations $a_{ij}=1$ if i=j. When the amount of rotation, $\theta = 90°$, 6 elements of a_{ij} become zero because of the orthogonality of the axes. The transformation matrices for rotation axis coincident with one of X,Y,Z axes are given below.

R on +X

1	0	0
0	$\cos\theta$	$\cos(\frac{\pi}{2}-\theta)$
0	$\cos(\frac{\pi}{2}+\theta)$	$\cos\theta$

R on -X

1	0	0
0	$\cos\theta$	$\cos(\frac{\pi}{2}+\theta)$
0	$\cos(\frac{\pi}{2}-\theta)$	0

R on +Y

$\cos\theta$	0	$\cos(\frac{\pi}{2}+\theta)$
0	1	0
$\cos(\frac{\pi}{2}-\theta)$	0	$\cos\theta$

R on -Y

$\cos\theta$	0	$\cos(\frac{\pi}{2}-\theta)$
0	1	0
$\cos(\frac{\pi}{2}+\theta)$	0	$\cos\theta$

R on +Z

$\cos\theta$	$\cos(\frac{\pi}{2}-\theta)$	0
$\cos(\frac{\pi}{2}+\theta)$	$\cos\theta$	0
0	0	1

R on -Z

Cos	$\cos(\frac{\pi}{2}+\theta)$	0
$\cos(\frac{\pi}{2}-\theta)$	$\cos\theta$	0
0	0	1

θ is the amount of rotation, $360°>\theta>0$.

Solution of simultaneous equations (E.4), (E.6), (E.7)

Let $\cos\alpha=a$, $\cos\beta=b$

General case:

$l \neq 0$, $m \neq 0$, $n \neq 0$.

For x axis, from (E.6)

$$l_f = b$$

$$n_f = \frac{-B \pm (B^2-4AC)^{\frac{1}{2}}}{2A}$$

where

$A=1-l^2$, $B=2n(bl-a)$, $C=(a-bl)^2-m^2(1-b^2)$,

$$m_f = \frac{(a-bl)-nn_f}{m} . \qquad \text{(E.9a-c)}$$

For Y axis, from (E.6)

$$m_f = b$$

$$l_f = \frac{-B \pm (B^2-4AC)^{\frac{1}{2}}}{2A}$$

where

$A=1-m^2$, $B=2l(bm-a)$, $C=(a-bm)^2-n^2(1-b^2)$,

$$n_f = \frac{(a-bm)-ll_f}{n} . \qquad \text{(E.10a-c)}$$

For Z axis, from (E.6)

$$n_f = b$$

$$l_f = \frac{-B \pm (B^2-4AC)^{\frac{1}{2}}}{2A}$$

where

$A=1-n^2$, $B=2l(bn-a)$, $C=(a-bn)^2-m^2(1-b^2)$,

$$m_f = \frac{(a-bn)-ll_f}{m} . \qquad \text{(E.11a-c)}$$

$\vec{R}$ on XY plane but not coinciding with X or Y:

$n=0$, $l \neq 0$, $m \neq 0$.

For X axis,

$l_f=b$

$$m_f = \frac{a-bl}{m}$$

$$n_f = (1-l_f^2-m_f^2)^{\frac{1}{2}}. \qquad \text{(E.12a-c)}$$

For Y axis,

$m_f=b$

$$l_f = \frac{a-bm}{l}$$

$$n_f = (1-l_f^2-m_f^2)^{\frac{1}{2}}. \qquad \text{(E.13a-c)}$$

For Z axis,

$n_f=b$

$$l_f = al \pm (a^2l^2-b^2m^2+m^2a^2)^{\frac{1}{2}}$$

$$m_f = \frac{a-ll_f}{m}. \qquad \text{(E.14a-c)}$$

$\vec{R}$ on XZ plane but $\vec{R}\neq\vec{X}$ or $\vec{R}\neq\vec{Z}$:

$l\neq 0$, $n\neq 0$, $m=0$.

For X axis,

$l_f=b$

$$n_f = \frac{a-bl}{n}$$

$$m_f = (1-l_f^2-n_f^2)^{\frac{1}{2}} \qquad \text{(E.15a-c)}$$

For Y axis,

$m_f=b$

$$n_f = an \pm (a^2n^2-b^2l^2+l^2-a^2)^{\frac{1}{2}}$$

$$l_f = \frac{a-nn_f}{l}. \qquad \text{(E.16a-c)}$$

For Z axis,

$n_f=b$

$l_f=(a-bn)/l$

$m_f=(1-l_f^2-n_f^2)^{\frac{1}{2}}$ (E.17a-c)

R on YZ plane but R≠Y or R≠Z:

$l=0$, $m\neq0$, $n\neq0$.

For X axis,

$m_f=b$

$n_f=(a-bm)/n$

$l_f = (1-m_f^2+n_f^2)^{\frac{1}{2}}$. (E.18a-c)

For Y axis,

$l_f=b$

$m_f=am\pm(a^2m^2-bn^2+n^2-a^2)^{\frac{1}{2}}$

$n_f= (a-mm_f)/n$. (E.19a-c)

For Z axis,

$n_f=b$

$m_f=(a-bn)/m$

$l_f=(1-m_f^2-n_f^2)^{\frac{1}{2}}$. (E.20a-c)

Program SPIN8

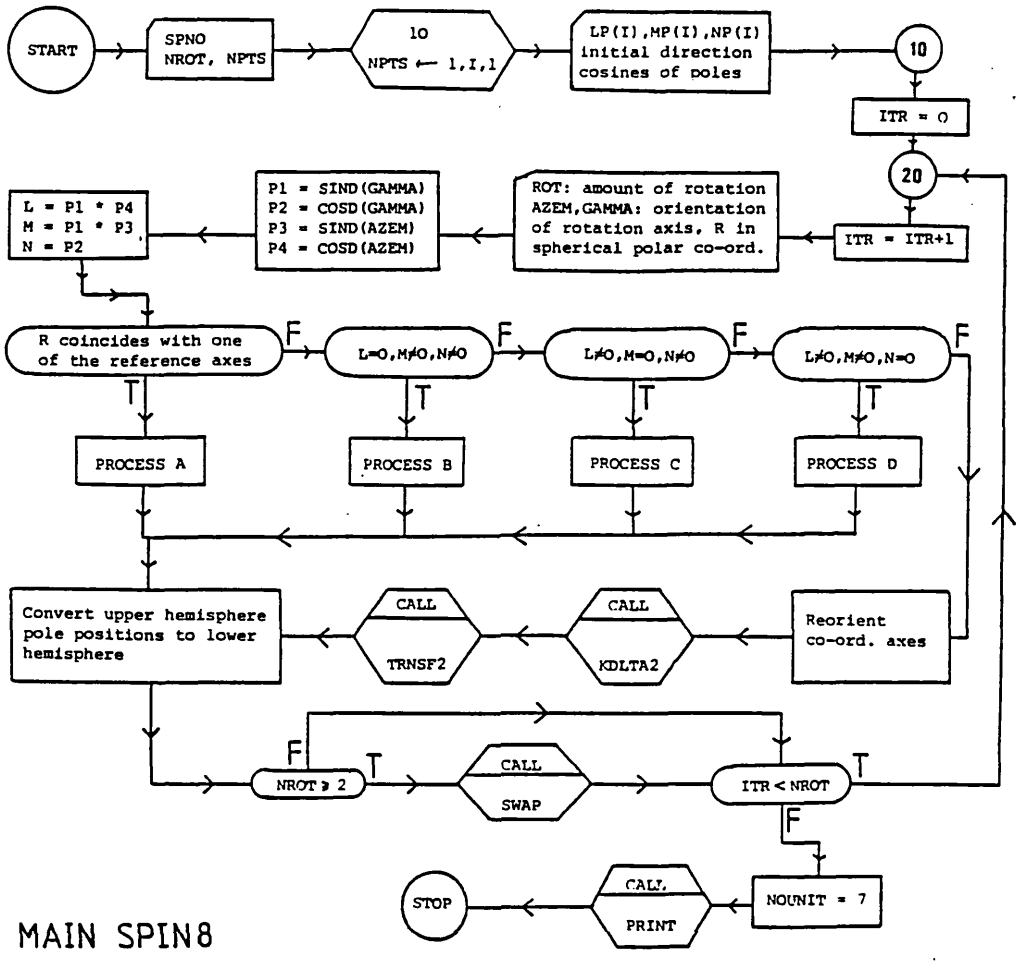
Based on the principles described above a Fortran 77 program SPIN8 is written. The orientation of the rotation axis in spherical polar co-ordinates, initial orientation of poles (direction cosines with respect to X,Y,Z axes), amount of rotation in degrees (ROT) and the number of rotations (NROT) have to be supplied as input data. One must bear in mind that the co-ordinate axes have to be rotated in a sense opposite to that required for the poles, i.e. for a clockwise rotation of poles rotate the co-ordinate axes in an anticlockwise sense. However, for a 'general' case solution of eqns. (E.4), (E.6), (E.7) should give two alternative sets of a_{ij} which satisfy Kronecker delta (ROT≠n.$\pi/_2$, integer n). The two sets of solutions correspond to clockwise and anticlockwise rotation of poles.

Subroutine KDLTA2 in the version of the program considered here writes two alternative solutions on TAPE8. The sense of rotation of the poles is as in Table 4E.1.

Table 4E.I

ROT	First solution on TAPE8	Second solution on TAPE8
$2\pi<\theta<\pi$	Clockwise	Anticlockwise
$0<\theta<\pi$	Anticlockwise	Clockwise

For $\theta = n.\frac{\pi}{2}$ (where n is an integer) the two solutions are identical and performs clockwise rotation of poles. Subroutine PRINT writes the direction cosines of poles after rotation on to TAPE7. Notice that only one set of solution is written on to TAPE7. The program flow is shown in Fig. 4E.4.



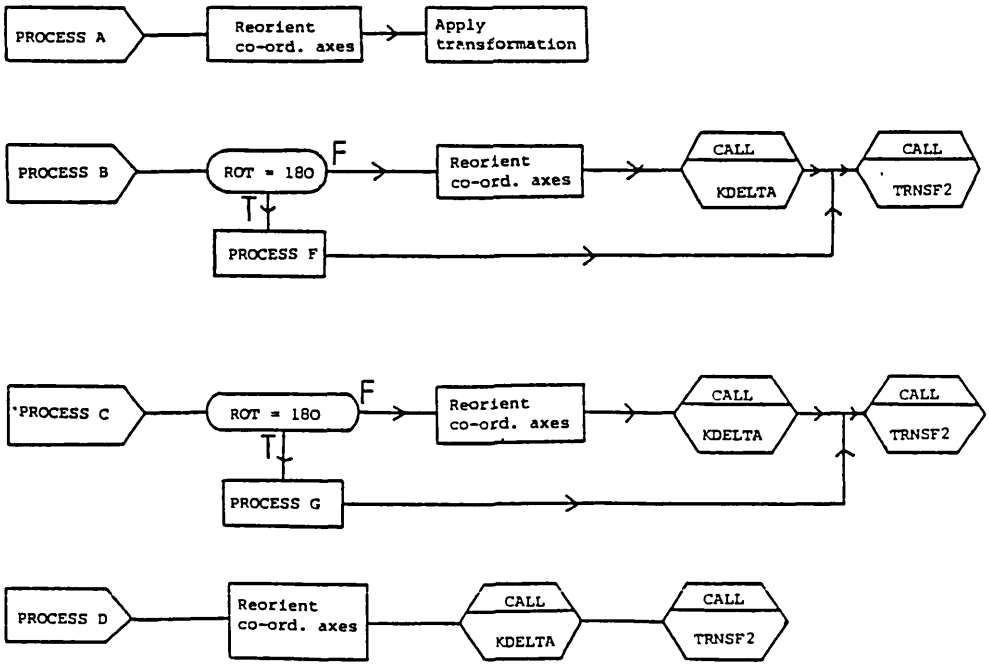


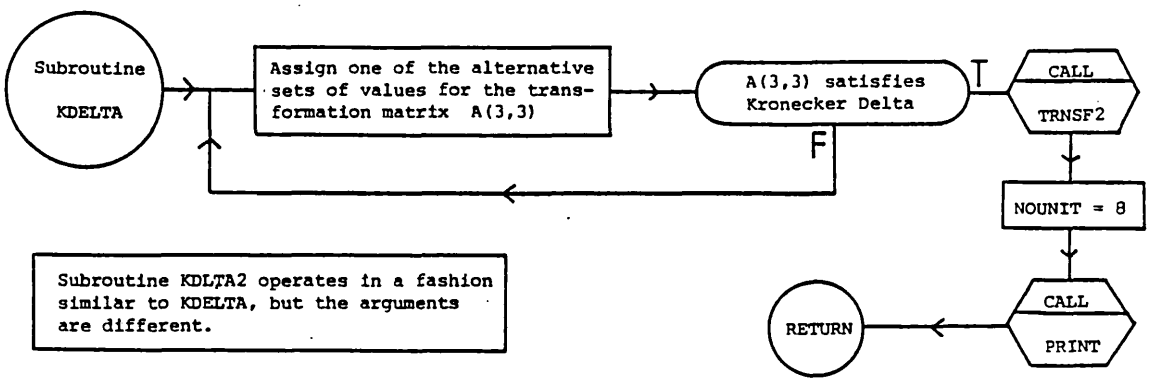
Figure 4E.4. Flowchart for program SPIN8.

```
PROCESS F

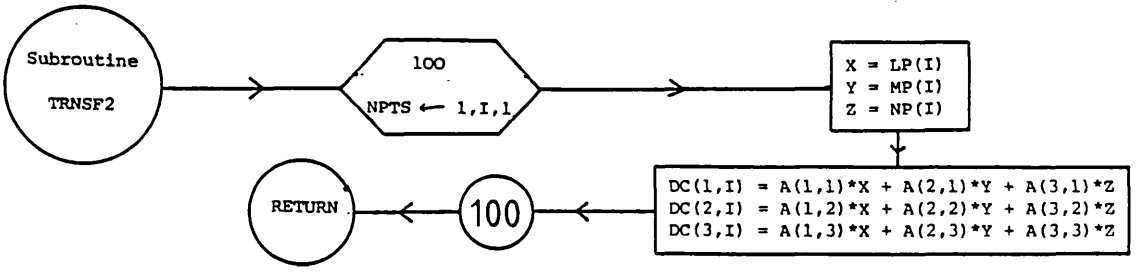
PLUNGE = 90-GAMMA
IF(AZEM.EQ.270) PLUNGE = 90+GAMMA
A(1,1) = -1
A(2,1) = 0
A(3,1) = 0
A(2,2) = COSD(2*PLUNGE)
A(3,2) = COSD(90 - 2*PLUNGE)
A(1,3) = 0
A(2,3) = A(3,2)
A(3,3) = COSD(180 - 2*PLUNGE)
A(1,2) = 0
```

```
PROCESS G

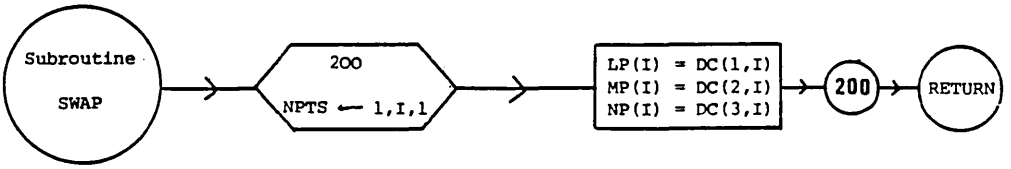
PLUNGE = 90 - GAMMA
IF(AZEM.EQ.180) PLUNGE = 90+GAMMA
A(1,1) = COSD(2*PLUNGE)
A(2,1) = 0
A(3,1) = COSD(90 - 2*PLUNGE)
A(1,2) = 0
A(2,2) = -1
A(3,2) = 0
A(1,3) = A(3,1)
A(2,3) = 0
A(3,3) = COSD(180 - 2*PLUNGE)
```

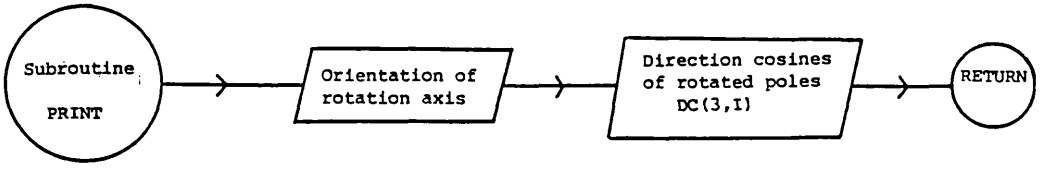


Subroutine KDLTA2 operates in a fashion similar to KDELTA, but the arguments are different.

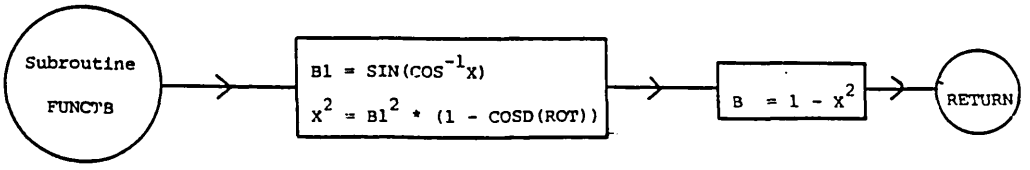


IN CASE OF MULTI-ROTATION REPLACE CURRENT DIRECTION COSINES OF POLES BY THOSE OF THE ROTATED POLES AFTER SUCCESSIVE ROTATION





SOLVE A PLANE TRIANGLE BY COSINE RULE



4E.4 contd.

APPENDIX - 4F

ESTIMATION OF POINT-DENSITY

The plotting and contouring of orientation data of crystallographic directions say, c-axis in quartz on stereographic (Wulff net) or equal-area (Schmidt net) projections is a common procedure for representing preferred orientation. Various methods of contouring have been described and their relative merits and demerits have been discussed (Flinn 1958, Stauffer 1966, Turner and Weiss 1963). The contoured pole-figure diagram graphically represents the distribution of the nearest-neighbour-density of poles over the projection space. Detailed description of the various methods are avoided here. In essence most of the procedures for counting selects a counter-size (neighbourhood) equal to 1% of the total projection area and counts the number of points (poles) falling within the counter area centred around either, each grid intersection of an arbitrarily chosen rectangular or squared grid superimposed on the scatter diagram (Schmidt method, squared grid method) or, each pole on the diagram (Mellis circle method, Mellis variable circle method, variable ellipse method).

The objection raised against the use of an arbitrary square-grid is that the same scatter diagram may appear different after contouring depending on the actual positioning of the grid with respect to the reference axes on the pole-figure diagram. However, such variation is only slight (Stauffer 1966) and can be avoided by considering a large number of grid intersections (Flinn 1958). The point-density estimate also depends on the shape of the count-area if equal-area projection is used. Ideally in this projection circular areas on the sphere should appear as ellipses of variable eccentricity depending on the closeness of the count-area to the primitive circle. When stereographic projection is used e.g. Mellis-variable-circle method, the radius of the counting circle has to be increased with increasing distance from the centre of the net.

To circumvent these problems to a large extent, we adopted a method which considers the distribution of lines (poles) on the hemispherical volume rather than their projection on the equal-area diagram. Although we still use a grid which projects as a rectangular-grid on an

equal-area projection, the neighbourhood around each grid intersection is given by a cone; the axis of this cone coincides with the position vector of the grid-intersection on the hemisphere (Fig. 4F.1). The semi-vertical angle (α) of the cone varies with sample size (total number of poles). The method of obtaining α is discussed in the following section. The angle (θ_i) between each pole ($\vec{N}_i$) and the axis of the cone ($\vec{N}_j$) is determined by means of vector algebra,

$$\theta_i = \text{Arcos}(\vec{N}_i \cdot \vec{N}_j) \quad . \tag{4F.1a}$$

If we assume a sphere of unit radius, all poles and position vectors of the grid-intersections are unit vectors and equation (4F.1a) can be rewritten as

$$\theta_i = \text{Arcos}(l_i l_j + m_i m_j + n_i n_j) \tag{4F.1b}$$

where l,m,n represent the direction cosines of $\vec{N}_i$ or $\vec{N}_j$ with respect to x,y,z axes respectively for a rectangular cartesian co-ordinate frame. If the orientation of $\vec{N}_i$ is given in spherical polar co-ordinates (ϕ,γ,1), (l,m,n) can be obtained from following relations (see Fig. 4F.2).

ϕ = azimuth measured clockwise from horizontal north (+x)

γ = compliment of plunge, i.e. angle between downwards vertical (+z) and the pole

$$l_i = \sin\gamma_i \cos\phi_i; \quad m_i = \sin\gamma_i \sin\phi_i \quad n_i = \cos\gamma_i \tag{4F.2a-c}$$

For any particular grid intersection, the total number of poles, t, falling within the defined neighbourhood will be given by

$$t = \sum_{i=1}^{n} F(\theta_i) \tag{4F.3}$$

where $F(\theta_i)=1$ for $\theta_i < \alpha$

$F(\theta_i)=0$ for $\theta_i > \alpha$

n = sample size.

The point-density, d, is given by

$$d = t/(an) \tag{4F.4}$$

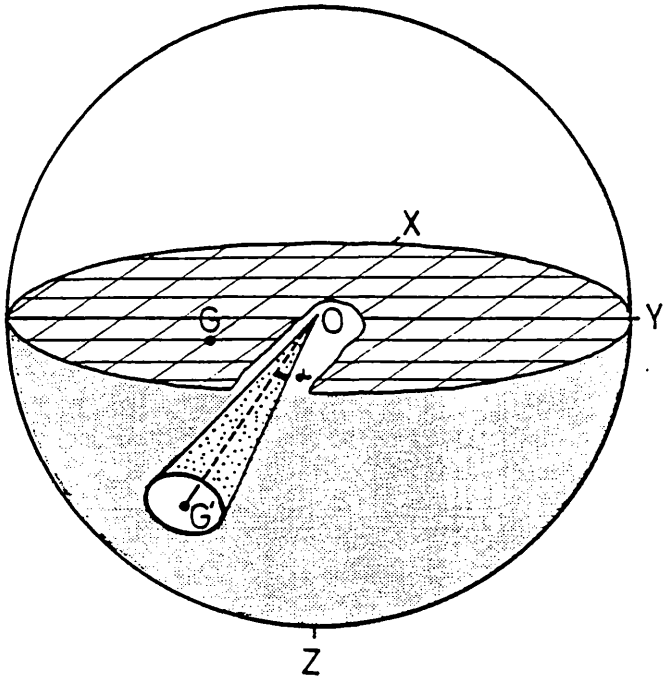


Figure 4F.1. Definition of the count-volume (nearest neighbourhood) around each grid-intersection, G. OG' is the position vector of G on the lower hemisphere. Nearest neighbourhood is defined by a cone with semivertical angle α.

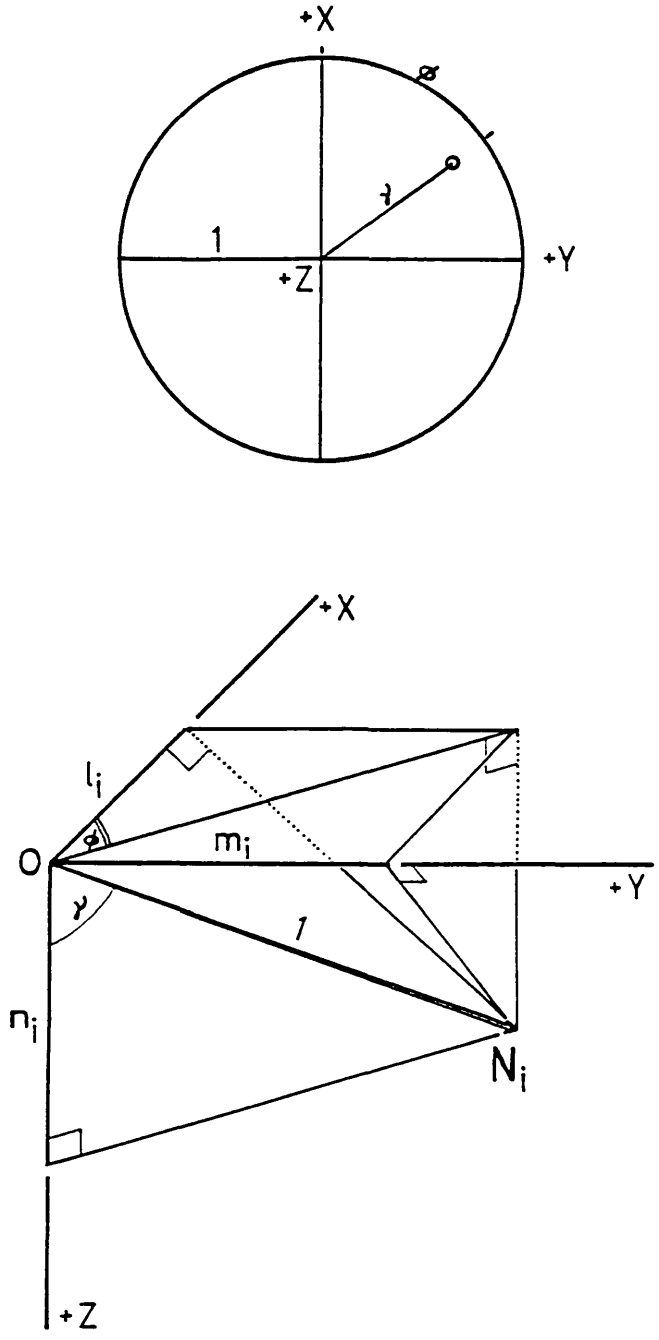


Figure 4F.2. Relationship between spherical polar co-ordinates (ø, ɣ ,1) and the direction cosines (l_i, m_i, n_i) of a pole considered as a unit vector ON_i. The spherical polar co-ordinates are also shown in an equal-area projection (top).

where a is the area of the intersection between the cone defined above and the spherical surface.

Equations of the type (4F.4) are used by statisticians as a nonparametric estimator of a probability density function (Fukunga and Hostetler 1973, Ramsden and Cruden 1979, Watson 1970). Contoured orientation diagrams thus provide statistical estimate of the probability density function represented by the sample in question (Ramsden and Cruden 1979).

$F(\theta_1)$ in equation (4F.3) is a binominal variable. Kamb (1959) noted that the coefficient of variation of d is given by

$$v = [(1-p)/np]^{\frac{1}{2}} \qquad (4F.5)$$

where p is the proportion of poles inside the count volume. Thus in any contouring procedure the coefficient of variation of point-density depends on the size of the neighbourhood. Variance of the density estimate becomes smaller by increasing a, which in its turn increases p. Setting $v = \frac{1}{3}$, Kamb (1959) suggested that all values of t which satisfy

$$t > E + 3\sigma$$

indicate significant preferred orientation; E is the expection for a random sample drawn from isotropic population, σ is the standard deviation. The argument is: although random sampling of an isotropic population may give the impression of an apparent preferred orientation in the contoured diagram, the density estimate at any point should lie within 3σ of the mean value (E; with a confidence limit of 90%).

Putting $v = \frac{1}{3}$ in (4F.5), one gets the proportion of poles (p') that should lie within the count volume, had the sample represented an isotropic population.

$$p' = \frac{9}{n+9}. \qquad (4F.6)$$

$$E = n.p'. \qquad (4F.7)$$

For the purpose of actual density estimates, α can be derived knowing that the count area on the hemispherical surface is given by $2\pi R^2(1-\cos\alpha)$, R is the radius of the sphere. Since the count area which contains E points equals to $2\pi R^2 p'$,

$$\alpha = \text{Arcos}(1-p') \qquad (4F.8)$$

and the point-density in terms of expected value for an isotropic population is given by

$$d = \frac{1}{E} \sum_{i=1}^{n} F(\theta_i) \qquad (4F.9)$$

where $F(\theta_i)$ is as defined earlier.

Fortran Program POLEV3X

POLEV3X is a FORTRAN-77 program which computes point-density related to a pole-figure diagram and prints on a line printer a semifinished fabric diagram. The fabric diagram shows the point-density value at each grid intersection by an alphanumeric character corresponding to a certain range of density values expressed as multiples of E, expectation for uniform distribution; contour lines have to be hand-drawn, if necessary. The method used in point-density estimation is outlined in the above section. The program also gives the maximum value of point-density (subroutine CTMAX) and writes the point-density values (array CTUNT) for each grid intersection on to a file TAPE7 which can be SAVE'd for further use (see Appendix 4G).

Input data can be one of the following:

(i) U-stage data on the orientation of crystallographic axes or planes; in the case of planar elements poles to planes are plotted;

(ii) Orientation of linear elements in spherical polar co-ordinate.

(iii) Field orientation of foliation or lination.

(iv) Direction cosines of poles. Program SPIN8 returns the orientation of rotated poles in terms of direction cosines. These may be used in POLEV3X.

For different types of raw data the main program calls appropriate subroutines e.g. for data type (i) subroutine USTAGE is called, for data type (iii) subroutine AZDIP is called. Both USTAGE and AZDIP return the orientation of poles in spherical polar co-ordinates (arrays AZEM and GAMA). Data of type (ii) and (iv) above are read in the main program itself rather than in the subroutines. The decision activity for this stage of the program is determined by the supplied values of the control variables, KOUNT, KIN and KONTRL. The values that have to be set for these variables depend on the data type and are shown in Table 4F.I.

TABLE 4F.I

	Data Type	KIN	KOUNT	KONTRL
	I Planar	2	0	-
USTAGE	I			
	I Linear	1	0	-
SPHERICAL POLAR CO-ORD.		1	-1	-
	I Planar	-	1	2
FIELD	I			
	I Linear	-	1	1
DIRECTION COSINES		-	2	-

For the purpose of point density estimation following relations are utilised in the program (eqns. 4F.6-9).

$\text{Cos}\,\alpha = 1-p'$, $p' = 9/(n+9)$.

The variables corresponding to Cosα, p' and n in the program are CTLIM, DELTA and NPTS respectively. A rectangular grid of size 21 x 24 is considered.

(X,Y) co-ordinate of each grid intersection is assigned considering two points:

(1) The projection sphere is of unit radius.

(2) Outline of the plot should approximate a circle when the results are printed with a spacing of 12 character/inch and 6 lines/inch.

For computation of point-density from eqn. (4F.9), grid intersections falling inside the projection circle of unit radius are considered. Array CTUNT stores the point-density values. A negative value is assigned to array elements falling outside the projection circle. Both (X,Y) co-ordinate of each grid intersection and the spherical polar co-ordinates (except for data type (iv) above) of each pole are converted to respective direction cosines before the inequality $\theta_i \leq \alpha$ is tested in a "LOGICAL IF".

Once point-density is estimated subroutine CTMAX is called. CTMAX returns the maximum value of the point density.

For plotting, the CTUNT array is converted to a character array CHAR so that a range of density value is represented by a single alphanumeric character (Table 4F.II). Subroutine circle is provided to initiate the array CHAR, size 28x25 and draw the outline of the projection circle.

TABLE 4F.II

PRINT SYMBOL	' '	X	S	1	2	3	4	5	6	7	8	9	A	B	C	H
POINT-DENSITY (X UNIFORM)	0	-2/3	-1.	-2.	-3.	-4.	-5.	-6.	-7.	-8.	-9.	-10	-11	-12	12	>12

Flowchart for POLEV3X is shown in Fig. 4F.3.

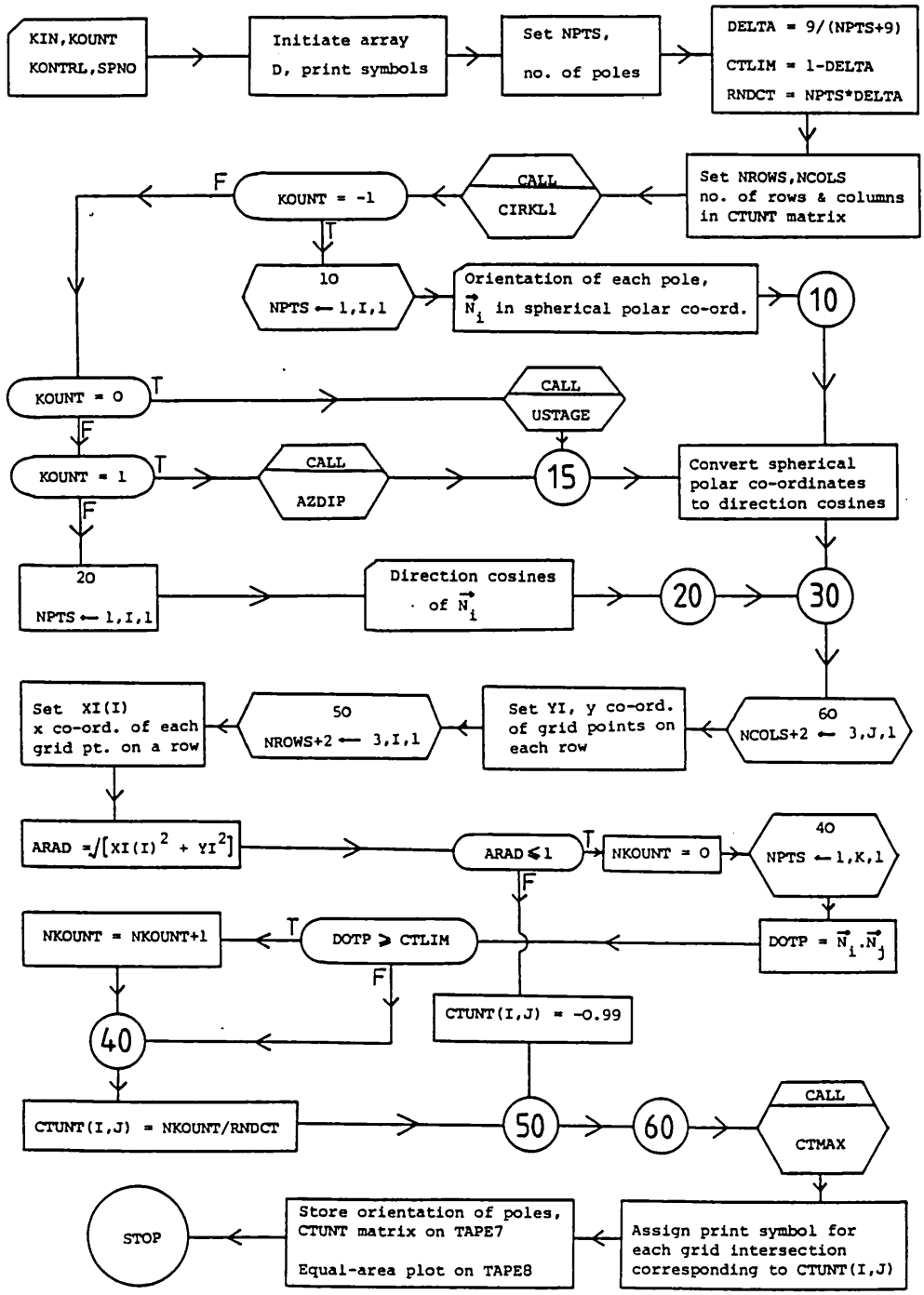


Figure 4F.3. Flowchart for program POLEV3X.

APPENDIX - 4G

PROBABILITY DISTRIBUTION OF THE POINT-DENSITY

In program POLEV3X, the variable CTUNT is a two-dimensional array variable of size 21x24. The array elements correspond to grid intersections at which point-density is estimated. In actual computation grid-intersections falling within the equal-area plot are considered for the purpose of counting, those outside the equal-area plot are given a constant negative value (see Table 4G.I for a listing of the CTUNT matrix). Out of 504 grid intersections (matrix elements), 372 elements fall within the equal-area plot and are used for estimating parameters related to the point-density distribution.

In essence, we have a smaple of size 372 corresponding to the variate point-density. The range of point-density is arbitrarily divided into a number of classes and the frequency in each class is determined. The probability of having the point-density value equal to or below a class upper limit is then given by the cumulative frequency up to a particular class.

The various statistic corresponding to a sample are computed using formulas given below.

$$\text{Mean, } \mu = \frac{\sum_{i=1}^{n} X_i}{n}; \quad \text{variance} \quad 2 = \frac{1}{n} \sum_{i=1}^{n} (X_i - \mu)^2$$

$$N^{th} \text{ moment } \mu_N = \frac{1}{n} \sum_{i=1}^{n} (X_i - \mu)^n$$

$$\text{Coefficient of Skewness, } \eta_3 = \mu_3/\sigma^3$$

$$\text{Coefficient of Kurtosis, } \eta_4 = \mu_4/\sigma^4$$

X_i is an observed value corresponding to the point-density variate, sample size = n. Fortran program PDFUNC3 is written for the purpose of computation.

PRINT OUT OF POINT DENSITIES*** CTUNT MATRIX SP. 577A
X EXPECTATION FOR UNIFORM DISTRIBUTION

TABLE 4G-I

3	-.99	-.99	-.99	-.99	-.99	-.99	-.99	-.99	-.99	0.00	0.00	.12	.35	.58	.70	-.99	-.99	-.99	-.99	-.99	-.99	-.99	-.99
4	-.99	-.99	-.99	-.99	-.99	-.99	.35	.46	.35	.35	.35	0.00	.12	.46	.58	.93	1.05	1.51	-.99	-.99	-.99	-.99	-.99	-.99
5	-.99	-.99	-.99	-.99	-.99	1.51	1.16	1.16	1.28	.93	.70	.46	.12	.12	.12	.23	.70	1.05	.93	-.99	-.99	-.99	-.99	-.99
6	-.99	-.99	-.99	-.99	2.09	1.39	1.28	1.39	1.39	.81	.81	.35	.12	.12	.23	.35	.46	.46	1.05	1.05	-.99	-.99	-.99	-.99
7	-.99	-.99	-.99	1.97	1.97	1.63	1.28	1.51	1.05	.81	.70	.12	.12	0.00	.12	.35	.46	.46	.46	.70	.58	-.99	-.99	-.99
8	-.99	-.99	2.32	1.97	1.51	.70	.93	.81	.46	.35	.12	0.00	0.00	0.00	0.00	.23	.46	.46	.46	.35	.46	.70	-.99	-.99
9	-.99	2.21	1.97	1.63	1.16	.46	.46	.23	.23	.12	0.00	0.00	0.00	.23	.23	.12	.12	.23	.35	.23	.23	.46	.93	-.99
10	-.99	2.09	1.63	1.39	1.16	.81	.46	.35	.35	.12	0.00	.12	.23	.35	.46	.81	.70	.58	.23	.23	1.05	1.16	.93	-.99
11	-.99	1.86	1.51	1.51	.81	.58	.58	.35	.35	.23	0.00	.12	.35	.70	.93	1.16	1.05	.58	.23	.81	1.63	1.74	1.63	-.99
12	-.99	1.51	1.39	1.05	.70	.70	.93	.46	.35	.35	.12	.12	.23	.81	1.39	1.51	1.28	1.05	.35	.93	1.63	1.97	1.86	-.99
13	1.63	1.39	1.28	1.28	.70	.81	.93	.46	.46	.35	.12	.12	.12	.81	1.28	1.74	1.63	1.16	.46	1.39	1.86	2.32	1.97	1.63
14	-.99	1.16	1.51	1.16	1.16	.93	.58	.70	.58	.12	.12	.23	.35	.81	1.63	1.39	1.05	.93	.93	1.51	2.32	2.67	1.97	-.99
15	-.99	1.28	1.51	1.39	1.05	1.05	.58	.46	.58	.23	.12	.35	.58	.81	1.28	1.63	1.74	1.28	1.74	1.97	2.32	2.67	1.39	-.99
16	-.99	1.28	1.51	1.51	1.28	.93	.58	.46	.35	.35	.35	.35	.70	.93	1.63	2.09	2.09	2.32	2.44	2.32	2.79	2.55	1.51	-.99
17	-.99	1.16	1.74	1.86	1.39	.93	.46	.35	.35	.23	.35	.23	.46	.93	1.63	2.32	2.44	3.72	3.37	3.37	3.60	3.02	2.44	-.99
18	-.99	-.99	1.74	1.39	1.05	.81	.23	.46	.23	.23	.23	.23	.12	.81	1.86	2.55	3.60	4.06	4.53	3.95	3.60	2.79	-.99	-.99
19	-.99	-.99	-.99	1.28	1.63	.93	.58	.35	.23	.12	.23	.35	.35	.58	1.51	2.55	3.37	3.83	3.95	3.48	3.02	-.99	-.99	-.99
20	-.99	-.99	-.99	-.99	1.63	1.74	.70	.46	.23	.23	.12	.12	.23	.35	.93	1.74	2.44	2.55	3.02	3.14	-.99	-.99	-.99	-.99
21	-.99	-.99	-.99	-.99	-.99	1.39	1.28	.81	.46	.35	.12	.12	.23	.23	.23	.70	.93	1.16	1.63	-.99	-.99	-.99	-.99	-.99
22	-.99	-.99	-.99	-.99	-.99	-.99	1.39	1.05	1.05	.70	.58	.23	.12	0.00	0.00	0.00	.12	.35	-.99	-.99	-.99	-.99	-.99	-.99
23	-.99	-.99	-.99	-.99	-.99	-.99	-.99	-.99	-.99	.70	.58	.35	.12	0.00	0.00	-.99	-.99	-.99	-.99	-.99	-.99	-.99	-.99	-.99

APPENDIX - 4H

CALCULATION OF THE EIGENVALUES OF THE ORIENTATION TENSOR

The orientation tensor is obtained from the matrix

$$a = \begin{pmatrix} \sum n_{ix}^2 & \sum n_{ix}\sum n_{iy} & \sum n_{ix}\sum n_{iz} \\ \sum n_{ix}\sum n_{iy} & \sum n_{iy}^2 & \sum n_{iy}\sum n_{iz} \\ \sum n_{ix}\sum n_{iz} & \sum n_{iy}\sum n_{iz} & \sum n_{iz}^2 \end{pmatrix}$$

where N axes are denoted by $\vec{n}_i$ with components n_{ix}, n_{iy}, n_{iz} in x,y,z directions respectively.

x,y,z are the three axes in rectangular cartesian co-ordinates. The convention used here is

+x towards horizontal north,
+y towards horizontal east,
+z vertically downwards.

$\vec{n}_i$ represents unit vector. Therefore, the direction cosines of each pole give n_{ix}, n_{iy} and n_{iz}. Once the elements of the 3x3 matrix a is known the eigenvalues and eigenvectors are obtained by using NAG routines from fortran libraries supported by the Imperial College Computer Centre (ICCC). For procedures related to NAG routines, see ICCC documentation. A fortran program EIGENV3 is written, which calls appropriate NAG routine after the elements of the matrix a are initiated.

When the azimuth and plunge of the axes are used as input values, these have to be converted to direction cosines before computing the elements of a.

APPENDIX - 4I

LINEAR REGRESSION ANALYSIS

A simple linear model given by equation (4.1a) is assumed. The model is

$$Y = \alpha + \beta x + e \qquad (4I.1)$$

where e is an unobservable random variable such that E(e)=0, and var(e) $=\sigma^2$.

Let (X_1,Y_1), (X_2,Y_2), ..., (X_n,Y_n) denote n pairs of observed values that fit the simple linear model. We wish to do the following:

1. Find the point estimate of the slope β.
2. Find the point estimate of the intercept α.
3. An answer to the question: How "good" is the quantity X as a predictor of the quantity Y?

Below are the formulas for calculating α and β (from Krumbein and Graybill 1965).

$$SS\ X^2 = \sum_{i=1}^{n} (X_i-\bar{X})^2 = \sum_{i=1}^{n} X_i^2 - \frac{\left(\sum_{i=1}^{n} X_i\right)^2}{n} \qquad (4I.2a)$$

$$SS\ Y^2 = \sum_{i=1}^{n} (Y_i-\bar{Y})^2 = \sum_{i=1}^{n} Y_i^2 - \frac{\left(\sum_{i=1}^{n} Y_i\right)^2}{n} \qquad (4I.2b)$$

$$SS\ XY = \sum_{i=1}^{n} (Y_i-\bar{Y})(X_i-\bar{X})$$

$$= \sum_{i=1}^{n} Y_i X_i - \frac{\sum_{i=1}^{n} Y_i \sum_{i=1}^{n} X_i}{n} \qquad (4I.2c)$$

$$\beta = \frac{SS\ XY}{SS\ X^2} \qquad (4I.2d)$$

$$\alpha = \bar{Y} - \beta \bar{X} \qquad (4I.2e)$$

A measure of how good a quantity X is when used to predict another quantity Y can be obtained from ρ, the (linear) correlation coefficient.

$$\rho^2 = \frac{\sigma_Y^2 - \sigma^2}{\sigma_Y^2} \qquad (4I.3a)$$

where $\sigma_Y 2$ is the variance of the normal population formed by Y's.

$100\rho^2$ is the percentage of variance of the population of Y's that is "accounted for" by using a related variable X. $\sigma_Y 2$, σ^2 etc. are usually unknown but ρ can be estimated from the sample values (X_i, Y_i). The estimator is

$$R = \frac{SS\ XY}{\sqrt{[(SS\ X^2)(SS\ Y^2)]}} \qquad (4I.3b)$$

The above formulas are translated into a FORTRAN program COEFFR2.

MAP I

PHOTO-INTERPRETED FRACTURE PATTERN W ISLAY

1:27000

Loch Laingeadail

LOCH GRUINART

LOCH GORM

LOCH INDAAL

Dilip Saha 1982

MAP II

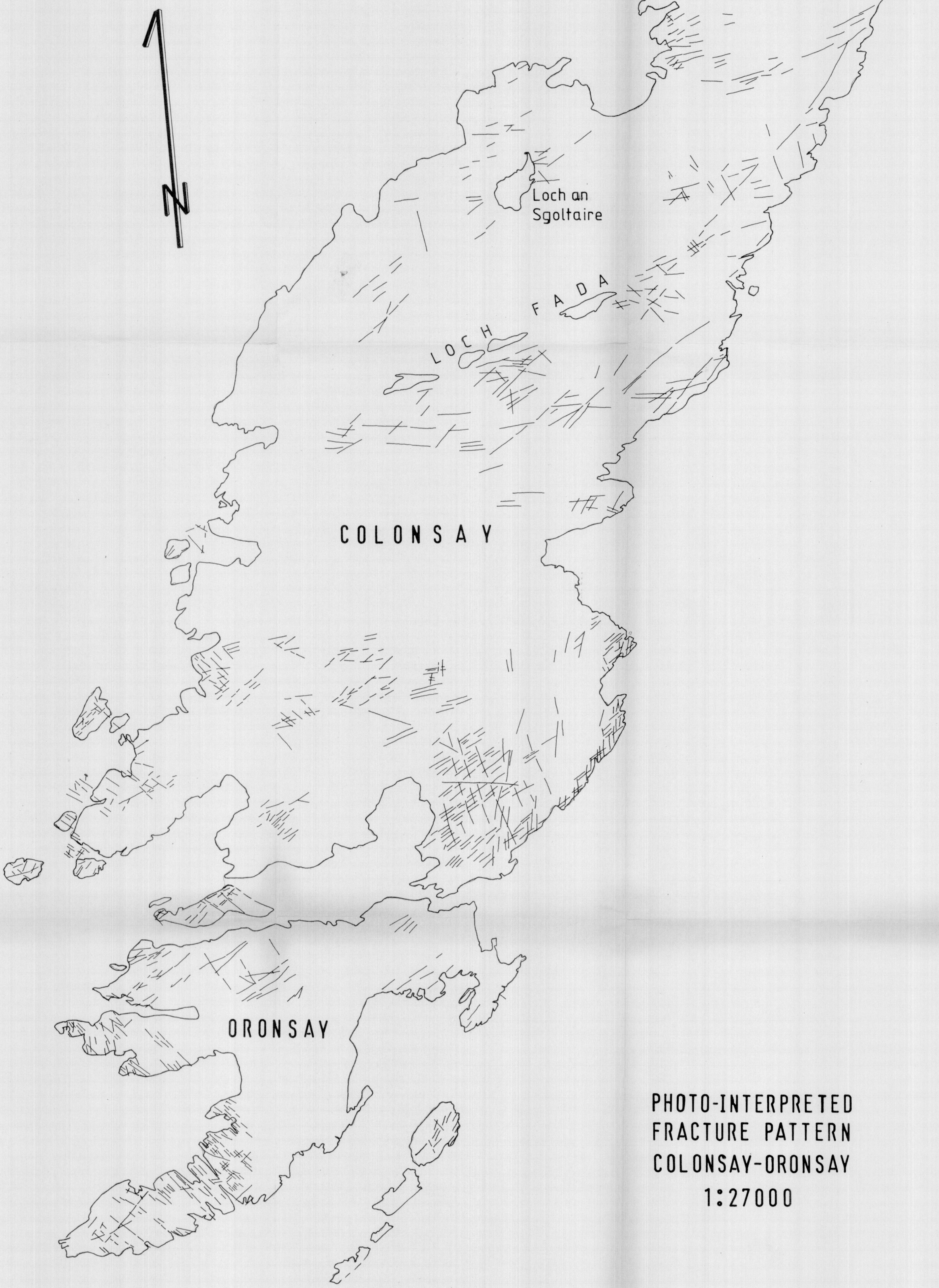


PHOTO-INTERPRETED
FRACTURE PATTERN
COLONSAY-ORONSAY
1:27000

Dilip Saha 1982

STRUCTURE MAP OF W ISLAY

LEWISIAN NOT INCLUDED 1:10560

MAP III

Loch Laingeadail

Sanaigmore

LOCH CORR

Smaull

LOCH GORM

Traigh Mhachir

Kilchoman

CROSPRIG

Kilchiaran Bay

Carn Mor

Kilchiaran Ho

Dun Midrig

Bruichladdich

COLONSAY GROUP

LEWISIAN

Eilean Liath

Port Charlotte

Loch an Fhir Mhor

Loch Gruinart

Sanaigmore Bay

Ardnave

Kilchiaran House

Coul

Lighthouse

Appinite with explosion breccia

Phyllite Grit

phyllite greywacke

grit phyllite

6°28′ 6°26′ 6°24′ 6°22′W

55°50′

55°45′ N

LITHOLOGICAL MAP OF W ISLAY
1: 100 000

10	Ardnave Formation
9	Sanaigmore Greywacke
8	Sanaigmore Phyllite
7	Smaull Greywacke
6	Kilchoman Phyllite
5	Crosprig Grit
4	Rubha na-h-Airde Moire Phyllite
3	Rubha Gaidhealach Grit
2	Kilchiaran Phyllite
1	Eilean Liath Grit

0 KM 2

- Crenulation cleavage, S_3
- .... S_2
- Schistosity S_1
- Mylonite foliation
- Bedding
- Grain elongation
- Intersection lin.
- Fold axis

axial trace of folds
- Antiform
- Synform

Dilip Saha 1983

MAP IV

STRUCTURE MAP OF COLONSAY

1:10000

- Bedding
- Cross-bedding
- Mylonite fol.
- Schistosity S_1
- Crenulation/P.S. cleavage S_2
- S_3
- Fold axis with style of fold indicated
- Stretching lineation
- Intersection lin.
- Fold interference
- Kink band

Leac Bhuidhe
pebbly grit
LEWISIAN
Rubh a' Geodha
Port an Obain
Balnahard
Carnan Eoin
Syenite
KILORAN BAY
Uragaig
limestone bands
Loch an Sgoltaire
Colonsay House
LOCH FADA
Upper Kilchattan
Riasg Buidhe
SCALASAIG
Pier
DOLOMITE
platonic intrusion
QUEENS BAY
Loch Staosnaig
MACHRINS
Milbuie
Baleromindubh
Loch Cholla
Baleromin-more
To Ardskenish
To Oronsay
LAT 56°02'N
THE STRAND

LITHOLOGIC MAP OF COLONSAY ORONSAY

Colonsay
Oronsay
1KM

- Plutonic intrusive
- Phyllite
- Epidotic grits
- Sandstone
- Mudstone
- Limestone
- Lewisian

Dilip Saha 1983

MAP V

STRUCTURE MAP OF IONA TORRIDONIAN

1 : 10 000

7 26

7 25

7 24

7 23

7 22

1 26

1 27

1 28

1 29

Port Bàn

Iona

A' Mhachair

Loch Staoinaig

St Mary's Abbey

Port an Diseart

Port a' Mhuilinn

Port na Muinntirr

St Ronan's Bay

Slipway

Port Lòrachan

Port an Fhir-bheilg

Port na Curraich

Port Gorrach an Ime

CONGLOMERATE

GRIT

FLAGGY GRIT

SCHISTOSE

ARKOSE

slate

slate

ONE KILOMETRE

- gneissic fol.
- bedding
- slaty cleavage
- mylonite fol.
- brittle shear zone
  - dextral
  - sinistral
- kink
- axial trace of fold
- thrust
- cataclasite

Dilip Saha 1983